SYNTHESIS AND SPECTROSCOPIC CHARACTERIZATION OF LOW- AND HIGH-VALENT WEAK-FIELD LANTHANIDE COMPLEXES

A Dissertation
Presented to
The Academic Faculty

by

Thaige P. Gompa

In Partial Fulfillment
of the Requirements for the Degree
Doctor of Philosophy in the
School of Chemistry and Biochemistry

Georgia Institute of Technology
December 2021

SYNTHESIS AND SPECTROSCOPIC CHARACTERIZATION OF LOW- AND HIGH-VALENT WEAK-FIELD LANTHANIDE COMPLEXES

Approved by:

Dr. Henry S. La Pierre, Advisor
School of Chemistry and Biochemistry
Georgia Institute of Technology

Dr. Joseph P. Sadighi
School of Chemistry and Biochemistry
Georgia Institute of Technology

Dr. Angus P. Wilkinson
School of Chemistry and Biochemistry
Georgia Institute of Technology

Dr. John Zhang
School of Chemistry and Biochemistry
Georgia Institute of Technology

Dr. Jake D. Soper
School of Chemistry and Biochemistry
Georgia Institute of Technology

Dr. Martin Mourigal
School of Physics
Georgia Institute of Technology

Date Approved: October 18, 2021

To my mom and dad.

ACKNOWLEDGEMENTS

It would like to express my utmost heartfelt gratitude to all the people who have helped me reach this point. Many people, both here at Georgia Tech and elsewhere, helped me along the way and I would like to use this opportunity to acknowledge and thank them for their support.

First, I would like to thank Dr. Henry La Pierre. As his first graduate student at Georgia Tech, he took a chance on me, and I am eternally grateful for that. He was a fantastic advisor who involved himself greatly in my PhD work as well as my thesis. Without any senior members in the lab, he had to train me personally so that I could move from breaking glassware to making molecules. On top of that, he provided invaluable professional and personal advice throughout my years in the PhD program, much of which I intend to follow as I move to the next stages of my career and life. I couldn't have asked for a better advisor, mentor, or friend.

I had the great fortune to be a part of an amazing cohort of lab mates in the La Pierre lab. I would like to thank Natalie Rice, Brandon Yik, Luis Aguirre Quintana, Andrew Boggiano, Ningxin Jiang, Arun Ramanathan, Dominic Russo, Julie Niklas, Haruko Tateyama, Tiffany Barker, and Grant Wilkinson for being wonderful and supportive lab mates.

I would like to thank my committee, Dr. Joseph Sadighi, Dr. Angus Wilkinson, Dr. John Zhang, Dr. Jake Soper, and Dr. Martin Mourigal for their help and guidance throughout my Ph.D.

I would also like to thank my high school teachers, Mr. Richie and Coach West who inspired and fostered my interest in STEM.

Finally, I would like to thank my parents, Vijaya and Raghu. Their support and love were invaluable and integral to my success in life as much as in graduate school.

Thank you, everyone.

TABLE OF CONTENTS

ACKNOWLEDGEMENTS **iv**

LIST OF TABLES **x**

LIST OF FIGURES **xx**

LIST OF SCHEMES **xxviii**

LIST OF SYMBOLS AND ABBREVIATIONS **xxix**

SUMMARY **xxxiv**

CHAPTER 1. Introduction **1**
1.1.1 Lanthanide starting materials 2
1.1.2 Redox chemistry in the lanthanides 3
1.1.3 Bonding in the lanthanides 7

CHAPTER 2. Diethyl Ether Adducts of Trivalent Lanthanide Iodides **10**
2.1 Background **10**
2.2 Results and Discussion **11**
2.2.1 Synthesis of $LnI_3(Et_2O)_x$, 1-Ln 11
2.2.2 Synthesis of $LnI_3(THF)_4$, 2-Ln, and $[LnI_2(THF)_5][LnI_4(THF)_2]$, 3-Ln 12
2.2.3 UV/vis Spectroscopy of colored 1-Ln complexes 13
2.2.4 Crystallography of 1-Ln 15
2.2.5 Test reactivity of 2-Ln and 3-Ln 21
2.3 Conclusion **22**
2.4 Experimental **22**
2.4.1 General Considerations 22
2.4.2 Synthesis of $LaI_3(Et_2O)_3$, 1-La 24
2.4.3 Synthesis $LaI_3(THF)_4$, 2-La 24
2.4.4 Synthesis of $CeI_3(Et_2O)_3$, 1-Ce 24
2.4.5 Synthesis $CeI_3(THF)_4$, 2-Ce 25
2.4.6 Synthesis of $PrI_3(Et_2O)_3$, 1-Pr 25
2.4.7 Synthesis $PrI_3(THF)_4$, 2-Pr 26
2.4.8 Synthesis of $NdI_3(Et_2O)_3$, 1-Nd 27
2.4.9 Synthesis $[NdI_2(THF)_5][NdI_4(THF)_2]$, 3-Nd 27
2.4.10 Synthesis of $SmI_3(Et_2O)_3$, 1-Sm 27
2.4.11 Synthesis $[SmI_2(THF)_5][SmI_4(THF)_2]$, 3-Sm 27
2.4.12 Direct Synthesis of $[EuI_2(THF)_5][EuI_4(THF)_2]$, 3-Eu 28
2.4.13 Synthesis of $GdI_3(Et_2O)_3$, 1-Gd 28
2.4.14 Synthesis $[GdI_2(THF)_5][GdI_4(THF)_2]$, 3-Gd 28
2.4.15 Synthesis of $TbI_3(Et_2O)_3$, 1-Tb 29
2.4.16 Synthesis $[TbI_2(THF)_5][TbI_4(THF)_2]$, 3-Tb 29
2.4.17 Synthesis of $DyI_3(Et_2O)_3$, 1-Dy 29

2.4.18 Synthesis $[DyI_2(THF)_5][DyI_4(THF)_2]$, 3-Dy 30
2.4.19 Synthesis of $HoI_3(Et_2O)_3$, 1-Ho 30
2.4.20 Synthesis $[HoI_2(THF)_5][HoI_4(THF)_2]$, 3-Ho 30
2.4.21 Synthesis of $ErI_3(Et_2O)_3$, 1-Er 30
2.4.22 Synthesis $[ErI_2(THF)_5][ErI_4(THF)_2]$, 3-Er 31
2.4.23 Synthesis of $TmI_3(Et_2O)_3$, 1-Tm 31
2.4.24 Synthesis $[TmI_2(THF)_5][TmI_4(THF)_2]$, 3-Tm 31
2.4.25 Direct Synthesis of $[YbI_2(THF)_5][YbI_4(THF)_2]$, 3-Yb 31
2.4.26 Synthesis of $Ce[N(Si(Me_3)_3)_2]_3$ 32
2.4.27 Synthesis of $Ce(C_7H_7)_3(THF)_3$ 33
2.5 Crystallographic Information 35
2.5.1 1-Ce 37
2.5.2 1-Pr 41
2.5.3 1-Nd 44
2.5.4 1-Sm 49
2.5.5 1-Gd 52
2.5.6 1-Tb 56
2.5.7 3-Tb 59

CHAPTER 3. Synthesis of Homoleptic, Divalent Lanthanide (Sm, Eu) Complexes via Oxidative Transmetallation 64
3.1 Background 64
3.2 Results and Discussion 65
3.2.1 Synthesis of the bis(tri-tert-butoxysilyl)amide complexes, 2-Eu and 2-Sm 66
3.2.2 Crystallographic analysis 67
3.2.3 SQUID measurements 69
3.2.4 UV/vis spectroscopy 70
3.3 Conclusion 71
3.4 Experimental 72
3.4.1 General Considerations 72
3.4.2 Synthesis of $(^tBuO)_3SiCl$ 74
3.4.3 Synthesis of $(^tBuO)_3SiNH_2$ 76
3.4.4 Synthesis of $(^tBuO)_3SiNHLi$ 78
3.4.5 Synthesis of $((^tBuO)_3Si)_2NH$, BTTSA-H 80
3.4.6 Synthesis of $((^tBuO)_3Si)_2NK$ 82
3.4.7 Synthesis of $[((^tBuO)_3Si)_2NCu]_2KCl$, 1 84
3.4.8 Synthesis of $[((^tBuO)_3Si)_2N]_2Sm$, 2-Sm 87
3.4.9 Synthesis of $[((^tBuO)_3Si)_2N]_2Eu$, 2-Eu 88
3.5 Crystallographic Information 90
3.5.1 BTTSA-H 91
3.5.2 BTTSA-Cu, 1 97
3.5.3 2-Sm 112
3.5.4 2-Eu 126

CHAPTER 4. High-frequency and -Field Electron Paramagnetic Resonance Spectroscopic Analysis of Metal-Ligand Covalency in $4f^7$ Valency Series (Eu^{2+}, Gd^{3+}, and Tb^{4+}) 139

4.1 Background 139
4.2 Results and Discussion 142
4.2.1 Analyte complexes 142
4.2.2 Crystallographic analysis 142
4.2.3 HFEPR and SQUID measurements 144
4.2.4 Quantum chemical calculations 150
4.3 Conclusion 155
4.4 Experimental 156
4.4.1 General Considerations 156
4.4.2 Synthesis of 1-Eu^{2+} 159
4.4.3 Synthesis of 2-Gd^{3+} 160
4.4.4 Synthesis of 3-Gd^{3+} 161
4.5 Crystallographic Information 162
4.5.1 1-Eu^{2+} 163
4.5.2 2-Gd^{3+} 181
4.5.3 3-Gd^{3+} 194
4.6 Magnetic data fits 219
4.6.1 1-Eu^{2+} 219
4.6.2 2-Gd^{3+} 223
4.6.3 3-Gd^{3+} 226
4.6.4 4-Tb^{4+} 229
4.7 EPR Spectra and Fits 232
4.8 Explicit Strain Model for EPR Linewidth 238
4.9 Model Geometries 243

CHAPTER 5. Intervalence Charge Transfer in Homobimetallic Ytterbium Complexes 252
5.1 Background 252
5.2 Results and Discussion 254
5.2.1 Crystallographic Analysis 254
5.2.2 Uv/vis Spectroscopy 260
5.2.3 SQUID measurements 268
5.3 Conclusion 270
5.4 Experimental 272
5.4.1 General Considerations 272
5.4.2 Synthesis of 1-Yb^{6+} 274
5.4.3 Synthesis of 2-Yb^{6+} 274
5.4.4 Synthesis of 3-Yb^{5+} 275
5.4.5 Synthesis of 5-Yb^{3+} 276
5.4.6 Synthesis of 1-Sm^{6+} 277
5.4.7 Synthesis of 2-Sm^{6+} 277
5.4.8 Synthesis of 4-$Sm^{5+}(Et_2O)$ 278
5.5 Crystallographic Information 280
5.5.1 1-Yb^{6+} 280
5.5.2 2-Yb^{6+} 290
5.5.3 3-Yb^{5+} 314
5.5.4 4-Yb^{5+}(DME) 328

5.5.5 5-Yb^{3+} 340
5.5.6 1-Sm^{6+} 358
5.5.7 2-Sm^{6+} 375
5.5.8 4-Sm^{5+}(Et2O) 391

CHAPTER 6. Conclusion 413
6.1 Thesis Overview 413
6.2 Future Work 415
6.2.1 New Low-Valent f-element Complexes Supported by Bulky Disilyl Amides 415
6.2.2 Mixed-Valent Template for Exploring Metal-Metal Bonding in the Lanthanides 416

APPENDIX A. Collaborator Contributions 418
A.1 Diethyl Ether Adducts of Trivalent Lanthanide Iodides 418
A.2 Synthesis of Homoleptic, Divalent Lanthanide (Sm, Eu) Complexes via Oxidative Transmetallation 418
A.3 High-Frequency and -Field Electron Paramagnetic Spectroscopic Analysis of Metal-Ligand Covalency in $4f^7$ Valency Series (Eu^{2+}, Gd^{3+}, Tb^{4+}) 418
A.4 Intervalence Charge Transfer in Homobimetallic Ytterbium Complexes 418

APPENDIX B. Permissions to Reproduce Published Materials 419
B.1 Introduction 419
B.2 Diethyl Ether Adducts of Trivalent Lanthanide Iodides 419
B.3 Synthesis of Homoleptic, Divalent Lanthanide (Sm, Eu) Complexes via Oxidative Transmetallation 419
B.4 High-Frequency and -Field Electron Paramagnetic Spectroscopic Analysis of Metal-Ligand Covalency in $4f^7$ Valency Series (Eu^{2+}, Gd^{3+}, Tb^{4+}) 420

References 421

LIST OF TABLES

Table 2.1	Coordination Geometry Parameters for 1-Ln.	20
Table 2.2	Table 2.2 General crystallographic data for 1-Ln.	36
Table 2.3	Fractional Atomic Coordinates ($\times 10^4$) and Equivalent Isotropic Displacement Parameters ($Å^2 \times 10^3$) for 1-Ce. U_{eq} is defined as 1/3 of the trace of the orthogonalised U_{ij}.	37
Table 2.4	Anisotropic Displacement Parameters ($\times 10^4$) for 1-Ce. The anisotropic displacement factor exponent takes the form: $-2\pi^2[h^2a^{*2} \times U_{11} + ... + 2hka^* \times b^* \times U_{12}]$.	38
Table 2.5	Bond Lengths in Å for 1-Ce.	38
Table 2.6	Bond Angles in ° for 1-Ce.	38
Table 2.7	Hydrogen Fractional Atomic Coordinates ($\times 10^4$) and Equivalent Isotropic Displacement Parameters ($Å^2 \times 10^3$) for 1-Ce. U_{eq} is defined as 1/3 of the trace of the orthogonalised U_{ij}.	39
Table 2.8	Fractional Atomic Coordinates ($\times 10^4$) and Equivalent Isotropic Displacement Parameters ($Å^2 \times 10^3$) for 1-Pr. U_{eq} is defined as 1/3 of the trace of the orthogonalised U_{ij}.	41
Table 2.9	Anisotropic Displacement Parameters ($\times 10^4$) 1-Pr. The anisotropic displacement factor exponent takes the form: $-2\pi^2[h^2a^{*2} \times U_{11} + ... + 2hka^* \times b^* \times U_{12}]$.	41
Table 2.10	Bond Lengths in Å for 1-Pr.	42
Table 2.11	Bond Angles in ° for 1-Pr.	42
Table 2.12	Hydrogen Fractional Atomic Coordinates ($\times 10^4$) and Equivalent Isotropic Displacement Parameters ($Å^2 \times 10^3$) for 1-Pr. U_{eq} is defined as 1/3 of the trace of the orthogonalised U_{ij}.	43
Table 2.13	Fractional Atomic Coordinates ($\times 10^4$) and Equivalent Isotropic Displacement Parameters ($Å^2 \times 10^3$) for 1-Nd. U_{eq} is defined as 1/3 of the trace of the orthogonalised U_{ij}.	44

Table 2.14	Anisotropic Displacement Parameters ($\times 10^4$) 1-Nd. The anisotropic displacement factor exponent takes the form: $-2\pi^2[h^2a^{*2} \times U_{11} + ... + 2hka^* \times b^* \times U_{12}]$.	45
Table 2.15	Bond Lengths in Å for 1-Nd.	45
Table 2.16	Bond Angles in ° for 1-Nd.	46
Table 2.17	Hydrogen Fractional Atomic Coordinates ($\times 10^4$) and Equivalent Isotropic Displacement Parameters ($Å^2 \times 10^3$) for 1-Nd. U_{eq} is defined as 1/3 of the trace of the orthogonalised U_{ij}.	46
Table 2.18	Fractional Atomic Coordinates (×104) and Equivalent Isotropic Displacement Parameters (Å2×103) for 1-Sm. Ueq is defined as 1/3 of the trace of the orthogonalised Uij.	49
Table 2.19	Anisotropic Displacement Parameters ($\times 10^4$) 1-Sm. The anisotropic displacement factor exponent takes the form: $-2\pi^2[h^2a^{*2} \times U_{11} + ... + 2hka^* \times b^* \times U_{12}]$.	50
Table 2.20	Bond Lengths in Å for 1-Sm.	50
Table 2.21	Bond Angles in ° for 1-Sm.	50
Table 2.22	Hydrogen Fractional Atomic Coordinates ($\times 10^4$) and Equivalent Isotropic Displacement Parameters ($Å^2 \times 10^3$) for 1-Sm. U_{eq} is defined as 1/3 of the trace of the orthogonalised U_{ij}.	51
Table 2.23	Atomic Occupancies for all atoms that are not fully occupied in 1-Sm.	51
Table 2.24	Fractional Atomic Coordinates ($\times 10^4$) and Equivalent Isotropic Displacement Parameters ($Å^2 \times 10^3$) for 1-Gd. U_{eq} is defined as 1/3 of the trace of the orthogonalised U_{ij}.	52
Table 2.25	Anisotropic Displacement Parameters ($\times 10^4$) 1-Gd. The anisotropic displacement factor exponent takes the form: $-2\pi^2[h^2a^{*2} \times U_{11} + ... + 2hka^* \times b^* \times U_{12}]$.	53
Table 2.26	Bond Lengths in Å for 1-Gd.	53
Table 2.27	Bond Angles in ° for 1-Gd.	53

Table 2.28	Hydrogen Fractional Atomic Coordinates ($\times 10^4$) and Equivalent Isotropic Displacement Parameters ($Å^2 \times 10^3$) for 1-Gd. U_{eq} is defined as 1/3 of the trace of the orthogonalised U_{ij}.	54
Table 2.29	Fractional Atomic Coordinates ($\times 10^4$) and Equivalent Isotropic Displacement Parameters ($Å^2 \times 10^3$) for 1-Tb. U_{eq} is defined as 1/3 of the trace of the orthogonalised U_{ij}.	56
Table 2.30	Anisotropic Displacement Parameters ($\times 10^4$) 1-Tb. The anisotropic displacement factor exponent takes the form: $-2\pi^2[h^2a^{*2} \times U_{11} + ... + 2hka^* \times b^* \times U_{12}]$	57
Table 2.31	Bond Lengths in Å for 1-Tb.	57
Table 2.32	Bond Angles in ° for 1-Tb.	57
Table 2.33	Hydrogen Fractional Atomic Coordinates ($\times 10^4$) and Equivalent Isotropic Displacement Parameters ($Å^2 \times 10^3$) for 1-Tb. U_{eq} is defined as 1/3 of the trace of the orthogonalised U_{ij}.	58
Table 2.34	Fractional Atomic Coordinates ($\times 10^4$) and Equivalent Isotropic Displacement Parameters ($Å^2 \times 10^3$) for 3-Tb. U_{eq} is defined as 1/3 of the trace of the orthogonalised U_{ij}.	59
Table 2.35	Anisotropic Displacement Parameters ($\times 10^4$) 3-Tb. The anisotropic displacement factor exponent takes the form: $-2\pi^2[h^2a^{*2} \times U_{11} + ... + 2hka^* \times b^* \times U_{12}]$.	60
Table 2.36	Bond Lengths in Å for 3-Tb.	60
Table 2.37	Bond Angles in ° for 3-Tb.	61
Table 2.38	Hydrogen Fractional Atomic Coordinates ($\times 10^4$) and Equivalent Isotropic Displacement Parameters ($Å^2 \times 10^3$) for 3-Tb. U_{eq} is defined as 1/3 of the trace of the orthogonalised U_{ij}.	62
Table 3.1	Selected bond lengths (Å) and angles (°) for 2-Sm and 2-Eu.	69
Table 3.2	Crystal data and structure refinement for BTTSA-H.	91

Table 3.3	Fractional Atomic Coordinates ($\times10^4$) and Equivalent Isotropic Displacement Parameters ($Å^2\times10^3$) for BTTSA-H. U_{eq} is defined as 1/3 of the trace of the orthogonalised U_{IJ} tensor.	92
Table 3.4	Anisotropic Displacement Parameters ($Å^2\times10^3$) for BTTSA-H. The Anisotropic displacement factor exponent takes the form: $-2\pi^2[h^2a^{*2}U_{11}+2hka^*b^*U_{12}+\ldots]$.	93
Table 3.5	Bond Lengths for BTTSA-H.	94
Table 3.6	Bond Angles for BTTSA-H.	94
Table 3.7	Hydrogen Atom Coordinates ($Å\times10^4$) and Isotropic Displacement Parameters ($Å^2\times10^3$) for BTTSA-H.	95
Table 3.8	Crystal data and structure refinement for 1.	97
Table 3.9	Fractional Atomic Coordinates ($\times10^4$) and Equivalent Isotropic Displacement Parameters ($Å^2\times10^3$) for 1. U_{eq} is defined as 1/3 of the trace of the orthogonalised U_{IJ} tensor.	98
Table 3.10	Anisotropic Displacement Parameters ($Å^2\times10^3$) for 1. The Anisotropic displacement factor exponent takes the form: $-2\pi^2[h^2a^{*2}U_{11}+2hka^*b^*U_{12}+\ldots]$.	100
Table 3.11	Bond Lengths for 1.	102
Table 3.12	Bond Angles for 1.	104
Table 3.13	Hydrogen Atom Coordinates ($Å\times10^4$) and Isotropic Displacement Parameters ($Å^2\times10^3$) for 1.	106
Table 3.14	Atomic Occupancy for 1.	110
Table 3.15	Solvent masks information for 1.	111
Table 3.16	Crystal data and structure refinement for 2-Sm.	112
Table 3.17	Fractional Atomic Coordinates (×104) and Equivalent Isotropic Displacement Parameters (Å2×103) for 2-Sm. Ueq is defined as 1/3 of the trace of the orthogonalised UIJ tensor.	113
Table 3.18	Anisotropic Displacement Parameters ($Å^2\times10^3$) for 2-Sm. The Anisotropic displacement factor exponent takes the form: $-2\pi^2[h^2a^{*2}U_{11}+2hka^*b^*U_{12}+\ldots]$.	115

Table 3.19	Bond Lengths for 2-Sm.	117
Table 3.20	Bond Angles for 2-Sm.	118
Table 3.21	Hydrogen Atom Coordinates ($Å \times 10^4$) and Isotropic Displacement Parameters ($Å^2 \times 10^3$) for 2-Sm.	121
Table 3.22	Atomic Occupancy for 2-Sm.	124
Table 3.23	Crystal data and structure refinement for 2-Eu.	126
Table 3.24	Fractional Atomic Coordinates ($\times 10^4$) and Equivalent Isotropic Displacement Parameters ($Å^2 \times 10^3$) for 2-Eu. U_{eq} is defined as 1/3 of the trace of the orthogonalised U_{ij} tensor.	127
Table 3.25	Anisotropic Displacement Parameters ($Å^2 \times 10^3$) for 2-Eu. The Anisotropic displacement factor exponent takes the form: $-2\pi^2[h^2a^{*2}U_{11}+2hka^*b^*U_{12}+\ldots]$.	129
Table 3.26	Bond Lengths for 2-Eu.	131
Table 3.27	Bond Angles for 2-Eu.	132
Table 3.28	Hydrogen Atom Coordinates ($Å \times 10^4$) and Isotropic Displacement Parameters ($Å^2 \times 10^3$) for 2-Eu.	135
Table 3.29	Atomic Occupancy for 2-Eu.	138
Table 4.1	Spin Hamiltonian Parameters Extracted from EPR Spectroscopy of Solution Samples.	146
Table 4.2	Metrics Derived from AILFT and CASSCF/NEVPT2 Calculations.	153
Table 4.3	Crystal data and structure refinement.	162
Table 4.4	Fractional Atomic Coordinates (×104) and Equivalent Isotropic Displacement Parameters (Å2×103) for 1-Eu^{2+}. U_{eq} is defined as 1/3 of the trace of the orthogonalised U_{IJ} tensor.	163
Table 4.5	Anisotropic Displacement Parameters ($Å^2 \times 10^3$) for 1-Eu^{2+}. The Anisotropic displacement factor exponent takes the form: $-2\pi^2[h^2a^{*2}U_{11} + 2hka^*b^*U_{12} + \ldots]$.	166
Table 4.6	Bond Lengths for 1-Eu^{2+}.	169

Table 4.7	Bond Angles for 1-Eu^{2+}.	170
Table 4.8	Hydrogen Atom Coordinates ($Å \times 10^4$) and Isotropic Displacement Parameters ($Å^2 \times 10^3$) for 1-Eu^{2+}.	174
Table 4.9	Atomic Occupancy for 1-Eu^{2+}.	179
Table 4.10	Fractional Atomic Coordinates ($\times 10^4$) and Equivalent Isotropic Displacement Parameters ($Å^2 \times 10^3$) for 2-Gd^{3+}. U_{eq} is defined as 1/3 of the trace of the orthogonalised U_{IJ} tensor.	181
Table 4.11	Anisotropic Displacement Parameters ($Å^2 \times 10^3$) for 2-Gd^{3+}. The Anisotropic displacement factor exponent takes the form: $-2\pi^2[h^2a^{*2}U_{11} + 2hka^*b^*U_{12} + \ldots]$.	184
Table 4.12	Bond Lengths for 2-Gd^{3+}.	186
Table 4.13	Bond Angles for 2-Gd^{3+}.	187
Table 4.14	Hydrogen Atom Coordinates ($Å \times 10^4$) and Isotropic Displacement Parameters ($Å^2 \times 10^3$) for 2-Gd^{3+}.	189
Table 4.15	Fractional Atomic Coordinates ($\times 10^4$) and Equivalent Isotropic Displacement Parameters ($Å^2 \times 10^3$) for 3-Gd^{3+}. U_{eq} is defined as 1/3 of the trace of the orthogonalised U_{IJ} tensor.	194
Table 4.16	Anisotropic Displacement Parameters ($Å^2 \times 10^3$) for 3-Gd^{3+}. The Anisotropic displacement factor exponent takes the form: $-2\pi^2[h^2a^{*2}U_{11} + 2hka^*b^*U_{12} + \ldots]$.	198
Table 4.17	Bond Lengths for 3-Gd^{3+}.	201
Table 4.18	Bond Angles for 3-Gd^{3+}.	203
Table 4.19	Torsion Angles for 3-Gd^{3+}.	207
Table 4.20	Hydrogen Atom Coordinates ($Å \times 10^4$) and Isotropic Displacement Parameters ($Å^2 \times 10^3$) for 3-Gd^{3+}.	211
Table 4.21	Atomic Occupancy for 3-Gd^{3+}.	216
Table 4.22	Fit parameters from dc susceptibility measurements.	219
Table 4.23	Spin Hamiltonian parameters extracted from EPR spectroscopy of polycrystalline samples.	235

Table 4.24	AILFT Results including the Condon-Shortley-Slater interelectronic repulsion parameters (F^i), SOC Constants (z), and Reductions from the Free Ion For CASSCF (normal print) and NEVPT2 (*italics*) Calculations.	236
Table 4.25	CASSCF/NEVPT2 calculated values of $\Delta_{\mathbf{8_S}}$with and without the spin-spin coupling (SSC) contribution (cm^{-1}) for truncated models, Ln^M (see Figure 4.25).	236
Table 4.26	Model Geometry for Eu^M.	243
Table 4.27	Model Geometry for Gd^M.	246
Table 4.28	Model Geometry for Tb^M.	248
Table 5.1	Select bond lengths for 1-Yb^{6+}, 2-Yb^{6+}, and 3-Yb^{5+}. Subscript of a denotes terminal ligand and subscript of b denotes bridging ligand.	255
Table 5.2	Gaussian fit parameters for 3-Yb^{5+} spectra in hexanes (Figure 5.6).	264
Table 5.3	Crystal data and structure refinement for 1-Yb^{6+}.	280
Table 5.4	Fractional Atomic Coordinates ($\times10^4$) and Equivalent Isotropic Displacement Parameters ($Å^2\times10^3$) for 1-Yb^{6+}. U_{eq} is defined as 1/3 of the trace of the orthogonalised U_{IJ} tensor.	281
Table 5.5	Anisotropic Displacement Parameters ($Å^2\times10^3$) for 1-Yb^{6+}. The Anisotropic displacement factor exponent takes the form: $-2\pi^2[h^2a^{*2}U_{11}+2hka^*b^*U_{12}+\ldots]$.	283
Table 5.6	Bond Lengths for 1-Yb^{6+}.	284
Table 5.7	Bond Angles for 1-Yb^{6+}.	285
Table 5.8	Hydrogen Atom Coordinates ($Å\times10^4$) and Isotropic Displacement Parameters ($Å^2\times10^3$) for 1-Yb^{6+}.	287
Table 5.9	Crystal data and structure refinement for 2-Yb^{6+}.	290
Table 5.10	Fractional Atomic Coordinates ($\times10^4$) and Equivalent Isotropic Displacement Parameters ($Å^2\times10^3$) for 2-Yb^{6+}. U_{eq} is defined as 1/3 of the trace of the orthogonalised U_{IJ} tensor.	291

Table 5.11	Anisotropic Displacement Parameters ($Å^2×10^3$) for 2-Yb^{6+}. The Anisotropic displacement factor exponent takes the form: $-2\pi^2[h^2a^{*2}U_{11}+2hka^*b^*U_{12}+\ldots]$.	294
Table 5.12	Bond Lengths for 2-Yb^{6+}.	297
Table 5.13	Bond Angles for 2-Yb^{6+}.	299
Table 5.14	Torsion Angles for 2-Yb^{6+}.	301
Table 5.15	Hydrogen Atom Coordinates ($Å×10^4$) and Isotropic Displacement Parameters ($Å^2×10^3$) for 2-Yb^{6+}.	308
Table 5.16	Atomic Occupancy for 2-Yb^{6+}.	312
Table 5.17	Solvent masks information for 2-Yb^{6+}.	313
Table 5.18	Crystal data and structure refinement for 3-Yb^{5+}.	314
Table 5.19	Fractional Atomic Coordinates ($×10^4$) and Equivalent Isotropic Displacement Parameters ($Å^2×10^3$) for 3-Yb^{5+}. U_{eq} is defined as 1/3 of the trace of the orthogonalised U_{IJ} tensor.	315
Table 5.20	Anisotropic Displacement Parameters ($Å^2×10^3$) for 3-Yb^{5+}. The Anisotropic displacement factor exponent takes the form: $-2\pi^2[h^2a^{*2}U_{11}+2hka^*b^*U_{12}+\ldots]$.	318
Table 5.21	Bond Lengths for 3-Yb^{5+}.	320
Table 5.22	Bond Angles for 3-Yb^{5+}.	322
Table 5.23	Torsion Angles for 3-Yb^{5+}.	324
Table 5.24	Crystal data and structure refinement for 4-Yb^{5+}(DME).	328
Table 5.25	Fractional Atomic Coordinates ($×10^4$) and Equivalent Isotropic Displacement Parameters ($Å^2×10^3$) for 4-Yb^{5+}(DME). U_{eq} is defined as 1/3 of the trace of the orthogonalised U_{IJ} tensor.	329
Table 5.26	Anisotropic Displacement Parameters ($Å^2×10^3$) for 4-Yb^{5+}(DME). The Anisotropic displacement factor exponent takes the form: $-2\pi^2[h^2a^{*2}U_{11}+2hka^*b^*U_{12}+\ldots]$.	332
Table 5.27	Hydrogen Atom Coordinates ($Å×10^4$) and Isotropic Displacement Parameters ($Å^2×10^3$) for 4-Yb^{5+}(DME).	335

Table 5.28	Atomic Occupancy for 4-Yb^{5+}(DME).	339
Table 5.29	Crystal data and structure refinement for 5-Yb^{3+}.	340
Table 5.30	Fractional Atomic Coordinates ($\times10^4$) and Equivalent Isotropic Displacement Parameters ($Å^2\times10^3$) for 5-Yb^{3+}. U_{eq} is defined as 1/3 of the trace of the orthogonalised U_{IJ} tensor.	341
Table 5.31	Anisotropic Displacement Parameters ($Å^2\times10^3$) for 5-Yb^{3+}. The Anisotropic displacement factor exponent takes the form: $-2\pi^2[h^2a^{*2}U_{11}+2hka^*b^*U_{12}+\ldots]$.	344
Table 5.32	Bond Lengths for 5-Yb^{3+}.	347
Table 5.33	Bond Angles for 5-Yb^{3+}.	349
Table 5.34	Hydrogen Atom Coordinates ($Å\times10^4$) and Isotropic Displacement Parameters ($Å^2\times10^3$) for 5-Yb^{3+}.	352
Table 5.35	Atomic Occupancy for 5-Yb^{3+}.	357
Table 5.36	Crystal data and structure refinement for 1-Sm^{6+}.	358
Table 5.37	Fractional Atomic Coordinates ($\times10^4$) and Equivalent Isotropic Displacement Parameters ($Å^2\times10^3$) for 1-Sm^{6+}. U_{eq} is defined as 1/3 of the trace of the orthogonalised U_{IJ} tensor.	359
Table 5.38	Anisotropic Displacement Parameters ($Å^2\times10^3$) for 1-Sm^{6+}. The Anisotropic displacement factor exponent takes the form: $-2\pi^2[h^2a^{*2}U_{11}+2hka^*b^*U_{12}+\ldots]$.	362
Table 5.39	Bond Lengths for 1-Sm^{6+}.	365
Table 5.40	Bond Angles for 1-Sm^{6+}.	367
Table 5.41	Hydrogen Atom Coordinates ($Å\times10^4$) and Isotropic Displacement Parameters ($Å^2\times10^3$) for 1-Sm^{6+}.	370
Table 5.42	Solvent masks information for 1-Sm^{6+}.	374
Table 5.43	Crystal data and structure refinement for 2-Sm^{6+}.	375
Table 5.44	Fractional Atomic Coordinates ($\times10^4$) and Equivalent Isotropic Displacement Parameters ($Å^2\times10^3$) for 2-Sm^{6+}. U_{eq} is defined as 1/3 of the trace of the orthogonalised U_{IJ} tensor.	376

Table 5.45	Anisotropic Displacement Parameters ($Å^2×10^3$) for 2-Sm^{6+}. The Anisotropic displacement factor exponent takes the form: $-2\pi^2[h^2a^{*2}U_{11}+2hka^*b^*U_{12}+\ldots]$.	379
Table 5.46	Bond Lengths for 2-Sm^{6+}.	382
Table 5.47	Bond Angles for 2-Sm^{6+}.	383
Table 5.48	Hydrogen Atom Coordinates ($Å×10^4$) and Isotropic Displacement Parameters ($Å^2×10^3$) for 2-Sm^{6+}.	386
Table 5.49	Crystal data and structure refinement for 4-Sm^{5+}(Et_2O).	391
Table 5.50	Fractional Atomic Coordinates ($×10^4$) and Equivalent Isotropic Displacement Parameters ($Å^2×10^3$) for 4-Sm^{5+}(Et_2O). U_{eq} is defined as 1/3 of the trace of the orthogonalised U_{IJ} tensor.	392
Table 5.51	Anisotropic Displacement Parameters ($Å^2×10^3$) for 4-Sm^{5+}(Et_2O). The Anisotropic displacement factor exponent takes the form: $-2\pi^2[h^2a^{*2}U_{11}+2hka^*b^*U_{12}+\ldots]$.	395
Table 5.52	Bond Lengths for 4-Sm^{5+}(Et_2O).	398
Table 5.53	Bond Angles for 4-Sm^{5+}(Et_2O).	400
Table 5.54	Torsion Angles for 4-Sm^{5+}(Et_2O).	403
Table 5.55	Hydrogen Atom Coordinates ($Å×10^4$) and Isotropic Displacement Parameters ($Å^2×10^3$) for 4-Sm^{5+}(Et_2O).	407
Table 5.56	Atomic Occupancy for 4-Sm^{5+}(Et_2O).	412

LIST OF FIGURES

Figure 1.1	Thermodynamic cycle for the binding of 3,4,3-LI(1,2-HOPO) to Ce^{3+} and Ce^{4+}. Figure adapted from ref 94.	6
Figure 2.1	Molecular structure of 3-Tb with thermal ellipsoids shown at 50% probability and H atoms are omitted for clarity.	12
Figure 2.2	UV/vis spectra for varied concentrations for 1-Sm in diethyl ether.	14
Figure 2.3	UV/vis spectra for varied concentrations for 1-Nd in diethyl ether.	15
Figure 2.4	UV/vis spectra of saturated solutions of 1-Nd and 1-Sm in diethyl ether.	16
Figure 2.5	Molecular structure of 1-Pr with thermal ellipsoids shown at 50% probability and H atoms are omitted for clarity.	17
Figure 2.6	Plot of the equatorial Ln–I bond distance relative to trivalent metal ionic radii in structurally characterized 1-Ln compounds in the Pbcn space group. Error bars are smaller than the point size.	18
Figure 2.7	^{1}H NMR of 1-Ce in C_6D_6 (no precipitation observed, all of the complex is dissolved).	25
Figure 2.8	^{1}H NMR of 1-Pr in C_6D_6 (no precipitation observed, all of the complex is dissolved).	26
Figure 2.9	^{1}H NMR of $Ce[N(Si(Me)_3)_2]_3$ in C_6D_6. Peak of C_6D_5H is noted as *.	33
Figure 2.10	^{13}C NMR of $Ce[N(Si(Me_3)_3)_2]_3$ in C_6D_6. Peak of C_6D_5H is noted as *.	33
Figure 2.11	Powder XRD pattern for $Ce(C_7H_7)_3(THF)_3$. Simulated pattern is based on previously reported single crystal XRD data from ref. 143.	34
Figure 2.12	Molecular structure of 1-Ce with thermal ellipsoids shown at 50% probability and H atoms are omitted for clarity.	37

Figure 2.13	Molecular structure of 1-Pr with thermal ellipsoids shown at 50% probability and H atoms are omitted for clarity.	41
Figure 2.14	Molecular structure of 1-Nd with thermal ellipsoids shown at 50% probability and H atoms are omitted for clarity.	44
Figure 2.15	Molecular structure of 1-Sm with thermal ellipsoids shown at 50% probability and H atoms are omitted for clarity.	49
Figure 2.16	Molecular structure of 1-Gd with thermal ellipsoids shown at 50% probability and H atoms are omitted for clarity.	52
Figure 2.17	Molecular structure of 1-Tb with thermal ellipsoids shown at 50% probability and H atoms are omitted for clarity.	56
Figure 2.18	Molecular structure of 3-Tb with thermal ellipsoids shown at 50% probability and H atoms are omitted for clarity.	59
Figure 3.1	Molecular structure of BTTSA-H. Thermal ellipsoids are shown at 50% probability and H atoms (except for N–H) are omitted for clarity.	66
Figure 3.2	Molecular structure of 2-Eu with thermal ellipsoids shown at 50% probability with hydrogen atoms omitted for clarity.	67
Figure 3.3	Temperature dependence of magnetic moment (μ_{eff}) for 2-Sm and 2-Eu collected under dc field of 1 T.	69
Figure 3.4	UV/vis spectra of 2-Sm and 2-Eu in diethyl ether.	70
Figure 3.5	^{1}H NMR for (^{t}BuO)$_3$SiCl in C_6D_6. C_6D_5H is noted as *.	75
Figure 3.6	^{13}C NMR for (^{t}BuO)$_3$SiCl in C_6D_6. C_6D_5H is noted as *.	75
Figure 3.7	^{1}H NMR for (^{t}BuO)$_3$SINH$_2$ in C_6D_6. Peak of C_6D_5H is noted as *.	77
Figure 3.8	^{13}C NMR for (^{t}BuO)$_3$SiNH$_2$ in C_6D_6. C_6D_5H is noted as *.	77
Figure 3.9	^{1}H NMR for (^{t}BuO)$_3$SiNHLi in C_6D_6. Peak of C_6D_5H is noted as *.	79
Figure 3.10	^{13}C NMR for (^{t}BuO)$_3$SiNHLi in C_6D_6. Peaks of C_6D_5H is noted as *.	79
Figure 3.11	^{1}H NMR for ((^{t}BuO)$_3$Si)$_2$NH in C_6D_6. Peak of C_6D_5H is noted as *. Unidentified impurities are marked as #.	81

Figure 3.12	^{13}C NMR for $((^{t}BuO)_3Si)_2NH$ in C_6D_6. Peak of C_6D_5H is noted as *. Unidentified impurities are marked as #.	81
Figure 3.13	^{1}H NMR for $((^{t}BuO)_3Si)_2NK$ in pyridine-d_5. Residual NMR solvent peaks are noted as *. BTTSA-H impurity is marked as #. Diethyl ether impurity is labeled with &.	83
Figure 3.14	^{13}C NMR for $((^{t}BuO)_3Si)_2NK$ in pyridine-d_5. Residual NMR solvent peaks are noted as *. BTTSA-H impurity are marked as #.	83
Figure 3.15	Molecular structure of 2. One subunit of a polymeric chain is shown. Thermal ellipsoids are shown at 50% probability and H atoms are omitted for clarity.	84
Figure 3.16	^{1}H NMR for 1 in C_6D_6. Peak of C_6D_5H is noted as *. BTTSA-H impurity is marked as #. THF impurity is labeled with &.	86
Figure 3.17	^{13}C NMR for 1 in C_6D_6. Peak of C_6D_5H is noted as *. BTTSA-H impurity is marked as #. THF impurity is labeled with &.	86
Figure 3.18	Molecular structure of 2-Sm. Thermal ellipsoids are shown at 50% probability and H atoms are omitted for clarity.	87
Figure 3.19	Molecular structure of 2-Eu. Thermal ellipsoids are shown at 50% probability and H atoms are omitted for clarity.	88
Figure 3.20	Molecular structure of BTTSA-H. Thermal ellipsoids are shown at 50% probability and H atoms (except for N–H) are omitted for clarity.	91
Figure 3.21	Molecular structure of 1. One subunit of a polymeric chain is shown. Thermal ellipsoids are shown at 50% probability and H atoms are omitted for clarity.	97
Figure 3.22	Molecular structure of 2-Sm. Thermal ellipsoids are shown at 50% probability and H atoms are omitted for clarity.	112
Figure 3.23	Molecular structure of 2-Eu. Thermal ellipsoids are shown at 50% probability and H atoms are omitted for clarity.	126
Figure 4.1	Molecular structures of 1-Eu^{2+}, 2-Gd^{3+}, 3-Gd^{3+}, and 4-Tb^{4+}.	141

Figure 4.2	Variable-temperature molar magnetic susceptibility times temperature ($\chi_M T$) for 1-Eu^{2+}, 2-Gd^{3+}, 3-Gd^{3+}, and 4-Tb^{4+} collected under dc field of 1 T.	144
Figure 4.3	a) Experimental (black traces) and simulated (red traces) X-band EPR spectra at 9.36 GHz and 5 K. b) Experimental (black traces) and simulated (red traces) HFEPR spectra at 260 GHz and 5 K. In these spectra the frequency of the central transition is subtracted in order to facilitate a direct comparison of the observed spectral extent for each compound. Simulation parameters are given in Table 4.1.	145
Figure 4.4	Energy levels for the ground ^8S state and excited sextet states calculated at the CASSCF/NEVPT2 level of theory. For each metal ion, the free ion and model structure energy levels are shown.	154
Figure 4.5	Molecular structure of 1-Eu^{2+} with thermal ellipsoids shown at 50% probability with hydrogen atoms omitted for clarity. Color code: C, black; N, blue; O, red; P, orange; K, purple; Eu, magenta.	163
Figure 4.6	Molecular structure of 2-Gd^{3+} with thermal ellipsoids shown at 50% probability with hydrogen atoms omitted for clarity. Color code: C, black; N, blue; O, red; P, orange; K, purple; Gd, magenta.	181
Figure 4.7	Molecular structure of 3-Gd^{3+} with thermal ellipsoids shown at 50% probability with hydrogen atoms omitted for clarity. Color code: C, black; N, blue; O, red; P, orange; K, purple; Gd, magenta.	194
Figure 4.8	Experimental (circles) and Fit (lines) χT data for 1-Eu^{2+} at 3 T (green) and 1 T (blue).	221
Figure 4.9	Experimental (circles) and Fit (lines) χ data for 1-Eu^{2+} at 3 T (green) and 1 T (blue).	221
Figure 4.10	Experimental (circles) and Fit (lines) $1/\chi$ data for 1-Eu^{2+} at 3 T (green) and 1 T (blue).	222
Figure 4.11	Experimental (circles) and Fit (lines) χT data for 2-Gd^{3+} at 3 T (green) and 1 T (blue).	224
Figure 4.12	Experimental (circles) and Fit (lines) χ data for 2-Gd^{3+} at 3 T (green) and 1 T (blue).	224

Figure 4.13	Experimental (circles) and Fit (lines) $1/\chi$ data for 2-Gd^{3+} at 3 T (green) and 1 T (blue).	225
Figure 4.14	Experimental (circles) and Fit (lines) χT data for 3-Gd^{3+} at 3 T (green) and 1 T (blue).	227
Figure 4.15	Experimental (circles) and Fit (lines) χ data for 3-Gd^{3+} at 3 T (green) and 1 T (blue).	227
Figure 4.16	Experimental (circles) and Fit (lines) $1/\chi$ data for 3-Gd^{3+} at 3 T (green) and 1 T (blue).	228
Figure 4.17	Experimental (circles) and Fit (lines) χT data for 4-Tb^{4+} at 3 T (green) and 1 T (blue).	230
Figure 4.18	Experimental and Fit χ data for 4-Tb^{4+} at 3 T (green) and 1 T (blue).	230
Figure 4.19	Experimental (circles) and Fit (lines) $1/\chi$ data for 4-Tb^{4+} at 3 T (green) and 1 T (blue).	231
Figure 4.20	Experimental Multi-frequency EPR spectra (black traces) and corresponding simulations (red traces) of 1-Eu^{2+}. a) Solutions (explicit strain model); b) Polycrystalline powders.	233
Figure 4.21	Experimental Multi-frequency EPR spectra (black traces) and corresponding simulations (red traces) of 2-Gd^{3+}. a) Solutions; b) Polycrystalline powders.	233
Figure 4.22	Experimental Multi-frequency EPR spectra (black traces) and corresponding simulations (red traces) of 3-Gd^{3+}. a) Solutions; b) Polycrystalline powders. The solid samples exhibit propagation artifacts at lower frequencies and the parameters are estimated from the 361 GHz spectrum only.	234
Figure 4.23	Experimental Multi-frequency EPR spectra (black traces) and corresponding simulations (red traces) of 4-Tb^{4+}. a) Solutions (explicit strain model); b) Polycrystalline powders (explicit strain model). Features marked by * indicate Tb^{3+} impurities while those marked with ^ correspond to molecular oxygen.	235

Figure 4.24 Energy levels for the ground ^{8}S state and excited sextet states (^{6}L) calculated at the CASSCF/NEVPT2 level of theory. For each metal ion the free ion (FI), hypothetical $[LnCl_4]^{-1/0/+1}$, (Cl_4) and model structure (L_4) energy levels are shown. 237

Figure 4.25 Truncated model Ln^{M} for quantum calculations. 237

Figure 5.1 A) Molecular structure of 1-Yb^{6+} with thermal ellipsoids shown at 50% probability with hydrogen and carbon atoms omitted for clarity. B) Molecular structure of 2-Yb^{6+} with thermal ellipsoids shown at 50% probability with hydrogen and carbon atoms omitted for clarity. C) Molecular structure of 3-Yb^{5+} with thermal ellipsoids shown at 50% probability with hydrogen and carbon atoms omitted for clarity. 253

Figure 5.2 A) Molecular structure of 4-Sm^{5+}(Et_2O) with thermal ellipsoids shown at 50% probability with hydrogen and non-solvent carbon atoms omitted for clarity. B) Molecular structure of 4-Yb^{5+}(DME) with thermal ellipsoids shown at 50% probability with hydrogen and non-solvent carbon atoms omitted for clarity. 257

Figure 5.3 UV/vis/NIR spectra for 1-Yb^{6+} (red) and 3-Yb^{5+} (black). 259

Figure 5.4 NIR spectra of 1-Yb^{6+} (red) and 5-Yb^{3+} (blue). 260

Figure 5.5 UV/vis spectra of 3-Yb^{5+} in various solvents at various temperatures. 261

Figure 5.6 Gaussian fits of UV/vis spectra for 3-Yb^{5+} at various temperatures in hexanes. 263

Figure 5.7 Gaussian fits of UV/vis spectra for 3-Yb^{5+} at high and low temperatures in hexanes, toluene, and diethyl ether. 265

Figure 5.8 Calculated optical spectra of 5-Yb^{3+}. a) TDDFT calculated absorption spectrum of 5-Yb^{3+}. The diagrams within the figure are electron difference densities and show where electron density is lost in the ground state (blue) and gained in the excited state (purple). b) Calculated absorption spectrum of 5-Yb^{3+} at the CASSCF + SOC level of theory. In both figures the black trace is the experimental spectrum while the red trace is the calculated spectrum. The vertical lines show the calculated oscillator strength of each transition. 266

Figure 5.9 Calculated optical spectra of 1-Yb^{6+}. a) TDDFT calculated absorption spectrum of 1-Yb^{6+}. The diagrams within the figure are electron difference densities and show where electron density is lost in the ground state (blue) and gained in the excited state (purple). b) Calculated absorption spectrum of 1-Yb^{6+} at the CASSCF + SOC level of theory. In both figures the black trace is the experimental spectrum while the red trace is the calculated spectrum. The vertical lines show the calculated oscillator strength of each transition. 267

Figure 5.10 Calculated optical spectra of 3-Yb^{5+}. a) TDDFT calculated absorption spectrum of 3-Yb^{5+}. The diagrams within the figure are electron difference densities and show where electron density is lost in the ground state (blue) and gained in the excited state (purple). b) Calculated absorption spectrum of 3-Yb^{5+} at the CASSCF + SOC level of theory. In both figures the black trace is the experimental spectrum while the red trace is the calculated spectrum. The vertical lines show the calculated oscillator strength of each transition. 267

Figure 5.11 Variable-temperature molar magnetic susceptibility times temperature ($\chi_M T$) for 1-Yb^{6+} (black), 5-Yb^{3+}(blue), and 3-Yb^{5+} (red) collected under dc field of 1 T. 269

Figure 5.12 Molecular structure of 1-Yb^{6+} with thermal ellipsoids shown at 50% probability with hydrogen atoms omitted for clarity. Color code: C, black; N, blue; O, red; P, orange; Yb, blue. 280

Figure 5.13 Molecular structure of 2-Yb^{6+} with thermal ellipsoids shown at 50% probability with hydrogen atoms omitted for clarity. Color code: C, black; N, blue; O, red; P, orange; I, purple; Yb, blue. 290

Figure 5.14 Molecular structure of 3-Yb^{5+} with thermal ellipsoids shown at 50% probability with hydrogen atoms omitted for clarity. Color code: C, black; N, blue; P, orange; Yb, blue. 314

Figure 5.15 Molecular structure of 4-Yb^{5+}(DME) with thermal ellipsoids shown at 50% probability with hydrogen atoms omitted for clarity. Color code: C, black; N, blue; O, red; P, orange; Yb, blue. Structure contains approximately 10% Iodide heavy atom impurity. 328

Figure 5.16 Molecular structure of 3-Yb^{5+} with thermal ellipsoids shown at 50% probability with hydrogen atoms omitted for clarity. Color code: C, black; N, blue; O, red; P, orange; K, green; Yb, blue. 340

Figure 5.17 Molecular structure of 1-Sm^{6+} with thermal ellipsoids shown at 50% probability with hydrogen atoms omitted for clarity. Color code: C, black; N, blue; O, red; P, orange; Sm, blue. 358

Figure 5.18 Molecular structure of 2-Sm^{6+} with thermal ellipsoids shown at 50% probability with hydrogen atoms omitted for clarity. Color code: C, black; N, blue; O, red; P, orange; I, purple; Sm, blue. 375

Figure 5.19 Molecular structure of 4-$Sm^{5+}(Et_2O)$ with thermal ellipsoids shown at 50% probability with hydrogen atoms omitted for clarity. Color code: C, black; N, blue; O, red; P, orange; Sm, blue. 391

LIST OF SCHEMES

Scheme 2.1	Two-step reaction scheme for synthesis of 2-Ln and 3-Ln through diethyl ether adduct, 1-Ln. Yields are shown for the two-step process and metals depicted in red are structurally characterized as 1-Ln.	11
Scheme 3.1	Multi-step reaction scheme for the synthesis of the copper salt, 1.	65
Scheme 3.2	Reaction scheme for the oxidation of zero-valent lanthanide metal with 1.	67
Scheme 4.1	Reaction scheme for the synthesis of 1-Eu^{2+}, 2-Gd^{3+}, 3-Gd^{3+}, and 4-Tb^{4+}.	142

LIST OF SYMBOLS AND ABBREVIATIONS

ζ	Spin-Orbit Coupling Constant
$\hat{S}_{\mu}$	Spin Operator Component (x,y,z)
$\vec{\mathbf{B}}$	Magnetic Field Vector
$\hat{\mathbf{S}}$	Electronic Spin Operator
$\tilde{g}$	Isotropic g-tensor
°	Degrees
°C	Degrees Celsius
μ_B	Bohr Magneton
μ_{eff}	Effective Magnetic Moment
Å	Angstrom
AILFT	ab initio Ligand Field Theory
Ax	Axial
C_6D_6	Deuterated Benzene
C_7H_7	Benzyl Group/Ligand
CASSCF	Complete Active Space Self-Consistent Field
CF	Crystal Field
cm	Centimeter
Cp^{1-}	Cyclopentadienyl Group/Ligand
Cp_3'	$C_5H_4SiMe_3$ Ligand
D	Axial ZFS Term
dc	Direct Current
DME	1,2-dimethoxyethane

E	Rhombic ZFS Term
EDTA	disodium salt of ethylenediaminetetraacetic acid
emu	Electromagnetic Unit
EPR	Electron Paramagnetic Resonance
Eq	Equatorial
Et_2O	Diethyl Ether
FWHM	Full Width at High Maximum
g_e	g-value of a Free Electron
HFEPR	High-Frequency and -Field EPR
^{i}Pr	Isopropyl Group
IR	Infrared
IVCT	Intervalence Charge Transfer
K	Kelvin
L	Total Orbital Quantum Number
LMCT	Ligand-to-Metal Charge Transfer
Ln	Lanthanide
M	Molarity
mer	Meridional
mL	Milliliter
mol	Mole
m_s	Projection of Electronic Spin
NEVPT2	N-electron Valence Perturbation Theory to Second Order
NHE	Normal Hydrogen Electrode
NIR	Near-Infrared
nm	Nanometer

NMR	Nuclear Magnetic Resonance
NP*	$[(NP(1,2\text{-}bis\text{-}^{t}Bu\text{-}diamidoethane)(NEt_2))]^{1-}$ Ligand
Rsd	Radii of Spherical Domain
S	Total Spin Quantum Number
SCXRD	Single-Crystal X-ray Diffraction
SHE	Standard Hydrogen Electrode
SOC	Spin-Orbit Coupling
SSC	Spin-Spin Coupling
SQUID	Superconducting Quantum Interference Device
T	Tesla
T	Temperature
^{t}Bu	Tert-butyl Group
TDDFT	Time-Dependent Density Functional Theory
THF	Tetrahydrofuran
TMS	Trimethyl Silyl Group
UHP	Ultra-High Purity
UV	Ultraviolet
V	Volt
VDP	Voronoi–Dirichlet polyhedron
Vis	Visible
XANES	X-ray Absorption Near-Edge Spectroscopy
XAS	X-ray Absorption Spectroscopy
XRD	X-ray Diffraction
ZFS	Zero-Field Splitting
β_e	Electron Bohr Magneton

Δ_{8s}	Energetic Separation Between the Highest and Lowest m_s states for S = 7/2
Δ_{LF}	Ligand Field Splitting
λ_{oct}	Quadratic Elongation
$\Sigma_{109.5}$	Total Deviation from Idealized Tetrahedral Angles
σ^2_{oct}	Bong Angle Variance
τ_4	Index for Four-Coordinate Complexes
1-La	$LaI_3(Et_2O)_3$
2-La	$LaI_3(THF)_4$
1-Ce	$CeI_3(Et_2O)_3$
2-Ce	$CeI_3(THF)_4$
1-Pr	$PrI_3(Et_2O)_3$
2-Pr	$PrI_3(THF)_4$
1-Nd	$NdI_3(Et_2O)_3$
3-Nd	$[NdI_2(THF)_5][NdI_4(THF)_2]$
1-Sm	$SmI_3(Et_2O)_3$
3-Sm	$[SmI_2(THF)_5][SmI_4(THF)_2]$
3-Eu	$[EuI_2(THF)_5][EuI_4(THF)_2]$
1-Gd	$GdI_3(Et_2O)_3$
3-Gd	$[GdI_2(THF)_5][GdI_4(THF)_2]$
1-Tb	$TbI_3(Et_2O)_3$
3-Tb	$[TbI_2(THF)_5][TbI_4(THF)_2]$
1-Dy	$DyI_3(Et_2O)_3$
3-Dy	$[TbI_2(THF)_5][TbI_4(THF)_2]$
1-Ho	$HoI_3(Et_2O)_3$

3-Ho	$[HoI_2(THF)_5][HoI_4(THF)_2]$
1-Er	$ErI_3(Et_2O)_3$
3-Er	$[ErI_2(THF)_5][ErI_4(THF)_2]$
1-Tm	$TmI_3(Et_2O)_3$
3-Tm	$[TmI_2(THF)_5][TmI_4(THF)_2]$
3-Yb	$[YbI_2(THF)_5][YbI_4(THF)_2]$
BTTSA	bis(tri-tert-butoxysilyl)amide Ligand
BTTSA-H	bis(tri-tert-butoxysilyl)amine
1	$[((^tBuO)_3Si)_2NCu]_2KCl$
2-Sm	$[((^tBuO)_3Si)_2N]_2Sm$
2-Eu	$[((^tBuO)_3Si)_2N]_2Eu$
1-Eu^{2+}	$[(NP(1,2\text{-}bis\text{-}^tBu\text{-diamidoethane})(NEt_2))]_4EuK_2$
2-Gd^{3+}	$[(NP(1,2\text{-}bis\text{-}^tBu\text{-diamidoethane})(NEt_2))]_4GdK$
3-Gd^{3+}	$[(NP(1,2\text{-}bis\text{-}^tBu\text{-diamidoethane})(NEt_2))]_4Gd[(2.2.2\text{-cryptand})K]$
4-Tb^{4+}	$[(NP(1,2\text{-}bis\text{-}^tBu\text{-diamidoethane})(NEt_2))]_4Tb$
1-Yb^{6+}	$[((CH_2)_5N)_3PN]_6Yb_2$
2-Yb^{6+}	$[((CH_2)_5N)_3PN]_5Yb_2I$
3-Yb^{5+}	$[((CH_2)_5N)_3PN]_5Yb_2$
5-Yb^{3+}	$[((CH_2)_5N)_3PN]_4Yb[(2.2.2\text{-cryptand})K]$
4-Yb^{5+}(DME)	$[((CH_2)_5N)_3PN]_5Yb_2(DME)$
1-Sm^{6+}	$[((CH_2)_5N)_3PN]_6Sm_2$
2-Sm^{6+}	$[((CH_2)_5N)_3PN]_5Sm_2I$
4-Sm^{5+}(Et$_2$O)	$[((CH_2)_5N)_3PN]_5Sm_2(Et_2O)$

SUMMARY

Redox chemistry and valence electronic structure of the lanthanides in molecular complexes is a rapidly expanding field of research. The contemporary understanding of the accessible oxidation states of the lanthanide elements and the variability in their electronic structure is the result of several groundbreaking fundamental discoveries. While the lanthanide elements have already found widespread use in technical and consumer applications, the continued reevaluation of basic redox properties is a central chemical concern to establish a more complete description of periodic properties. This continuous development of understanding of valence electronic structure and its connection to oxidation state and coordination environment is essential for the continued development of lanthanides in quantum information science and quantum materials research.

Due, in part, to the minimal extension of the valence 4*f* orbitals in lanthanide complexes, covalent bonding and electronic communication between metal centers, in particular lanthanide-lanthanide metal centers, is nearly non-existent and unexplored. This thesis details the development of new methodology for lanthanide triiodide starting materials for salt metathesis reactions. This thesis also outlines the development of novel lanthanide complexes that exhibit unique electronic structure properties such as vibronic coupling in neutral divalent complexes and intervalence charge transfer in mixed-valent, homobimetallic complexes. Additionally, the first isostructural molecular valences series spanning three oxidation states (Eu^{2+}, Gd^{3+}, and $Tb4^{+)}$ is synthesized and interrogated through high-field and -frequency electronic paramagnetic resonance. This work correlates formal charge, zero-field splitting, and covalency in these lanthanide complexes.

CHAPTER 1. INTRODUCTION

Part of this thesis chapter has been adapted with permission from an article co-written by the author:

Gompa, T. P., Ramanathan, A., Rice, N. T., La Pierre, H. S. The chemical and physical properties of tetravalent lanthanides: Pr, Nd, Tb, and Dy. Dalton Trans., **2020**,*49*, 15945-15987

f-elements are well integrated into our society and their use ranges from everyday consumer goods to high specialized applications such as catalysts for oil refining[1] and transportation, phosphors for lighting and electronic displays,[2] nuclear materials, and magnets for medicine and alternative energy,[3] and the list goes on. Despite their wide-spread use, fundamental f-element chemistry is a still rapidly growing and fertile area of research. The current understanding of fundamental f-block chemistry and electronic structure is the direct result of many paradigm shifts, some as recent as the past few years. Despite these advances, there is still much progress to be had. Understanding electron delocalization phenomena is crucial for classic problems in actinide science including the valence electronic structure of plutonium metal and its materials. These phenomena are also key to understanding the physical properties of quantum materials such as topological insulators[4, 5] and exchange coupled single molecule magnets.[6] The goal of this body of work is to examine the physical basis of electron delocalization phenomena in the f-block to address central technical concerns for nuclear security and enable the design and application of quantum materials for quantum information science. One way to begin to clearly understand how these coincident electronic phenomena combine to give rise to the

electronic structure of lanthanide and actinide materials as a whole is to truncate materials to more addressable molecular systems.

1.1.1 *Lanthanide starting materials*

For transition metals, anhydrous halides are readily and cheaply available, however, for the lanthanides this is not necessarily the case. Due to the specific needs for clean complex formation with certain ligand sets, new methodologies are needed to be developed for production of anhydrous trivalent lanthanide halide precursors. Lanthanide halide precursors are convenient for transmetallation and salt metathesis reactions as well as organic transformation reactions as Lewis acid catalysts.[7] However, lanthanide halide hydrates can't be dried simply by heating due to the propensity of the chlorides to be hydrolyzed to oxyhalides. Chloride hydrates are readily available as they are produced through the Rhône-Poulenc separation process and are widely used when dried as a trivalent lanthanide precursor.[8] The standard drying method employed utilizes ammonium chloride to prevent hydrolysis of the lanthanide chloride during the heating process.[9] A common impurity in precursors prepared by this method is ammonium chloride, which can be deemed unacceptable given the basicity of the certain ligand systems. Additionally, chlorides are not ideal as they are only mild leaving groups and may interfere with clean complex formation, resulting in anionic "ate" complexes. Similarly, it has been observed that reactions anhydrous lanthanide chlorides produced low yields and unwanted side products, or just exhibited general inertness.[10] As a result, lanthanide iodides are far more attractive because iodide, being larger and able to more spread out the incurred negative charge, is a much better leaving group and a worse nucleophile (in aprotic solvents) than chloride.

Thermal dehydration of hydrated lanthanide triiodides is exhibits similar problems to that of hydrated lanthanide chlorides and results in undesirable side-products.[11] Over time, multiple routes have been developed to cleanly synthesize anhydrous (solvated) lanthanide halides. Zero-valent samarium and ytterbium metal has been used to reduce of mercuric iodide in THF to give $SmI_3(THF)_{3.5}$ and $YbI_3(THF)_{3.5}$, respectively.[12] Similarly, zero-valent metal sources have been used to reduce alkyl iodides, such as CH_2I_2 or EtI, in THF to give $LnI_3(THF)_n$ (Ln = La, Ce, n = 4; Nd, n = 3.5).[13] Finally, the straightforward reaction between elemental iodine and lanthanide metals in THF to yield $LnI_3(THF)_n$.[14] Many of these routes suffer from significant drawbacks, including the separation and disposal of elemental mercury, the potential formation of organo-lanthanide side-products, low yields, and the incorporation of Lewis basic ligands in the product which may interfere with further metathesis reactions. Development of a robust lanthanide triiodide synthetic method in low polarity, weak Lewis basic solvents opens a more versatile area for lanthanide metathesis reactions.

1.1.2 *Redox chemistry in the lanthanides*

The understanding of lanthanide oxidation states, valence electronic structure, and redox chemistry in condensed phases has been through waves of reconstruction. These paradigm shifts began when the lanthanides were first available in pure form and in significant quantities starting in the 1950's with Frank Spending's development of ion exchange purification methodologies.[15-23] Prior to this innovation, Klemm established an empirical model of systematic valences that rationalized the aqueous stability of trivalent lanthanides across the series along with exceptions for divalent Sm, Eu, and Yb ions and tetravalent Ce ions in solution.[24] This framework also contended with the observed stability

of tetravalent Pr and Tb in the solid state. The accessibility of non-trivalent oxidation states was rationalized on achieving (or approximately achieving) empty, filled, or half-filled shells (*e.g.*, $4f^0$, $4f^{14}$, $4f^7$).

The emergence and rationalization of lanthanide oxidation states outside of Klemm's model can be traced to the work of John D. Corbett on solid-state lanthanide halides.[25] These studies guided the field from Klemm's empirically derived model of systematic valences of the lanthanides, to the classification of divalent lanthanide halides in insulating phases, $(R^{2+})(X^-)_2$, (R = rare-earth and X = halide) and semi-metallic phases $(R^{3+}e^-)(X^-)_2$. The latter phases were proposed to have an electron delocalized in the conduction band. These dichotomous valence electronic structure models for divalent lanthanides were refined through both the synthesis and characterization of solid-state and molecular systems to the contemporary nomenclature: insulating $4f^{n+1}5d^0$ and semi-metallic $4f^n5d^1$. This current model was built from the close relationship between solid-state and molecular practitioners.[25, 26] In contrast to molecular transition metal chemistry, where biological inspiration has historically driven the field, molecular lanthanide redox chemistry has built on the materials, techniques, and analysis established for solid-state systems. With the advent of bioinorganic lanthanide chemistry, this synergy is evolving.[27-34] However, there are significant signposts in the solid-state literature to guide the further development of molecular lanthanide redox chemistry.

This intellectual approach has precedent. Corbett and Meyer mapped the phases of accessible divalent lanthanide halide and oxide-halide materials.[35-46] The divalent lanthanide phases have yielded unique magnetic properties.[47] The identity of the products of these reactions were often governed by the equilibrium $M + MX_3 \rightleftharpoons 2MX_2$ which

defined two synthetic targets for the molecular synthetic community: isolation of zero-valent and divalent complexes. Cloke and co-workers established molecular zero-valent complexes of the rare-earth elements (Sc, Y, and Ln = lanthanide)[48-53] and established the framework for the analysis of mixed-valent magnetism (ground state population of the *f* and *d* shell).[50] Bocharev and co-workers employed the divalent iodide extended solids of Tm, Nd, and Dy to open the field of non-traditional divalent lanthanide complexes with the isolation of their ethereal adducts.[54-57] These leads led to the consideration of organometallic divalent lanthanide complexes. Lappert and Evans built a complete series of lanthanide divalent anions, and, concurrently, a wide range of structural types for anionic divalent lanthanides and actinides were isolated.[58-87] These methodological developments have even led to the isolation of neutral, non-traditional divalent lanthanide and actinide complexes, with some electrochemical evidence for a monovalent uranium complex.[88, 89] The latter possibility is foreshadowed by the isolation of monovalent [LaI] and a monovalent Sc complex.[90, 91] These results portend the development of lanthanide and actinide monovalent molecular chemistry.

The flexibility of oxidation potential of the lanthanide elements is demonstrated by the substantial changes in cerium ions dissolved in a variety of mineral acids that principally differ in the Lewis basicity of the supporting anion. Ce(III/IV) redox couple is measured to be 1.70 V, 1.61 V, 1.44 V, and 1.28 V (vs SHE) in 1 M $HClO_4$, HNO_3, H_2SO_4, and HCl, respectively.[92] These shifts in redox potential imply a difference in stabilities of the trivalent species and the tetravalent species that is dependent on the complexing anion present. Even for cerium, which is the most readily oxidizable lanthanide, oxidation in 1 M mineral acids is challenging because the relevant reduction potentials exceed the

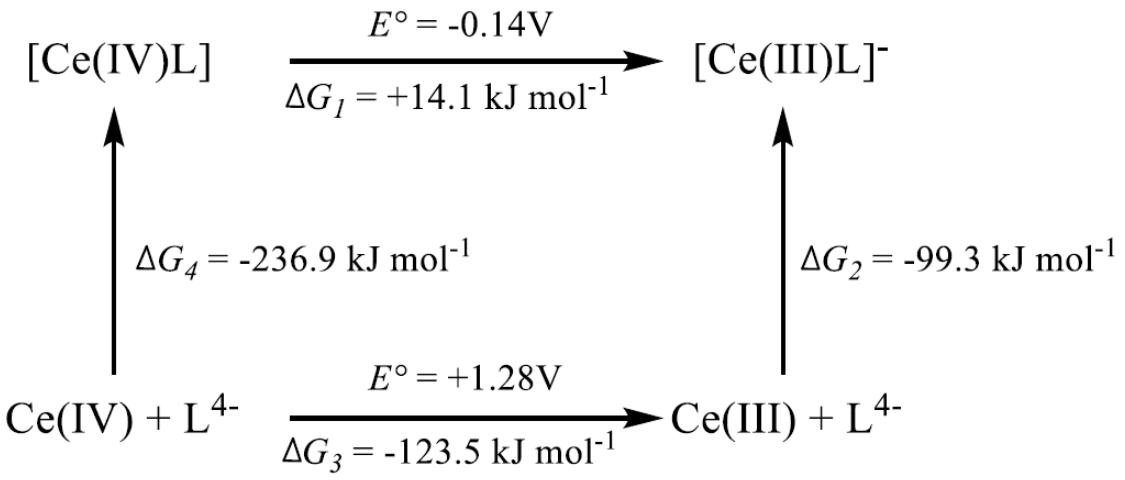

Figure 1.1 Thermodynamic cycle for the binding of 3,4,3-LI(1,2-HOPO) to Ce^{3+} and Ce^{4+}. Figure adapted from ref 94.

oxidation potential of water (1.23 V vs SHE). Weak field chelating ligands can shift the Ce(III/IV) couple even further. For example, tetrakis(catecholate) cerium compounds, have a measured redox potential of -0.69 V, a shift of nearly 2.4 V from the free ion potential.[93] Figure 1.1 depicts a thermodynamic cycle for a novel octadente ligand system, 3,4,3-LI(1,2- HOPO).[94] In the cycle, the ligand shows obvious preference for tetravalent cerium, a free energy change on complexation of -236.9 kJ mol^{-1} for the tetravalent versus only a change of -99.3 kJ mol^{-1} for the trivalent. The free energy of the reduction of free Ce(IV), ΔG3 in Figure 1.1, can be calculated from the measured potential. Based on these values, the free energy of the reduction of complexed Ce(IV) to complexed Ce(III) by the following equation:

$$\Delta G_1 = \Delta G_3 - (\Delta G_4 - \Delta G_2) \quad (1.1)$$

From the free energy change, the expected shift in potential can be calculated. The experimentally observed potential for this reduction for this specific system is -0.021 ±

0.010 V which is in good agreement with this estimate. Based on this argument, it is reasonable to conclude that a strongly donating, oxidatively stable ligand would be able to lift the thermodynamic barrier of oxidation potential by either destabilizing the trivalent state, and in turn increasing ΔG2, or by stabilizing the tetravalent state, resulting in a decrease in ΔG4. Further evidence for ligand control of lanthanide redox potentials has recently been demonstrated by Evans and co-workers.[61] The divalent complexes, $LnCp'_3$ ($Cp' = C_5H_4SiMe_3$), were demonstrated to have the electronic configuration $4f^n5d^1$. This accessible divalent oxidation state is dependent on the 3-fold symmetric, strong field ligand architecture which stabilizes the low valent oxidation state by lowering the $5dz^2$ orbital with respect to the 4*f* manifold. This unique valence electronic structure leads to the highest magnetic moments observed for any ion in the cases of $DyCp'_3$and $HoCp'_3$.[65] Not only do these results confirm the dependence of redox potential on coordination environment, but they also demonstrate the latent potential of the lanthanides when new oxidation states and electronic ground states are established.

1.1.3 *Bonding in the lanthanides*

The 4*f* orbitals are core-like in the trivalent oxidation state, as they are eclipsed by the [Xe] core in the bonding region.[95-100] As a result, most bonding is treated as ionic interaction rather than covalent. This model was challenged by Kozimor and co-workers through ligand based X-ray absorption spectroscopy (XAS).[101] These Cl K-edge results suggest that, upon oxidation, there is differential compression of the core orbitals versus the valence orbitals. As a result, the 4*f* orbitals are able to more readily participate in covalent bonding. This is also seen in spectra of tetravalent ions typically containing a weak pre-edge feature, which has been attributed to a quadrupole allowed $2p_{3/2} \rightarrow 4f$

transition, and has been described as a consequence of the emergence of covalent bonding between orbitals of *p* character in the ligand and 4*f* character in the lanthanide.[102-104] This is seen further through comprehensive O K-edge XAS studies have been performed by Minasian and co-workers on the entire series of trivalent lanthanide sesquioxides[105] as well as the stable tetravalent dioxides, CeO_2, PrO_2, and TbO_2.[106] Utilizing pre-edge features in the O K-edge spectra for the sesquioxides, the covalent mixing between O 2*p* orbitals and Ln 5*d*/4*f*/6*p* orbitals was investigated. As seen in the Cl K-edge XAS studies of $[LnCl_6]^{x-}$, little 4*f* mixing is observed and there is a substantial amount of ligand 2*p* – Ln 5*d*/6*p* mixing.[101] Furthermore, 2*p* – 5*d* mixing is resolved to explicit σ- and π-symmetry. While π-symmetry mixing remains relatively constant across the series, σ-symmetry mixing is maximized for La, Gd, Tb, Dy, Ho, and Er. In these cases, the covalent part of the Ln–O bond can best be described as an O 2*p* → 5*d* charge transfer since there are no $4f^n$ or $4f^{n+1}$ states in the gap between filled O 2*p* and Ln $5d^1$ states. Reduced mixing in the other elements can be ascribed to 4*f*/5*d* hybridization (such as in the case with Ce, Pr, and Nd) and better energy parity between O 2*p* and Ln 4*f* orbitals which enhanced the amount of 2*p* → 4*f* charge transfer possible. This increased covalency can be used to stabilize complexes utilizing weak field ligands such as nitrides, oxides, and fluorides. However, in order to study the solution behavior of these species more solubilizing weak field ligands must be developed.

Metal-metal bonding in the lanthanides is far more elusive. Owing largely to the core-like nature of the 4*f* orbitals, spatial overlap of occupied metal-based orbitals is very unlikely. As a result, there has been few reports of lanthanide-lanthanide bonding, which consistent primarily of multi-centered one electron bonding inside of endohedral fullerene

cages.[107] Despite this, there have been no complexes featuring lanthanide-lanthanide bonding of any order that have be substantiated through external spectroscopic means. This is due, in part, to the stability and complexity of the proposed endohedral fullerene complexes. As a result, new and simpler systems need to be developed that exhibit strong electronic communication or bonding between lanthanide metal centers.

CHAPTER 2. DIETHYL ETHER ADDUCTS OF TRIVALENT LANTHANIDE IODIDES

Part of this thesis chapter has been adapted with permission from an article co-written by the author:

Gompa, T. P., Rice, N. T., Russo, D. R., Quintana L. M. A., Yik, B. J. Bacsa, J., La Pierre, H. S. Diethyl ether adducts of trivalent lanthanide iodides. Dalton Trans., **2019**, *48,* 8030-8033.

2.1 Background

Starting material development and characterization remains an important technical issue facilitating discoveries across the f-block including the development of single-molecule magnets[108-115] and low-valent transuranic complexes.[68, 73, 116, 117] These studies are facilitated by anhydrous, hydrocarbon-soluble starting materials that are well-defined and supported by weakly-coordinating supporting ligands, often solvent adducts. Numerous methods have been reported for the preparation of trivalent lanthanide and actinide halides starting from other metal halides,[9, 118-124] metal oxides,[125] or bulk metal[14, 126-135] and an appropriate oxidant.

In order to access divergent properties of low-coordinate and low-valent lanthanide and actinide complexes, precursor complexes prepared in low-polarity solvents, including diethyl ether, have been developed.[126, 127, 136] These materials are typically isolated as partial solvates $[MI_3(Et_2O)_x]$, where the amount of diethyl ether remaining is dependent on isolation conditions and is variable from batch-to-batch and no structural information has

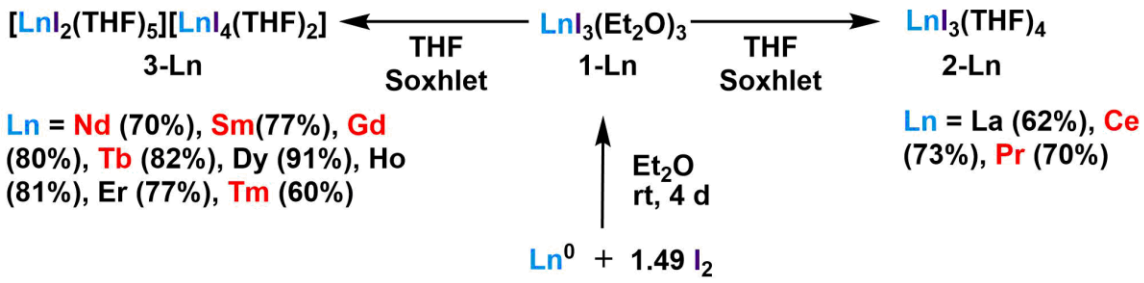

Scheme 2.1 Two-step reaction scheme for synthesis of 2-Ln and 3-Ln through diethyl ether adduct, 1-Ln. Yields are shown for the two-step process and metals depicted in red are structurally characterized as 1-Ln.

been reported to-date. In our application of these methods, it was discovered that the lanthanide triiodides exhibited noticeable, albeit sparing, solubility in diethyl ether. Herein we report a bulk synthetic method for the preparation of diethyl ether supported lanthanide triiodides, their crystallographic characterization, and their conversion to more stable precursors.

2.2 Results and Discussion

2.2.1 *Synthesis of $LnI_3(Et_2O)_x$, 1-Ln*

The diethyl ether complexes of the lanthanide iodides are prepared by treating lanthanide metal turnings (up to 1 gram) slurried in diethyl ether with a slightly substoichiometric amount of iodine (< 1.5 equivalents) dissolved in diethyl ether (Scheme 2.1). A substoichiometic amount of iodine is essential to avoid the formation of red brown $[I_3]^{1-}$. Due to the use of substoichiometric iodine, it is crucial that high-quality metal turnings are used to avoid incorporation of Ln_2O_3 in the product. After 4 days, the complex, $[LnI_3(Et_2O)_x]$, **1-Ln**, is isolated on a frit. This material can be used directly in further reactions but must be characterized by elemental analysis to determine amount of coordinated diethyl ether for reactions that require careful control of stoichiometry and

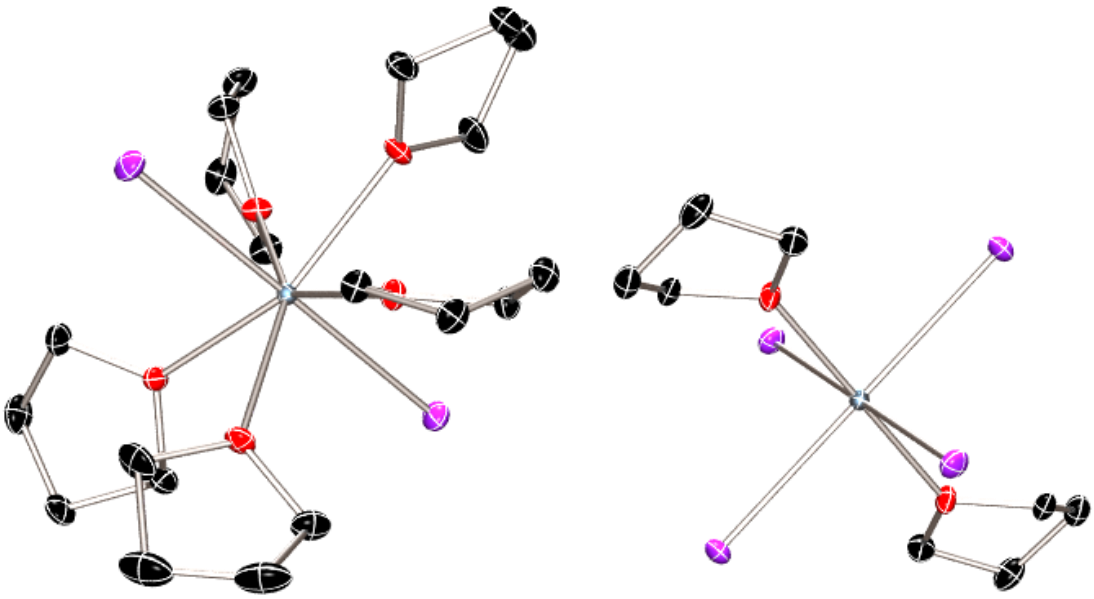

Figure 2.1 Molecular structure of 3-Tb with thermal ellipsoids shown at 50% probability and H atoms are omitted for clarity.

have any residual metal removed mechanically. In our laboratory, ether content after exposure to vacuum depended on the surface area, absolute vacuum, and metal identity and varied between 1.9 and 0.6 ethers per metal ion. In practice, well-defined solvento-complexes are obtained by tetrahydrofuran

2.2.2 *Synthesis of $LnI_3(THF)_4$, 2-Ln, and $[LnI_2(THF)_5][LnI_4(THF)_2]$, 3-Ln*

Soxhlet extraction of the $[LnI_3(Et_2O)_x]$ residue to afford the THF adducts of the lanthanide iodides, $[LnI_3(THF)_4]$, **2-Ln**, or $[LnI_2(THF)_5][LnI_4(THF)_2]$, **3-Ln**. The residual metal and metal oxide remain on the frit. The yield for this two-step process is good to excellent (60-91%). The neutral, **2-Ln**, or charge-separated form, **3-Ln**, was established by comparison of lattice parameters with known structures or full structural characterization (Figure 2.1).[14, 122, 137]

There is, however, flexibility in this dichotomy of structures as it has been demonstrated that recrystallization from toluene will lead to the isolation of all lanthanides in the charge-separated system.[127] Bulk phase purity was established by complexometric titration (see Experimental section).[138] The isolation of the trivalent lanthanide, diethyl ether adducts proved to be unsuitable for metals with accessible divalent oxidation states – namely Eu and Yb. Oxidation of the lanthanide metal in diethyl ether resulted in the formation in a mixture of divalent and trivalent products. This product mixture suggests that the divalent intermediate is only slowly oxidized to the trivalent state. Instead, a direct route to **3-Ln** in tetrahydrofuran is used for these two elements.

2.2.3 *UV/vis Spectroscopy of colored 1-Ln complexes*

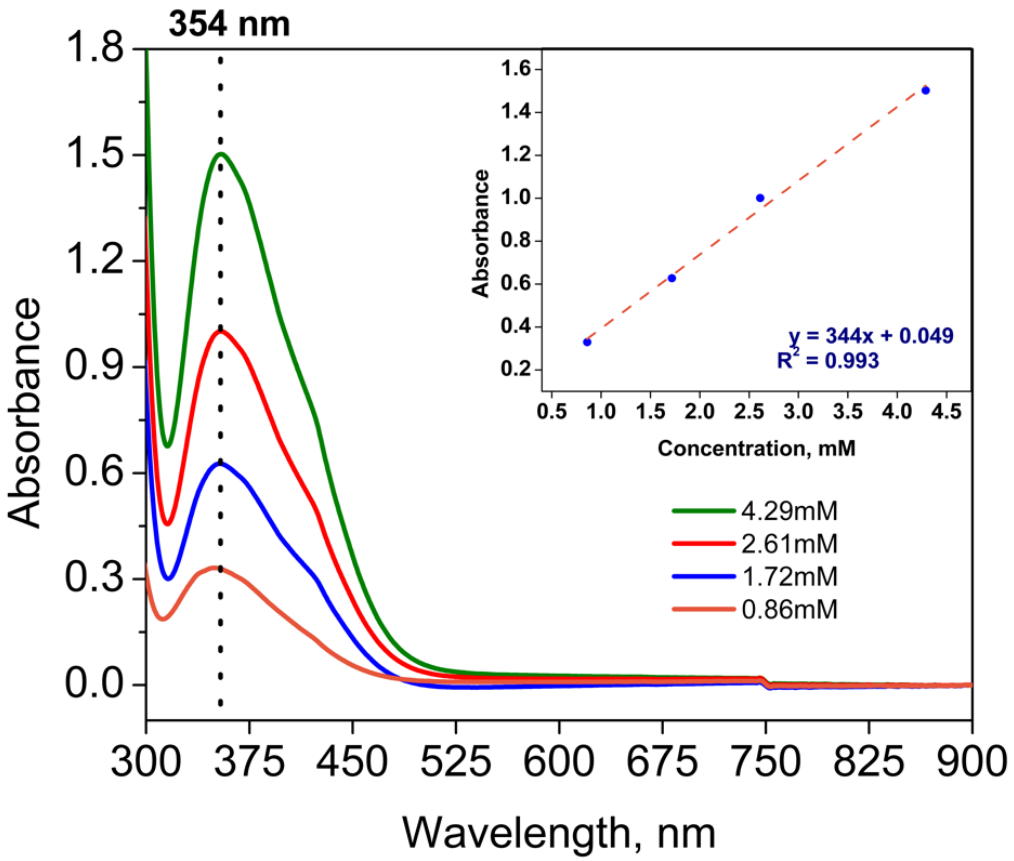

Figure 2.2 UV/vis spectra for varied concentrations for 1-Sm in diethyl ether.

In the case of Pr, Nd, and Sm, the final reaction mixtures of the iodine oxidation in diethyl ether were definitively colored (pale green, pale blue, and yellow, respectively), indicating partial solubility of the trivalent iodide complex in diethyl ether. UV/vis spectra for these compounds were obtained to accurately determine molar absorptivity of the observed features. Figure 2.2 and Figure 2.3 depict absorption spectra at varied concentration and calculation of the molar absorptivity of prominent features. Figure 2.4 shows the UV/vis spectra for saturated solutions of **1-Sm** and **1-Nd** in diethyl ether. The saturated solution concentrations obtained by this method for **1-Sm** and **1-Nd** were 6.65 mM and 29.1 mM, respectively. Due to the low solubility and low molar absorptivity of the *f-f* transitions for **1-Pr**, accurate determination of concentration is difficult. However,

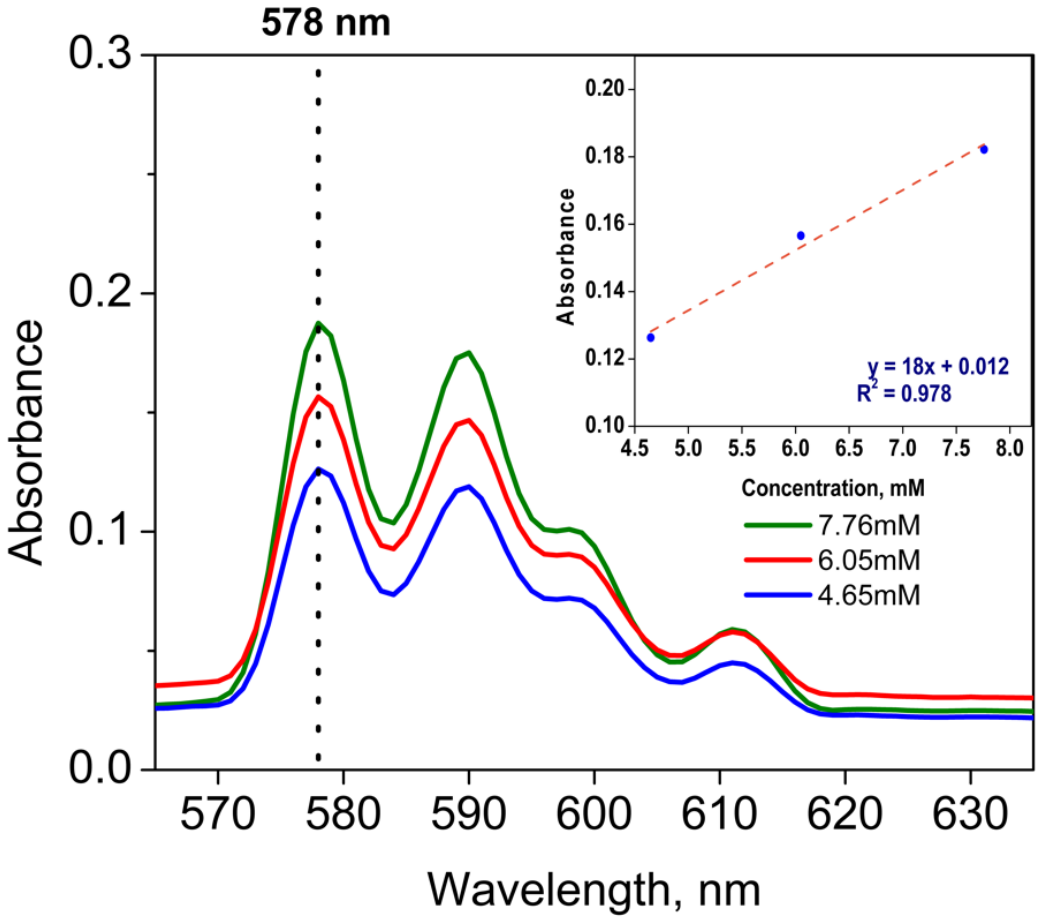

Figure 2.3 UV/vis spectra for varied concentrations for 1-Nd in diethyl ether.

the saturated solution concentration can be estimated at around 3 mM. This observed solubility suggested that the etherate complexes could be isolated and structurally characterized.

2.2.4 *Crystallography of 1-Ln*

For **1-Ln** (Ln = Ce, Pr, Nd, Sm, Gd, Tb, and Tm), X-ray diffraction quality single crystals are grown by cooling saturated diethyl ether solutions to -35°C. Each of the lanthanide iodide ether adduct complexes adopt a pseudo-octahedral geometry and with a meridional orientation of the iodides and diethyl ether ligands (Figure 1). The complexes, **1-Ln** (Ln = Ce, Pr, Sm, Gd, and Tb), crystallize in the *Pbcn* space group, giving isomorphic structures. Complexes **1-Nd** and **1-Tm** diverge. Complex **1-Nd** is isolated in Pna21, while **1-Tm** crystallizes in P-1 and does not yield a satisfactory refinement (however, connectivity was confirmed: a representation of connectivity and initial lattice parameters are included in Crystallographic Information section). These divergent crystal systems

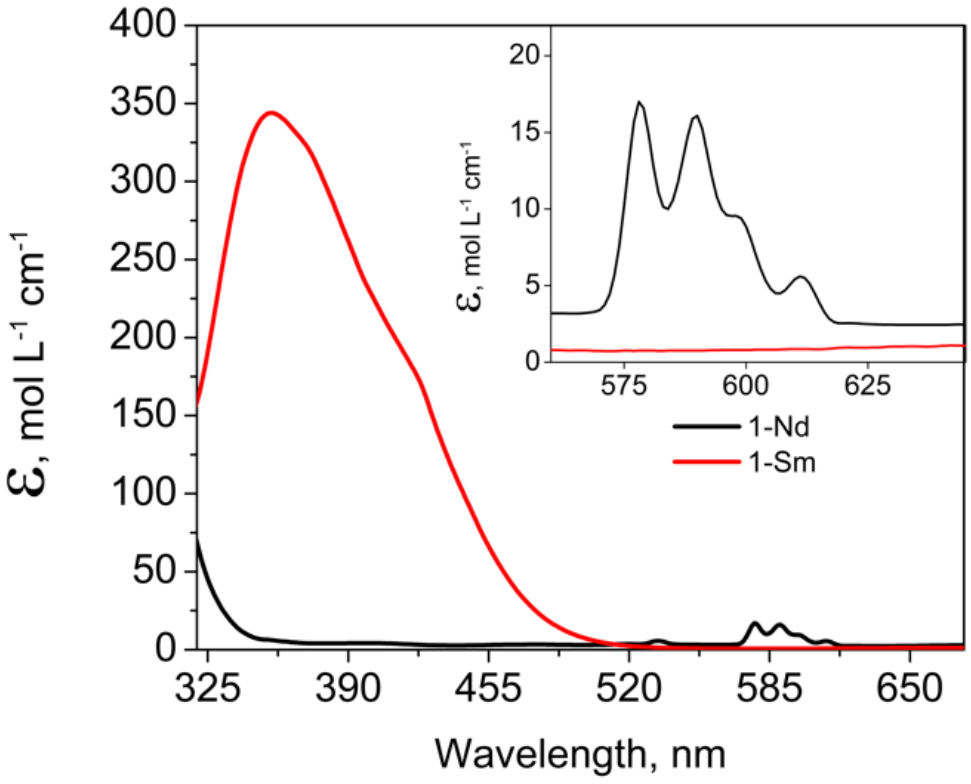

Figure 2.4 UV/vis spectra of saturated solutions of 1-Nd and 1-Sm in diethyl ether.

demonstrate the relatively soft potential the complexes have for crystallization and the sensitivity to diethyl ether loss.

The crystal structure of **1-Pr**, [PrI_3(*mer*-$Et_2O)_3$], is shown in Figure 2.5. This complex is isostructural with the other **1-Ln** complexes and is representative for the series. The praseodymium atom is coordinated by the three iodides and three diethyl ether molecules, forming a pseudo-octahedral coordination sphere. The I_{ax}–Pr–I_{eq} bond angles are both 89.124(6)° and the I_{ax}–Pr–I_{ax} bond angle is 178.248(12)°. The Pr–I_{ax} bond lengths are 3.0812(3) Å while the Pr–I_{eq} bond length is 3.0441(4) Å, giving an average length of 3.069(3) Å. There is similar variation in the Pr–O distances which span 2.406(2) to 2.522(4) Å and average 2.445(3) Å. The average Ln–I bond length for each structurally

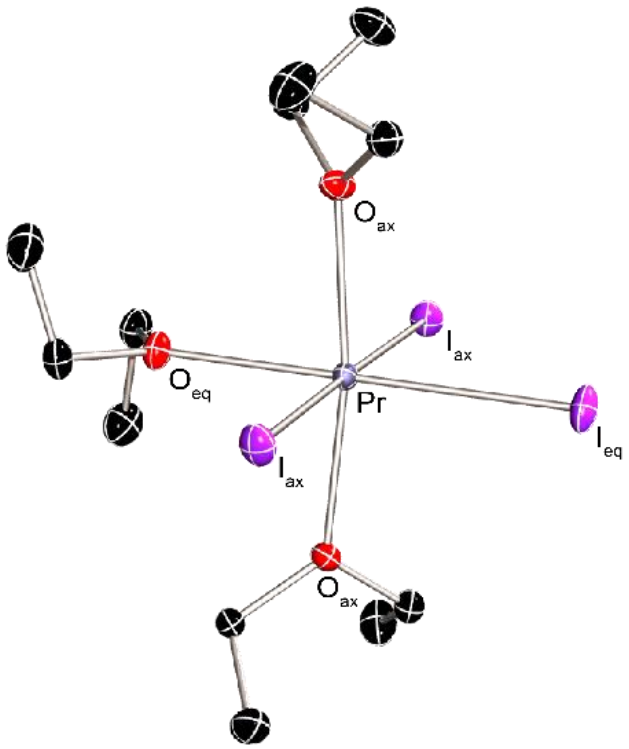

Figure 2.5 Molecular structure of 1-Pr with thermal ellipsoids shown at 50% probability and H atoms are omitted for clarity.

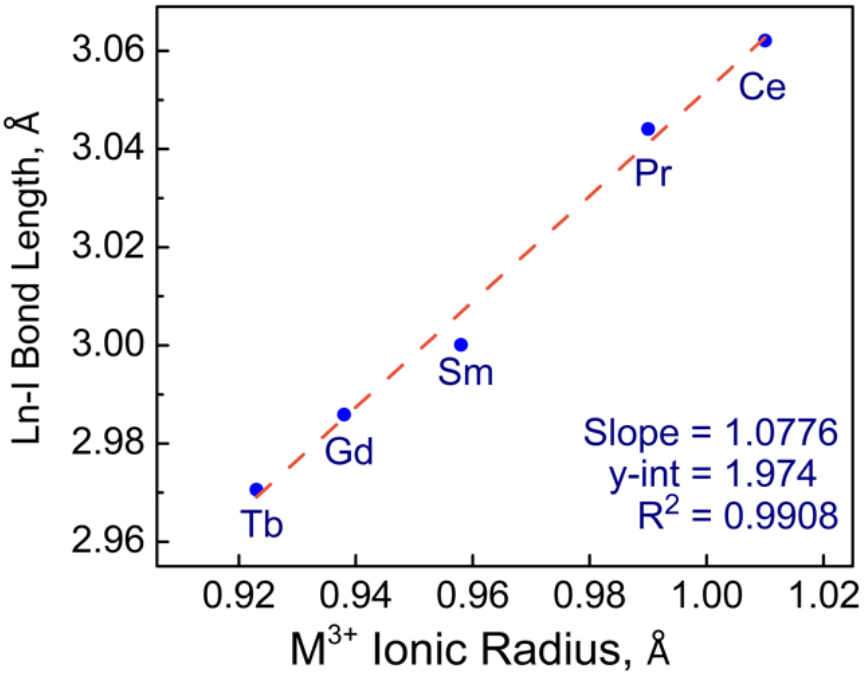

Figure 2.6 Plot of the equatorial Ln–I bond distance relative to trivalent metal ionic radii in structurally characterized 1-Ln compounds in the Pbcn space group. Error bars are smaller than the point size.

characterized complex is consistent with lanthanide ion contraction as atomic number increases. Figure 2.6 demonstrates the linear decrease in bond length of analogous equatorial iodide of the crystallographically characterized **1-Ln** complexes in the *Pbcn* space group (Ln = Ce, Pr, Sm, Gd, Tb). A linear fit to the data (with an R^2 value of 0.9908) gives a slope of 1.0776. The y-intercept is 1.974, slightly shorter than the iodide ionic radii.[139] This model is consistent with structural indications of ionic bonding.[140]

In these complexes, the Ln ion was six coordinate, and the correct space group was *Pbcn* (or its chiral enantiomer Pna21, except for **1-Tm**) with the Ln atom located at a special position with point symmetry 2. Thus, the coordination polyhedron has C_2 symmetry. The coordination geometry is severely distorted from a regular octahedron because of the very different donor properties of the diethyl ether and iodide ligands. Not

surprisingly, the ether molecules (and the I atoms) bind to the Ln atom with substantially different Ln-O distances (and Ln-I distances) despite having identical donor characteristics because the trans pair of Ln-O bonds will form substantially stronger bonds than the ether trans to the Ln-I bond. For example, the Ce-O distance is 2.3518(11) for the trans ethers and 2.4480(15) Å for the third ether. There is a correlation between the asymmetric binding of the ether molecules and the binding of the iodine atoms. The distortion of the geometry of the octahedra from regularity was measured by the quadratic elongation (λ_{oct}) and the bond angle variance (σ^2_{oct}). The distortions are presented in Table 2.1.

Table 2.1 Coordination Geometry Parameters for 1-Ln.

	Ce	Pr	Nd	Sm	Gd	Tb	Tm
Average bond length (Å)	2.7737	2.7565	2.7423	2.7113	2.6945	2.6773	2.6196
Polyhedral volume ($Å^3$)	27.9371	27.4178	26.60	26.067	25.605	25.1107	23.5003
Distortion index	0.11291	0.1130	0.11414	0.11551	0.11527	0.11699	0.12424
Quadratic elongation	1.0254	1.0254	1.0289	1.0267	1.0260	1.0266	1.0289
Bond angle variance ($°^2$)	7.6874	7.6874	8.066	7.5856	7.3546	6.7864	8.0661
Volume of the Ln VDP ($Å^3$)	21.230	20.822	20.780	19.805	19.451	19.057	17.976
Radius of the Spherical Lanthanum Voronoi–Dirichlet Domain (Rsd, Å)	1.718	1.707	1.706	1.678	1.668	1.657	1.625
Solid angles from the Voronoi–Dirichlet Polyhedron (S, °) with Ln as the central atom	O2 20.12	O1 20.17	O3 20.85	O3 20.27	O1 20.15	O2 20.21	O2 20.25
	O3 20.12	O3 20.17	O2 19.38	O1 20.27	O3 20.15	O1 20.21	O1 20.14
	O1 17.23	O2 17.20	O1 17.89	O2 17.15	O2 17.34	O3 17.40	O3 17.78
	I2 15.36	I3 15.31	I3 13.80	I3 15.26	I3 15.25	I2 15.17	I1 15.37
	I3 13.59	I2 13.57	I2 13.23	I2 13.52	I2 13.55	I1 13.50	I3 13.19
	I1 13.59	I1 13.57	I1 14.85	I1 13.52	I1 13.55	I3 13.50	I2 13.27

A useful method of quantifying the size and distortion of the coordination geometry is by analyzing the Voronoi–Dirichlet polyhedron (the dual of the coordination polyhedron). The values of solid angles of corresponding Dirichlet domain faces characterize the lanthanide interactions in the complexes. They correlate well with the bond valences of the bonds. The volumes of Dirichlet domains (V, $Å^3$) and the corresponding radii of spherical domains (Rsd, Å) are characteristic for the atoms in a given oxidation state.[141] There is a systematic reduction in the polyhedral volumes, average bond lengths, VDP's and Rsd's across the series. The solid angles for the same atom types stays relatively constant across the series. The significant result is that the VDP's and Rsd's reflects the atomic sizes of the lanthanide atom in these compounds. The solid angle is proportional to the portion of the valence electron density from the lanthanide atom which is taking part in the formation of bonds. This relationship has been interpreted as an analogue of valence-electron density in the volume between the interacting atoms.[142] Since the sum of the bond valences is equal to the oxidation state of the metal atom (+3 in all these compounds), the valences to the same atom types and the solid angles are expected to be constant for all these compounds.

2.2.5 *Test reactivity of 2-Ln and 3-Ln*

After Soxhlet extraction, **2-Ln** or **3-Ln** can be utilized to produce synthetically useful quantities of standard lanthanide complexes. The tris-benzyl complex, $[Ce(C_7H_7)_3(THF)_3]$, is produced in comparable yields as reported with similar starting reagents,[143] while increased yields are reported for materials such as $[Ce[N(Si(Me)_3)_2]_3]$,[144] see Experimental section. These reactions are accomplished by reacting **2-Ln** or **3-Ln**

with an alkali metal salt of the ligand, i.e., potassium benzyl or potassium bis(trimethylsilyl)amide in appropriate stoichiometries.

2.3 Conclusion

In summary, a standard methodology to produce lanthanide triiodide etherate complexes is established for early- and late-lanthanides, La, Ce, Pr, Nd, Sm, Gd, Tb, Dy, Ho, Er, and Tm. This method offers a consistent route for the production of trivalent lanthanide iodide precursors on reasonable scales for bulk synthesis (~1 g). Crystallographic investigation of the 1-Ln complexes reveal that these solvated lanthanide triiodides are isostructural with three weakly bound diethyl ethers to each lanthanide metal center.

2.4 Experimental

2.4.1 *General Considerations*

Unless otherwise noted, all reagents were obtained from commercial suppliers and the syntheses and manipulations were conducted under argon with exclusion of oxygen and water using Schlenk techniques or in an inert atmosphere box (Vigor) under a dinitrogen (<0.1 ppm O_2/H_2O) atmosphere. The glovebox is equipped with two -35 ˚C freezers. All glassware and cannula were stored in an oven over-night (>8 h) at a temperature of ca. 160˚C. Celite and molecular sieves were dried under vacuum at a temperature >250˚C for a minimum of 24 h. C_6D_6 was stored over 3 Å molecular sieves and then vacuum-transferred from purple sodium/benzophenone prior to use. Diethyl ether and tetrahydrofuran were purged with UHP-grade argon (Airgas) and passed through

columns containing Q-5 and molecular sieves in a solvent purification system (JC Meyer Solvent Systems). All solvents in the glovebox were stored in bottles over 3 Å molecular sieves. NMR spectra were obtained on a Bruker Advance III 400 MHz spectrometer at 298 K, unless otherwise noted. ^{1}H NMR chemical shifts are reported in δ, parts per million. ^{1}H NMR are references to the residual ^{1}H resonances of the solvent. Peak position is listed, followed by peak multiplicity, integration value, and proton assignment, where applicable. Multiplicity and shape are indicated by one or more of the following abbreviations: s (singlet); d (doublet); t (triplet); q (quartet); dd (doublet of doublets); td (triplet of doublets); m (multiplet); br (broad). Elemental analyses were determined at Robertson Microlit Laboratories (Ledgewood, NJ). Powder X-ray diffraction measurements were conducted in reflection mode with a PANalytical Empyrean diffractometer with Cu-Kα radiation. A continuous scan with a gonio axis and a scan rate of 0.0423 (degree/s) was used. An Anton Paar Domed sample holder was used for the measurement. The broad peak centered around 17° 2θ is due to the background from the Kapton dome.

Lanthanide metal content of **2-Ln**, $[LnI_3(THF)_4]$, and **3-Ln**, $[LnI_2(THF)_5][LnI_4(THF)_2]$ were determined by complexometric titration using the disodium salt of ethylenediaminetetraacetic acid (EDTA). A buffer solution was made using hexamethylenetetramine as the buffer and Xylenol Orange as the indicator. Roughly 20-70 mg of either **2-Ln** or **3-Ln** was dissolved in the buffer solution. Then, a 0.150 M solution of EDTA in H_2O was used to titrate the sample. EDTA binds to lanthanides to form a Ln-EDTA complex. The endpoint of the titration is determined visually, when the solution changes color to yellow, signalling that the endpoint has been reached. Titrations for each metal complex was completed in triplicate over a range of metal complex masses

and the averages of the triplicate are reported. This procedure was developed based on a previous report.[138]

2.4.2 *Synthesis of $LaI_3(Et_2O)_3$, 1-La*

To a slurry of lanthanum powder (1.15 g, 8.31 mmol, 1.0 equiv.) in 80 mL of diethyl ether in a 250 mL Schlenk flask was added a solution of iodine (3.143 g, 12.38 mmol, 1.49 equiv.) in diethyl ether (40 mL). The reaction mixture was stirred for 4 days at room temperature and a grey solid precipitated. The solid was isolated on a fine porosity, sintered glass frit, and washed with diethyl ether (2x40 mL). The solid was dried *in vacuo* to yield a free flowing, gray microcrystalline powder (3.354 g). The precise composition of $LaI_3(Et_2O)_x$ after exposure to dynamic vacuum is dependent on absolute vacuum.

2.4.3 *Synthesis $LaI_3(THF)_4$, 2-La*

$LaI_3(Et_2O)_x$ (3.354g) is subjected to Soxhlet extraction with THF yielding a white powder (4.133 g, 62% for two steps based on iodine as limiting reagent). Found: La, 17.34%. $LaI_3(THF)_4$ requires 17.19%.

2.4.4 *Synthesis of $CeI_3(Et_2O)_3$, 1-Ce*

To a slurry of cerium powder (0.500 g, 3.54 mmol, 1.0 equiv.) in 30 mL of diethyl ether in a 100 mL Schlenk flask was added a solution of iodine (1.339 g, 5.27 mmol, 1.49 equiv.) in diethyl ether (30 mL). The reaction mixture was stirred for 4 days at room temperature and an off-white solid precipitated. The solid was isolated on a fine porosity, sintered glass frit, and washed with diethyl ether (2x35 mL). The solid was dried *in vacuo* to yield a free flowing, off-white microcrystalline powder (1.83 g). The precise composition of

$CeI_3(Et_2O)_x$ depends on absolute vacuum and duration of exposure to vacuum. After three hours at 400 mtorr, elemental analysis found(calc'd) for $CeI_3(Et_2O)_{1.00}$: C, 8.15(8.08) H, 1.70(1.69). After nine hours at 30 mtorr, elemental analysis found(calc'd) for $CeI_3(Et_2O)_{0.62}$: C, 4.39(5.23), H, 1.09(1.10).

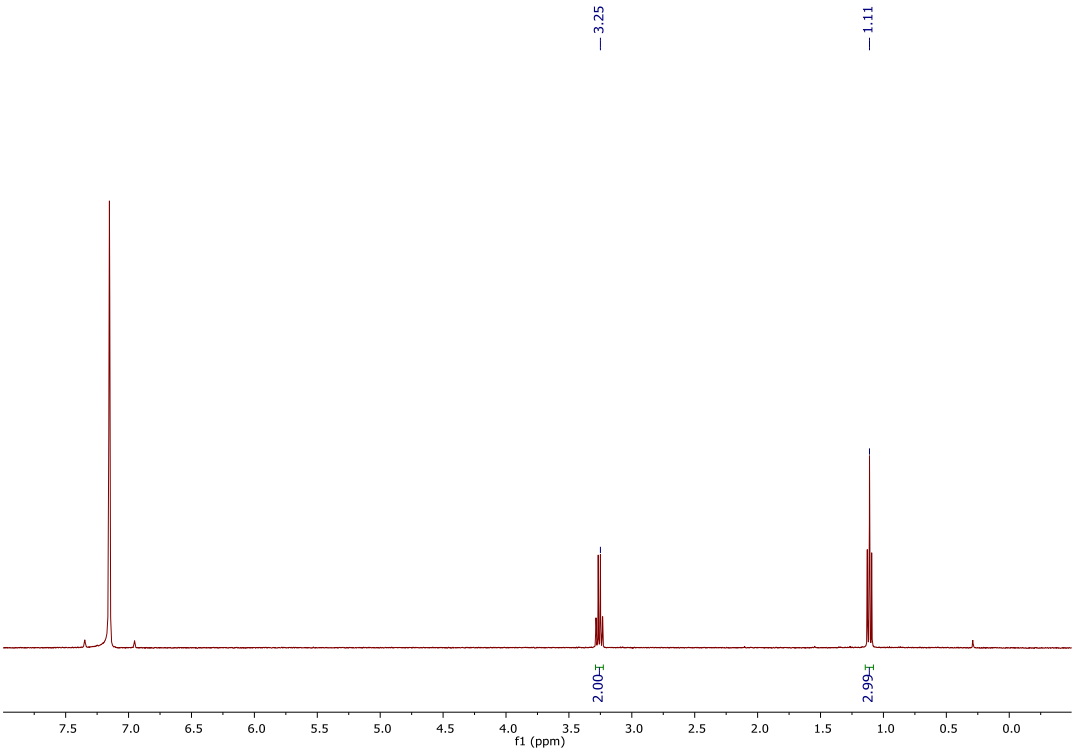

Figure 2.7 ^{1}H NMR of 1-Ce in C_6D_6 (no precipitation observed, all of the complex is dissolved).

2.4.5 *Synthesis $CeI_3(THF)_4$, 2-Ce*

$CeI_3(Et_2O)_x$ (1.83g) is subjected to Soxhlet extraction with THF yielding an off-white powder (2.08 g, 73%). Found: Ce, 17.55%. $CeI_3(THF)_4$ requires 17.31%.

2.4.6 *Synthesis of $PrI_3(Et_2O)_3$, 1-Pr*

To a slurry of praseodymium powder (300 mg, 2.13 mmol, 1.0 equiv.) in 20 mL of diethyl ether in a 50 mL Schlenk flask was added a solution of iodine (806 mg, 3.17 mmol, 1.49 equiv.) in diethyl ether (16 mL). The reaction mixture was stirred for 4 days at room temperature and a pale green solid precipitated. The solid was isolated on a fine porosity, sintered glass frit, and washed with diethyl ether (2x25 mL). The solid was dried *in vacuo* to yield a free flowing, pale green microcrystalline powder (945 mg). The precise composition of $PrI_3(Et_2O)_x$ depends on absolute vacuum.

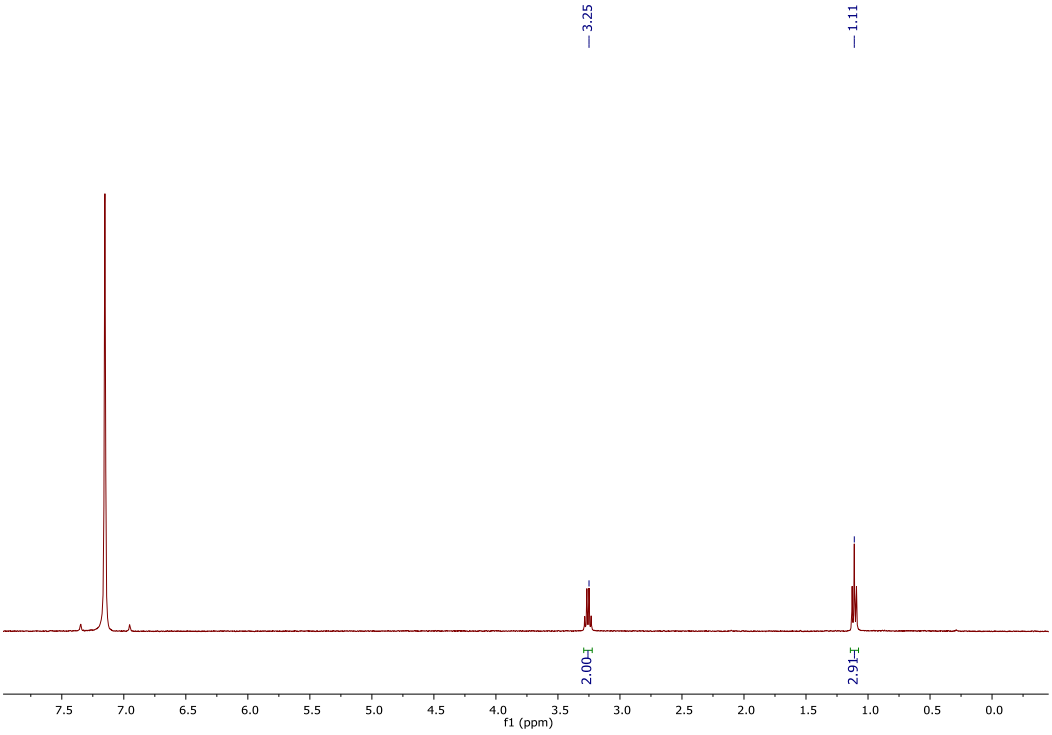

Figure 2.8 ^{1}H NMR of 1-Pr in C_6D_6 (no precipitation observed, all of the complex is dissolved).

2.4.7 *Synthesis $PrI_3(THF)_4$, 2-Pr*

$PrI_3(Et_2O)_x$ (945 mg) is subjected to Soxhlet extraction with THF yielding a gray-green powder (1.195 g, 70%). Found: Pr, 17.49%. $PrI_3(THF)_4$ requires 17.40%.

2.4.8 *Synthesis of $NdI_3(Et_2O)_3$, 1-Nd*

To a slurry of neodymium powder (1.081 g, 7.50 mmol, 1.0 equiv.) in 80 mL of diethyl ether in a 200 mL Schlenk flask was added a solution of iodine (2.817 g, 11.1 mmol, 1.48 equiv.) in diethyl ether (40 mL). The reaction mixture was stirred for 4 days at room temperature and a brown solid remained in a deep blue solution. The solid was isolated on a fine porosity, sintered glass frit, and washed with diethyl ether (2x40 mL). Volatiles are removed from the combined filtrates to yield a blue microcrystalline powder (3.713 g). The precise composition of $NdI_3(Et_2O)_x$ depends on absolute vacuum.

2.4.9 *Synthesis $[NdI_2(THF)_5][NdI_4(THF)_2]$, 3-Nd*

$NdI_3(Et_2O)_x$ (3.713g) is subjected to Soxhlet extraction with THF yielding a blue powder (4.038 g, 70%). Found: Nd, 18.61%. $NdI_3(THF)_{3.5}$ requires 18.56%.

2.4.10 *Synthesis of $SmI_3(Et_2O)_3$, 1-Sm*

To a slurry of samarium powder (1.038 g, 6.90 mmol, 1.0 equiv.) in 80 mL of diethyl ether in a 200 mL Schlenk flask was added a solution of iodine (2.590 g, 10.2 mmol, 1.48 equiv.) in diethyl ether (40 mL). The reaction mixture was stirred for 4 days at room temperature and a yellow solid precipitated. The solid was isolated on a fine porosity, sintered glass frit, and washed with diethyl ether (2x40 mL). The solid was dried *in vacuo* to yield a free flowing, yellow microcrystalline powder (3.810 g). The precise composition of $SmI_3(Et_2O)_x$ depends on absolute vacuum.

2.4.11 *Synthesis $[SmI_2(THF)_5][SmI_4(THF)_2]$, 3-Sm*

$SmI_3(Et_2O)_x$ (3.810 g) is subjected to Soxhlet extraction with THF yielding a yellow powder (4.175 g, 77%). Found: Sm, 19.31%. $[SmI_2(THF)_5][SmI_4(THF)_2]$ requires 19.19%.

2.4.12 *Direct Synthesis of $[EuI_2(THF)_5][EuI_4(THF)_2]$, 3-Eu*

To a slurry of europium powder (201 mg, 1.32 mmol, 1.0 equiv.) in 10 mL of THF in a 50 mL Schlenk flask was added a solution of iodine (495 mg, 1.95 mmol, 1.48 equiv.) in THF (14 mL). The reaction mixture was stirred for 4 days at room temperature and a tan-brown solid precipitated. The solid was isolated on a fine porosity, sintered glass frit, and washed with THF (2x10 mL) until filtrate no longer had a greenish color to it. The solid was dried *in vacuo* to yield a free flowing, tan -brown microcrystalline powder (725 mg, 71%). Found: Eu, 19.12%. $[EuI_2(THF)_5][EuI_4(THF)_2]$ requires 19.35%.

2.4.13 *Synthesis of $GdI_3(Et_2O)_3$, 1-Gd*

To a slurry of gadolinium powder (204 mg, 1.30 mmol, 1.0 equiv.) in 10 mL of diethyl ether in a 50 mL Schlenk flask was added a solution of iodine (488 mg, 1.92 mmol, 1.48 equiv.) in diethyl ether (14 mL). The reaction mixture was stirred for 4 days at room temperature and a tan solid precipitated. The solid was isolated on a fine porosity, sintered glass frit, and washed with diethyl ether (2x10 mL). The solid was dried *in vacuo* to yield a free flowing, tan microcrystalline powder (675 mg). The precise composition of $GdI_3(Et_2O)_x$ depends on absolute vacuum.

2.4.14 *Synthesis $[GdI_2(THF)_5][GdI_4(THF)_2]$, 3-Gd*

$GdI_3(Et_2O)_x$ (675 mg) is subjected to Soxhlet extraction with THF yielding a tan powder (815 mg, 80%). Found: Gd, 19.78%. $[GdI_2(THF)_5][GdI_4(THF)_2]$ requires 19.90%.

2.4.15 *Synthesis of $TbI_3(Et_2O)_3$, 1-Tb*

To a slurry of terbium powder (1.039 g, 6.29 mmol, 1.0 equiv.) in 40 mL of diethyl ether in a 200 mL Schlenk flask was added a solution of iodine (2.378 g, 9.37 mmol, 1.49 equiv.) in diethyl ether (80 mL). The reaction mixture was stirred for 4 days at room temperature and a tan solid precipitated. The solid was isolated on a fine porosity, sintered glass frit, and washed with diethyl ether (2x40 mL). The solid was dried *in vacuo* to yield a free flowing, white microcrystalline powder (4.067 g). The precise composition of $TbI_3(Et_2O)_x$ depends on absolute vacuum and duration of exposure to vacuum. After three hours at 400 mtorr, elemental analysis found(calc'd) for $TbI_3(Et_2O)_{1.88}$: C, 12.02(13.30) H, 2.79(2.79). After nine hours at 30 mtorr, elemental analysis found(calc'd) for $TbI_3(Et_2O)_{1.07}$: C, 7.33(8.84), H, 1.99(1.99).

2.4.16 *Synthesis $[TbI_2(THF)_5][TbI_4(THF)_2]$, 3-Tb*

$TbI_3(Et_2O)_x$ (4.067 mg) is subjected to Soxhlet extraction with THF yielding a white powder (4.071 g, 82%). Found: 20.10%. $[TbI_2(THF)_5][TbI_4(THF)_2]$ requires 20.06%.

2.4.17 *Synthesis of $DyI_3(Et_2O)_3$, 1-Dy*

To a slurry of dysprosium powder (1.020 g, 6.28 mmol, 1.0 equiv.) in 80 mL of diethyl ether in a 250 mL Schlenk flask was added a solution of iodine (2.374 g, 9.35 mmol, 1.49 equiv.) in diethyl ether (40 mL). The reaction mixture was stirred for 4 days at room temperature and a gray solid precipitated. The solid was isolated on a fine porosity, sintered glass frit, and washed with diethyl ether (2x40 mL). The solid was dried *in vacuo* to yield

a free flowing, gray microcrystalline powder (3.5067 g). The precise composition of $DyI_3(Et_2O)_x$ depends on absolute vacuum.

2.4.18 *Synthesis $[DyI_2(THF)_5][DyI_4(THF)_2]$, 3-Dy*

$DyI_3(Et_2O)_x$ (3.5067 g) is subjected to Soxhlet extraction with THF yielding a gray powder (4.533 g, 91%). Found: Dy, 20.45%. $[DyI_2(THF)_5][DyI_4(THF)_2]$ requires 20.43%.

2.4.19 *Synthesis of $HoI_3(Et_2O)_3$, 1-Ho*

To a slurry of holmium powder (1.010 g, 6.12 mmol, 1.0 equiv.) in 80 mL of diethyl ether in a 250 mL Schlenk flask was added a solution of iodine (2.314 g, 9.12 mmol, 1.49 equiv.) in diethyl ether (40 mL). The reaction mixture was stirred for 4 days at room temperature and a gray solid precipitated. The solid was isolated on a fine porosity, sintered glass frit, and washed with diethyl ether (2x40 mL). The solid was dried *in vacuo* to yield a free flowing, gray microcrystalline powder (3.3164 g). The precise composition of $HoI_3(Et_2O)_x$ depends on absolute vacuum.

2.4.20 *Synthesis $[HoI_2(THF)_5][HoI_4(THF)_2]$, 3-Ho*

$HoI_3(Et_2O)_x$ (3.3164 g) is subjected to Soxhlet extraction with THF yielding a gray powder (3.957 g, 81%). Found: Ho, 20.52%. $[HoI_2(THF)_5][HoI_4(THF)_2]$ requires 20.65%.

2.4.21 *Synthesis of $ErI_3(Et_2O)_3$, 1-Er*

To a slurry of erbium powder (221 mg, 1.32 mmol, 1.0 equiv.) in 14 mL of diethyl ether in a 50 mL Schlenk flask was added a solution of iodine (496 mg, 1.95 mmol, 1.48 equiv.) in diethyl ether (12 mL). The reaction mixture was stirred for 4 days at room temperature

and a gray solid precipitated. The solid was isolated on a fine porosity, sintered glass frit, and washed with diethyl ether (2x25 mL). The solid was dried *in vacuo* to yield a free flowing, gray-brown microcrystalline powder (682 mg). The precise composition of $ErI_3(Et_2O)_x$ depends on absolute vacuum.

2.4.22 *Synthesis $[ErI_2(THF)_5][ErI_4(THF)_2]$, 3-Er*

$ErI_3(Et_2O)_x$ (682 mg) is subjected to Soxhlet extraction with THF yielding a gray powder (804 mg, 77%). Found 20.99%. $[ErI_2(THF)_5][ErI_4(THF)_2]$ requires 20.90%.

2.4.23 *Synthesis of $TmI_3(Et_2O)_3$, 1-Tm*

To a slurry of thulium powder (200 mg, 1.184 mmol, 1.0 equiv.) in 12 mL of diethyl ether in a 50 mL Schlenk flask was added a solution of iodine (447 mg, 1.764 mmol, 1.49 equiv.) in diethyl ether (18 mL). The reaction mixture was stirred for 4 days at room temperature and a gray solid precipitated. The solid was isolated on a fine porosity, sintered glass frit, and washed with diethyl ether (2x25 mL). The solid was dried *in vacuo* to yield a free flowing, gray-brown microcrystalline powder (860 mg). The precise composition of $TmI_3(Et_2O)_x$ depends on absolute vacuum.

2.4.24 *Synthesis $[TmI_2(THF)_5][TmI_4(THF)_2]$, 3-Tm*

$TmI_3(Et_2O)_x$ (860 mg) is subjected to Soxhlet extraction with THF yielding a gray powder (570 mg, 60%). Found: Tm, 21.48%. $[TmI_2(THF)_5][TmI_4(THF)_2]$ requires 21.06%.

2.4.25 *Direct Synthesis of $[YbI_2(THF)_5][YbI_4(THF)_2]$, 3-Yb*

To a slurry of ytterbium powder (250 mg, 1.44 mmol, 1.0 equiv.) in 12 mL of THF in a 50 mL Schlenk flask was added a solution of iodine (542 mg, 2.14 mmol, 1.48 equiv.) in THF (20 mL). The reaction mixture was stirred for 4 days at room temperature and a red-brown solid precipitated. The solid was isolated on a fine porosity, sintered glass frit, and washed with THF (2x10 mL). The solid was dried *in vacuo* to yield a free flowing, tan -brown microcrystalline powder (836 mg, 72%). Found: Yb, 21.31%. $[YbI_2(THF)_5][YbI_4(THF)_2]$ requires 21.45%.

2.4.26 *Synthesis of $Ce[N(Si(Me_3)_3)_2]_3$*

$CeI_3(THF)_4$ (2.20 g, 2.72 mmol, 1.00 equiv.) was suspended in 20 mL of toluene inside a 100-mL round-bottomed flask inside a glovebox. A 20 mL toluene solution of $K[N(SiMe_3)_2]$ (1.63 g, 8.16 mmol, 3.00 equiv.) was added to the stirring suspension of $CeI_3(THF)_4$. The reaction mixture was stirred at room temperature for 24 hours. The resulting cloudy yellow solution was filtered through a fine-porosity glass frit with a plug of Celite. The product solution was dried *in vacuo* and collected as a free-flowing crystalline bright yellow solid (1.61 g, 95%). ^{1}H NMR, C_6D_6, δ (br-s) -3.39 ppm.

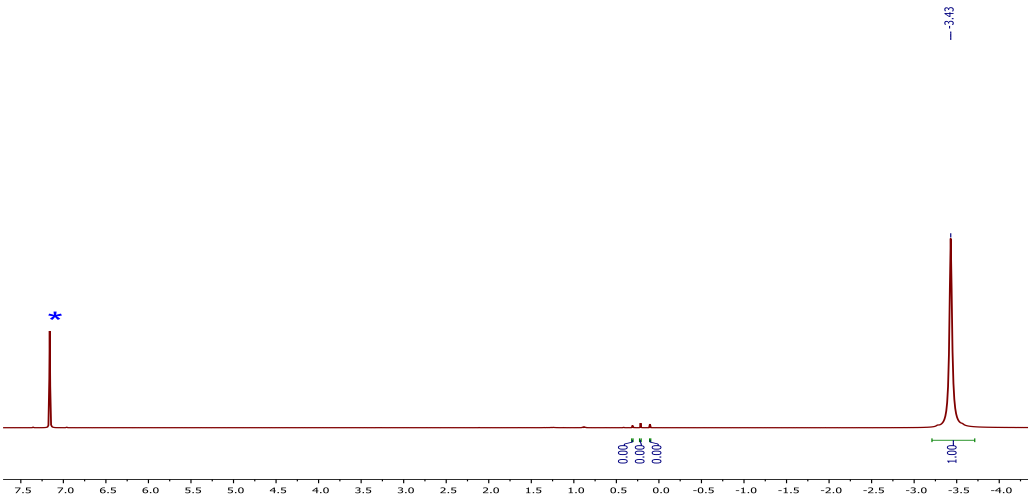

Figure 2.9 ^{1}H NMR of Ce[N(Si(Me)$_3$)$_2$]$_3$ in C_6D_6. Peak of C_6D_5H is noted as *.

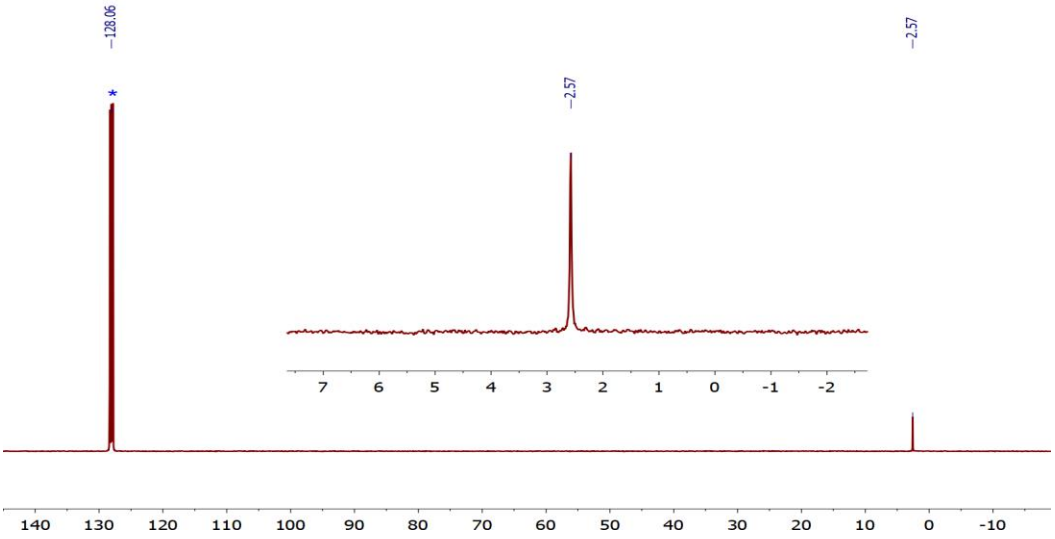

Figure 2.10 ^{13}C NMR of Ce[N(Si(Me$_3$)$_3$)$_2$]$_3$ in C_6D_6. Peak of C_6D_5H is noted as *.

2.4.27 *Synthesis of Ce(C$_7$H$_7$)$_3$(THF)$_3$*

$CeI_3(THF)_4$ (441 mg, 0.545 mmol, 1.00 equiv.) was suspended in 5 mL of THF and chilled to -35°C. Potassium benzyl (213 mg, 1.63 mmol, 3.00 equiv.) was dissolved separately in 8 mL of THF and chilled to -35°C. The solution of potassium benzyl was added to the slurry of $CeI_3(THF)_4$ while cold. The reaction mixture is stirred for 4 hours at -35°C. The mixture is filtered over Celite using pre-chilled glass equipment. The filtrate is concentrated to approximately 5 mL of THF. The solution is layered with approximately 2 mL of cold hexanes and set to crystalize overnight at -35°C. The supernatant is decanted, and the dark orange crystals are collected and dried (203 mg, 59%). Powder XRD, shown in Figure 2.11, is used to confirm purity based on previous SCXRD result.[143]

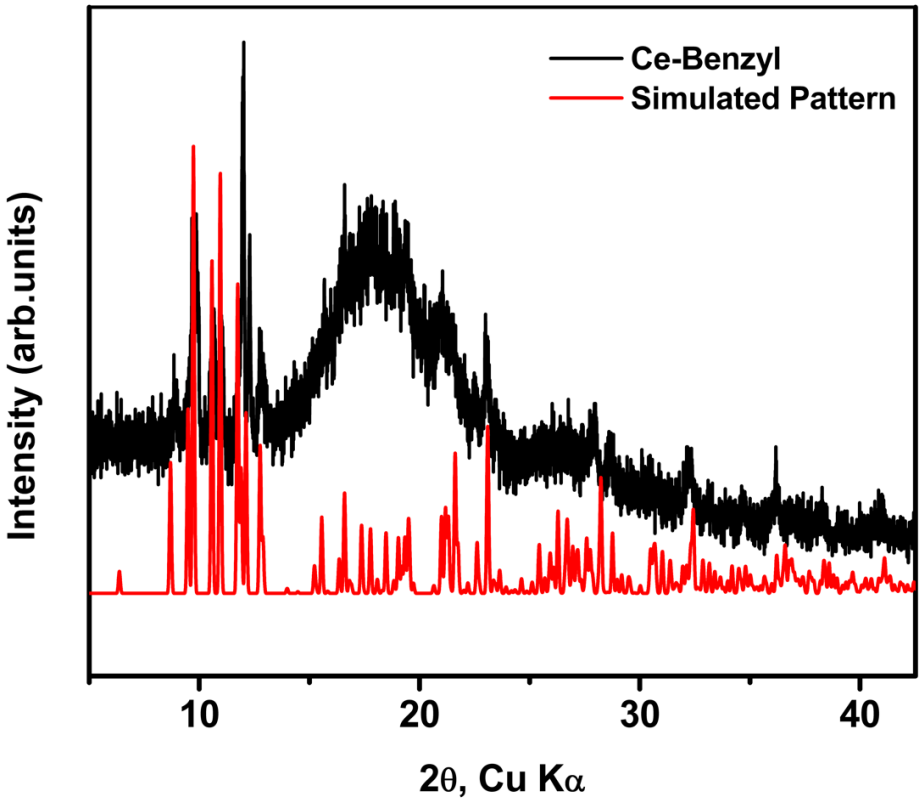

Figure 2.11 Powder XRD pattern for $Ce(C_7H_7)_3(THF)_3$. Simulated pattern is based on previously reported single crystal XRD data from ref. 143.

2.5 Crystallographic Information

Crystals suitable for X-ray diffraction were covered in paratone oil in a glove box and transferred to the diffractometer in a 20 mL capped vial. Crystals were mounted on a loop with paratone oil on a Bruker D8 VENTURE diffractometer. The crystals were cooled and kept at T = 100(2) K during data collections. The structures were solved with the ShelXT structure solution program using the Intrinsic Phasing solution method and by using Olex2 as the graphical interface.[145, 146] The model was refined with version 2014/7 of XL using Least Squares minimization.[147] XRD graphics are generated using POV-Ray.[148]

Table 2.2 General crystallographic data for 1-Ln.

	1-Ce	***1-Pr***	***1-Nd***	***1-Sm***	***1-Gd***	***1-Tb***	***1-Tm***
Formula	$C_{12}H_{30}I_3O_3Ce$	$C_{12}H_{30}I_3O_3Pr$	$C_{12}H_{30}I_3O_3Nd$	$C_{12}H_{30}I_3O_3Sm$	$C_{12}H_{30}I_3O_3Gd$	$C_{12}H_{30}I_3O_3Tb$	$C_{12}H_{30}I_3O_3Tm$
Molecular weight	743.18	743.91	747.30	753.41	760.31	761.98	771.99
Color, Shape	Colorless Prism	Colorless Prism	Blue Prism	Yellow Prism	Colorless Prism	Colorless Prism	Colorless Prism
Size/mm	0.233×0.216×0.158	0.34×0.33×0.13	0.747×0.355×0.15	0.38×0.22×0.11	0.302×0.295×0.254	0.747×0.6×0.15	0.285×0.221×0.12
T/K	100(2)	100(2)	100(2)	100(2)	100(2)	100(2)	100(2)
Crystal System	Orthorhombic	Orthorhombic	Orthorhombic	Orthorhombic	Orthorhombic	Orthorhombic	Triclinic
Space Group	Pbcn	Pbcn	$Pna2_1$	Pbcn	Pbcn	Pbcn	P-1
a/Å	10.1423	10.1152(4)	10.3268(6)	10.0662(7)	10.0525(12)	10.0273(6)	13.695(2)
b/Å	13.9652	13.9216(7)	16.1190(10)	13.8437(10)	13.8205(17)	13.7816(9)	17.532(3)
c/Å	15.8918	15.8716(8)	13.6707(10)	15.8345(11)	15.8047(19)	15.7910(11)	20.912(4)
α/°	90	90	90	90	90	90	65.386(7)
β/°	90	90	90	90	90	90	87.540(7)
γ/°	90	90	90	90	90	90	87.044(7)
V/Å³	2250.90(16)	2235.04(18)	2275.6(3)	2206.6(3)	2195.8(5)	2182.2(2)	4557.7(15)
Z	4	4	4	4	4	4	8
Wavelength/Å	0.71073	0.71073	0.71073	0.71073	0.71073	0.71073	0.71073
Measured Reflections	24517	40923	63656	50414	114756	45138	140106
Unique Reflections	5427	3418	10888	5322	8912	3344	27718
Refl. I > 2σ	4012	2762	8725	3816	7567	2965	21667
R_{int}	0.0391	0.0567	0.0462	0.0619	0.0421	0.0606	0.0436
wR_2 *(all data)*	0.0645	0.0747	0.1497	0.1051	0.0547	0.0571	0.2680
wR_2	0.0556	0.0653	0.1332	0.0815	0.0501	0.0552	0.2493
R_1 *(all data)*	0.0494	0.0369	0.0772	0.0616	0.0320	0.0280	0.1232
R_1	0.0291	0.0255	0.0571	0.0342	0.0240	0.0235	0.1021
GooF	1.020	1.090	1.044	1.112	1.198	1.069	1.081

2.5.1 *1-Ce*

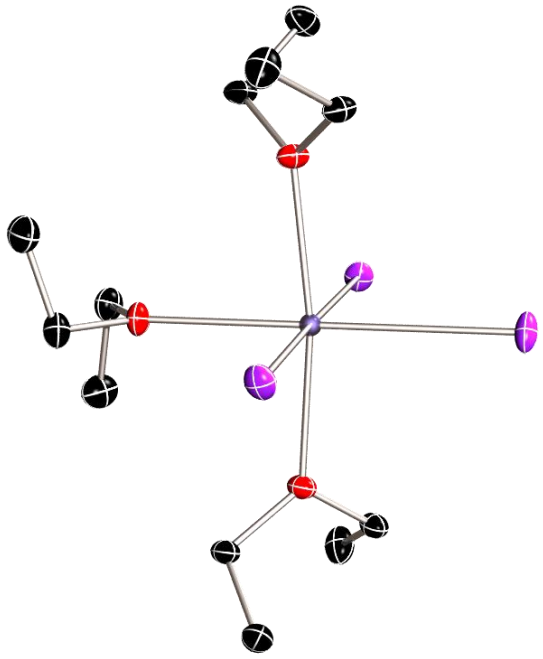

Figure 2.12 Molecular structure of 1-Ce with thermal ellipsoids shown at 50% probability and H atoms are omitted for clarity.

Table 2.3 Fractional Atomic Coordinates ($\times 10^4$) and Equivalent Isotropic Displacement Parameters ($Å^2 \times 10^3$) for 1-Ce. U_{eq} is defined as 1/3 of the trace of the orthogonalised U_{ij}.

Atom	x	y	z	U_{eq}
Ce1	5000	3716.1(2)	2500	10.89(4)
I1	7219.9(2)	3749.7(2)	3839.9(2)	19.35(4)
I2	5000	5908.8(2)	2500	21.22(6)
O1	5000	1903.0(19)	2500	18.5(4)
O2	3390.3(18)	3582.2(14)	3622.0(11)	16.7(3)
C5	3456(3)	4202(2)	4368.3(16)	18.0(4)
C3	2286(3)	2909(2)	3612.3(17)	18.3(4)
C4	970(3)	3405(2)	3587(2)	25.3(5)
C6	3747(3)	3654(2)	5159.7(18)	26.5(6)
C1	4201(3)	1316(2)	1929.0(18)	21.8(5)
C2	4943(3)	1097(2)	1132(2)	28.5(6)

Table 2.4 Anisotropic Displacement Parameters (×10^4) for 1-Ce. The anisotropic displacement factor exponent takes the form: $-2\pi^2[h^2a^{*2} \times U_{11} + ... + 2hka^* \times b^* \times U_{12}]$.

Atom	U_{11}	U_{22}	U_{33}	U_{23}	U_{13}	U_{12}
Ce1	10.50(7)	10.42(8)	11.75(7)	0	0.12(6)	0
I1	15.54(7)	20.41(8)	22.09(8)	-0.37(7)	-6.38(6)	2.05(7)
I2	35.71(14)	10.57(10)	17.4(1)	0	-5.97(10)	0
O1	21.9(10)	11.8(9)	21.8(8)	0	-2.4(8)	0
O2	14.3(6)	20.4(7)	15.5(5)	-2.7(5)	2.5(5)	-3.6(5)
C5	19.0(10)	19.9(7)	15.0(6)	-2.2(5)	2.5(6)	-4.3(6)
C3	13.8(6)	20.2(7)	21.0(10)	-4.9(6)	4.3(6)	-3.3(5)
C4	14.3(6)	25.3(10)	36.5(15)	-6.2(11)	2.9(7)	-1.5(6)
C6	38.8(16)	24.6(11)	16.0(5)	-0.8(7)	-0.5(7)	-1.7(11)
C1	25.5(10)	16.8(10)	23.1(8)	-2.7(7)	-2.0(7)	-2.6(7)
C2	33.9(13)	26.0(14)	25.6(8)	-7.0(8)	1.7(8)	-4.1(11)

Table 2.5 Bond Lengths in Å for 1-Ce.

Atom	Atom	Length/Å
Ce1	I1	3.09923(18)
Ce1	I1	3.09924(19)
Ce1	I2	3.0620(3)
Ce1	O1	2.532(3)
Ce1	O2	2.4248(18)
Ce1	O2	2.4248(18)
O1	C1	1.467(3)
O1	C1	1.467(3)
O2	C5	1.470(3)
O2	C3	1.463(3)
C5	C6	1.501(4)
C3	C4	1.504(4)
C1	C2	1.504(4)

Table 2.6 Bond Angles in ° for 1-Ce.

Atom	Atom	Atom	Angle/°
I1	Ce1	I1	178.265(10)
I2	Ce1	I1	89.132(5)
I2	Ce1	I1	89.133(5)
O1	Ce1	I1	90.868(5)
O1	Ce1	I1	90.867(5)
O1	Ce1	I2	180.0
O2	Ce1	I1	90.99(4)
O2	Ce1	$I1^1$	90.99(4)
O2	Ce1	$I1^1$	89.15(4)
O2	Ce1	I1	89.15(4)
O2	Ce1	I2	94.42(4)
O2	Ce1	I2	94.42(4)
O2	Ce1	O1	85.58(4)
O2	Ce1	O1	85.58(4)
O2	Ce1	O2	171.15(9)
C1	O1	Ce1	124.00(15)

Atom	Atom	Atom	Angle/°
C1	O1	Ce1	124.00(15)
C1	O1	C1	112.0(3)
C5	O2	Ce1	121.17(15)
C3	O2	Ce1	123.88(15)
C3	O2	C5	114.94(19)
O2	C5	C6	112.6(2)
O2	C3	C4	112.6(2)
O1	C1	C2	111.0(2)

Table 2.7 Hydrogen Fractional Atomic Coordinates (×10^4) and Equivalent Isotropic Displacement Parameters (Å^2×10^3) for 1-Ce. U_{eq} is defined as 1/3 of the trace of the orthogonalised U_{ij}.

Atom	x	y	z	U_{eq}
H5A	2603.98	4540.51	4433.81	22
H5B	4149.91	4690.68	4282.46	22
H3A	2329.69	2500.49	4120.7	22
H3B	2366.79	2487.26	3114.13	22
H4A	965.32	3877.43	3131.22	38
H4B	813.69	3729.73	4125.14	38
H4C	272.61	2932.15	3489.85	38
H6A	4558.32	3283.36	5085.13	40
H6B	3013.49	3219.15	5282.25	40
H6C	3858.04	4103.42	5628.28	40
H1A	3377.12	1660.36	1789.47	26
H1B	3960.56	709.19	2212.77	26
H2A	4417.89	664.86	780.43	43
H2B	5784.05	789.25	1272.3	43
H2C	5111.86	1692.74	825.45	43

Coordination polyhedron

Ce1-I1 = 3.0993(3) Å

Ce1-O2 = 2.4248(18) Å

Ce1-I2 = 3.0621(5) Å

Ce1-O1 = 2.532(3) Å

Ce1-O2 = 2.4248(18) Å

Ce1-I1 = 3.0993(3) Å

The ether molecules bind highly asymmetrical. There is a correlation between the asymmetric binding of the ether molecules and the binding of the iodine atoms. The distortion index is 0.11291 and the bond angle variance is 7.7°.

Average bond length = 2.7737 Å

Polyhedral volume = 27.9370 $Å^3$

Distortion index (bond length) = 0.11291

Quadratic elongation = 1.0254

Bond angle variance = 7.6979 $deg.^2$

Effective coordination number = 3.3401

2.5.2 *1-Pr*

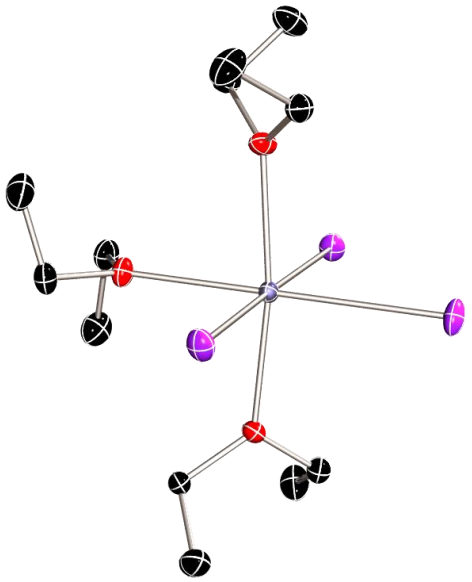

Figure 2.13 Molecular structure of 1-Pr with thermal ellipsoids shown at 50% probability and H atoms are omitted for clarity.

Table 2.8 Fractional Atomic Coordinates ($\times 10^4$) and Equivalent Isotropic Displacement Parameters ($Å^2 \times 10^3$) for 1-Pr. U_{eq} is defined as 1/3 of the trace of the orthogonalised U_{ij}.

Atom	x	y	Z	U_{eq}
Pr1	5000	6287.7(2)	2500	12.42(7)
I1	7216.7(2)	6253.8(2)	1168.8(2)	20.93(7)
I2	5000	4101.1(2)	2500	22.37(9)
O1	5000	8099(3)	2500	18.6(7)
O2	6596(2)	6416.6(17)	3617.9(16)	18.0(5)
C3	6535(4)	5797(2)	4360(2)	20.4(7)
C5	7707(3)	7093(3)	3607(2)	19.3(7)
C1	4201(4)	8685(3)	3068(3)	23.1(7)
C2	4945(5)	8903(3)	3869(3)	30.9(9)
C4	6252(5)	6344(3)	5158(3)	29.6(9)
C6	9025(4)	6600(3)	3584(3)	28.7(8)

Table 2.9 Anisotropic Displacement Parameters ($\times 10^4$) 1-Pr. The anisotropic displacement factor exponent takes the form: $-2\pi^2[h^2a^{*2} \times U_{11} + ... + 2hka^* \times b^* \times U_{12}]$.

Atom	U_{11}	U_{22}	U_{33}	U_{23}	U_{13}	U_{12}
Pr1	12.16(12)	10.66(12)	14.43(12)	0	-0.06(8)	0
I1	17.14(11)	20.67(12)	24.97(13)	-0.07(9)	6.30(8)	-1.77(9)

Atom	U_{11}	U_{22}	U_{33}	U_{23}	U_{13}	U_{12}
I2	36.14(19)	10.91(14)	20.05(16)	0	5.47(13)	0
O1	24.9(17)	13.7(15)	17.1(16)	0	3.1(14)	0
O2	14.5(11)	18.6(12)	20.9(12)	2.7(9)	-2.8(9)	-2.8(9)
C3	22.0(16)	17.4(16)	21.7(17)	2.2(13)	-1.8(13)	-1.4(13)
C5	18.1(15)	16.9(16)	22.8(17)	4.6(13)	-5.6(13)	-3.8(12)
C1	26.0(17)	15.6(16)	27.6(19)	-1.0(14)	2.5(14)	3.6(14)
C2	41(2)	23.8(19)	28(2)	-5.0(16)	0.3(17)	4.1(17)
C4	45(2)	28.4(19)	15.6(16)	-0.6(15)	0.2(17)	-6.1(17)
C6	18.6(16)	31(2)	36(2)	9.4(18)	-1.0(16)	-0.4(15)

Table 2.10 Bond Lengths in Å for 1-Pr.

Atom	Atom	Length/Å
Pr1	I1	3.0812(2)
Pr1	I1	3.0812(2)
Pr1	I2	3.0441(4)
Pr1	O1	2.521(4)
Pr1	O2	2.406(2)
Pr1	O2	2.406(2)
O1	C1	1.460(4)
O1	C1	1.460(4)
O2	C3	1.461(4)
O2	C5	1.466(4)
C3	C4	1.506(5)
C5	C6	1.501(5)
C1	C2	1.509(6)

Table 2.11 Bond Angles in ° for 1-Pr.

Atom	Atom	Atom	Angle/°
I1	Pr1	I1	178.248(12)
I2	Pr1	I1	89.124(6)
I2	Pr1	I1	89.124(6)
O1	Pr1	I1	90.876(6)
O1	Pr1	I1	90.876(6)
O1	Pr1	I2	180.0
O2	Pr1	I1	91.06(6)
O2	Pr1	I1	91.06(6)
O2	Pr1	I1	89.08(6)
O2	Pr1	I1	89.07(6)
O2	Pr1	I2	94.28(6)
O2	Pr1	I2	94.28(6)
O2	Pr1	O1	85.72(6)
O2	Pr1	O1	85.72(6)
O2	Pr1	O2	171.45(12)
C1	O1	Pr1	124.01(19)
C1	O1	Pr1	124.01(19)
C1	O1	C1	112.0(4)
C3	O2	Pr1	121.5(2)
C3	O2	C5	114.9(3)
C5	O2	Pr1	123.6(2)
O2	C3	C4	112.8(3)

Atom	Atom	Atom	Angle/°
O2	C5	C6	112.7(3)
O1	C1	C2	110.9(3)

Table 2.12 Hydrogen Fractional Atomic Coordinates (×10^4) and Equivalent Isotropic Displacement Parameters (Å^2×10^3) for 1-Pr. U_{eq} is defined as 1/3 of the trace of the orthogonalised U_{ij}.

Atom	x	y	z	U_{eq}
H3A	7388	5455	4421	24
H3B	5836	5309	4275	24
H5A	7661	7504	4116	23
H5B	7625	7515	3108	23
H1A	3373	8340	3206	28
H1B	3963	9294	2784	28
H2A	5097	8306	4181	46
H2B	4425	9346	4216	46
H2C	5796	9200	3730	46
H4A	6965	6806	5262	44
H4B	6194	5895	5632	44
H4C	5412	6689	5100	44
H6A	9180	6273	4122	43
H6B	9722	7076	3488	43
H6C	9033	6127	3126	43

2.5.3 *1-Nd*

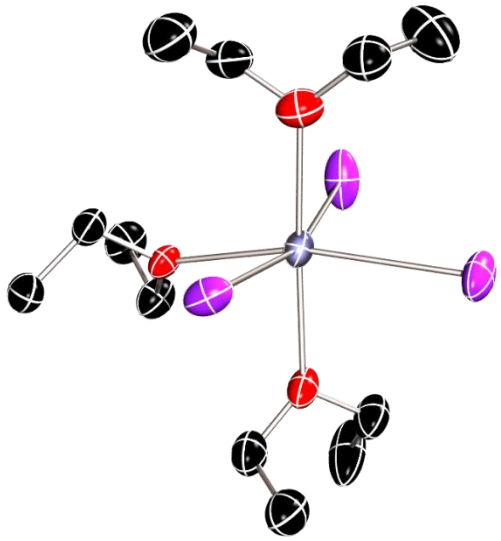

Figure 2.14 Molecular structure of 1-Nd with thermal ellipsoids shown at 50% probability and H atoms are omitted for clarity.

Table 2.13 Fractional Atomic Coordinates ($\times 10^4$) and Equivalent Isotropic Displacement Parameters ($Å^2 \times 10^3$) for 1-Nd. U_{eq} is defined as 1/3 of the trace of the orthogonalised U_{ij}.

Atom	x	y	z	U_{eq}
Nd1	2919.1(5)	5136.3(4)	4588.5(5)	29.56(13)
I1	5085.4(7)	4146.0(5)	3609.0(7)	41.63(19)
I2	2061.9(9)	6020.6(7)	2719.2(7)	54.4(3)
I3	1246.4(11)	6125.9(8)	6010.8(8)	62.9(3)
O1	3231(7)	4177(5)	5985(6)	31.6(15)
O2	1300(8)	4101(5)	4205(7)	39.4(18)
O3	4540(10)	6158(6)	4871(9)	56(3)
C2	4693(14)	3017(9)	6294(12)	50(3)
C4	2212(19)	4097(12)	7598(12)	64(4)
C6	1665(18)	3029(11)	2903(13)	64(4)
C10	6620(20)	5851(14)	5603(17)	83(5)
C5	1614(18)	3232(9)	3971(12)	58(3)
C9	5161(19)	6141(12)	5814(16)	73(4)
C11	4867(16)	6921(12)	4256(14)	66(4)
C12	3970(20)	7577(13)	4470(30)	102(8)
C8	-1020(17)	3914(16)	4500(20)	101(9)
C7	-2(17)	4338(14)	3903(16)	77(6)
C3	2125(18)	3835(12)	6514(13)	61(4)
C1	4462(15)	3962(9)	6362(12)	50(3)

Table 2.14 Anisotropic Displacement Parameters (×10^4) 1-Nd. The anisotropic displacement factor exponent takes the form: $-2\pi^2[h^2a^{*2} \times U_{11} + ... + 2hka^* \times b^* \times U_{12}]$.

Atom	U_{11}	U_{22}	U_{33}	U_{23}	U_{13}	U_{12}
Nd1	24.4(2)	38.7(3)	25.6(2)	7.0(3)	3.2(2)	2.2(2)
I1	31.1(3)	57.8(4)	35.9(4)	-15.6(4)	8.5(3)	-1.6(3)
I2	47.8(5)	70.5(6)	44.8(5)	30.8(5)	-8.4(4)	-10.5(4)
I3	59.7(6)	82.6(7)	46.4(5)	18.8(5)	24.5(5)	36.7(5)
O1	28(3)	38(4)	28(4)	-1(3)	0(3)	-7(3)
O2	26(4)	48(4)	44(5)	18(4)	-5(3)	-7(3)
O3	44(5)	53(5)	70(6)	-18(4)	11(4)	-8(4)
C2	42(7)	47(6)	62(9)	7(6)	-2(6)	4(5)
C4	76(11)	77(11)	40(7)	15(7)	26(7)	4(8)
C6	68(10)	62(9)	61(7)	3(6)	-6(7)	-19(8)
C10	73(9)	91(13)	83(13)	1(11)	-37(8)	-9(8)
C5	71(9)	47(5)	55(7)	19(5)	-3(6)	0(5)
C9	80(9)	56(9)	82(9)	30(8)	-8(7)	-15(7)
C11	50(8)	79(8)	70(10)	3(7)	-2(7)	-14(6)
C12	66(10)	82(10)	160(20)	2(13)	20(13)	-8(8)
C8	38(8)	150(20)	118(19)	74(17)	-10(9)	2(9)
C7	48(8)	90(13)	92(15)	36(11)	-18(8)	-8(8)
C3	65(10)	69(10)	50(8)	9(7)	-1(7)	-2(8)
C1	44(6)	52(6)	53(8)	-3(6)	-16(6)	-1(5)

Table 2.15 Bond Lengths in Å for 1-Nd.

Atom	Atom	Length/Å
Nd1	I1	3.0537(9)
Nd1	I2	3.0534(10)
Nd1	I3	3.0475(11)
Nd1	O1	2.475(8)
Nd1	O2	2.417(8)
Nd1	O3	2.377(10)
O1	C3	1.458(19)
O1	C1	1.413(16)
O2	C5	1.472(18)
O2	C7	1.456(18)
O3	C9	1.44(2)
O3	C11	1.53(2)
C2	C1	1.54(2)
C4	C3	1.54(2)
C6	C5	1.50(2)
C10	C9	1.60(3)
C11	C12	1.44(3)
C8	C7	1.49(3)

Table 2.16 Bond Angles in ° for 1-Nd.

Atom	Atom	Atom	Angle/°
I1	Nd1	I2	95.13(3)
I3	Nd1	I1	165.11(4)
I3	Nd1	I2	97.17(3)
O1	Nd1	I1	85.21(19)
O1	Nd1	I2	166.59(17)
O1	Nd1	I3	84.77(19)
O2	Nd1	I1	92.9(2)
O2	Nd1	I2	86.6(2)
O2	Nd1	I3	96.2(2)
O2	Nd1	O1	80.0(3)
O3	Nd1	I1	85.3(2)
O3	Nd1	I2	91.0(3)
O3	Nd1	I3	86.2(2)
O3	Nd1	O1	102.4(3)
O3	Nd1	O2	176.8(4)
C3	O1	Nd1	121.0(8)
C1	O1	Nd1	123.4(8)
C1	O1	C3	115.5(12)
C5	O2	Nd1	123.4(9)
C5	O2	C7	121.3(10)
C7	O2	Nd1	113.0(13)
C9	O3	Nd1	116.5(9)
C9	O3	C11	114.2(12)
C11	O3	Nd1	128.6(10)
O2	C5	C6	115.3(12)
O3	C9	C10	105.2(17)
O3	C11	C12	109.7(16)
O2	C7	C8	112.1(14)
O1	C3	C4	109.1(14)
O1	C1	C2	111.1(11)

Table 2.17 Hydrogen Fractional Atomic Coordinates ($\times 10^4$) and Equivalent Isotropic Displacement Parameters ($Å^2 \times 10^3$) for 1-Nd. U_{eq} is defined as 1/3 of the trace of the orthogonalised U_{ij}.

Atom	x	y	z	U_{eq}
H2A	5300.38	2900.43	5759.12	76
H2B	3868.74	2735.12	6166.1	76
H2C	5057.96	2816.25	6912.58	76
H4A	2253.81	4703.9	7642.21	97
H4B	2993.08	3856.25	7892.56	97
H4C	1445.02	3896.86	7949.89	97
H6A	1909.85	3525.88	2532.46	96
H6B	810.59	2836.65	2685.3	96
H6C	2306.9	2590.35	2790.97	96
H10A	7120.59	6322.48	5352.61	124
H10B	6616.16	5404.26	5115.62	124
H10C	7013	5649.38	6211.25	124
H5A	959.4	2869.78	4284.59	69
H5B	2465.58	3097.04	4265.1	69

Atom	x	y	z	U_{eq}
H9A	4719.63	5743.77	6256.6	87
H9B	5146.79	6698.52	6119.8	87
H11A	5760.73	7106.69	4403.5	79
H11B	4820.47	6778.52	3551.67	79
H12A	3879.23	7635.79	5183.05	153
H12B	3120.87	7444.34	4185.78	153
H12C	4287.64	8099.32	4193.17	153
H8A	-1876.77	4046.64	4230.32	152
H8B	-967.67	4106.27	5177.44	152
H8C	-882.51	3312.45	4474.98	152
H7A	-123.67	4193.97	3203.72	92
H7B	-102.1	4946.6	3969.68	92
H3A	2127.52	3222.11	6463.19	74
H3B	1308.24	4044.92	6224.84	74
H1A	4520.98	4139.4	7054.52	60
H1B	5142.82	4257.27	5988.29	60

Coordination polyhedron

Nd1-O2 = 2.417(9) Å

Nd1-I3 = 3.0475(14) Å

Nd1-O1 = 2.475(9) Å

Nd1-I2 = 3.0533(13) Å

Nd1-I1 = 3.0538(10) Å

Nd1-O3 = 2.377(11) Å

The ether molecules bind highly asymmetrically. There is a correlation between the asymmetric binding of the ether molecules and the binding of the iodine atoms. The distortion index is 0.11414 and the bond angle variance is 46.38°

Average bond length = 2.7373 Å

Polyhedral volume = 26.4709 $Å^3$

Distortion index (bond length) = 0.1148

Quadratic elongation = 1.0355

Bond angle variance = 43.5 deg^2

Effective coordination number = 3.31

2.5.4 *1-Sm*

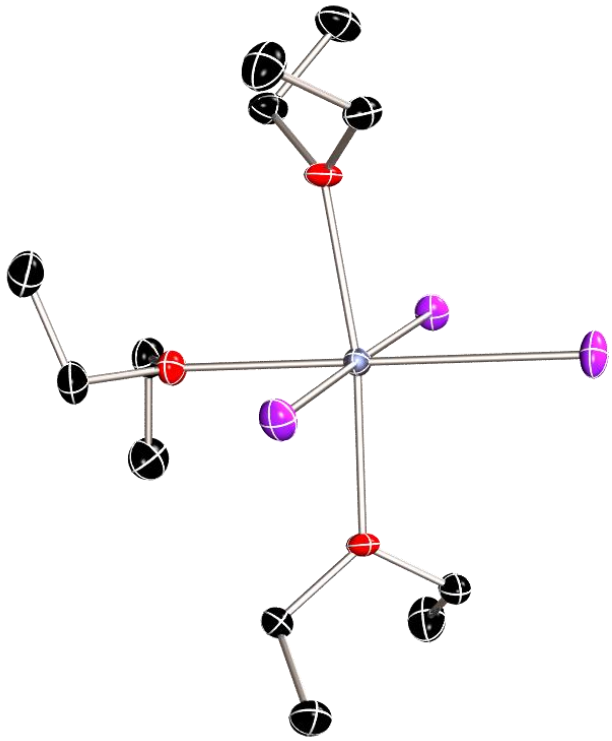

Figure 2.15 Molecular structure of 1-Sm with thermal ellipsoids shown at 50% probability and H atoms are omitted for clarity.

Table 2.18 Fractional Atomic Coordinates (×104) and Equivalent Isotropic Displacement Parameters (Å2×103) for 1-Sm. Ueq is defined as 1/3 of the trace of the orthogonalised Uij.

Atom	x	y	Z	U_{eq}
Sm1	5000	6292.4(2)	2500	13.12(6)
I1	7203.5(3)	6256.1(2)	1191.3(2)	20.98(7)
I2	5000	4124.5(2)	2500	22.41(9)
O1	5000	8083(3)	2500	19.4(7)
O2	6570(3)	6423(2)	3598.5(19)	17.2(5)
C3	6517(4)	5795(3)	4350(3)	20.0(6)
C5	7689(4)	7099(3)	3592(3)	21.2(7)
C1	4198(5)	8677(3)	3071(3)	24.3(7)
C2	4948(6)	8899(4)	3870(3)	31.1(9)
C4	6249(6)	6349(3)	5145(3)	30.3(9)
C6	9020(4)	6601(4)	3580(3)	28.5(9)
I1'	7150(40)	6280(30)	3800(30)	20.98(7)

Table 2.19 Anisotropic Displacement Parameters (×10^4) 1-Sm. The anisotropic displacement factor exponent takes the form: $-2\pi^2[h^2a^{*2} \times U_{11} + ... + 2hka^* \times b^* \times U_{12}]$.

Atom	U_{11}	U_{22}	U_{33}	U_{23}	U_{13}	U_{12}
Sm1	12.39(11)	11.87(10)	15.10(11)	0	0.01(8)	0
I1	16.97(12)	21.32(12)	24.64(13)	0.20(9)	5.92(9)	-1.57(9)
I2	34.7(2)	11.98(13)	20.54(17)	0	4.65(14)	0
O1	20.6(17)	13.9(14)	23.8(16)	0	-0.9(13)	0
O2	12.5(10)	20.9(11)	18.1(11)	3.3(8)	-5.7(8)	-1.3(8)
C3	20.6(16)	20.1(13)	19.2(12)	2.9(10)	-4.1(11)	-3.7(11)
C5	16.9(12)	20.8(13)	25.8(18)	5.3(12)	-3.9(11)	-4.3(10)
C1	27.4(17)	16.1(15)	29.5(16)	-2.8(12)	1.9(13)	2.6(12)
C2	38(2)	24.7(19)	30.1(17)	-6.7(14)	-1.9(15)	2.3(17)
C4	44(3)	27.1(18)	20.3(14)	0.2(12)	-0.6(14)	-3.6(17)
C6	17.5(13)	31.1(19)	37(2)	6.9(18)	-2.7(13)	-0.4(12)
I1'	16.97(12)	21.32(12)	24.64(13)	0.20(9)	5.92(9)	-1.57(9)

Table 2.20 Bond Lengths in Å for 1-Sm.

Atom	Atom	Length/Å
Sm1	I1	3.0359(3)
Sm1	I1	3.0359(3)
Sm1	I2	3.0012(5)
Sm1	O1	2.479(4)
Sm1	O2	2.357(3)
Sm1	O2	2.357(3)
O1	C1	1.465(5)
O1	C1	1.465(5)
O2	C3	1.474(5)
O2	C5	1.466(5)
C3	C4	1.499(6)
C5	C6	1.507(6)
C1	C2	1.505(7)

Table 2.21 Bond Angles in ° for 1-Sm.

Atom	Atom	Atom	Angle/°
I1^1	Sm1	I1	178.101(13)
I2	Sm1	I1	89.051(7)
I2	Sm1	I1	89.051(7)
O1	Sm1	I1	90.949(7)
O1	Sm1	I1	90.949(7)
O1	Sm1	I2	180.0
O2^1	Sm1	I1	89.27(8)
O2	Sm1	I1	89.28(8)
O2^1	Sm1	I1	90.87(8)
O2	Sm1	I1	90.87(8)
O2	Sm1	I2	94.39(7)
O2^1	Sm1	I2	94.39(7)
O2	Sm1	O1	85.61(7)
O2^1	Sm1	O1	85.61(7)
O2^1	Sm1	O2	171.22(14)

Atom	Atom	Atom	Angle/°
C1	O1	Sm1	124.2(2)
C1[1]	O1	Sm1	124.2(2)
C1	O1	C1	111.7(4)
C3	O2	Sm1	121.8(2)
C5	O2	Sm1	124.0(2)
C5	O2	C3	114.2(3)
O2	C3	C4	112.6(3)
O2	C5	C6	113.0(4)
O1	C1	C2	110.9(4)

Table 2.22 Hydrogen Fractional Atomic Coordinates (×10^4) and Equivalent Isotropic Displacement Parameters (Å^2×10^3) for 1-Sm. U_{eq} is defined as 1/3 of the trace of the orthogonalised U_{ij}.

Atom	x	y	z	U_{eq}
H3A	7374	5450	4407	24
H3B	5811	5306	4271	24
H5A	7636	7517	4098	25
H5B	7617	7520	3088	25
H1A	3367	8331	3212	29
H1B	3956	9288	2785	29
H2A	5077	8303	4193	47
H2B	4440	9362	4210	47
H2C	5814	9178	3728	47
H4A	6967	6814	5241	45
H4B	6201	5900	5623	45
H4C	5403	6694	5092	45
H6A	9157	6262	4117	43
H6B	9724	7081	3502	43
H6C	9045	6134	3115	43

Table 2.23 Atomic Occupancies for all atoms that are not fully occupied in 1-Sm.

Atom	Occupancy
I1	0.9926(10)
I1'	0.0074(10)

2.5.5 *1-Gd*

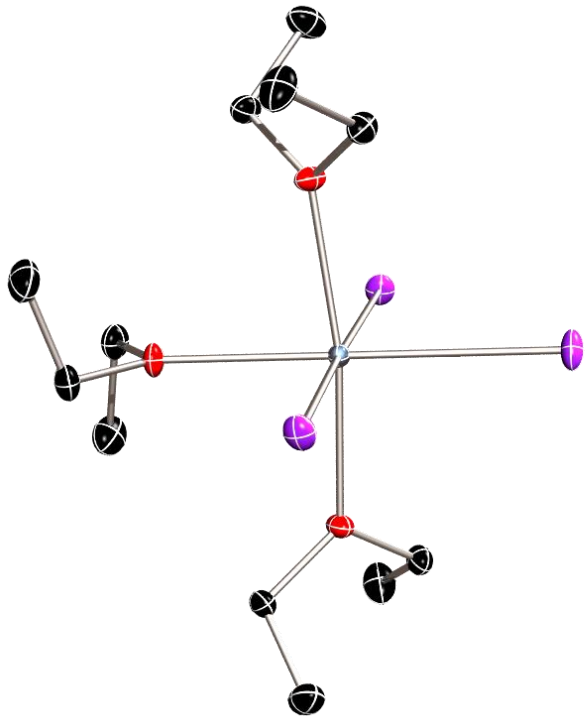

Figure 2.16 Molecular structure of 1-Gd with thermal ellipsoids shown at 50% probability and H atoms are omitted for clarity.

Table 2.24 Fractional Atomic Coordinates (×10^4) and Equivalent Isotropic Displacement Parameters (Å^2×10^3) for 1-Gd. U_{eq} is defined as 1/3 of the trace of the orthogonalised U_{ij}.

Atom	x	y	Z	U_{eq}
Gd1	5000	3703.0(2)	2500	9.26(2)
I1	7195.7(2)	3740.7(2)	3798.8(2)	16.49(2)
I2	5000	5863.5(2)	2500	17.11(3)
O1	5000	1931.9(11)	2500	15.0(2)
O2	3432.2(11)	3574.6(8)	3598.7(7)	13.92(16)
C5	3491.7(17)	4202.7(11)	4342.2(9)	15.7(2)
C3	2322.3(15)	2898.9(11)	3587.7(11)	16.0(2)
C4	985.9(18)	3394.9(15)	3577.2(13)	23.1(3)
C6	3746(2)	3648.2(14)	5143.1(11)	24.9(3)
C1	4195.9(18)	1329.5(11)	1932.6(11)	18.6(2)
C2	4939(2)	1104.5(14)	1129.0(13)	25.9(3)

Table 2.25 Anisotropic Displacement Parameters (×10^4) 1-Gd. The anisotropic displacement factor exponent takes the form: $-2\pi^2[h^2a^{*2} \times U_{11} + ... + 2hka^* \times b^* \times U_{12}]$.

Atom	U_{11}	U_{22}	U_{33}	U_{23}	U_{13}	U_{12}
Gd1	9.68(3)	8.24(3)	9.85(3)	0	-0.17(2)	0
I1	14.19(4)	17.02(4)	18.28(4)	0.08(3)	-5.56(3)	1.43(3)
I2	28.63(7)	8.39(4)	14.31(5)	0	-4.15(4)	0
O1	19.5(6)	7.6(4)	17.8(6)	0	-1.9(5)	0
O2	12.5(4)	15.8(4)	13.4(4)	-2.7(3)	3.0(3)	-3.0(3)
C5	19.0(6)	14.4(5)	13.8(5)	-2.4(4)	1.1(4)	-2.3(4)
C3	14.1(5)	14.5(5)	19.5(6)	-3.5(4)	2.3(4)	-3.6(4)
C4	14.8(6)	25.1(7)	29.5(8)	-7.4(6)	0.6(6)	-0.4(5)
C6	40.3(10)	21.9(7)	12.6(5)	1.0(5)	-0.3(6)	-4.2(7)
C1	21.4(7)	12.4(5)	22.0(6)	-2.3(4)	-2.4(5)	-3.4(5)
C2	36.5(10)	19.4(7)	21.8(7)	-6.0(6)	2.2(7)	-3.1(6)

Table 2.26 Bond Lengths in Å for 1-Gd.

Atom	Atom	Length/Å
Gd1	I1	3.0144(2)
Gd1	I1	3.0145(3)
Gd1	I2	2.9849(3)
Gd1	O1	2.4470(15)
Gd1	O2	2.3517(11)
Gd1	O2	2.3517(11)
O1	C1	1.4663(18)
O1	C1	1.4663(18)
O2	C5	1.4622(18)
O2	C3	1.4546(18)
C5	C6	1.502(2)
C3	C4	1.508(2)
C1	C2	1.506(3)

Table 2.27 Bond Angles in ° for 1-Gd.

Atom	Atom	Atom	Angle/°
I1	Gd1	I1	178.022(5)
I2	Gd1	I1	89.011(2)
I2	Gd1	I1	89.011(2)
O1	Gd1	I1	90.989(2)
O1	Gd1	I1	90.989(2)
O1	Gd1	I2	180.0
O2^1	Gd1	I1	89.35(3)
O2	Gd1	I1	89.35(3)
O2	Gd1	I1	90.79(3)
O2^1	Gd1	I1	90.79(3)
O2^1	Gd1	I2	94.33(3)
O2	Gd1	I2	94.33(3)
O2^1	Gd1	O1	85.67(3)
O2	Gd1	O1	85.67(3)
O2	Gd1	O2	171.34(6)
C1	O1	Gd1	124.58(8)

Atom	Atom	Atom	Angle/°
C1[1]	O1	Gd1	124.58(8)
C1	O1	C1	110.83(16)
C5	O2	Gd1	121.43(9)
C3	O2	Gd1	123.60(9)
C3	O2	C5	114.95(11)
O2	C5	C6	112.45(13)
O2	C3	C4	113.05(13)
O1	C1	C2	111.09(14)

Table 2.28 Hydrogen Fractional Atomic Coordinates (×10^4) and Equivalent Isotropic Displacement Parameters (Å^2×10^3) for 1-Gd. U_{eq} is defined as 1/3 of the trace of the orthogonalised U_{ij}.

Atom	x	y	z	U_{eq}
H5A	2639.92	4557.35	4395.97	19
H5B	4208.49	4685.71	4262.39	19
H3A	2376.69	2477.76	4093.27	19
H3B	2398.27	2480.59	3081.48	19
H4A	969.21	3878.9	3124.18	35
H4B	834.05	3713.76	4122.55	35
H4C	285.75	2914.27	3478.21	35
H6A	4585.72	3292.07	5092.11	37
H6B	3016.57	3190.9	5240.14	37
H6C	3802.46	4099.84	5619.88	37
H1A	3359.13	1672.4	1793.41	22
H1B	3961.49	717.69	2222.71	22
H2A	4425.37	641.82	791.06	39
H2B	5807.11	823.64	1268.57	39
H2C	5067.89	1701.57	804.55	39

Coordination polyhedron

l(Gd1-O2) = 2.3519(12) Å

l(Gd1-I1) = 3.0147(4) Å

l(Gd1-O1) = 2.4479(16) Å

l(Gd1-I2) = 2.9859(6) Å

l(Gd1-I1) = 3.0147(4) Å

l(Gd1-O2) = 2.3519(12) Å

The ether molecules bind highly asymmetrically. There is a correlation between the asymmetric binding of the ether molecules and the binding of the iodine atoms. The distortion index is 0.11528 and the bond angle variance is 7.3°

.----------

Average bond length = 2.6945 Å

Polyhedral volume = 25.6050 $Å^3$

Distortion index (bond length) = 0.11528

Quadratic elongation = 1.0260

Bond angle variance = 7.3546 deg^2

Effective coordination number = 3.3106

2.5.6 *1-Tb*

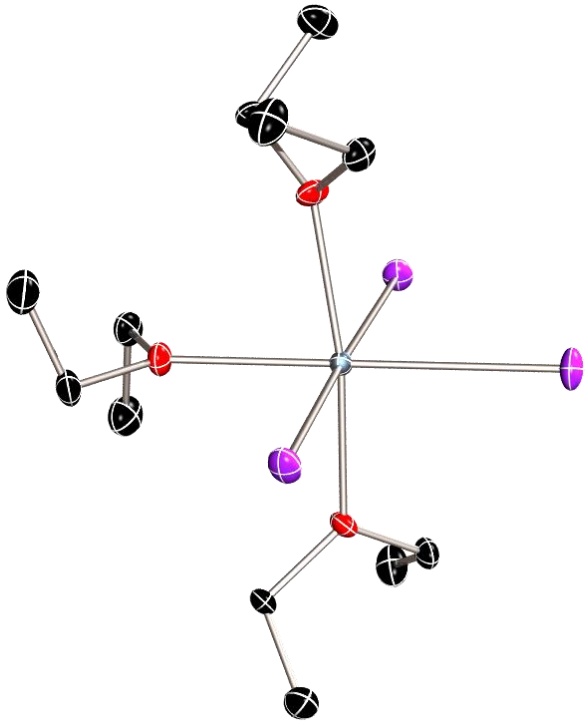

Figure 2.17 Molecular structure of 1-Tb with thermal ellipsoids shown at 50% probability and H atoms are omitted for clarity.

Table 2.29 Fractional Atomic Coordinates ($\times 10^4$) and Equivalent Isotropic Displacement Parameters ($Å^2 \times 10^3$) for 1-Tb. U_{eq} is defined as 1/3 of the trace of the orthogonalised U_{ij}.

Atom	x	y	z	U_{eq}
Tb1	5000	3695.9(2)	2500	10.79(6)
I1	7191.6(2)	3737.3(2)	3793.1(2)	18.17(6)
I2	5000	5851.4(2)	2500	18.78(7)
O1	5000	1933(2)	2500	16.7(5)
O2	3441.5(19)	3574.2(13)	3590.4(12)	15.6(4)
C5	3506(3)	4204.5(18)	4338.2(16)	16.7(5)
C3	2332(3)	2892.2(19)	3578.4(18)	17.5(5)
C4	996(3)	3393(2)	3575(2)	24.6(6)
C6	3743(4)	3647(2)	5140.5(18)	26.0(6)
C1	4193(3)	1329.4(18)	1931.4(19)	20.3(5)
C2	4938(3)	1105(2)	1127(2)	27.8(7)

Table 2.30 Anisotropic Displacement Parameters (×10^4) 1-Tb. The anisotropic displacement factor exponent takes the form: $-2\pi^2[h^2a^{*2} \times U_{11} + ... + 2hka^* \times b^* \times U_{12}]$

Atom	U_{11}	U_{22}	U_{33}	U_{23}	U_{13}	U_{12}
Tb1	9.59(9)	8.92(9)	13.87(9)	0	-0.10(5)	0
I1	14.14(10)	17.81(10)	22.55(10)	0.22(6)	-5.84(6)	1.40(6)
I2	28.64(15)	9.16(11)	18.53(12)	0	-4.44(9)	0
O1	19.2(14)	10.4(12)	20.5(13)	0	-1.4(10)	0
O2	12.9(9)	15.8(9)	18.2(8)	-1.9(7)	2.8(7)	-5.2(6)
C5	19.3(13)	14.1(11)	16.7(11)	-3.7(9)	0.5(9)	-4.5(9)
C3	12.9(12)	14.7(12)	25.0(13)	-4.0(10)	4.1(9)	-5.1(9)
C4	16.0(14)	25.0(14)	32.9(15)	-7.8(12)	-0.9(11)	-1.7(11)
C6	38.2(18)	22.5(14)	17.4(12)	-0.3(10)	1.0(12)	-3.9(11)
C1	20.4(14)	12.3(12)	28.1(14)	-3.5(10)	-2.1(10)	-3.1(9)
C2	35.4(19)	19.9(14)	28.2(16)	-4.9(12)	2.0(11)	-2.4(11)

Table 2.31 Bond Lengths in Å for 1-Tb.

Atom	Atom	Length/Å
Tb1	I1	3.0003(2)
Tb1	I1	3.0003(2)
Tb1	I2	2.9706(3)
Tb1	O1	2.430(3)
Tb1	O2	2.3313(19)
Tb1	O2	2.3313(19)
O1	C1	1.467(3)
O1	C1	1.467(3)
O2	C5	1.467(3)
O2	C3	1.457(3)
C5	C6	1.501(4)
C3	C4	1.507(4)
C1	C2	1.506(4)

Table 2.32 Bond Angles in ° for 1-Tb.

Atom	Atom	Atom	Angle/°
I1	Tb1	I1	177.822(8)
I2	Tb1	I1	88.911(4)
I2	Tb1	I1	88.911(4)
O1	Tb1	I1	91.089(4)
O1	Tb1	I1	91.089(4)
O1	Tb1	I2	180.0
O2	Tb1	I1	90.75(5)
O2	Tb1	I1	90.75(5)
O2	Tb1	I1	89.41(5)
O2	Tb1	I1	89.41(5)
O2	Tb1	I2	94.13(4)
O2	Tb1	I2	94.13(4)
O2	Tb1	O1	85.87(4)

Atom	Atom	Atom	Angle/°
O2	Tb1	O2	171.75(9)
C1	O1	Tb1	124.52(14)
C1	O1	Tb1	124.52(14)
C1	O1	C1	111.0(3)
C5	O2	Tb1	121.47(14)
C3	O2	Tb1	123.29(15)
C3	O2	C5	115.23(19)
O2	C5	C6	112.5(2)
O2	C3	C4	112.6(2)
O1	C1	C2	111.1(2)
O2	Tb1	O2	171.75(9)

Table 2.33 Hydrogen Fractional Atomic Coordinates (×10^4) and Equivalent Isotropic Displacement Parameters (Å^2×10^3) for 1-Tb. U_{eq} is defined as 1/3 of the trace of the orthogonalised U_{ij}.

Atom	x	y	z	U_{eq}
H5A	2659.02	4568.66	4388.82	20
H5B	4234.57	4681.48	4261.34	20
H3A	2389.95	2466.43	4082	21
H3B	2404.58	2477.2	3068.76	21
H4A	971.38	3871.65	3116.08	37
H4B	857.63	3720.75	4118.34	37
H4C	289.32	2911.78	3487.17	37
H6A	4581.15	3285.15	5094.47	39
H6B	3005.22	3192.26	5232.56	39
H6C	3796.31	4098.67	5618.49	39
H1A	3354.83	1673.64	1792.45	24
H1B	3958.1	715.81	2221.19	24
H2A	4423.6	641.38	787.98	42
H2B	5808.35	823.31	1266.16	42
H2C	5067.27	1703.83	802.41	42

2.5.7 *3-Tb*

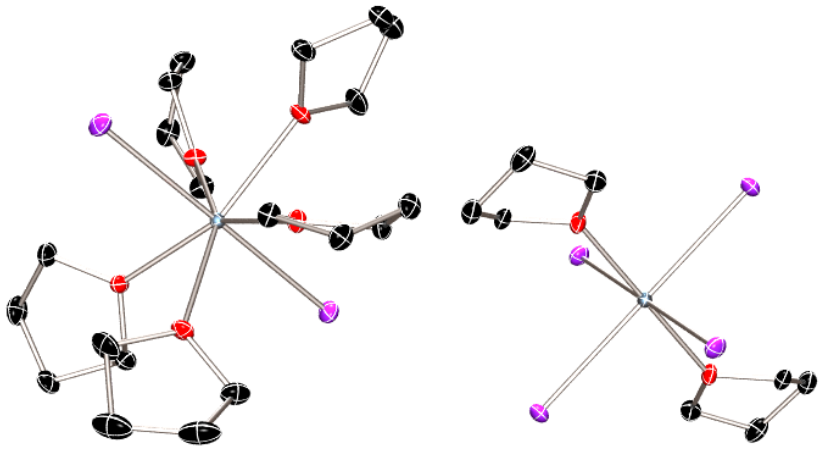

Figure 2.18 Molecular structure of 3-Tb with thermal ellipsoids shown at 50% probability and H atoms are omitted for clarity.

Table 2.34 Fractional Atomic Coordinates ($\times 10^4$) and Equivalent Isotropic Displacement Parameters ($Å^2 \times 10^3$) for 3-Tb. U_{eq} is defined as 1/3 of the trace of the orthogonalised U_{ij}.

Atom	x	y	z	U_{eq}
Tb2	5000	4993.3(2)	2500	8.73(4)
Tb1	0	5000	5000	10.92(4)
I2	875.4(2)	5978.3(2)	5952.6(2)	17.23(5)
I1	297.2(2)	2669.7(2)	5379.6(2)	17.76(5)
I3	2888.1(2)	4978.6(2)	2831.8(2)	17.20(5)
O3	5000	6985(3)	2500	13.7(6)
O2	4520.4(19)	3391.2(19)	2021.7(8)	13.9(4)
O1	1728(2)	5042(2)	4833.2(9)	16.2(5)
O4	5831(2)	5622(2)	3265.4(8)	15.4(5)
C5	5227(3)	2517(3)	1889.3(13)	18.2(7)
C12	6792(3)	6311(3)	3349.5(13)	20.3(7)
C8	3422(3)	3135(3)	1814.1(12)	16.2(6)
C13	4462(3)	7690(3)	2810.7(12)	15.6(6)
C2	2760(3)	4699(3)	4236.7(13)	20.1(7)
C3	3318(3)	5625(3)	4545.4(15)	23.7(8)
C14	4899(3)	8845(3)	2757.2(12)	17.6(7)
C1	2154(3)	4132(3)	4579.6(13)	17.5(7)
C9	5449(4)	5423(4)	3720.1(12)	24.6(8)
C4	2482(3)	5984(3)	4850.9(13)	18.2(7)
C7	3521(3)	2249(3)	1448.5(13)	19.8(7)
C11	6745(4)	6865(4)	3815.1(15)	31.4(9)
C6	4491(3)	1609(3)	1672.8(14)	22.0(8)

Atom	x	y	z	U_{eq}
C10	6268(4)	5964(4)	4089.3(15)	33.6(9)

Table 2.35 Anisotropic Displacement Parameters (×10⁴) 3-Tb. The anisotropic displacement factor exponent takes the form: $-2\pi^2[h^2a^{*2} \times U_{11} + ... + 2hka^* \times b^* \times U_{12}]$.

Atom	U_{11}	U_{22}	U_{33}	U_{23}	U_{13}	U_{12}
Tb2	9.31(9)	8.97(8)	7.95(9)	0	1.33(7)	0
Tb1	9.98(9)	12.19(9)	10.52(9)	-1.43(7)	1.24(7)	1.28(7)
I2	18.03(11)	20.86(10)	12.01(9)	-3.84(8)	-0.49(8)	-0.32(8)
I1	17.61(11)	15.23(9)	20.08(11)	2.27(8)	1.60(8)	4.50(8)
I3	12.94(10)	21.22(10)	18.45(11)	-2.34(8)	5.66(8)	-0.95(8)
O3	16.2(17)	10.2(14)	15.6(16)	0	4.6(13)	0
O2	12.8(11)	12.2(10)	15.9(11)	-3.0(9)	-0.3(9)	1.4(8)
O1	13.2(11)	15.7(11)	20.9(12)	-5.3(9)	6.8(10)	-0.5(9)
O4	18.8(12)	16.6(11)	9.7(10)	-2.7(8)	-1.1(9)	-1.2(9)
C5	19.3(17)	15.2(15)	20.5(17)	-3.8(13)	4.2(14)	2.4(12)
C12	20.5(16)	16.9(15)	21.8(15)	-5.4(12)	-2.8(12)	-0.4(12)
C8	15.2(16)	15.2(15)	17.6(16)	-3.5(12)	0.1(13)	-1.2(12)
C13	17.3(16)	13.5(14)	16.8(16)	-2.3(12)	4.6(13)	-0.3(12)
C2	23.7(19)	20.9(16)	16.5(16)	2.8(13)	6.1(14)	7.4(14)
C3	17.4(18)	22.8(17)	33(2)	3.7(16)	10.3(16)	2.1(14)
C14	19.5(17)	11.9(14)	21.8(17)	-2.9(12)	4.1(14)	-2.0(12)
C1	15.2(16)	17.7(15)	20.4(16)	-2.4(13)	4.9(13)	4.3(13)
C9	31.5(19)	32.1(19)	10.5(14)	-2.5(13)	3.9(13)	2.9(15)
C4	15.7(16)	16.2(15)	23.0(17)	-2.2(13)	4.1(14)	-4.1(13)
C7	20.8(18)	17.9(16)	19.9(17)	-8.3(13)	0.7(14)	-6.0(14)
C11	23.2(19)	39(2)	28.6(18)	-18.0(15)	-6.2(15)	5.1(15)
C6	27(2)	12.3(15)	27.9(19)	-5.2(14)	9.9(16)	-1.5(14)
C10	29(2)	51(2)	19.6(16)	-11.4(15)	-2.7(14)	10.0(17)

Table 2.36 Bond Lengths in Å for 3-Tb.

Atom	Atom	Length/Å
Tb2	I3	2.9824(6)
Tb2	I3	2.9824(6)
Tb2	O3	2.393(3)
Tb2	$O2^1$	2.389(2)
Tb2	O2	2.389(2)
Tb2	$O4^1$	2.411(2)
Tb2	O4	2.411(2)
Tb1	I2	3.0284(5)
Tb1	I2	3.0285(5)
Tb1	I1	3.0074(6)
Tb1	I1	3.0073(6)
Tb1	O1	2.321(2)
Tb1	O1	2.321(2)
O3	C13	1.469(4)
O3	C13	1.469(4)
O2	C5	1.469(4)

Atom	Atom	Length/Å
O2	C8	1.470(4)
O1	C1	1.460(4)
O1	C4	1.480(4)
O4	C12	1.468(4)
O4	C9	1.475(4)
C5	C6	1.511(5)
C12	C11	1.499(5)
C8	C7	1.511(5)
C13	C14	1.512(5)
C2	C3	1.530(6)
C2	C1	1.499(5)
C3	C4	1.536(5)
C14	C14	1.532(7)
C9	C10	1.519(6)
C7	C6	1.516(6)
C11	C10	1.516(7)

Table 2.37 Bond Angles in ° for 3-Tb.

Atom	Atom	Atom	Angle/°
I3	Tb2	I3	179.322(12)
O3	Tb2	I3	90.340(6)
O3	Tb2	I3	90.339(6)
O3	Tb2	O4	71.75(6)
O3	Tb2	O4	71.75(6)
O2	Tb2	I3	88.83(6)
O2	Tb2	I3	90.63(6)
O2	Tb2	I3	90.63(6)
O2	Tb2	I3	88.83(6)
O2	Tb2	O3	143.68(6)
O2	Tb2	O3	143.68(6)
O2	Tb2	O2	72.64(11)
O2	Tb2	O4	71.95(8)
O2	Tb2	O4	144.54(8)
O2	Tb2	O4	144.54(8)
O2	Tb2	O4	71.95(8)
O4	Tb2	I3	90.50(6)
O4	Tb2	I3	89.71(6)
O4	Tb2	I3	90.50(6)
O4	Tb2	I3	89.71(6)
O4	Tb2	O4	143.50(12)
I2	Tb1	I2	180.0
I1	Tb1	I2	88.523(13)
I1	Tb1	I2	91.476(13)
I1	Tb1	I2	91.478(13)
I1	Tb1	I2	88.522(13)
I1	Tb1	I1	180.0
O1	Tb1	I2	93.34(6)
O1	Tb1	I2	86.66(6)
O1	Tb1	I2	93.34(6)
O1	Tb1	I2	86.66(6)
O1	Tb1	I1	88.76(6)
O1	Tb1	I1	91.24(6)

Atom	Atom	Atom	Angle/°
O1	Tb1	I1	88.75(6)
O1	Tb1	I1	91.25(6)
O1	Tb1	O1	180.00(11)
C13	O3	Tb2	125.21(17)
C13	O3	Tb2	125.21(17)
C13	O3	C13	109.6(3)
C5	O2	Tb2	127.5(2)
C5	O2	C8	109.2(2)
C8	O2	Tb2	123.28(18)
C1	O1	Tb1	121.3(2)
C1	O1	C4	107.6(3)
C4	O1	Tb1	129.8(2)
C12	O4	Tb2	124.7(2)
C12	O4	C9	108.8(3)
C9	O4	Tb2	126.4(2)
O2	C5	C6	104.8(3)
O4	C12	C11	104.8(3)
O2	C8	C7	104.9(3)
O3	C13	C14	104.9(3)
C1	C2	C3	101.1(3)
C2	C3	C4	103.3(3)
C13	C14	C14[1]	102.3(2)
O1	C1	C2	104.5(3)
O4	C9	C10	105.2(3)
O1	C4	C3	105.5(3)
C8	C7	C6	102.1(3)
C12	C11	C10	102.4(3)
C5	C6	C7	103.0(3)
C11	C10	C9	103.4(3)

Table 2.38 Hydrogen Fractional Atomic Coordinates (×10^4) and Equivalent Isotropic Displacement Parameters (Å^2×10^3) for 3-Tb. U_{eq} is defined as 1/3 of the trace of the orthogonalised U_{ij}.

Atom	x	y	z	U_{eq}
H5A	5699	2238	2170	22
H5B	5668	2802	1658	22
H12A	6794	6870	3096	24
H12B	7437	5845	3364	24
H8A	3064	3805	1665	19
H8B	3013	2854	2058	19
H13A	4621	7435	3142	19
H13B	3684	7676	2712	19
H2A	2279	5005	3964	24
H2B	3276	4189	4122	24
H3A	3512	6251	4350	28
H3B	3966	5343	4743	28
H14A	5564	8966	2977	21
H14B	4377	9424	2812	21
H1A	1574	3670	4412	21
H1B	2627	3653	4799	21
H9A	5397	4615	3781	30
H9B	4742	5765	3721	30

Atom	x	y	z	U_{eq}
H4A	2816	6127	5180	22
H4B	2114	6668	4723	22
H7A	3634	2582	1143	24
H7B	2885	1767	1398	24
H11A	6288	7534	3777	38
H11B	7462	7077	3972	38
H6A	4312	1088	1917	26
H6B	4813	1186	1433	26
H10A	5931	6287	4349	40
H10B	6814	5420	4223	40

CHAPTER 3. SYNTHESIS OF HOMOLEPTIC, DIVALENT LANTHANIDE (SM, EU) COMPLEXES VIA OXIDATIVE TRANSMETALLATION

Part of this thesis chapter has been adapted with permission from an article co-written by the author:

Gompa, T. P., Jiang, N., J. Bacsa, J., La Pierre, H. S. Synthesis of Homoleptic, Divalent Lanthanide (Sm, Eu) Complexes via Oxidative Transmetallation. Dalton Trans., **2019**, *48*, 16869-16872.

3.1 Background

Synthetic methods for the preparation of lanthanide complexes supported by low-coordination number ligand spheres or high-symmetry planar ligands are crucial technologies for the development and application of molecular lanthanide complexes in quantum information sciences.[88, 149-158] Current approaches rely on salt metathesis reactions which can be complicated by solubility limitations and aggregation issues including the formation anionic, -ate, complexes supported by outer sphere alkali counter cations. Oxidative transmetallation can potentially avoid these issues. Historically, this method, in particular the reaction of Cu^{1+} reagents with bulk lanthanide metals, is a synthetic technique that has been explored to prepare lanthanide complexes with small supporting ligands such as cyclopentadienyl (Cp^{1-}), alkynolates ($R\text{-}C{\equiv}C^{1-}$), or amides ($[TMS)_2N]^{1-}$).[159-164] This methodology is related to Hg amalgation and $HgCl_2$ activation procedures for activated metal reactions and to the use alkyl mercurials and thallium in oxidative transmetallation.[161, 165-170] It should be noted that these approaches have been combined

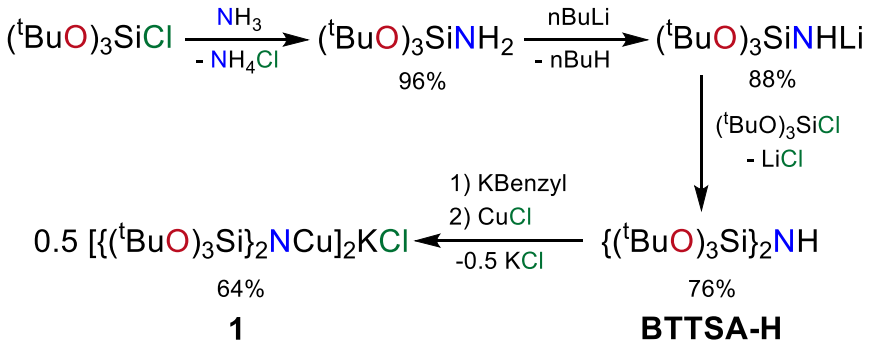

Scheme 3.1 Multi-step reaction scheme for the synthesis of the copper salt, 1.

with an internal base (e.g. $Hg(C_6F_5)_2$) to afford the alkali- metal free metalation of bulky, heterotopic calix[4]pyrrole and calix[4]arene ligands in redox transmetallation/protonolysis reactions.[171] A similar methodology and reagents were used to synthesize a number of lanthanide complexes, both di- and trivalent.[172] Further refinement of these techniques has led to applications in the synthesis of organometallic, pentavalent uranium complexes via oxidative transmetallation processes using Cu^{1+} or Au^{1+} reagents.[173-175]

Our group is broadly interested in the control of f-block metal oxidation state and valence electronic configuration via ligand design.[176, 177] In order to design a redox stable ligand, capable supporting lanthanides in a range of oxidation states, a ligand framework incorporating the oxidative stability of tris-(tert-butoxy)siloxides and the reductive stability and low-coordination number of bulky amides was designed to facilitate the stabilization of monomeric complexes across a range of redox states. This goal was achieved in the synthesis of bis(tris-tert-butoxysilyl)amine, **BTTSA-H**, a bulky monoanionic, polydentate amide ligand. These features help prevent dimerization and as shown herein, stabilize low-valent lanthanide complexes. The metalation of these bulky ligands is facilitated by oxidative transmetallation.

3.2 Results and Discussion

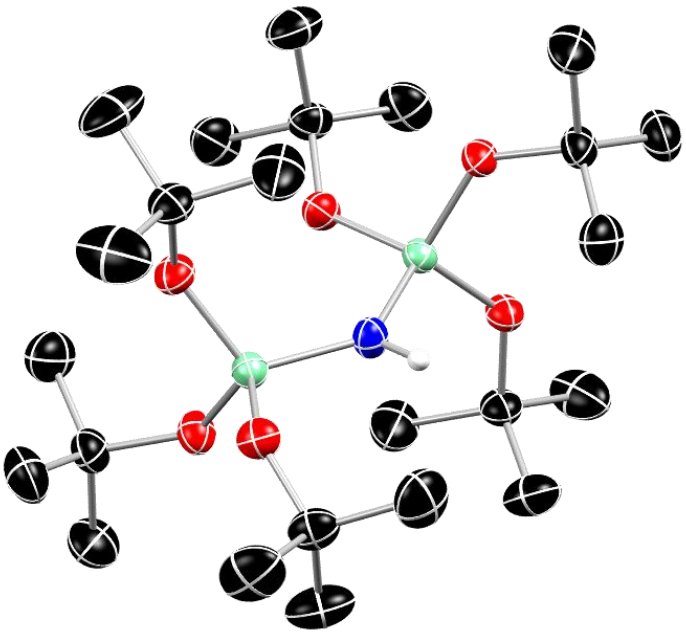

Figure 3.1 Molecular structure of BTTSA-H. Thermal ellipsoids are shown at 50% probability and H atoms (except for N–H) are omitted for clarity.

3.2.1 *Synthesis of the bis(tri-tert-butoxysilyl)amide complexes, 2-Eu and 2-Sm*

Synthesis of the bis(tri-tert-butoxysilyl)amine, **BTTSA-H**, is shown in Scheme 3.1. Single crystal XRD confirms the connectivity (Figure 3.1). In contrast to bulky bis(tris-alkyl)silylamides, the Si–N–Si angle is significantly more open at 134.90(7)°, in comparision to 126.3(1)° for the lithium salt of bis(tert-butyldimethylsilyl)amine.[178] While the size of the silyl substituents changes significantly between the two amines, a key distinction is the incorporation of alkoxide rather than alkyl silyl substituents. The pro-ligand is converted to the active copper(I) species in two steps including deprotonation with potassium benzyl and transmetallation with copper(I) chloride. This copper salt, **1**, is stirred in THF with a glass stir bar over freshly ground lanthanide (Eu or Sm) metal shavings in a 2:1 stoichiometric ratio for 60 h to yield the divalent lanthanide complexes **2-Eu** and **2-Sm** in 83% and 68% yield, respectively (Scheme 3.2).

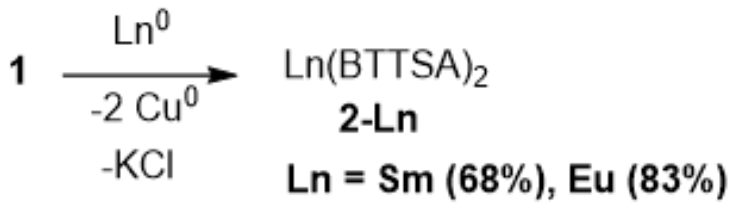

Scheme 3.2 Reaction scheme for the oxidation of zero-valent lanthanide metal with 1.

3.2.2 *Crystallographic analysis*

The molecular structure of **2-Eu** (isotypic to **2-Sm**) is shown in Figure 3.2 and crystalizes in the *P21/n* space group (Table 3.1 includes relevant bonding metrics for both complexes). Two tert-butoxy arms from each ligand coordinate the metal ion, leading to an overall 6-coordinate ion. Further inspection of the bond metrics reveals uniquely long M–N distances, which on average are 2.712(5) Å and 2.7181(17) Å for **2-Sm** and **2-Eu**, respectively. These are particularly long when compared to the M–N bond lengths in related divalent Sm and Eu amides, which range from 2.483(5) to 2.500(2) Å.[151, 179] The

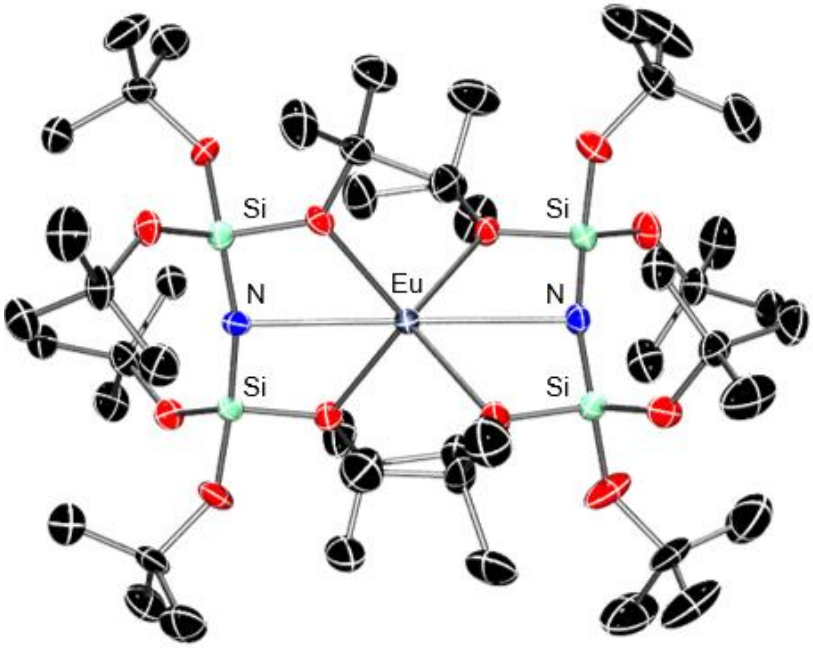

Figure 3.2 Molecular structure of 2-Eu with thermal ellipsoids shown at 50% probability with hydrogen atoms omitted for clarity.

M–O bonds in 2-Sm and 2-Eu are shorter than in related anionic tris-(tert-butoxy)siloxide complexes of divalent Eu and Sm. In the complexes reported here, the bond distance to coordinated tert-butoxy oxygen ranges from 2.6381(19) to 2.6659(18) Å.[180] As expected, there is variation in the Si–O bond lengths within the structures of 2-Sm and 2-Eu, with the Si–O bond lengths for coordinated O atoms longer on average than the Si–O bond of non-coordinated O atoms. The average Si–O bond length for coordinated O atoms is 1.692(5) Å in both **2-Sm** and **2-Eu** compared to 1.634(5) Å for the non-coordinated O atoms.

These divalent complexes present a near linear geometry along the N–M–N axis. The N-M-N bond angle is 179.21(14)° and 179.20(6)° for 2-Sm and 2-Eu, respectively. Additionally, the Si–N–Si bond angle in both complexes is more linear when compared to the structure for the proligand, **BTTSA-H**. When compared to analogous bis(tris-alkyl)silylamide complexes, this metric is significantly more linear. For example, bis(tert-butyl-dimethylsilyl)amine which has a Si–N–Si bond angle of 126.3(1)° in the lithium salt and 133.68° in the lanthanum complex,31 while the Si–N–Si bond angle is 134.90(7)° in the pro-ligand, **BTTSA-H**, and 169.6(1)° and 168.4(3)° in the **2-Eu** and **2-Sm**, respectively. Similarly, in divalent Sm complexes supported by bis(tris-isopropyl)silylamides in $Sm[N(Si^iPr_3)_2]_2$, the Si–N–Si bond angles average 138.7(4).[151]

Since N–M–N angles are nearly linear, the M–N are notable long, and the M–O bond lengths are short, a $\tau 4$ index for the "equatorial" O donors can quantify the extent of distortion.[181] For a perfect octahedron, this index would be 0.0 (i.e. square planar for the 4 oxygen donors). For both **2-Sm** and **2-Eu**, the index is calculated to be 0.89 – indicating strong distortion in the equatorial region of the coordination octahedron to a pseudo-tetrahedral geometry for the oxygen donors. This analysis is supported by the non-orthogonal relationship between the planes defined by the ONO donor atoms of each ligand which affords an angle between the planes of 89.3(3)° and 88.8(2)° for 2-Sm and 2-Eu, respectively.

Table 3.1 Selected bond lengths (Å) and angles (°) for 2-Sm and 2-Eu.

	2-Sm	2-Eu
M–N (Å)	2.712(5)	2.7181(17)
M–O_{Coord} (Å)	2.540(5)	2.526(4)
Si–O_{Coord} (Å)	1.692(5)	1.692(5)
N–M–N (°)	179.21(14)	179.20(6)
Si–N–Si (°)	168.4(3)	169.6(1)

3.2.3 *SQUID measurements*

The dc magnetic susceptibility data for **2-Sm** and **2-Eu** are shown in Figure 3.3. The complex, **2-Sm**, has a $^7F_0$ ground state and a calculated room temperature moment of 0 μ_B based on Landé equations. However, a substantial moment is observed due to temperature-dependent population of low-lying excited j-states. This phenomenon also contributes to the general curve shape observed since as temperature increases, the gradual

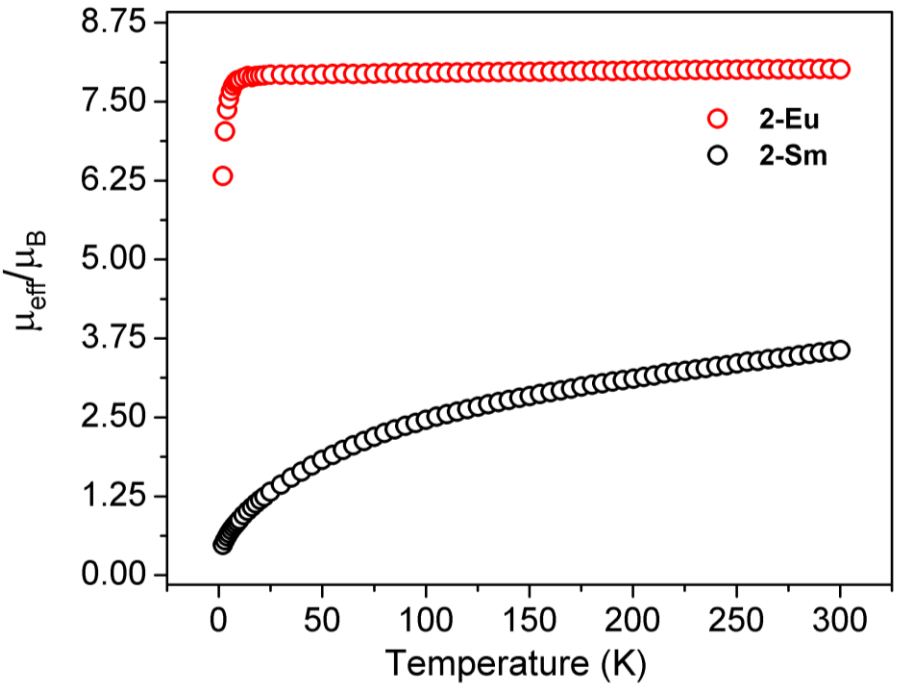

Figure 3.3 Temperature dependence of magnetic moment (μ_{eff}) for 2-Sm and 2-Eu collected under dc field of 1 T.

population of low-lying magnetic excited states increases. At room temperature, the moment for **2-Sm** is 3.45 μ_B, and is consistent with the experimentally observed moments for other divalent samarium and isoelectronic Eu^{3+} compounds.[65] The complex, **2-Eu**, isoelectronic to Gd^{3+} complexes, has an isotropic $^8S_{7/2}$ ground state and exhibits a room temperature moment of 8.01 μ_B, which is in good agreement with the expected moment for the ion of 7.94 μ_B. In contrast to **2-Sm**, the moment remains constant from 300 K to 14 K, at which point the moment drops rapidly as it approaches 2K. This behavior can be rationalized since the f^7 ion contains no low-lying excited j-states and the moment is purely produced through the population of the singular $^8S_{7/2}$ ground state.

3.2.4 *UV/vis spectroscopy*

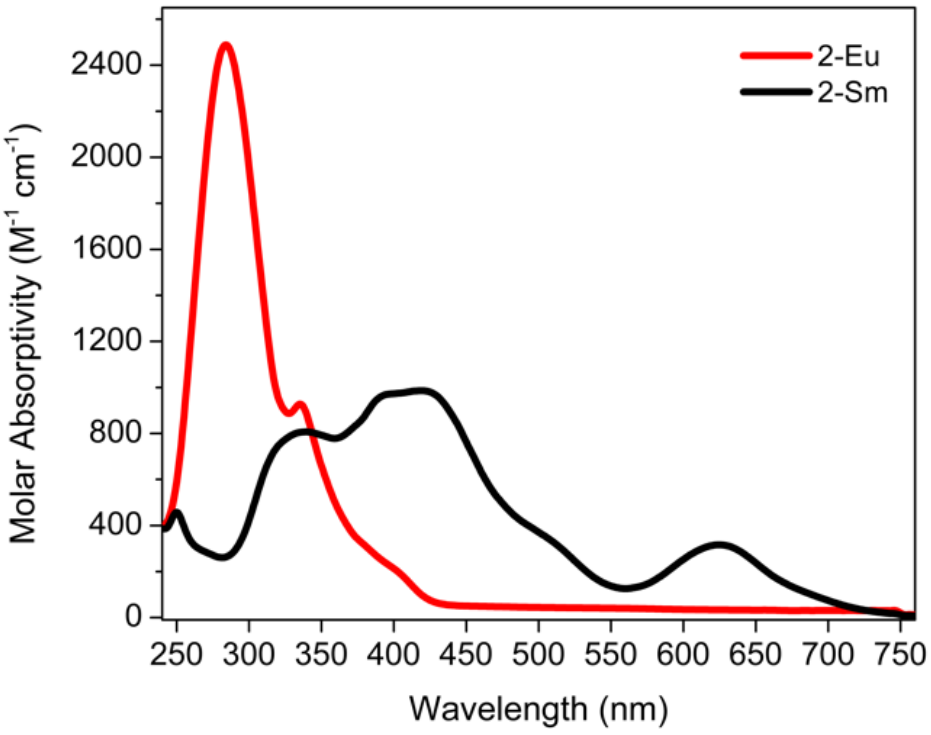

Figure 3.4 UV/vis spectra of 2-Sm and 2-Eu in diethyl ether

Due to the stabilization of the 5*d* orbitals in the divalent lanthanides in comparison to their trivalent counterparts, spin-allowed f-d transitions give "traditional" divalent

complexes (i.e. those with $4f^{n+1}$ ground state configurations) strong colors.[65] Divalent europium complexes are excluded, as these strong absorbances are typically centered in the UV and trail into the visible giving them a pale color. The complexes **2-Sm** and **2-Eu** follow this trend: their solutions are deep forest green and pale lime green, respectively. Their UV/vis spectra in diethyl ether are shown in Figure 3.4. The spectrum of **2-Sm** contains four noteworthy absorbance bands, ranging from a molar absorptivity of 350 to 1000 M^{-1} cm^{-1}, centered at 625 nm, 420 nm, 338 nm, and 249 nm. The broad low energy peak at 625 is likely attributable to a $^7F_0$ to $^5D_0$ transition. The most intense feature for **2-Sm** is an imperfect Gaussian and appears to contain two contributing transitions, most likely $^7F_0$ to $^5D_1$ and $^7F_0$ to $^5D_2$ due to their proximity in energy. The higher energy transitions are more difficult to assign as they lie in a crowded manifold for metal-based transitions for a divalent samarium compound.[182] The spectrum for **2-Eu** contains two prominent absorbance bands, ranging from a molar absorptivity of 950 to 2500 M^{-1} cm^{-1} and centered at 335 and 284 nm, respectively. The feature at 335 is assignable as an $^8S_{7/2}$ to ^6P transition and the feature at 284 is an $^8S_{7/2}$ to ^6I transition. Despite the forbidden nature of these transitions, their molar absorptivity is substantially higher than what is observed for allowed transitions for **2-Sm**. This phenomenon has been noted previously for amide supported divalent europium complexes and has been suggested to be attributable to vibronic coupling in near linear coordination environments.[179] Such an analysis would suggest a strong topological homology between **2-Sm** and **2-Eu** and the $Ln[N(Si^iPr_3)_2]$ complexes.

3.3 Conclusion

The synthesis and characterization of divalent complexes of Eu and Sm supported the bulky, polydentate ligand bis(tris-tert-butoxysilyl)amide are reported. This synthetic approach is dependent on the use of a copper(I) species as an oxidative transmetallation reagent to prepare the neutral, divalent complexes directly from bulk metal as conventional

metathesis reactions with lanthanide halides and alkali metals salts of BTTSA proved unsuccessful. Absorbance studies and variable-temperature dc magnetic susceptibility measurements confirm the divalent nature of the compounds and suggest that the observed distorted coordination polyhedra enforced by the linear Si–N–Si ligand backbone support a homologous structure to the formally two-coordinate Ln[N(Si^{i}Pr$_3$)$_2$] complexes.[151, 179]

3.4 Experimental

3.4.1 *General Considerations*

Unless otherwise noted, all reagents were obtained from commercial suppliers. The syntheses and manipulations were conducted under argon with exclusion of oxygen and water using Schlenk techniques or in an inert atmosphere box (Vigor) under a dinitrogen (8 h) at a temperature of ca. 160˚C. Celite and molecular sieves were dried under vacuum at a temperature >250˚C for a minimum of 24 h. C_6D_6 was stored over 3 Å molecular sieves and then vacuum-transferred from purple sodium/benzophenone prior to use. Pyridine-d_5 was degassed by three freeze-pump-thaw cycles stored over 3 Å molecular sieves for at least 24 h prior to use. Hexanes, diethyl ether and tetrahydrofuran were purged with UHPgrade argon (Airgas) and passed through columns containing Q-5 and molecular sieves in a solvent purification system (JC Meyer Solvent Systems). All solvents in the glovebox were stored in bottles over 3 Å molecular sieves. NMR spectra were obtained on a Bruker Advance III 400 MHz spectrometer at 298 K, unless otherwise noted. ^{1}H NMR chemical shifts are reported in δ, parts per million. ^{1}H NMR are references to the residual ^{1}H resonances of the deuterated solvent. Peak position is listed, followed by peak multiplicity, integration value, and proton assignment, where applicable. Multiplicity and shape are indicated by one or more of the following abbreviations: s (singlet); d (doublet);

t (triplet); q (quartet); dd (doublet of doublets); td (triplet of doublets); m (multiplet); br (broad). Infrared (IR) samples were taken on a Bruker ALPHA FTIR spectrometer from 400 to 4000 cm^{-1}. IR samples were prepared as Nujol mulls sandwiched between two KBr plates. The peaks are listed in wavenumber [cm^{-1}] and intensity by using the following abbreviations: vw (very weak); w (weak); m (medium); s (strong); vs (very strong); br (broad). UV/vis/NIR spectroscopy was performed in Teflon-valve sealed quartz cuvettes with a 1 cm path length on a Hitachi UH4150 UV–vis–NIR scanning spectrophotometer between 2500 and 240 nm. Elemental analyses were determined at Robertson Microlit Laboratories (Ledgewood, NJ). Magnetic measurements were performed on a Quantum Design MPMS-5S magnetometer. Inside of a glovebox, a measured amount of quartz wool (10–20 mg) was loaded and packed tightly into a quartz tube. Powdered samples were loaded inside of the tube and onto the glass wool plug by tapping the compound through a glass pipet. Another pre-massed amount of quartz wool (10–20 mg) was loaded on top of the sample, and the contents were packed tightly again. The top of the tube was affixed to an Ultra Torr Swagelok adaptor while the bottom was plugged with a piece of snug tubing tightly closed with a stopper and copper wire. This was transported from the glovebox to a Schlenk line where it was sealed above and below the sample using a O_2/H_2 torch while the sample was under vacuum. The vacuum sealed tubing was taped to a straw, and the straw was loaded into the instrument. Diamagnetic corrections for the quartz wool and the complex were performed using Pascal's constants.[183]

3.4.2 *Synthesis of (^{t}BuO)$_3$SiCl*

This procedure was adapted from a literature procedure.[184] $SiCl_4$ (23 mL, 34 g, 200 mmol, 1.0 equiv.) was added to 300 mL of hexanes in a 3-neck, 1L round-bottom flask via syringe. The solution was stirred vigorously and cooled to 0 °C with an ice-water bath. Solid potassium *tert*-butoxide (72.1 g, 640 mmol, 3.2 equiv.) was added in small portions to the solution over 1h. Once the addition is complete, the reaction mixture was allowed to warm to room temperature and is stirred for an additional 2 h and then refluxed overnight. The reaction mixture was filtered through Celite on a glass frit and the volatiles are removed *in vacuo*. The yellowish oil was distilled (3 torr, 55°C) yielding a clear, colorless liquid (49.65 g, 176 mmol, 88%). ^{1}H NMR (400 MHz, C_6D_6): δ 1.37 (s, 27 H, *tert*-butyl -CH_3). ^{13}C NMR (400 MHz, C_6D_6): δ 74.76 (s), 30.93 (s). IR (cm^{-1}): *v* 2980 (s), 2936 (m), 2917 (m), 2876 (w), 1472 (m), 1392 (m), 1368 (s), 1244 (s), 1186 (s), 1080 (s), 1031 (m), 915 (vw), 832 (m), 806 (m), 697 (m), 637 (m). Elem anal. Found (calculated) for $C_{12}H_{27}O_3SiCl$: C, 51.20 (50.95); H, 9.70 (9.62); N, <0.10 (0.00).

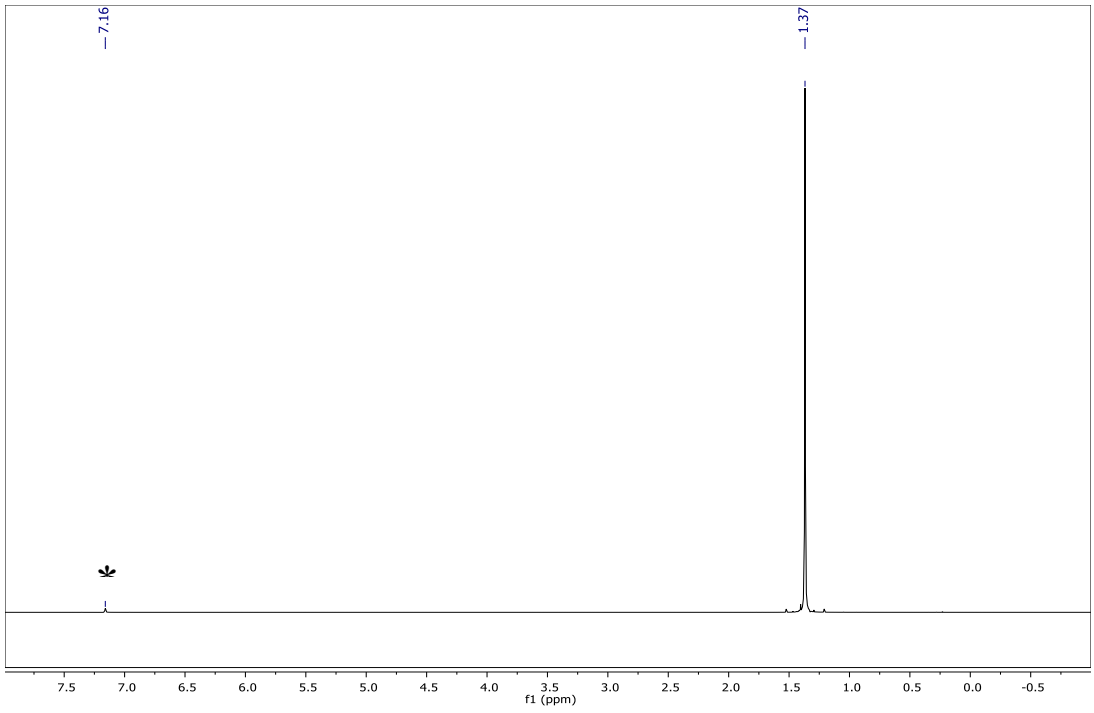

Figure 3.5 ^{1}H NMR for (^{t}BuO)$_3$SiCl in C_6D_6. C_6D_5H is noted as *.

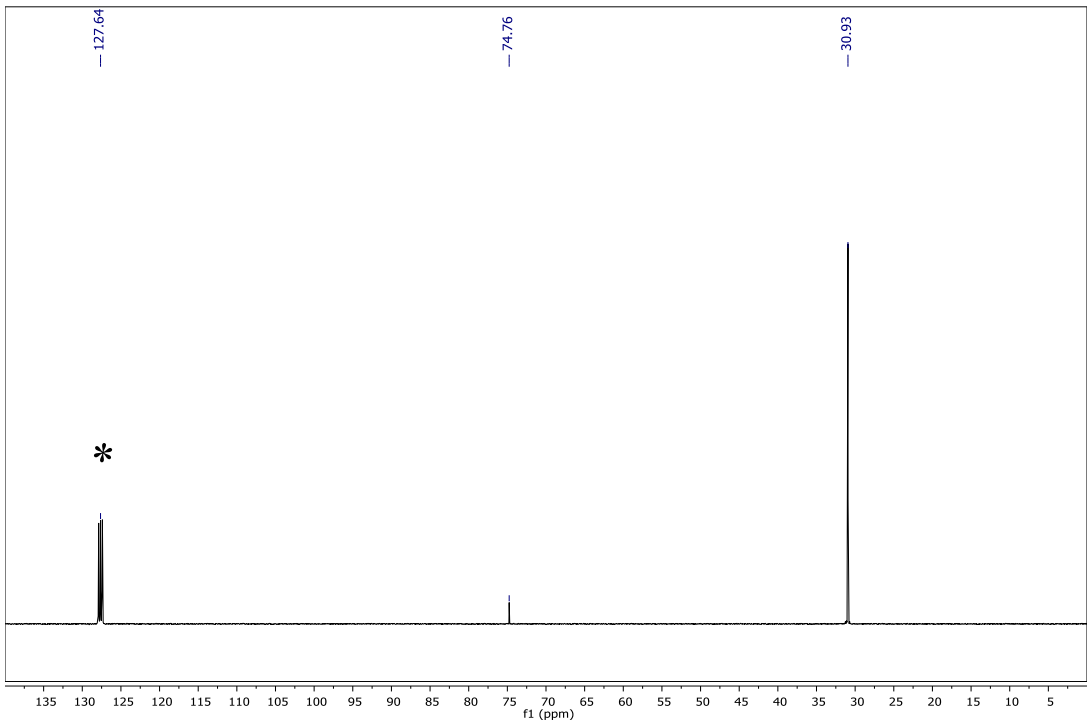

Figure 3.6 ^{13}C NMR for (^{t}BuO)$_3$SiCl in C_6D_6. C_6D_5H is noted as *.

3.4.3 *Synthesis of (^{t}BuO)$_3$SiNH$_2$*

In a 2-neck 5L round-bottom flask, (^{t}BuO)$_3$SiCl (29g, 102 mmol, 1.0 equiv.) was added to 500 mL of diethyl ether. The solution was stirred vigorously as anhydrous ammonia is bubbled through the solution for 20 minutes. A white precipitate was observed at this time. The flask is sealed under a slight positive pressure of ammonia and stirred overnight. The reaction mixture was subjected to these same conditions (20 minutes of bubbling anhydrous ammonia and overnight stirring) two more times in order to achieve a stoichiometric amount of ammonia. The mixture was filtered through Celite, and the volatiles are removed *in vacuo*. The yellowish oil was purified via distillation (3 torr, 69°C) yielding a colorless liquid (25.8g, 97.9 mmol, 96%). ^{1}H NMR (400 MHz, C_6D_6): δ 1.39 (s, 27 H, *tert*-butyl -CH_3), 0.52 (s, 2 H, -NH_2). ^{13}C NMR (400 MHz, C_6D_6): δ 71.80 (s), 31.34 (s). IR (cm^{-1}): *v* 3497 (w), 3420 (w), 2975 (s), 2934 (m), 2874 (m), 1549 (m), 1473 (m), 1389 (m), 1365 (m), 1244 (m), 1193 (m), 1065 (s), 1027 (m), 871 (m), 830 (m), 804 (w), 794 (w), 696 (m), 640 (s). Elem anal. Found (calculated) for $C_{12}H_{28}O_3SiNLi$: C, 52.50 (54.71); H, 10.77 (11.10); N, 5.06 (5.32).

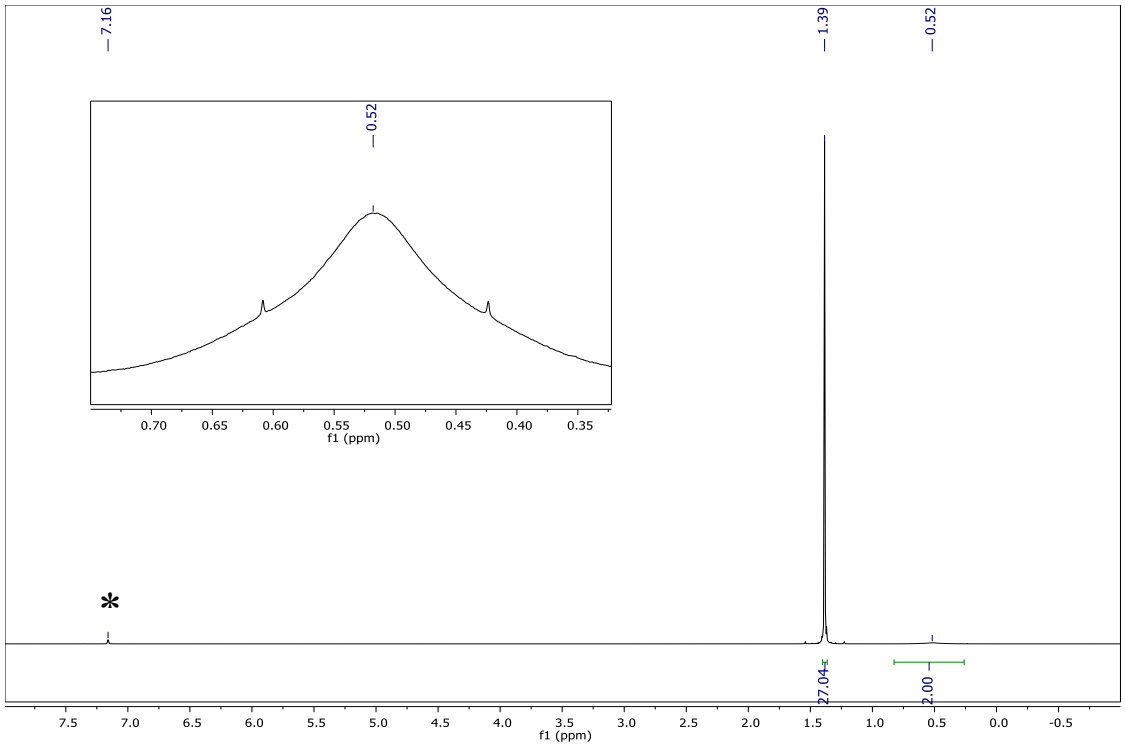

Figure 3.7 ^{1}H NMR for (^{t}BuO)$_3$SINH$_2$ in C_6D_6. Peak of C_6D_5H is noted as *.

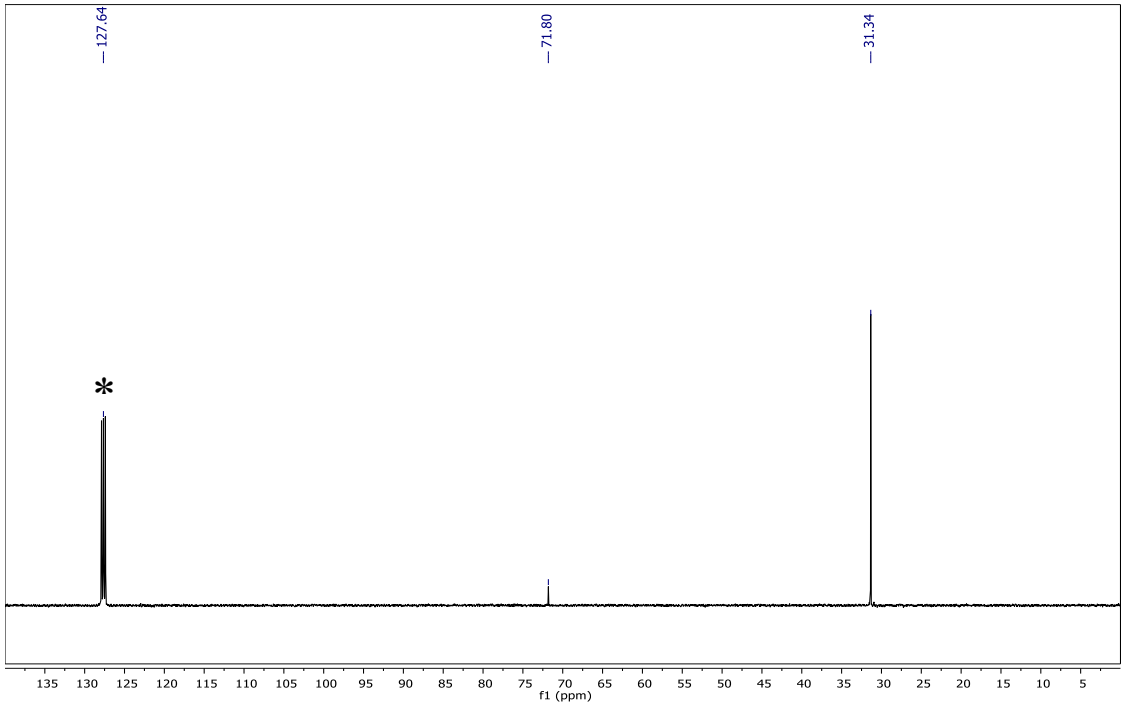

Figure 3.8 ^{13}C NMR for (^{t}BuO)$_3$SiNH$_2$ in C_6D_6. C_6D_5H is noted as *.

3.4.4 *Synthesis of (^{t}BuO)$_3$SiNHLi*

In a 1 L round-bottom Schlenk flask, (^{t}BuO)$_3$SiNH$_2$ (25.794g, 97.9 mmol, 1.0 equiv.) was dissolved to 200 mL of hexanes. The solution was cooled to 0°C using an ice-water bath. The solution is stirred vigorously and nBuLi (42.8 mL, 2.40 M, 103 mmol, 1.05 equiv.) was added dropwise via addition funnel over 25 minutes. After the addition was complete, the solution was allowed to warm to room temperature. The mixture was stirred for 16 h. All volatiles were removed *in vacuo* and the solid is redissolved in approximately 120 mL of n-pentane, and the solution is filtered through Celite. The solution was concentrated *in vacuo* and chilled to -80°C yielding the title compound as a white crystalline solid (23.253 g, 86.24 mmol, 88%) after decantation. ^{1}H NMR (400 MHz, C_6D_6): δ 1.56 (s, 27 H, *tert*-butyl -CH_3), -1.29 (s, 1 H, -NH). ^{13}C NMR (400 MHz, C_6D_6): δ 71.81 (s), 31.99 (s). IR (cm^{-1}): *v* 1361 (s), 1241 (s), 1213 (s), 1196 (s), 1055 (s), 1038 (s), 1018 (s), 992 (s), 956 (m), 941 (m), 931 (m), 817 (m), 694 (m), 624 (w). Elem. anal. Found (calculated) for $C_{12}H_{28}O_3SiNLi$: C, 52.05 (53.50); H, 10.48 (10.48); N, 4.99 (5.20). Carbon consistently low on multiple burns.

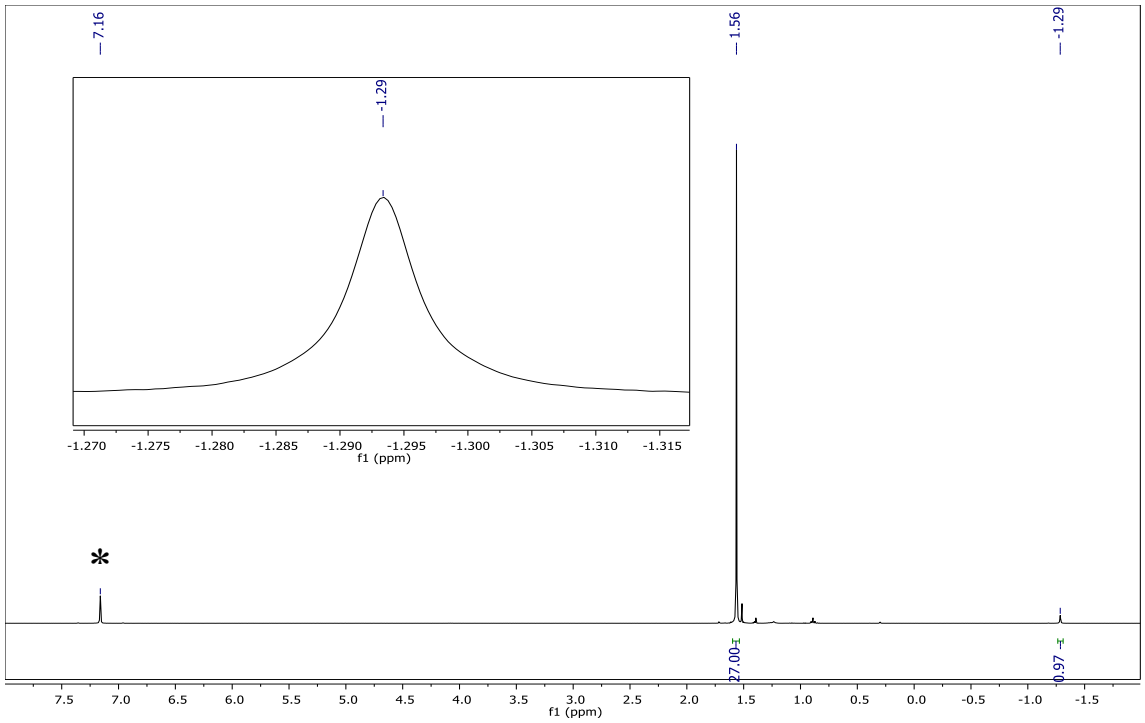

Figure 3.9 ^{1}H NMR for (^{t}BuO)$_3$SiNHLi in C_6D_6. Peak of C_6D_5H is noted as *.

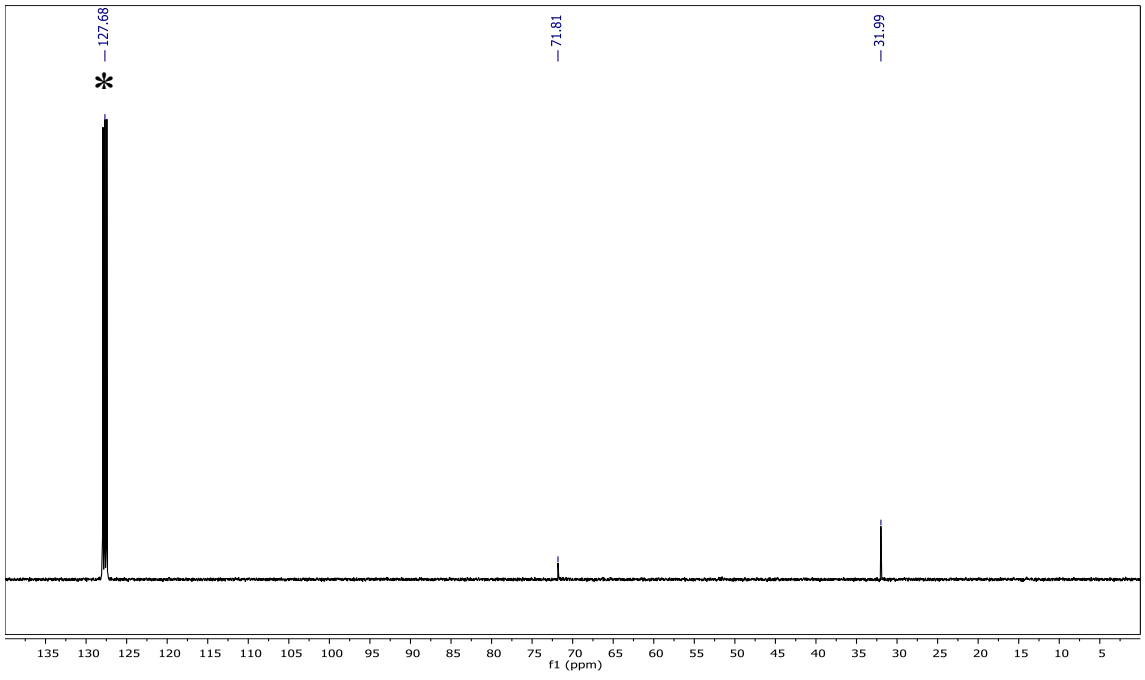

Figure 3.10 ^{13}C NMR for (^{t}BuO)$_3$SiNHLi in C_6D_6. Peaks of C_6D_5H is noted as *.

3.4.5 *Synthesis of ((ᵗBuO)₃Si)₂NH, BTTSA-H*

(^{t}BuO)$_3$SiNHLi (18.5629g, 68.9 mmol, 1.0 equiv.) was slurried in 300 mL of toluene in a 1 L round-bottom Schlenk flask. Separately, (^{t}BuO)$_3$SiCl was dissolved in 100 mL of toluene and the solution is added to the stirring slurry via cannula. The reaction mixture was stirred for an hour and then the reaction is brought to reflux (after all solid is dissolved) for 24h. The mixture was filtered through Celite and the solid was washed with toluene. The filtrate was concentrated *in vacuo* and crystalized at -80°C yielding the title compound as a white crystalline solid (26.78 g, 76%) after decantation. ^{1}H NMR (400 MHz, C_6D_6): δ 1.46 (s, 54 H, *tert*-butyl -CH_3), 0.63 (s, 1 H, -NH). ^{13}C NMR (400 MHz, C_6D_6): δ 72.03 (s), 31.49 (s). IR (cm^{-1}): *v* 3409 (m), 3246 (w), 3192 (w), 2713 (w), 2272 (w), 1874 (w), 1365 (s), 1242 (s), 1203 (s), 1062 (s), 1002 (s), 969 (s), 934 (m), 830 (s), 800 (m), 700 (s), 624 (m). Elem. anal. Found (calculated) for $C_{24}H_{55}NO_6Si_2$: C, 54.31 (56.54); H, 10.41 (10.87); N, 2.71 (2.75). Carbon consistently low on multiple burns.

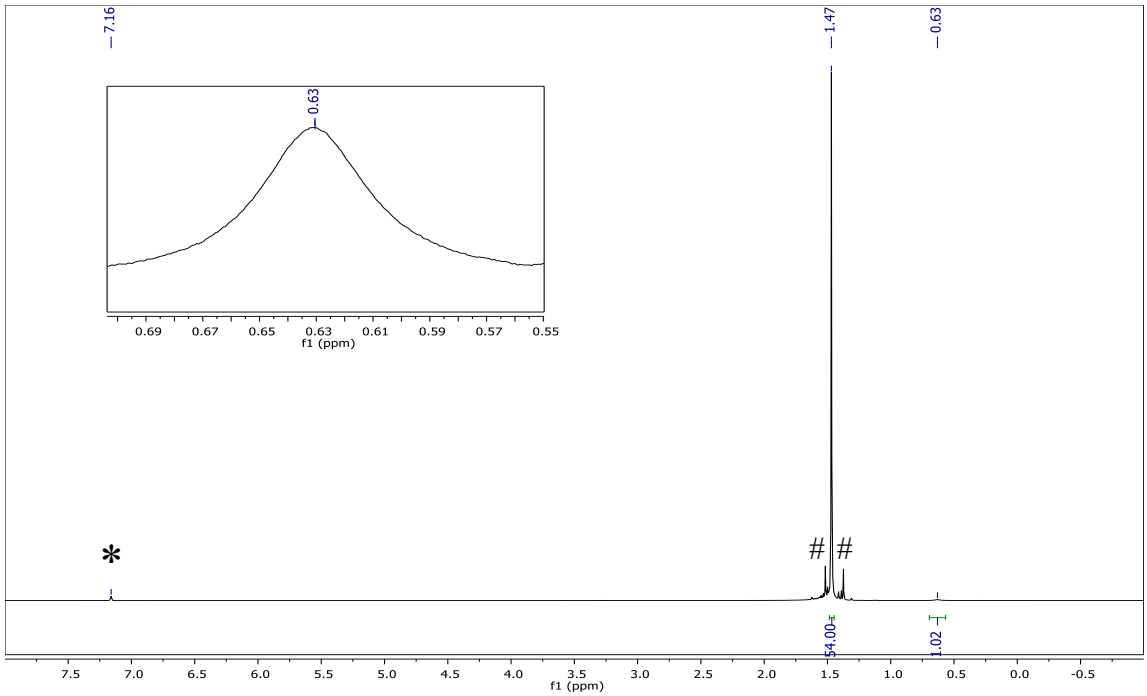

Figure 3.11 ^{1}H NMR for $((^{t}BuO)_3Si)_2NH$ in C_6D_6. Peak of C_6D_5H is noted as *. Unidentified impurities are marked as #.

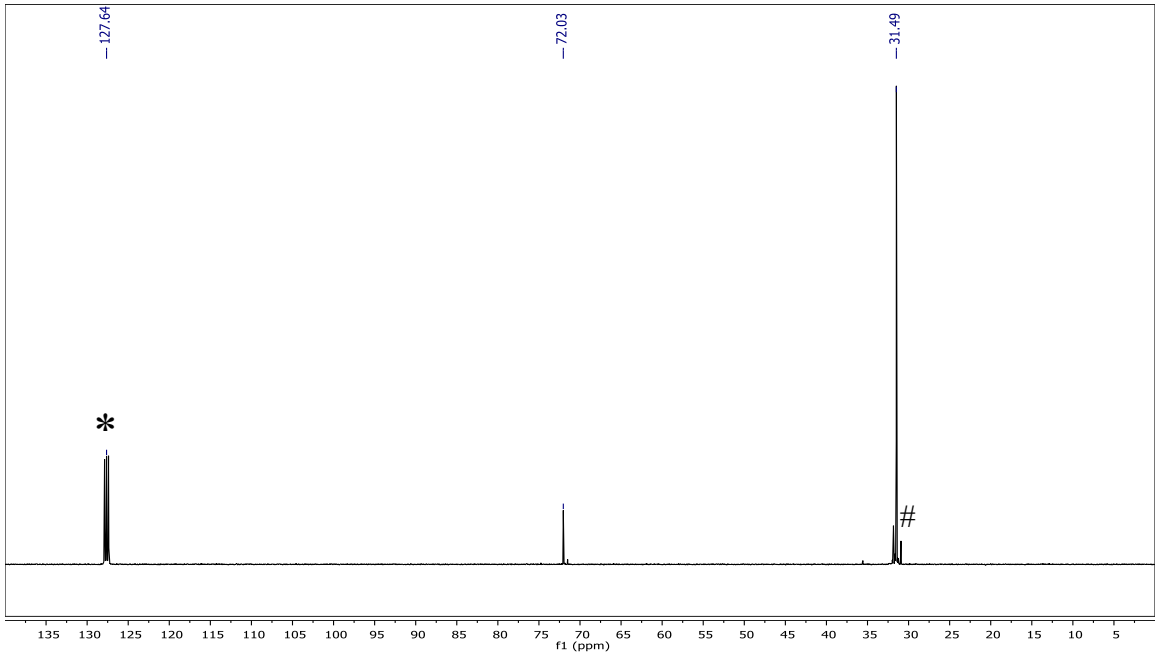

Figure 3.12 ^{13}C NMR for $((^{t}BuO)_3Si)_2NH$ in C_6D_6. Peak of C_6D_5H is noted as *. Unidentified impurities are marked as #.

3.4.6 *Synthesis of* $((^tBuO)_3Si)_2NK$

$((^tBuO)_3Si)_2NH$ (2.045g, 3.92 mmol, 1.0 equiv.) was added to a 100 mL pear Schlenk flask with 20 mL of toluene. Potassium benzyl (548 mg, 4.12 mmol, 1.05 equiv.) was added to the flask as a solid. 30 mL toluene was added to assist in the transfer. The reaction mixture was brought to reflux for 12h. After about 1h, the solution began to turn from cherry-red to light brown. After the reflux, volatiles were removed *in vacuo* and the solid was extracted with diethyl ether. The solution is filtered over celite and crystalized at -80°C yielding white crystalline material (1.82 g, 83%). ^1H NMR (400 MHz, pyridine-d_5): δ 1.61 (s, 54 H, *tert*-butyl -CH_3). ^{13}C NMR (400 MHz, pyridine-d_5): δ 70.19 (s), 32.16 (s). IR (cm^{-1}): *v* 2713 (w), 2272 (w), 1874 (w), 1365 (s), 1242 (s), 1203 (s), 1062 (s), 1002 (s), 969 (s), 934 (m), 830 (s), 800 (m), 700 (s), 624 (m). Elem. anal. Found (calculated) for $C_{24}H_{54}NO_6Si_2K$: C, 51.39 (52.61); H, 10.02 (9.93); N, 2.54 (2.56). Carbon consistently low on multiple burns.

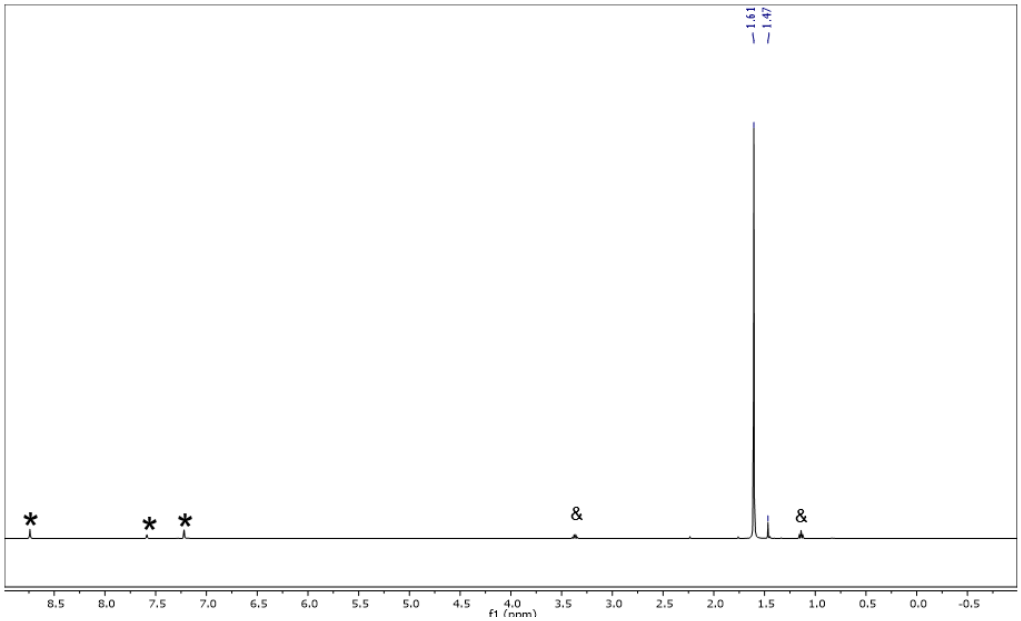

Figure 3.13 ^{1}H NMR for $(({}^{t}BuO)_3Si)_2NK$ in pyridine-d_5. Residual NMR solvent peaks are noted as *. BTTSA-H impurity is marked as #. Diethyl ether impurity is labeled with &.

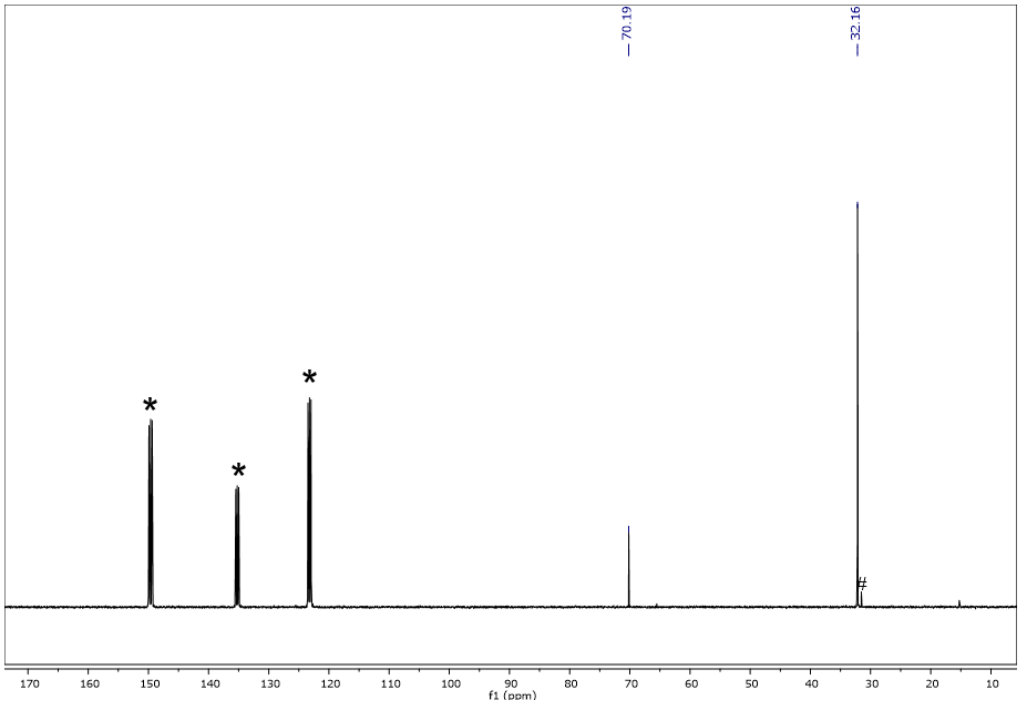

Figure 3.14 ^{13}C NMR for $(({}^{t}BuO)_3Si)_2NK$ in pyridine-d_5. Residual NMR solvent peaks are noted as *. BTTSA-H impurity are marked as #.

3.4.7 *Synthesis of [((ᵗBuO)₃Si)₂NCu]₂KCl, 1*

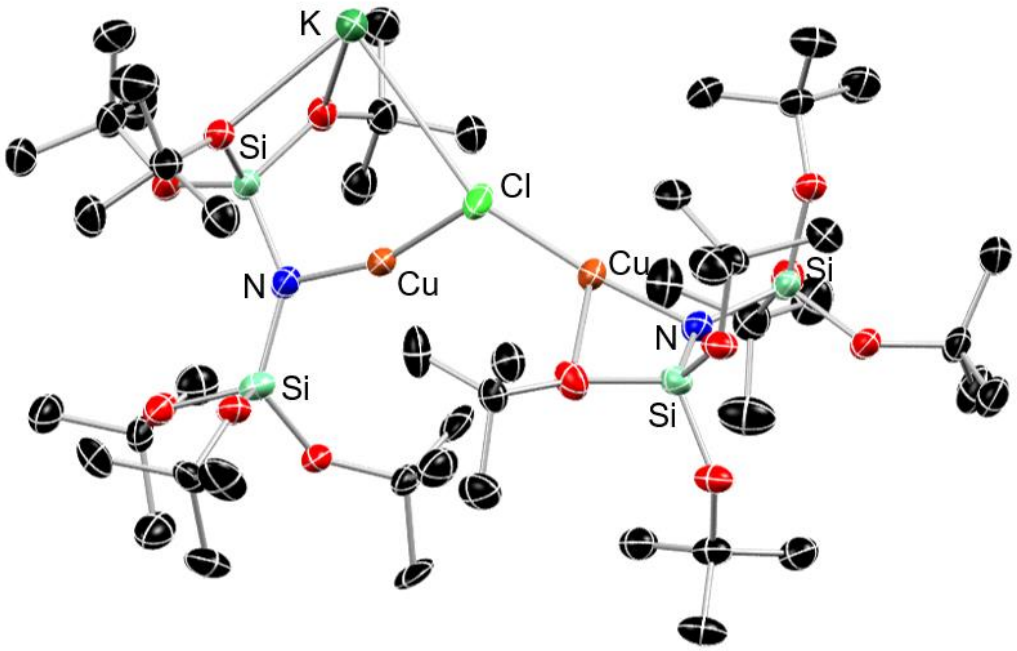

Figure 3.15 Molecular structure of 2. One subunit of a polymeric chain is shown. Thermal ellipsoids are shown at 50% probability and H atoms are omitted for clarity.

((ᵗBuO)₃Si)₂NK (917 mg, 1.67 mmol, 1.0 equiv.) was dissolved in 8 mL of THF and added to a stirring slurry of CuCl (166 mg, 1.67 mmol, 1.0 equiv.) in 2 mL THF. Upon addition, the solution adopted a yellow-orange color. The reaction mixture was stirred for 16h. The mixture was filtered through Celite and washed with THF. The volatiles were removed *in vacuo*. The resultant solid was dissolved in approximately 7 mL of *n*-pentane and filtered through Celite, and the filter cake was washed with n-pentane. The volatiles are removed *in vacuo* yielding title compound as a tan solid (781 mg, 77%). XRD quality crystals were obtained by the slow evaporation of a hexanes solution at -35 °C. ^{1}H NMR (400 MHz, C_6D_6): δ 1.64 (s, 108 H, *tert*-butyl -CH_3). ^{13}C NMR (400 MHz, C_6D_6): δ 72.03 (s), 32.39

(s). IR (cm^{-1}): *v* 2720 (m), 2272 (w), 1364 (s), 1304 (m), 1241 (s), 1192 (s), 1065 (s), 990 (s), 909 (m), 826 (s), 813 (s), 755 (m), 684 (m), 608 (w). Elem anal. Found (calculated) for $C_{48}H_{108}N_2ClCu_2O_{12}Si_4K$: C, 46.39 (47.28); H, 8.45 (8.93); N, 2.26 (2.30). Carbon consistently low on multiple burns.

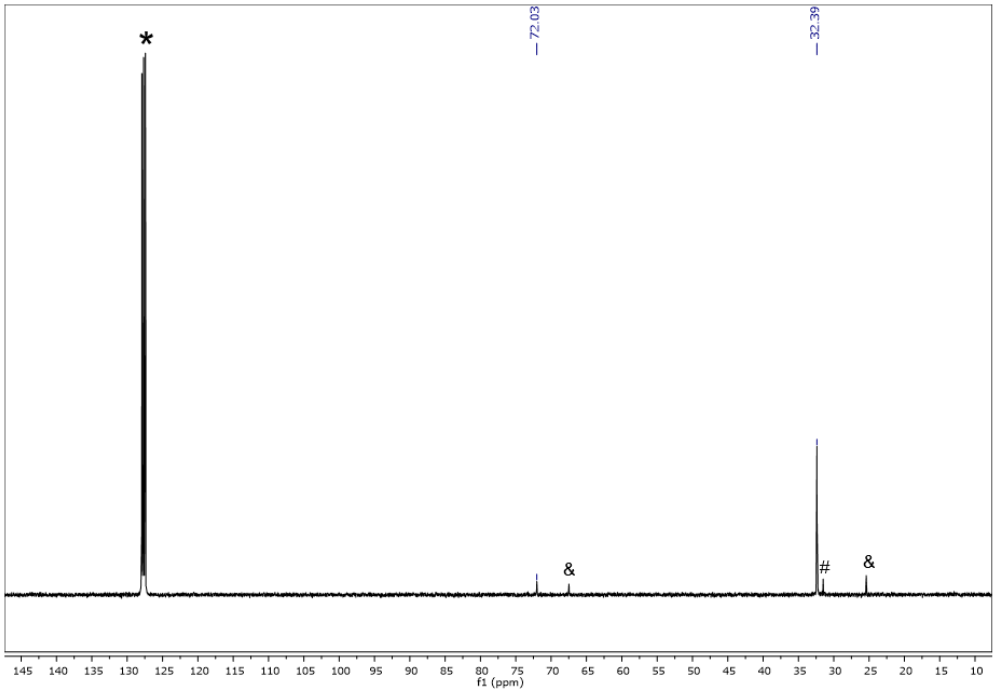

Figure 3.16 ^{1}H NMR for 1 in C_6D_6. Peak of C_6D_5H is noted as *. BTTSA-H impurity is marked as #. THF impurity is labeled with &.

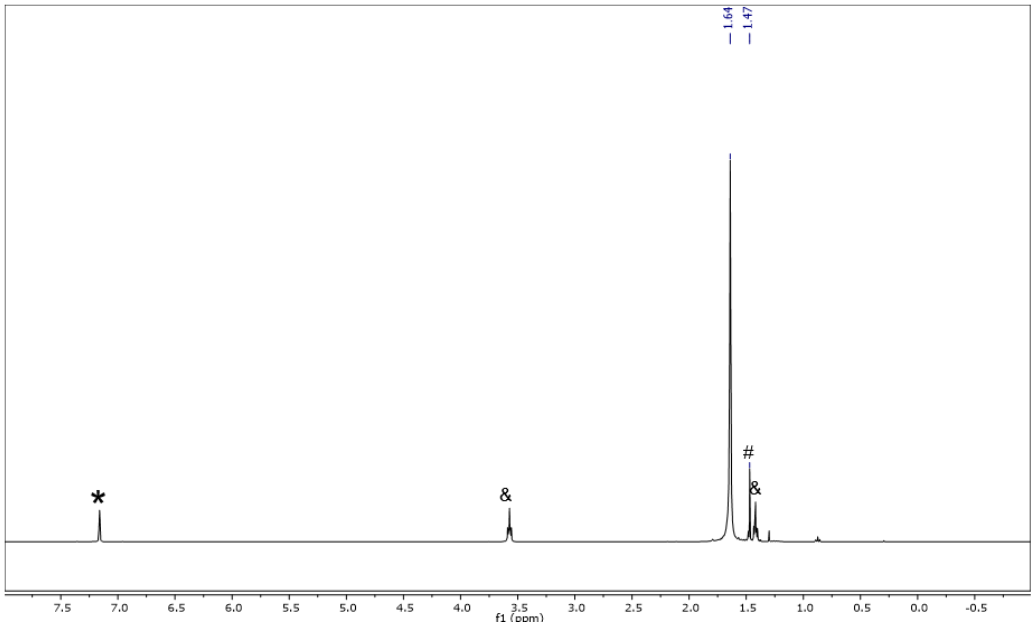

Figure 3.17 ^{13}C NMR for 1 in C_6D_6. Peak of C_6D_5H is noted as *. BTTSA-H impurity is marked as #. THF impurity is labeled with &.

3.4.8 *Synthesis of [((^{t}BuO)$_3$Si)$_2$N]$_2$Sm, 2-Sm*

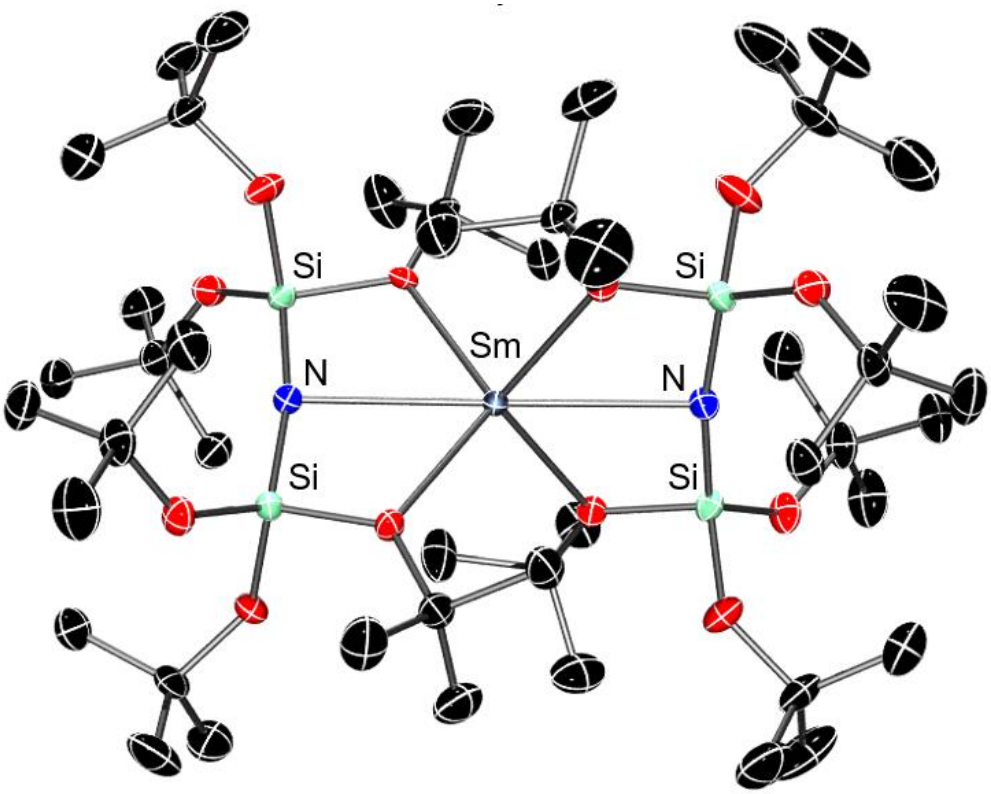

Figure 3.18 Molecular structure of 2-Sm. Thermal ellipsoids are shown at 50% probability and H atoms are omitted for clarity.

[((^{t}BuO)$_3$Si)$_2$NCu]$_2$KCl (200 mg, 0.164, 1.0 equiv.) was dissolved in 4 mL of THF and added to a slurry of Sm metal (24.7 mg, 0.164, 1.0 equiv.) in 1 mL of THF. The reaction mixture was stirred with a glass stir bar for 60 h. The solution changed color from yellow-tan to red to finally dark green over the reaction period. The mixture was filtered through Celite and washed with THF. The volatiles were removed *in vacuo*. The solid was extracted with 5 mL *n*-pentane and filtered through Celite. Volatiles were again removed *in vacuo* yielding the title compound as a dark green solid (131 mg, 68%). XRD quality

crystals were obtained via the slow evaporation of a diethyl either solution at -35°C. No ^{1}H NMR signal observed due to paramagnetic broadening. IR (cm^{-1}): *v* 2364 (w), 1362 (m), 1276 (m), 1261 (m), 1242 (m), 1193 (s), 1065 (s), 1058 (s), 1038 (m), 967 (m), 914 (w), 819 (w), 801 (m), 732 (w), 685 (w), 661 (w), 649 (w). Elem anal. Found (calculated) for $C_{48}H_{108}N_2O_{12}Si_4Sm$: C, 46.32 (49.36); H, 9.11 (9.32); N, 2.31 (2.40). Carbon consistently low on multiple burns.

3.4.9 *Synthesis of [((^{t}BuO)$_3$Si)$_2$N]$_2$Eu, 2-Eu*

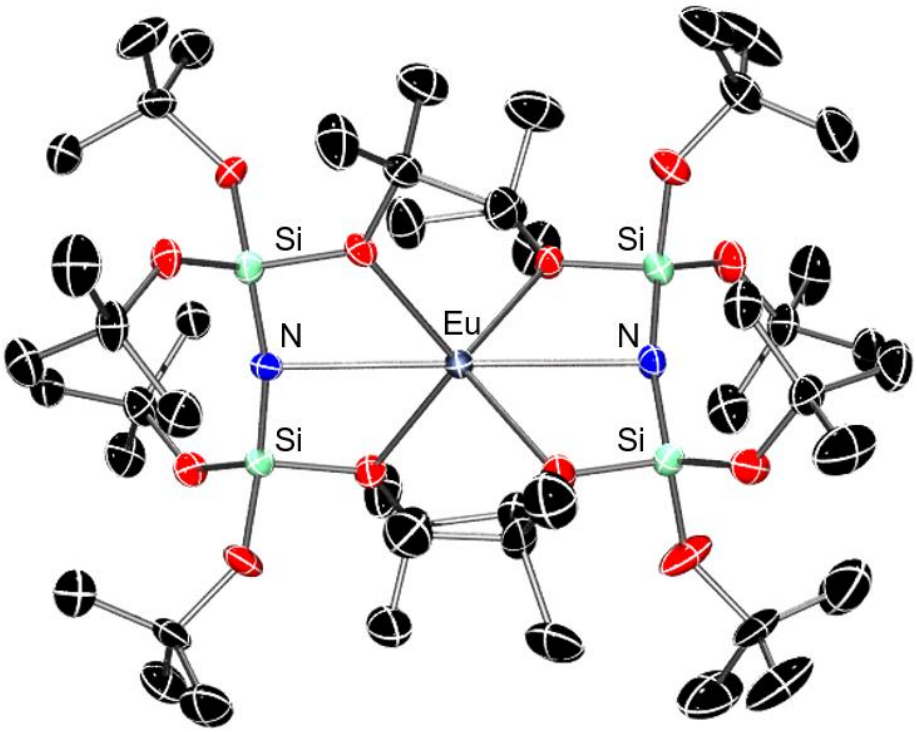

Figure 3.19 Molecular structure of 2-Eu. Thermal ellipsoids are shown at 50% probability and H atoms are omitted for clarity.

[((^{t}BuO)$_3$Si)$_2$NCu]$_2$KCl (431.7 mg, 0.354, 1.0 equiv.) was dissolved in 6 mL of THF and added to a slurry of Eu metal (53.8 mg, 0.354, 1.0 equiv.) in 1 mL of THF. The reaction was stirred with a glass stir bar for 60 h. The solution color turned from yellow-tan to red

to finally light green/colorless over the reaction period. The mixture was filtered through Celite, and the filter was washed with THF. Volatiles were removed *in vacuo.* The product was extracted with 5 mL *n*-pentane and filtered through Celite. Volatiles were removed *in vacuo* yielding the title compound as a pale green solid (341 mg, 82%). XRD quality crystals were obtained from a concentrated diethyl either at -35°C. No ^{1}H NMR signal observed due to paramagnetic broadening. IR (cm^{-1}): *v* 2364 (w), 1362 (m), 1276 (m), 1261 (m), 1242 (m), 1193 (s), 1065 (s), 1058 (s), 1038 (m), 967 (m), 914 (w), 819 (w), 801 (m), 732 (w), 685 (w), 661 (w), 649 (w). Elem anal. Found (calculated) for $C_{48}H_{108}N_2O_{12}Si_4Eu$: C, 48.45 (49.29); H, 9.60 (9.31); N, 2.31 (2.39). Carbon consistently low on multiple burns.

3.5 Crystallographic Information

Crystals suitable for X-ray diffraction were covered in paratone oil in a glove box and transferred to the diffractometer in a 20 mL capped vial. Crystals were mounted on a loop 3 with paratone oil on a Bruker D8 VENTURE diffractometer. The crystals were cooled and kept at T = 100(2) K during data collections. The structures were solved with the ShelXT structure solution program using the Intrinsic Phasing solution method and by using Olex2 as the graphical interface.[145, 146] The model was refined with version 2014/7 of XL using Least Squares minimization.[147] Structures are visualized in Ortep3 and graphics are generated with POV-ray.[185]

3.5.1 *BTTSA-H*

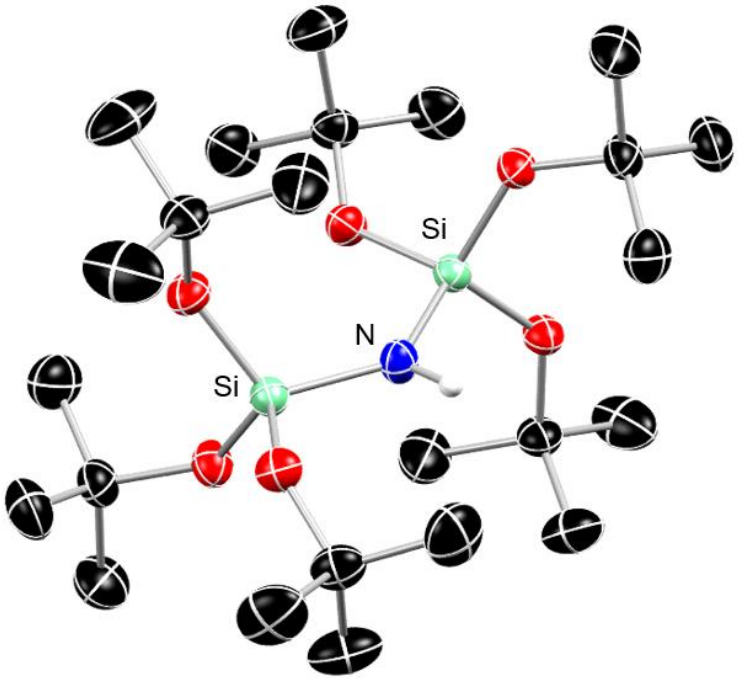

Figure 3.20 Molecular structure of BTTSA-H. Thermal ellipsoids are shown at 50% probability and H atoms (except for N–H) are omitted for clarity.

Table 3.2 Crystal data and structure refinement for BTTSA-H.

Identification code	**BTTSA-H**
Empirical formula	$C_{24}H_{55}NO_6Si_2$
Formula weight	509.87
Temperature/K	185(2)
Crystal system	triclinic
Space group	P-1
a/Å	9.2019(9)
b/Å	9.4820(10)
c/Å	20.813(2)
α/°	79.543(4)
β/°	79.198(4)
γ/°	64.407(3)
Volume/Å^3	1598.4(3)
Z	2
ρ_{calc}g/cm^3	1.059

μ/mm^{-1}	0.143
F(000)	564.0
Crystal size/mm^3	0.333 × 0.258 × 0.14
Radiation	MoKα (λ = 0.71073)
2Θ range for data collection/°	4.794 to 61.016
Index ranges	$-13 \leq h \leq 13$, $-13 \leq k \leq 13$, $-29 \leq l \leq 29$
Reflections collected	41132
Independent reflections	9720 [R_{int} = 0.0413, R_{sigma} = 0.0391]
Data/restraints/parameters	9720/1/319
Goodness-of-fit on F^2	1.031
Final R indexes [I>=2σ (I)]	R_1 = 0.0438, wR_2 = 0.1021
Final R indexes [all data]	R_1 = 0.0660, wR_2 = 0.1171
Largest diff. peak/hole / e $Å^{-3}$	0.41/-0.29

Table 3.3 Fractional Atomic Coordinates (×10^4) and Equivalent Isotropic Displacement Parameters (Å^2×10^3) for BTTSA-H. U_{eq} is defined as 1/3 of the trace of the orthogonalised U_{IJ} tensor.

Atom	*x*	*y*	*z*	U(eq)
Si2	7221.8(4)	7588.3(4)	3266.4(2)	22.18(8)
Si1	8757.5(4)	7591.3(4)	1781.8(2)	23.81(9)
O4	9015.6(10)	7301.3(11)	3391.3(4)	27.60(19)
O2	9545.6(11)	8837.9(11)	1746.2(5)	30.9(2)
O1	10221.3(11)	5851.5(11)	1842.3(5)	30.1(2)
O5	5952.0(10)	9238.9(10)	3540.7(5)	26.78(19)
N1	7323.4(13)	7635.0(13)	2436.6(5)	26.7(2)
C13	9569.1(16)	7554.1(16)	3946.4(7)	30.5(3)
O3	7918.9(12)	8007.2(11)	1109.8(5)	31.0(2)
C14	11383.4(18)	6533(2)	3891.3(9)	46.5(4)
C18	3651(2)	9282(2)	4325.3(8)	45.1(4)
C21	7133.2(17)	4622.4(15)	3610.9(7)	29.8(3)
C22	8954.1(19)	3844.7(18)	3425.3(10)	50.5(4)
C8	9975(3)	11037(2)	1872.9(12)	65.3(6)
C15	8705(2)	7079(2)	4590.4(7)	43.8(4)
C12	7587(3)	5656(2)	1000.4(10)	58.2(5)
C1	11918.1(16)	5251.9(17)	1584.6(7)	33.5(3)
C19	3463.3(18)	9754(2)	3111.8(9)	42.8(4)
C17	4204.4(15)	9978.2(15)	3659.1(7)	31.0(3)
C4	12818(2)	5624(2)	2023.2(10)	51.0(4)
C16	9237(2)	9284.0(19)	3891.0(10)	47.8(4)
C7	9122(4)	10874(2)	838.4(10)	75.3(7)
C9	6990.5(19)	7425.8(18)	837.1(7)	36.6(3)

Atom	*x*	*y*	*z*	U(eq)
C24	6621(3)	3916(2)	4280.6(9)	54.8(5)
C20	3778.9(19)	11715.3(17)	3662.0(10)	47.3(4)
C2	12147(2)	5962(2)	876.5(8)	49.5(4)
C3	12462(2)	3482.4(18)	1619.6(9)	47.1(4)
C5	8930.5(19)	10517.9(16)	1578.4(7)	35.4(3)
C10	7233(3)	7861(3)	99.7(9)	62.2(5)
C6	7176(2)	11304.6(19)	1865.2(12)	61.2(6)
C11	5208(2)	8248(3)	1103.3(10)	58.3(5)
C23	6250(2)	4475(2)	3096.9(9)	50.4(4)
O6	6598.3(11)	6272.3(10)	3666.8(4)	26.87(19)

Table 3.4 Anisotropic Displacement Parameters ($Å^2×10^3$) for BTTSA-H. The Anisotropic displacement factor exponent takes the form: $-2\pi^2[h^2a^{*2}U_{11}+2hka^*b^*U_{12}+\ldots]$.

Atom	U_{11}	U_{22}	U_{33}	U_{23}	U_{13}	U_{12}
Si2	20.62(15)	20.71(16)	23.87(17)	-2.93(12)	-2.21(12)	-7.33(12)
Si1	23.81(16)	22.01(16)	24.37(17)	-1.76(13)	-2.02(13)	-8.99(13)
O4	23.5(4)	31.1(5)	28.3(5)	-6.3(4)	-4.8(3)	-9.5(4)
O2	30.0(5)	24.9(4)	38.8(5)	-2.4(4)	-3.2(4)	-13.1(4)
O1	25.4(4)	25.2(4)	35.0(5)	-1.5(4)	-0.5(4)	-8.0(4)
O5	21.6(4)	23.0(4)	33.9(5)	-6.0(4)	-1.3(4)	-7.3(3)
N1	21.5(5)	32.2(6)	26.3(5)	-3.0(4)	-3.8(4)	-10.6(4)
C13	29.3(6)	30.4(7)	33.3(7)	-6.9(5)	-9.6(5)	-10.1(5)
O3	37.2(5)	30.0(5)	27.2(5)	0.6(4)	-7.1(4)	-15.3(4)
C14	30.4(7)	56.4(10)	51.7(10)	-15.6(8)	-15.3(7)	-9.1(7)
C18	40.3(8)	44.2(9)	46.1(9)	-10.1(7)	12.2(7)	-18.2(7)
C21	34.0(7)	21.6(6)	33.6(7)	-4.4(5)	-0.4(5)	-12.3(5)
C22	35.5(8)	26.3(7)	81.9(13)	-11.6(8)	-0.5(8)	-6.0(6)
C8	73.3(13)	44.9(10)	96.6(17)	-2.9(10)	-24.6(12)	-38.1(10)
C15	48.7(9)	51.8(10)	30.7(8)	-4.1(7)	-9.7(7)	-18.6(8)
C12	80.7(14)	41.3(9)	64.4(12)	-4.0(8)	-27.0(10)	-29.8(9)
C1	24.1(6)	31.7(7)	39.6(8)	-7.6(6)	0.3(5)	-7.0(5)
C19	26.0(7)	45.0(9)	54.5(10)	-8.5(7)	-8.1(6)	-9.4(6)
C17	21.6(6)	25.5(6)	40.9(8)	-6.3(5)	1.5(5)	-6.3(5)
C4	33.7(8)	52.5(10)	67.7(12)	-16.4(9)	-10.9(8)	-13.0(7)
C16	50.5(9)	36.5(8)	65.0(11)	-9.8(8)	-15.8(8)	-21.0(7)
C7	133(2)	49.5(11)	43.4(10)	7.1(9)	-1.1(12)	-46.1(13)
C9	46.1(8)	37.3(8)	31.3(7)	-1.0(6)	-12.8(6)	-19.6(6)
C24	84.7(14)	33.7(8)	42.6(9)	-0.5(7)	6.2(9)	-28.4(9)
C20	34.7(8)	25.5(7)	73.1(12)	-11.7(7)	1.4(8)	-5.2(6)

Atom	U_{11}	U_{22}	U_{33}	U_{23}	U_{13}	U_{12}
C2	43.2(9)	50.2(10)	44.5(9)	-7.5(7)	10.5(7)	-14.9(8)
C3	37.5(8)	30.9(8)	62.1(11)	-10.3(7)	-4.9(7)	-2.5(6)
C5	43.3(8)	24.8(6)	39.1(8)	-1.7(6)	-2.1(6)	-17.0(6)
C10	88.9(15)	80.8(14)	32.6(9)	1.5(9)	-18.9(9)	-47.9(12)
C6	47.1(10)	25.3(8)	101.4(16)	-10.4(9)	3.9(10)	-9.7(7)
C11	43.8(10)	75.1(13)	61.5(12)	-8.6(10)	-16.7(9)	-25.1(9)
C23	62.1(11)	48.3(10)	54.0(10)	-12.7(8)	-11.5(9)	-30.6(9)
O6	28.6(4)	20.8(4)	29.0(5)	-3.8(3)	0.6(4)	-9.4(3)

Table 3.5 Bond Lengths for BTTSA-H.

Atom	Atom	Length/Å	Atom	Atom	Length/Å
Si2	O4	1.6166(9)	C18	C17	1.520(2)
Si2	O5	1.6233(9)	C21	C22	1.515(2)
Si2	N1	1.7055(12)	C21	C24	1.517(2)
Si2	O6	1.6255(10)	C21	C23	1.517(2)
Si1	O2	1.6178(10)	C21	O6	1.4432(15)
Si1	O1	1.6187(10)	C8	C5	1.511(2)
Si1	N1	1.7028(11)	C12	C9	1.516(2)
Si1	O3	1.6274(10)	C1	C4	1.516(2)
O4	C13	1.4416(16)	C1	C2	1.522(2)
O2	C5	1.4398(16)	C1	C3	1.521(2)
O1	C1	1.4418(16)	C19	C17	1.521(2)
O5	C17	1.4417(15)	C17	C20	1.521(2)
C13	C14	1.520(2)	C7	C5	1.509(2)
C13	C15	1.524(2)	C9	C10	1.516(2)
C13	C16	1.520(2)	C9	C11	1.522(2)
O3	C9	1.4346(17)	C5	C6	1.510(2)

Table 3.6 Bond Angles for BTTSA-H.

Atom	Atom	Atom	Angle/°	Atom	Atom	Atom	Angle/°
O4	Si2	O5	107.46(5)	O6	C21	C24	105.56(11)
O4	Si2	N1	105.32(5)	O6	C21	C23	108.31(12)
O4	Si2	O6	114.34(5)	O1	C1	C4	108.49(12)
O5	Si2	N1	113.03(5)	O1	C1	C2	110.62(12)
O5	Si2	O6	105.41(5)	O1	C1	C3	105.01(12)
O6	Si2	N1	111.40(5)	C4	C1	C2	111.25(14)
O2	Si1	O1	106.96(5)	C4	C1	C3	110.62(13)
O2	Si1	N1	115.24(6)	C3	C1	C2	110.65(13)
O2	Si1	O3	106.44(5)	O5	C17	C18	108.85(11)

Atom	Atom	Atom	Angle/°	Atom	Atom	Atom	Angle/°
O1	Si1	N1	106.96(5)	O5	C17	C19	110.43(11)
O1	Si1	O3	113.02(5)	O5	C17	C20	105.28(11)
O3	Si1	N1	108.39(5)	C18	C17	C19	111.19(13)
C13	O4	Si2	130.82(8)	C18	C17	C20	110.75(13)
C5	O2	Si1	132.45(9)	C20	C17	C19	110.17(13)
C1	O1	Si1	132.58(9)	O3	C9	C12	110.93(13)
C17	O5	Si2	132.88(8)	O3	C9	C10	105.49(13)
Si1	N1	Si2	134.90(7)	O3	C9	C11	108.99(13)
O4	C13	C14	105.57(11)	C12	C9	C11	110.67(15)
O4	C13	C15	110.65(12)	C10	C9	C12	110.54(15)
O4	C13	C16	108.51(12)	C10	C9	C11	110.09(15)
C14	C13	C15	110.92(13)	O2	C5	C8	105.60(13)
C16	C13	C14	110.73(13)	O2	C5	C7	108.77(13)
C16	C13	C15	110.34(13)	O2	C5	C6	110.69(12)
C9	O3	Si1	135.99(9)	C7	C5	C8	110.23(16)
C22	C21	C24	111.36(14)	C7	C5	C6	111.02(17)
C22	C21	C23	110.69(14)	C6	C5	C8	110.38(16)
C24	C21	C23	109.63(14)	C21	O6	Si2	132.15(8)
O6	C21	C22	111.11(11)				

Table 3.7 Hydrogen Atom Coordinates (Å×10^4) and Isotropic Displacement Parameters (Å^2×10^3) for BTTSA-H.

Atom	*x*	*y*	*z*	U(eq)
H14A	11573	5426	3917	70
H14B	11839	6675	4252	70
H14C	11909	6840	3469	70
H18A	3992	8151	4321	68
H18B	2465	9796	4416	68
H18C	4139	9450	4669	68
H22A	9502	3961	3760	76
H22B	9251	4346	2998	76
H22C	9287	2724	3398	76
H8A	9862	10776	2352	98
H8B	9629	12177	1766	98
H8C	11114	10495	1692	98
H15A	7538	7744	4613	66
H15B	9132	7214	4962	66
H15C	8891	5975	4611	66
H12A	8733	5148	823	87
H12B	6946	5285	805	87

Atom	*x*	*y*	*z*	U(eq)
H12C	7469	5392	1479	87
H19A	3895	10149	2686	64
H19B	2281	10335	3179	64
H19C	3736	8632	3117	64
H4A	12419	6768	2010	76
H4B	13983	5177	1867	76
H4C	12635	5169	2476	76
H16A	9780	9579	3471	72
H16B	9653	9465	4254	72
H16C	8065	9924	3912	72
H7A	10263	10320	663	113
H7B	8780	12010	719	113
H7C	8448	10522	653	113
H24A	6940	2790	4272	82
H24B	5440	4442	4387	82
H24C	7151	4059	4615	82
H20A	4307	11841	4002	71
H20B	2599	12286	3756	71
H20C	4156	12138	3231	71
H2A	11512	5745	609	74
H2B	13298	5496	701	74
H2C	11777	7102	863	74
H3A	12255	3054	2076	71
H3B	13625	2988	1467	71
H3C	11854	3265	1339	71
H10A	6888	9003	4	93
H10B	6584	7536	-115	93
H10C	8383	7326	-67	93
H6A	6514	10954	1671	92
H6B	6798	12449	1767	92
H6C	7077	11021	2343	92
H11A	5049	7895	1573	87
H11B	4546	7989	866	87
H11C	4880	9389	1042	87
H23A	6581	4935	2665	76
H23B	5076	5034	3213	76
H23C	6523	3361	3081	76
H1	6379(16)	7878(18)	2334(8)	32

3.5.2 *BTTSA-Cu, 1*

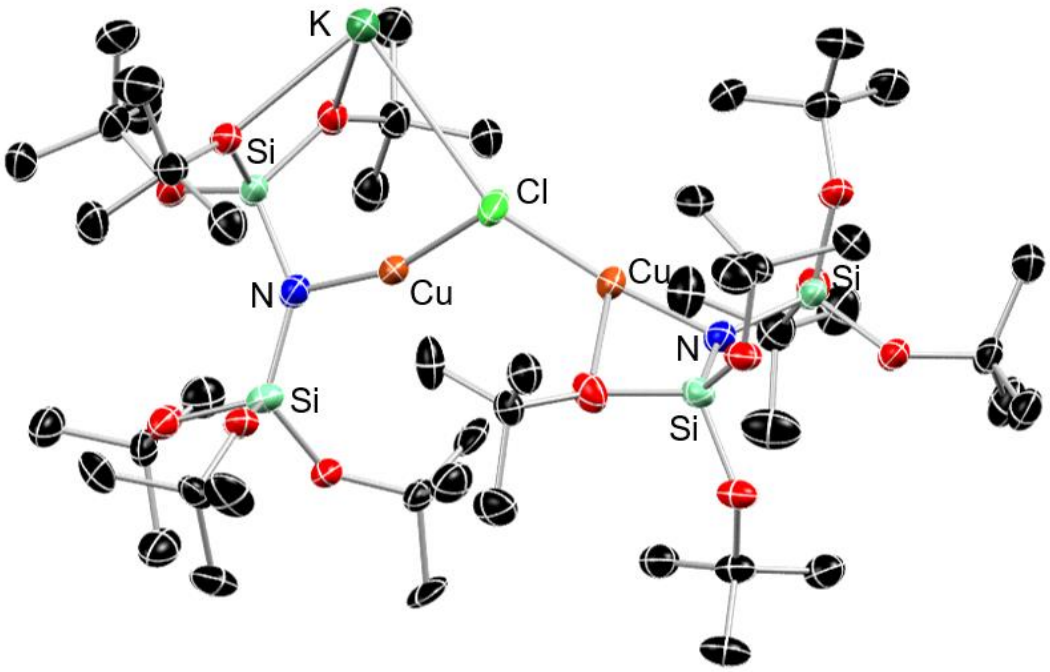

Figure 3.21 Molecular structure of 1. One subunit of a polymeric chain is shown. Thermal ellipsoids are shown at 50% probability and H atoms are omitted for clarity.

Table 3.8 Crystal data and structure refinement for 1.

Identification code	BTTSA-Cu
Empirical formula	$C_{48}H_{108}ClCu_2KN_2O_{12}Si_4$
Formula weight	1219.35
Temperature/K	191.07
Crystal system	monoclinic
Space group	$P2_1/c$
a/Å	20.524(8)
b/Å	19.826(9)
c/Å	19.692(8)
α/°	90
β/°	112.541(15)
γ/°	90
Volume/Å^3	7401(6)
Z	4
ρ_{calc}g/cm^3	1.094

μ/mm^{-1}	0.777
F(000)	2624.0
Crystal size/mm^3	0.549 × 0.29 × 0.258
Radiation	MoKα (λ = 0.71073)
2Θ range for data collection/°	4.638 to 60.708
Index ranges	$-26 \leq h \leq 28$, $-27 \leq k \leq 27$, $-27 \leq l \leq 27$
Reflections collected	182799
Independent reflections	21842 [R_{int} = 0.0802, R_{sigma} = 0.0519]
Data/restraints/parameters	21842/32/741
Goodness-of-fit on F^2	1.071
Final R indexes [I>=2σ (I)]	R_1 = 0.0552, wR_2 = 0.1280
Final R indexes [all data]	R_1 = 0.1125, wR_2 = 0.1719
Largest diff. peak/hole / e $Å^{-3}$	0.61/-1.03

Table 3.9 Fractional Atomic Coordinates (×10^4) and Equivalent Isotropic Displacement Parameters (Å^2×10^3) for 1. U_{eq} is defined as 1/3 of the trace of the orthogonalised U_{IJ} tensor.

Atom	*x*	*y*	*z*	U(eq)
Cu1	7891.8(2)	3204.4(2)	7502.0(2)	31.70(10)
Cu2	7130.4(2)	4647.1(2)	8127.5(2)	29.79(10)
K1	7614.5(4)	1014.3(4)	5070.9(4)	35.68(16)
Cl1	7583.2(5)	3644.1(5)	8337.4(5)	46.9(2)
Si1	9083.5(4)	2597.8(5)	7114.6(4)	27.70(17)
Si2	7488.3(4)	2305.3(4)	6275.5(4)	27.79(17)
Si3	6238.4(5)	5824.7(4)	7416.9(4)	30.79(18)
Si4	6970.0(4)	5557.1(5)	9137.7(4)	29.23(18)
O1	9580.0(11)	3280.6(12)	7351.4(12)	34.6(5)
O2	9431.1(11)	2091.6(12)	7830.1(11)	33.5(5)
O3	9186.0(10)	2182.9(11)	6432.8(11)	30.9(5)
O4	7475.7(11)	1460.5(11)	6347.6(11)	31.9(5)
O5	7328.6(11)	2312.7(11)	5382.3(11)	32.8(5)
O6	6837.0(11)	2660.3(12)	6441.9(13)	35.9(5)
O10	6585.0(11)	4944.2(12)	9443.6(11)	34.5(5)
O11	7800.9(10)	5321.5(11)	9646.5(11)	32.6(5)
O12	6795.9(12)	6309.9(12)	9386.5(11)	37.9(5)
N2	6798.0(13)	5529.3(13)	8236.5(13)	28.9(5)
N1	8206.6(12)	2726.3(13)	6842.8(13)	28.5(5)
C1	9534.0(17)	4001.5(18)	7177.6(19)	38.0(7)
C2	10297.7(19)	4239(2)	7369(2)	50.7(9)
C3	9225(2)	4375(2)	7663(2)	53.1(10)
C4	9097(2)	4120(2)	6371(2)	55.9(11)

Atom	*x*	*y*	*z*	U(eq)
C5	9805.9(17)	2190(2)	8613.0(16)	40.5(8)
C6	9792(2)	1500(2)	8960(2)	55.3(10)
C7	10569.2(18)	2404(2)	8780.3(19)	51.0(10)
C8	9430(2)	2719(2)	8898.2(19)	53.2(10)
C9	9792.1(16)	1941.6(18)	6298.0(17)	34.7(7)
C10	10338.0(19)	1605(2)	6972(2)	52.5(10)
C11	10115.0(19)	2546(2)	6044(2)	47.8(9)
C12	9491.8(17)	1420.8(19)	5681.3(18)	39.5(7)
C13	7694.6(16)	1000.1(16)	6978.2(17)	32.8(6)
C14	7765.7(18)	1368.1(18)	7687.4(17)	37.8(7)
C15	8401.6(18)	687.9(18)	7046.1(19)	40.4(8)
C16	7126.6(19)	444.0(18)	6795(2)	44.1(8)
C17	7316.3(16)	2868.2(16)	4884.0(16)	32.0(6)
C18	8030.8(17)	2871.0(18)	4802.1(17)	36.4(7)
C19	6725.4(19)	2703.1(18)	4144.9(17)	42.1(8)
C20	7178.2(17)	3551.5(17)	5175.5(17)	35.3(7)
C37	5847.5(16)	4721.2(19)	9167.9(17)	38.1(7)
C38	5754(2)	4371(3)	9815(2)	73.6(16)
C39	5717.1(18)	4217.9(18)	8535(2)	41.4(8)
C40	5340.2(17)	5323(2)	8912(2)	45.0(9)
C41	8468.8(15)	5581.5(19)	9648.5(17)	35.9(7)
C42	8782.9(17)	5053(2)	9290.6(19)	41.9(8)
C43	8955.4(17)	5663(2)	10460.7(19)	47.0(9)
C44	8383.9(18)	6257.8(19)	9240(2)	41.2(8)
C45	6854.7(19)	6628(2)	10078.3(17)	45.0(9)
C46	7480(2)	7116(3)	10320(2)	64.2(13)
C47	6944(3)	6093(2)	10675(2)	63.2(13)
C48	6166.6(19)	7021(2)	9911.2(19)	45.8(9)
C21A	6092(7)	2644(5)	6364(4)	29.7(13)
C22A	5900(20)	1906(3)	6458(7)	37.9(12)
C23A	5662(4)	2884(5)	5585(4)	45.3(13)
C24A	5967(4)	3104(4)	6920(4)	43.9(12)
O7A	6520(2)	6034(2)	6791(2)	29.4(6)
C25A	6963(3)	5733(3)	6457(3)	28.9(11)
C26A	7746(3)	5847(6)	6947(7)	40.2(16)
C27A	6795(5)	4976(3)	6353(4)	47.2(12)
C28A	6793(7)	6083(4)	5710(5)	41.8(14)
O9A	5790(2)	6574.6(19)	7470(2)	32.0(6)
C33A	5965(3)	7281(2)	7444(3)	30.2(13)
C34A	6757(3)	7388(4)	7864(4)	42.7(14)
C35A	5542(4)	7694(3)	7797(4)	45.1(12)

Atom	*x*	*y*	*z*	U(eq)
C36A	5744(5)	7486(4)	6633(3)	47.8(15)
O8A	5571(3)	5294(3)	7087(3)	32.3(8)
C29A	4862(4)	5281(6)	6526(6)	32.3(18)
C30A	4641(6)	4550(6)	6295(8)	55(2)
C31A	4855(6)	5700(5)	5859(4)	51.4(19)
C32A	4380(6)	5625(11)	6854(10)	42.1(18)
C21B	6070(5)	2564(4)	6150(3)	29.7(13)
C22B	5903(15)	1974(3)	6569(5)	37.9(12)
C23B	5724(3)	2439(4)	5324(3)	45.3(13)
C24B	5820(3)	3232(3)	6342(4)	43.9(12)
O7B	6483(2)	5408.0(19)	6783.9(19)	29.4(6)
C25B	6994(3)	5547(3)	6467(3)	28.9(11)
C26B	7686(3)	5804(5)	7063(6)	40.2(16)
C27B	7122(4)	4890(3)	6124(4)	47.2(12)
C28B	6687(6)	6094(4)	5876(5)	41.8(14)
O9B	6332(2)	6593.0(19)	7265(2)	32.0(6)
C33B	6232(3)	7237(2)	7561(3)	30.2(13)
C34B	6911(3)	7443(3)	8198(4)	42.7(14)
C35B	5623(3)	7167(3)	7830(4)	45.1(12)
C36B	6034(4)	7759(3)	6936(4)	47.8(15)
O8B	5463(2)	5561(3)	7265(2)	32.3(8)
C29B	4831(4)	5481(4)	6604(5)	32.3(18)
C31B	4808(5)	6011(5)	6028(4)	51.4(19)
C32B	4186(4)	5559(10)	6824(8)	42.1(18)
C30B	4849(6)	4759(5)	6320(7)	55(2)

Table 3.10 Anisotropic Displacement Parameters ($Å^2×10^3$) for 1. The Anisotropic displacement factor exponent takes the form: $-2\pi^2[h^2a^{*2}U_{11}+2hka^*b^*U_{12}+\ldots]$.

Atom	U_{11}	U_{22}	U_{33}	U_{23}	U_{13}	U_{12}
Cu1	29.30(19)	43.0(2)	27.64(18)	3.53(15)	16.29(15)	6.99(16)
Cu2	30.51(19)	39.4(2)	21.55(17)	2.16(14)	12.34(14)	8.42(15)
K1	31.6(3)	47.2(4)	29.3(3)	-1.7(3)	12.8(3)	-6.0(3)
Cl1	64.0(6)	52.8(5)	39.7(4)	17.7(4)	37.5(4)	30.1(4)
Si1	19.7(3)	44.5(5)	19.7(3)	-2.1(3)	8.5(3)	0.5(3)
Si2	20.3(4)	38.0(4)	23.7(4)	4.4(3)	6.8(3)	-0.5(3)
Si3	35.8(4)	36.4(4)	19.7(4)	0.8(3)	10.2(3)	-2.2(3)
Si4	21.6(4)	45.8(5)	20.1(3)	-4.3(3)	7.7(3)	5.6(3)
O1	23.1(10)	47.3(13)	32.7(11)	-6.0(10)	9.8(9)	-1.5(9)
O2	24.0(10)	54.8(14)	19.8(9)	-0.7(9)	6.2(8)	4.0(9)
O3	23.2(10)	48.8(13)	21.7(9)	-2.5(9)	9.6(8)	1.8(9)

Atom	U_{11}	U_{22}	U_{33}	U_{23}	U_{13}	U_{12}
O4	28.4(10)	40.9(12)	24.2(10)	6.9(9)	7.7(8)	1.6(9)
O5	30.5(11)	38.8(12)	24.1(10)	7.2(9)	5.1(8)	-3.4(9)
O6	19.7(10)	43.5(13)	43.8(13)	5.2(10)	11.3(9)	0.2(9)
O10	23.5(10)	57.4(14)	23.9(10)	4.0(9)	10.6(8)	7.3(9)
O11	22.8(10)	46.8(13)	27.1(10)	-6.0(9)	8.2(8)	4.2(9)
O12	35.1(12)	54.5(14)	22.0(10)	-7.7(9)	8.8(9)	13.2(10)
N2	25.4(12)	38.3(14)	24.2(11)	-4.4(10)	10.7(9)	1.1(10)
N1	23.5(11)	39.8(14)	24.0(11)	-0.1(10)	10.9(9)	0.5(10)
C1	29.8(15)	47.4(19)	37.5(17)	-6.3(14)	13.8(13)	-7.8(14)
C2	38.9(19)	63(2)	52(2)	-16.8(19)	20.1(17)	-16.0(17)
C3	48(2)	53(2)	67(3)	-6(2)	32(2)	0.2(18)
C4	55(2)	55(2)	43(2)	5.8(17)	1.8(18)	-16.6(19)
C5	32.1(16)	68(2)	18.0(13)	-0.6(14)	5.7(12)	10.3(15)
C6	51(2)	78(3)	28.5(17)	10.8(18)	5.1(16)	13(2)
C7	32.9(18)	83(3)	29.0(17)	-9.1(18)	3.4(14)	2.8(18)
C8	51(2)	85(3)	23.1(15)	-0.8(17)	14.4(15)	23(2)
C9	23.8(14)	57(2)	27.6(14)	-5.6(14)	14.4(12)	2.6(13)
C10	35.2(18)	89(3)	34.3(18)	-1.6(18)	14.4(15)	20.2(19)
C11	38.3(18)	65(2)	52(2)	-12.3(18)	30.1(17)	-8.6(17)
C12	33.8(16)	55(2)	35.4(16)	-10.3(15)	20.0(14)	-3.4(15)
C13	29.1(15)	37.3(16)	29.3(15)	9.6(12)	8.4(12)	4.2(12)
C14	37.3(17)	46.5(19)	29.7(15)	10.1(14)	12.9(13)	6.1(14)
C15	36.7(17)	45.4(19)	36.8(17)	6.1(14)	11.5(14)	10.3(14)
C16	39.9(18)	44(2)	46(2)	11.2(16)	14.6(16)	-1.1(15)
C17	31.4(15)	38.4(16)	22.0(13)	3.5(12)	5.6(11)	-4.6(12)
C18	37.3(17)	44.3(18)	27.5(15)	0.0(13)	12.5(13)	-3.6(14)
C19	42.8(18)	44.5(19)	25.9(15)	6.2(14)	-1.4(13)	-4.9(15)
C20	33.1(16)	42.5(18)	28.2(14)	3.6(13)	9.4(12)	-0.5(13)
C37	21.3(14)	65(2)	29.4(15)	9.5(15)	11.7(12)	5.6(14)
C38	31.9(19)	145(5)	50(2)	36(3)	22.2(18)	7(2)
C39	33.9(17)	42.3(19)	50(2)	4.2(15)	18.6(15)	-2.1(14)
C40	24.7(15)	67(2)	41.6(18)	-8.0(17)	10.7(14)	7.7(15)
C41	20.5(13)	56(2)	29.9(15)	-6.2(14)	7.8(11)	2.8(13)
C42	28.4(15)	62(2)	35.6(17)	-1.4(16)	12.9(13)	10.9(15)
C43	26.3(16)	76(3)	32.7(17)	-12.2(17)	4.8(13)	-0.9(16)
C44	30.9(16)	51(2)	43.9(19)	-8.6(16)	16.6(14)	-3.5(14)
C45	42.0(18)	65(2)	25.0(15)	-13.0(15)	9.5(13)	20.5(17)
C46	41(2)	92(3)	51(2)	-42(2)	7.2(17)	6(2)
C47	80(3)	80(3)	25.1(17)	-4.4(18)	14.5(18)	35(2)
C48	40.4(18)	62(2)	32.9(17)	-8.7(16)	11.5(14)	19.1(17)
C21A	16.9(15)	40(3)	32(4)	2(3)	10(3)	1.4(18)

Atom	U_{11}	U_{22}	U_{33}	U_{23}	U_{13}	U_{12}
C22A	27.3(16)	45(2)	43(3)	0(2)	16(4)	0(3)
C23A	25(2)	69(4)	36(3)	6(2)	5.5(19)	-3(2)
C24A	28(2)	42(3)	68(3)	-11(3)	25(3)	1.8(19)
O7A	35.8(15)	33.0(14)	22.3(13)	3.4(12)	14.5(12)	7.6(13)
C25A	44.6(19)	22(3)	26.2(15)	3.1(18)	21.0(14)	9(2)
C26A	41(2)	60(3)	32(3)	1(2)	28.1(19)	-1.0(19)
C27A	65(4)	42(3)	37(3)	-4(2)	24(2)	9(3)
C28A	63(4)	51(2)	24(4)	9(2)	31(3)	7(2)
O9A	42.0(17)	30.7(15)	27.5(14)	0.3(12)	18.0(13)	3.9(13)
C33A	36(4)	27.4(18)	34(2)	1.9(16)	20(3)	10(2)
C34A	50(4)	36(2)	41(4)	-6(3)	16(3)	-4(2)
C35A	62(3)	41(2)	41(3)	3(2)	29(2)	17(2)
C36A	71(5)	38(3)	42(4)	12(2)	30(3)	15(3)
O8A	27.7(16)	46(3)	21.0(18)	1.1(15)	6.6(12)	3.9(16)
C29A	27.8(17)	32(6)	27(2)	-2(3)	-0.1(16)	9(2)
C30A	44(6)	53(6)	42(2)	-18(4)	-11(4)	4(4)
C31A	41(3)	73(6)	29(3)	14(3)	1(2)	12(4)
C32A	8(5)	65(4)	44(2)	-2(3)	-1(4)	1(5)
C21B	16.9(15)	40(3)	32(4)	2(3)	10(3)	1.4(18)
C22B	27.3(16)	45(2)	43(3)	0(2)	16(4)	0(3)
C23B	25(2)	69(4)	36(3)	6(2)	5.5(19)	-3(2)
C24B	28(2)	42(3)	68(3)	-11(3)	25(3)	1.8(19)
O7B	35.8(15)	33.0(14)	22.3(13)	3.4(12)	14.5(12)	7.6(13)
C25B	44.6(19)	22(3)	26.2(15)	3.1(18)	21.0(14)	9(2)
C26B	41(2)	60(3)	32(3)	1(2)	28.1(19)	-1.0(19)
C27B	65(4)	42(3)	37(3)	-4(2)	24(2)	9(3)
C28B	63(4)	51(2)	24(4)	9(2)	31(3)	7(2)
O9B	42.0(17)	30.7(15)	27.5(14)	0.3(12)	18.0(13)	3.9(13)
C33B	36(4)	27.4(18)	34(2)	1.9(16)	20(3)	10(2)
C34B	50(4)	36(2)	41(4)	-6(3)	16(3)	-4(2)
C35B	62(3)	41(2)	41(3)	3(2)	29(2)	17(2)
C36B	71(5)	38(3)	42(4)	12(2)	30(3)	15(3)
O8B	27.7(16)	46(3)	21.0(18)	1.1(15)	6.6(12)	3.9(16)
C29B	27.8(17)	32(6)	27(2)	-2(3)	-0.1(16)	9(2)
C31B	41(3)	73(6)	29(3)	14(3)	1(2)	12(4)
C32B	8(5)	65(4)	44(2)	-2(3)	-1(4)	1(5)
C30B	44(6)	53(6)	42(2)	-18(4)	-11(4)	4(4)

Table 3.11 Bond Lengths for 1.

Atom	Atom	Length/Å	Atom	Atom	Length/Å

Cu1	Cl1	2.1601(11)	C9	C11	1.543(5)
Cu1	Si2	2.8572(13)	C9	C12	1.532(5)
Cu1	N1	1.909(2)	C13	C14	1.532(5)
Cu2	Cl1	2.1667(13)	C13	C15	1.535(4)
Cu2	N2	1.919(3)	C13	C16	1.543(5)
K1	Cl1[1]	3.4565(17)	C17	C18	1.535(5)
K1	Si2	3.5659(16)	C17	C19	1.531(4)
K1	Si4[1]	3.6012(18)	C17	C20	1.539(5)
K1	O4	2.781(2)	C37	C38	1.527(5)
K1	O5	2.761(3)	C37	C39	1.537(5)
K1	O10[1]	2.757(2)	C37	C40	1.535(5)
K1	O11[1]	2.847(3)	C41	C42	1.535(5)
Si1	O1	1.650(2)	C41	C43	1.535(4)
Si1	O2	1.652(2)	C41	C44	1.539(5)
Si1	O3	1.655(2)	C45	C46	1.531(6)
Si1	N1	1.689(3)	C45	C47	1.539(6)
Si2	O4	1.682(2)	C45	C48	1.534(5)
Si2	O5	1.661(2)	C21A	C22A	1.545(5)
Si2	O6	1.651(2)	C21A	C23A	1.524(7)
Si2	N1	1.690(3)	C21A	C24A	1.521(7)
Si3	N2	1.687(3)	O7A	C25A	1.439(5)
Si3	O7A	1.604(4)	C25A	C26A	1.542(5)
Si3	O9A	1.773(4)	C25A	C27A	1.535(7)
Si3	O8A	1.650(5)	C25A	C28A	1.540(6)
Si3	O7B	1.722(4)	O9A	C33A	1.451(5)
Si3	O9B	1.578(4)	C33A	C34A	1.530(7)
Si3	O8B	1.591(5)	C33A	C35A	1.538(7)
Si4	O10	1.682(3)	C33A	C36A	1.538(6)
Si4	O11	1.679(2)	O8A	C29A	1.450(4)
Si4	O12	1.652(2)	C29A	C30A	1.534(13)
Si4	N2	1.672(3)	C29A	C31A	1.549(16)
O1	C1	1.464(4)	C29A	C32A	1.53(2)
O2	C5	1.448(4)	C21B	C22B	1.545(5)
O3	C9	1.449(3)	C21B	C23B	1.524(7)
O4	C13	1.466(3)	C21B	C24B	1.521(7)
O5	C17	1.469(4)	O7B	C25B	1.439(5)
O6	C21A	1.477(14)	C25B	C26B	1.541(5)
O6	C21B	1.466(10)	C25B	C27B	1.535(7)
O10	C37	1.467(4)	C25B	C28B	1.539(6)
O11	C41	1.463(4)	O9B	C33B	1.451(5)
O12	C45	1.463(4)	C33B	C34B	1.531(7)
C1	C2	1.539(5)	C33B	C35B	1.538(7)

C1	C3	1.526(5)	C33B	C36B	1.538(6)
C1	C4	1.513(5)	O8B	C29B	1.450(4)
C5	C6	1.534(6)	C29B	C31B	1.534(13)
C5	C7	1.532(5)	C29B	C32B	1.550(16)
C5	C8	1.531(5)	C29B	C30B	1.542(13)
C9	C10	1.523(5)			

Table 3.12 Bond Angles for 1.

Atom	Atom	Atom	Angle/°	Atom	Atom	Atom	Angle/°
Cl1	Cu1	Si2	145.18(4)	O1	C1	C4	110.9(3)
N1	Cu1	Cl1	173.10(8)	C3	C1	C2	109.1(3)
N1	Cu1	Si2	34.85(8)	C4	C1	C2	110.4(3)
N2	Cu2	Cl1	163.75(8)	C4	C1	C3	111.1(3)
$Cl1^1$	K1	$Cu2^1$	34.33(2)	O2	C5	C6	105.2(3)
$Cl1^1$	K1	Si2	122.53(4)	O2	C5	C7	110.4(3)
$Cl1^1$	K1	$Si4^1$	78.55(3)	O2	C5	C8	110.3(3)
Si2	K1	$Cu2^1$	149.32(3)	C7	C5	C6	110.1(3)
Si2	K1	$Si4^1$	148.68(3)	C8	C5	C6	110.5(3)
$Si4^1$	K1	$Cu2^1$	44.311(16)	C8	C5	C7	110.4(3)
O4	K1	$Cu2^1$	160.47(5)	O3	C9	C10	112.4(2)
O4	K1	$Cl1^1$	149.42(6)	O3	C9	C11	107.9(3)
O4	K1	Si2	27.32(5)	O3	C9	C12	104.8(2)
O4	K1	$Si4^1$	126.28(5)	C10	C9	C11	111.0(3)
O4	K1	$O11^1$	129.29(7)	C10	C9	C12	109.5(3)
O5	K1	$Cu2^1$	123.34(5)	C12	C9	C11	111.1(3)
O5	K1	$Cl1^1$	96.40(5)	O4	C13	C14	111.5(3)
O5	K1	Si2	26.77(4)	O4	C13	C15	107.3(2)
O5	K1	$Si4^1$	148.45(5)	O4	C13	C16	106.7(2)
O5	K1	O4	53.02(6)	C14	C13	C15	110.9(3)
O5	K1	$O11^1$	175.23(6)	C14	C13	C16	110.7(3)
$O10^1$	K1	$Cu2^1$	56.72(5)	C15	C13	C16	109.6(3)
$O10^1$	K1	$Cl1^1$	88.38(5)	O5	C17	C18	107.5(2)
$O10^1$	K1	Si2	123.65(6)	O5	C17	C19	106.2(2)
$O10^1$	K1	$Si4^1$	26.69(5)	O5	C17	C20	111.7(2)
$O10^1$	K1	O4	107.33(7)	C18	C17	C20	110.8(3)
$O10^1$	K1	O5	123.41(7)	C19	C17	C18	110.0(3)
$O10^1$	K1	$O11^1$	52.66(7)	C19	C17	C20	110.5(3)
$O11^1$	K1	$Cu2^1$	52.84(4)	O10	C37	C38	105.7(3)
$O11^1$	K1	$Cl1^1$	81.15(5)	O10	C37	C39	109.3(2)
$O11^1$	K1	Si2	156.24(5)	O10	C37	C40	111.2(3)
$O11^1$	K1	$Si4^1$	27.10(5)	C38	C37	C39	110.0(4)

Atom	Atom	Atom	Angle/°	Atom	Atom	Atom	Angle/°
Cu1	Cl1	Cu2	117.04(4)	C38	C37	C40	110.0(3)
Cu1	Cl1	K1[2]	158.64(4)	C40	C37	C39	110.6(3)
Cu2	Cl1	K1[2]	81.53(3)	O11	C41	C42	108.4(3)
O1	Si1	O2	103.84(12)	O11	C41	C43	105.9(3)
O1	Si1	O3	112.35(12)	O11	C41	C44	112.8(2)
O1	Si1	N1	115.68(13)	C42	C41	C43	109.3(3)
O2	Si1	O3	104.02(12)	C42	C41	C44	109.7(3)
O2	Si1	N1	114.91(12)	C43	C41	C44	110.5(3)
O3	Si1	N1	105.62(12)	O12	C45	C46	108.8(3)
O4	Si2	N1	118.28(12)	O12	C45	C47	110.9(3)
O5	Si2	O4	95.45(11)	O12	C45	C48	106.2(3)
O5	Si2	N1	117.62(12)	C46	C45	C47	111.0(3)
O6	Si2	O4	111.59(12)	C46	C45	C48	109.8(3)
O6	Si2	O5	111.12(12)	C48	C45	C47	110.1(3)
O6	Si2	N1	103.05(13)	O6	C21A	C22A	108.1(14)
N2	Si3	O9A	114.41(16)	O6	C21A	C23A	106.0(8)
N2	Si3	O7B	104.22(16)	O6	C21A	C24A	111.5(8)
O7A	Si3	N2	120.75(18)	C23A	C21A	C22A	109.9(5)
O7A	Si3	O9A	100.2(2)	C24A	C21A	C22A	111.1(5)
O7A	Si3	O8A	110.6(2)	C24A	C21A	C23A	110.2(4)
O8A	Si3	N2	108.3(2)	C25A	O7A	Si3	136.1(4)
O8A	Si3	O9A	100.7(3)	O7A	C25A	C26A	110.0(3)
O9B	Si3	N2	115.36(18)	O7A	C25A	C27A	108.5(4)
O9B	Si3	O7B	103.63(19)	O7A	C25A	C28A	107.3(4)
O9B	Si3	O8B	117.8(2)	C27A	C25A	C26A	110.7(4)
O8B	Si3	N2	109.35(18)	C27A	C25A	C28A	110.8(4)
O8B	Si3	O7B	104.7(2)	C28A	C25A	C26A	109.4(4)
Cu2	Si4	K1[2]	71.61(4)	C33A	O9A	Si3	131.8(4)
O10	Si4	Cu2	89.33(9)	O9A	C33A	C34A	109.9(4)
O10	Si4	K1[2]	47.42(8)	O9A	C33A	C35A	107.9(4)
O11	Si4	Cu2	82.84(8)	O9A	C33A	C36A	108.3(4)
O11	Si4	K1[2]	50.55(8)	C34A	C33A	C35A	110.4(4)
O11	Si4	O10	95.42(12)	C34A	C33A	C36A	110.7(5)
O12	Si4	Cu2	153.06(9)	C36A	C33A	C35A	109.6(4)
O12	Si4	K1[2]	135.16(9)	C29A	O8A	Si3	138.6(7)
O12	Si4	O10	111.21(12)	O8A	C29A	C30A	109.8(7)
O12	Si4	O11	111.09(12)	O8A	C29A	C31A	108.4(9)
O12	Si4	N2	111.28(13)	O8A	C29A	C32A	106.9(8)
N2	Si4	Cu2	42.14(9)	C30A	C29A	C31A	110.5(7)
N2	Si4	K1[2]	113.56(10)	C30A	C29A	C32A	112.3(10)
N2	Si4	O10	114.79(13)	C32A	C29A	C31A	108.7(11)

Atom	Atom	Atom	Angle/°	Atom	Atom	Atom	Angle/°
N2	Si4	O11	112.14(12)	O6	C21B	C22B	108.3(11)
C1	O1	Si1	139.2(2)	O6	C21B	C23B	115.6(6)
C5	O2	Si1	134.9(2)	O6	C21B	C24B	101.7(6)
C9	O3	Si1	134.23(18)	C23B	C21B	C22B	109.8(4)
Si2	O4	K1	103.31(9)	C24B	C21B	C22B	111.1(4)
C13	O4	K1	117.60(18)	C24B	C21B	C23B	110.1(4)
C13	O4	Si2	133.0(2)	C25B	O7B	Si3	133.3(3)
Si2	O5	K1	104.74(10)	O7B	C25B	C26B	110.2(3)
C17	O5	K1	120.10(17)	O7B	C25B	C27B	107.8(4)
C17	O5	Si2	131.3(2)	O7B	C25B	C28B	107.9(4)
C21A	O6	Si2	148.7(4)	C27B	C25B	C26B	110.8(4)
C21B	O6	Si2	134.1(3)	C27B	C25B	C28B	110.8(4)
Si4	O10	$K1^2$	105.89(10)	C28B	C25B	C26B	109.4(4)
C37	O10	$K1^2$	117.6(2)	C33B	O9B	Si3	136.6(3)
C37	O10	Si4	130.17(19)	O9B	C33B	C34B	109.8(4)
Si4	O11	$K1^2$	102.35(10)	O9B	C33B	C35B	108.5(4)
C41	O11	$K1^2$	123.93(18)	O9B	C33B	C36B	107.8(4)
C41	O11	Si4	129.8(2)	C34B	C33B	C35B	110.3(4)
C45	O12	Si4	135.6(2)	C34B	C33B	C36B	110.8(5)
Si3	N2	Cu2	110.51(13)	C36B	C33B	C35B	109.6(4)
Si4	N2	Cu2	102.08(13)	C29B	O8B	Si3	133.7(6)
Si4	N2	Si3	142.48(16)	O8B	C29B	C31B	110.6(7)
Si1	N1	Cu1	117.18(14)	O8B	C29B	C32B	107.7(9)
Si1	N1	Si2	133.53(16)	O8B	C29B	C30B	106.9(6)
Si2	N1	Cu1	104.94(13)	C31B	C29B	C32B	110.4(7)
O1	C1	C2	105.8(3)	C31B	C29B	C30B	111.5(9)
O1	C1	C3	109.4(3)	C30B	C29B	C32B	109.6(8)

Table 3.13 Hydrogen Atom Coordinates (Å×10^4) and Isotropic Displacement Parameters (Å^2×10^3) for 1.

Atom	*x*	*y*	*z*	U(eq)
H2A	10581.13	4133.69	7885.03	76
H2B	10302.36	4726.73	7292.03	76
H2C	10496.18	4006.85	7052.69	76
H3A	8748.2	4207.7	7563.59	80
H3B	9205.32	4859.32	7555.4	80
H3C	9523.7	4299.2	8181.11	80
H4A	9318.55	3893.13	6072.51	84
H4B	9067.79	4605.44	6268.76	84
H4C	8621.23	3938.95	6249.67	84

Atom	*x*	*y*	*z*	U(eq)
H6A	9302.97	1371.52	8858.89	83
H6B	10055.59	1526.4	9493.11	83
H6C	10010.28	1162.05	8751.13	83
H7A	10816.18	2041.62	8638.41	76
H7B	10808	2494.91	9307.54	76
H7C	10571.74	2813.28	8501.82	76
H8A	9433.1	3154.12	8662.57	80
H8B	9674.62	2764.89	9432	80
H8C	8941.49	2578.12	8782.68	80
H10A	10542.78	1942.43	7359.94	79
H10B	10711.47	1407.76	6840.56	79
H10C	10110.8	1249.94	7149.08	79
H11A	9753.87	2755.13	5612.44	72
H11B	10506.8	2390.02	5916.99	72
H11C	10289.26	2878.37	6442.34	72
H12A	9289.58	1042.91	5855.55	59
H12B	9870.04	1254.67	5537.22	59
H12C	9123.69	1631.52	5256.58	59
H14A	8148.16	1699.41	7811.26	57
H14B	7872.07	1040.84	8088.49	57
H14C	7322.19	1599.46	7615.89	57
H15A	8338.93	437.58	6596.21	61
H15B	8566.82	380.2	7467.64	61
H15C	8750.2	1046.69	7117.8	61
H16A	6684.89	638.87	6786.96	66
H16B	7285.23	89.29	7169.4	66
H16C	7048.98	250.85	6311.94	66
H18A	8410.68	2925.89	5286.91	55
H18B	8044.32	3245.23	4482.72	55
H18C	8093.35	2443.54	4584.53	55
H19A	6812.51	2259.83	3976.02	63
H19B	6713.37	3046.74	3782.54	63
H19C	6272.08	2697.01	4202.89	63
H20A	6711.49	3545.43	5202.92	53
H20B	7195.82	3912.1	4842.53	53
H20C	7539.44	3631.97	5666.48	53
H38A	6095.94	4001.99	9991.67	110
H38B	5274.74	4189.12	9657.05	110
H38C	5832.35	4696.68	10213.31	110
H39A	5758.4	4451.36	8115.11	62
H39B	5242.52	4026.69	8389.66	62

Atom	*x*	*y*	*z*	U(eq)
H39C	6067.14	3854.93	8698.4	62
H40A	5423.47	5632.29	9324.51	67
H40B	4852.27	5159.96	8733.01	67
H40C	5421.02	5559.38	8514.18	67
H42A	8807.36	4616.34	9531.58	63
H42B	9258.23	5193.11	9344.46	63
H42C	8483.52	5013.72	8767.21	63
H43A	8750.66	5992.77	10693.44	70
H43B	9419.47	5821.86	10495.54	70
H43C	9006.67	5228.13	10711.69	70
H44A	8074.92	6195.94	8722.05	62
H44B	8847.17	6416.75	9272.24	62
H44C	8175.71	6591.43	9464.1	62
H46A	7921.35	6860.18	10472.42	96
H46B	7475.55	7388.72	10733.77	96
H46C	7443.36	7413.35	9909.2	96
H47A	6535.89	5789.55	10509.25	95
H47B	6976.82	6317.29	11130.37	95
H47C	7374.67	5833.44	10763.51	95
H48A	6121.37	7368.05	9541.68	69
H48B	6173.52	7234.92	10362.5	69
H48C	5765.23	6710.44	9722.76	69
H22A	6013.63	1616.09	6115.04	57
H22B	5393.83	1875.01	6353.74	57
H22C	6169.04	1758.13	6963.02	57
H23A	5775.41	3356.83	5533.77	68
H23B	5157.93	2843.37	5486.79	68
H23C	5775.3	2606.98	5232.85	68
H24A	6229.46	2933.01	7417.99	66
H24B	5462.01	3113.33	6825.51	66
H24C	6128.07	3560.59	6875.78	66
H26A	7827.64	6327.47	7063.92	60
H26B	8041.21	5697.08	6685.17	60
H26C	7866.34	5587.83	7402.71	60
H27A	6922.91	4760.93	6834.64	71
H27B	7065.15	4770.6	6090.47	71
H27C	6289.46	4914.09	6066.92	71
H28A	6295.67	6007.72	5396.82	63
H28B	7092.3	5895.05	5471.15	63
H28C	6881.42	6567.81	5787.49	63
H34A	6896.32	7211.62	8364.64	64

Atom	*x*	*y*	*z*	U(eq)
H34B	6864.66	7870.91	7884.09	64
H34C	7018.12	7149.74	7611.54	64
H35A	5037	7613.21	7528.62	68
H35B	5643.73	8174.45	7776.35	68
H35C	5677.35	7555.9	8310.92	68
H36A	5978.54	7192.22	6396.6	72
H36B	5882.28	7955.61	6605.45	72
H36C	5231.76	7442.36	6381.54	72
H30A	4937.12	4363.41	6050.92	82
H30B	4145.88	4539.63	5955.76	82
H30C	4700.07	4279.83	6731.64	82
H31A	4977.34	6169.58	6011.02	77
H31B	4383.86	5682.62	5467.78	77
H31C	5200.55	5513.75	5677.93	77
H32A	4412.63	5387.35	7302.47	63
H32B	3891.7	5612.81	6496.46	63
H32C	4527.99	6094.93	6973.55	63
H22D	6061.17	1549.15	6427.71	57
H22E	5393.77	1953.88	6446.8	57
H22F	6149.45	2043.75	7099.58	57
H23D	5791.66	2834.58	5059.63	68
H23E	5217.7	2359.72	5186.15	68
H23F	5938.37	2043.35	5195.31	68
H24D	6035.33	3302.32	6875.12	66
H24E	5304.93	3224.64	6183.32	66
H24F	5956.88	3600.28	6092.27	66
H26D	7593.62	6224.91	7272.82	60
H26E	8033.62	5887.25	6844.07	60
H26F	7868.84	5464.95	7452.41	60
H27D	7326.86	4551.85	6510.18	71
H27E	7447.25	4976.71	5877.07	71
H27F	6672.61	4722.48	5764.74	71
H28D	6239.7	5936.73	5505.22	63
H28E	7020.68	6188.28	5640.86	63
H28F	6605.68	6507.32	6105.67	63
H34D	7015.83	7115.54	8599.25	64
H34E	6850.89	7891.45	8375.27	64
H34F	7301.73	7453.31	8028.6	64
H35D	5180.25	7091.19	7407.18	68
H35E	5585.49	7580.37	8084.57	68
H35F	5715.29	6783.38	8167.9	68

Atom	*x*	*y*	*z*	U(eq)
H36D	6406.81	7778.23	6741.46	72
H36E	5979.99	8203.51	7126.19	72
H36F	5588.33	7627.34	6543.3	72
H31D	4814.71	6463.17	6231.91	77
H31E	4375.08	5953.33	5589.48	77
H31F	5218.7	5955.12	5895.74	77
H32D	4213.25	5223.31	7198.34	63
H32E	3751.22	5491.67	6389.54	63
H32F	4186.13	6013	7021.22	63
H30D	5268.45	4703.63	6202.87	82
H30E	4424.63	4680.95	5876.75	82
H30F	4863.38	4432.68	6699.8	82

Table 3.14 Atomic Occupancy for 1.

Atom	*Occupancy*	Atom	*Occupancy*	Atom	*Occupancy*
C21A	0.444(5)	C22A	0.444(5)	H22A	0.444(5)
H22B	0.444(5)	H22C	0.444(5)	C23A	0.444(5)
H23A	0.444(5)	H23B	0.444(5)	H23C	0.444(5)
C24A	0.444(5)	H24A	0.444(5)	H24B	0.444(5)
H24C	0.444(5)	O7A	0.472(3)	C25A	0.472(3)
C26A	0.472(3)	H26A	0.472(3)	H26B	0.472(3)
H26C	0.472(3)	C27A	0.472(3)	H27A	0.472(3)
H27B	0.472(3)	H27C	0.472(3)	C28A	0.472(3)
H28A	0.472(3)	H28B	0.472(3)	H28C	0.472(3)
O9A	0.481(3)	C33A	0.481(3)	C34A	0.481(3)
H34A	0.481(3)	H34B	0.481(3)	H34C	0.481(3)
C35A	0.481(3)	H35A	0.481(3)	H35B	0.481(3)
H35C	0.481(3)	C36A	0.481(3)	H36A	0.481(3)
H36B	0.481(3)	H36C	0.481(3)	O8A	0.463(4)
C29A	0.463(4)	C30A	0.463(4)	H30A	0.463(4)
H30B	0.463(4)	H30C	0.463(4)	C31A	0.463(4)
H31A	0.463(4)	H31B	0.463(4)	H31C	0.463(4)
C32A	0.463(4)	H32A	0.463(4)	H32B	0.463(4)
H32C	0.463(4)	C21B	0.556(5)	C22B	0.556(5)
H22D	0.556(5)	H22E	0.556(5)	H22F	0.556(5)
C23B	0.556(5)	H23D	0.556(5)	H23E	0.556(5)
H23F	0.556(5)	C24B	0.556(5)	H24D	0.556(5)
H24E	0.556(5)	H24F	0.556(5)	O7B	0.528(3)
C25B	0.528(3)	C26B	0.528(3)	H26D	0.528(3)
H26E	0.528(3)	H26F	0.528(3)	C27B	0.528(3)

Atom	*Occupancy*	Atom	*Occupancy*	Atom	*Occupancy*
H27D	0.528(3)	H27E	0.528(3)	H27F	0.528(3)
C28B	0.528(3)	H28D	0.528(3)	H28E	0.528(3)
H28F	0.528(3)	O9B	0.519(3)	C33B	0.519(3)
C34B	0.519(3)	H34D	0.519(3)	H34E	0.519(3)
H34F	0.519(3)	C35B	0.519(3)	H35D	0.519(3)
H35E	0.519(3)	H35F	0.519(3)	C36B	0.519(3)
H36D	0.519(3)	H36E	0.519(3)	H36F	0.519(3)
O8B	0.537(4)	C29B	0.537(4)	C31B	0.537(4)
H31D	0.537(4)	H31E	0.537(4)	H31F	0.537(4)
C32B	0.537(4)	H32D	0.537(4)	H32E	0.537(4)
H32F	0.537(4)	C30B	0.537(4)	H30D	0.537(4)
H30E	0.537(4)	H30F	0.537(4)		

Table 3.15 Solvent masks information for 1.

Number	X	Y	Z	Volume	Electron count	Content
1	0.000	0.000	0.000	619.8	97.0	?
2	0.000	0.500	0.500	619.8	97.0	?

3.5.3 *2-Sm*

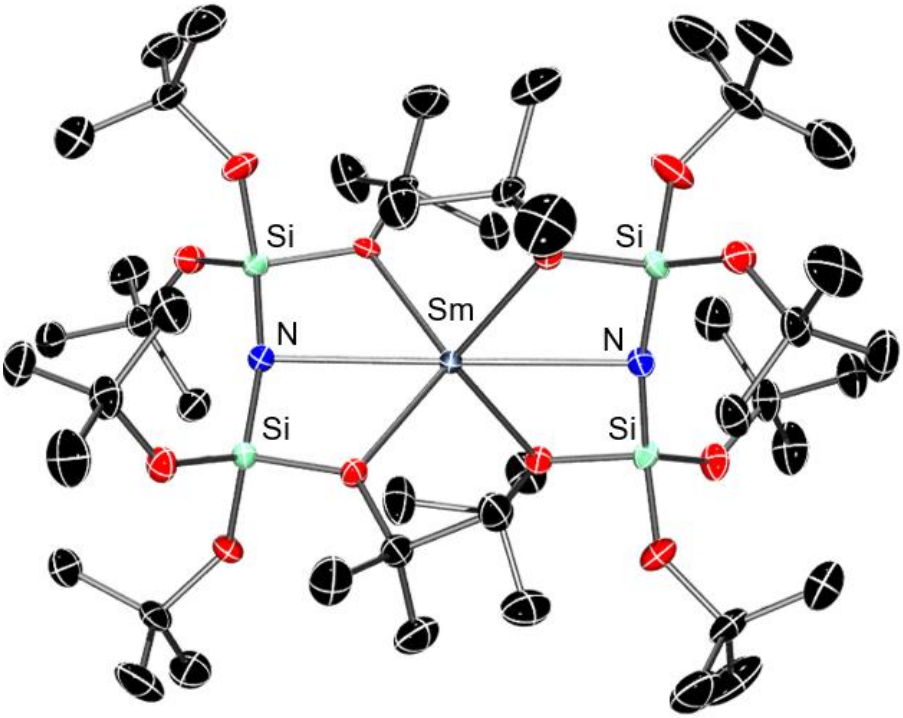

Figure 3.22 Molecular structure of 2-Sm. Thermal ellipsoids are shown at 50% probability and H atoms are omitted for clarity.

Table 3.16 Crystal data and structure refinement for 2-Sm.

Identification code	2-Sm
Empirical formula	$C_{2.34}H_{5.27}N_{0.1}O_{0.59}Si_{0.2}Sm_{0.05}$
Formula weight	56.98
Temperature/K	106.92
Crystal system	monoclinic
Space group	$P2_1/n$
a/Å	21.438(5)
b/Å	15.090(3)
c/Å	21.412(4)
α/°	90
β/°	111.444(6)
γ/°	90
Volume/Å^3	6447(2)
Z	82

ρ_{calc}g/cm^3	1.203
μ/mm^{-1}	1.035
F(000)	2496.0
Crystal size/mm^3	0.158 × 0.126 × 0.109
Radiation	MoKα (λ = 0.71073)
2Θ range for data collection/°	4.694 to 56.564
Index ranges	-28 ≤ h ≤ 28, -20 ≤ k ≤ 20, -28 ≤ l ≤ 28
Reflections collected	85838
Independent reflections	15980 [R_{int} = 0.1689, R_{sigma} = 0.1267]
Data/restraints/parameters	15980/60/679
Goodness-of-fit on F^2	1.010
Final R indexes [I>=2σ (I)]	R_1 = 0.0714, wR_2 = 0.1099
Final R indexes [all data]	R_1 = 0.1395, wR_2 = 0.1360
Largest diff. peak/hole / e Å^{-3}	1.34/-1.44

Table 3.17 Fractional Atomic Coordinates (×104) and Equivalent Isotropic Displacement Parameters (Å2×103) for 2-Sm. Ueq is defined as 1/3 of the trace of the orthogonalised UIJ tensor.

Atom	*x*	*y*	*z*	U(eq)
Sm1	5021.2(2)	6202.6(2)	7472.7(2)	19.38(9)
Si1	4146.1(9)	4341.0(11)	7284.0(8)	23.1(4)
Si2	5775.5(9)	4287.4(11)	7996.4(8)	22.9(4)
Si3	4813.2(8)	7928.1(11)	6469.8(8)	20.8(4)
Si4	5367.0(8)	8241.4(11)	8087.0(8)	21.2(4)
O2	3855(2)	4029(3)	6502(2)	47.6(14)
O3	3712.3(19)	3781(3)	7631.6(19)	30.2(10)
O4	6061.1(19)	5233(3)	7776(2)	23.4(9)
O5	6163(2)	3453(3)	7812(2)	31.4(10)
O6	6071(2)	4331(3)	8820(2)	31.2(10)
O8	4010(2)	8098(3)	6082(2)	30.5(10)
O9	5170(2)	8494(3)	6040.4(19)	25.4(9)
O10	5224.7(19)	7288(3)	8433.9(18)	21.8(9)
O11	6180(2)	8386(3)	8434.7(19)	24.7(9)
O12	5057(2)	9069(3)	8370.5(19)	25.9(9)
N1	4962(2)	4424(3)	7638(2)	22.0(11)
N2	5081(2)	7972(3)	7291(2)	21.5(11)
C00K	5382(3)	7018(4)	9126(3)	30.4(15)
C00L	6640(3)	9096(4)	8763(3)	28.1(14)
C00N	6720(3)	5544(5)	7824(3)	31.8(16)
C00O	4250(3)	4062(4)	8831(3)	34.6(16)
C00P	4445(3)	9563(4)	8149(3)	31.9(15)

Atom	*x*	*y*	*z*	U(eq)
C00Q	3844(3)	3424(4)	8289(3)	29.7(15)
C00R	4999(3)	6161(4)	9090(3)	36.0(16)
C00S	3586(3)	8732(5)	5618(3)	33.1(15)
C00T	5537(3)	2108(4)	7416(3)	37.5(17)
C00U	5994(3)	2808(4)	7287(3)	32.2(15)
C00V	6386(4)	3740(5)	9382(3)	38.1(16)
C00W	6365(3)	8471(4)	6712(3)	33.9(16)
C00X	6644(4)	6521(5)	7677(4)	51(2)
C00Y	3450(4)	3332(5)	6094(3)	41.0(18)
C01A	5176(4)	7710(5)	9511(3)	48(2)
C01B	5909(3)	9013(5)	5526(3)	40.3(18)
C01C	6136(3)	6797(5)	9445(3)	45.7(19)
C01D	3725(4)	9664(5)	5911(4)	50(2)
C01E	4205(4)	2547(4)	8340(4)	50(2)
C01F	3691(4)	8703(5)	4944(3)	51(2)
C01G	7250(4)	5335(6)	8487(4)	57(2)
C01H	2877(3)	8452(5)	5519(4)	57(2)
C01I	5989(4)	2898(5)	9295(4)	56(2)
C01J	6374(4)	4247(6)	9989(3)	59(2)
C01K	6914(4)	5086(5)	7277(4)	52(2)
C01L	6583(4)	9326(5)	9432(3)	49(2)
C01M	4381(4)	9957(5)	8779(4)	50(2)
C01N	3156(4)	3275(6)	8331(4)	62(3)
C01O	3785(5)	2453(6)	6286(5)	85(3)
C01P	3363(5)	3591(7)	5381(4)	80(3)
C01Q	2761(4)	3298(6)	6147(4)	71(3)
C01R	7101(4)	3544(7)	9446(4)	79(3)
C010	3847(3)	8958(5)	7786(4)	40.4(18)
C011	5648(4)	3234(5)	6600(3)	44.7(19)
C012	5796(3)	8957(4)	6187(3)	30.4(15)
C014	5709(4)	9891(4)	6423(3)	39.2(17)
C015	4504(4)	10297(4)	7681(4)	44.2(19)
C016	6663(4)	2379(5)	7334(4)	53(2)
C017	6487(3)	9912(4)	8307(3)	39.9(17)
C018	7329(3)	8732(5)	8861(4)	46.0(19)
O1A	3915(3)	5411(3)	7263(14)	33.2(11)
C1A	3280(5)	5855(7)	7143(8)	39(2)
C2A	3400(10)	6820(7)	7025(14)	49(3)
C3A	3067(11)	5751(17)	7740(10)	54(3)
C4A	2749(10)	5474(17)	6519(10)	64(3)
O1B	3912(2)	5411(3)	7247(6)	33.2(11)

Atom	*x*	*y*	*z*	U(eq)
C1B	3281(3)	5892(4)	7019(4)	39(2)
C2B	3446(5)	6806(5)	7329(6)	49(3)
C3B	2770(5)	5429(7)	7241(6)	54(3)
C4B	3018(5)	5969(8)	6261(4)	64(3)
O7A	4905(7)	6833(3)	6340(3)	25.5(10)
C25A	4882(5)	6310(5)	5766(3)	32.0(19)
C26A	4875(7)	5347(5)	5975(5)	33(3)
C27A	5503(6)	6484(8)	5598(6)	52(3)
C28A	4247(7)	6508(9)	5165(6)	58(4)
O7B	4891(10)	6831(3)	6336(4)	25.5(10)
C25B	4747(6)	6316(6)	5729(4)	32.0(19)
C26B	5096(9)	5429(6)	5952(7)	33(3)
C27B	5030(10)	6775(10)	5257(6)	52(3)
C28B	3995(7)	6168(14)	5386(9)	58(4)

Table 3.18 Anisotropic Displacement Parameters ($Å^2×10^3$) for 2-Sm. The Anisotropic displacement factor exponent takes the form: $-2\pi^2[h^2a^{*2}U_{11}+2hka^*b^*U_{12}+\ldots]$.

Atom	U_{11}	U_{22}	U_{33}	U_{23}	U_{13}	U_{12}
Sm1	20.57(14)	17.77(14)	19.20(14)	0.63(15)	6.55(11)	-0.23(15)
Si1	23.3(9)	21.9(9)	22.9(8)	-0.3(7)	7.1(7)	-3.6(7)
Si2	23.8(9)	21.5(9)	24.9(8)	3.8(7)	10.9(8)	3.0(7)
Si3	21.6(9)	20.8(9)	19.2(8)	1.6(7)	6.4(7)	-1.5(7)
Si4	23.4(9)	18.9(8)	21.5(8)	0.9(7)	8.6(7)	-0.4(7)
O2	52(3)	64(4)	26(2)	-17(2)	14(2)	-35(3)
O3	24(2)	39(3)	28(2)	9(2)	8.8(19)	-8(2)
O4	19(2)	20(2)	30(2)	2.1(18)	7.2(19)	-2.0(18)
O5	32(3)	22(2)	43(3)	1(2)	17(2)	7(2)
O6	31(3)	37(3)	25(2)	10(2)	10(2)	5(2)
O8	21(2)	36(3)	29(2)	15(2)	2.4(19)	4(2)
O9	29(2)	28(2)	22(2)	4.6(18)	11.7(19)	-2.9(19)
O10	27(2)	23(2)	17.0(19)	4.6(17)	9.5(18)	2.1(18)
O11	23(2)	21(2)	26(2)	-3.4(18)	5.2(19)	-6.0(18)
O12	32(2)	18(2)	30(2)	-2.0(18)	14(2)	4.3(18)
N1	23(3)	16(2)	27(3)	1(2)	9(2)	2(2)
N2	20(3)	23(3)	19(2)	2(2)	4(2)	-1(2)
C00K	38(4)	32(4)	18(3)	5(3)	7(3)	-5(3)
C00L	23(3)	33(4)	24(3)	2(3)	2(3)	-5(3)
C00N	16(3)	40(4)	41(4)	10(3)	13(3)	1(3)
C00O	47(4)	28(4)	35(4)	-2(3)	23(3)	-1(3)
C00P	39(4)	20(3)	45(4)	1(3)	26(4)	5(3)

Atom	U_{11}	U_{22}	U_{33}	U_{23}	U_{13}	U_{12}
C00Q	35(4)	30(4)	27(3)	3(3)	14(3)	-9(3)
C00R	49(4)	32(4)	28(3)	7(3)	15(3)	-13(4)
C00S	26(3)	34(4)	30(3)	12(3)	0(3)	7(3)
C00T	40(4)	25(4)	49(4)	2(3)	18(4)	2(3)
C00U	41(4)	21(3)	39(4)	-4(3)	19(3)	0(3)
C00V	42(4)	43(4)	31(3)	13(3)	16(3)	5(4)
C00W	33(4)	28(4)	38(4)	4(3)	10(3)	0(3)
C00X	32(4)	39(5)	83(6)	18(4)	20(4)	0(3)
C00Y	40(4)	44(5)	35(4)	-19(3)	8(3)	-21(4)
C01A	85(6)	36(4)	33(4)	4(3)	32(4)	2(4)
C01B	44(4)	43(5)	42(4)	13(3)	25(4)	-8(3)
C01C	38(4)	59(5)	37(4)	14(4)	10(4)	-2(4)
C01D	54(5)	37(5)	52(5)	-2(4)	11(4)	2(4)
C01E	80(6)	25(4)	41(4)	-6(3)	18(4)	-5(4)
C01F	64(5)	51(5)	28(3)	16(4)	6(4)	6(4)
C01G	29(4)	86(7)	51(5)	18(5)	7(4)	-3(4)
C01H	27(4)	60(6)	69(6)	16(5)	1(4)	1(4)
C01I	66(6)	45(5)	59(5)	24(4)	24(5)	5(4)
C01J	68(6)	66(6)	34(4)	18(4)	7(4)	9(5)
C01K	47(5)	53(5)	70(6)	-12(4)	39(5)	1(4)
C01L	55(5)	53(5)	36(4)	-17(4)	11(4)	-27(4)
C01M	59(5)	43(5)	62(5)	-7(4)	40(5)	9(4)
C01N	54(5)	89(7)	45(5)	0(5)	21(4)	-35(5)
C01O	61(6)	46(6)	122(9)	-19(6)	2(6)	-3(5)
C01P	94(8)	105(9)	32(4)	-4(5)	9(5)	-44(7)
C01Q	62(6)	88(7)	63(6)	-45(5)	25(5)	-40(5)
C01R	44(5)	128(9)	66(6)	59(6)	21(5)	32(6)
C010	29(4)	39(4)	54(4)	-1(4)	16(3)	7(3)
C011	63(5)	38(4)	42(4)	-4(3)	30(4)	8(4)
C012	34(4)	30(4)	32(3)	9(3)	17(3)	-1(3)
C014	38(4)	28(4)	44(4)	5(3)	6(3)	-3(3)
C015	46(5)	29(4)	53(5)	6(4)	13(4)	10(3)
C016	47(5)	37(4)	94(6)	-4(4)	47(5)	11(4)
C017	39(4)	28(4)	45(4)	3(3)	7(4)	-8(3)
C018	29(4)	45(5)	54(4)	7(4)	2(3)	-11(4)
O1A	15(2)	26(3)	56(3)	8(2)	9(2)	0.0(19)
C1A	15(3)	28(4)	66(6)	9(4)	5(4)	-5(3)
C2A	41(4)	46(4)	57(5)	-1(3)	13(3)	7(3)
C3A	44(4)	55(4)	65(4)	6(3)	22(3)	6(3)
C4A	34(6)	70(9)	64(7)	18(6)	-8(5)	7(6)
O1B	15(2)	26(3)	56(3)	8(2)	9(2)	0.0(19)

Atom	U_{11}	U_{22}	U_{33}	U_{23}	U_{13}	U_{12}
C1B	15(3)	28(4)	66(6)	9(4)	5(4)	-5(3)
C2B	41(4)	46(4)	57(5)	-1(3)	13(3)	7(3)
C3B	44(4)	55(4)	65(4)	6(3)	22(3)	6(3)
C4B	34(6)	70(9)	64(7)	18(6)	-8(5)	7(6)
O7A	36(3)	22(2)	18(2)	-2.2(17)	8.5(19)	-1.3(19)
C25A	47(6)	28(4)	20(3)	-5(3)	12(4)	2(4)
C26A	44(10)	28(4)	29(4)	-2(3)	17(5)	-4(5)
C27A	94(11)	33(7)	37(7)	-7(5)	34(7)	-7(7)
C28A	77(11)	43(9)	34(7)	-4(6)	-3(6)	6(7)
O7B	36(3)	22(2)	18(2)	-2.2(17)	8.5(19)	-1.3(19)
C25B	47(6)	28(4)	20(3)	-5(3)	12(4)	2(4)
C26B	44(10)	28(4)	29(4)	-2(3)	17(5)	-4(5)
C27B	94(11)	33(7)	37(7)	-7(5)	34(7)	-7(7)
C28B	77(11)	43(9)	34(7)	-4(6)	-3(6)	6(7)

Table 3.19 Bond Lengths for 2-Sm.

Atom	Atom	Length/Å	Atom	Atom	Length/Å
Sm1	Si1	3.3196(18)	C00L	C01L	1.523(9)
Sm1	Si2	3.3012(18)	C00L	C017	1.530(8)
Sm1	Si3	3.2999(17)	C00L	C018	1.516(9)
Sm1	Si4	3.3214(18)	C00N	C00X	1.503(9)
Sm1	O4	2.544(4)	C00N	C01G	1.493(9)
Sm1	O10	2.541(4)	C00N	C01K	1.543(9)
Sm1	N1	2.716(5)	C00O	C00Q	1.513(8)
Sm1	N2	2.707(5)	C00P	C01M	1.525(9)
Sm1	O1A	2.545(4)	C00P	C010	1.534(9)
Sm1	O1B	2.545(4)	C00P	C015	1.529(9)
Sm1	O7A	2.531(4)	C00Q	C01E	1.516(9)
Sm1	O7B	2.531(4)	C00Q	C01N	1.526(9)
Si1	O2	1.627(4)	C00S	C01D	1.525(9)
Si1	O3	1.625(4)	C00S	C01F	1.541(9)
Si1	N1	1.637(5)	C00S	C01H	1.515(9)
Si1	O1A	1.685(5)	C00T	C00U	1.535(9)
Si1	O1B	1.685(5)	C00U	C011	1.525(9)
Si2	O4	1.687(4)	C00U	C016	1.543(9)
Si2	O5	1.634(4)	C00V	C01I	1.502(10)
Si2	O6	1.642(4)	C00V	C01J	1.517(10)
Si2	N1	1.641(5)	C00V	C01R	1.517(10)
Si3	O8	1.636(4)	C00W	C012	1.512(8)
Si3	O9	1.635(4)	C00Y	C01O	1.493(11)

Atom	Atom	Length/Å	Atom	Atom	Length/Å
Si3	N2	1.640(5)	C00Y	C01P	1.519(10)
Si3	O7A	1.699(4)	C00Y	C01Q	1.523(10)
Si3	O7B	1.699(4)	C01B	C012	1.523(8)
Si4	O10	1.696(4)	C012	C014	1.531(9)
Si4	O11	1.640(4)	O1A	C1A	1.452(8)
Si4	O12	1.633(4)	C1A	C2A	1.516(5)
Si4	N2	1.637(5)	C1A	C3A	1.516(5)
O2	C00Y	1.439(7)	C1A	C4A	1.516(5)
O3	C00Q	1.436(7)	O1B	C1B	1.452(7)
O4	C00N	1.456(7)	C1B	C2B	1.516(5)
O5	C00U	1.430(7)	C1B	C3B	1.516(5)
O6	C00V	1.451(7)	C1B	C4B	1.515(5)
O8	C00S	1.438(7)	O7A	C25A	1.447(7)
O9	C012	1.442(7)	C25A	C26A	1.523(5)
O10	C00K	1.453(6)	C25A	C27A	1.522(5)
O11	C00L	1.451(7)	C25A	C28A	1.522(5)
O12	C00P	1.431(7)	O7B	C25B	1.447(7)
C00K	C00R	1.517(8)	C25B	C26B	1.522(5)
C00K	C01A	1.494(9)	C25B	C27B	1.522(5)
C00K	C01C	1.545(9)	C25B	C28B	1.522(5)

Table 3.20 Bond Angles for 2-Sm.

Atom	Atom	Atom	Angle/°	Atom	Atom	Atom	Angle/°
Si1	Sm1	Si4	150.04(4)	C00N	O4	Si2	134.0(4)
Si2	Sm1	Si1	59.03(4)	C00U	O5	Si2	135.2(4)
Si2	Sm1	Si4	131.73(4)	C00V	O6	Si2	138.3(4)
Si3	Sm1	Si1	130.74(4)	C00S	O8	Si3	137.5(4)
Si3	Sm1	Si2	147.64(4)	C012	O9	Si3	136.1(4)
Si3	Sm1	Si4	58.96(4)	Si4	O10	Sm1	101.37(16)
O4	Sm1	Si1	87.01(9)	C00K	O10	Sm1	123.5(3)
O4	Sm1	Si2	30.15(9)	C00K	O10	Si4	132.3(4)
O4	Sm1	Si3	121.14(9)	C00L	O11	Si4	137.7(4)
O4	Sm1	Si4	112.57(9)	C00P	O12	Si4	136.4(4)
O4	Sm1	N1	58.46(14)	Si1	N1	Sm1	96.2(2)
O4	Sm1	N2	121.36(13)	Si1	N1	Si2	168.4(3)
O4	Sm1	O1A	116.64(15)	Si2	N1	Sm1	95.3(2)
O4	Sm1	O1B	116.72(13)	Si3	N2	Sm1	95.6(2)
O10	Sm1	Si1	124.50(9)	Si4	N2	Sm1	96.6(2)
O10	Sm1	Si2	111.82(9)	Si4	N2	Si3	167.7(3)
O10	Sm1	Si3	87.74(9)	O10	C00K	C00R	105.5(5)

Atom	Atom	Atom	Angle/°	Atom	Atom	Atom	Angle/°
O10	Sm1	Si4	30.05(9)	O10	C00K	C01A	111.1(5)
O10	Sm1	O4	106.82(13)	O10	C00K	C01C	109.1(5)
O10	Sm1	N1	122.26(13)	C00R	C00K	C01C	107.3(6)
O10	Sm1	N2	58.48(13)	C01A	C00K	C00R	111.2(6)
O10	Sm1	O1A	108.6(5)	C01A	C00K	C01C	112.3(6)
O10	Sm1	O1B	109.1(2)	O11	C00L	C01L	110.5(5)
N1	Sm1	Si1	29.36(11)	O11	C00L	C017	109.6(5)
N1	Sm1	Si2	29.67(11)	O11	C00L	C018	104.8(5)
N1	Sm1	Si3	149.66(10)	C01L	C00L	C017	110.1(6)
N1	Sm1	Si4	151.38(10)	C018	C00L	C01L	111.1(6)
N2	Sm1	Si1	150.61(10)	C018	C00L	C017	110.5(6)
N2	Sm1	Si2	150.32(11)	O4	C00N	C00X	105.9(5)
N2	Sm1	Si3	29.64(10)	O4	C00N	C01G	112.4(5)
N2	Sm1	Si4	29.32(10)	O4	C00N	C01K	109.0(6)
N2	Sm1	N1	179.23(14)	C00X	C00N	C01K	108.7(6)
O1A	Sm1	Si1	29.83(10)	C01G	C00N	C00X	113.1(7)
O1A	Sm1	Si2	87.6(2)	C01G	C00N	C01K	107.7(6)
O1A	Sm1	Si3	111.1(4)	O12	C00P	C01M	106.2(6)
O1A	Sm1	Si4	124.3(3)	O12	C00P	C010	110.6(5)
O1A	Sm1	N1	58.28(19)	O12	C00P	C015	107.9(5)
O1A	Sm1	N2	121.84(19)	C01M	C00P	C010	110.6(6)
O1B	Sm1	Si1	29.83(10)	C01M	C00P	C015	110.7(6)
O1B	Sm1	Si2	87.79(12)	C015	C00P	C010	110.7(6)
O1B	Sm1	Si3	110.62(18)	O3	C00Q	C00O	111.4(5)
O1B	Sm1	Si4	124.58(14)	O3	C00Q	C01E	108.0(5)
O1B	Sm1	N1	58.41(15)	O3	C00Q	C01N	105.3(5)
O1B	Sm1	N2	121.70(15)	C00O	C00Q	C01E	111.4(6)
O7A	Sm1	Si1	110.4(2)	C00O	C00Q	C01N	110.3(6)
O7A	Sm1	Si2	121.25(16)	C01E	C00Q	C01N	110.3(6)
O7A	Sm1	Si3	30.40(9)	O8	C00S	C01D	110.4(5)
O7A	Sm1	Si4	87.76(13)	O8	C00S	C01F	110.9(5)
O7A	Sm1	O4	103.3(3)	O8	C00S	C01H	105.0(5)
O7A	Sm1	O10	117.48(14)	C01D	C00S	C01F	109.8(6)
O7A	Sm1	N1	120.24(14)	C01H	C00S	C01D	110.5(6)
O7A	Sm1	N2	59.01(14)	C01H	C00S	C01F	110.2(6)
O7B	Sm1	Si1	110.0(3)	O5	C00U	C00T	108.8(5)
O7B	Sm1	Si2	121.5(2)	O5	C00U	C011	111.4(5)
O7B	Sm1	Si3	30.40(10)	O5	C00U	C016	105.8(6)
O7B	Sm1	Si4	87.95(16)	C00T	C00U	C016	109.8(5)
O7B	Sm1	O4	103.8(4)	C011	C00U	C00T	110.2(6)
O7B	Sm1	O10	117.61(15)	C011	C00U	C016	110.7(6)

Atom	Atom	Atom	Angle/°	Atom	Atom	Atom	Angle/°
O7B	Sm1	N1	120.11(15)	O6	C00V	C01I	110.3(6)
O7B	Sm1	N2	59.14(15)	O6	C00V	C01J	104.7(6)
O2	Si1	Sm1	110.94(18)	O6	C00V	C01R	110.1(5)
O2	Si1	N1	116.2(3)	C01I	C00V	C01J	110.2(6)
O2	Si1	O1A	104.5(9)	C01I	C00V	C01R	110.7(7)
O2	Si1	O1B	103.5(4)	C01J	C00V	C01R	110.8(7)
O3	Si1	Sm1	141.02(17)	O2	C00Y	C01O	111.0(6)
O3	Si1	O2	104.6(2)	O2	C00Y	C01P	104.3(6)
O3	Si1	N1	121.4(2)	O2	C00Y	C01Q	111.4(6)
O3	Si1	O1A	107.4(6)	C01O	C00Y	C01P	112.0(8)
O3	Si1	O1B	108.0(3)	C01O	C00Y	C01Q	109.4(7)
N1	Si1	Sm1	54.44(16)	C01P	C00Y	C01Q	108.6(7)
N1	Si1	O1A	101.2(3)	O9	C012	C00W	111.1(5)
N1	Si1	O1B	101.4(3)	O9	C012	C01B	106.1(5)
O1A	Si1	Sm1	48.72(15)	O9	C012	C014	107.6(5)
O1B	Si1	Sm1	48.71(15)	C00W	C012	C01B	111.0(5)
O4	Si2	Sm1	49.26(14)	C00W	C012	C014	111.3(6)
O5	Si2	Sm1	145.22(17)	C01B	C012	C014	109.6(5)
O5	Si2	O4	108.4(2)	Si1	O1A	Sm1	101.5(2)
O5	Si2	O6	105.0(2)	C1A	O1A	Sm1	124.5(5)
O5	Si2	N1	122.1(2)	C1A	O1A	Si1	134.0(6)
O6	Si2	Sm1	106.19(17)	O1A	C1A	C2A	105.5(6)
O6	Si2	O4	103.3(2)	O1A	C1A	C3A	110.8(6)
N1	Si2	Sm1	55.02(17)	O1A	C1A	C4A	109.6(6)
N1	Si2	O4	101.3(2)	C3A	C1A	C2A	111.2(8)
N1	Si2	O6	115.1(2)	C4A	C1A	C2A	109.7(8)
O8	Si3	Sm1	108.70(16)	C4A	C1A	C3A	110.0(8)
O8	Si3	N2	115.4(2)	Si1	O1B	Sm1	101.46(19)
O8	Si3	O7A	103.5(5)	C1B	O1B	Sm1	121.3(3)
O8	Si3	O7B	102.5(7)	C1B	O1B	Si1	136.0(4)
O9	Si3	Sm1	142.93(16)	O1B	C1B	C2B	105.6(5)
O9	Si3	O8	104.8(2)	O1B	C1B	C3B	110.7(6)
O9	Si3	N2	122.0(2)	O1B	C1B	C4B	109.6(6)
O9	Si3	O7A	108.0(3)	C3B	C1B	C2B	111.2(7)
O9	Si3	O7B	108.6(4)	C4B	C1B	C2B	109.6(7)
N2	Si3	Sm1	54.73(17)	C4B	C1B	C3B	110.1(7)
N2	Si3	O7A	101.4(3)	Si3	O7A	Sm1	100.68(17)
N2	Si3	O7B	101.7(3)	C25A	O7A	Sm1	124.8(4)
O7A	Si3	Sm1	48.92(13)	C25A	O7A	Si3	134.4(4)
O7B	Si3	Sm1	48.92(14)	O7A	C25A	C26A	105.7(5)
O10	Si4	Sm1	48.58(13)	O7A	C25A	C27A	110.2(6)

Atom	Atom	Atom	Angle/°	Atom	Atom	Atom	Angle/°
O11	Si4	Sm1	110.47(16)	O7A	C25A	C28A	110.7(6)
O11	Si4	O10	104.2(2)	C27A	C25A	C26A	109.8(7)
O12	Si4	Sm1	142.53(17)	C28A	C25A	C26A	109.6(7)
O12	Si4	O10	108.8(2)	C28A	C25A	C27A	110.8(8)
O12	Si4	O11	103.8(2)	Si3	O7B	Sm1	100.69(18)
O12	Si4	N2	121.9(2)	C25B	O7B	Sm1	125.1(4)
N2	Si4	Sm1	54.07(17)	C25B	O7B	Si3	132.3(6)
N2	Si4	O10	100.7(2)	O7B	C25B	C26B	105.7(5)
N2	Si4	O11	115.9(2)	O7B	C25B	C27B	110.2(6)
C00Y	O2	Si1	139.1(4)	O7B	C25B	C28B	110.7(6)
C00Q	O3	Si1	134.8(4)	C27B	C25B	C26B	109.8(7)
Si2	O4	Sm1	100.60(18)	C28B	C25B	C26B	109.6(7)
C00N	O4	Sm1	124.7(3)	C28B	C25B	C27B	110.8(8)

Table 3.21 Hydrogen Atom Coordinates (Å×10^4) and Isotropic Displacement Parameters (Å^2×10^3) for 2-Sm.

Atom	*x*	*y*	*z*	U(eq)
H00A	4671.57	4197.77	8771.14	52
H00B	4345.94	3791.92	9272.21	52
H00C	3994.32	4609.96	8798.71	52
H00D	4517.55	6272.89	8871.99	54
H00E	5094.79	5934.48	9544.1	54
H00F	5138.58	5722.31	8828.97	54
H00G	5769.26	1827.74	7853.06	56
H00H	5423.4	1656.6	7063	56
H00I	5125.14	2391.16	7415.74	56
H00J	6265.72	8406.28	7121.41	51
H00K	6781.14	8807.85	6812.28	51
H00L	6416.96	7883.13	6542.09	51
H00M	6300.17	6617	7231.95	77
H00N	7072.08	6764.1	7688.8	77
H00O	6511.03	6818.53	8016.12	77
H01A	5424.04	8258.61	9519.05	73
H01B	5275.08	7504.04	9971.04	73
H01C	4694.29	7822.9	9294.59	73
H01D	5958.92	8414.85	5372.71	60
H01E	6316.6	9355.91	5591.19	60
H01F	5524.67	9305.77	5188.66	60
H01G	6243.69	6320.19	9190.18	69
H01H	6244.16	6605.35	9910.24	69

Atom	*x*	*y*	*z*	U(eq)
H01I	6399.29	7324.96	9437.37	69
H01J	3639.95	9684.91	6330.69	75
H01K	3431.49	10087.49	5590.76	75
H01L	4194.27	9818.53	6001.73	75
H01M	3935.19	2154.9	7976.64	75
H01N	4271.65	2270.36	8773.36	75
H01O	4640.64	2650.48	8301.3	75
H01P	4162.77	8824.92	5020.62	76
H01Q	3407.84	9151.08	4640.33	76
H01R	3571.08	8114.43	4741.95	76
H01S	7130.42	5598.8	8846.26	86
H01T	7679.83	5577.25	8503.1	86
H01U	7288.54	4690.58	8547.44	86
H01V	2798.96	7847.51	5338.87	85
H01W	2558.33	8856.91	5202.95	85
H01X	2816.18	8469.57	5950.3	85
H01Y	5535.69	3036.45	9274.84	84
H	6208.91	2503.78	9676.42	84
HA	5965.07	2605.18	8878.73	84
H01Z	6654.49	4777.4	10055.19	89
HB	6546.75	3868.74	10387.87	89
HC	5912.46	4422.33	9916.96	89
H01	6962.98	4447.24	7365.48	78
HD	7339.25	5329.11	7280.92	78
HE	6563.09	5189.16	6836.55	78
H0AA	6122.62	9508.68	9357.91	74
HF	6891.13	9811.89	9643.86	74
HG	6698.66	8805.48	9726.39	74
H1AA	4340.39	9476.81	9070.61	75
HH	3981.14	10333.32	8652.43	75
HI	4778.98	10312.09	9018.93	75
H2AA	2935.02	3847.58	8314.91	92
HJ	3208.68	2972.93	8752.18	92
HK	2882.48	2908.75	7951.48	92
H3AA	4223.51	2469.44	6239.29	128
HL	3507.17	1992.97	5991.11	128
HM	3846.08	2320.06	6752.14	128
H4AA	3155.67	4178.43	5280.46	121
HN	3076.27	3156.18	5066.64	121
HO	3802.6	3605.8	5337.62	121
H5AA	2812.95	3217.51	6617.9	106

Atom	*x*	*y*	*z*	U(eq)
HP	2505.22	2801.19	5880.52	106
HQ	2522.55	3853.54	5978.24	106
H6AA	7097.89	3227.28	9045.12	119
HR	7318.35	3175.74	9843.52	119
HS	7347.81	4101.17	9490.27	119
H7AA	3895.92	8713.45	7382.14	61
HT	3431.09	9300.25	7659.16	61
HU	3833.58	8472.31	8084.84	61
H8AA	5237.01	3530.32	6588.41	67
HV	5535.36	2775.29	6252.45	67
HW	5948.89	3669.17	6518.98	67
H9AA	5346.42	10195.01	6068.55	59
HX	6127	10223.82	6524.67	59
HY	5598.11	9850.42	6827.49	59
H0BA	4858.3	10711.56	7934.3	66
HZ	4077.11	10614.38	7493.7	66
H5BA	4615.35	10034.86	7316.29	66
H1BA	6956.72	2830.73	7260.35	80
H6BA	6576.37	1915.06	6992.44	80
H7BA	6880.48	2116.84	7780.58	80
H2BA	6519.99	9754.88	7876.06	60
H8BA	6810.16	10381.33	8521.34	60
H9BA	6032.56	10121.85	8231.85	60
H3BA	7414.11	8202.03	9144.15	69
H0CA	7668.73	9182.11	9078.46	69
H1CA	7348.69	8578.32	8424.09	69
H2AB	3793.01	7036.25	7397.62	74
H2AC	3006.36	7170.16	6998.87	74
H2AD	3478.65	6876.62	6604.21	74
H3AB	3101.22	5126.12	7874.21	81
H3AC	2602.01	5949.49	7617.5	81
H3AD	3359	6108.83	8114.43	81
H4AB	2947.71	5341.29	6184.53	95
H4AC	2386.32	5906.34	6334.46	95
H4AD	2567.99	4928.78	6636.19	95
H2BB	3627.59	6753.42	7819.56	74
H2BC	3037.34	7167.08	7189.93	74
H2BD	3778.02	7089.43	7179.72	74
H3BB	2689.26	4830.07	7050.84	81
H3BC	2350.18	5764.6	7084.85	81
H3BD	2941.58	5391.28	7732.19	81

Atom	*x*	*y*	*z*	U(eq)
H4BA	3245.66	6459.12	6130.84	95
H4BB	2535.07	6083.16	6094.04	95
H4BC	3104.68	5415.22	6067.49	95
H26A	5282.09	5221.69	6364.65	49
H26B	4858.15	4957.94	5602.85	49
H26C	4480.58	5241.45	6093.04	49
H27A	5513.08	7109.75	5478.55	78
H27B	5489.2	6111.55	5218.31	78
H27C	5904.7	6344.09	5988.32	78
H28A	3855.61	6432.48	5292.81	86
H28B	4214.46	6100.66	4797.99	86
H28C	4262.1	7119.99	5016.91	86
H26D	5576.66	5528.04	6191.11	49
H26E	5028.29	5056.46	5557.94	49
H26F	4907.91	5133.09	6250.84	49
H27D	4761.65	7301.81	5064.16	78
H27E	5017.05	6367.17	4896.65	78
H27F	5494.93	6951.82	5508.06	78
H28D	3825.65	5857.54	5693.3	86
H28E	3908.28	5810.19	4980.86	86
H28F	3768.72	6741.47	5262.89	86

Table 3.22 Atomic Occupancy for 2-Sm.

Atom	*Occupancy*	Atom	*Occupancy*	Atom	*Occupancy*
O1A	0.270(8)	C1A	0.270(8)	C2A	0.270(8)
H2AB	0.270(8)	H2AC	0.270(8)	H2AD	0.270(8)
C3A	0.270(8)	H3AB	0.270(8)	H3AC	0.270(8)
H3AD	0.270(8)	C4A	0.270(8)	H4AB	0.270(8)
H4AC	0.270(8)	H4AD	0.270(8)	O1B	0.730(8)
C1B	0.730(8)	C2B	0.730(8)	H2BB	0.730(8)
H2BC	0.730(8)	H2BD	0.730(8)	C3B	0.730(8)
H3BB	0.730(8)	H3BC	0.730(8)	H3BD	0.730(8)
C4B	0.730(8)	H4BA	0.730(8)	H4BB	0.730(8)
H4BC	0.730(8)	O7A	0.582(9)	C25A	0.582(9)
C26A	0.582(9)	H26A	0.582(9)	H26B	0.582(9)
H26C	0.582(9)	C27A	0.582(9)	H27A	0.582(9)
H27B	0.582(9)	H27C	0.582(9)	C28A	0.582(9)
H28A	0.582(9)	H28B	0.582(9)	H28C	0.582(9)
O7B	0.418(9)	C25B	0.418(9)	C26B	0.418(9)
H26D	0.418(9)	H26E	0.418(9)	H26F	0.418(9)

Atom	***Occupancy***	**Atom**	***Occupancy***	**Atom**	***Occupancy***
C27B	0.418(9)	H27D	0.418(9)	H27E	0.418(9)
H27F	0.418(9)	C28B	0.418(9)	H28D	0.418(9)
H28E	0.418(9)	H28F	0.418(9)		

3.5.4 *2-Eu*

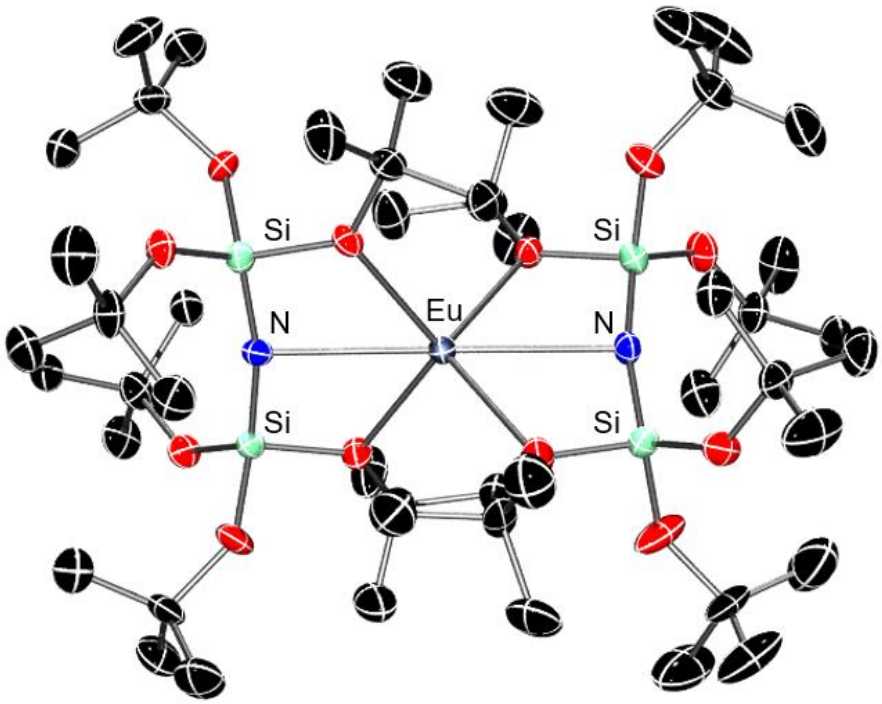

Figure 3.23 Molecular structure of 2-Eu. Thermal ellipsoids are shown at 50% probability and H atoms are omitted for clarity.

Table 3.23 Crystal data and structure refinement for 2-Eu.

Identification code	2-Eu
Empirical formula	$C_{32}H_{72}Eu_{0.67}N_{1.33}O_8Si_{2.67}$
Formula weight	779.79
Temperature/K	102.5
Crystal system	monoclinic
Space group	$P2_1/n$
a/Å	21.372(3)
b/Å	15.061(2)
c/Å	21.461(3)
α/°	90
β/°	111.428(5)
γ/°	90
Volume/Å^3	6430.3(16)
Z	6

ρ_{calc}g/cm^3	1.208
μ/mm^{-1}	1.100
F(000)	2500.0
Crystal size/mm^3	0.26 × 0.258 × 0.154
Radiation	MoKα (λ = 0.71073)
2Θ range for data collection/°	4.604 to 58.26
Index ranges	$-29 \leq h \leq 29$, $-20 \leq k \leq 20$, $-29 \leq l \leq 29$
Reflections collected	169239
Independent reflections	17268 [R_{int} = 0.0794, R_{sigma} = 0.0383]
Data/restraints/parameters	17268/29/684
Goodness-of-fit on F^2	1.034
Final R indexes [I>=2σ (I)]	R_1 = 0.0321, wR_2 = 0.0673
Final R indexes [all data]	R_1 = 0.0431, wR_2 = 0.0728
Largest diff. peak/hole / e Å^{-3}	0.89/-0.74

Table 3.24 Fractional Atomic Coordinates (×10^4) and Equivalent Isotropic Displacement Parameters (Å^2×10^3) for 2-Eu. U_{eq} is defined as 1/3 of the trace of the orthogonalised U_{ij} tensor.

Atom	*x*	*y*	*z*	U(eq)
Eu1	7475.5(2)	6202.2(2)	5025.3(2)	13.78(3)
Si1	8088.7(3)	8238.2(4)	5371.0(3)	15.45(11)
Si2	6470.4(3)	7924.0(4)	4816.1(3)	15.96(11)
Si4	7285.2(3)	4347.9(4)	4148.2(3)	17.15(11)
Si3	8000.5(3)	4289.4(4)	5776.6(3)	16.96(11)
O1	8434.3(7)	7284.8(9)	5235.8(7)	17.5(3)
O5	6041.0(7)	8487.6(10)	5172.3(7)	22.1(3)
O11	7631.4(8)	3779.3(10)	3712.8(7)	24.7(3)
O6	6078.1(8)	8086.6(11)	4013.8(7)	25.6(3)
O9	7818.7(8)	3454.4(10)	6167.9(7)	24.9(3)
O8	8825.2(8)	4335.1(11)	6075.0(8)	26.3(3)
O12	6500.6(8)	4036.2(13)	3849.9(9)	35.8(4)
O10A	7293(6)	5424.2(14)	3927.1(16)	24.1(4)
C37A	7187(4)	5877(4)	3298(2)	25.2(7)
C38A	6534(5)	5559(8)	2769(5)	53.4(11)
C39A	7777(5)	5732(9)	3075(5)	59(4)
C40A	7129(8)	6850(3)	3453(5)	48.2(12)
O10B	7246(2)	5425.0(11)	3919.7(9)	24.1(4)
O2	8435.9(7)	8382.3(10)	6183.0(7)	21.3(3)
O3	8374.2(8)	9065.6(10)	5061.3(7)	22.5(3)
O4A	6323(3)	6818.2(15)	4823(9)	14.9(12)
O4B	6359.3(16)	6835.3(11)	4950(4)	14.9(12)

Atom	*x*	*y*	*z*	U(eq)
O7	7780.5(7)	5238.7(9)	6059.9(7)	18.0(3)
N1	7289.7(8)	7979.2(11)	5082.4(8)	16.8(3)
N2	7643.1(9)	4417.6(11)	4963.8(8)	18.2(3)
C25	7827.2(12)	5546.4(15)	6718.6(10)	25.0(5)
C1	9126.4(11)	7004.6(15)	5383.4(11)	24.0(4)
C21	5621.3(12)	8726.5(16)	3592.4(11)	28.3(5)
C41	8286.2(12)	3426.3(15)	3835.6(12)	26.0(5)
C42	8825.1(12)	4070.0(16)	4244.5(13)	29.7(5)
C20	6709.0(12)	8461.6(16)	6371.4(11)	28.4(5)
C2	9082.7(12)	6156.0(15)	4993.3(13)	29.9(5)
C9	8151.7(13)	9567.0(15)	4449.4(12)	28.2(5)
C5	8756.5(11)	9087.6(15)	6636.3(11)	25.5(5)
C33	7292.0(13)	2802.3(15)	5998.3(12)	28.7(5)
C26	7691.0(17)	6524.1(17)	6645.6(12)	41.3(7)
C17	6183.0(12)	8955.2(15)	5794.5(11)	24.9(5)
C45	6099.1(13)	3335.0(18)	3449.2(13)	35.6(6)
C29	9379.9(12)	3748.9(17)	6381.8(12)	30.5(5)
C37B	6999.3(15)	5890.5(18)	3282.1(12)	25.2(7)
C22	5921.4(16)	9650.0(19)	3739.0(15)	44.1(7)
C27	7271.1(15)	5090.4(19)	6902.8(13)	38.8(6)
C32	9298.6(16)	2899(2)	5989.2(17)	50.8(8)
C11	7786.9(15)	8973.5(17)	3854.2(12)	37.7(6)
C44	8338.2(15)	2546.5(17)	4190.2(17)	46.9(7)
C24	5526.0(16)	8447(2)	2882.6(12)	46.5(7)
C3	9514.7(13)	7703.6(18)	5185.2(15)	39.9(6)
C10	8781.7(15)	9962.6(19)	4386.7(15)	43.7(7)
C8	8860.0(16)	8729.6(19)	7329.4(12)	41.6(7)
C19	5524.9(13)	9002.0(19)	5910.3(13)	37.2(6)
C6	9431.0(13)	9323(2)	6585.6(15)	45.1(7)
C48	6322(2)	2456(2)	3785.0(18)	66.7(10)
C30	9458.4(18)	3555(3)	7100.9(15)	63.0(10)
C46	6139.6(17)	3323(2)	2753.0(15)	55.5(9)
C43	8327.9(16)	3296(2)	3150.6(15)	53.8(9)
C31	9998.5(14)	4252(2)	6374.6(17)	52.0(8)
C47	5383.9(16)	3561(3)	3379(2)	68.5(11)
C38B	6237.6(18)	5940(3)	3033(2)	53.4(11)
C39B	7238(3)	5437(3)	2777.3(16)	45.3(11)
C40B	7299(3)	6814(2)	3445(2)	48.2(12)
C13A	5701(11)	6342(17)	4721(8)	21.8(14)
C13B	5782(6)	6282(9)	4896(4)	21.8(14)
C14A	5267(4)	6753(5)	5028(5)	42.5(10)

Atom	*x*	*y*	*z*	U(eq)
C14B	5613(2)	6472(3)	5520(3)	42.5(10)
C15A	5406(4)	6159(6)	3986(4)	44.6(10)
C15B	5164(2)	6507(3)	4268(2)	44.6(10)
C16A	5955(7)	5424(10)	5072(6)	26.9(11)
C16B	5985(4)	5335(5)	4875(3)	26.9(11)
C18	6422.1(14)	9882.6(16)	5713.1(13)	33.6(6)
C4	9441.8(13)	6787(2)	6134.8(13)	38.1(6)
C34	6610.2(14)	3227.3(18)	5644.3(15)	39.9(6)
C23	4950.6(13)	8700.4(19)	3687.8(14)	40.0(6)
C28	8492.6(14)	5328(2)	7247.9(13)	43.3(7)
C36	7429.8(14)	2104.0(16)	5549.4(13)	34.7(6)
C12	7695.3(14)	10302.9(16)	4521.9(13)	36.4(6)
C7	8308.0(14)	9903.9(17)	6493.3(13)	35.9(6)
C35	7337.5(17)	2386.8(18)	6660.5(14)	44.1(7)

Table 3.25 Anisotropic Displacement Parameters ($Å^2×10^3$) for 2-Eu. The Anisotropic displacement factor exponent takes the form: $-2\pi^2[h^2a^{*2}U_{11}+2hka^*b^*U_{12}+\ldots]$.

Atom	U_{11}	U_{22}	U_{33}	U_{23}	U_{13}	U_{12}
Eu1	14.55(5)	12.39(5)	13.18(5)	-0.32(4)	3.61(3)	0.85(4)
Si1	15.6(3)	13.8(3)	16.6(2)	-0.4(2)	5.4(2)	0.0(2)
Si2	14.6(3)	16.3(3)	15.6(2)	-0.4(2)	3.8(2)	2.7(2)
Si4	18.4(3)	15.9(3)	16.4(3)	-3.6(2)	5.4(2)	-0.8(2)
Si3	20.4(3)	15.8(3)	15.5(3)	2.7(2)	7.6(2)	3.4(2)
O1	13.5(7)	15.6(7)	23.3(7)	-0.9(6)	6.5(6)	1.8(5)
O5	18.9(7)	24.8(8)	21.7(7)	-5.2(6)	6.2(6)	3.3(6)
O11	24.0(8)	28.3(8)	20.9(7)	-6.4(6)	7.2(6)	3.7(7)
O6	24.1(8)	31.4(9)	17.3(7)	0.9(6)	3.0(6)	12.6(7)
O9	36.7(9)	18.2(7)	22.6(7)	4.2(6)	14.1(7)	0.7(7)
O8	21.2(8)	29.2(9)	27.4(8)	9.5(7)	7.5(6)	7.9(7)
O12	23.3(8)	44.3(11)	38.7(10)	-24.7(8)	10.2(7)	-10.1(8)
O10A	35.0(10)	19.7(7)	14.6(6)	0.4(6)	5.6(6)	4.6(6)
C37A	30.3(16)	23.6(10)	16.1(9)	2.4(8)	2.1(10)	7.5(11)
C38A	49(2)	54(3)	39(2)	9.4(18)	-4.9(17)	17.5(19)
C39A	81(11)	74(10)	37(7)	11(6)	38(7)	8(8)
C40A	82(4)	31.4(15)	26.1(14)	6.6(12)	13.9(18)	0.3(17)
O10B	35.0(10)	19.7(7)	14.6(6)	0.4(6)	5.6(6)	4.6(6)
O2	22.5(7)	19.9(8)	18.0(7)	-4.4(6)	3.2(6)	-2.6(6)
O3	23.5(8)	18.0(7)	27.4(8)	2.6(6)	10.8(6)	-2.1(6)
O4A	12.7(7)	18.0(7)	12(4)	-3.7(7)	2.2(12)	-2.5(6)
O4B	12.7(7)	18.0(7)	12(4)	-3.7(7)	2.2(12)	-2.5(6)

Atom	U_{11}	U_{22}	U_{33}	U_{23}	U_{13}	U_{12}
O7	22.5(7)	18.3(7)	13.1(6)	0.3(5)	6.3(6)	1.9(6)
N1	17.2(8)	15.5(8)	17.0(8)	0.4(6)	5.3(6)	1.1(7)
N2	21.3(9)	16.2(8)	17.4(8)	-0.7(7)	7.5(7)	-0.4(7)
C25	34.4(12)	26.5(12)	13.3(9)	-1.5(8)	7.8(9)	6.4(10)
C1	15.6(10)	23.0(11)	32.9(12)	-4.8(9)	8.3(9)	2.5(8)
C21	29.6(12)	28.3(12)	19.8(10)	3.9(9)	0.7(9)	10.1(10)
C41	25.3(11)	23.2(11)	33.5(12)	-8.5(9)	15.4(10)	1.5(9)
C42	27.0(12)	25.9(12)	41.1(14)	-8.8(10)	18.2(11)	-2.5(10)
C20	34.4(13)	29.3(12)	20.5(10)	-1.1(9)	8.7(9)	8.7(10)
C2	21.3(11)	25.6(12)	43.5(14)	-8.4(10)	12.7(10)	0.7(9)
C9	39.7(14)	20.6(11)	27.7(11)	4.8(9)	16.3(10)	-3.1(10)
C5	25.5(11)	23.6(11)	22.7(10)	-10.6(9)	3.2(9)	-1.7(9)
C33	40.9(14)	17.3(11)	35.6(13)	3.6(9)	23.2(11)	-1.9(10)
C26	76(2)	27.1(13)	23.4(12)	-1.1(10)	21.0(13)	8.1(13)
C17	28.4(11)	24.6(11)	22.4(10)	-4.7(9)	10.1(9)	6.3(9)
C45	26.3(12)	40.5(15)	38.5(14)	-20.3(12)	10.0(11)	-15.6(11)
C29	26.2(12)	37.3(14)	26.5(11)	8.2(10)	8.1(9)	15.8(10)
C37B	30.3(16)	23.6(10)	16.1(9)	2.4(8)	2.1(10)	7.5(11)
C22	48.1(17)	34.4(15)	42.6(16)	6.7(12)	7.7(13)	1.3(13)
C27	47.0(16)	42.4(16)	33.8(13)	-1.6(12)	23.0(12)	-4.4(13)
C32	48.4(18)	38.4(16)	62(2)	3.8(14)	15.2(15)	16.6(14)
C11	59.6(18)	29.7(13)	25.6(12)	2.2(10)	17.6(12)	-7.1(12)
C44	37.0(15)	20.5(13)	81(2)	1.6(14)	18.7(15)	1.9(11)
C24	55.7(18)	52.9(18)	21.6(12)	4.9(12)	3.2(12)	18.1(15)
C3	27.9(13)	34.5(14)	62.9(18)	2.2(13)	23.3(13)	0.6(11)
C10	53.8(18)	34.1(15)	53.5(17)	8.2(13)	31.9(15)	-9.8(13)
C8	50.9(17)	42.5(16)	21.3(11)	-8.5(11)	1.1(11)	5.2(13)
C19	34.9(14)	45.1(16)	37.2(14)	-4.3(12)	20.0(11)	11.9(12)
C6	29.3(14)	48.8(18)	53.8(17)	-24.0(14)	11.1(12)	-15.8(13)
C48	78(3)	46(2)	61(2)	-8.3(17)	7.5(19)	-22.6(18)
C30	59(2)	95(3)	34.7(15)	30.3(17)	16.8(15)	45(2)
C46	52.5(19)	68(2)	44.5(17)	-31.6(16)	16.2(14)	-27.6(17)
C43	48.2(18)	77(2)	43.4(16)	-28.3(16)	25.3(14)	2.5(16)
C31	27.7(14)	57(2)	66(2)	9.3(16)	10.7(14)	12.7(14)
C47	30.6(16)	91(3)	79(3)	-48(2)	14.3(16)	-16.8(17)
C38B	49(2)	54(3)	39(2)	9.4(18)	-4.9(17)	17.5(19)
C39B	79(3)	37(2)	21.4(17)	7.5(15)	20.3(19)	12(2)
C40B	82(4)	31.4(15)	26.1(14)	6.6(12)	13.9(18)	0.3(17)
C13A	9(3)	20(2)	29(5)	5(4)	-1(3)	-1(2)
C13B	9(3)	20(2)	29(5)	5(4)	-1(3)	-1(2)
C14A	42(2)	37(2)	63(3)	-13(2)	37(2)	-15.2(18)

Atom	U_{11}	U_{22}	U_{33}	U_{23}	U_{13}	U_{12}
C14B	42(2)	37(2)	63(3)	-13(2)	37(2)	-15.2(18)
C15A	21.9(19)	45(2)	54(3)	6.5(19)	-2.4(16)	-7.3(16)
C15B	21.9(19)	45(2)	54(3)	6.5(19)	-2.4(16)	-7.3(16)
C16A	20.4(14)	22(2)	45(4)	-6(3)	19(3)	-3.1(14)
C16B	20.4(14)	22(2)	45(4)	-6(3)	19(3)	-3.1(14)
C18	39.8(14)	22.5(12)	32.9(13)	-3.9(10)	6.6(11)	6.1(11)
C4	30.4(13)	46.1(16)	33.3(13)	0.3(12)	6.2(11)	13.8(12)
C34	37.6(15)	31.9(14)	57.7(17)	2.0(13)	26.2(13)	-4.4(12)
C23	25.9(12)	43.0(16)	42.4(15)	4.7(12)	2.1(11)	16.1(12)
C28	40.2(15)	63(2)	23.9(12)	-2.5(12)	8.7(11)	5.7(14)
C36	49.3(16)	20.5(12)	40.1(14)	-1.8(10)	23.0(12)	-2.7(11)
C12	46.4(16)	21.5(12)	38.8(14)	6.4(10)	12.5(12)	4.6(11)
C7	40.7(15)	25.7(12)	35.6(13)	-11.1(10)	7.3(11)	3.3(11)
C35	71(2)	30.2(14)	46.4(16)	7.9(12)	39.3(16)	-1.4(14)

Table 3.26 Bond Lengths for 2-Eu.

Atom	Atom	Length/Å	Atom	Atom	Length/Å
Eu1	Si1	3.3106(7)	O3	C9	1.437(3)
Eu1	Si2	3.2917(7)	O4A	C13A	1.46(2)
Eu1	Si4	3.3088(7)	O4B	C13B	1.458(13)
Eu1	Si3	3.2918(7)	O7	C25	1.456(2)
Eu1	O1	2.5268(14)	C25	C26	1.498(3)
Eu1	O10A	2.531(2)	C25	C27	1.544(3)
Eu1	O10B	2.5279(16)	C25	C28	1.497(3)
Eu1	O4A	2.518(4)	C1	C2	1.512(3)
Eu1	O4B	2.518(2)	C1	C3	1.495(3)
Eu1	O7	2.5306(14)	C1	C4	1.539(3)
Eu1	N1	2.7149(17)	C21	C22	1.516(4)
Eu1	N2	2.7211(18)	C21	C24	1.521(3)
Si1	O1	1.6877(15)	C21	C23	1.521(4)
Si1	O2	1.6400(15)	C41	C42	1.516(3)
Si1	O3	1.6319(16)	C41	C44	1.512(4)
Si1	N1	1.6368(18)	C41	C43	1.518(3)
Si2	O5	1.6307(15)	C20	C17	1.527(3)
Si2	O6	1.6349(15)	C9	C11	1.520(3)
Si2	O4A	1.6961(19)	C9	C10	1.522(4)
Si2	O4B	1.6961(19)	C9	C12	1.521(3)
Si2	N1	1.6334(18)	C5	C8	1.521(3)
Si4	O11	1.6307(16)	C5	C6	1.527(4)
Si4	O12	1.6302(17)	C5	C7	1.520(3)

Atom	Atom	Length/Å	Atom	Atom	Length/Å
Si4	O10A	1.691(2)	C33	C34	1.517(4)
Si4	O10B	1.6879(17)	C33	C36	1.526(3)
Si4	N2	1.6375(17)	C33	C35	1.523(3)
Si3	O9	1.6361(16)	C17	C19	1.517(3)
Si3	O8	1.6421(17)	C17	C18	1.519(3)
Si3	O7	1.6864(15)	C45	C48	1.499(4)
Si3	N2	1.6401(17)	C45	C46	1.528(4)
O1	C1	1.457(2)	C45	C47	1.519(4)
O5	C17	1.441(3)	C29	C32	1.507(4)
O11	C41	1.429(3)	C29	C30	1.519(4)
O6	C21	1.433(3)	C29	C31	1.529(4)
O9	C33	1.437(3)	C37B	C38B	1.518(4)
O8	C29	1.431(3)	C37B	C39B	1.517(3)
O12	C45	1.433(3)	C37B	C40B	1.518(3)
O10A	C37A	1.456(3)	C13A	C14A	1.45(3)
C37A	C38A	1.519(3)	C13A	C15A	1.495(19)
C37A	C39A	1.517(3)	C13A	C16A	1.57(3)
C37A	C40A	1.518(3)	C13B	C14B	1.538(13)
O10B	C37B	1.454(3)	C13B	C15B	1.542(8)
O2	C5	1.434(3)	C13B	C16B	1.495(15)

Table 3.27 Bond Angles for 2-Eu.

Atom	Atom	Atom	Angle/°	Atom	Atom	Atom	Angle/°
Si2	Eu1	Si1	59.075(17)	O10A	C37A	C39A	111.1(3)
Si2	Eu1	Si4	130.458(16)	O10A	C37A	C40A	104.3(3)
Si2	Eu1	Si3	147.661(15)	C39A	C37A	C38A	111.3(4)
Si4	Eu1	Si1	149.948(15)	C39A	C37A	C40A	110.6(4)
Si3	Eu1	Si1	131.651(16)	C40A	C37A	C38A	110.0(4)
Si3	Eu1	Si4	59.273(17)	Si4	O10B	Eu1	101.55(7)
O1	Eu1	Si1	29.95(3)	C37B	O10B	Eu1	122.63(14)
O1	Eu1	Si2	87.84(3)	C37B	O10B	Si4	134.36(16)
O1	Eu1	Si4	124.71(3)	C5	O2	Si1	137.50(14)
O1	Eu1	Si3	111.59(3)	C9	O3	Si1	136.50(14)
O1	Eu1	O10A	107.7(2)	Si2	O4A	Eu1	100.94(15)
O1	Eu1	O10B	109.46(9)	C13A	O4A	Eu1	128.8(10)
O1	Eu1	O7	106.32(5)	C13A	O4A	Si2	130.2(10)
O1	Eu1	N1	58.56(5)	Si2	O4B	Eu1	100.90(11)
O1	Eu1	N2	122.24(5)	C13B	O4B	Eu1	122.8(5)
O10A	Eu1	Si1	123.45(11)	C13B	O4B	Si2	134.9(5)
O10A	Eu1	Si2	111.51(19)	Si3	O7	Eu1	100.72(6)

Atom	Atom	Atom	Angle/°	Atom	Atom	Atom	Angle/°
O10A	Eu1	Si4	30.07(5)	C25	O7	Eu1	125.01(12)
O10A	Eu1	Si3	87.71(9)	C25	O7	Si3	133.69(13)
O10A	Eu1	N1	121.53(8)	Si1	N1	Eu1	95.88(7)
O10A	Eu1	N2	58.39(8)	Si2	N1	Eu1	95.15(7)
O10B	Eu1	Si1	124.36(5)	Si2	N1	Si1	168.91(12)
O10B	Eu1	Si2	110.10(7)	Si4	N2	Eu1	95.55(8)
O10B	Eu1	Si4	29.99(4)	Si4	N2	Si3	169.56(12)
O10B	Eu1	Si3	88.22(5)	Si3	N2	Eu1	94.77(7)
O10B	Eu1	O7	117.23(5)	O7	C25	C26	105.63(17)
O10B	Eu1	N1	121.16(5)	O7	C25	C27	108.71(19)
O10B	Eu1	N2	58.73(5)	O7	C25	C28	112.08(19)
O4A	Eu1	Si1	88.84(11)	C26	C25	C27	109.0(2)
O4A	Eu1	Si2	30.39(5)	C28	C25	C26	112.9(2)
O4A	Eu1	Si4	107.7(3)	C28	C25	C27	108.3(2)
O4A	Eu1	Si3	122.96(18)	O1	C1	C2	105.78(17)
O4A	Eu1	O1	118.14(7)	O1	C1	C3	111.04(19)
O4A	Eu1	O7	106.6(3)	O1	C1	C4	108.11(18)
O4A	Eu1	N1	59.63(9)	C2	C1	C4	108.3(2)
O4A	Eu1	N2	119.57(9)	C3	C1	C2	111.5(2)
O4B	Eu1	Si1	87.24(6)	C3	C1	C4	111.9(2)
O4B	Eu1	Si2	30.40(4)	O6	C21	C22	110.3(2)
O4B	Eu1	Si4	111.48(13)	O6	C21	C24	104.91(19)
O4B	Eu1	Si3	120.54(10)	O6	C21	C23	110.8(2)
O4B	Eu1	O1	117.03(6)	C22	C21	C24	110.7(2)
O4B	Eu1	O7	102.00(17)	C22	C21	C23	110.1(2)
O4B	Eu1	N1	58.60(6)	C24	C21	C23	109.9(2)
O4B	Eu1	N2	120.61(6)	O11	C41	C42	110.77(18)
O7	Eu1	Si1	112.36(3)	O11	C41	C44	107.81(19)
O7	Eu1	Si2	121.16(3)	O11	C41	C43	105.6(2)
O7	Eu1	Si4	87.36(3)	C42	C41	C43	110.0(2)
O7	Eu1	Si3	30.22(3)	C44	C41	C42	111.6(2)
O7	Eu1	O10A	117.01(7)	C44	C41	C43	110.8(2)
O7	Eu1	N1	121.38(5)	O3	C9	C11	110.84(19)
O7	Eu1	N2	58.66(5)	O3	C9	C10	106.2(2)
N1	Eu1	Si1	29.46(4)	O3	C9	C12	107.45(19)
N1	Eu1	Si2	29.62(4)	C11	C9	C10	110.8(2)
N1	Eu1	Si4	150.24(4)	C11	C9	C12	111.3(2)
N1	Eu1	Si3	150.44(4)	C12	C9	C10	110.2(2)
N1	Eu1	N2	179.20(5)	O2	C5	C8	105.29(19)
N2	Eu1	Si1	151.33(4)	O2	C5	C6	110.69(19)
N2	Eu1	Si2	149.59(4)	O2	C5	C7	110.63(18)

Atom	Atom	Atom	Angle/°	Atom	Atom	Atom	Angle/°
N2	Eu1	Si4	29.51(4)	C8	C5	C6	110.4(2)
N2	Eu1	Si3	29.77(4)	C7	C5	C8	109.9(2)
O2	Si1	O1	103.81(8)	C7	C5	C6	109.9(2)
O3	Si1	O1	109.11(8)	O9	C33	C34	111.02(19)
O3	Si1	O2	103.91(8)	O9	C33	C36	108.48(19)
O3	Si1	N1	121.44(8)	O9	C33	C35	105.5(2)
N1	Si1	O1	101.17(8)	C34	C33	C36	110.3(2)
N1	Si1	O2	115.99(8)	C34	C33	C35	111.3(2)
O5	Si2	O6	104.82(8)	C35	C33	C36	110.2(2)
O5	Si2	O4A	111.6(4)	O5	C17	C20	110.91(17)
O5	Si2	O4B	106.6(2)	O5	C17	C19	106.30(19)
O5	Si2	N1	121.62(9)	O5	C17	C18	107.98(18)
O6	Si2	O4A	97.5(6)	C19	C17	C20	110.0(2)
O6	Si2	O4B	105.9(3)	C19	C17	C18	110.3(2)
N1	Si2	O6	115.63(9)	C18	C17	C20	111.2(2)
N1	Si2	O4A	103.07(19)	O12	C45	C48	110.3(2)
N1	Si2	O4B	100.86(12)	O12	C45	C46	111.1(2)
O11	Si4	O10A	106.8(3)	O12	C45	C47	104.7(2)
O11	Si4	O10B	108.83(11)	C48	C45	C46	109.7(3)
O11	Si4	N2	120.91(9)	C48	C45	C47	112.2(3)
O12	Si4	O11	103.92(9)	C47	C45	C46	108.7(3)
O12	Si4	O10A	106.2(4)	O8	C29	C32	111.1(2)
O12	Si4	O10B	103.18(16)	O8	C29	C30	110.6(2)
O12	Si4	N2	116.74(9)	O8	C29	C31	105.3(2)
N2	Si4	O10A	100.95(15)	C32	C29	C30	110.6(3)
N2	Si4	O10B	101.72(9)	C32	C29	C31	109.8(2)
O9	Si3	O8	104.74(8)	C30	C29	C31	109.3(3)
O9	Si3	O7	108.46(8)	O10B	C37B	C38B	109.2(3)
O9	Si3	N2	122.06(9)	O10B	C37B	C39B	110.7(2)
O8	Si3	O7	102.99(8)	O10B	C37B	C40B	104.3(2)
N2	Si3	O8	115.24(9)	C39B	C37B	C38B	111.6(3)
N2	Si3	O7	101.59(8)	C39B	C37B	C40B	110.7(3)
Si1	O1	Eu1	101.68(6)	C40B	C37B	C38B	110.1(3)
C1	O1	Eu1	122.98(12)	O4A	C13A	C15A	104.9(15)
C1	O1	Si1	133.01(13)	O4A	C13A	C16A	103.0(14)
C17	O5	Si2	136.47(14)	C14A	C13A	O4A	114.8(18)
C41	O11	Si4	135.12(14)	C14A	C13A	C15A	117.6(14)
C21	O6	Si2	137.24(14)	C14A	C13A	C16A	108.9(13)
C33	O9	Si3	134.94(14)	C15A	C13A	C16A	106.4(17)
C29	O8	Si3	138.09(16)	O4B	C13B	C14B	106.6(8)
C45	O12	Si4	138.82(16)	O4B	C13B	C15B	112.0(7)

Atom	Atom	Atom	Angle/°	Atom	Atom	Atom	Angle/°
Si4	O10A	Eu1	101.33(10)	O4B	C13B	C16B	107.6(9)
C37A	O10A	Eu1	124.5(3)	C14B	C13B	C15B	108.7(8)
C37A	O10A	Si4	134.1(3)	C16B	C13B	C14B	111.6(6)
O10A	C37A	C38A	109.5(3)	C16B	C13B	C15B	110.4(8)

Table 3.28 Hydrogen Atom Coordinates (Å×10^4) and Isotropic Displacement Parameters (Å^2×10^3) for 2-Eu.

Atom	*x*	*y*	*z*	U(eq)
H38A	6617.96	5018.31	2557.91	80
H38B	6354.65	6021.29	2429.46	80
H38C	6206.92	5430.72	2980.3	80
H39A	8184.45	5983.62	3409.25	89
H39B	7686.2	6025.14	2643.29	89
H39C	7839.97	5094.42	3029.59	89
H40A	6702.71	6950.79	3514.7	72
H40B	7144.1	7215.16	3080.12	72
H40C	7503.41	7013	3862.74	72
H42A	8769	4637.17	4006.36	45
H42B	9269.42	3823.85	4311.29	45
H42C	8785.11	4165.25	4680.16	45
H20A	6542.09	7866.79	6412.26	43
H20B	6796.21	8790.06	6788.91	43
H20C	7126.3	8411.28	6283.09	43
H2A	8845.64	5702.97	5150.29	45
H2B	9536.85	5946.27	5060.67	45
H2C	8837.15	6268.87	4516.12	45
H26A	8054.22	6821.98	6550.86	62
H26B	7666.66	6759.61	7061.82	62
H26C	7263.12	6630.37	6276.36	62
H22A	6005.78	9802.61	4206.67	66
H22B	5606.94	10079.59	3443.86	66
H22C	6345.53	9664.98	3661.3	66
H27A	6831.64	5218.22	6557.15	58
H27B	7282.16	5316.14	7334.98	58
H27C	7346.54	4447.39	6933.19	58
H32A	8894.34	2587.33	5984.75	76
H32B	9692.9	2520.39	6198.71	76

Atom	*x*	*y*	*z*	U(eq)
H32C	9255.55	3036.14	5529.02	76
H11A	8093.32	8509.44	3818.11	57
H11B	7633.6	9330.01	3443.87	57
H11C	7398.52	8698.33	3916.97	57
H44A	8274.66	2639.64	4615.17	70
H44B	8782.77	2287.16	4277.52	70
H44C	7990.74	2142.34	3907.74	70
H24A	5960.3	8461.71	2825.29	70
H24B	5213.66	8856.9	2563.74	70
H24C	5342.69	7843.83	2801.26	70
H3A	9304.61	7815.41	4703.27	60
H3B	9977.99	7500.99	5291.34	60
H3C	9516.1	8252.34	5431.05	60
H10A	9026.46	10307.11	4789.74	66
H10B	8654.35	10351.76	3994	66
H10C	9069.76	9483.46	4336.08	66
H8A	8423.07	8584.83	7355.33	62
H8B	9085.22	9179.86	7666.47	62
H8C	9138.33	8193.3	7413.2	62
H19A	5185.67	9300.12	5530.2	56
H19B	5591.27	9336.55	6321.2	56
H19C	5372.53	8399.63	5954.15	56
H6A	9724.83	8801.02	6697.3	68
H6B	9642.08	9805.19	6898.66	68
H6C	9359.09	9514.78	6128.11	68
H48A	6804.56	2380.02	3886.35	100
H48B	6074.04	1978.1	3486.77	100
H48C	6232.83	2434.99	4201.48	100
H30A	9527.05	4112.84	7352.28	95
H30B	9846.95	3165.68	7306.45	95
H30C	9051.84	3261.52	7108.1	95
H46A	5987.15	3895.13	2532.8	83
H46B	5852.18	2847.6	2486.01	83
H46C	6605.45	3217.34	2793.81	83
H43A	7952.25	2924.12	2875.11	81
H43B	8753.54	3004.6	3200.18	81
H43C	8304.72	3874.18	2934.13	81
H31A	9942.65	4394.89	5911.82	78
H31B	10399.16	3881.75	6575.18	78
H31C	10050.26	4802.56	6632.32	78
H47A	5348.25	3553.53	3821.8	103

Atom	*x*	*y*	*z*	U(eq)
H47B	5074.14	3122.91	3089.5	103
H47C	5267.92	4153.75	3181.78	103
H38D	6051.36	5338.49	2985.21	80
H38E	6068.1	6241.82	2598.94	80
H38F	6101.65	6272.61	3355.87	80
H39D	7728.86	5388.44	2962.63	68
H39E	7098.84	5788.42	2364.4	68
H39F	7039.43	4843.01	2678.72	68
H40D	7171.38	7075.32	3799.73	72
H40E	7128.58	7187.1	3043.68	72
H40F	7789.62	6776.19	3596.25	72
H14A	5526.59	6868.92	5501.83	64
H14B	4893.19	6352.72	4988.42	64
H14C	5090.71	7313.54	4799.72	64
H14D	6011.31	6367.83	5923.53	64
H14E	5248.56	6078.97	5523.45	64
H14F	5469.99	7092.14	5512.39	64
H15A	5309.74	6722.31	3740.42	67
H15B	4988.68	5820.37	3882.16	67
H15C	5726.73	5815.24	3854.09	67
H15D	5010.55	7109.63	4308.8	67
H15E	4801.98	6083.41	4226.2	67
H15F	5284.63	6469.45	3870.31	67
H16A	6262.11	5153.43	4881.35	40
H16B	5570.06	5029.76	4999.66	40
H16C	6191.44	5517.22	5553.19	40
H16D	6088.42	5235.97	4471.37	40
H16E	5615	4944.21	4866.17	40
H16F	6382.86	5204.55	5272.07	40
H18A	6821.24	9840.92	5592.36	50
H18B	6534.54	10208.49	6135.26	50
H18C	6064.62	10196.74	5359.15	50
H4A	9416.73	7309.83	6396.1	57
H4B	9913.23	6616.87	6248.49	57
H4C	9196.18	6293.93	6238.38	57
H34A	6530.55	3680.14	5934.72	60
H34B	6259.37	2771.94	5541.7	60
H34C	6600.36	3504.29	5227.57	60
H23A	4750.64	8109.03	3570.83	60
H23B	4647.71	9145.07	3397.93	60
H23C	5021.25	8830.13	4156.15	60

Atom	*x*	*y*	*z*	U(eq)
H28A	8541.49	4682.04	7295.98	65
H28B	8517.75	5589.67	7674.48	65
H28C	8854.1	5569.58	7119.63	65
H36A	7442.13	2389.04	5143.57	52
H36B	7072.46	1656.16	5426.34	52
H36C	7863.22	1818.28	5789.96	52
H12A	7326.52	10042.61	4629.15	55
H12B	7510.96	10634.1	4100.83	55
H12C	7954.4	10705.92	4882.26	55
H7A	8218.08	10107.02	6034.82	54
H7B	8533.94	10376.89	6808.85	54
H7C	7882.87	9754.1	6543.86	54
H35A	7782.1	2117.89	6877.34	66
H35B	6990.61	1928.94	6577.49	66
H35C	7269.09	2846.28	6952.65	66

Table 3.29 Atomic Occupancy for 2-Eu.

Atom	*Occupancy*	Atom	*Occupancy*	Atom	*Occupancy*
O10A	0.257(5)	C37A	0.257(5)	C38A	0.257(5)
H38A	0.257(5)	H38B	0.257(5)	H38C	0.257(5)
C39A	0.257(5)	H39A	0.257(5)	H39B	0.257(5)
H39C	0.257(5)	C40A	0.257(5)	H40A	0.257(5)
H40B	0.257(5)	H40C	0.257(5)	O10B	0.743(5)
O4A	0.370(4)	O4B	0.630(4)	C37B	0.743(5)
C38B	0.743(5)	H38D	0.743(5)	H38E	0.743(5)
H38F	0.743(5)	C39B	0.743(5)	H39D	0.743(5)
H39E	0.743(5)	H39F	0.743(5)	C40B	0.743(5)
H40D	0.743(5)	H40E	0.743(5)	H40F	0.743(5)
C13A	0.370(4)	C13B	0.630(4)	C14A	0.370(4)
H14A	0.370(4)	H14B	0.370(4)	H14C	0.370(4)
C14B	0.630(4)	H14D	0.630(4)	H14E	0.630(4)
H14F	0.630(4)	C15A	0.370(4)	H15A	0.370(4)
H15B	0.370(4)	H15C	0.370(4)	C15B	0.630(4)
H15D	0.630(4)	H15E	0.630(4)	H15F	0.630(4)
C16A	0.370(4)	H16A	0.370(4)	H16B	0.370(4)
H16C	0.370(4)	C16B	0.630(4)	H16D	0.630(4)
H16E	0.630(4)	H16F	0.630(4)		

CHAPTER 4. HIGH-FREQUENCY AND -FIELD ELECTRON PARAMAGNETIC RESONANCE SPECTROSCOPIC ANALYSIS OF METAL-LIGAND COVALENCY IN $4F^7$ VALENCY SERIES (EU^{2+}, GD^{3+}, AND TB^{4+})

Part of this thesis chapter has been adapted with permission from an article co-written by the author:

Gompa, T. P., Greer, S. M., Rice, N. T., Jiang, N., Telser, J., Ozarowski, A., Stein, B. W., La Pierre, H. S. High-Frequency and -Field Electron Paramagnetic Resonance Spectroscopic Analysis of Metal–Ligand Covalency in a $4f^7$ Valence Series (Eu^{2+}, Gd^{3+}, and Tb^{4+}). Inorg. Chem., **2021**, *60*, 12, 9064-9073.

4.1 Background

The accessible molecular oxidation states of the lanthanides have rapidly expanded.[186-189] The synthesis and characterization of novel divalent complexes has enabled a detailed understanding of lanthanide electronic structure[54, 56-59, 61, 64, 70-72, 153, 179, 190-194] and reactivity,[180, 195-204] and, as a result, has demonstrated significant opportunities to improve our knowledge of the magnetic properties of the lanthanides.[65, 88, 151, 152, 205-207] Until 2019, molecular tetravalent lanthanide complexes were limited to cerium.[176, 177, 208-211] Recently developed weak-field ligand systems, such as imidophosphoranes $[N=P(NR_2)_3]^{1-}$ (R = alkyl), decrease the thermodynamic barrier for oxidation thereby making oxidation potential more accessible within the solvent window.[186, 187] We have recently reported the synthesis and characterization of novel lanthanide complexes featuring weak-field dialkylamide imidophosphorane ligands. This class of compounds

includes the most reducing Ce^{3+} complex to date as well as one of the first isolable Tb^{4+} complexes. Similarly, the Mazzanti group has isolated a pair of Tb^{4+} complexes featuring weak-field siloxide ligands.[209, 210]

Magnetic susceptibility measurements on both the imidophosphorane and siloxide supported Tb^{4+} complexes demonstrate results consistent with a $4f^7$ ion formulation. Concurrent X-band electron paramagnetic resonance (EPR) measurements resulted in broad, complex spectra that were difficult to interpret and, thus, a quantitative evaluation of the zero-field splitting (ZFS) has not yet been possible for these molecular compounds. ZFS refers to the energetic separation between spin projection (m_S) levels in the absence of an applied magnetic field and originates from the mixing of low-lying excited electronic states facilitated by spin-orbit coupling (SOC) and, to a lesser extent, the spin-spin coupling (SSC) of unpaired electron spins.[212] As a result, ZFS is sensitive to the interplay between the ligand field, spin-orbit coupling, and inter-electronic repulsion, and therefore offers unique insight into the ground state electronic structure and magnetic properties. A detailed understanding of ZFS as function of metal identity and oxidation state in the lanthanides is a crucial reference for understanding and rationalizing the behavior of actinide $5f^7$ ions including Cm^{3+} and Bk^{4+}.[213-216] Most importantly, this analysis is crucial to guide design principles for lanthanide single-molecule magnets, qubits, magnetocaloric effect coolants, and frustrated magnetic materials based on significant variations in metal-ligand covalency as a function of lanthanide oxidation state.

To address the challenge of ascertaining reliable ZFS parameters in these lanthanide systems, we have employed high-frequency and -field EPR (HFEPR). HFEPR has proven to be a powerful technique capable of directly determining ZFS parameters.[217-219] To analyze the effects of the oxidation state on physical properties, we have prepared a valence series of $4f^7$ complexes consisting of Eu^{2+}, Gd^{3+}, and Tb^{4+}. Herein, we report the synthesis, structural analysis, magnetic measurements, HFEPR analysis, and quantum chemical

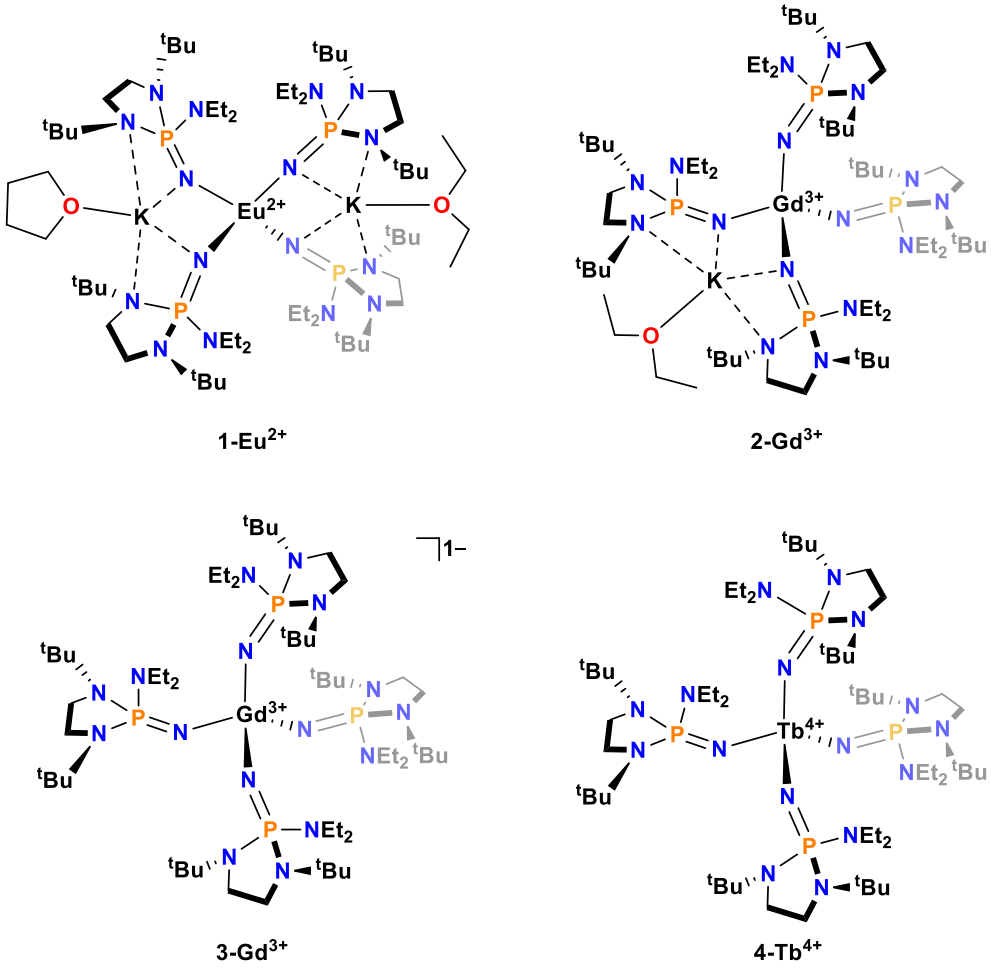

Figure 4.1 Molecular structures of 1-Eu^{2+}, 2-Gd^{3+}, 3-Gd^{3+}, and 4-Tb^{4+}.

calculations for this imidophosphorane valence series with the lanthanide ion spanning three oxidation states. These complexes exhibit an ^{8}S ground state and consequently are expected to exhibit small ZFS parameters (typically $|D| < \sim 0.1$ cm^{-1}, where D is the axial, second order ZFS[220, 221]) due to the lack of other octet states and large separation between the ground octet and first excited sextet state.[222-225] Until now, there has not been a series of pseudo-isostructural molecular compounds of Eu^{2+}, Gd^{3+}, and Tb^{4+} to interrogate the dependence of S = 7/2 spin Hamiltonian parameters (i.e., isotropic g values and ZFS) on metal identity and charge. The present HFEPR studies on the Tb^{4+} complex demonstrate ZFS ~8 times greater than its closest structural analog Gd^{3+} complex.

4.2 Results and Discussion

4.2.1 *Analyte complexes*

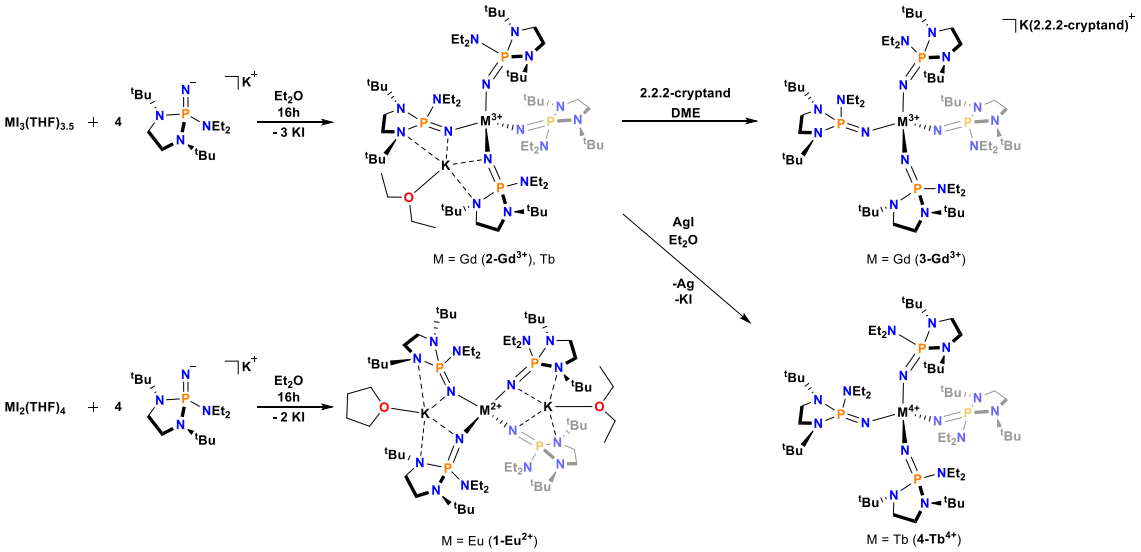

Scheme 4.1 Reaction scheme for the synthesis of 1-Eu^{2+}, 2-Gd^{3+}, 3-Gd^{3+}, and 4-Tb^{4+}.

The four homoleptic compounds investigated here are supported by the [(NP(1,2-*bis*-^{t}Bu-diamidoethane)(NEt$_2$))]$^{1-}$ ligand, [NP*]$^{1-}$,[177, 208] and include [(THF)K][(Et$_2$O)K][Eu^{2+}(NP*)4], (**1-Eu^{2+}**), [(Et$_2$O)K][Gd^{3+}(NP*)$_4$], (**2-Gd^{3+}**), [(2.2.2-crypt)K][Gd^{3+}(NP*)4], (**3-Gd^{3+}**), and the previously reported [Tb(NP*)$_4$],[177] (**4-Tb^{4+}**, Figure 4.1). The synthesis of each of these complexes is detailed in the Experimental section and depicted in Scheme 4.1.

4.2.2 *Crystallographic analysis*

All four complexes have a similar primary coordination sphere with four imidophosphorane ligands coordinated in a pseudo-tetrahedral fashion. However, due to the interactions of the bound or unbound potassium counter cations in the second

coordination sphere, both gadolinium structures and the europium structure deviate from the S4 point group observed in the solid-state structure of neutral **4-Tb^{4+}**.[226] This deviation from a tetrahedral structure is quantified by two parameters in this study: (1) τ_4, where a value of 1.0 implies a perfect tetrahedral structure and a value of 0.0 implies a square planar structure,[181] and (2) $\Sigma_{109.5}$, which is the sum of the absolute difference from each of the six angles in the primary coordination sphere from the tetrahedral angle (109.5°). This latter parameter is useful as it represents absolute deviance from a tetrahedral configuration while τ4 represents average deviation. As expected, the neutral complex **4-Tb^{4+}** has a coordination geometry closest to tetrahedral of the four (τ_4 of 0.99, $\Sigma_{109.5}$ of 9.8^o). In contrast, the dianionic complex **1-Eu^{2+}** is furthest from a tetrahedral geometry (τ_4 of 0.82, $\Sigma_{109.5}$ of 60.6^o). The two monoanionic gadolinium complexes fall in between these extremes (**2-Gd^{3+}** and **3-Gd^{3+}**: τ_4 of 0.94 and 0.98, $\Sigma_{109.5}$ of 28.4 and 6.0^o, respectively).

The average Ln–N bond lengths are 2.483(4), 2.271(6), 2.267(4), and 2.106(3) Å for **1-Eu^{2+}**, **2-Gd^{3+}**, **3-Gd^{3+}**, and **4-Tb^{4+}**, respectively. The change in bond lengths across the series follows that expected based on the six-coordinate Shannon ionic radii: Eu^{2+} (1.17 Å), Gd^{3+} (0.938 Å), and Tb^{4+} (0.76 Å).[227] The average P–N_{imide} bond length (1.555(4) Å) for **4-Tb^{4+}** is longer than those for the other compounds in this series, which are 1.519(4), 1.521(6), and 1.523(4) Å for **1-Eu^{2+}**, **2-Gd^{3+}**, and **3-Gd^{3+}**, respectively. This difference is greater than the error of the respective measurements, but not greater than 3σ. The P–N bond lengths for **1-Eu^{2+}**, **2-Gd^{3+}**, and **3-Gd^{3+}** are more in line with the P–N_{imide} bond lengths observed in the solid-state structure for the potassium salt of the ligand, 1.526(7) Å.[177] This result could be indicative of increased electron donation to the metal center for **4-Tb^{4+}** in comparison to **1-Eu^{2+}**, **2-Gd^{3+}**, and **3-Gd^{3+}**.

4.2.3 *HFEPR and SQUID measurements*

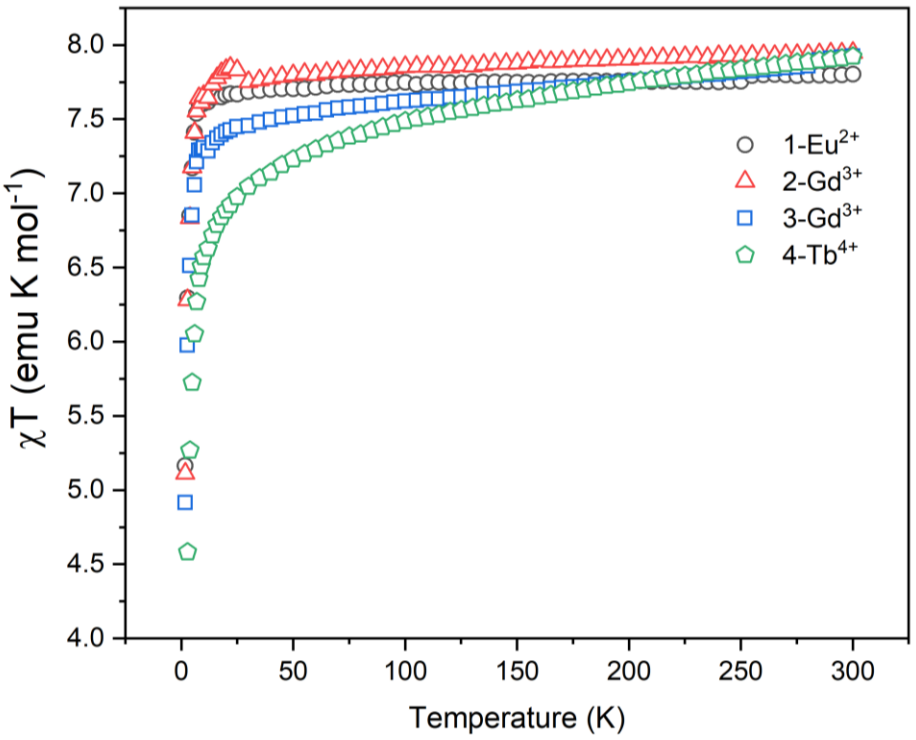

Figure 4.2 Variable-temperature molar magnetic susceptibility times temperature ($\chi_M T$) for 1-Eu^{2+}, 2-Gd^{3+}, 3-Gd^{3+}, and 4-Tb^{4+} collected under dc field of 1 T.

Variable-temperature dc magnetic susceptibility data for all compounds in this series is shown in Figure 4.2 and Figure 4.20-Figure 4.23. All four complexes exhibit a consistent room-temperature $\chi_m T$ value, ranging from 7.80 to 7.93 emu K/mol, with a theoretical value of 7.88 emu K/mol for an isotropic $4f^7$ complex (g = 2, S = 7/2; L = 0, J = 7/2, μ_{eff} = 7.94 μ_B). The distinguishing feature of the magnetic behavior of these compounds is their low temperature susceptibility and is a direct result of varied ZFS parameters among these europium, gadolinium, and terbium complexes. Utilizing multi-field data and accounting for increased Zeeman splitting at higher fields, the isotropic g and D values for each of these compounds can be extracted from their fit using PHI software (results are summarized in Table 4.22).[228] As expected, for **1-Eu^{2+}**, **2-Gd^{3+}**, and **3-Gd^{3+}** the absolute

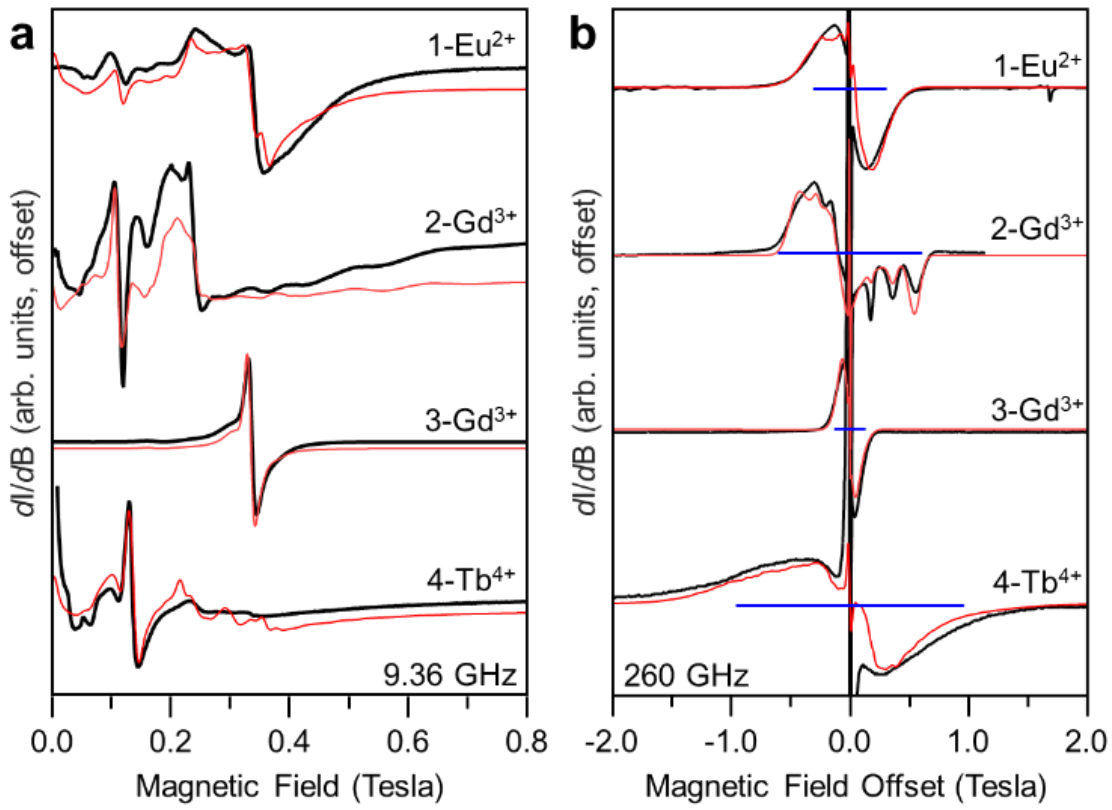

Figure 4.3 a) Experimental (black traces) and simulated (red traces) X-band EPR spectra at 9.36 GHz and 5 K. b) Experimental (black traces) and simulated (red traces) HFEPR spectra at 260 GHz and 5 K. In these spectra the frequency of the central transition is subtracted in order to facilitate a direct comparison of the observed spectral extent for each compound. Simulation parameters are given in Table 4.1.

values of D obtained from the fit are relatively small, ranging from 0.03(7) to 0.19(5) cm^{-1}. On the other hand, **4-Tb^{4+}** exhibits a strikingly large |D| value of 6.3(3) cm^{-1}, which is in agreement with previously reported analyses.[177]

The X-band and representative HFEPR spectra of **1-Eu^{2+}**, **2-Gd^{3+}**, **3-Gd^{3+}**, and **4-Tb^{4+}** in solution (toluene) along with their respective simulations (using the Matlab toolbox EasySpin[229]) are shown in Figure 4.3. The spectra of the solid-state samples and additional solution experiments along with their spectral simulations are shown in Figure 4.20-4.23

and Table 4.23. All of the recorded HFEPR spectra exhibit broad linewidths away from the central transition that are indicative of strain in the ZFS parameters.[223, 230] Here, strain refers to a distribution in ZFS that results from a variation in the local coordination sphere of the molecular species under investigation. This effect manifests as a broadening of spectral

Table 4.1 Spin Hamiltonian Parameters Extracted from EPR Spectroscopy of Solution Samples.

Sample	$\Sigma_{109.5}$	g	D (cm^{-1})	E (cm^{-1})	σ_D (cm^{-1})	σ_E (cm^{-1})	Δ_{8S} (cm^{-1})	Δ_{8S} (cm^{-1})
1-Eu^{2+}	60.6	1.990(5)	0.045(5)	0.008(5)	0.020	0.020	0.58	0.596
2-Gd^{3+}	28.4	1.990(5)	0.086(3)	0.018(3)	0.017	0.017	1.14	1.181
3-Gd^{3+}	6.0	1.990(5)	0.018(3)	0.005(3)	0.020	0.010	0.25	0.271
4-Tb^{4+}	9.8	2.010(5)	0.140(5)	0.025(5)	0.095	0.035	1.81	1.857

features. The narrow central feature arises from the transition from m_S = -1/2 to m_S = +1/2 and is, to first order, immune from the effects of strain.[231] Note that in these samples the strain is often of comparable magnitude to the ZFS parameter itself. This situation makes spectral simulation tedious because the often-used approximation for the effect of strain on the spectrum is strictly valid only when the strain is small compared to the central value.[229] Testing of the typical/approximate model of strain compared to an explicit model of strain showed that differences in the ZFS parameters are smaller than the estimated error in all cases except for **1-Eu^{2+}** and **4-Tb^{4+}**. For this reason, the approximate model has been employed for all compounds except for **1-Eu^{2+}** and **4-Tb^{4+}** to expedite the data analysis. The procedures for the explicit modeling of strain are detailed in the SI along with the Matlab® script.

EPR spectrum of a well-isolated spin ground state can be described in terms of the following spin Hamiltonian[220, 221]:

$$\hat{\mathrm{H}}_{\mathrm{S}} = \beta_e \vec{\mathbf{B}} \cdot \tilde{\boldsymbol{g}} \cdot \hat{\mathbf{S}} + D\left[\hat{\mathrm{S}}_{\mathrm{z}}^2 - \frac{S(S+1)}{3} + \frac{E}{D}\left(\hat{\mathrm{S}}_{\mathrm{x}}^2 - \hat{\mathrm{S}}_{\mathrm{y}}^2\right)\right] \qquad (4.2)$$

The first term is the electronic Zeeman interaction where β_e is the electron Bohr magneton, $\vec{\mathbf{B}}$ is the magnetic field vector, $\tilde{\boldsymbol{g}}$ is the g-tensor (assumed to be isotropic), and $\hat{\mathbf{S}}$ represents the electron spin operator. The second term describe the 2nd order ZFS interactions and are parameterized by D (axial term) and E (rhombic term), respectively. Here $\hat{\mathrm{S}}_{\mu}$ is the component of the spin operator (μ = x, y, z). Note that in the present case where the strain is significant, there is a distribution of positive and negative D parameters.[223] In cases where S > 2, the spin system may need to be characterized by 4th and/or higher-order ZFS terms.[220, 221] In this work we have limited the analysis to only second-order terms as not to over parameterize the results. In extended lattice systems containing $4f^7$ ions as dopants in high symmetry sites, e.g., the Y^{3+} site in yttrium aluminum garnet ($Y_3Al_5O_{12}$) and the Pb^{2+} site in $PbWO_4$ (both materials have been used as hosts for Eu^{2+} and Gd^{3+})[232-235] or thoria (host for Tb^{4+}),[236] it is possible to extract fourth and sixth order ZFS terms, although these are much smaller than the D (= $3B^2_0$) term. The final term in eq. 1 parameterizes the Zeeman interaction where the external magnetic field is given by $\vec{\mathbf{B}}$, β_e the electron Bohr magneton, Sˆthe total spin operator, and $\tilde{g}$ is the g-tensor which is assumed to be isotropic. To simplify the analysis, a new parameter, Δ_{8s}, defined as the energetic separation between the highest and lowest m_S states of the S = 7/2 ground state, is employed (vide infra). This parameter is defined to capture the effect of ZFS, without the distraction that results from ambiguity of the sign of D for a highly strained system. It

corresponds to 12|D| at zero-field for an axial system, and to [12|D| + 39.6E^2/|D|] for a rhombic system.[237]

A qualitative analysis of the anisotropy of this series can be achieved by comparing the spectral extent of each compound in Figure 4.3b Here, each spectrum is offset according to the resonance condition of the $\Delta m_S = \pm 1/2$ transition. This presentation allows simultaneous examination of the entire series of spectra and shows how the ZFS produces peak separations that are independent of magnetic field (Figure 4.20Figure 4.23). It also allows a direct comparison of the spectral extent, and thus the anisotropy of each compound (Figure 4.3b). Examination of Figure 4.3 clearly shows that the spectrum of **4-Tb^{4+}** extends much further to either side of the central transition than in the spectra of the other compounds, indicating comparatively larger anisotropy. This expectation is confirmed by the parameters extracted from the spectral simulations (Figure 4.3, Table 4.1), which determined that the Δ_{8s} parameters for **1-Eu^{2+}** (Δ_{8s} = 0.58 cm^{-1}), **2-Gd^{3+}** (Δ_{8s} = 1.14 cm^{-1}), and **3-Gd^{3+}** (Δ_{8s} = 0.25 cm^{-1}) are all significantly smaller than that of **4-Tb^{4+}** (Δ_{8s} = 1.81 cm^{-1}).

Additionally, the g-values are isotropic and nearly equal for **1-Eu^{2+}**, **2-Gd^{3+}**, and **3-Gd^{3+}** with g = 1.990(5) (the g value for free ion Eu^{2+} and Gd^{3+} are 1.9926[238, 239] and 1.991[240], respectively). Interestingly the g value for **4-Tb^{4+}**, g = 2.010(5), is not only larger than those for the Eu^{2+}/Gd^{3+} complexes but is larger than the free electron value (g_e = 2.0023). This unusual observation, however, is not without precedent. Although scarce, some solid-state materials containing Tb^{4+} have been investigated through EPR and has yielded a diverse range of g values.[236, 241-243] In these cases, the g values in different host lattices span 1.997(5) to 2.0146(4). The highest values were obtained in ThO2 and ThSiO4

host lattices, where g = 2.0146(4) and 2.011(5), respectively.[236, 242] Similarly, g values for Eu^{2+} and closely related Gd^{3+} complexes exhibit a reduced g value when compared to g_e.[232, 233, 235, 243] Qualitative comparison between values between among materials containing Eu^{2+}, Gd^{3+}, or Tb^{4+} is available only in pairs (e.g. Eu^{2+}/Gd^{3+} or Gd^{3+}/Tb^{4+} in related hosts/sites). The lack of close structural similarity, combined with the dependence on local structure, makes it difficult to definitively determine the effect of metal identity and highlights the importance of the close structural congeners in this work.

The two Gd complexes, **2-Gd^{3+}** and **3-Gd^{3+}**, highlight the significant impact that associated counter ions can have on the resultant spectrum. Both complexes have the same coordination environment but differ in the binding or sequestration of the potassium counter ion. If the counter ion were not associated with the structure in solution, then both compounds would be expected to give identical EPR spectra. However, the spectra are quite different as is reflected by the Δ_{8s} value which increases by ~4.5 times from **3-Gd^{3+}** to **2-Gd^{3+}**. Insight into this difference can be gleaned from comparison of the crystal structures of these two complexes. The $\Sigma_{109.5}$ value for **3-Gd^{3+}** is 6.0°, meaning that the structure adopts a nearly tetrahedral geometry while the **2-Gd^{3+}** structure has a $\Sigma_{109.5}$ of 28.4°. The large difference in $\Sigma_{109.5}$ values for these two complexes arises from the K^+ counter ion in **2-Gd^{3+}** that is bound inner sphere and distorts the ligand field about the Gd^{3+}, while the sequestration of the K^+ in **3-Gd^{3+}** only minimally perturbs the ligand geometry via charge-pairing. These metrics are useful, since for an f^7 ion (S = 7/2, L = 0), in a perfect tetrahedron, there can be no ZFS. Therefore, one would expect that the closer to an ideal tetrahedron, the smaller the anisotropy would be observed. This simplistic expectation is found to be true in the comparison of the measured ZFS parameters of **2-Gd^{3+}** and **3-Gd^{3+}**.

Importantly, the expected reduction in the observed ZFS with decreasing deviation from ideal tetrahedral symmetry is not found for **4-Tb^{4+}**. This complex reveals the largest ZFS of the series despite the very small distortion from an ideal tetrahedron. This observation implicates the significant changes in the electronic structure of the Tb^{4+} ion in comparison to both Eu^{2+} and Gd^{3+}. The high symmetry of the tetrakisimidophosphorane coordination is reflected in the ZFS of the Gd^{3+} and Eu^{2+} complexes being smaller magnitude than even for these ions in the Pb^{2+} site in PbWO4 where the lanthanide ion is in octa-coordination by tungstate oxygen atoms.[234, 235] This comparison highlights the significance of the relatively large ZFS in **4-Tb^{4+}** in this coordination environment.

4.2.4 *Quantum chemical calculations*

To understand the basis of the divergent properties of the Tb^{4+} ion and the link between spectroscopic properties and electronic structure, a series of Complete Active Space Self-Consistent Field (CASSCF) calculations were performed followed by N-electron valence perturbation theory to second order (NEVPT2) to account for dynamic correlation.[244-250] To gain insight into the differences in bonding across the series, the results of these calculations were analyzed in terms of ab initio ligand field theory (AILFT).[251-253] Specifically, the energies and AILFT parameters of the free ions Eu^{2+}, Gd^{3+}, and Tb^{4+} and a series of truncated models of **1-Eu^{2+}**, **2-Gd^{3+}**/**3-Gd^{3+}**, and **4-Tb^{4+}** (referred to as **Eu^{M}**, **Gd^{M}**, and **Tb^{M}**) were compared. The truncated models were optimized starting with the crystallographically determined atomic coordinates where all methyl groups more than four bonds from the metal center were replaced with hydrogen atoms and all counter ions removed (Figure 4.25). This suite of calculations forms a convenient framework to systematically evaluate the interplay between bonding, inter-electronic repulsion, and spin-

orbit coupling (SOC). The goal of these calculations is not to reproduce the experimental ZFS values but rather to understand how the electronic structure changes across the series. The accurate calculation of ZFS parameters for $4f^7$ systems is extremely challenging due to the numerous excited states that mix via SOC into the ground state and make significant contributions to the phenomenologically observed ZFS. This scenario makes the quantitative determination of D extremely sensitive to the accuracy of the calculated excited state energies that in turn are extremely sensitive to geometry. Given these caveats, it is unreasonable to assume that the truncated geometries will model the exact magnitude of a given observed ZFS. The focus is on the trend of the energetics and mixing of the sextet states as well as the effects of covalent interactions.

The definition and evaluation of covalency is not unique and trends are sensitive to the choice of method. Here, covalency is considered as a one electron interaction that is analyzed in terms of the nephelauxetic reduction.[251, 252, 254] This effect was originally used to explain why the SOC and electron repulsion parameters in coordination complexes were reduced compared to those of the free ion.[255, 256] The nephelauxetic reduction results from two effects. The first is termed 'symmetry restricted' and arises from orbital mixing, specifically, the dilution of metal orbitals with ligand character. The second is 'central field' and results from the change in the radial extent of the *f* (or *d*) orbital wave functions due to the complexation of the metal with a ligand. The central field covalency will contribute mostly to the reduction of inter-electronic repulsion while the symmetry restricted covalency will manifest itself primarily in the reduction of the SOC constant, ζ.[254, 257]

Comparing the percent reduction of the SOC parameter, defined as [100 × (1 - ζ/ζ_{free})], across the series reveals that all three model complexes exhibit very little reduction, ~1% compared to the calculated free ion value (please note that the Tb^{4+} free ion value is greater than that of Eu^{2+} due to its greater effective nuclear charge).[258] This limited change in the SOC parameter in the model complexes is not unanticipated given the small radial extent of the 4*f* orbitals in the lanthanide series. Importantly, we find that **Tb^{M}** has a slightly greater reduction than either **Gd^{M}** or **Eu^{M}** which are nearly equal. To confirm this result, the same calculations were performed on the hypothetical series of $[LnCl_4]^{-1/0/+1}$ complexes. In this much simpler ligand field, it is again found that the reduction of the SOC parameter for the Tb^{4+} ion is greatest while the reductions in ζ for the Gd^{3+} and Eu^{2+} ions are smaller and essentially the same (Figure 4.24 and Table 4.24). It is important to note that the SOC constant is only mapped onto the CASSCF wave function and that, for now, evaluation of the effects of dynamic correlation are not possible. However, as noted by Aravena and coworkers, since the goal is to evaluate the effects of covalency as a one-electron property, the neglect of dynamic correlations - a multi-electron interaction, is not a limitation.[252] A similar analysis can be performed for the reduction of the inter-electronic repulsion. In this case, the CASSCF and CASSCF + NEVPT2 wave functions can be mapped onto the ligand field model. Here, no trend in the reduction of inter-electronic repulsion is found across the series. However, the inclusion of dynamic correlation further reduces the inter-electronic repulsion parameters by ~0.5 – 1%. Interestingly, in the hypothetical $[LnCl_4]^{-1/0/+1}$ series we again find that the reduction is approximately equal for Gd^{3+} and Eu^{2+}, while the Tb^{4+} model exhibits a larger reduction. Overall, our computational results suggest that both symmetry restricted and central field covalency are larger in Tb^{4+}

than in the Gd^{3+} and Eu^{2+} compounds. This observation trends with the AILFT calculated ligand field splitting (Δ_{LF}), defined as the difference between highest and lowest AILFT orbital, which increases across the series: Δ_{LF} = 334, 438, and 914 cm^{-1} for **Eu^{M}**, **Gd^{M}**, and **Tb^{M}**, respectively.

Since the quantitative calculation of the ZFS parameters is not possible for this $4f^7$ series, the AILFT model can be used to gain insight into the origins of the ZFS. The largest contribution to the magnitude of the ZFS is from SOC between the ground ^8S state and excited states of the ^6P manifold and is proportional to $\zeta^2/E(^6P_i)$ where $E(^6P_i)$ is the energy difference between the ^8S and one of the three ^6P excited states.[224, 254, 257, 259] The separation of the ^8S and ^6P states is predominately governed by the strength of the inter-electronic repulsion that increases from Eu^{2+} to Tb^{4+} (Figure 4.4). However, the calculations also show that the SOC constant increases from Eu^{2+} to Tb^{4+}. This increase in SOC means that the magnitude of the ZFS is a competition between contributions from inter-electronic repulsion and spin-orbit interactions. The ratio $\zeta^2/E(^6P)$ increases across the series (Table 4.2) from Eu^{2+} to Tb^{4+}. This trend suggests that the contribution from larger spin-orbit

Table 4.2 Metrics Derived from AILFT and CASSCF/NEVPT2 Calculations.

	ζ (cm^{-1})	ζ/ζ_{free}[a]	$E(^6P)$ (cm^{-1})	$\zeta^2/E(^6P)$	Ground State Char.	
					^8S (%)	^6P (%)
Eu^{M}	1259.5	98.9	30698.2	51.7	97.76	2.22
Gd^{M}	1545.9	99.1	35351.7	67.6	97.48	2.51
Tb^{M}	1848.1	98.7	38909.0	87.8	97.05	2.92

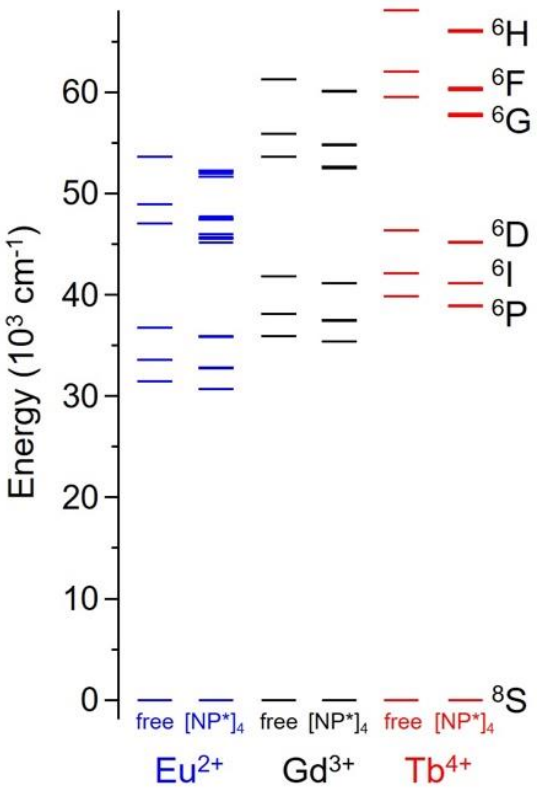

Figure 4.4 Energy levels for the ground ^{8}S state and excited sextet states calculated at the CASSCF/NEVPT2 level of theory. For each metal ion, the free ion and model structure energy levels are shown.

interaction in Tb^{4+} overwhelms that from increased inter-electronic repulsion, and thus results in larger ZFS. The trend of increasing $\zeta^2/E(^6P)$ from Eu^{2+} to Tb^{4+} is also reflected in the composition of the ground state that increases in ^{6}P character moving from Eu^{2+} to Tb^{4+} (Table 4.2). This analysis demonstrates the competing interactions (spin-orbit coupling, inter-electron repulsion, ligand field splitting) that lead Tb^{4+} to exhibit larger ZFS values than formally isoelectronic Eu^{2+} and Gd^{3+}. The ZFS is mostly determined by the splitting within the ^{6}P state, e.g., in the T_d point group, microstates within P terms are triply degenerate while in lower symmetry groups this degeneracy is lifted. The magnitude of the splitting among these ^{6}P microstates is then governed by the ligand field strength. Since each of these microstates make a different contribution to the ZFS, the computed ZFS

values are extremely sensitive to the geometry of the molecule. This situation is particularly challenging because the magnitude of each individual contribution is often much larger than the ZFS. While these factors limit the quantitative analysis of the experimental results, the significantly larger value of Δ_{8S} observed for the Tb complex is rationalized by the single-ion properties of the Tb^{4+} ion wherein the increased inter-electronic repulsion, shown by the increased separation between ^8S and ^6P states, is compensated by a larger SOC interaction in Tb^{4+}.

4.3 Conclusion

The isolation of tetravalent terbium complexes facilitated the first ever series of isostructural, isoelectronic lanthanide complexes spanning three oxidation states. Despite an isotropic ground state (^8S), conventional X-band EPR measurements of the tetravalent terbium compound in this study, as well as other tetravalent terbium complexes, exhibited strongly anisotropic spectra. The spectra contained broad, complex resonances and, using low frequency EPR, the quantitative value of ZFS in these compounds was impossible to determine. Multi-field fitting of the dc magnetometry data for all four compounds in this study highlights the increase in ZFS (as given by Δ_{8S}, which gives the effect of ZFS absent the complication of signage of traditional parameters) for Tb^{4+} when compared to Eu^{2+} and Gd^{3+} in a nearly conserved ligand environment. This trend is replicated in the analysis of the solution and solid-state HFEPR of the **1-Eu^{2+}**, **2-Gd^{3+}**, **3-Gd^{3+}**, and **4-Tb^{4+}** complexes which demonstrate similar ZFS parameters for the Eu^{2+} and Gd^{3+} complexes, although the Gd^{3+} parameters depending strongly on the deviation from tetrahedral coordination. As in

the trend seen in the fit of the dc susceptibility data, the $|D|$ and Δ_{8_S} values increase by ~8 times between **3-Gd^{3+}** and **4-Tb^{4+}**.

These experimental results were rationalized through CASSCF-NEVPT2 calculations on series of model complexes (**Eu^{M}**, **Gd^{M}**, and **Tb^{M}**) and simplified tetrahedral structures ($[LnCl_4]^{-1/0/+1}$ complexes). These calculations reveal that the similarity of the Eu^{2+} and Gd^{3+} single-ion properties and the divergence of the Tb^{4+} properties are driven by competition between electron-electron repulsion and spin orbit coupling. Specifically, in Tb^{4+} the increase in inter-electronic repulsion is compensated by a comparatively large increase in SOC (from Gd^{3+} to Tb^{4+} versus Eu^{2+} to Gd^{3+}). Additionally, these studies contribute to recent spectroscopic reevaluation[101, 106, 260] of lanthanide covalent bonding and reveal that tetravalent lanthanides, even mid-lanthanides, have greater metal-ligand bond covalency than in their di- and trivalent counterparts.

4.4 Experimental

4.4.1 *General Considerations*

Unless otherwise noted, all reagents were obtained from commercial suppliers. The syntheses and manipulations were conducted under argon with exclusion of oxygen and water using Schlenk techniques or in an inert atmosphere box (Vigor) under a dinitrogen (<0.1 ppm O_2/H_2O) atmosphere. The glovebox is equipped with two -35 ˚C freezers. All glassware and cannula were stored in an oven over-night (>8 h) at a temperature of ca. 160˚C. Celite and molecular sieves were dried under vacuum at a temperature >250˚C for a minimum of 24 h. C_6D_6 was stored over 3 Å molecular sieves and then vacuum-transferred from purple sodium/benzophenone prior to use. Hexanes, diethyl ether and

tetrahydrofuran were purged with UHP-grade argon (Airgas) and passed through columns containing Q-5 and molecular sieves in a solvent purification system (JC Meyer Solvent Systems). All solvents in the glovebox were stored in bottles over 3 Å molecular sieves. The starting materials $EuI_2(THF)_4$, $GdI_3(THF)_{3.5}$, and $[(CH_2N^tBu)_2(Et_2N)PN]K$ were prepared according to the literature procedures.[177, 261, 262] Compound **4-Tb^{4+}** (Tb[(NP(1,2-*bis*-^{t}Bu-diamidoethane)(NEt_2))]$_4$) was prepared according to previously reported procedures.[177]

Infrared (IR) samples were taken on a Bruker ALPHA FTIR spectrometer from 400 to 4000 cm^{-1}. IR samples were prepared as Nujol mulls sandwiched between two KBr plates. The peaks are listed in wavenumber [cm^{-1}] and intensity by using the following abbreviations: vw (very weak); w (weak); m (medium); s (strong); vs (very strong); br (broad).

Magnetic measurements were performed on a Quantum Design MPMS-5S magnetometer. Inside of a glovebox, a measured amount of quartz wool (10–20 mg) was loaded and packed tightly into a quartz tube. Powdered samples were loaded inside of the tube and onto the glass wool plug by tapping the compound through a glass pipet. Another pre-massed amount of quartz wool (10–20 mg) was loaded on top of the sample, and the contents were packed tightly again. The top of the tube was affixed to an Ultra Torr Swagelok adaptor while the bottom was plugged with a piece of snug tubing tightly closed with a stopper and copper wire. This was transported from the glovebox to a Schlenk line where it was sealed above and below the sample using a O_2/H_2 torch while the sample was under vacuum. The vacuum sealed tubing was taped to a straw, and the straw was loaded into the instrument. Diamagnetic corrections for the quartz wool and the complex were

performed using Pascal's constants.[183] Fit of the magnetic data was determined using Phi software.[228] All data collected in this study was collected roughly during the same time and utilized identical sample preparation. Susceptibility data for **4-Tb^{4+}** was recollected in this study on a different instrument than the previously reported data.

Crystals suitable for X-ray diffraction were covered in Paratone® oil in a glove box and transferred to the diffractometer in a 20 mL capped vial. Crystals were mounted on a loop with Paratone® oil on a Bruker D8 VENTURE diffractometer. The crystals were cooled and kept at T = 100(2) K during data collections. The structures were solved with the ShelXT structure solution program using the Intrinsic Phasing solution method and by using Olex2 as the graphical interface.[263, 264] The model was refined with version 2014/7 of XL using Least Squares minimization.[265] Structures are visualized in Ortep3 and graphics are generated with POV-ray.[266]

X-band EPR spectra were recorded using a commercial Bruker E680 X-band spectrometer. The sample temperature was controlled using an Oxford Instruments CF935 helium flow cryostat and ITC503 temperature controller. Measurements were performed with samples prepared as both polycrystalline powders and solutions (in toluene). New measurements were performed on **4-Tb^{4+}** and a wider field range was possible on this instrument compared to what was acquired in the previously reported spectra.

High-Frequency / High-Field Electron Paramagnetic Resonance (HFEPR) Spectra were recorded on a transmission-type spectrometer equipped with a 17 T superconducting magnet.[218] Microwaves were generated using a phase locked Virginia Diodes (Charlottesville, VA) source combined with a series of frequency multipliers and detected

with an InSb hot-electron bolometer (QMC Ltd., Cardiff, U.K.). Temperature control was accomplished using an Oxford Instruments (Oxford, U.K.) continuous-flow cryostat. All simulations of EPR spectra were performed using EasySpin software, which uses the Matlab® toolbox.[229]

To facilitate a direct comparison across the series, truncated models of **1-Eu**, **2-Gd**, **3-Gd**, and **4-Tb** as well as the hypothetical f^7 series $[LnCl_4]^{-/0/+}$ (Ln = Eu^{2+}, Gd^{3+}, Tb^{4+}) were optimized using the BP86 functional with the following basis sets: SARC-zora-TZVP (Eu, Gd, Tb) / zora-def2-TZVP (P,N,C,H).[16–19] Dispersion was accounted for by Grimme's DFT-D3(BJ) method. In all DFT calculations, relativistic effects were taken into account using the ZORA procedure.[267, 268]

In the complete active space self-consistent field (CASSCF) calculations, scalar relativistic effects were accounted for using the second-order Douglas-Kroll-Hess (DKH) procedure.[244-246, 269] To account for dynamic correlation, the converged wave functions were subjected to N-electron valence perturbation theory to second order (NEVPT2).[248-250, 270] In these calculations, spin-orbit coupling was accounted for with quasi-degenerate perturbation theory.[271] In all three models, the active space consisted of seven electrons in seven 4*f* orbitals averaged over the single octet state and all 48 sextet states where each state was weighted equally. All calculations were performed using the Orca 4.2.1 program package.[272]

4.4.2 *Synthesis of 1-Eu^{2+}*

Inside a glovebox, $EuI_2(THF)_2$ (0.246 g, 0.447 mmol) was added to a 20 mL scintillation vial charged with a glass stir bar and 2 mL of diethyl ether. [PN*]K (0.584 g,

1.79 mmol, 4.0 eq.) was added as a solution in diethyl ether (5 mL) and the reaction mixture was stirred overnight. The mixture was filtered through a fine porosity frit packed with Celite. The filtrate was concentrated in vacuo to give an orange solid. The residue was triturated three times with 1 mL of n-pentane and then taken up in 5 mL of diethyl ether and filtered through a pipet filter packed with Celite and glass filter paper. The dark orange solution was concentrated in vacuo and placed inside a −35 °C freezer overnight, during which time dark orange crystals were obtained (0.531 g, 86%). No ^{1}H, ^{13}C, or ^{31}P NMR signals were observed. IR: ν [cm^{-1}] = 1266 (m), 1246 (m), 1204 (s), 1180 (m), 1147 (s), 1093 (s), 1076 (s), 1047 (m), 1023 (m), 969 (w), 911 (w), 866 (w), 795 (w), 705 (s), 680 (m), 614 (w). Elemental analysis found (calculated): C, 49.15 (50.37), H, 9.60 (9.64), N, 14.65 (14.69). Carbon was consistently low on multiple burns. XRD quality crystals were grown from concentrated solution of diethyl ether at −35 °C.

4.4.3 *Synthesis of 2-Gd^{3+}*

Inside a glovebox, $GdI_3(THF)_{3.5}$ (0.313 g, 0.396 mmol) was added to a 20 mL scintillation vial charged with a stir bar and 2 mL of diethyl ether. [PN*]K (0.518 g, 1.58 mmol, 4.0 eq.) was added as a solution in diethyl ether (5 mL) and the reaction mixture was stirred overnight. The mixture was filtered through a fine porosity frit packed with Celite. The filtrate was concentrated in vacuo to give a pale tan solid. The residue was triturated three times with 1 mL of n-pentane and then taken up in 5 mL of diethyl ether and filtered through a pipet filter packed with Celite and glass filter paper. The pale orange solution was concentrated in vacuo and placed inside a −35 °C freezer overnight, during which time colorless crystals were obtained (0.407 g, 71%). No ^{1}H, ^{13}C, or ^{31}P NMR signals were observed. IR: ν [cm–1] = 1266 (m), 1246 (m), 1217 (s), 1200 (s), 1171 (s),

1151 (s), 1113 (m), 1051 (m), 1031 (m), 977 (w), 928 (w), 866 (w), 795 (w), 725 (w), 692 (m), 626 (w). Elemental analysis found (calculated): C, 50.12 (49.97), H, 9.66 (9.59), N, 16.48 (16.65). XRD quality crystals were grown from concentrated solution of diethyl ether at −35 °C.

4.4.4 *Synthesis of 3-Gd^{3+}*

Inside a glovebox, **1-Gd^{3+}** (0.164 g, 0.122 mmol) was added to a 20 mL scintillation vial charged with a stir bar and 2 mL of 1,2-dimethoxyethane. [2.2.2]-Cryptand (0.046 g, 0.122 mmol) was added as a solution in 1,2-dimethoxyethane (2 mL) and the reaction was stirred overnight. The mixture was filtered through a fine porosity frit packed with Celite. The volume of the solution was reduced to around 3 mL in vacuo and crystals were grown through slow evaporation at room temperature. The solution was decanted, and the colorless crystals were dried in vacuo to give the title compound (0.165 g, 79%). No ^{1}H, ^{13}C, or ^{31}P NMR signals were observed. IR: ν [cm−1] = 1258 (m), 1250 (m), 1217 (s), 1200 (s), 1180 (s), 1155 (m), 1134 (m), 1105 (m), 1080 (w), 1051 (m), 1023 (m), 977 (w), 952 (w), 923 (w), 866 (w), 795 (w), 688 (m). Elemental analysis found (calculated): C, 50.81 (51.60), H, 9.49 (9.60), N, 14.61 (14.64). Carbon was consistently low on multiple burns. XRD quality crystals were grown from evaporating solution of 1,2-dimethoxyethane at room temperature.

4.5 Crystallographic Information

Table 4.3 Crystal data and structure refinement.

Identification code	**1-Eu^{2+}**	**2-Gd^{3+}**	**3-Gd^{3+}**
Empirical formula	$C_{68}H_{153.95}EuK_2N_{16}O_3P_4$	$C_{64}H_{148}GdKN_{16}O_2P_4$	$C_{296}H_{656}Gd_4K_4N_{72}O_{24}P_{16}$
Formula weight	1598.05	1494.21	6889.81
Temperature/K	99.99	100.01	100.06
Crystal system	orthorhombic	monoclinic	orthorhombic
Space group	$P2_12_12_1$	$P2_1/n$	Pbca
a/Å	18.5834(14)	22.581(4)	19.756(2)
b/Å	21.5499(16)	15.4593(19)	26.462(2)
c/Å	21.6496(17)	25.693(4)	35.130(3)
α/°	90	90	90
β/°	90	114.850(7)	90
γ/°	90	90	90
Volume/Å^3	8670.0(11)	8139(2)	18365(3)
Z	4	4	2
ρ_{calc}g/cm^3	1.224	1.219	1.246
μ/mm^{-1}	0.943	0.993	0.893
F(000)	3436.0	3212.0	7400.0
Crystal size/mm^3	0.29 × 0.23 × 0.228	0.383 × 0.258 × 0.248	0.157 × 0.121 × 0.114
Radiation	MoKα (λ = 0.71073)	MoKα (λ = 0.71073)	MoKα (λ = 0.71073)
2Θ range for data collection/°	4.354 to 61.018	4.106 to 55.188	4.552 to 56.672
Index ranges	-26 ≤ h ≤ 26, -30 ≤ k ≤ 30, -30 ≤ l ≤ 30	-29 ≤ h ≤ 29, -19 ≤ k ≤ 20, -33 ≤ l ≤ 32	-26 ≤ h ≤ 26, -34 ≤ k ≤ 35, -46 ≤ l ≤ 46
Reflections collected	123450	55131	169161
Independent reflections	26365 [R_{int} = 0.0574, R_{sigma} = 0.0447]	18224 [R_{int} = 0.0591, R_{sigma} = 0.0702]	22804 [R_{int} = 0.1112, R_{sigma} = 0.0703]
Data/restraints/parameters	26365/86/942	18224/60/829	22804/206/1096
Goodness-of-fit on F^2	1.034	1.138	1.158
Final R indexes [I>=2σ (I)]	R_1 = 0.0398, wR_2 = 0.0906	R_1 = 0.0722, wR_2 = 0.1654	R_1 = 0.0694, wR_2 = 0.1350
Final R indexes [all data]	R_1 = 0.0477, wR_2 = 0.0962	R_1 = 0.0896, wR_2 = 0.1733	R_1 = 0.1063, wR_2 = 0.1495
Largest diff. peak/hole / e Å^{-3}	1.01/-0.80	2.51/-3.22	1.60/-1.19
Flack parameter	0.199(9)	- -	

4.5.1 *1-Eu*$^{2+}$

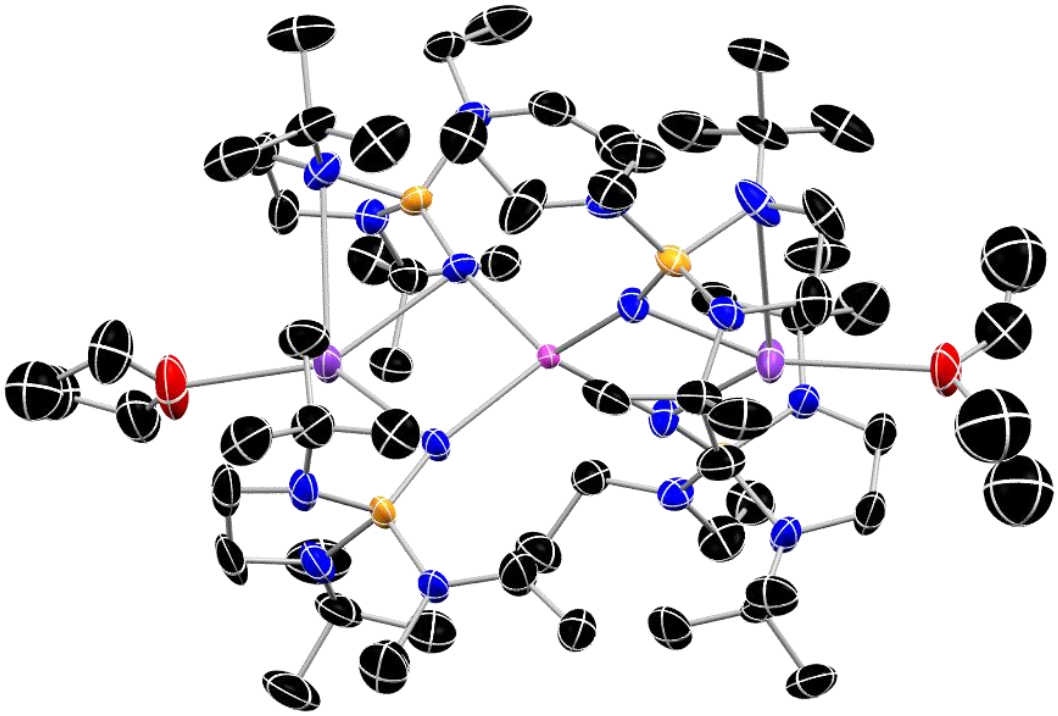

Figure 4.5 Molecular structure of 1-Eu^{2+} with thermal ellipsoids shown at 50% probability with hydrogen atoms omitted for clarity. Color code: C, black; N, blue; O, red; P, orange; K, purple; Eu, magenta.

Table 4.4 Fractional Atomic Coordinates (×104) and Equivalent Isotropic Displacement Parameters (Å2×103) for 1-Eu^{2+}. U_{eq} is defined as 1/3 of the trace of the orthogonalised U_{IJ} tensor.

Atom	*x*	*y*	*z*	*U*(eq)
Eu1	5094.0(2)	5039.9(2)	5362.5(2)	18.47(4)
K1	3892.9(7)	6201.4(5)	6078.3(6)	43.2(3)
K2	6321.5(6)	3959.8(5)	4536.3(5)	38.6(2)
P1	4329.4(5)	6582.3(4)	4608.3(6)	24.21(19)
P2	4232.2(6)	5049.1(7)	7048.6(5)	31.8(2)
P3	7213.8(5)	4969.8(6)	5464.9(5)	31.0(2)
P4	4623.5(6)	3585.1(5)	4301.3(6)	28.8(2)
O2	7222(3)	3318(3)	3714(3)	82.7(18)
N1	4591(2)	6031.2(18)	4980.7(19)	34.8(8)
N2	4483(2)	7327.3(19)	4857(2)	42.9(11)

Atom	*x*	*y*	*z*	*U*(eq)
N3	3423(2)	6736.4(17)	4571(2)	37.6(9)
N4	4617(2)	6605.6(18)	3868.2(19)	34.7(8)
N5	4563(2)	5128.0(18)	6411.7(18)	34.3(8)
N6	4421(2)	5565(2)	7645.0(19)	35.4(9)
N7	3332(2)	5190(3)	7123(2)	53.6(14)
N8	4385(3)	4351(2)	7381(2)	47.4(12)
N9	6404.3(16)	4903.8(16)	5379.7(18)	29.6(7)
N10	7714(2)	4388(2)	5812(2)	43.3(11)
N11	7750(2)	4943(3)	4828(2)	48.8(11)
N12	7479(2)	5606.5(19)	5855(2)	36.0(9)
N13	4878(2)	4155.4(16)	4651(2)	34.1(7)
N14	5098(3)	2906.3(17)	4432(2)	41.8(9)
N15	4750(2)	3505.4(19)	3516.6(19)	35.8(9)
N16	3740(2)	3435.0(18)	4377.2(19)	33.9(8)
C1	5185(3)	7561(2)	5067(3)	40.6(12)
C2	5801(3)	7213(3)	4748(4)	68(2)
C3	5252(4)	8250(3)	4892(3)	58.7(17)
C4	5266(4)	7498(3)	5768(3)	58.5(17)
C5	3849(3)	7650(2)	5035(3)	50.3(14)
C6	3217(3)	7302(3)	4850(4)	57.5(18)
C7	2863(3)	6279(2)	4405(2)	35.8(10)
C8	2545(5)	5989(4)	4983(3)	83(3)
C9	3179(3)	5754(3)	4016(4)	60.3(19)
C10	2265(4)	6600(4)	4052(5)	84(3)
C11	4458(4)	7131(3)	3465(3)	57.9(17)
C13	4980(3)	6082(2)	3589(2)	42.7(12)
C14	5698(4)	6229(3)	3282(3)	58.6(16)
C15	5144(3)	5861(3)	7683(3)	46.3(12)
C16	5226(4)	6138(4)	8332(3)	71(2)
C17	5247(4)	6373(3)	7204(3)	54.9(15)
C18	5722(3)	5369(3)	7587(3)	50.7(15)
C19	3802(4)	5957(3)	7778(3)	52.5(15)
C20	3150(3)	5558(4)	7662(3)	57.7(17)
C25	4683(3)	4208(3)	8504(3)	53.1(15)
C26	4119(4)	4208(3)	8002(3)	53.2(15)
C27	4910(6)	3938(3)	7129(3)	77(3)
C29	7436(3)	4048(3)	6363(3)	54.0(15)
C30	7082(4)	4498(4)	6807(3)	61.7(17)
C31	6880(4)	3554(3)	6178(4)	65(2)
C32	8078(4)	3734(3)	6698(4)	75(2)
C33	8069(3)	4015(3)	5342(4)	62.1(18)

Atom	*x*	*y*	*z*	*U*(eq)
C34	8304(3)	4460(3)	4847(4)	63(2)
C35	7724(3)	5363(3)	4292(3)	58.4(17)
C36	7370(5)	5041(5)	3744(3)	81(2)
C37	7304(4)	5964(3)	4444(4)	68(2)
C38	8489(4)	5556(5)	4105(4)	87(3)
C39	8561(4)	5709(4)	6542(4)	74(2)
C40	8242(3)	5768(3)	5903(3)	56.3(17)
C41	6958(4)	5961(3)	6219(4)	69(2)
C43	5094(4)	2551(2)	5023(3)	54.7(16)
C44	4926(6)	2973(3)	5560(3)	80(2)
C45	5853(4)	2292(3)	5132(4)	75(2)
C46	4562(5)	2007(4)	5007(4)	77(2)
C47	5195(3)	2544(2)	3868(3)	49.9(14)
C48	5250(3)	3017(3)	3363(3)	48.1(13)
C49	4749(3)	4057(2)	3102(2)	40.2(11)
C50	5443(3)	4433(3)	3170(3)	50.0(14)
C51	4663(4)	3836(4)	2431(3)	60.5(17)
C52	4108(3)	4474(3)	3262(3)	42.9(12)
C53	2743(5)	3150(4)	3648(4)	82(3)
C54	3375(3)	2936(2)	4047(3)	43.7(13)
C55	3308(4)	3782(3)	4803(4)	73(2)
O1	619(3)	4460(2)	5611(2)	61.0(12)
C11S	194(4)	4296(4)	6627(4)	72(2)
C12S	153(4)	4688(4)	6056(4)	70.2(19)
C13S	625(4)	4816(4)	5048(4)	78(2)
C14S	1138(5)	4544(4)	4601(4)	85(2)
C21S	7493(6)	2772(4)	3971(5)	94(3)
C23S	7772(7)	2775(5)	2901(5)	109(4)
C24S	7409(5)	3352(4)	3058(4)	79(2)
C12A	3874(12)	7140(15)	2977(10)	61(3)
C28A	4889(15)	3238(4)	7180(8)	73(3)
C42A	7032(13)	6557(7)	6518(12)	51(2)
C56A	3069(8)	4371(6)	4711(8)	82(4)
C22S	8107(10)	2605(14)	3556(7)	99(4)
C31A	3340(17)	8168(11)	6859(14)	139(7)
C32A	3168(18)	7661(13)	7063(14)	160(8)
O3A	2994(8)	7141(12)	6688(19)	63(3)
C33A	2282(10)	7267(9)	6433(11)	93(4)
C34A	1746(11)	6945(11)	6383(13)	123(6)
C21A	2756(4)	4859(6)	6845(4)	51(3)
C22A	2450(6)	4383(6)	7303(5)	65(3)

Atom	*x*	*y*	*z*	*U*(eq)
C23A	2135(6)	5291(7)	6643(6)	75(4)
C24A	3040(6)	4515(7)	6266(5)	75(4)
C12B	4042(10)	6939(9)	2894(5)	61(3)
C28B	4538(13)	3314(7)	7176(10)	73(3)
C42B	7002(5)	6626(3)	6130(5)	51(2)
C56B	2793(9)	3464(8)	5119(9)	82(4)
C12	7472(10)	2337(7)	3432(7)	99(4)
C31B	3781(14)	7736(13)	7085(13)	139(7)
C32B	3218(12)	7636(12)	6812(17)	160(8)
O3B	3022(7)	7049(12)	6567(18)	63(3)
C33B	2272(10)	6952(8)	6740(11)	93(4)
C34B	1840(12)	7294(11)	6995(12)	123(6)
C21B	2750(10)	4620(13)	6860(8)	51(3)
C22B	2271(18)	4296(16)	7339(11)	65(3)
C23B	2261(16)	5025(18)	6446(13)	75(4)
C24B	3114(14)	4124(15)	6448(14)	75(4)

Table 4.5 Anisotropic Displacement Parameters ($Å^2 \times 10^3$) for 1-Eu^{2+}. The Anisotropic displacement factor exponent takes the form: $-2\pi^2[h^2a^{*2}U_{11} + 2hka^*b^*U_{12} + \ldots]$.

Atom	U_{11}	U_{22}	U_{33}	U_{23}	U_{13}	U_{12}
Eu1	15.80(7)	16.96(7)	22.66(7)	-0.27(7)	0.76(6)	0.99(6)
K1	48.5(6)	37.6(5)	43.5(6)	2.9(5)	14.5(5)	16.7(5)
K2	30.4(5)	35.7(5)	49.9(7)	-15.7(4)	1.1(4)	5.5(4)
P1	25.1(4)	19.0(4)	28.5(5)	0.0(4)	-3.1(5)	0.8(3)
P2	29.7(5)	39.4(6)	26.4(5)	2.3(5)	7.6(4)	-3.4(5)
P3	17.0(4)	33.0(5)	43.1(6)	-9.8(6)	-1.4(3)	2.7(4)
P4	29.7(5)	24.3(5)	32.4(6)	-5.3(4)	-3.1(4)	-3.9(4)
O2	64(3)	94(4)	90(4)	-41(3)	5(3)	34(3)
N1	39(2)	31.0(18)	34(2)	3.7(15)	2.9(17)	10.3(16)
N2	32(2)	28.3(19)	69(3)	-15.8(19)	-8.6(19)	2.4(16)
N3	26.5(17)	30.7(17)	56(3)	-8.9(19)	-8.4(19)	1.1(14)
N4	40(2)	32.0(18)	32(2)	4.6(16)	2.9(17)	-2.8(16)
N5	36.1(19)	32.5(19)	34.3(19)	5.0(15)	10.5(15)	4.8(15)
N6	34(2)	43(2)	30(2)	-3.4(17)	9.1(17)	-4.0(17)
N7	28.6(19)	100(4)	33(2)	-16(2)	7.7(16)	-3(2)
N8	63(3)	42(2)	37(2)	10.6(19)	6(2)	-13(2)
N9	19.4(13)	32.9(16)	36.4(17)	-8.0(17)	-2.1(13)	1.9(12)
N10	26(2)	42(2)	61(3)	-12(2)	-11(2)	12.2(18)
N11	27.1(17)	62(3)	57(3)	-13(3)	10.4(16)	3(2)
N12	20.1(18)	36(2)	52(3)	-13.7(18)	-4.2(17)	-1.5(15)

Atom	U_{11}	U_{22}	U_{33}	U_{23}	U_{13}	U_{12}
N13	33.5(18)	29.8(15)	39(2)	-8.0(15)	-1(2)	-7.9(14)
N14	48(2)	29.7(17)	47(2)	-2.6(15)	-10(2)	1.3(18)
N15	37(2)	34.6(19)	36(2)	-5.8(16)	3.9(17)	0.6(16)
N16	34(2)	31.3(18)	37(2)	-5.0(15)	-0.9(16)	-9.3(16)
C1	39(3)	28(2)	54(3)	-5.8(19)	-7(2)	-10(2)
C2	31(3)	75(4)	99(6)	-39(4)	-5(3)	-11(3)
C3	61(4)	40(3)	76(4)	3(3)	-11(3)	-18(3)
C4	45(3)	67(4)	63(4)	10(3)	-19(3)	-13(3)
C5	42(3)	33(2)	76(4)	-17(3)	-14(3)	11(2)
C6	35(3)	39(3)	98(5)	-24(3)	-12(3)	8(2)
C7	29(2)	41(2)	37(2)	-9(2)	-3.6(18)	-2.5(19)
C8	103(6)	83(5)	61(4)	-29(4)	27(4)	-56(5)
C9	45(3)	56(3)	79(5)	-36(3)	8(3)	-22(3)
C10	65(5)	76(5)	112(7)	-15(5)	-60(5)	1(4)
C11	69(4)	54(3)	51(4)	28(3)	2(3)	6(3)
C13	53(3)	38(2)	37(2)	-5.7(18)	16(2)	-7(2)
C14	48(3)	69(4)	59(4)	-6(3)	14(3)	-9(3)
C15	47(3)	49(3)	44(3)	0(2)	1(2)	-15(3)
C16	81(5)	88(5)	45(3)	-9(3)	-8(3)	-37(4)
C17	65(4)	46(3)	53(3)	3(3)	8(3)	-16(3)
C18	30(3)	69(4)	53(3)	15(3)	-1(2)	-12(3)
C19	56(4)	61(4)	40(3)	-10(3)	13(3)	13(3)
C20	36(3)	104(5)	33(3)	-10(3)	13(2)	9(3)
C25	55(3)	64(4)	40(3)	18(3)	4(3)	-6(3)
C26	56(4)	64(4)	40(3)	17(3)	3(3)	-23(3)
C27	136(8)	38(3)	57(4)	15(3)	31(5)	13(4)
C29	42(3)	52(3)	69(4)	3(3)	-23(3)	4(3)
C30	65(4)	70(4)	50(4)	6(3)	-14(3)	4(3)
C31	47(4)	57(4)	91(6)	7(4)	-22(4)	-10(3)
C32	60(4)	57(4)	107(6)	10(4)	-47(4)	5(3)
C33	37(3)	58(3)	91(5)	-27(4)	-14(3)	23(2)
C34	24(2)	85(5)	81(5)	-37(4)	7(3)	12(3)
C35	43(3)	70(4)	63(4)	-9(3)	22(3)	-20(3)
C36	91(5)	93(6)	58(4)	-2(5)	-4(4)	-35(6)
C37	67(4)	64(4)	74(5)	12(4)	17(4)	-8(4)
C38	53(4)	108(7)	100(7)	-19(5)	35(4)	-34(4)
C39	40(3)	85(5)	96(6)	-22(4)	-30(4)	1(3)
C40	25(2)	58(3)	86(5)	-25(3)	-5(3)	-3(2)
C41	43(3)	57(4)	107(6)	-36(4)	-3(4)	0(3)
C43	65(4)	37(2)	62(4)	10(2)	-32(3)	-9(3)
C44	118(7)	71(4)	50(4)	15(3)	-24(4)	0(5)

Atom	U_{11}	U_{22}	U_{33}	U_{23}	U_{13}	U_{12}
C45	70(5)	49(3)	108(6)	24(4)	-48(4)	-6(3)
C46	84(5)	68(4)	79(5)	27(4)	-38(4)	-38(4)
C47	47(3)	33(2)	70(4)	-19(2)	-10(3)	8(2)
C48	47(3)	44(3)	54(3)	-20(2)	4(2)	10(2)
C49	42(3)	45(3)	33(2)	-2(2)	6(2)	-5(2)
C50	47(3)	48(3)	56(4)	4(3)	11(3)	-9(3)
C51	69(4)	76(4)	36(3)	-2(3)	1(3)	-3(4)
C52	43(3)	39(3)	47(3)	8(2)	-4(2)	-2(2)
C53	80(5)	58(4)	108(7)	12(4)	-57(5)	-32(4)
C54	37(3)	32(2)	63(4)	-8(2)	-11(2)	-11(2)
C55	60(4)	66(4)	93(6)	-41(4)	39(4)	-29(3)
O1	58(3)	57(3)	68(3)	-12(2)	-12(2)	5(2)
C11S	52(4)	93(5)	72(5)	-24(4)	-4(4)	-11(4)
C12S	49(4)	87(5)	74(5)	-9(4)	-9(4)	22(4)
C13S	53(4)	90(6)	93(6)	15(5)	-6(4)	10(4)
C14S	114(7)	58(4)	82(5)	-6(4)	11(6)	-3(4)
C21S	110(7)	81(6)	91(7)	-33(5)	17(6)	21(5)
C23S	115(8)	95(7)	117(8)	-42(6)	59(7)	-17(6)
C24S	60(4)	84(5)	94(6)	-26(5)	16(4)	4(4)
C12A	56(4)	64(4)	61(4)	19(3)	-5(3)	0(3)
C28A	80(5)	66(4)	74(4)	0(3)	-1(4)	6(3)
C42A	50(3)	43(3)	58(4)	-2(3)	-1(3)	5(2)
C56A	68(7)	85(8)	93(9)	-16(7)	32(6)	-15(6)
C22S	99(5)	98(5)	101(5)	-4(3)	3(3)	2(3)
C31A	140(8)	139(8)	138(8)	1(3)	0(3)	3(3)
C32A	162(9)	159(8)	161(9)	-1(3)	0(3)	-5(3)
O3A	58(3)	62(7)	70(13)	-34(5)	13(4)	18(3)
C33A	91(5)	95(5)	94(5)	0(3)	1(3)	0(3)
C34A	123(6)	124(6)	123(6)	2(3)	1(3)	3(3)
C21A	35(3)	85(9)	34(3)	-6(4)	8(2)	-25(4)
C22A	50(7)	91(7)	54(4)	7(4)	-4(4)	-38(5)
C23A	44(5)	133(12)	47(7)	18(7)	-2(5)	-22(6)
C24A	68(6)	104(10)	54(6)	-28(6)	-1(5)	-42(7)
C12B	56(4)	64(4)	61(4)	19(3)	-5(3)	0(3)
C28B	80(5)	66(4)	74(4)	0(3)	-1(4)	6(3)
C42B	50(3)	43(3)	58(4)	-2(3)	-1(3)	5(2)
C56B	68(7)	85(8)	93(9)	-16(7)	32(6)	-15(6)
C12	99(5)	98(5)	101(5)	-4(3)	3(3)	2(3)
C31B	140(8)	139(8)	138(8)	1(3)	0(3)	3(3)
C32B	162(9)	159(8)	161(9)	-1(3)	0(3)	-5(3)
O3B	58(3)	62(7)	70(13)	-34(5)	13(4)	18(3)

Atom	U_{11}	U_{22}	U_{33}	U_{23}	U_{13}	U_{12}
C33B	91(5)	95(5)	94(5)	0(3)	1(3)	0(3)
C34B	123(6)	124(6)	123(6)	2(3)	1(3)	3(3)
C21B	35(3)	85(9)	34(3)	-6(4)	8(2)	-25(4)
C22B	50(7)	91(7)	54(4)	7(4)	-4(4)	-38(5)
C23B	44(5)	133(12)	47(7)	18(7)	-2(5)	-22(6)
C24B	68(6)	104(10)	54(6)	-28(6)	-1(5)	-42(7)

Table 4.6 Bond Lengths for 1-Eu^{2+}

Atom	Atom	Length/Å	Atom	Atom	Length/Å
Eu1	K1	3.6944(10)	N16	C55	1.434(7)
Eu1	K2	3.7177(10)	C1	C2	1.533(9)
Eu1	N1	2.474(4)	C1	C3	1.536(7)
Eu1	N5	2.483(4)	C1	C4	1.531(9)
Eu1	N9	2.453(3)	C5	C6	1.452(8)
Eu1	N13	2.483(3)	C7	C8	1.518(9)
K1	P1	3.3853(17)	C7	C9	1.528(8)
K1	P2	3.3131(17)	C7	C10	1.516(8)
K1	N1	2.732(4)	C11	C12A	1.515(11)
K1	N5	2.725(4)	C11	C12B	1.517(11)
K1	N7	3.309(6)	C13	C14	1.524(8)
K1	O3A	2.939(15)	C15	C16	1.533(8)
K1	O3B	2.659(13)	C15	C17	1.526(8)
K2	P3	3.3954(15)	C15	C18	1.523(9)
K2	P4	3.2966(16)	C19	C20	1.506(9)
K2	O2	2.807(5)	C25	C26	1.510(9)
K2	N9	2.738(4)	C27	C28A	1.513(11)
K2	N11	3.456(5)	C27	C28B	1.515(11)
K2	N13	2.726(4)	C29	C30	1.515(10)
K2	N14	3.221(4)	C29	C31	1.537(9)
P1	N1	1.515(4)	C29	C32	1.552(8)
P1	N2	1.717(4)	C33	C34	1.502(11)
P1	N3	1.719(4)	C35	C36	1.524(10)
P1	N4	1.690(4)	C35	C37	1.548(10)
P2	N5	1.520(4)	C35	C38	1.537(8)
P2	N6	1.739(4)	C39	C40	1.510(10)
P2	N7	1.708(5)	C41	C42A	1.445(10)
P2	N8	1.693(5)	C41	C42B	1.447(10)
P3	N9	1.522(3)	C43	C44	1.509(11)
P3	N10	1.731(5)	C43	C45	1.534(10)
P3	N11	1.703(4)	C43	C46	1.535(9)

Atom	Atom	Length/Å	Atom	Atom	Length/Å
P3	N12	1.685(4)	C47	C48	1.498(9)
P4	N13	1.519(3)	C49	C50	1.531(8)
P4	N14	1.732(4)	C49	C51	1.537(8)
P4	N15	1.724(4)	C49	C52	1.531(8)
P4	N16	1.681(4)	C53	C54	1.530(9)
O2	C21S	1.396(11)	C55	C56A	1.359(12)
O2	C24S	1.464(11)	C55	C56B	1.361(12)
N2	C1	1.470(7)	O1	C12S	1.384(9)
N2	C5	1.421(7)	O1	C13S	1.440(9)
N3	C6	1.412(7)	C11S	C12S	1.500(11)
N3	C7	1.478(6)	C13S	C14S	1.479(11)
N4	C11	1.460(7)	C21S	C22S	1.496(15)
N4	C13	1.446(6)	C21S	C12	1.496(15)
N6	C15	1.490(7)	C23S	C24S	1.455(12)
N6	C19	1.456(7)	C23S	C22S	1.592(17)
N7	C20	1.451(7)	C23S	C12	1.590(17)
N7	C21A	1.421(10)	C31A	C32A	1.221(16)
N7	C21B	1.73(2)	C32A	O3A	1.42(2)
N8	C26	1.466(7)	O3A	C33A	1.46(2)
N8	C27	1.427(9)	C33A	C34A	1.220(16)
N10	C29	1.492(9)	C21A	C22A	1.536(11)
N10	C33	1.457(8)	C21A	C23A	1.545(12)
N11	C34	1.464(8)	C21A	C24A	1.548(12)
N11	C35	1.471(9)	C31B	C32B	1.221(17)
N12	C40	1.464(6)	C32B	O3B	1.42(2)
N12	C41	1.463(8)	O3B	C33B	1.46(2)
N14	C43	1.491(7)	C33B	C34B	1.222(16)
N14	C47	1.461(7)	C21B	C22B	1.536(11)
N15	C48	1.442(6)	C21B	C23B	1.545(12)
N15	C49	1.489(7)	C21B	C24B	1.548(12)
N16	C54	1.458(6)			

Table 4.7 Bond Angles for 1-Eu^{2+}

Atom	Atom	Atom	Angle/°	Atom	Atom	Atom	Angle/°
K1	Eu1	K2	175.37(3)	C20	N7	P2	113.7(4)
N1	Eu1	K1	47.69(10)	C20	N7	C21B	120.4(7)
N1	Eu1	K2	127.72(10)	C21A	N7	K1	106.1(5)
N1	Eu1	N5	95.13(13)	C21A	N7	P2	127.5(5)
N1	Eu1	N13	113.23(13)	C21A	N7	C20	116.1(5)
N5	Eu1	K1	47.52(9)	C21B	N7	K1	116.0(7)

Atom	Atom	Atom	Angle/°	Atom	Atom	Atom	Angle/°
N5	Eu1	K2	137.02(9)	C26	N8	P2	121.3(5)
N9	Eu1	K1	132.42(8)	C27	N8	P2	120.4(4)
N9	Eu1	K2	47.41(8)	C27	N8	C26	116.9(5)
N9	Eu1	N1	118.92(13)	Eu1	N9	K2	91.31(11)
N9	Eu1	N5	112.92(13)	P3	N9	Eu1	166.3(2)
N9	Eu1	N13	94.46(12)	P3	N9	K2	101.88(16)
N13	Eu1	K1	133.05(9)	C29	N10	P3	121.1(4)
N13	Eu1	K2	47.15(9)	C33	N10	P3	109.8(4)
N13	Eu1	N5	124.19(13)	C33	N10	C29	116.4(5)
P1	K1	Eu1	67.98(3)	P3	N11	K2	73.65(15)
P2	K1	Eu1	69.09(3)	C34	N11	K2	96.3(4)
P2	K1	P1	137.07(4)	C34	N11	P3	114.3(5)
N1	K1	Eu1	42.04(8)	C34	N11	C35	118.9(5)
N1	K1	P1	25.98(8)	C35	N11	K2	102.0(3)
N1	K1	P2	111.13(9)	C35	N11	P3	126.7(4)
N1	K1	N7	130.97(12)	C40	N12	P3	120.8(4)
N1	K1	O3A	138.9(9)	C41	N12	P3	120.1(4)
N5	K1	Eu1	42.24(8)	C41	N12	C40	118.6(4)
N5	K1	P1	110.20(9)	Eu1	N13	K2	90.94(12)
N5	K1	P2	26.96(8)	P4	N13	Eu1	168.6(2)
N5	K1	N1	84.22(11)	P4	N13	K2	97.83(18)
N5	K1	N7	53.41(11)	P4	N14	K2	77.03(14)
N5	K1	O3A	136.6(9)	C43	N14	K2	107.8(3)
N7	K1	Eu1	91.77(9)	C43	N14	P4	124.9(4)
N7	K1	P1	151.37(10)	C47	N14	K2	110.4(3)
N7	K1	P2	29.88(8)	C47	N14	P4	112.1(3)
O3A	K1	Eu1	177.3(5)	C47	N14	C43	116.4(4)
O3A	K1	P1	113.0(9)	C48	N15	P4	112.8(4)
O3A	K1	P2	109.9(9)	C48	N15	C49	116.4(4)
O3A	K1	N7	88.2(8)	C49	N15	P4	120.9(3)
O3B	K1	Eu1	178.6(9)	C54	N16	P4	123.3(4)
O3B	K1	P1	110.7(9)	C55	N16	P4	120.6(4)
O3B	K1	P2	112.2(9)	C55	N16	C54	116.0(5)
O3B	K1	N1	136.6(9)	N2	C1	C2	110.8(4)
O3B	K1	N5	139.1(9)	N2	C1	C3	109.1(5)
O3B	K1	N7	89.4(9)	N2	C1	C4	111.3(5)
P3	K2	Eu1	67.26(2)	C2	C1	C3	107.5(6)
P3	K2	N11	28.77(7)	C4	C1	C2	109.2(6)
P4	K2	Eu1	68.92(3)	C4	C1	C3	108.8(5)
P4	K2	P3	135.71(4)	N2	C5	C6	110.0(4)
P4	K2	N11	156.05(9)	N3	C6	C5	110.2(5)

Atom	Atom	Atom	Angle/°	Atom	Atom	Atom	Angle/°
O2	K2	Eu1	168.29(15)	N3	C7	C8	110.3(5)
O2	K2	P3	113.58(13)	N3	C7	C9	110.9(4)
O2	K2	P4	110.61(13)	N3	C7	C10	109.6(5)
O2	K2	N11	87.70(15)	C8	C7	C9	107.4(5)
O2	K2	N14	91.68(16)	C10	C7	C8	108.5(7)
N9	K2	Eu1	41.27(7)	C10	C7	C9	110.0(5)
N9	K2	P3	26.02(7)	N4	C11	C12A	124.9(12)
N9	K2	P4	109.80(7)	N4	C11	C12B	112.3(8)
N9	K2	O2	139.05(15)	N4	C13	C14	115.4(4)
N9	K2	N11	51.63(10)	N6	C15	C16	107.9(5)
N9	K2	N14	127.60(12)	N6	C15	C17	112.6(5)
N11	K2	Eu1	89.98(8)	N6	C15	C18	109.3(4)
N13	K2	Eu1	41.90(7)	C17	C15	C16	109.2(5)
N13	K2	P3	109.11(8)	C18	C15	C16	109.0(6)
N13	K2	P4	27.17(7)	C18	C15	C17	108.8(5)
N13	K2	O2	136.08(15)	N6	C19	C20	105.8(5)
N13	K2	N9	83.09(10)	N7	C20	C19	104.9(4)
N13	K2	N11	130.12(11)	N8	C26	C25	115.2(5)
N13	K2	N14	54.62(11)	N8	C27	C28A	125.1(12)
N14	K2	Eu1	92.40(9)	N8	C27	C28B	102.5(12)
N14	K2	P3	146.93(9)	N10	C29	C30	110.0(5)
N14	K2	P4	30.79(8)	N10	C29	C31	111.4(6)
N14	K2	N11	170.93(12)	N10	C29	C32	108.8(6)
N1	P1	K1	52.17(16)	C30	C29	C31	108.5(6)
N1	P1	N2	120.8(2)	C30	C29	C32	108.4(6)
N1	P1	N3	119.4(2)	C31	C29	C32	109.7(5)
N1	P1	N4	115.2(2)	N10	C33	C34	106.1(5)
N2	P1	K1	88.37(18)	N11	C34	C33	105.7(5)
N2	P1	N3	89.80(19)	N11	C35	C36	110.4(6)
N3	P1	K1	81.70(18)	N11	C35	C37	111.4(5)
N4	P1	K1	167.01(14)	N11	C35	C38	110.1(6)
N4	P1	N2	102.5(2)	C36	C35	C37	109.2(7)
N4	P1	N3	105.1(2)	C36	C35	C38	108.5(6)
N5	P2	K1	54.40(15)	C38	C35	C37	107.2(6)
N5	P2	N6	121.4(2)	N12	C40	C39	115.1(6)
N5	P2	N7	117.6(2)	C42A	C41	N12	130.0(11)
N5	P2	N8	114.7(2)	C42B	C41	N12	114.1(7)
N6	P2	K1	91.74(16)	N14	C43	C44	110.7(5)
N7	P2	K1	74.9(2)	N14	C43	C45	108.3(6)
N7	P2	N6	90.8(2)	N14	C43	C46	112.1(5)
N8	P2	K1	165.52(18)	C44	C43	C45	107.0(6)

Atom	Atom	Atom	Angle/°	Atom	Atom	Atom	Angle/°
N8	P2	N6	102.6(2)	C44	C43	C46	110.1(7)
N8	P2	N7	106.4(3)	C45	C43	C46	108.5(5)
N9	P3	K2	52.10(13)	N14	C47	C48	104.8(4)
N9	P3	N10	121.0(2)	N15	C48	C47	106.5(5)
N9	P3	N11	118.5(2)	N15	C49	C50	111.3(5)
N9	P3	N12	115.2(2)	N15	C49	C51	108.8(5)
N10	P3	K2	93.17(16)	N15	C49	C52	109.5(4)
N11	P3	K2	77.58(17)	C50	C49	C51	110.0(5)
N11	P3	N10	90.8(3)	C50	C49	C52	108.8(4)
N12	P3	K2	164.08(16)	C52	C49	C51	108.4(5)
N12	P3	N10	102.4(2)	N16	C54	C53	114.3(5)
N12	P3	N11	105.2(2)	C56A	C55	N16	125.3(9)
N13	P4	K2	55.01(15)	C56B	C55	N16	117.0(9)
N13	P4	N14	116.3(2)	C12S	O1	C13S	113.9(6)
N13	P4	N15	122.0(2)	O1	C12S	C11S	110.0(6)
N13	P4	N16	114.3(2)	O1	C13S	C14S	110.4(7)
N14	P4	K2	72.18(16)	O2	C21S	C22S	103.9(12)
N15	P4	K2	92.62(15)	O2	C21S	C12	102.0(10)
N15	P4	N14	90.4(2)	C24S	C23S	C22S	99.8(12)
N16	P4	K2	165.16(15)	C24S	C23S	C12	100.1(9)
N16	P4	N14	108.6(2)	C23S	C24S	O2	107.1(8)
N16	P4	N15	102.2(2)	C21S	C22S	C23S	100.4(10)
C21S	O2	K2	112.2(5)	C31A	C32A	O3A	124(3)
C21S	O2	C24S	110.0(6)	C32A	O3A	K1	132.1(14)
C24S	O2	K2	137.1(5)	C32A	O3A	C33A	106.1(11)
Eu1	N1	K1	90.27(13)	C33A	O3A	K1	118.2(15)
P1	N1	Eu1	167.3(3)	C34A	C33A	O3A	132.0(16)
P1	N1	K1	101.85(19)	N7	C21A	C22A	109.9(7)
C1	N2	P1	124.4(3)	N7	C21A	C23A	112.4(9)
C5	N2	P1	113.9(3)	N7	C21A	C24A	109.1(6)
C5	N2	C1	118.9(4)	C22A	C21A	C23A	107.9(6)
C6	N3	P1	114.4(3)	C22A	C21A	C24A	109.2(9)
C6	N3	C7	119.2(4)	C23A	C21A	C24A	108.3(8)
C7	N3	P1	124.9(3)	C21S	C12	C23S	100.5(10)
C11	N4	P1	121.7(4)	C31B	C32B	O3B	124(3)
C13	N4	P1	121.4(3)	C32B	O3B	K1	127.2(11)
C13	N4	C11	116.7(5)	C32B	O3B	C33B	106.0(11)
Eu1	N5	K1	90.24(12)	C33B	O3B	K1	125.9(13)
P2	N5	Eu1	169.2(2)	C34B	C33B	O3B	131.2(16)
P2	N5	K1	98.64(18)	C22B	C21B	N7	117.5(14)
C15	N6	P2	119.8(3)	C22B	C21B	C23B	107.9(7)

Atom	Atom	Atom	Angle/°	Atom	Atom	Atom	Angle/°
C19	N6	P2	111.0(4)	C22B	C21B	C24B	109.2(9)
C19	N6	C15	116.9(4)	C23B	C21B	N7	99.1(17)
P2	N7	K1	75.19(18)	C23B	C21B	C24B	108.3(8)
P2	N7	C21B	117.0(8)	C24B	C21B	N7	114.0(13)
C20	N7	K1	105.3(4)				

Table 4.8 Hydrogen Atom Coordinates (Å×10^4) and Isotropic Displacement Parameters (Å^2×10^3) for 1-Eu^{2+}.

Atom	*x*	*y*	*z*	*U*(eq)
H2A	5761.37	6768.57	4837.33	102
H2B	6262.66	7368.91	4901.81	102
H2C	5772.21	7279.31	4300.8	102
H3A	5157.51	8299.78	4449.31	88
H3B	5739.44	8395.22	4985.85	88
H3C	4902.1	8492.8	5128.6	88
H4A	4832.9	7657.53	5971.52	88
H4B	5685.67	7736.88	5905.44	88
H4C	5332.38	7060.29	5875.7	88
H5A	3841.76	8064.71	4838	60
H5B	3846.78	7709.54	5488.85	60
H6A	2914.01	7215.8	5216.82	69
H6B	2929.15	7549.6	4555.1	69
H8A	2911.8	5737.5	5189.75	124
H8B	2135.78	5726.07	4869.47	124
H8C	2381.5	6317.97	5262.91	124
H9A	3339.26	5918.73	3617.55	91
H9B	2811.14	5435.35	3948.3	91
H9C	3589.72	5570.57	4234.06	91
H10A	2020.5	6895.89	4323.69	126
H10B	1918.37	6289.57	3905.98	126
H10C	2468.73	6820.74	3696.96	126
H11A	4912.73	7229.52	3247.83	70
H11B	4358.29	7487.02	3741.4	70
H11C	4915.07	7329.56	3337.73	70
H11D	4174.21	7441.87	3697.79	70
H13A	4656	5897.89	3275.78	51
H13B	5062.17	5764.92	3911.93	51
H14A	5619.93	6518.07	2938.74	88
H14B	5912.29	5844.81	3124.02	88
H14C	6022.67	6417.91	3584.46	88

Atom	*x*	*y*	*z*	*U*(eq)
H16A	4885.55	6481.5	8382.74	107
H16B	5718.02	6291.44	8386	107
H16C	5125.71	5817.41	8641.5	107
H17A	5200.88	6196.86	6788.58	82
H17B	5726.12	6556.4	7252.33	82
H17C	4879.92	6693.73	7263.88	82
H18A	5667.57	5042.13	7898.99	76
H18B	6198.54	5559.23	7627.42	76
H18C	5671.6	5188.13	7174.23	76
H19A	3798.56	6324.38	7503.81	63
H19B	3813.24	6099.27	8212.41	63
H20A	3051.12	5287.62	8022.09	69
H20B	2721.1	5818.08	7581.35	69
H25A	5082.35	3937.69	8383.25	80
H25B	4470.47	4055.92	8889.92	80
H25C	4861.83	4631.73	8565.79	80
H26A	3886.78	3794.93	7993.29	64
H26B	3743.86	4515.83	8111.55	64
H27A	5359.79	3944.8	7372.96	92
H27B	5020.46	4043.69	6693.96	92
H30A	7422.22	4828.84	6912.13	93
H30B	6940.37	4276.86	7183.16	93
H30C	6654.75	4678.72	6611.94	93
H31A	6479.66	3752.34	5959.22	98
H31B	6698.11	3346.65	6549.29	98
H31C	7107.69	3246.98	5906.66	98
H32A	8300.34	3427.75	6423.66	112
H32B	7905.32	3527.18	7073	112
H32C	8434.95	4049.91	6810.35	112
H33A	7732.64	3703	5170.4	74
H33B	8489.88	3796.23	5518.43	74
H34A	8778.48	4641.8	4949.39	76
H34B	8339.35	4247.04	4443.37	76
H36A	7641.97	4665.92	3639.22	121
H36B	7366.68	5322.86	3388.29	121
H36C	6875.08	4928.32	3851.02	121
H37A	6820.53	5857.39	4589.6	102
H37B	7267.11	6221.02	4071.47	102
H37C	7559.01	6195.59	4766.44	102
H38A	8745.58	5715.79	4467.02	131
H38B	8463.95	5880.44	3787.97	131

Atom	*x*	*y*	*z*	*U*(eq)
H38C	8746.82	5195.72	3939.36	131
H39A	9070.13	5825.59	6529.82	110
H39B	8515.35	5279.13	6683.99	110
H39C	8303.02	5984.51	6826.13	110
H40A	8305.25	6200.91	5760.58	68
H40B	8517.25	5497.11	5618.71	68
H41A	6534.72	6006.47	5945.36	83
H41B	6806.73	5674.87	6552.28	83
H41C	6467.21	5821.23	6109.11	83
H41D	7034.44	5867.84	6662.01	83
H44A	5236.65	3339.55	5542.76	120
H44B	5009.76	2750.49	5948.58	120
H44C	4420.68	3102.16	5538.46	120
H45A	5967.44	1988.86	4808.81	113
H45B	5871.86	2088.67	5536.69	113
H45C	6202.69	2631.38	5119.62	113
H46A	4070.21	2167.62	4971.89	116
H46B	4606.93	1764.24	5387.76	116
H46C	4668.43	1741.83	4650.79	116
H47A	4778.56	2266.04	3798.15	60
H47B	5638.02	2290.71	3890.58	60
H48A	5746.03	3183.28	3338.07	58
H48B	5124.2	2829.9	2959.62	58
H50A	5470.4	4606.15	3587.78	75
H50B	5445.72	4771.1	2867.36	75
H50C	5858.43	4161.88	3097.97	75
H51A	5089.37	3598.68	2309.01	91
H51B	4608.83	4196.26	2159.21	91
H51C	4235.1	3571.89	2398.45	91
H52A	3659.76	4241.39	3207.97	64
H52B	4106.84	4836.6	2988.6	64
H52C	4148.43	4611.83	3692.22	64
H53A	2908.21	3469.56	3358.14	123
H53B	2365.17	3322.41	3912.84	123
H53C	2551.49	2796.19	3416.38	123
H54A	3196.48	2630.53	4352.23	52
H54B	3729.19	2722.27	3780.15	52
H55A	2873.87	3527.51	4879.94	87
H55B	3579.79	3790.3	5195.99	87
H55C	3633.1	3979.31	5107.35	87
H55D	3068.49	4120.04	4570.8	87

Atom	*x*	*y*	*z*	*U*(eq)
H11E	8.34	3879.76	6537.15	109
H11F	-96.14	4486.03	6954.5	109
H11G	695.41	4265.73	6762.96	109
H12S	-149.3	5039.92	6005.65	84
H13C	764.19	5249.44	5138.75	94
H13D	135.94	4819.65	4865.91	94
H14D	1164.68	4808.23	4233.62	127
H14E	974.16	4128.42	4482.17	127
H14F	1615.02	4514.77	4791.88	127
H21A	7123.79	2441.51	3972.9	113
H21B	7661.89	2842.68	4398.84	113
H21C	7186.29	2622.8	4313.41	113
H21D	7991.09	2830.29	4123.4	113
H23A	8149.87	2839.4	2584.19	131
H23B	7429.75	2454.95	2756.12	131
H23C	8302.24	2818.23	2922.02	131
H23D	7632.79	2624.96	2485.42	131
H24A	6969.48	3402.84	2804.51	95
H24B	7730.27	3710.63	2980.35	95
H12A	3948.2	6795.32	2688.95	91
H12B	3893.21	7533.81	2750.89	91
H12C	3402.63	7097.31	3175.51	91
H28A	4746.32	3120.16	7599.82	110
H28B	5366.65	3068.65	7089.67	110
H28C	4539.55	3071.72	6883.87	110
H42A	6945.43	6511.4	6961.71	76
H42B	6681.02	6848.16	6343.22	76
H42C	7519.46	6717.07	6450.13	76
H56A	3467.2	4663.02	4770.16	123
H56B	2685.25	4463.97	5008.14	123
H56C	2881.12	4410.8	4290.27	123
H22A	8228.06	2158.05	3584.67	119
H22B	8541.15	2855.11	3646.8	119
H31D	2908	8419.42	6792.19	209
H31E	3594.42	8113.29	6466.01	209
H31F	3656.7	8376.95	7154.98	209
H32D	2746.06	7732.75	7332.88	192
H32E	3565.2	7526.58	7336.03	192
H33C	2114.52	7637.4	6661.7	112
H33D	2379.4	7411.84	6007.33	112
H34C	1597.13	6930.21	5948.92	185

Atom	*x*	*y*	*z*	*U*(eq)
H34D	1356.27	7121.42	6632.62	185
H34E	1852.09	6523.51	6527.4	185
H22C	2826.74	4086.85	7416.82	97
H22D	2048.06	4161.41	7109.97	97
H22E	2279.07	4598.57	7673.65	97
H23E	1960.99	5525.13	7001.23	112
H23F	1741.64	5041.71	6472.63	112
H23G	2309.56	5580.59	6327.55	112
H24C	3241.79	4816.94	5974.78	113
H24D	2643.22	4291.33	6068.04	113
H24E	3414.62	4220.12	6388.89	113
H12D	4335.13	6654.64	2645.96	91
H12E	3925.85	7308.02	2648.06	91
H12F	3595.73	6731.03	3017.19	91
H28D	4481.94	3201.18	7611.34	110
H28E	4828.19	2998.79	6965.21	110
H28F	4062.92	3339	6980.29	110
H42D	7467.5	6776.27	6281.27	76
H42E	6613.42	6828.69	6360.23	76
H42F	6954.65	6721.82	5689.92	76
H56D	2590.47	3140.43	4852.91	123
H56E	2411.16	3750.06	5245.95	123
H56F	3008.48	3272.42	5485.69	123
H12G	6975.62	2195.76	3343.5	119
H12H	7786.02	1972.21	3498.5	119
H31G	3839.55	8184.36	7143.9	209
H31H	4184.53	7574.96	6842.62	209
H31I	3769.21	7530.26	7488.64	209
H32F	3202.35	7931.91	6462.4	192
H32G	2825.86	7758.05	7096.54	192
H33E	2031.77	6829.29	6350.76	112
H33F	2279.47	6574.13	6999.77	112
H34F	1684.29	7106.52	7385.09	185
H34G	1421.28	7354.85	6726.04	185
H34H	2066.58	7696.28	7078.31	185
H22F	2566.66	4021.56	7596.22	97
H22G	1902.04	4050.92	7127.07	97
H22H	2038.95	4608.4	7601.07	97
H23H	1972.07	5301.58	6706.14	112
H23I	1941.98	4757.2	6204.02	112
H23J	2559.74	5273.22	6166.55	112

Atom	*x*	*y*	*z*	*U*(eq)
H24F	3452.96	4325.82	6165.22	113
H24G	2746.52	3903.43	6209.21	113
H24H	3374.5	3827.78	6709.39	113

Table 4.9 Atomic Occupancy for 1-Eu^{2+}

Atom	*Occupancy*	Atom	*Occupancy*	Atom	*Occupancy*
H11A	0.38(4)	H11B	0.38(4)	H11C	0.62(4)
H11D	0.62(4)	H27A	0.48(3)	H27B	0.48(3)
H41A	0.277(14)	H41B	0.277(14)	H41C	0.723(14)
H41D	0.723(14)	H55A	0.521(12)	H55B	0.521(12)
H55C	0.479(12)	H55D	0.479(12)	H21A	0.364(15)
H21B	0.364(15)	H21C	0.636(15)	H21D	0.636(15)
H23A	0.364(15)	H23B	0.364(15)	H23C	0.636(15)
H23D	0.636(15)	C12A	0.38(4)	H12A	0.38(4)
H12B	0.38(4)	H12C	0.38(4)	C28A	0.52(3)
H28A	0.52(3)	H28B	0.52(3)	H28C	0.52(3)
C42A	0.277(14)	H42A	0.277(14)	H42B	0.277(14)
H42C	0.277(14)	C56A	0.521(12)	H56A	0.521(12)
H56B	0.521(12)	H56C	0.521(12)	C22S	0.364(15)
H22A	0.364(15)	H22B	0.364(15)	C31A	0.485(10)
H31D	0.485(10)	H31E	0.485(10)	H31F	0.485(10)
C32A	0.485(10)	H32D	0.485(10)	H32E	0.485(10)
O3A	0.485(10)	C33A	0.485(10)	H33C	0.485(10)
H33D	0.485(10)	C34A	0.485(10)	H34C	0.485(10)
H34D	0.485(10)	H34E	0.485(10)	C21A	0.725(17)
C22A	0.725(17)	H22C	0.725(17)	H22D	0.725(17)
H22E	0.725(17)	C23A	0.725(17)	H23E	0.725(17)
H23F	0.725(17)	H23G	0.725(17)	C24A	0.725(17)
H24C	0.725(17)	H24D	0.725(17)	H24E	0.725(17)
C12B	0.62(4)	H12D	0.62(4)	H12E	0.62(4)
H12F	0.62(4)	C28B	0.48(3)	H28D	0.48(3)
H28E	0.48(3)	H28F	0.48(3)	C42B	0.723(14)
H42D	0.723(14)	H42E	0.723(14)	H42F	0.723(14)
C56B	0.479(12)	H56D	0.479(12)	H56E	0.479(12)
H56F	0.479(12)	C12	0.636(15)	H12G	0.636(15)
H12H	0.636(15)	C31B	0.515(10)	H31G	0.515(10)
H31H	0.515(10)	H31I	0.515(10)	C32B	0.515(10)
H32F	0.515(10)	H32G	0.515(10)	O3B	0.515(10)
C33B	0.515(10)	H33E	0.515(10)	H33F	0.515(10)
C34B	0.515(10)	H34F	0.515(10)	H34G	0.515(10)

Atom	***Occupancy***	**Atom**	***Occupancy***	**Atom**	***Occupancy***
H34H	0.515(10)	C21B	0.275(17)	C22B	0.275(17)
H22F	0.275(17)	H22G	0.275(17)	H22H	0.275(17)
C23B	0.275(17)	H23H	0.275(17)	H23I	0.275(17)
H23J	0.275(17)	C24B	0.275(17)	H24F	0.275(17)
H24G	0.275(17)	H24H	0.275(17)		

4.5.2 *2-Gd*$^{3+}$

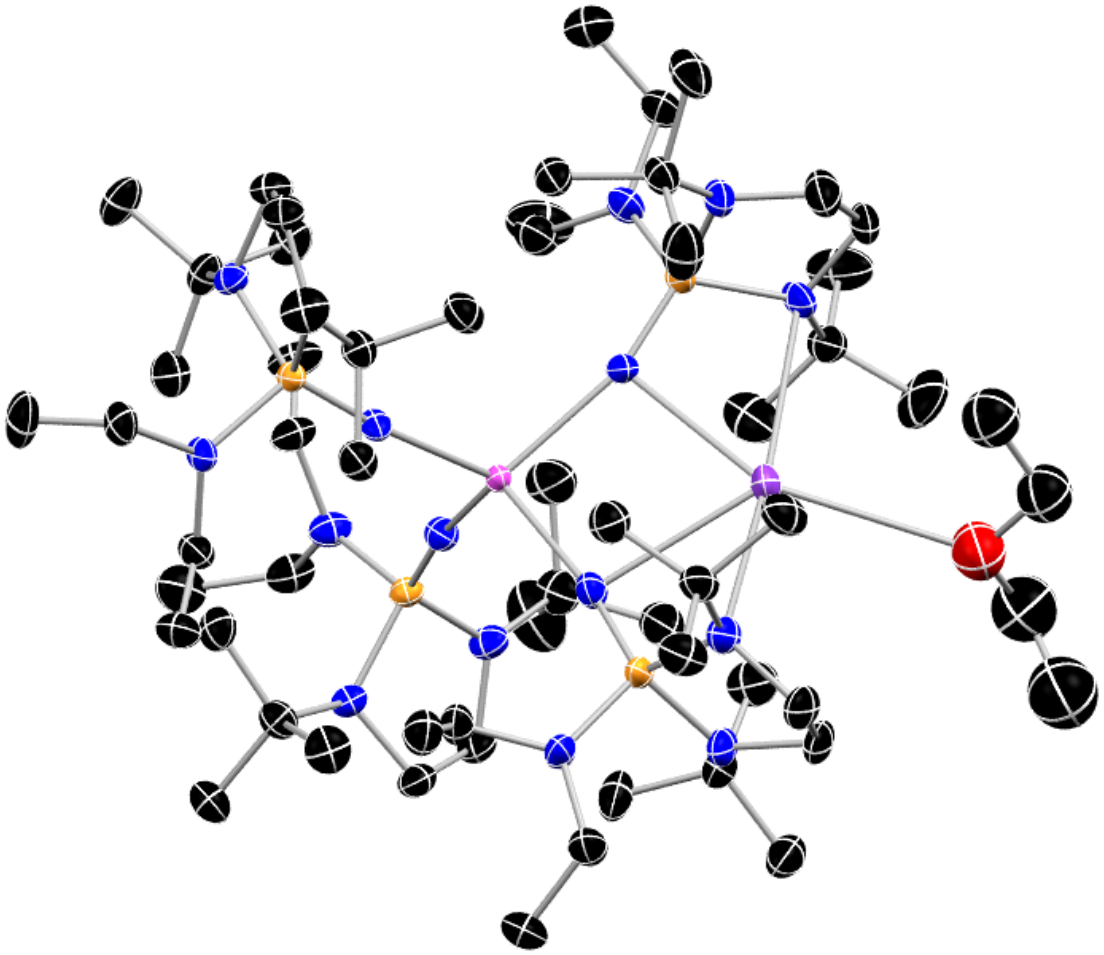

Figure 4.6 Molecular structure of 2-Gd^{3+} with thermal ellipsoids shown at 50% probability with hydrogen atoms omitted for clarity. Color code: C, black; N, blue; O, red; P, orange; K, purple; Gd, magenta.

Table 4.10 Fractional Atomic Coordinates (×10^4) and Equivalent Isotropic Displacement Parameters (Å^2×10^3) for 2-Gd^{3+}. U_{eq} is defined as 1/3 of the trace of the orthogonalised U_{IJ} tensor.

Atom	*x*	*y*	*z*	*U*(eq)
Gd1	4953.5(2)	7070.6(2)	7404.0(2)	15.77(8)
K1	4995.9(7)	4638.6(9)	7360.6(7)	31.9(3)
P1	5627.7(7)	8209.8(10)	8820.8(6)	19.8(3)

Atom	*x*	*y*	*z*	*U*(eq)
P2	4342.1(7)	8666.1(10)	6181.9(6)	18.2(3)
P3	3581.7(8)	5539.1(10)	7239.7(7)	23.8(3)
P4	6294.4(8)	5633.6(10)	7372.2(7)	22.0(3)
N1	5272(2)	7777(3)	8244(2)	24.0(11)
N2	5930(3)	7602(4)	9424(2)	27.3(12)
N3	6367(2)	8695(3)	9000(2)	21.1(10)
N4	5187(3)	8990(4)	8954(2)	28.5(12)
N5	4640(2)	8008(3)	6664(2)	21.6(10)
N6	3672(2)	9267(3)	6114(2)	23.2(11)
N7	3962(3)	8343(3)	5489(2)	24.0(11)
N8	4879(2)	9409(3)	6169(2)	23.0(11)
N9	4201(2)	6013(3)	7310(2)	24.7(11)
N10	3704(3)	4550(4)	7588(3)	32.2(13)
N11	3079(3)	5071(3)	6604(2)	28.8(12)
N12	3067(3)	6139(4)	7407(3)	31.0(13)
N13	5725(3)	6137(3)	7394(2)	25.5(11)
N14	6767(3)	4984(3)	7925(2)	28.9(12)
N15	6070(3)	4766(3)	6903(3)	29.2(12)
N16	6846(3)	6255(3)	7270(2)	26.4(12)
C1	5564(4)	7088(5)	9676(3)	39.5(17)
C2	4834(4)	7128(6)	9289(4)	53(2)
C3	5779(4)	6143(6)	9722(4)	54(2)
C4	5683(6)	7429(7)	10270(4)	72(3)
C5	6614(3)	7730(4)	9773(3)	30.8(15)
C6	6887(3)	8131(4)	9387(3)	27.5(14)
C7	6527(3)	9199(4)	8584(3)	28.4(14)
C8	7068(4)	9849(5)	8927(3)	35.0(16)
C9	5931(4)	9709(5)	8195(3)	32.9(15)
C10	6760(4)	8627(5)	8222(3)	37.9(17)
C11	5564(4)	10431(5)	9442(4)	45(2)
C12	5447(4)	9469(5)	9489(3)	34.2(16)
C13	4562(3)	9276(5)	8517(3)	33.2(16)
C14	4033(4)	9375(6)	8732(4)	47(2)
C15	3602(3)	9652(4)	6609(3)	28.6(14)
C16	3118(4)	10405(5)	6391(3)	39.5(18)
C17	4259(4)	10005(5)	7031(3)	34.8(16)
C18	3359(4)	8994(5)	6919(3)	36.0(17)
C19	3085(3)	8850(5)	5675(3)	33.8(16)
C20	3286(3)	8593(5)	5213(3)	31.1(15)
C21	4230(3)	7791(4)	5173(3)	26.3(13)
C22	4008(4)	8133(5)	4564(3)	39.7(18)

Atom	*x*	*y*	*z*	*U*(eq)
C23	3981(4)	6870(4)	5160(3)	34.6(16)
C24	4976(3)	7792(4)	5460(3)	30.7(15)
C25	6071(3)	9567(5)	6478(4)	41.8(19)
C26	5511(3)	9519(4)	6647(3)	29.3(14)
C27	4703(4)	10029(4)	5697(3)	30.3(15)
C28	4662(5)	10969(5)	5859(4)	47(2)
C29	3962(3)	4441(5)	8216(3)	36.9(17)
C30	4449(5)	5150(6)	8517(3)	56(3)
C31	4332(5)	3580(6)	8378(4)	64(3)
C32	3428(4)	4445(7)	8432(4)	60(3)
C33	3203(4)	3924(4)	7251(3)	37.3(17)
C34	3044(4)	4147(5)	6636(3)	42.9(19)
C35	2968(3)	5444(4)	6039(3)	28.1(14)
C36	2972(3)	6427(4)	6059(3)	31.3(15)
C37	3498(5)	5143(5)	5859(4)	52(2)
C38	2297(4)	5142(5)	5606(3)	48(2)
C39	1872(4)	6465(6)	6912(4)	50(2)
C40	2410(3)	5858(5)	7291(4)	38.7(17)
C41	3253(4)	6997(5)	7664(3)	39.5(17)
C42	3134(4)	7125(7)	8199(4)	61(3)
C43	6873(3)	5158(4)	8522(3)	33.3(16)
C44	7048(4)	6115(4)	8660(3)	39.9(18)
C45	7444(4)	4613(5)	8931(3)	39.9(18)
C46	6273(4)	4959(6)	8627(4)	46(2)
C47	6745(4)	4070(4)	7764(3)	37.0(17)
C48	6553(4)	4072(4)	7132(3)	37.7(17)
C49	5764(3)	4849(4)	6270(3)	31.7(15)
C50	5351(4)	5654(5)	6088(3)	35.9(16)
C51	6270(4)	4871(5)	6015(3)	41.0(18)
C52	5307(4)	4065(5)	6022(3)	40.7(18)
C53	8048(4)	6567(5)	7729(4)	47(2)
C54	7497(3)	5958(5)	7371(3)	34.5(16)
C55	6678(3)	7140(4)	7038(3)	30.7(14)
C56	6775(4)	7287(5)	6494(3)	39.6(17)
O1	5419(4)	2811(5)	7862(3)	68.3(19)
C1S	6347(7)	2127(10)	8527(6)	104(4)
C2S	5767(7)	2528(9)	8485(6)	89(4)
C3S	5049(5)	2158(7)	7509(4)	66(3)
C4S	4569(5)	2543(7)	6956(5)	69(3)
O2	7220(7)	3038(9)	10025(6)	142(4)
C5S	6397(13)	3803(18)	10077(12)	227(12)

Atom	*x*	*y*	*z*	*U*(eq)
C6S	6811(11)	3017(15)	10313(10)	164(8)
C7S	7656(6)	2414(9)	10193(6)	86(4)
C8S	8160(10)	2337(14)	9963(9)	160(8)

Table 4.11 Anisotropic Displacement Parameters ($Å^2×10^3$) for 2-Gd^{3+}. The Anisotropic displacement factor exponent takes the form: $-2\pi^2[h^2a^{*2}U_{11} + 2hka^*b^*U_{12} + \ldots]$.

Atom	U_{11}	U_{22}	U_{33}	U_{23}	U_{13}	U_{12}
Gd1	14.89(13)	14.13(13)	18.88(14)	1.71(11)	7.68(10)	0.14(10)
K1	31.4(7)	17.8(6)	45.1(9)	0.9(6)	14.5(6)	-2.4(6)
P1	18.4(7)	23.5(7)	16.4(7)	0.6(6)	6.3(6)	1.7(6)
P2	18.0(7)	18.9(7)	17.3(7)	3.0(5)	7.1(6)	-1.0(6)
P3	18.7(7)	21.7(8)	29.4(9)	8.5(6)	8.4(6)	-2.3(6)
P4	19.6(7)	15.1(7)	31.9(9)	-2.6(6)	11.3(7)	1.0(6)
N1	24(3)	25(3)	22(3)	3(2)	8(2)	-1(2)
N2	24(3)	33(3)	23(3)	6(2)	8(2)	4(2)
N3	21(2)	26(3)	16(2)	-0.8(19)	8(2)	4(2)
N4	25(3)	36(3)	23(3)	-4(2)	8(2)	3(2)
N5	22(2)	22(2)	15(2)	2(2)	1.1(19)	-4(2)
N6	21(3)	25(3)	21(3)	4(2)	7(2)	3(2)
N7	22(3)	25(3)	23(3)	-1(2)	8(2)	2(2)
N8	24(3)	23(3)	22(3)	9(2)	9(2)	-3(2)
N9	17(2)	24(3)	30(3)	6(2)	6(2)	0(2)
N10	27(3)	30(3)	36(3)	13(2)	9(2)	-9(2)
N11	29(3)	22(3)	28(3)	6(2)	6(2)	-4(2)
N12	25(3)	31(3)	41(3)	4(2)	18(3)	-5(2)
N13	27(3)	19(3)	31(3)	-3(2)	13(2)	-3(2)
N14	30(3)	16(2)	35(3)	-6(2)	8(2)	2(2)
N15	28(3)	21(3)	38(3)	-7(2)	13(2)	1(2)
N16	23(3)	19(3)	40(3)	1(2)	16(2)	4(2)
C1	42(4)	44(4)	31(4)	9(3)	15(3)	-3(4)
C2	39(4)	62(6)	64(6)	26(5)	28(4)	1(4)
C3	39(4)	48(5)	59(6)	21(4)	4(4)	-6(4)
C4	103(9)	80(7)	53(6)	4(5)	52(6)	-19(6)
C5	27(3)	31(4)	26(3)	4(3)	3(3)	3(3)
C6	23(3)	29(3)	27(3)	-1(2)	6(3)	5(2)
C7	30(3)	31(3)	28(3)	-1(3)	16(3)	-5(3)
C8	36(4)	34(4)	36(4)	-3(3)	16(3)	-10(3)
C9	40(4)	31(4)	27(3)	8(3)	14(3)	0(3)
C10	47(4)	42(4)	33(4)	-6(3)	24(3)	0(3)

Atom	U_{11}	U_{22}	U_{33}	U_{23}	U_{13}	U_{12}
C11	48(5)	46(5)	45(5)	-16(4)	22(4)	-3(4)
C12	32(4)	45(4)	27(4)	-8(3)	14(3)	7(3)
C13	24(3)	40(4)	31(4)	-3(3)	7(3)	8(3)
C14	27(4)	61(5)	51(5)	3(4)	16(4)	13(4)
C15	34(4)	26(3)	32(4)	6(3)	20(3)	8(3)
C16	46(4)	34(4)	46(4)	6(3)	27(4)	18(3)
C17	43(4)	31(4)	34(4)	-3(3)	20(3)	-1(3)
C18	41(4)	43(4)	33(4)	15(3)	24(3)	9(3)
C19	22(3)	37(4)	38(4)	0(3)	9(3)	2(3)
C20	26(3)	36(4)	25(3)	1(3)	5(3)	1(3)
C21	30(3)	25(3)	24(3)	-3(2)	12(3)	-3(3)
C22	43(4)	50(5)	29(4)	1(3)	17(3)	2(3)
C23	34(4)	30(4)	38(4)	-7(3)	14(3)	-7(3)
C24	32(3)	29(4)	36(4)	-5(3)	19(3)	-2(3)
C25	25(4)	40(4)	58(5)	-2(4)	15(4)	-3(3)
C26	26(3)	29(3)	29(3)	4(3)	7(3)	-6(3)
C27	39(4)	27(3)	27(3)	9(3)	16(3)	-3(3)
C28	64(5)	27(4)	60(5)	17(4)	36(5)	6(4)
C29	29(4)	39(4)	35(4)	17(3)	7(3)	-3(3)
C30	54(5)	73(6)	29(4)	16(4)	6(4)	-17(5)
C31	72(7)	59(6)	54(6)	33(5)	18(5)	19(5)
C32	38(5)	101(8)	44(5)	23(5)	19(4)	-1(5)
C33	36(4)	22(3)	45(4)	11(3)	8(3)	-6(3)
C34	47(5)	28(4)	41(4)	2(3)	6(4)	-8(3)
C35	30(3)	27(3)	26(3)	2(3)	11(3)	-6(3)
C36	32(4)	30(3)	25(3)	5(3)	5(3)	-2(3)
C37	67(6)	38(4)	70(6)	8(4)	47(5)	3(4)
C38	52(5)	41(4)	32(4)	4(3)	-2(4)	-20(4)
C39	35(4)	52(5)	58(5)	1(4)	16(4)	4(4)
C40	27(4)	36(4)	57(5)	4(3)	22(3)	-4(3)
C41	33(4)	38(4)	49(5)	-5(3)	19(3)	-5(3)
C42	43(5)	86(7)	59(6)	-25(5)	27(4)	-5(5)
C43	30(4)	25(3)	42(4)	2(3)	13(3)	5(3)
C44	53(5)	24(3)	32(4)	1(3)	7(3)	5(3)
C45	39(4)	31(4)	39(4)	-1(3)	6(3)	6(3)
C46	42(4)	58(5)	42(5)	9(4)	20(4)	2(4)
C47	39(4)	17(3)	45(4)	-1(3)	9(3)	7(3)
C48	38(4)	21(3)	49(5)	-10(3)	14(3)	6(3)
C49	26(3)	28(3)	40(4)	-9(3)	13(3)	-2(3)
C50	37(4)	33(4)	36(4)	-4(3)	14(3)	0(3)
C51	37(4)	47(5)	43(4)	-14(3)	21(4)	-4(3)

Atom	U_{11}	U_{22}	U_{33}	U_{23}	U_{13}	U_{12}
C52	36(4)	37(4)	47(5)	-17(3)	15(4)	-8(3)
C53	28(4)	44(5)	62(5)	-1(4)	13(4)	-9(3)
C54	28(4)	29(4)	49(4)	-2(3)	19(3)	0(3)
C55	33(3)	22(3)	42(4)	1(3)	21(3)	1(3)
C56	41(4)	33(4)	46(4)	6(3)	20(4)	2(3)
O1	70(2)	60(2)	70(2)	2.6(17)	24.3(17)	-5.5(18)
C1S	105(5)	98(5)	108(5)	-2(4)	45(4)	-5(4)
C2S	89(4)	88(4)	91(4)	-1(2)	36(2)	-1(2)
C3S	69(3)	60(3)	66(3)	-2.3(19)	25(2)	-1.1(19)
C4S	71(3)	66(3)	69(3)	-1.7(19)	28(2)	-0.4(19)
O2	142(5)	143(5)	142(5)	1(2)	61(2)	-2(2)
C5S	228(12)	228(12)	227(12)	0(2)	96(5)	0(2)
C6S	164(8)	164(8)	163(8)	-0.2(10)	69(3)	0.3(10)
C7S	86(4)	86(4)	85(4)	0.0(10)	36.3(17)	0.8(10)
C8S	160(8)	161(8)	159(8)	2(2)	68(4)	-2(2)

Table 4.12 Bond Lengths for 2-Gd^{3+}.

Atom	Atom	Length/Å	Atom	Atom	Length/Å
Gd1	K1	3.7638(14)	N16	C55	1.478(8)
Gd1	N1	2.249(5)	C1	C2	1.528(11)
Gd1	N5	2.254(5)	C1	C3	1.528(12)
Gd1	N9	2.296(5)	C1	C4	1.529(12)
Gd1	N13	2.272(5)	C5	C6	1.504(10)
K1	N9	2.748(5)	C7	C8	1.540(9)
K1	N13	2.823(5)	C7	C9	1.516(9)
P1	N1	1.513(5)	C7	C10	1.527(9)
P1	N2	1.692(5)	C11	C12	1.525(11)
P1	N3	1.708(5)	C13	C14	1.520(10)
P1	N4	1.688(6)	C15	C16	1.532(9)
P2	N5	1.524(5)	C15	C17	1.524(10)
P2	N6	1.720(5)	C15	C18	1.530(9)
P2	N7	1.693(5)	C19	C20	1.491(10)
P2	N8	1.681(5)	C21	C22	1.522(9)
P3	N9	1.522(5)	C21	C23	1.527(9)
P3	N10	1.733(6)	C21	C24	1.528(9)
P3	N11	1.710(6)	C25	C26	1.501(10)
P3	N12	1.678(6)	C27	C28	1.526(10)
P4	N13	1.523(6)	C29	C30	1.515(11)
P4	N14	1.700(6)	C29	C31	1.533(11)
P4	N15	1.730(6)	C29	C32	1.524(11)

Atom	Atom	Length/Å	Atom	Atom	Length/Å
P4	N16	1.679(6)	C33	C34	1.507(11)
N2	C1	1.476(9)	C35	C36	1.520(9)
N2	C5	1.436(8)	C35	C37	1.526(11)
N3	C6	1.466(8)	C35	C38	1.527(10)
N3	C7	1.484(8)	C39	C40	1.519(11)
N4	C12	1.452(8)	C41	C42	1.521(11)
N4	C13	1.454(8)	C43	C44	1.533(10)
N6	C15	1.473(8)	C43	C45	1.529(9)
N6	C19	1.478(8)	C43	C46	1.520(11)
N7	C20	1.439(8)	C47	C48	1.493(11)
N7	C21	1.475(8)	C49	C50	1.507(10)
N8	C26	1.448(8)	C49	C51	1.536(10)
N8	C27	1.464(8)	C49	C52	1.546(9)
N10	C29	1.477(9)	C53	C54	1.522(10)
N10	C33	1.464(9)	C55	C56	1.518(10)
N11	C34	1.435(9)	O1	C2S	1.521(14)
N11	C35	1.483(8)	O1	C3S	1.380(12)
N12	C40	1.451(8)	C1S	C2S	1.412(18)
N12	C41	1.463(9)	C3S	C4S	1.501(14)
N14	C43	1.474(9)	O2	C6S	1.41(2)
N14	C47	1.468(8)	O2	C7S	1.315(16)
N15	C48	1.466(8)	C5S	C6S	1.50(3)
N15	C49	1.481(9)	C7S	C8S	1.49(2)
N16	C54	1.456(8)			

Table 4.13 Bond Angles for 2-Gd^{3+}.

Atom	Atom	Atom	Angle/°	Atom	Atom	Atom	Angle/°
N1	Gd1	K1	120.76(13)	P4	N15	K1	80.4(2)
N1	Gd1	N5	110.92(19)	C48	N15	K1	111.6(4)
N1	Gd1	N9	111.78(19)	C48	N15	P4	109.7(4)
N1	Gd1	N13	112.43(19)	C48	N15	C49	115.4(5)
N5	Gd1	K1	128.32(13)	C49	N15	K1	110.0(4)
N5	Gd1	N9	114.37(18)	C49	N15	P4	124.2(4)
N5	Gd1	N13	111.68(19)	C54	N16	P4	123.5(4)
N9	Gd1	K1	46.56(13)	C54	N16	C55	115.6(5)
N13	Gd1	K1	48.38(13)	C55	N16	P4	120.8(4)
N13	Gd1	N9	94.79(19)	N2	C1	C2	110.1(6)
N9	K1	N13	74.22(16)	N2	C1	C3	109.3(7)
N1	P1	N2	119.7(3)	N2	C1	C4	110.9(7)
N1	P1	N3	120.9(3)	C3	C1	C2	108.0(7)

Atom	Atom	Atom	Angle/°	Atom	Atom	Atom	Angle/°
N1	P1	N4	113.5(3)	C4	C1	C2	108.9(8)
N2	P1	N3	91.4(3)	C4	C1	C3	109.6(7)
N4	P1	N2	104.8(3)	N2	C5	C6	106.1(5)
N4	P1	N3	103.0(3)	N3	C6	C5	105.0(5)
N5	P2	N6	120.8(3)	N3	C7	C8	107.8(5)
N5	P2	N7	120.9(3)	N3	C7	C9	109.2(5)
N5	P2	N8	113.4(3)	N3	C7	C10	112.6(6)
N7	P2	N6	90.9(3)	C9	C7	C8	108.0(6)
N8	P2	N6	103.9(3)	C9	C7	C10	109.8(6)
N8	P2	N7	103.5(3)	C10	C7	C8	109.4(6)
N9	P3	K1	53.2(2)	N4	C12	C11	115.9(6)
N9	P3	N10	115.1(3)	N4	C13	C14	114.0(6)
N9	P3	N11	121.7(3)	N6	C15	C16	108.2(5)
N9	P3	N12	113.9(3)	N6	C15	C17	109.4(5)
N10	P3	K1	69.5(2)	N6	C15	C18	112.0(6)
N11	P3	K1	97.8(2)	C17	C15	C16	108.7(6)
N11	P3	N10	91.0(3)	C17	C15	C18	108.8(6)
N12	P3	K1	159.2(2)	C18	C15	C16	109.7(6)
N12	P3	N10	109.4(3)	N6	C19	C20	104.3(5)
N12	P3	N11	103.0(3)	N7	C20	C19	107.0(5)
N13	P4	K1	58.6(2)	N7	C21	C22	109.3(5)
N13	P4	N14	121.0(3)	N7	C21	C23	108.6(5)
N13	P4	N15	114.6(3)	N7	C21	C24	111.0(5)
N13	P4	N16	114.0(3)	C22	C21	C23	110.0(6)
N14	P4	K1	88.6(2)	C22	C21	C24	108.5(6)
N14	P4	N15	91.2(3)	C23	C21	C24	109.5(6)
N15	P4	K1	68.5(2)	N8	C26	C25	114.2(6)
N16	P4	K1	168.6(2)	N8	C27	C28	115.1(6)
N16	P4	N14	102.8(3)	N10	C29	C30	110.1(6)
N16	P4	N15	110.7(3)	N10	C29	C31	108.4(7)
P1	N1	Gd1	168.1(3)	N10	C29	C32	112.8(6)
C1	N2	P1	128.0(5)	C30	C29	C31	107.1(7)
C5	N2	P1	114.1(4)	C30	C29	C32	109.1(8)
C5	N2	C1	117.0(5)	C32	C29	C31	109.2(7)
C6	N3	P1	109.6(4)	N10	C33	C34	104.6(6)
C6	N3	C7	115.7(5)	N11	C34	C33	107.0(6)
C7	N3	P1	122.9(4)	N11	C35	C36	111.0(5)
C12	N4	P1	121.2(4)	N11	C35	C37	110.3(6)
C12	N4	C13	116.7(5)	N11	C35	C38	107.5(6)
C13	N4	P1	121.7(4)	C36	C35	C37	108.8(6)
P2	N5	Gd1	171.7(3)	C36	C35	C38	108.7(6)

Atom	Atom	Atom	Angle/°	Atom	Atom	Atom	Angle/°
C15	N6	P2	122.7(4)	C37	C35	C38	110.6(7)
C15	N6	C19	116.5(5)	N12	C40	C39	114.8(6)
C19	N6	P2	108.1(4)	N12	C41	C42	113.5(7)
C20	N7	P2	113.8(4)	N14	C43	C44	109.3(6)
C20	N7	C21	118.7(5)	N14	C43	C45	109.7(6)
C21	N7	P2	127.3(4)	N14	C43	C46	112.3(6)
C26	N8	P2	121.7(4)	C45	C43	C44	108.2(6)
C26	N8	C27	116.9(5)	C46	C43	C44	108.4(7)
C27	N8	P2	121.1(4)	C46	C43	C45	108.9(6)
Gd1	N9	K1	96.11(18)	C43	C46	K1	109.0(5)
P3	N9	Gd1	163.4(3)	N14	C47	C48	105.3(6)
P3	N9	K1	100.5(2)	N15	C48	C47	105.3(6)
P3	N10	K1	80.1(2)	N15	C49	C50	110.8(6)
C29	N10	K1	103.4(4)	N15	C49	C51	112.5(6)
C29	N10	P3	124.7(5)	N15	C49	C52	107.9(6)
C33	N10	K1	117.1(5)	C50	C49	C51	108.9(6)
C33	N10	P3	111.3(4)	C50	C49	C52	107.5(6)
C33	N10	C29	115.0(5)	C51	C49	C52	109.2(6)
C34	N11	P3	113.4(5)	N16	C54	C53	114.9(6)
C34	N11	C35	116.9(6)	N16	C55	C56	113.5(6)
C35	N11	P3	122.8(4)	C2S	O1	K1	129.4(7)
C40	N12	P3	122.7(5)	C3S	O1	K1	113.6(6)
C40	N12	C41	116.1(6)	C3S	O1	C2S	112.5(8)
C41	N12	P3	121.2(5)	C1S	C2S	O1	105.0(11)
Gd1	N13	K1	94.64(18)	O1	C3S	C4S	109.2(9)
P4	N13	Gd1	171.2(3)	C3S	C4S	K1	95.1(6)
P4	N13	K1	94.0(2)	C7S	O2	C6S	112.1(15)
C43	N14	P4	122.2(4)	O2	C6S	C5S	102(2)
C47	N14	P4	113.4(4)	O2	C7S	C8S	121.2(15)
C47	N14	C43	116.2(6)				

Table 4.14 Hydrogen Atom Coordinates (Å×10^4) and Isotropic Displacement Parameters (Å^2×10^3) for 2-Gd^{3+}.

Atom	*x*	*y*	*z*	*U*(eq)
H2A	4667.77	7705.33	9312.44	79
H2B	4605.03	6694.88	9415.05	79
H2C	4760.83	7008.6	8892.17	79
H3A	5704.97	5926.77	9341.44	82
H3B	5525.78	5797.46	9876.5	82
H3C	6244.26	6099.89	9978.95	82

Atom	*x*	*y*	*z*	*U*(eq)
H4A	6133.55	7305.25	10540.29	108
H4B	5381.68	7145.79	10401.25	108
H4C	5609.31	8055.65	10250.17	108
H5A	6830.26	7170.44	9925.72	37
H5B	6679.33	8118.32	10098.6	37
H6A	7285.19	8469.1	9612.98	33
H6B	6997.13	7679.8	9168.24	33
H8A	6927.87	10195.75	9174.16	52
H8B	7151.97	10230.65	8660.63	52
H8C	7467.53	9534.09	9163.14	52
H9A	5581.1	9307.9	7968.25	49
H9B	6042.66	10073.1	7937.51	49
H9C	5782.79	10074.89	8428.9	49
H10A	7160.95	8327.09	8473.4	57
H10B	6846.52	8986.41	7947.75	57
H10C	6421.87	8200.68	8013.97	57
H11A	5156.25	10705.91	9178.96	68
H11B	5896.74	10506.61	9294.8	68
H11C	5713.41	10700.37	9821.23	68
H12A	5865.33	9200.46	9748.01	41
H12B	5140.83	9405.21	9672.14	41
H13A	4412.82	8855.18	8197.46	40
H13B	4624.56	9839.41	8363.66	40
H14A	3617.6	9515.83	8408.89	70
H14B	4151.61	9841.28	9016.3	70
H14C	3987.2	8832.29	8908.62	70
H16A	3263.08	10808.4	6174.52	59
H16B	3096.53	10706.21	6718.43	59
H16C	2684.81	10180.86	6141.82	59
H17A	4568.06	9525.45	7186.34	52
H17B	4205.56	10303.46	7344.43	52
H17C	4427	10411.51	6832.46	52
H18A	2941.27	8752.37	6649.19	54
H18B	3299.76	9280.98	7234.43	54
H18C	3679.66	8527.84	7073.39	54
H19A	2714.45	9260.31	5527.6	41
H19B	2957.56	8337.73	5835.32	41
H20A	3016.01	8103.58	4989.57	37
H20B	3229.78	9084.22	4949.15	37
H22A	3530.52	8112.34	4368.23	59
H22B	4194.35	7774.71	4355.67	59

Atom	*x*	*y*	*z*	*U*(eq)
H22C	4155.72	8731.7	4576.89	59
H23A	4128.14	6653.22	5552.95	52
H23B	4151.15	6496.24	4946.06	52
H23C	3502.64	6867.89	4972.01	52
H24A	5137.35	8364.68	5419.68	46
H24B	5141.79	7357.61	5277.18	46
H24C	5126.38	7653.62	5868.22	46
H25A	6048.92	9077.22	6228.81	63
H25B	6483.3	9546.71	6823.01	63
H25C	6045.64	10109.73	6272.29	63
H26A	5586.12	9029.95	6915.67	35
H26B	5503.04	10056.42	6853.72	35
H27A	4275.52	9858.6	5391.79	36
H27B	5029.68	9987.9	5534.27	36
H28A	4553.37	11337.84	5520.69	71
H28B	5082.96	11148.08	6159.62	71
H28C	4322.45	11025.96	6000.05	71
H30A	4807.74	5127.93	8397.38	84
H30B	4622.14	5067.34	8932.75	84
H30C	4232.27	5714.2	8414.85	84
H31A	4025.74	3101.34	8209.67	97
H31B	4536.82	3519.79	8796.48	97
H31C	4668.36	3568.49	8231.8	97
H32A	3218.75	5015.16	8362.9	91
H32B	3620.61	4320.73	8843.99	91
H32C	3102	4003.09	8227.74	91
H33A	2811.55	3979.55	7330.22	45
H33B	3371.38	3325.25	7340.24	45
H34A	3360.57	3870.72	6513.95	52
H34B	2600.31	3941.07	6381.6	52
H36A	2620.64	6628.65	6158.37	47
H36B	2903.79	6658.01	5682.74	47
H36C	3392.58	6628.9	6348.76	47
H37A	3920.26	5380.42	6123.97	78
H37B	3395.87	5344.69	5469.2	78
H37C	3519.8	4509.51	5869.46	78
H38A	2310.13	4519.1	5541.59	72
H38B	2179.4	5451.15	5243.14	72
H38C	1972.47	5262.57	5756.49	72
H39A	1890.8	6524.66	6539.32	74
H39B	1932.31	7033.57	7096.04	74

Atom	*x*	*y*	*z*	*U*(eq)
H39C	1446.94	6228.86	6855.99	74
H40A	2376.35	5789.8	7660.7	46
H40B	2335.59	5282.66	7104.99	46
H41A	3003.17	7439.06	7376.2	47
H41B	3722	7091.06	7763.33	47
H42A	2666.38	7071.58	8099.25	92
H42B	3285.29	7700.94	8358.51	92
H42C	3373.9	6684.03	8483.88	92
H44A	7447.12	6247.08	8612.27	60
H44B	7119.81	6232.05	9056.84	60
H44C	6690.07	6476.28	8399.21	60
H45A	7316.06	4002.39	8891.88	60
H45B	7563.22	4801.75	9326.34	60
H45C	7819.12	4685.35	8836.55	60
H46A	5925.72	5370.96	8413.13	69
H46B	6383.69	5009.26	9037.47	69
H46C	6124.14	4369.9	8497.62	69
H47A	6419.33	3751.42	7854.43	44
H47B	7176.84	3794.74	7970.1	44
H48A	6936.86	4186.85	7049.76	45
H48B	6361.43	3508.34	6961	45
H50A	5044.67	5663.28	6268.12	54
H50B	5106.04	5655.81	5669.87	54
H50C	5632.09	6165.75	6207.41	54
H51A	6580.26	5342.16	6192.61	62
H51B	6046.96	4966.87	5600.57	62
H51C	6504.17	4319.24	6090.63	62
H52A	5553.81	3528.72	6164.84	61
H52B	5129	4076.85	5602.46	61
H52C	4948.78	4092.2	6141.89	61
H53A	8004.92	7111.51	7521.15	71
H53B	8468.66	6298.39	7801.18	71
H53C	8025.13	6682.09	8095.13	71
H54A	7513.92	5869.66	6995.72	41
H54B	7573.93	5389.71	7566.27	41
H55A	6951.45	7557.77	7333.06	37
H55B	6216.67	7257.17	6955.85	37
H56A	6505.64	6877.43	6198.58	59
H56B	7235.68	7199.24	6575.49	59
H56C	6647.13	7879.76	6358.1	59
H1SA	6239.42	1663.98	8240.65	155

Atom	*x*	*y*	*z*	*U*(eq)
H1SB	6580.19	1882	8911.39	155
H1SC	6624.79	2556.06	8456.48	155
H2SA	5867.01	3032.42	8745.24	107
H2SB	5495.28	2115.57	8584.44	107
H3SA	4813.58	1840.85	7699.46	79
H3SB	5336.32	1743.35	7431.21	79
H4SA	4266.57	2092.86	6725.33	104
H4SB	4803.17	2782.8	6743.25	104
H4SC	4322.74	3003.79	7038.55	104
H5SA	5971.26	3628.94	9781.38	341
H5SB	6613.07	4190.05	9908.89	341
H5SC	6336.29	4104.12	10386.8	341
H6SA	7064.77	3059.57	10733.76	196
H6SB	6543.03	2483.91	10221.92	196
H7SA	7413.14	1860.66	10110.08	103
H7SB	7891.47	2457.86	10615.23	103
H8SA	7967.55	2060.51	9584.9	239
H8SB	8524.75	1985.9	10224.84	239
H8SC	8318.68	2914.51	9927.91	239

4.5.3 *3-Gd*$^{3+}$

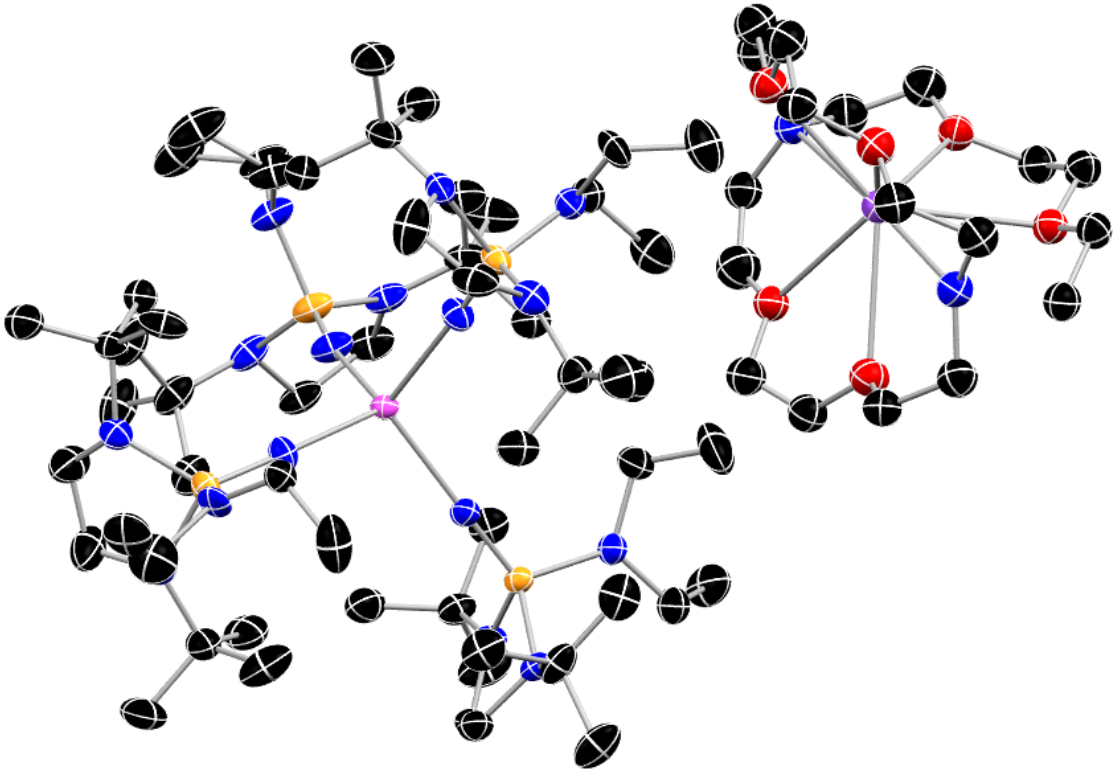

Figure 4.7 Molecular structure of 3-Gd^{3+} with thermal ellipsoids shown at 50% probability with hydrogen atoms omitted for clarity. Color code: C, black; N, blue; O, red; P, orange; K, purple; Gd, magenta.

Table 4.15 Fractional Atomic Coordinates (×10^4) and Equivalent Isotropic Displacement Parameters (Å^2×10^3) for 3-Gd^{3+}. U_{eq} is defined as 1/3 of the trace of the orthogonalised U_{IJ} tensor.

Atom	*x*	*y*	*z*	*U*(eq)
Gd1	7337.1(2)	5321.7(2)	8762.1(2)	19.76(6)
P1	5892.9(7)	6243.2(5)	8798.7(5)	31.5(3)
P2	7267.4(7)	4615.4(5)	7837.5(4)	26.6(3)
P3	7235.6(7)	4391.1(5)	9568.4(4)	27.3(3)
P4	8934.2(6)	6106.7(4)	8808.6(4)	22.6(3)
N1	6432(2)	5832.7(15)	8748.2(15)	33.0(10)
N2	5118(2)	6010.9(16)	8900.9(15)	35.9(11)
N3	5717(2)	6674.3(15)	8445.2(15)	34.4(11)

Atom	*x*	*y*	*z*	*U*(eq)
N4	6016(2)	6714.7(15)	9119.8(15)	33.5(11)
N5	7337(2)	4844.1(15)	8231.3(12)	29.1(9)
N7	6481(2)	4492.0(15)	7643.1(13)	29.7(10)
N8	7480(2)	4953.9(17)	7439.7(13)	34.0(11)
N9	7252(2)	4825.7(15)	9283.1(12)	30.3(10)
N11	7863(2)	3944.3(16)	9577.5(14)	35.2(11)
N12	6633(2)	3922.5(16)	9543.1(13)	32.2(10)
N13	8315(2)	5769.1(15)	8784.6(12)	26.8(9)
N14	9124(2)	6277.6(16)	9256.0(12)	28.2(9)
N15	8985(2)	6646.7(16)	8547.4(13)	29.0(10)
N16	9711(2)	5925.5(16)	8628.1(13)	27.9(9)
C1	4439(3)	5224(2)	8832(3)	63(2)
C2	5040(3)	5481(2)	9010(2)	47.5(17)
C3	4572(3)	6346(2)	9026(2)	44.0(16)
C4	4040(3)	6464(2)	8727(2)	55.8(19)
C5	5691(3)	6518(2)	8036(2)	41.1(15)
C6	5280(3)	6028(2)	7998(2)	49.7(17)
C7	5318(4)	6929(2)	7811(2)	57(2)
C8	6382(3)	6424(3)	7871(2)	52.0(17)
C9	6110(3)	7133(2)	8528.1(19)	39.1(14)
C10	6057(3)	7214(2)	8952.1(19)	42.0(15)
C11	6172(3)	6653(2)	9531.4(19)	40.1(14)
C12	5816(4)	7063(2)	9761(2)	54.8(19)
C13	6934(3)	6676(3)	9600(2)	54.5(18)
C14	5921(3)	6140(2)	9670(2)	44.7(15)
C19	8110(3)	5257(2)	7408.3(17)	39.2(14)
C20	8047(3)	5758(2)	7618(2)	49.9(17)
C21	8258(4)	5354(3)	6989(2)	74(3)
C22	8699(4)	4968(3)	7575(3)	67(2)
C23	6894(4)	5131(3)	7236(2)	58(2)
C24	6293(3)	4903(3)	7394(2)	53.5(19)
C25	5924(3)	4259.5(18)	7868.7(15)	28.4(11)
C26	5575(3)	4641.9(19)	8127.4(16)	32.2(12)
C27	5398(3)	4043(2)	7595.8(18)	43.0(15)
C28	6212(3)	3828(2)	8110.3(18)	40.9(15)
C33	8584(3)	4071(2)	9536.5(18)	39.0(14)
C34	8749(3)	4546(2)	9761(2)	49.3(16)
C35	8774(3)	4158(2)	9114.9(18)	43.4(15)
C36	9010(4)	3637(3)	9693(2)	59(2)
C37	7643(4)	3472(2)	9406.2(19)	46.3(16)
C38	6922(4)	3514(2)	9315(2)	55.6(19)

Atom	*x*	*y*	*z*	*U*(eq)
C39	5914(3)	4026(2)	9485.3(16)	37.3(13)
C40	5695(3)	4496(2)	9715.3(19)	46.1(16)
C41	5509(3)	3575(2)	9640(2)	49.8(17)
C42	5736(3)	4111(2)	9071.1(17)	40.8(14)
C43	9086(5)	5920(3)	9918(2)	68(2)
C44	8692(3)	6134(3)	9582.5(17)	44.7(15)
C45	9715(3)	6585(2)	9338.5(17)	38.6(14)
C46	9559(4)	7072(2)	9543(2)	55.8(19)
C47	8449(3)	7041.0(19)	8522.4(17)	32.6(12)
C48	8798(3)	7556(2)	8482(2)	56(2)
C49	8018(3)	7043(2)	8878.1(17)	38.6(14)
C50	7994(3)	6934(3)	8182.2(19)	49.0(16)
C51	9483(3)	6632(2)	8245.4(16)	31.9(12)
C52	9748(3)	6103(2)	8235.7(16)	34.3(12)
C53	10004(3)	5422(2)	8703.7(19)	38.2(14)
C54	10771(3)	5453(2)	8621(2)	51.7(18)
C55	9903(3)	5275(2)	9116.0(19)	46.2(16)
C56	9687(3)	5012(2)	8445(2)	45.9(16)
C15A	7707(10)	3355(6)	7371(5)	57(3)
C16A	7787(11)	3921(6)	7416(4)	74(7)
N6A	7640(20)	4067(11)	7813(5)	31(3)
C17A	7910(6)	3776(5)	8124(3)	30(3)
C18A	8680(8)	3726(7)	8137(5)	63(3)
C29A	7553(7)	5445(4)	10218(4)	52(2)
C30A	6969(5)	5087(4)	10118(4)	35(2)
N10A	7148(9)	4567(3)	10013(4)	29.6(16)
C31A	7140(20)	4191(5)	10321(7)	40(3)
C32A	7510(30)	4350(30)	10675(9)	59(5)
N17A	6450(9)	7776(5)	11170(4)	36.5(19)
C57A	5861(6)	7476(5)	11240(4)	46(2)
C58A	5895(7)	6891(5)	11291(4)	52(2)
O1A	6503(6)	6624(5)	11163(3)	40.9(17)
C59A	6479(7)	6118(5)	11333(4)	55(3)
C60A	7102(6)	5854(5)	11189(4)	42(2)
O2A	7696(4)	6103(3)	11380(2)	42.0(14)
C61A	8292(7)	5843(6)	11284(5)	48(2)
C62A	8867(6)	6070(4)	11511(4)	48(2)
C63A	6539(7)	8070(5)	10817(4)	40(2)
C64A	7092(8)	7986(6)	10579(4)	57(3)
O3A	7604(4)	7765(3)	10595(2)	35.7(13)
C65A	8031(7)	7661(5)	10293(4)	45(2)

Atom	*x*	*y*	*z*	*U*(eq)
C66A	8609(8)	7661(6)	10421(5)	44(2)
O4A	8793(4)	7359(3)	10746(3)	44.4(16)
C67A	9229(7)	6978(5)	10698(4)	43(2)
C68A	9491(7)	6756(5)	11058(4)	46(2)
C69A	6481(8)	8183(5)	11420(4)	54(3)
C70A	6719(7)	8095(5)	11797(4)	50(2)
O5A	7303(8)	7866(7)	11777(5)	35.5(17)
C71A	7845(6)	8110(4)	12006(3)	43(2)
C72A	8268(8)	7716(5)	12151(5)	40(2)
O6A	8615(4)	7455(3)	11858(2)	36.1(14)
C73A	9022(7)	7066(5)	12001(4)	38(2)
C74A	9442(6)	6862(5)	11674(3)	43(2)
N18A	8935(6)	6531(4)	11291(3)	37.8(19)
C15B	8248(5)	3544(4)	7276(3)	57(3)
C16B	7588(4)	3736(3)	7441(2)	23.1(17)
N6B	7728(13)	4070(7)	7769(3)	31(3)
C17B	8151(5)	3900(4)	8077(3)	46(3)
C18B	7990(6)	3380(4)	8241(3)	63(3)
C29B	6626(7)	5351(4)	10339(4)	52(2)
C30B	7220(6)	5151(4)	10103(4)	35(2)
N10B	7243(10)	4604(4)	10030(4)	29.6(16)
C31B	7070(20)	4273(5)	10351(7)	40(3)
C32B	7560(30)	4290(30)	10678(10)	59(5)
N17B	6440(10)	7698(6)	11100(5)	36.5(19)
C57B	5906(7)	7359(5)	11030(5)	46(2)
C58B	5843(8)	6968(6)	11055(5)	52(2)
O1B	6372(7)	6665(5)	11249(4)	40.9(17)
C59B	6377(8)	6178(6)	11055(5)	55(3)
C60B	6901(8)	5890(6)	11281(5)	42(2)
O2B	7559(5)	6090(3)	11149(3)	42.0(14)
C61B	8083(8)	5807(7)	11289(6)	48(2)
C62B	8768(7)	6012(5)	11152(4)	48(2)
C63B	6443(8)	7915(5)	10734(4)	40(2)
C64B	6922(9)	7810(6)	10468(5)	57(3)
O3B	7420(5)	7500(3)	10524(2)	35.7(13)
C65B	7981(9)	7467(6)	10274(5)	45(2)
C66B	8740(10)	7553(7)	10419(6)	44(2)
O4B	8736(5)	7117(4)	10655(3)	44.4(16)
C67B	9453(8)	7088(6)	10818(4)	43(2)
C68B	9412(8)	6557(6)	11020(5)	46(2)
C69B	6252(8)	7971(6)	11486(5)	54(3)

Atom	*x*	*y*	*z*	*U*(eq)
C70B	6880(8)	8269(6)	11642(5)	50(2)
O5B	7398(10)	7897(8)	11813(6)	35.5(17)
C71B	7627(7)	7759(5)	12169(4)	43(2)
C72B	8367(10)	7605(7)	12162(6)	40(2)
O6B	8424(4)	7180(3)	11911(3)	36.1(14)
C73B	9103(8)	7005(6)	11881(4)	38(2)
C74B	9147(7)	6511(5)	11681(4)	43(2)
N18B	9073(7)	6608(5)	11396(4)	37.8(19)
K1	7714.8(6)	7144.3(4)	11252.2(3)	29.1(2)

Table 4.16 Anisotropic Displacement Parameters ($Å^2 \times 10^3$) for 3-Gd^{3+}. The Anisotropic displacement factor exponent takes the form: $-2\pi^2[h^2a^{*2}U_{11} + 2hka^*b^*U_{12} + \ldots]$.

Atom	U_{11}	U_{22}	U_{33}	U_{23}	U_{13}	U_{12}
Gd1	21.34(11)	15.76(9)	22.17(11)	-0.01(9)	3.66(10)	-0.63(9)
P1	23.3(6)	19.2(6)	51.9(9)	-3.0(6)	7.3(7)	1.2(5)
P2	33.3(7)	24.0(6)	22.7(6)	-2.1(5)	0.3(6)	-0.1(5)
P3	36.8(8)	23.3(6)	21.7(6)	2.8(5)	1.6(6)	-6.5(5)
P4	22.5(6)	20.5(5)	24.8(7)	-2.4(5)	1.5(5)	-2.9(5)
N1	25(2)	21.1(19)	53(3)	-2(2)	8(2)	5.3(16)
N2	25(2)	22(2)	61(3)	-8(2)	7(2)	-1.1(17)
N3	24(2)	20(2)	60(3)	0(2)	-4(2)	-2.6(17)
N4	25(2)	21(2)	54(3)	-4(2)	9(2)	-3.2(17)
N5	36(2)	28(2)	23(2)	-3.4(16)	-2(2)	3.6(19)
N7	35(3)	24(2)	30(2)	2.8(17)	2(2)	-1.9(18)
N8	30(3)	39(2)	33(3)	4(2)	3.3(19)	-3(2)
N9	42(3)	23(2)	26(2)	4.9(16)	0(2)	-3.8(18)
N11	43(3)	27(2)	36(3)	3.4(19)	2(2)	1.7(19)
N12	42(3)	31(2)	23(2)	0.9(18)	-1(2)	-14(2)
N13	25(2)	31(2)	25(2)	-4.0(18)	2.8(19)	-3.4(17)
N14	29(2)	28(2)	27(2)	-5.2(18)	-0.7(19)	-4.2(18)
N15	25(2)	28(2)	34(3)	4.4(18)	5.8(19)	1.0(18)
N16	20(2)	28(2)	35(3)	-4.3(18)	2.6(18)	-1.3(17)
C1	40(4)	31(3)	118(7)	-2(4)	9(4)	-9(3)
C2	43(4)	22(3)	78(5)	-2(3)	16(3)	-4(2)
C3	26(3)	27(3)	79(5)	-15(3)	13(3)	-3(2)
C4	31(3)	47(4)	89(6)	-18(4)	6(4)	7(3)
C5	28(3)	30(3)	65(4)	2(3)	-6(3)	2(2)
C6	45(4)	36(3)	68(5)	-11(3)	-13(3)	0(3)
C7	54(4)	41(4)	77(5)	4(3)	-28(4)	4(3)

Atom	U_{11}	U_{22}	U_{33}	U_{23}	U_{13}	U_{12}
C8	37(4)	66(4)	52(4)	-2(3)	-4(3)	2(3)
C9	30(3)	25(3)	62(4)	-4(3)	5(3)	-9(2)
C10	43(4)	23(3)	61(4)	-3(3)	10(3)	-5(2)
C11	37(3)	34(3)	49(4)	-9(3)	17(3)	-4(2)
C12	71(5)	28(3)	66(5)	-11(3)	34(4)	-3(3)
C13	41(4)	78(5)	44(4)	-4(3)	7(3)	-12(3)
C14	43(4)	31(3)	60(4)	-1(3)	13(3)	-1(3)
C19	38(3)	44(3)	35(3)	-2(3)	3(3)	-11(3)
C20	46(4)	46(4)	58(4)	2(3)	7(3)	-18(3)
C21	73(6)	108(7)	42(4)	-4(4)	20(4)	-47(5)
C22	38(4)	63(5)	100(7)	-4(4)	6(4)	-11(4)
C23	57(4)	64(4)	55(4)	31(4)	-24(4)	-22(4)
C24	41(4)	64(4)	55(4)	35(4)	-8(3)	-8(3)
C25	31(3)	23(2)	30(3)	-1(2)	5(2)	-5(2)
C26	35(3)	27(3)	34(3)	-3(2)	0(2)	-1(2)
C27	45(4)	41(3)	43(4)	-11(3)	6(3)	-14(3)
C28	53(4)	25(3)	44(4)	8(2)	23(3)	4(3)
C33	36(3)	39(3)	42(4)	7(3)	-4(3)	2(3)
C34	44(4)	53(4)	51(4)	0(3)	-8(3)	-9(3)
C35	41(4)	42(3)	48(4)	8(3)	6(3)	5(3)
C36	55(4)	57(4)	64(5)	25(4)	-5(4)	9(3)
C37	58(4)	31(3)	50(4)	0(3)	17(3)	-12(3)
C38	63(5)	30(3)	74(5)	-11(3)	-28(4)	3(3)
C39	43(3)	41(3)	28(3)	1(2)	8(3)	-13(3)
C40	40(4)	49(4)	49(4)	-5(3)	8(3)	-5(3)
C41	54(4)	47(4)	49(4)	5(3)	9(3)	-21(3)
C42	39(3)	47(3)	36(3)	1(3)	-1(3)	-6(3)
C43	103(7)	69(5)	33(4)	6(3)	-15(4)	-25(5)
C44	48(4)	55(4)	31(3)	1(3)	5(3)	-16(3)
C45	41(3)	41(3)	34(3)	-8(3)	-2(3)	-7(3)
C46	55(4)	50(4)	62(5)	-29(3)	7(4)	-17(3)
C47	31(3)	23(2)	44(3)	8(2)	3(3)	-2(2)
C48	47(4)	26(3)	95(6)	9(3)	8(4)	-6(3)
C49	37(3)	31(3)	47(4)	-2(2)	3(3)	8(2)
C50	35(3)	64(4)	47(4)	15(3)	1(3)	1(3)
C51	30(3)	39(3)	27(3)	2(2)	5(2)	-7(2)
C52	29(3)	40(3)	34(3)	-6(2)	6(2)	-4(2)
C53	26(3)	31(3)	57(4)	-11(3)	-7(3)	3(2)
C54	28(3)	38(3)	88(6)	-6(3)	-5(3)	9(3)
C55	52(4)	27(3)	60(4)	2(3)	-8(3)	11(3)
C56	48(4)	29(3)	60(4)	-10(3)	4(3)	2(3)

Atom	U_{11}	U_{22}	U_{33}	U_{23}	U_{13}	U_{12}
C15A	55(6)	62(6)	53(6)	-16(5)	15(5)	17(5)
C16A	74(7)	74(7)	73(7)	0(2)	1(2)	0(2)
N6A	30(7)	38(2)	23(3)	-8(3)	9(4)	10(3)
C17A	31(4)	30(4)	30(4)	1.3(19)	0(2)	2(2)
C18A	79(8)	62(6)	50(6)	-15(5)	-24(6)	21(5)
C29A	73(7)	37(5)	48(6)	-11(4)	5(5)	-1(4)
C30A	36(3)	35(2)	35(2)	-0.8(17)	-0.3(19)	-0.1(19)
N10A	32(3)	29.7(19)	27.4(19)	-0.4(14)	-0.5(17)	-6.2(16)
C31A	63(8)	37(5)	19(4)	-5(4)	2(4)	-9(6)
C32A	84(9)	52(13)	42(4)	11(4)	-17(4)	12(7)
N17A	36(2)	36(3)	36(3)	0.9(19)	-0.7(18)	0.7(17)
C57A	45(3)	46(3)	47(3)	1.6(19)	-0.6(19)	1.2(18)
C58A	48(3)	52(3)	54(3)	1.5(19)	0(2)	-2.0(18)
O1A	42(2)	39(2)	42(3)	-0.4(18)	1.3(18)	-4.4(17)
C59A	55(3)	52(3)	57(3)	-0.1(19)	-0.4(19)	-2.6(19)
C60A	44(3)	36(2)	46(3)	-0.9(18)	4.5(19)	-4.8(19)
O2A	45(2)	37.4(18)	44(2)	-0.8(18)	0.1(18)	-0.8(16)
C61A	49(3)	45(3)	50(3)	0.3(18)	0(2)	2(2)
C62A	48(3)	46(3)	49(3)	0.2(18)	-0.3(19)	5.9(18)
C63A	40(3)	40(3)	40(3)	2.4(19)	-0.9(18)	2.0(19)
C64A	57(3)	57(3)	56(3)	2.8(19)	0.4(19)	0.6(19)
O3A	35(2)	37(2)	35.4(19)	2.9(16)	-0.4(16)	2.5(17)
C65A	44(3)	46(3)	44(3)	1(2)	1.2(18)	0(2)
C66A	44(3)	44(3)	43(3)	2.3(19)	1.7(19)	0.8(19)
O4A	44(2)	47(2)	43(2)	4.3(18)	2.0(17)	1.6(18)
C67A	42(3)	45(3)	43(3)	0.4(19)	2.4(19)	-0.5(19)
C68A	44(3)	46(3)	47(3)	-1(2)	1.5(18)	0(2)
C69A	52(3)	52(3)	56(3)	-1.1(19)	2.7(19)	3.4(19)
C70A	50(3)	49(3)	51(3)	-1.7(19)	2.6(19)	3.6(19)
O5A	35(3)	36(2)	36(2)	-3.6(16)	0.8(18)	3.1(18)
C71A	44(3)	43(2)	43(3)	-3.0(18)	1.3(18)	-2.0(18)
C72A	40(3)	40(3)	40(3)	-2.2(19)	-0.7(18)	-0.6(19)
O6A	36(2)	36(2)	37(2)	-1.9(17)	0.1(16)	-1.6(16)
C73A	37(3)	39(2)	37(3)	0.1(19)	-1.3(19)	2.0(17)
C74A	41(3)	45(3)	43(3)	2.5(18)	-2.1(18)	1.9(18)
N18A	38(2)	37(2)	39(3)	0.3(18)	0.1(18)	2.0(17)
C15B	55(6)	62(6)	53(6)	-16(5)	15(5)	17(5)
C16B	25(2)	21(2)	23(2)	-3.0(17)	-0.1(17)	0.6(17)
N6B	30(7)	38(2)	23(3)	-8(3)	9(4)	10(3)
C17B	46(3)	44(3)	46(3)	0.7(19)	-0.4(19)	0.6(19)
C18B	79(8)	62(6)	50(6)	-15(5)	-24(6)	21(5)

Atom	U_{11}	U_{22}	U_{33}	U_{23}	U_{13}	U_{12}
C29B	73(7)	37(5)	48(6)	-11(4)	5(5)	-1(4)
C30B	36(3)	35(2)	35(2)	-0.8(17)	-0.3(19)	-0.1(19)
N10B	32(3)	29.7(19)	27.4(19)	-0.4(14)	-0.5(17)	-6.2(16)
C31B	63(8)	37(5)	19(4)	-5(4)	2(4)	-9(6)
C32B	84(9)	52(13)	42(4)	11(4)	-17(4)	12(7)
N17B	36(2)	36(3)	36(3)	0.9(19)	-0.7(18)	0.7(17)
C57B	45(3)	46(3)	47(3)	1.6(19)	-0.6(19)	1.2(18)
C58B	48(3)	52(3)	54(3)	1.5(19)	0(2)	-2.0(18)
O1B	42(2)	39(2)	42(3)	-0.4(18)	1.3(18)	-4.4(17)
C59B	55(3)	52(3)	57(3)	-0.1(19)	-0.4(19)	-2.6(19)
C60B	44(3)	36(2)	46(3)	-0.9(18)	4.5(19)	-4.8(19)
O2B	45(2)	37.4(18)	44(2)	-0.8(18)	0.1(18)	-0.8(16)
C61B	49(3)	45(3)	50(3)	0.3(18)	0(2)	2(2)
C62B	48(3)	46(3)	49(3)	0.2(18)	-0.3(19)	5.9(18)
C63B	40(3)	40(3)	40(3)	2.4(19)	-0.9(18)	2.0(19)
C64B	57(3)	57(3)	56(3)	2.8(19)	0.4(19)	0.6(19)
O3B	35(2)	37(2)	35.4(19)	2.9(16)	-0.4(16)	2.5(17)
C65B	44(3)	46(3)	44(3)	1(2)	1.2(18)	0(2)
C66B	44(3)	44(3)	43(3)	2.3(19)	1.7(19)	0.8(19)
O4B	44(2)	47(2)	43(2)	4.3(18)	2.0(17)	1.6(18)
C67B	42(3)	45(3)	43(3)	0.4(19)	2.4(19)	-0.5(19)
C68B	44(3)	46(3)	47(3)	-1(2)	1.5(18)	0(2)
C69B	52(3)	52(3)	56(3)	-1.1(19)	2.7(19)	3.4(19)
C70B	50(3)	49(3)	51(3)	-1.7(19)	2.6(19)	3.6(19)
O5B	35(3)	36(2)	36(2)	-3.6(16)	0.8(18)	3.1(18)
C71B	44(3)	43(2)	43(3)	-3.0(18)	1.3(18)	-2.0(18)
C72B	40(3)	40(3)	40(3)	-2.2(19)	-0.7(18)	-0.6(19)
O6B	36(2)	36(2)	37(2)	-1.9(17)	0.1(16)	-1.6(16)
C73B	37(3)	39(2)	37(3)	0.1(19)	-1.3(19)	2.0(17)
C74B	41(3)	45(3)	43(3)	2.5(18)	-2.1(18)	1.9(18)
N18B	38(2)	37(2)	39(3)	0.3(18)	0.1(18)	2.0(17)
K1	33.5(6)	22.7(5)	31.1(6)	-0.4(4)	0.9(5)	1.4(4)

Table 4.17 Bond Lengths for 3-Gd^{3+}.

Atom	Atom	Length/Å	Atom	Atom	Length/Å
Gd1	N1	2.242(4)	C31A	C32A	1.505(15)
Gd1	N5	2.253(4)	N17A	C57A	1.43(2)
Gd1	N9	2.258(4)	N17A	C63A	1.47(2)
Gd1	N13	2.267(4)	N17A	C69A	1.391(19)
P1	N1	1.532(4)	N17A	K1	3.020(16)

Atom	Atom	Length/Å	Atom	Atom	Length/Å
P1	N2	1.689(5)	C57A	C58A	1.562(17)
P1	N3	1.722(5)	C58A	O1A	1.464(17)
P1	N4	1.700(5)	O1A	C59A	1.466(18)
P2	N5	1.516(4)	O1A	K1	2.781(12)
P2	N7	1.728(5)	C59A	C60A	1.504(18)
P2	N8	1.712(5)	C60A	O2A	1.504(16)
P2	N6A	1.629(11)	O2A	C61A	1.405(17)
P2	N6B	1.724(7)	O2A	K1	2.792(8)
P3	N9	1.526(4)	C61A	C62A	1.51(2)
P3	N11	1.713(5)	C62A	N18A	1.450(16)
P3	N12	1.722(4)	C63A	C64A	1.40(2)
P3	N10A	1.638(14)	C64A	O3A	1.170(16)
P3	N10B	1.718(14)	C64A	K1	3.474(15)
P4	N13	1.518(4)	O3A	C65A	1.383(16)
P4	N14	1.678(4)	O3A	K1	2.841(7)
P4	N15	1.701(4)	C65A	C66A	1.23(2)
P4	N16	1.728(4)	C66A	O4A	1.439(19)
N2	C2	1.461(7)	O4A	C67A	1.336(15)
N2	C3	1.464(7)	O4A	K1	2.832(9)
N3	C5	1.495(8)	C67A	C68A	1.486(19)
N3	C9	1.471(6)	C68A	N18A	1.494(18)
N4	C10	1.448(7)	C69A	C70A	1.424(19)
N4	C11	1.487(8)	C70A	O5A	1.30(2)
N7	C24	1.446(7)	O5A	C71A	1.49(2)
N7	C25	1.489(7)	O5A	K1	2.777(18)
N8	C19	1.485(7)	C71A	C72A	1.432(18)
N8	C23	1.439(8)	C72A	O6A	1.417(18)
N11	C33	1.471(7)	O6A	C73A	1.399(15)
N11	C37	1.454(7)	O6A	K1	2.893(8)
N12	C38	1.463(8)	C73A	C74A	1.516(17)
N12	C39	1.460(8)	C74A	N18A	1.891(15)
N14	C44	1.480(7)	N18A	K1	2.910(11)
N14	C45	1.452(7)	C15B	C16B	1.515(10)
N15	C47	1.489(7)	C16B	N6B	1.477(13)
N15	C51	1.448(7)	N6B	C17B	1.440(10)
N16	C52	1.458(7)	C17B	C18B	1.527(12)
N16	C53	1.478(7)	C29B	C30B	1.533(11)
C1	C2	1.504(9)	C30B	N10B	1.469(8)
C3	C4	1.518(9)	N10B	C31B	1.467(8)
C5	C6	1.536(8)	C31B	C32B	1.505(15)
C5	C7	1.535(8)	N17B	C57B	1.41(2)

Atom	Atom	Length/Å	Atom	Atom	Length/Å
C5	C8	1.505(9)	N17B	C63B	1.41(2)
C9	C10	1.508(9)	N17B	C69B	1.58(2)
C11	C12	1.525(8)	N17B	K1	2.963(19)
C11	C13	1.526(9)	C57B	C58B	1.046(19)
C11	C14	1.524(8)	C58B	O1B	1.48(2)
C19	C20	1.521(8)	O1B	C59B	1.46(2)
C19	C21	1.525(9)	O1B	K1	2.939(13)
C19	C22	1.511(10)	C59B	C60B	1.51(2)
C23	C24	1.444(9)	C60B	O2B	1.478(17)
C25	C26	1.525(7)	O2B	C61B	1.37(2)
C25	C27	1.527(8)	O2B	K1	2.830(9)
C25	C28	1.532(7)	C61B	C62B	1.54(2)
C33	C34	1.522(9)	C62B	N18B	1.894(19)
C33	C35	1.545(9)	C63B	C64B	1.36(2)
C33	C36	1.526(8)	C64B	O3B	1.295(18)
C37	C38	1.464(9)	O3B	C65B	1.414(19)
C39	C40	1.544(8)	O3B	K1	2.789(9)
C39	C41	1.535(8)	C65B	C66B	1.60(3)
C39	C42	1.514(8)	C66B	O4B	1.42(2)
C43	C44	1.521(9)	O4B	C67B	1.530(18)
C45	C46	1.507(8)	O4B	K1	2.911(10)
C47	C48	1.533(7)	C67B	C68B	1.58(2)
C47	C49	1.511(8)	C68B	N18B	1.49(2)
C47	C50	1.522(8)	C69B	C70B	1.57(2)
C51	C52	1.495(7)	C70B	O5B	1.54(3)
C53	C54	1.544(8)	O5B	C71B	1.38(2)
C53	C55	1.513(9)	O5B	K1	2.87(2)
C53	C56	1.546(8)	C71B	C72B	1.52(2)
C15A	C16A	1.514(11)	C72B	O6B	1.43(2)
C16A	N6A	1.477(13)	O6B	C73B	1.424(18)
N6A	C17A	1.440(10)	O6B	K1	2.707(9)
C17A	C18A	1.528(12)	C73B	C74B	1.49(2)
C29A	C30A	1.533(11)	C73B	K1	3.541(16)
C30A	N10A	1.470(8)	C74B	N18B	1.043(17)
N10A	C31A	1.467(8)	N18B	K1	3.077(14)

Table 4.18 Bond Angles for 3-Gd^{3+}.

Atom	Atom	Atom	Angle/°	Atom	Atom	Atom	Angle/°
N1	Gd1	N5	108.67(17)	C57A	N17A	K1	110.4(9)
N1	Gd1	N9	108.01(17)	C63A	N17A	K1	106.0(9)

Atom	Atom	Atom	Angle/°	Atom	Atom	Atom	Angle/°
N1	Gd1	N13	111.41(15)	C69A	N17A	C57A	110.9(14)
N5	Gd1	N9	110.17(15)	C69A	N17A	C63A	96.8(12)
N5	Gd1	N13	108.80(16)	C69A	N17A	K1	109.4(10)
N9	Gd1	N13	109.78(16)	N17A	C57A	C58A	122.4(11)
N1	P1	N2	113.4(2)	O1A	C58A	C57A	118.6(11)
N1	P1	N3	121.8(3)	C58A	O1A	C59A	106.8(10)
N1	P1	N4	119.8(3)	C58A	O1A	K1	115.6(8)
N2	P1	N3	102.2(2)	C59A	O1A	K1	115.7(8)
N2	P1	N4	104.8(2)	O1A	C59A	C60A	105.2(11)
N4	P1	N3	91.2(2)	O2A	C60A	C59A	106.6(10)
N5	P2	N7	121.2(2)	C60A	O2A	K1	111.9(7)
N5	P2	N8	120.9(2)	C61A	O2A	C60A	109.4(10)
N5	P2	N6A	111.3(4)	C61A	O2A	K1	115.8(8)
N5	P2	N6B	114.5(3)	O2A	C61A	C62A	107.9(13)
N8	P2	N7	89.8(2)	N18A	C62A	C61A	97.2(11)
N8	P2	N6B	101.2(8)	C64A	C63A	N17A	120.8(13)
N6A	P2	N7	102.5(15)	C63A	C64A	K1	88.4(8)
N6A	P2	N8	108.2(14)	O3A	C64A	C63A	136.7(14)
N6B	P2	N7	105.1(8)	O3A	C64A	K1	48.7(7)
N9	P3	N11	121.1(3)	C64A	O3A	C65A	126.1(11)
N9	P3	N12	121.6(2)	C64A	O3A	K1	113.3(9)
N9	P3	N10A	114.5(4)	C65A	O3A	K1	117.4(7)
N9	P3	N10B	111.9(4)	C66A	C65A	O3A	106.7(14)
N11	P3	N12	90.2(2)	C65A	C66A	O4A	121.6(15)
N11	P3	N10B	101.7(6)	C66A	O4A	K1	114.8(8)
N10A	P3	N11	104.7(6)	C67A	O4A	C66A	118.8(11)
N10A	P3	N12	100.4(6)	C67A	O4A	K1	114.4(7)
N10B	P3	N12	106.9(6)	O4A	C67A	C68A	114.6(11)
N13	P4	N14	113.0(2)	C67A	C68A	N18A	111.6(11)
N13	P4	N15	120.8(2)	N17A	C69A	C70A	118.4(13)
N13	P4	N16	122.2(2)	O5A	C70A	C69A	108.5(14)
N14	P4	N15	105.4(2)	C70A	O5A	C71A	113.9(15)
N14	P4	N16	102.7(2)	C70A	O5A	K1	127.9(12)
N15	P4	N16	89.0(2)	C71A	O5A	K1	116.6(10)
P1	N1	Gd1	168.5(3)	C72A	C71A	O5A	107.2(12)
C2	N2	P1	120.0(4)	O6A	C72A	C71A	112.3(13)
C2	N2	C3	115.2(5)	C72A	O6A	K1	112.1(8)
C3	N2	P1	120.7(3)	C73A	O6A	C72A	112.0(10)
C5	N3	P1	121.1(3)	C73A	O6A	K1	114.2(7)
C9	N3	P1	107.3(4)	O6A	C73A	C74A	107.6(10)
C9	N3	C5	115.9(5)	C73A	C74A	N18A	114.5(9)

Atom	Atom	Atom	Angle/°	Atom	Atom	Atom	Angle/°
C10	N4	P1	114.0(4)	C62A	N18A	C68A	134.1(11)
C10	N4	C11	119.0(5)	C62A	N18A	C74A	93.5(8)
C11	N4	P1	126.4(4)	C62A	N18A	K1	114.6(8)
P2	N5	Gd1	168.3(3)	C68A	N18A	C74A	79.5(8)
C24	N7	P2	109.2(4)	C68A	N18A	K1	111.1(8)
C24	N7	C25	116.3(5)	C74A	N18A	K1	102.3(6)
C25	N7	P2	122.1(4)	N6B	C16B	C15B	109.8(12)
C19	N8	P2	123.3(4)	C16B	N6B	P2	120.8(8)
C23	N8	P2	112.4(4)	C17B	N6B	P2	117.5(6)
C23	N8	C19	117.4(5)	C17B	N6B	C16B	120.6(7)
P3	N9	Gd1	166.4(3)	N6B	C17B	C18B	116.3(16)
C33	N11	P3	122.8(4)	N10B	C30B	C29B	117.2(9)
C37	N11	P3	111.8(4)	C30B	N10B	P3	119.1(11)
C37	N11	C33	116.3(5)	C31B	N10B	P3	121.9(12)
C38	N12	P3	106.8(4)	C31B	N10B	C30B	116.6(5)
C39	N12	P3	123.0(4)	N10B	C31B	C32B	114.6(9)
C39	N12	C38	116.3(5)	C57B	N17B	C63B	95.9(14)
P4	N13	Gd1	175.2(3)	C57B	N17B	C69B	105.4(15)
C44	N14	P4	121.8(4)	C57B	N17B	K1	110.7(11)
C45	N14	P4	121.2(4)	C63B	N17B	C69B	126.8(15)
C45	N14	C44	117.0(4)	C63B	N17B	K1	111.3(12)
C47	N15	P4	125.4(3)	C69B	N17B	K1	105.7(10)
C51	N15	P4	114.3(3)	C58B	C57B	N17B	134.9(18)
C51	N15	C47	117.4(4)	C57B	C58B	O1B	119.2(17)
C52	N16	P4	107.6(3)	C58B	O1B	K1	114.0(9)
C52	N16	C53	116.1(4)	C59B	O1B	C58B	105.5(12)
C53	N16	P4	122.2(4)	C59B	O1B	K1	112.2(9)
N2	C2	C1	114.2(6)	O1B	C59B	C60B	101.8(13)
N2	C3	C4	115.3(5)	O2B	C60B	C59B	104.9(12)
N3	C5	C6	109.6(5)	C60B	O2B	K1	114.2(8)
N3	C5	C7	108.4(5)	C61B	O2B	C60B	110.8(12)
N3	C5	C8	112.8(5)	C61B	O2B	K1	114.3(10)
C7	C5	C6	107.4(5)	O2B	C61B	C62B	111.1(14)
C8	C5	C6	107.8(5)	C61B	C62B	N18B	115.6(12)
C8	C5	C7	110.7(6)	C64B	C63B	N17B	123.1(16)
N3	C9	C10	106.0(5)	O3B	C64B	C63B	123.8(15)
N4	C10	C9	106.1(5)	C64B	O3B	C65B	122.8(12)
N4	C11	C12	109.8(5)	C64B	O3B	K1	120.7(9)
N4	C11	C13	110.6(5)	C65B	O3B	K1	112.6(8)
N4	C11	C14	110.0(5)	O3B	C65B	C66B	121.9(14)
C12	C11	C13	110.0(6)	O4B	C66B	C65B	93.7(14)

Atom	Atom	Atom	Angle/°	Atom	Atom	Atom	Angle/°
C14	C11	C12	108.4(5)	C66B	O4B	C67B	104.7(12)
C14	C11	C13	107.9(6)	C66B	O4B	K1	113.9(10)
N8	C19	C20	111.5(5)	C67B	O4B	K1	112.0(8)
N8	C19	C21	108.9(5)	O4B	C67B	C68B	99.6(11)
N8	C19	C22	110.0(5)	N18B	C68B	C67B	110.1(12)
C20	C19	C21	109.8(6)	C70B	C69B	N17B	110.1(14)
C22	C19	C20	108.4(6)	O5B	C70B	C69B	109.8(14)
C22	C19	C21	108.2(6)	C70B	O5B	K1	108.7(12)
N8	C23	C24	109.5(5)	C71B	O5B	C70B	137.8(18)
C23	C24	N7	109.6(5)	C71B	O5B	K1	111.5(13)
N7	C25	C26	112.2(4)	O5B	C71B	C72B	111.9(15)
N7	C25	C27	109.0(4)	O6B	C72B	C71B	107.2(14)
N7	C25	C28	109.2(4)	C72B	O6B	K1	120.9(9)
C26	C25	C27	108.4(5)	C73B	O6B	C72B	112.0(12)
C26	C25	C28	109.4(5)	C73B	O6B	K1	114.4(8)
C27	C25	C28	108.7(5)	O6B	C73B	C74B	112.0(13)
N11	C33	C34	110.2(5)	O6B	C73B	K1	44.1(6)
N11	C33	C35	111.3(5)	C74B	C73B	K1	80.8(8)
N11	C33	C36	109.2(5)	N18B	C74B	C73B	103.4(14)
C34	C33	C35	108.8(5)	C62B	N18B	K1	91.9(6)
C34	C33	C36	108.5(6)	C68B	N18B	C62B	70.4(9)
C36	C33	C35	108.8(5)	C68B	N18B	K1	106.8(9)
N11	C37	C38	108.3(5)	C74B	N18B	C62B	106.0(13)
N12	C38	C37	108.5(5)	C74B	N18B	C68B	140.1(16)
N12	C39	C40	110.5(5)	C74B	N18B	K1	113.1(12)
N12	C39	C41	108.2(5)	O1A	K1	O2A	61.2(3)
N12	C39	C42	112.8(5)	O1A	K1	O3A	97.4(3)
C41	C39	C40	107.1(5)	O1A	K1	O4A	132.5(3)
C42	C39	C40	108.5(5)	O1A	K1	O6A	138.9(3)
C42	C39	C41	109.7(5)	O1A	K1	N18A	116.3(3)
N14	C44	C43	113.6(6)	O2A	K1	O3A	134.4(2)
N14	C45	C46	114.2(5)	O2A	K1	O4A	108.0(3)
N15	C47	C48	108.0(5)	O2A	K1	O6A	99.8(2)
N15	C47	C49	110.7(4)	O2A	K1	N18A	56.8(3)
N15	C47	C50	109.6(5)	O3A	K1	O6A	118.7(2)
C49	C47	C48	109.0(5)	O3A	K1	N18A	115.1(3)
C49	C47	C50	108.5(5)	O4A	K1	O3A	55.4(2)
C50	C47	C48	111.0(5)	O4A	K1	O6A	86.7(2)
N15	C51	C52	106.3(4)	O4A	K1	N18A	61.2(3)
N16	C52	C51	105.2(4)	O5A	K1	O1A	99.4(4)
N16	C53	C54	107.6(5)	O5A	K1	O2A	124.6(4)

Atom	Atom	Atom	Angle/°	Atom	Atom	Atom	Angle/°
N16	C53	C55	110.7(5)	O5A	K1	O3A	96.9(4)
N16	C53	C56	111.5(5)	O5A	K1	O4A	120.0(4)
C54	C53	C56	109.0(5)	O5A	K1	O6A	59.8(4)
C55	C53	C54	108.9(5)	O5A	K1	N18A	126.5(4)
C55	C53	C56	109.2(5)	O6A	K1	N18A	67.3(3)
N6A	C16A	C15A	109.6(12)	O2B	K1	O4B	87.6(3)
C16A	N6A	P2	111.8(12)	O2B	K1	O5B	138.4(5)
C17A	N6A	P2	127.1(9)	O3B	K1	O2B	101.1(3)
C17A	N6A	C16A	120.3(7)	O3B	K1	O4B	59.4(3)
N6A	C17A	C18A	116.1(16)	O3B	K1	O5B	110.5(5)
N10A	C30A	C29A	117.0(9)	O5B	K1	O4B	131.6(5)
C30A	N10A	P3	122.1(11)	O6B	K1	O2B	101.6(3)
C31A	N10A	P3	120.7(10)	O6B	K1	O3B	151.7(3)
C31A	N10A	C30A	116.6(5)	O6B	K1	O4B	105.0(3)
N10A	C31A	C32A	114.6(9)	O6B	K1	O5B	60.1(4)
C57A	N17A	C63A	122.3(13)				

Table 4.19 Torsion Angles for 3-Gd^{3+}.

A	B	C	D	Angle/°	A	B	C	D	Angle/°
P1	N2	C2	C1	-138.0(5)	C38	N12	C39	C42	-53.0(7)
P1	N2	C3	C4	104.0(6)	C39	N12	C38	C37	179.1(5)
P1	N3	C5	C6	45.8(6)	C44	N14	C45	C46	-56.1(7)
P1	N3	C5	C7	162.8(4)	C45	N14	C44	C43	-48.7(7)
P1	N3	C5	C8	-74.3(6)	C47	N15	C51	C52	-155.4(5)
P1	N3	C9	C10	-41.6(5)	C51	N15	C47	C48	-54.5(7)
P1	N4	C10	C9	-10.9(6)	C51	N15	C47	C49	-173.8(5)
P1	N4	C11	C12	-143.2(4)	C51	N15	C47	C50	66.5(6)
P1	N4	C11	C13	95.1(6)	C52	N16	C53	C54	63.8(6)
P1	N4	C11	C14	-24.0(7)	C52	N16	C53	C55	-177.4(5)
P2	N7	C24	C23	29.1(7)	C52	N16	C53	C56	-55.6(6)
P2	N7	C25	C26	78.6(5)	C53	N16	C52	C51	-174.6(4)
P2	N7	C25	C27	-161.4(4)	C15A	C16A	N6A	P2	-145(3)
P2	N7	C25	C28	-42.8(5)	C15A	C16A	N6A	C17A	45(4)
P2	N8	C19	C20	-78.0(6)	C16A	N6A	C17A	C18A	58(4)
P2	N8	C19	C21	160.7(5)	N6A	P2	N5	Gd1	174(2)
P2	N8	C19	C22	42.3(7)	N6A	P2	N7	C24	-137.8(14)
P2	N8	C23	C24	-9.1(8)	N6A	P2	N7	C25	81.6(14)
P2	N6A	C17A	C18A	-111(4)	N6A	P2	N8	C19	-84.8(15)
P2	N6B	C17B	C18B	119.3(17)	N6A	P2	N8	C23	125.3(15)
P3	N11	C33	C34	41.2(7)	C29A	C30A	N10A	P3	-95.4(16)

A	B	C	D	Angle/°	A	B	C	D	Angle/°
P3	N11	C33	C35	-79.6(6)	C29A	C30A	N10A	C31A	94(2)
P3	N11	C33	C36	160.3(5)	C30A	N10A	C31A	C32A	-48(4)
P3	N11	C37	C38	-5.8(6)	N10A	P3	N9	Gd1	173.0(14)
P3	N12	C38	C37	37.4(6)	N10A	P3	N11	C33	-89.5(7)
P3	N12	C39	C40	-39.7(6)	N10A	P3	N11	C37	124.8(7)
P3	N12	C39	C41	-156.6(4)	N10A	P3	N12	C38	-140.0(7)
P3	N12	C39	C42	81.9(6)	N10A	P3	N12	C39	81.5(7)
P3	N10A	C31A	C32A	141(3)	N17A	C57A	C58A	O1A	-17(2)
P3	N10B	C31B	C32B	132(4)	N17A	C63A	C64A	O3A	-12(3)
P4	N14	C44	C43	132.8(5)	N17A	C63A	C64A	K1	-5.2(13)
P4	N14	C45	C46	122.5(5)	N17A	C69A	C70A	O5A	53(2)
P4	N15	C47	C48	146.1(5)	C57A	N17A	C63A	C64A	-121.4(16)
P4	N15	C47	C49	26.8(6)	C57A	N17A	C69A	C70A	79.3(18)
P4	N15	C47	C50	-92.8(5)	C57A	C58A	O1A	C59A	165.3(12)
P4	N15	C51	C52	6.3(6)	C57A	C58A	O1A	K1	35.0(15)
P4	N16	C52	C51	44.3(5)	C58A	O1A	C59A	C60A	179.0(11)
P4	N16	C53	C54	-161.2(4)	O1A	C59A	C60A	O2A	69.8(13)
P4	N16	C53	C55	-42.4(6)	C59A	C60A	O2A	C61A	174.7(11)
P4	N16	C53	C56	79.3(6)	C59A	C60A	O2A	K1	-55.7(11)
N1	P1	N2	C2	12.6(6)	C60A	O2A	C61A	C62A	-174.4(11)
N1	P1	N2	C3	168.8(5)	O2A	C61A	C62A	N18A	-74.9(13)
N1	P1	N3	C5	40.2(5)	C61A	C62A	N18A	C68A	-118.0(15)
N1	P1	N3	C9	-95.9(4)	C61A	C62A	N18A	C74A	163.3(10)
N1	P1	N4	C10	116.9(4)	C61A	C62A	N18A	K1	58.1(11)
N1	P1	N4	C11	-54.6(5)	C63A	N17A	C57A	C58A	117.5(16)
N2	P1	N1	Gd1	-126.6(15)	C63A	N17A	C69A	C70A	-152.3(14)
N2	P1	N3	C5	-87.6(4)	C63A	C64A	O3A	C65A	167.8(16)
N2	P1	N3	C9	136.3(4)	C63A	C64A	O3A	K1	9(2)
N2	P1	N4	C10	-114.3(4)	C64A	O3A	C65A	C66A	147.7(15)
N2	P1	N4	C11	74.2(5)	O3A	C65A	C66A	O4A	52.7(18)
N3	P1	N1	Gd1	110.8(15)	C65A	C66A	O4A	C67A	113.9(17)
N3	P1	N2	C2	145.5(5)	C65A	C66A	O4A	K1	-26.8(19)
N3	P1	N2	C3	-58.3(5)	C66A	O4A	C67A	C68A	168.4(12)
N3	P1	N4	C10	-11.4(4)	O4A	C67A	C68A	N18A	62.0(15)
N3	P1	N4	C11	177.1(4)	C67A	C68A	N18A	C62A	138.0(13)
N3	C9	C10	N4	32.7(6)	C67A	C68A	N18A	C74A	-137.4(11)
N4	P1	N1	Gd1	-1.8(16)	C67A	C68A	N18A	K1	-38.1(12)
N4	P1	N2	C2	-119.9(5)	C69A	N17A	C57A	C58A	-129.5(15)
N4	P1	N2	C3	36.3(6)	C69A	N17A	C63A	C64A	118.6(15)
N4	P1	N3	C5	167.0(4)	C69A	C70A	O5A	C71A	128.5(15)
N4	P1	N3	C9	30.8(4)	C69A	C70A	O5A	K1	-36(2)

A	B	C	D	Angle/°	A	B	C	D	Angle/°
N5	P2	N7	C24	97.5(5)	C70A	O5A	C71A	C72A	145.2(16)
N5	P2	N7	C25	-43.1(5)	O5A	C71A	C72A	O6A	65.3(16)
N5	P2	N8	C19	45.2(5)	C71A	C72A	O6A	C73A	-179.3(12)
N5	P2	N8	C23	-104.7(5)	C71A	C72A	O6A	K1	-49.5(13)
N5	P2	N6A	C16A	-160(2)	C72A	O6A	C73A	C74A	-172.1(11)
N5	P2	N6A	C17A	10(5)	O6A	C73A	C74A	N18A	-66.6(13)
N5	P2	N6B	C16B	164.8(15)	C73A	C74A	N18A	C62A	-78.5(11)
N5	P2	N6B	C17B	-3(3)	C73A	C74A	N18A	C68A	147.2(11)
N7	P2	N5	Gd1	-65.1(15)	C73A	C74A	N18A	K1	37.7(10)
N7	P2	N8	C19	172.1(5)	C15B	C16B	N6B	P2	139.6(17)
N7	P2	N8	C23	22.2(5)	C15B	C16B	N6B	C17B	-53(3)
N7	P2	N6A	C16A	69(3)	C16B	N6B	C17B	C18B	-49(3)
N7	P2	N6A	C17A	-121(4)	N6B	P2	N5	Gd1	167.3(18)
N7	P2	N6B	C16B	29(2)	N6B	P2	N7	C24	-130.8(8)
N7	P2	N6B	C17B	-138.4(19)	N6B	P2	N7	C25	88.6(8)
N8	P2	N5	Gd1	45.8(16)	N6B	P2	N8	C19	-82.5(9)
N8	P2	N7	C24	-29.2(5)	N6B	P2	N8	C23	127.6(9)
N8	P2	N7	C25	-169.8(4)	C29B	C30B	N10B	P3	120.8(13)
N8	P2	N6A	C16A	-25(3)	C29B	C30B	N10B	C31B	-42(3)
N8	P2	N6A	C17A	145(4)	C30B	N10B	C31B	C32B	-66(5)
N8	P2	N6B	C16B	-63(2)	N10B	P3	N9	Gd1	166.0(14)
N8	P2	N6B	C17B	129(2)	N10B	P3	N11	C33	-83.0(7)
N8	C23	C24	N7	-12.8(9)	N10B	P3	N11	C37	131.3(7)
N9	P3	N11	C33	41.8(6)	N10B	P3	N12	C38	-137.3(6)
N9	P3	N11	C37	-103.9(4)	N10B	P3	N12	C39	84.2(7)
N9	P3	N12	C38	92.5(5)	N17B	C57B	C58B	O1B	9(4)
N9	P3	N12	C39	-45.9(5)	N17B	C63B	C64B	O3B	0(3)
N9	P3	N10A	C30A	11.3(16)	N17B	C69B	C70B	O5B	-74.9(18)
N9	P3	N10A	C31A	-178(2)	C57B	N17B	C63B	C64B	-105.0(19)
N9	P3	N10B	C30B	3.8(16)	C57B	N17B	C69B	C70B	167.4(14)
N9	P3	N10B	C31B	165(2)	C57B	C58B	O1B	C59B	-146.8(19)
N11	P3	N9	Gd1	46.1(14)	C57B	C58B	O1B	K1	-23(2)
N11	P3	N12	C38	-35.0(4)	C58B	O1B	C59B	C60B	-177.4(12)
N11	P3	N12	C39	-173.4(4)	O1B	C59B	C60B	O2B	-76.6(15)
N11	P3	N10A	C30A	146.3(12)	C59B	C60B	O2B	C61B	-170.6(14)
N11	P3	N10A	C31A	-43(2)	C59B	C60B	O2B	K1	58.5(13)
N11	P3	N10B	C30B	134.5(12)	C60B	O2B	C61B	C62B	179.8(13)
N11	P3	N10B	C31B	-64(2)	O2B	C61B	C62B	N18B	75.6(18)
N11	C37	C38	N12	-20.1(7)	C61B	C62B	N18B	C68B	-158.1(14)
N12	P3	N9	Gd1	-66.1(13)	C61B	C62B	N18B	C74B	63.8(18)
N12	P3	N11	C33	169.7(5)	C61B	C62B	N18B	K1	-50.9(12)

A	B	C	D	Angle/°	A	B	C	D	Angle/°
N12	P3	N11	C37	24.0(4)	C63B	N17B	C57B	C58B	126(3)
N12	P3	N10A	C30A	-120.7(12)	C63B	N17B	C69B	C70B	-83(2)
N12	P3	N10A	C31A	50(2)	C63B	C64B	O3B	C65B	-167.8(15)
N12	P3	N10B	C30B	-131.6(12)	C63B	C64B	O3B	K1	-12(2)
N12	P3	N10B	C31B	30(2)	C64B	O3B	C65B	C66B	122.6(17)
N13	P4	N14	C44	-3.8(5)	O3B	C65B	C66B	O4B	65.7(17)
N13	P4	N14	C45	177.7(4)	C65B	C66B	O4B	C67B	176.5(12)
N13	P4	N15	C47	48.9(5)	C65B	C66B	O4B	K1	-60.9(13)
N13	P4	N15	C51	-111.0(4)	C66B	O4B	C67B	C68B	-172.1(13)
N13	P4	N16	C52	91.2(4)	O4B	C67B	C68B	N18B	-80.8(14)
N13	P4	N16	C53	-47.0(5)	C67B	C68B	N18B	C62B	139.1(14)
N14	P4	N15	C47	-80.6(5)	C67B	C68B	N18B	C74B	-129(2)
N14	P4	N15	C51	119.5(4)	C67B	C68B	N18B	K1	53.1(13)
N14	P4	N16	C52	-140.9(3)	C69B	N17B	C57B	C58B	-104(3)
N14	P4	N16	C53	80.9(4)	C69B	N17B	C63B	C64B	140.8(19)
N15	P4	N14	C44	130.1(4)	C69B	C70B	O5B	C71B	-108(3)
N15	P4	N14	C45	-48.3(5)	C69B	C70B	O5B	K1	54.0(15)
N15	P4	N16	C52	-35.3(4)	C70B	O5B	C71B	C72B	-148(2)
N15	P4	N16	C53	-173.5(4)	O5B	C71B	C72B	O6B	-60.6(19)
N15	C51	C52	N16	-31.3(6)	C71B	C72B	O6B	C73B	179.7(12)
N16	P4	N14	C44	-137.3(4)	C71B	C72B	O6B	K1	40.1(17)
N16	P4	N14	C45	44.2(5)	C72B	O6B	C73B	C74B	169.3(13)
N16	P4	N15	C47	176.5(5)	C72B	O6B	C73B	K1	-142.4(14)
N16	P4	N15	C51	16.6(4)	O6B	C73B	C74B	N18B	75.3(17)
C2	N2	C3	C4	-98.7(7)	C73B	C74B	N18B	C62B	-157.6(11)
C3	N2	C2	C1	64.5(8)	C73B	C74B	N18B	C68B	124(2)
C5	N3	C9	C10	179.6(5)	C73B	C74B	N18B	K1	-58.4(14)
C9	N3	C5	C6	178.5(5)	K1	N17A	C57A	C58A	-8.1(16)
C9	N3	C5	C7	-64.6(6)	K1	N17A	C63A	C64A	6.2(15)
C9	N3	C5	C8	58.4(6)	K1	N17A	C69A	C70A	-42.7(17)
C10	N4	C11	C12	45.7(7)	K1	O1A	C59A	C60A	-50.7(12)
C10	N4	C11	C13	-75.9(6)	K1	O2A	C61A	C62A	58.2(14)
C10	N4	C11	C14	164.9(5)	K1	C64A	O3A	C65A	159.2(15)
C11	N4	C10	C9	161.3(5)	K1	O3A	C65A	C66A	-53.9(13)
C19	N8	C23	C24	-160.9(6)	K1	O4A	C67A	C68A	-50.7(14)
C23	N8	C19	C20	70.5(7)	K1	O5A	C71A	C72A	-48.3(15)
C23	N8	C19	C21	-50.8(8)	K1	O6A	C73A	C74A	59.1(11)
C23	N8	C19	C22	-169.2(6)	K1	N17B	C57B	C58B	10(3)
C24	N7	C25	C26	-59.4(7)	K1	N17B	C63B	C64B	10(2)
C24	N7	C25	C27	60.5(6)	K1	N17B	C69B	C70B	50.1(14)
C24	N7	C25	C28	179.1(5)	K1	O1B	C59B	C60B	57.9(13)

A	B	C	D	Angle/°	A	B	C	D	Angle/°
C25	N7	C24	C23	172.3(6)	K1	O2B	C61B	C62B	-49.5(17)
C33	N11	C37	C38	-153.9(5)	K1	O3B	C65B	C66B	-35.1(16)
C37	N11	C33	C34	-174.5(5)	K1	O4B	C67B	C68B	64.0(11)
C37	N11	C33	C35	64.7(6)	K1	O5B	C71B	C72B	50.9(16)
C37	N11	C33	C36	-55.5(7)	K1	O6B	C73B	C74B	-48.3(14)
C38	N12	C39	C40	-174.6(5)	K1	C73B	C74B	N18B	43.6(13)
C38	N12	C39	C41	68.4(6)					

Table 4.20 Hydrogen Atom Coordinates (Å×10^4) and Isotropic Displacement Parameters (Å^2×10^3) for 3-Gd^{3+}.

Atom	*x*	*y*	*z*	*U*(eq)
H1A	4460.13	5261.13	8554.94	95
H1B	4021.42	5378.07	8927.62	95
H1C	4444.67	4863.89	8898.32	95
H2A	4996.42	5461.31	9290.22	57
H2B	5454.69	5295.58	8936.77	57
H3A	4774.45	6668.44	9113.15	53
H3B	4344.5	6189.91	9247.94	53
H4A	4248.32	6652.61	8517.64	84
H4B	3679.25	6668.65	8841.61	84
H4C	3848.25	6148.28	8629.83	84
H6A	5509.9	5755.21	8135.23	75
H6B	5240.6	5937.59	7728.15	75
H6C	4827.36	6078.49	8105.32	75
H7A	4888.56	7008.63	7937.41	86
H7B	5227.26	6807.84	7552.23	86
H7C	5598.66	7234.1	7798.82	86
H8A	6620.55	6746.47	7840.7	78
H8B	6335.79	6260.84	7621.47	78
H8C	6640.44	6203.74	8041.37	78
H9A	5921.62	7426.45	8388.89	47
H9B	6588.52	7087.66	8451.92	47
H10A	6458.9	7396.48	9048.41	50
H10B	5647.11	7412.78	9014.38	50
H12A	6005.73	7393.73	9694.21	82
H12B	5881.48	7000.32	10033.06	82
H12C	5330.65	7059.64	9702.05	82
H13A	7158.38	6409.56	9453.06	82
H13B	7027.45	6628.21	9871.36	82
H13C	7106.17	7006.72	9518.84	82

Atom	*x*	*y*	*z*	*U*(eq)
H14A	5428.71	6120.12	9637.11	67
H14B	6033.47	6098.99	9939.77	67
H14C	6138.05	5871.38	9521.83	67
H20A	7622.53	5923.27	7546.05	75
H20B	8429.46	5975.89	7550.78	75
H20C	8049.26	5696.09	7893.39	75
H21A	8301.86	5030.61	6855.1	112
H21B	8680.61	5544.98	6964.78	112
H21C	7885.92	5548.78	6876.55	112
H22A	8632.31	4927.13	7849.63	101
H22B	9119.46	5153.88	7528.23	101
H22C	8726.8	4633.99	7454.73	101
H23A	6935.1	5041.64	6963.02	70
H23B	6863.88	5503.86	7255.77	70
H24A	6001.86	4774.75	7185.65	64
H24B	6032.99	5159.39	7538.12	64
H26A	5912.17	4803.03	8292.2	48
H26B	5237.33	4468.66	8284.55	48
H26C	5351.42	4899.83	7971.63	48
H27A	5203.33	4316.31	7442.86	64
H27B	5037.76	3877.23	7741.97	64
H27C	5613.43	3795.17	7427.49	64
H28A	6455.2	3590.53	7945.87	61
H28B	5840.89	3651.83	8239.2	61
H28C	6524.02	3966.46	8300.6	61
H34A	8494.34	4832.14	9656.89	74
H34B	9235.25	4616.38	9743.48	74
H34C	8624.53	4496.89	10028.89	74
H35A	8727.81	3839.86	8974.04	65
H35B	9242.76	4276.42	9098.63	65
H35C	8471.27	4412.07	9004.57	65
H36A	8882.16	3570.71	9957.48	88
H36B	9490.31	3728.61	9681.06	88
H36C	8931.88	3332.81	9539.59	88
H37A	7717.62	3188.68	9585.76	56
H37B	7906.6	3404.14	9171.87	56
H38A	6864.27	3588.41	9040.43	67
H38B	6689.07	3192.09	9372.15	67
H40A	5803.51	4444.46	9984.8	69
H40B	5206.85	4547.17	9686.56	69
H40C	5937.27	4793.48	9620.46	69

Atom	*x*	*y*	*z*	*U*(eq)
H41A	5626.68	3270.53	9496.39	75
H41B	5024.06	3643.39	9613.81	75
H41C	5619.26	3524.93	9909.65	75
H42A	5999.19	4396.47	8972.02	61
H42B	5251.9	4186.56	9048.88	61
H42C	5841.87	3806.63	8924.23	61
H43A	9332.62	5617.16	9836.77	103
H43B	8771.68	5831.8	10122.9	103
H43C	9408.71	6173.79	10009.67	103
H44A	8359.07	5878.54	9496.63	54
H44B	8437.39	6434.87	9668.59	54
H45A	9946.76	6665.99	9096.15	46
H45B	10032.66	6385.1	9495.92	46
H46A	9344.97	7309.43	9366.15	84
H46B	9979.98	7219.34	9640.72	84
H46C	9251.21	7003.98	9755.77	84
H48A	9097.05	7611.87	8700.62	84
H48B	8454.83	7823.12	8473.11	84
H48C	9064.63	7561.6	8247.02	84
H49A	7800.9	6712.87	8908.48	58
H49B	7670.69	7305.77	8856.51	58
H49C	8304.67	7112.54	9099.86	58
H50A	8270.34	6906.14	7951.65	74
H50B	7668.07	7210.55	8152.22	74
H50C	7749.44	6616.39	8223.82	74
H51A	9853.83	6873.19	8297.59	38
H51B	9272.24	6720.41	7998.56	38
H52A	9467.05	5888.36	8067.02	41
H52B	10220.88	6096.48	8142.85	41
H54A	10841.18	5529.67	8350.62	78
H54B	10984.59	5129.58	8682.58	78
H54C	10972.71	5721.34	8776.3	78
H55A	10097.99	5535.4	9281	69
H55B	10128.75	4951.04	9164.96	69
H55C	9418.46	5241.74	9168.95	69
H56A	9196.97	5000.3	8487.93	69
H56B	9885.74	4682.87	8505.59	69
H56C	9776.73	5094.99	8177.88	69
H15A	7658.93	3271.69	7100.49	85
H15B	7302.38	3243.07	7508.97	85
H15C	8106.26	3184.26	7474.53	85

Atom	*x*	*y*	*z*	*U*(eq)
H16A	8255	4021.12	7349.05	89
H16B	7472.84	4098.02	7241.1	89
H17A	7712.69	3432.86	8113.11	36
H17B	7758.13	3932.98	8365.54	36
H18A	8831.27	3504.32	7930.53	95
H18B	8816.1	3580.58	8382.36	95
H18C	8887.28	4059.98	8107.56	95
H29A	7847.51	5485.35	9995.13	79
H29B	7814.91	5303.07	10429.1	79
H29C	7370.36	5774.64	10291.84	79
H30A	6660.29	5072.19	10340.1	42
H30B	6712.23	5237.58	9904.67	42
H31A	7348.75	3874.7	10224.66	48
H31B	6667.45	4116.49	10388.46	48
H32A	7991.3	4411.86	10613.7	89
H32B	7481.43	4082.98	10866.56	89
H32C	7311.57	4661.66	10774.93	89
H57A	5543.97	7541.81	11027.11	55
H57B	5645.22	7613.46	11472.2	55
H58A	5834.01	6816.32	11564.87	62
H58B	5502.74	6742.66	11155.39	62
H59A	6065.43	5935.87	11252.04	66
H59B	6483.8	6139.76	11614.11	66
H60A	7086.57	5489.83	11254.81	50
H60B	7137.48	5886.81	10909.41	50
H61A	8383.61	5875.44	11008.19	58
H61B	8244.15	5479.23	11345.62	58
H62A	8738.86	6136.8	11778.7	57
H62B	9280.78	5859.63	11502.22	57
H63A	6125.6	8020.47	10662.21	48
H63B	6549.26	8431.69	10890.32	48
H64A	6880.1	7848.56	10345.26	68
H64B	7237.36	8332.04	10510.05	68
H65A	7921.69	7326.91	10181.74	53
H65B	7983.85	7921.22	10092.96	53
H66A	8721.22	8015.2	10484.63	52
H66B	8912.98	7560.04	10210.2	52
H67A	9617.51	7101.92	10546.44	52
H67B	9004.13	6708.58	10549.62	52
H68A	9721.88	7022.02	11207.37	55
H68B	9827.61	6491.18	10996.74	55

Atom	*x*	*y*	*z*	*U*(eq)
H69A	6021.45	8329.44	11439.13	64
H69B	6775.54	8443.83	11303.97	64
H70A	6769.25	8420.07	11933.96	60
H70B	6390.86	7883.17	11938.2	60
H71A	8111.68	8343.83	11845.51	52
H71B	7644.15	8305.39	12218.82	52
H72A	8603.34	7863.03	12329.09	48
H72B	7987.26	7472.77	12295.96	48
H73A	8736.83	6794.18	12109.61	45
H73B	9321.42	7197.08	12204.45	45
H74A	9779.95	6622.59	11776.77	51
H74B	9691.96	7146.51	11556.25	51
H15D	8154.05	3336.53	7051.06	85
H15E	8484.04	3338.82	7467.09	85
H15F	8533.22	3830.99	7203.81	85
H16C	7334.8	3924.91	7244.1	28
H16D	7306.33	3446.83	7524.27	28
H17C	8119.99	4150.86	8285.74	55
H17D	8626.2	3898.45	7987.36	55
H18D	7973.57	3131.21	8034.07	95
H18E	7551.16	3390.15	8370.29	95
H18F	8342.86	3283.04	8423.06	95
H29D	6201.43	5289.82	10203.02	79
H29E	6682.93	5714.93	10380.96	79
H29F	6615.12	5176.81	10585.32	79
H30C	7214.54	5326.22	9853.53	42
H30D	7645.25	5247.87	10232.7	42
H31C	7045.03	3921.08	10257.99	48
H31D	6617.36	4367.78	10447.03	48
H32D	8005.71	4166.72	10593.19	89
H32E	7396.89	4082.55	10886.91	89
H32F	7611.3	4642.96	10765.33	89
H57C	5528.36	7498.63	11181.75	55
H57D	5784.58	7426.9	10761.11	55
H58C	5787.09	6829.08	10795.34	62
H58D	5411.3	6908.85	11191.56	62
H59C	6512.36	6212.99	10784.86	66
H59D	5928.19	6011.66	11068.26	66
H60C	6842.2	5948.56	11557.15	50
H60D	6868.07	5522.5	11230.16	50
H61C	8030.67	5452.08	11203.91	58

Atom	*x*	*y*	*z*	*U*(eq)
H61D	8070.08	5811.05	11570.47	58
H62C	8736.51	6079.04	10874.9	57
H62D	9114.05	5745.24	11188.2	57
H63C	6000.39	7831.5	10616.67	48
H63D	6448.15	8285.65	10770.26	48
H64C	6677.3	7684.94	10240.65	68
H64D	7126.36	8137.29	10395.39	68
H65C	7900.5	7712.46	10066.52	53
H65D	7965.31	7126.48	10157.35	53
H66C	9077.42	7532.74	10210.91	52
H66D	8796.46	7871.09	10563.41	52
H67C	9542.88	7363.51	11001.03	52
H67D	9800.04	7092.33	10614.5	52
H68C	9154.99	6318.01	10858.53	55
H68D	9873.86	6420.03	11055.97	55
H69C	5870.96	8207.72	11443.39	64
H69D	6106.11	7717.04	11676.26	64
H70C	7093.11	8462.58	11432.87	60
H70D	6731.62	8511.98	11839.94	60
H71C	7352.26	7472.63	12264.53	52
H71D	7568.12	8045.47	12346.75	52
H72C	8649.88	7888.12	12069.63	48
H72D	8519.89	7511.67	12421.16	48
H73C	9297.5	6969.59	12139.54	45
H73D	9376.07	7258.31	11741.54	45
H74C	9595.29	6352.7	11719.01	51
H74D	8790.69	6276.53	11770.42	51

Table 4.21 Atomic Occupancy for 3-Gd^{3+}.

Atom	*Occupancy*	Atom	*Occupancy*	Atom	*Occupancy*
C15A	0.374(7)	H15A	0.374(7)	H15B	0.374(7)
H15C	0.374(7)	C16A	0.374(7)	H16A	0.374(7)
H16B	0.374(7)	N6A	0.374(7)	C17A	0.374(7)
H17A	0.374(7)	H17B	0.374(7)	C18A	0.374(7)
H18A	0.374(7)	H18B	0.374(7)	H18C	0.374(7)
C29A	0.510(8)	H29A	0.510(8)	H29B	0.510(8)
H29C	0.510(8)	C30A	0.510(8)	H30A	0.510(8)
H30B	0.510(8)	N10A	0.510(8)	C31A	0.510(8)
H31A	0.510(8)	H31B	0.510(8)	C32A	0.510(8)
H32A	0.510(8)	H32B	0.510(8)	H32C	0.510(8)

Atom	*Occupancy*	Atom	*Occupancy*	Atom	*Occupancy*
N17A	0.539(3)	C57A	0.539(3)	H57A	0.539(3)
H57B	0.539(3)	C58A	0.539(3)	H58A	0.539(3)
H58B	0.539(3)	O1A	0.539(3)	C59A	0.539(3)
H59A	0.539(3)	H59B	0.539(3)	C60A	0.539(3)
H60A	0.539(3)	H60B	0.539(3)	O2A	0.539(3)
C61A	0.539(3)	H61A	0.539(3)	H61B	0.539(3)
C62A	0.539(3)	H62A	0.539(3)	H62B	0.539(3)
C63A	0.539(3)	H63A	0.539(3)	H63B	0.539(3)
C64A	0.539(3)	H64A	0.539(3)	H64B	0.539(3)
O3A	0.539(3)	C65A	0.539(3)	H65A	0.539(3)
H65B	0.539(3)	C66A	0.539(3)	H66A	0.539(3)
H66B	0.539(3)	O4A	0.539(3)	C67A	0.539(3)
H67A	0.539(3)	H67B	0.539(3)	C68A	0.539(3)
H68A	0.539(3)	H68B	0.539(3)	C69A	0.539(3)
H69A	0.539(3)	H69B	0.539(3)	C70A	0.539(3)
H70A	0.539(3)	H70B	0.539(3)	O5A	0.539(3)
C71A	0.539(3)	H71A	0.539(3)	H71B	0.539(3)
C72A	0.539(3)	H72A	0.539(3)	H72B	0.539(3)
O6A	0.539(3)	C73A	0.539(3)	H73A	0.539(3)
H73B	0.539(3)	C74A	0.539(3)	H74A	0.539(3)
H74B	0.539(3)	N18A	0.539(3)	C15B	0.626(7)
H15D	0.626(7)	H15E	0.626(7)	H15F	0.626(7)
C16B	0.626(7)	H16C	0.626(7)	H16D	0.626(7)
N6B	0.626(7)	C17B	0.626(7)	H17C	0.626(7)
H17D	0.626(7)	C18B	0.626(7)	H18D	0.626(7)
H18E	0.626(7)	H18F	0.626(7)	C29B	0.490(8)
H29D	0.490(8)	H29E	0.490(8)	H29F	0.490(8)
C30B	0.490(8)	H30C	0.490(8)	H30D	0.490(8)
N10B	0.490(8)	C31B	0.490(8)	H31C	0.490(8)
H31D	0.490(8)	C32B	0.490(8)	H32D	0.490(8)
H32E	0.490(8)	H32F	0.490(8)	N17B	0.461(3)
C57B	0.461(3)	H57C	0.461(3)	H57D	0.461(3)
C58B	0.461(3)	H58C	0.461(3)	H58D	0.461(3)
O1B	0.461(3)	C59B	0.461(3)	H59C	0.461(3)
H59D	0.461(3)	C60B	0.461(3)	H60C	0.461(3)
H60D	0.461(3)	O2B	0.461(3)	C61B	0.461(3)
H61C	0.461(3)	H61D	0.461(3)	C62B	0.461(3)
H62C	0.461(3)	H62D	0.461(3)	C63B	0.461(3)
H63C	0.461(3)	H63D	0.461(3)	C64B	0.461(3)
H64C	0.461(3)	H64D	0.461(3)	O3B	0.461(3)
C65B	0.461(3)	H65C	0.461(3)	H65D	0.461(3)

Atom	***Occupancy***	**Atom**	***Occupancy***	**Atom**	***Occupancy***
C66B	0.461(3)	H66C	0.461(3)	H66D	0.461(3)
O4B	0.461(3)	C67B	0.461(3)	H67C	0.461(3)
H67D	0.461(3)	C68B	0.461(3)	H68C	0.461(3)
H68D	0.461(3)	C69B	0.461(3)	H69C	0.461(3)
H69D	0.461(3)	C70B	0.461(3)	H70C	0.461(3)
H70D	0.461(3)	O5B	0.461(3)	C71B	0.461(3)
H71C	0.461(3)	H71D	0.461(3)	C72B	0.461(3)
H72C	0.461(3)	H72D	0.461(3)	O6B	0.461(3)
C73B	0.461(3)	H73C	0.461(3)	H73D	0.461(3)
C74B	0.461(3)	H74C	0.461(3)	H74D	0.461(3)
N18B	0.461(3)				

4.6 Magnetic data fits

The Hamiltonian used is the sum of the electronic Zeeman (first term), utilizing an isotropic g value, and the ZFS interaction (second term), utilizing only second order (k) terms.

$$\hat{\mathrm{H}} = \beta_e \boldsymbol{B} \cdot \tilde{\boldsymbol{g}} \cdot \hat{\mathbf{S}} + \sum_{k=2,4,6..} \sum_{q=-k}^{k} B_k^q \hat{O}_k^q$$

β_e is the Bohr magneton, B_k^q are the Stevens operators for the crystal field parameters and $\hat{O}_{k_i}^q$ are the operator equivalents.

Table 4.22 Fit parameters from dc susceptibility measurements.

Complex	*g*	$3B_2^0 = D$ *(cm^{-1})*	$B_2^2 = E$ *(cm^{-1})*
1-Eu^{2+}	1.98779	-0.05553	-0.05561
2-Gd^{3+}	2.01057	0.06282	-0.00005
3-Gd^{3+}	1.97208	0.38913	0.00003
4-Tb^{4+}	1.99338	6.32910	-0.00002

4.6.1 *1-Eu^{2+}*

==========

Finished Simplex with 386 iterations

1.9877932743879176 +/- 0.00039468150838

GF 1 4 0

-0.0185088763040316 +/- 0.03718714981731

CF 1 2 0

-0.0556059204800335 +/- 0.03820289310540

CF 1 2 2

---------- Parameter Correlations ----------

If magnitude of correlation is > 0.8,

then a strong correllation is present.

1 2 -0.0

1 3 -0.0

2 3 -0.9

Residual: 0.34063576460962292

Residual reduced by: 59.033342828087221

or: 99.426287790234895%

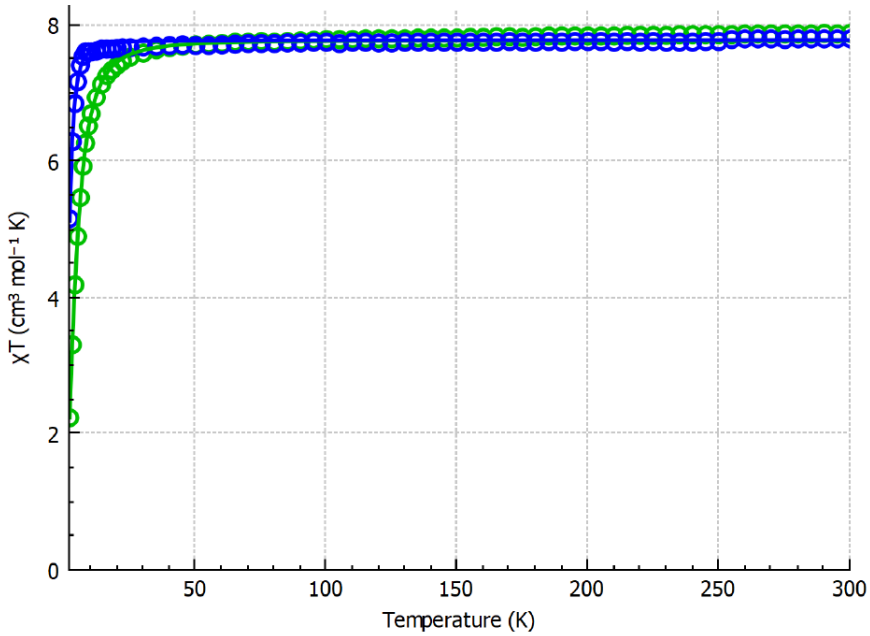

Figure 4.8 Experimental (circles) and Fit (lines) χT data for 1-Eu^{2+} at 3 T (green) and 1 T (blue).

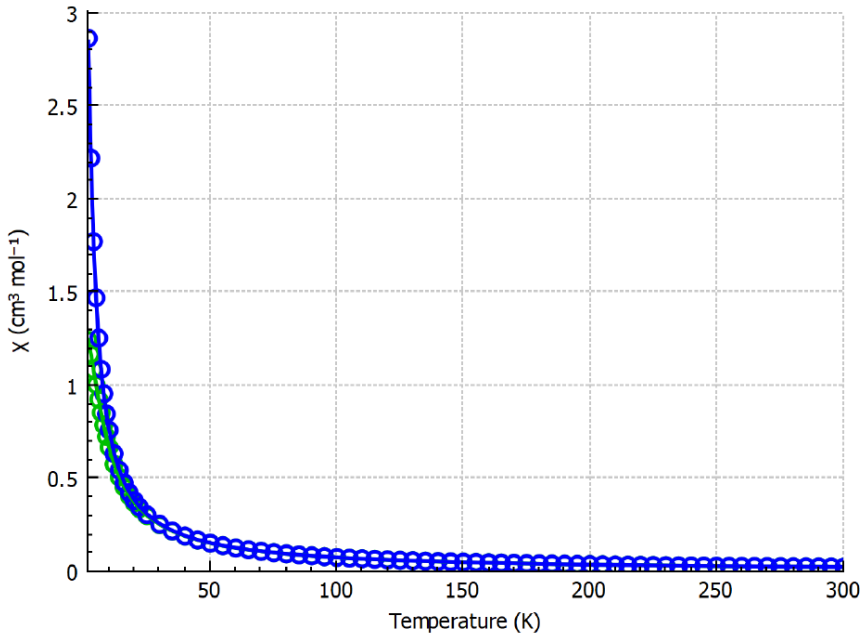

Figure 4.9 Experimental (circles) and Fit (lines) χ data for 1-Eu^{2+} at 3 T (green) and 1 T (blue).

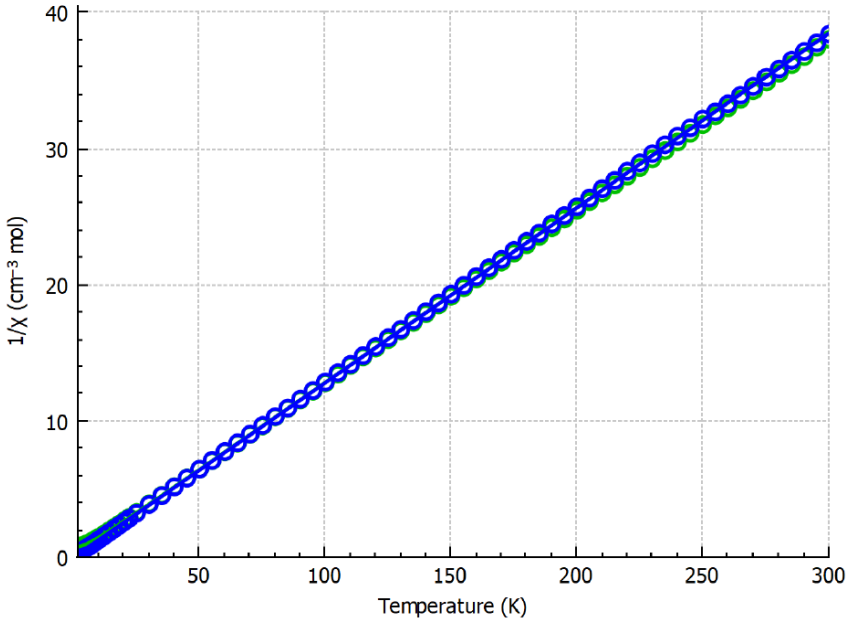

Figure 4.10 Experimental (circles) and Fit (lines) 1/χ data for 1-Eu^{2+} at 3 T (green) and 1 T (blue).

4.6.2 *2-Gd^{3+}*

==========

Finished Simplex with 399 iterations

2.0105725112715280 +/- 0.00040352587401

GF 1 4 0

-0.0209447790395919 +/- 0.00885387731238

CF 1 2 0

-0.5650373633881E-004 +/- 0.4743966528E-001

CF 1 2 2

---------- Parameter Correlations ----------

If magnitude of correlation is > 0.8,

then a strong correllation is present.

1 2 -0.1

1 3 0.0

2 3 -0.0

Residual: 0.36526901256918964

Residual reduced by: 94.934544039380242

or: 99.616715919085721%

==========

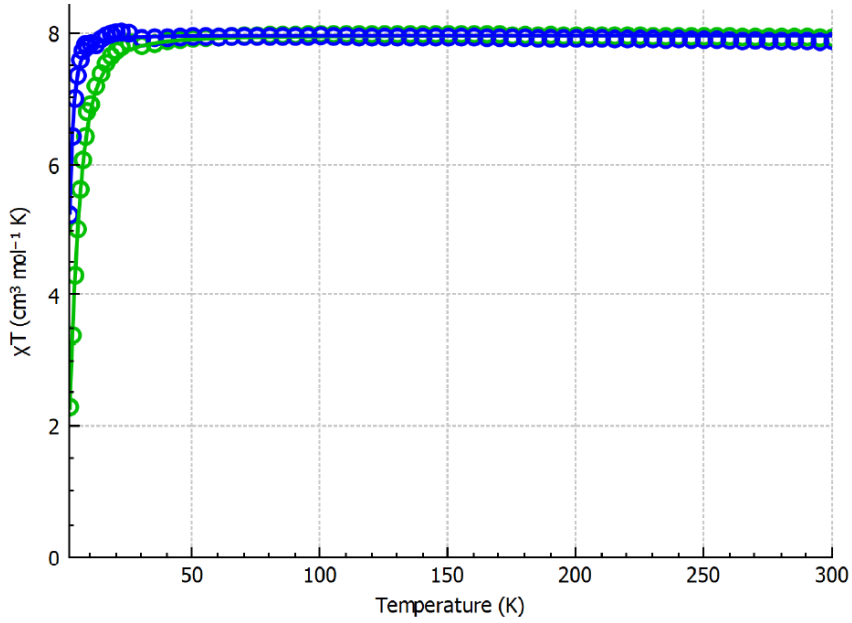

Figure 4.11 Experimental (circles) and Fit (lines) χT data for 2-Gd^{3+} at 3 T (green) and 1 T (blue).

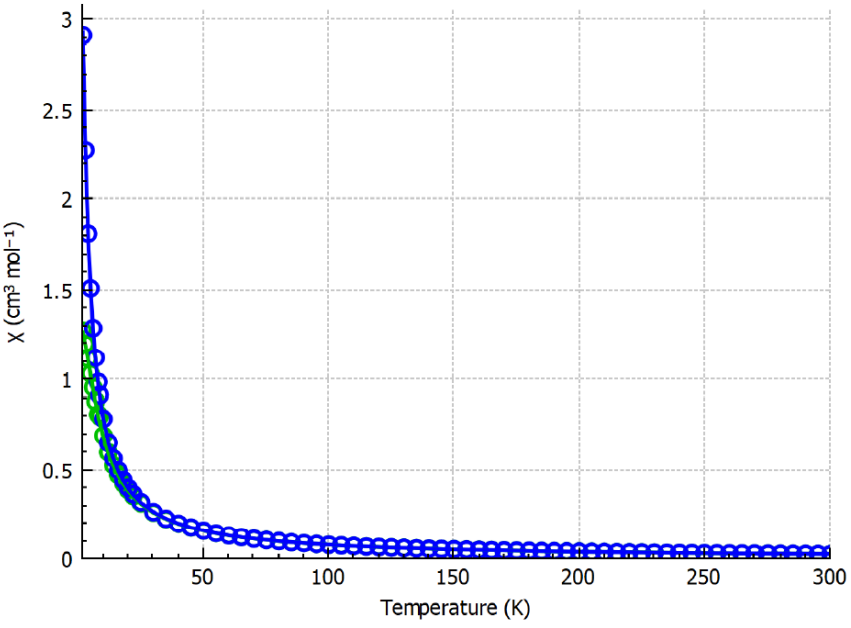

Figure 4.12 Experimental (circles) and Fit (lines) χ data for 2-Gd^{3+} at 3 T (green) and 1 T (blue).

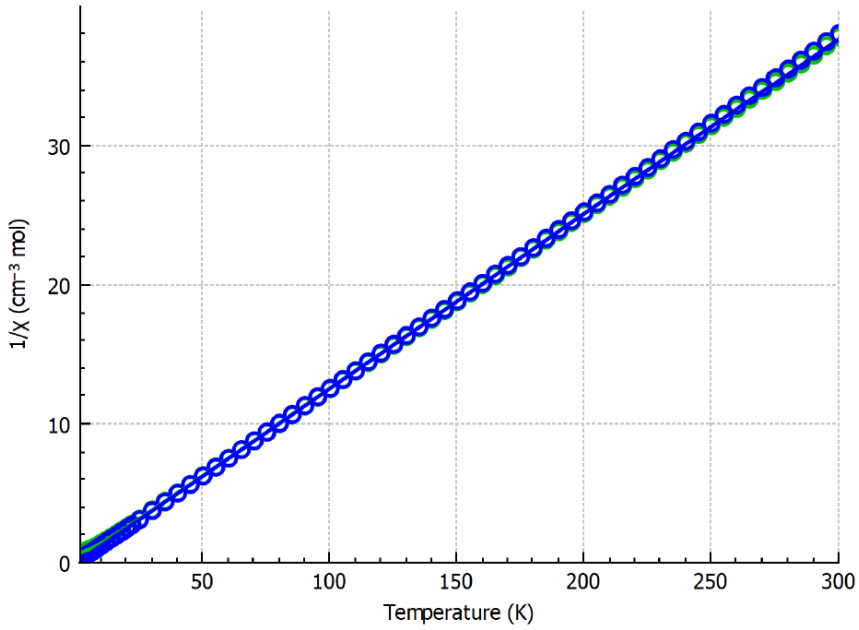

Figure 4.13 Experimental (circles) and Fit (lines) 1/χ data for 2-Gd^{3+} at 3 T (green) and 1 T (blue).

4.6.3 *3-Gd^{3+}*

==========

Finished Simplex with 402 iterations

1.9720758580132602 +/- 0.00102440899973

GF 1 4 0

0.1297080770319040 +/- 0.01405437547297

CF 1 2 0

0.3473915949406E-004 +/- 0.2373487188E-001

CF 1 2 2

---------- Parameter Correlations ----------

If magnitude of correlation is > 0.8,

then a strong correllation is present.

1 2 0.2

1 3 -0.0

2 3 -0.0

Residual: 2.1794367485082669

Residual reduced by: 38.421940173679133

or: 94.632111239268653%

==========

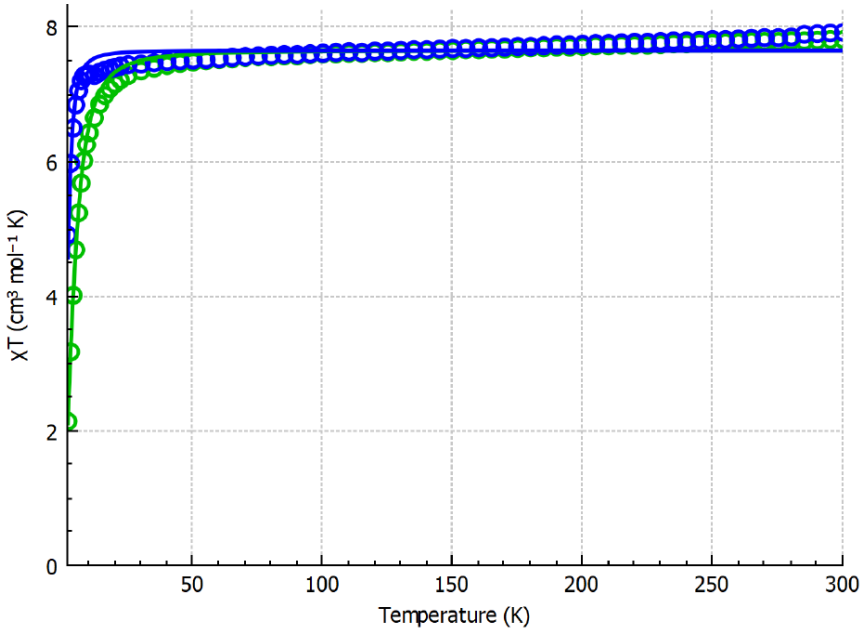

Figure 4.14 Experimental (circles) and Fit (lines) χT data for 3-Gd^{3+} at 3 T (green) and 1 T (blue).

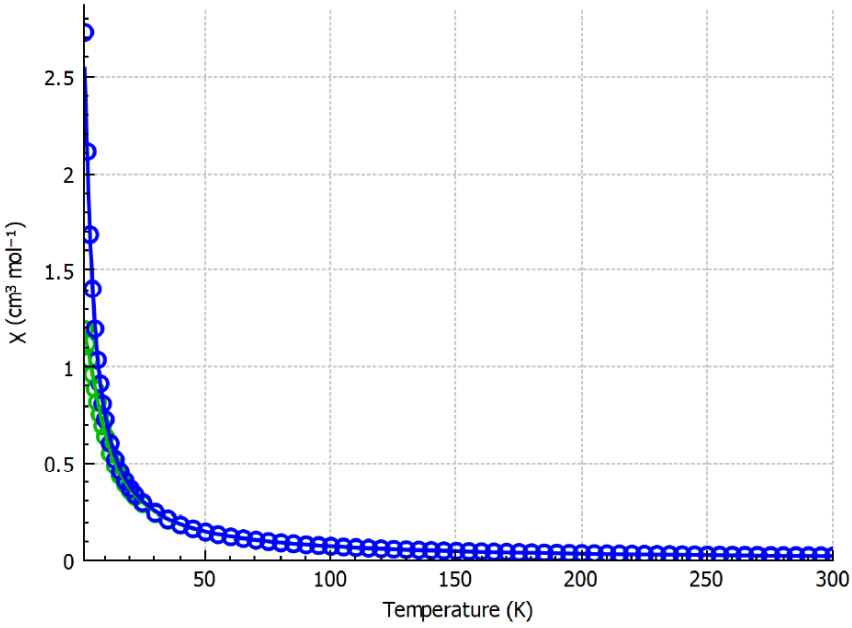

Figure 4.15 Experimental (circles) and Fit (lines) χ data for 3-Gd^{3+} at 3 T (green) and 1 T (blue).

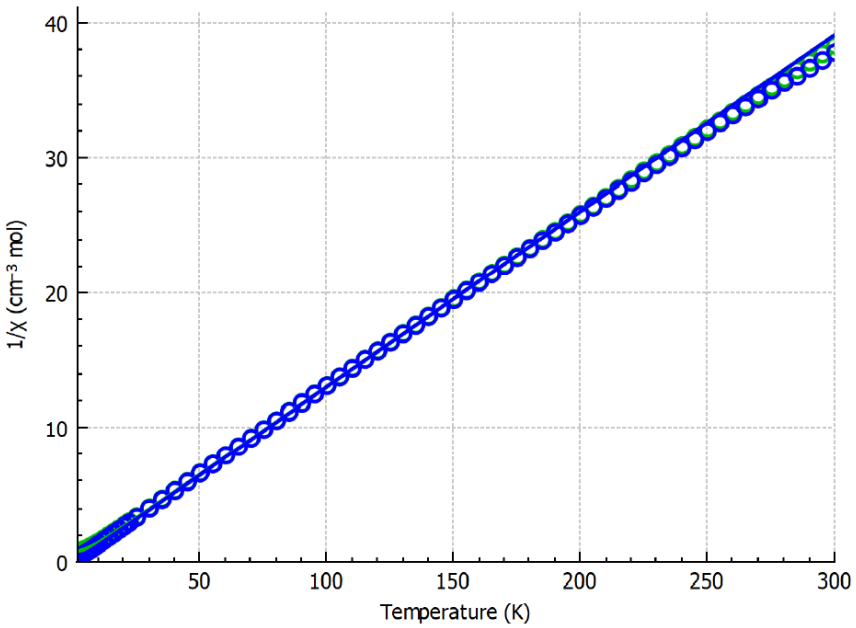

Figure 4.16 Experimental (circles) and Fit (lines) 1/χ data for 3-Gd^{3+} at 3 T (green) and 1 T (blue).

4.6.4 *4-Tb^{4+}*

==========

Finished Simplex with 405 iterations

1.9651680123841979 +/- 0.00189021971044

GF 1 4 0

2.1096877014924349 +/- 0.08840892627420

CF 1 2 0

-0.2468112921451E-004 +/- 0.6022470609E-001

CF 1 2 2

---------- Parameter Correlations ----------

If magnitude of correlation is > 0.8,

then a strong correllation is present.

1 2 0.5

1 3 -0.0

2 3 -0.0

Residual: 5.5432395913651469

Residual reduced by: 16.588412693733751

or: 74.953340491900946%

==========

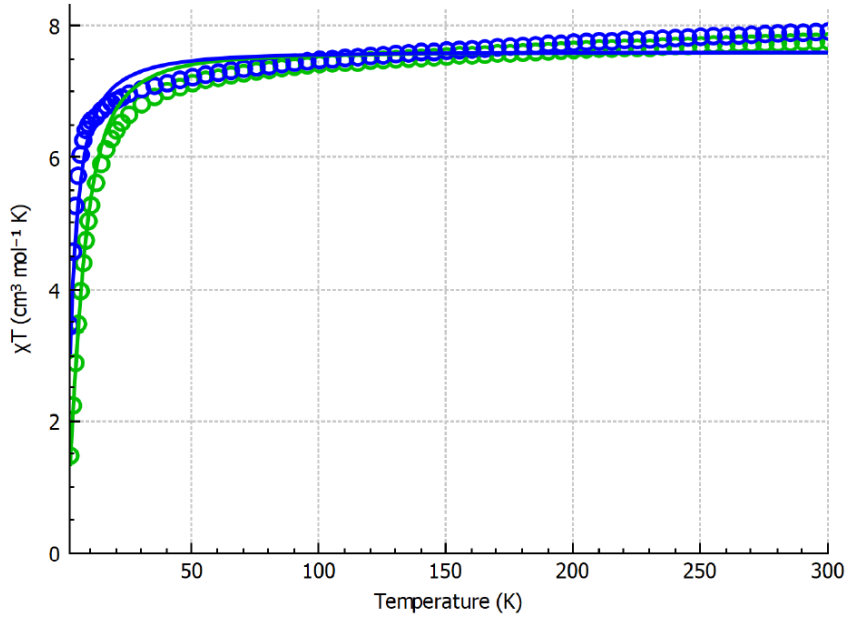

Figure 4.17 Experimental (circles) and Fit (lines) χT data for 4-Tb^{4+} at 3 T (green) and 1 T (blue).

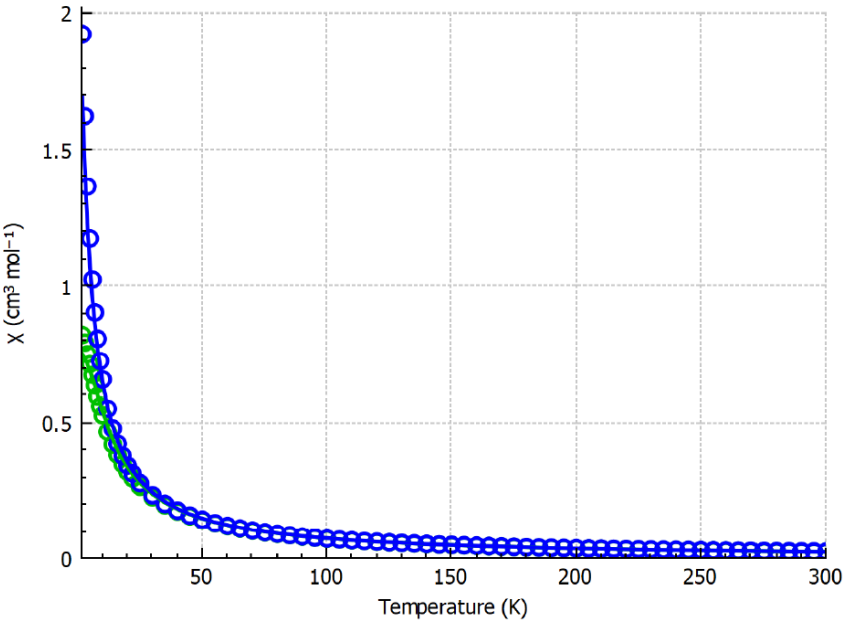

Figure 4.18 Experimental and Fit χ data for 4-Tb^{4+} at 3 T (green) and 1 T (blue).

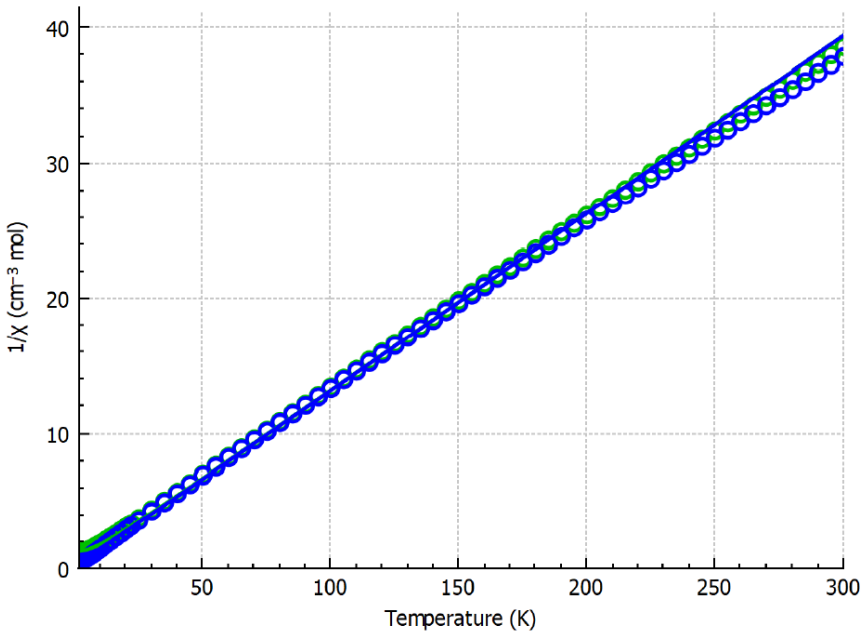

Figure 4.19 Experimental (circles) and Fit (lines) 1/χ data for 4-Tb^{4+} at 3 T (green) and 1 T (blue).

4.7 EPR Spectra and Fits

Simulations that employ the explicit strain model are noted in the caption. In these models, the exaggerated intensity of the low-field (near zero) field originates from a simulation artifact caused by spectral density expanding past zero field. In all of the following figures the features are centered at the central transition in order to facilitate a direct comparison of the observed spectral extent for each compound. All solution measurements were done in toluene. The entire series of spectra for a given compound are simulated using the same parameters. When the entire series is reasonably reproduced (in a "Chi-by-eye" fashion) the parameters are reported. The three decimal places (note the large error in the third) was settled on because these were the parameters that, to our judgment, best reproduced the entire series of spectra.

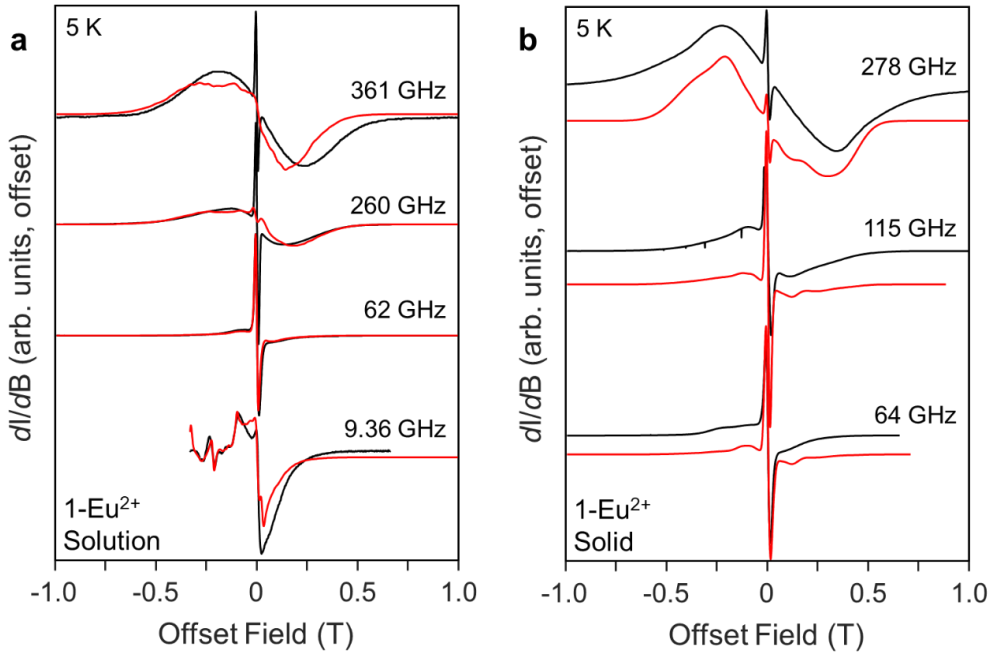

Figure 4.20 Experimental Multi-frequency EPR spectra (black traces) and corresponding simulations (red traces) of 1-Eu^{2+}. a) Solutions (explicit strain model); b) Polycrystalline powders.

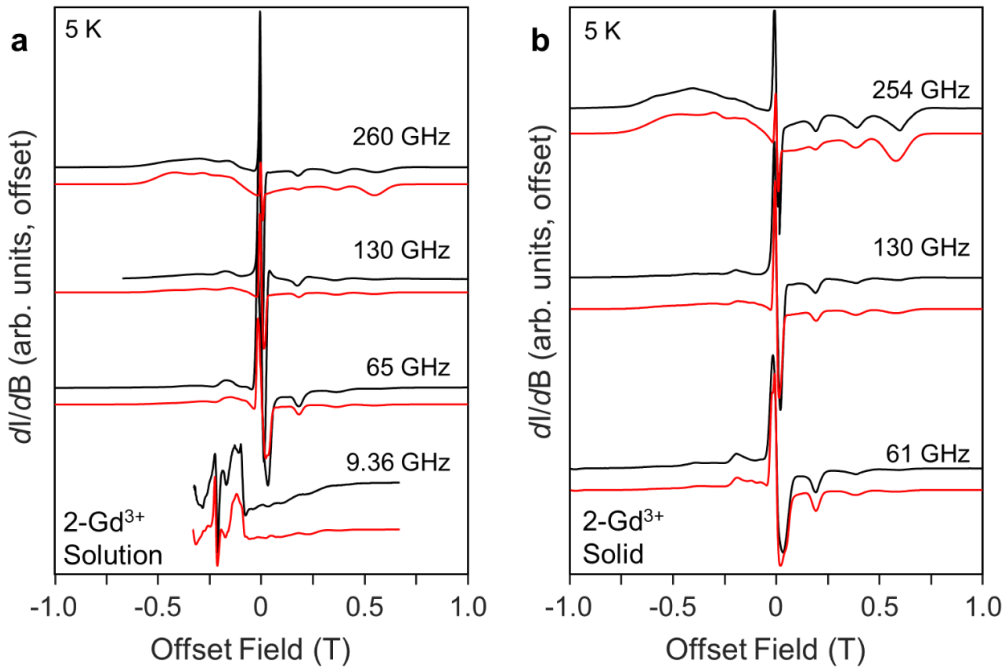

Figure 4.21 Experimental Multi-frequency EPR spectra (black traces) and corresponding simulations (red traces) of 2-Gd^{3+}. a) Solutions; b) Polycrystalline powders.

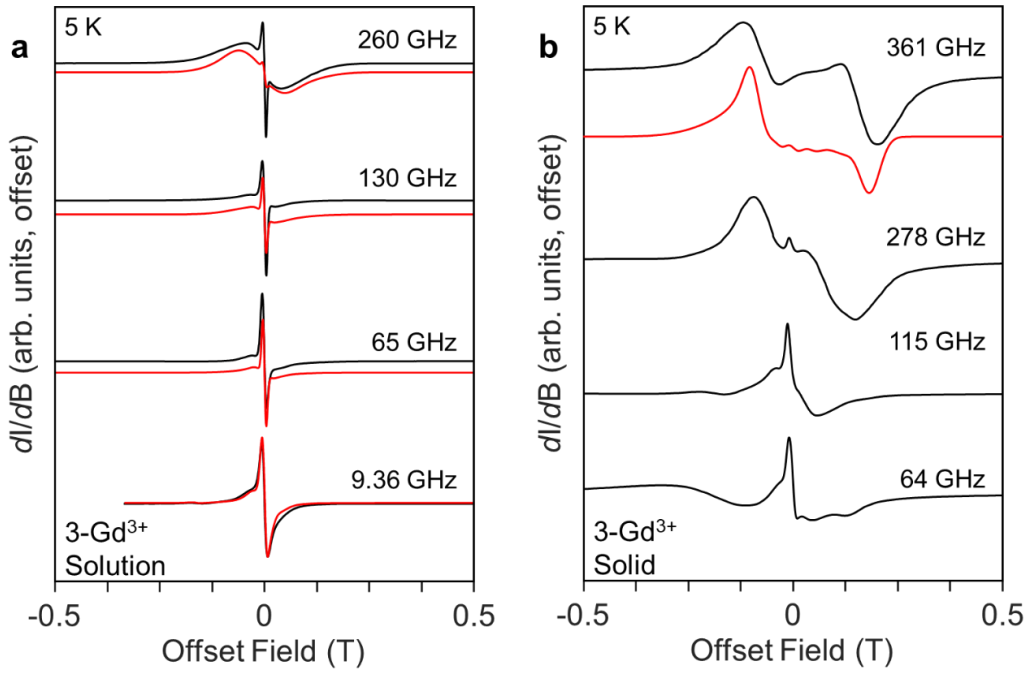

Figure 4.22 Experimental Multi-frequency EPR spectra (black traces) and corresponding simulations (red traces) of 3-Gd^{3+}. a) Solutions; b) Polycrystalline powders. The solid samples exhibit propagation artifacts at lower frequencies and the parameters are estimated from the 361 GHz spectrum only.

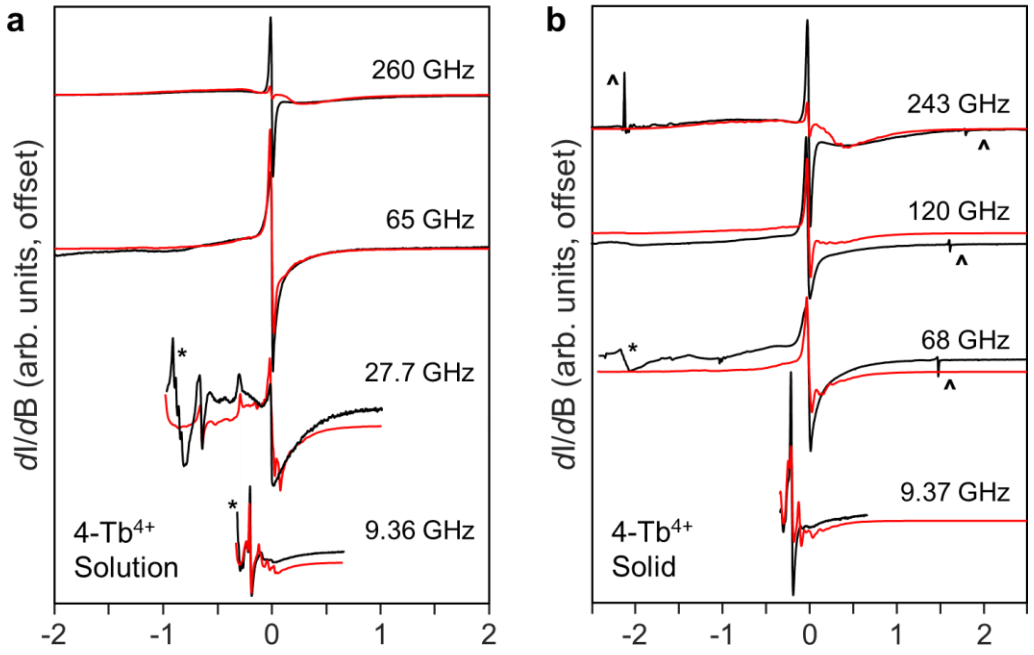

Figure 4.23 Experimental Multi-frequency EPR spectra (black traces) and corresponding simulations (red traces) of 4-Tb^{4+}. a) Solutions (explicit strain model); b) Polycrystalline powders (explicit strain model). Features marked by * indicate Tb^{3+} impurities while those marked with ^ correspond to molecular oxygen.

Table 4.23 Spin Hamiltonian parameters extracted from EPR spectroscopy of polycrystalline samples.

Sample	$\Sigma_{109.5}$ (°)	g	D (cm^{-1})	E (cm^{-1})	σ_D (cm^{-1})	σ_E (cm^{-1})	Δ_{8S} (cm^{-1})	Δ_{8S} (T)
1-Eu^{2+}	60.6	1.99(1)	0.060(5)	0.020(5)	0.030	0.025	0.87	0.93
2-Gd^{3+}	28.4	1.99(1)	0.091(3)	0.025(3)	0.018	0.025	1.26	1.35
3-Gd^{3+}	6.0	1.99(1)	0.029(3)	0.008(3)	0.008	0.02	0.40	0.43
4-Tb^{4+}	9.8	2.01(1)	0.14 (2)	0.04 (2)	0.09	0.04	1.96	2.09

Table 4.24 AILFT Results including the Condon-Shortley-Slater interelectronic repulsion parameters (F^i), SOC Constants (z), and Reductions from the Free Ion For CASSCF (normal print) and NEVPT2 (*italics*) Calculations.

	Eu^{2+}			Gd^{3+}			Tb^{4+}		
	Free	Cl_4	L_4	Free	Cl_4	L_4	Free	Cl_4	L_4
F^2 (cm^{-1})	106418.6 *78223.0*	*105402.7* *76616.9*	104450.0 *75193.4*	118237.0 *89804.0*	117029.9 *87949.1*	116721.7 *87582.7*	128783.0 *100011.5*	126352.6 *96016.1*	126260.6 *96265.5*
F^4 (cm^{-1})	66462.4 *59289.4*	65856.7 *58480.2*	65385.1 *57838.1*	74283.5 *67687.0*	73532.1 *66770.8*	73376.7 *66467.3*	81281.2 *75111.1*	79686.8 *68540.3*	79807.6 *73004.1*
F^6 (cm^{-1})	47728.7 *42090.4*	47267.0 *41582.8*	46897.0 *41033.2*	53469.7 *48099.7*	52899.8 *47528.2*	52775.0 *47358.8*	58614.9 *53442.8*	57466.0 *51619.1*	57481.6 *52234.7*
ζ (cm^{-1})	1273.0	1265.4	1259.5	1559.9	1548.3	1545.9	1872.7	1844.6	1848.1
Avg F^i Red.	- -	1.0 *1.6*	1.7 *3.0*	- -	1.0 *1.6*	1.3 *2.0*	- -	1.9 *4.0*	2.0 *3.7*
ζ Red.	-	0.6	1.1	-	0.7	0.9	-	1.5	1.3

Table 4.25 CASSCF/NEVPT2 calculated values of Δ_{8S} with and without the spin-spin coupling (SSC) contribution (cm^{-1}) for truncated models, Ln^M (see Figure 4.25).

	D_{SOC}	$D_{SOC} + D_{SSC}$
Eu^M	0.349	0.342
Gd^M	0.175	0.198
Tb^M	0.325	0.405

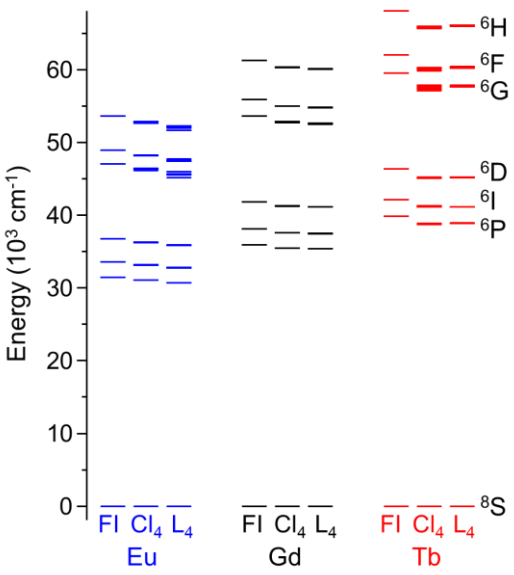

Figure 4.24 Energy levels for the ground ^{8}S state and excited sextet states (^{6}L) calculated at the CASSCF/NEVPT2 level of theory. For each metal ion the free ion (FI), hypothetical $[LnCl_4]^{-1/0/+1}$, (Cl_4) and model structure (L_4) energy levels are shown.

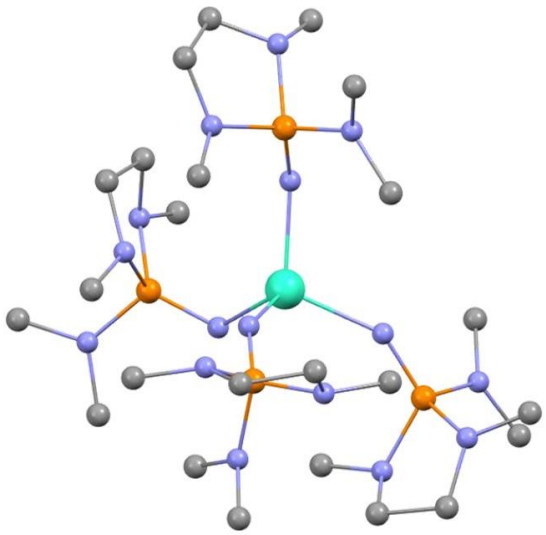

Figure 4.25 Truncated model Ln^M for quantum calculations.

4.8 Explicit Strain Model for EPR Linewidth

Strain functions in EPR simulation software use an approximation to treat the line broadening resulting from strain, whether from *g* strain (most relevant to $S = 1/2$ systems) or *D*,*E* strain (relevant to $S > 1/2$ systems). These methods are very robust when the strain is small compared to the magnitude of the parameter. When this is not the case it can become necessary to develop an explicit model. There are a few different models that have been reported, all of which follow a similar recipe. The model we have chosen requires four parameters and considers only the strain in the ZFS parameters. The four parameters are: *D*, *E*, σ_D ('sigmaD' in the script) and σ_E ('sigmaE' in the script). The first two values have their standard meaning while σ_D and σ_E represent the width of the Gaussian distribution of parameters about the central values. In the following script pairs of *D* and *E* values are generated pseudo-randomly using the Matlab function 'rand'. The values are constrained by the variable 'xsigma' that tells the program how many Gaussian widths away from the central value of *D* (or *E*) to sample. The probability of a molecule having the selected value of *D* (or *E*) is then computed by calculating the intensity of that value on its Gaussian curve. The probability of each pair is then assumed to be the product of the probability of each ZFS parameter. The program then loops over each parameter pair and sums the product of the individual spectra and associated probability for the set of ZFS parameters. The number of spectra to sum for the simulation is given by the variable 'sample'.

We include here the Matlab script used to simulate the **4-Tb^{4+}** spectra. This script makes use of the Matlab toolbox EasySpin.[229]

```
clear all,

clf,



D = -0.092; %Central value of D in cm-1

E = 0.03; %Central value of E in cm-1

sigmaD = 0.01; %Width of the Gaussian distribution of D

sigmaE = 0.01; %Width of the Gaussian distribution of E

xsigma = 3; %Number of Gaussian widths to sample

samples = 5; %Number of samples



%Standard definition of parameters for spin system and experimental

%settings in Easyspin

Sys.S=7/2;

Sys.g = 2;

Sys.lwpp = 20;

Exp.Range = [0 1]*1000;

Exp.Temperature =5;
```

```
Exp.mwFreq = 9.6;

Exp.nPoints = 4096;



%No more input is required

E_min = E - xsigma*sigmaE; %Defines minimum value for E

E_max = E + xsigma*sigmaE; %Defines maximum value for E

D_min = D - xsigma*sigmaD; %Defines minimum value for D

D_max = D + xsigma*sigmaD; %Defines maximum value for D



Sample = zeros(samples,5); %defines a place to store values

for i = 1:samples

    Sample(i,4) = D_min+rand(1)*(D_max-D_min); %Selects D

    Sample(i,5) = E_min+rand(1)*(E_max-E_min); %Selects E

    Sample(i,1) = gauss_dist(Sample(i,4), D, sigmaD); %Prob. of D

    Sample(i,2) = gauss_dist(Sample(i,5), E, sigmaE); %Prob. of E

    Sample(i,3) = Sample(i,1) * Sample(i,2); %Probability of D and E pair

end
```

```
%loop over parameter pairs and sum all spectra

Spec = zeros(1,Exp.nPoints);

for i = 1:samples

Sys.D = [Sample(i,4) Sample(i,5)]* 29.97925*1000;

[b,sim] = pepper(Sys,Exp);

Spec = Spec + sim*Sample(i,3);

end

plot(b/1000,Spec./max(Spec)) %Plot Intensity Normalized Simulated Spectrum




function f = gauss_dist(x, mu, s)

p1 = -.5 * ((x - mu)/s) .^ 2;

p2 = (s * sqrt(2*pi));

f = exp(p1) ./ p2;

end
```

Example ORCA Input Files

CASSCF/NEVPT2 + SOC Calculation

```
!DKH dkh-def2-SVP autoaux tightscf nofrozencore normalprint

%maxcore 14000
```

%basis

newgto Tb "sarc2-DKH-QZVP" end

newauxgto Tb "autoaux" end

end

%rel

picturechange 2

end

%casscf

nel 7

norb 7

nroots 1,48

mult 8,6

trafostep rimo

bweight 0.02040816, 0.97959184

actorbs forbs

rel

dosoc true

dossc true

gtensor true

end

end

*xyz 0 8

xyz coordinates

*

4.9 Model Geometries

Table 4.26 Model Geometry for Eu^{M}.

Eu	0	0	0
P	0.070417	1.065491	3.438527
P	-1.92252	-2.9423	0.25879
P	2.927465	-1.43197	-0.36778
P	-0.7464	3.4486	-0.89752
N	1.372369	2.184298	3.254638
N	0.113266	0.527498	5.093721
N	-1.22752	2.147056	3.816036
N	0	0	2.351819
N	-3.40689	-2.27769	0.832594
N	-2.49341	-4.46657	-0.38634
N	-1.20712	-3.77708	1.594536
N	-1.10823	-1.99563	-0.62117
N	4.644346	-1.35666	-0.15331
N	2.444281	-2.43534	0.923724
N	2.6709	-2.72497	-1.51056
N	2.314885	-0.04367	-0.59468
N	-1.09556	4.082627	-2.45975
N	0.819379	4.139543	-0.61355
N	-1.42753	4.575584	0.219072
N	-1.08821	1.964945	-0.76631
C	2.569107	1.765591	2.546096
C	1.594449	3.236602	4.221382
C	1.320049	-0.0662	5.606874

C	-0.69348	1.32568	5.982384
C	-1.83212	1.844379	5.0992
C	-2.15838	2.454761	2.743852
C	-3.48198	-0.83313	0.992214
C	-4.20857	-3.02471	1.777518
C	-2.66564	-4.48475	-1.8264
C	-1.70847	-5.56659	0.149647
C	-1.45162	-5.19595	1.611079
C	-0.91547	-3.11626	2.847206
C	5.409955	-2.58122	-0.11545
C	5.333524	-0.23097	-0.74744
C	2.77412	-2.13505	2.291838
C	2.110122	-3.79388	0.56697
C	1.797769	-3.75227	-0.92991
C	2.23909	-2.29502	-2.83352
C	-1.91896	3.305955	-3.35632
C	-0.9953	5.491667	-2.74374
C	1.95486	3.315817	-1.01576
C	0.856867	4.636751	0.760837
C	-0.47298	5.377026	0.938554
C	-2.81401	4.927645	0.216374
H	0.627825	3.589021	4.607604
H	2.23054	2.923109	5.079768
H	2.102842	4.091381	3.735536
H	3.338422	1.337534	3.224941
H	2.321571	1.018693	1.779047
H	3.023908	2.634397	2.037046
H	-3.89005	-2.89171	2.833534
H	-5.26693	-2.70544	1.711045
H	-4.15952	-4.09445	1.529658
H	-4.54119	-0.51584	0.970053
H	-3.02819	-0.47623	1.937207
H	-2.95849	-0.34561	0.15938
H	1.815126	-0.61679	4.79411
H	2.041383	0.678602	6.012516
H	1.09323	-0.78719	6.414173
H	-2.98068	1.713767	2.685891
H	-2.60466	3.452671	2.905115
H	-1.64637	2.452923	1.770387
H	3.094363	-1.08846	2.362258
H	1.894212	-2.25415	2.943731
H	3.595897	-2.78295	2.672348
H	1.152474	-2.08306	-2.8666

H	2.766955	-1.37203	-3.10968
H	2.468114	-3.0782	-3.58012
H	-1.74131	-3.22289	3.583994
H	-0.00951	-3.55501	3.305726
H	-0.71696	-2.04008	2.686182
H	-3.15449	-3.55341	-2.14231
H	-1.70035	-4.55091	-2.36956
H	-3.29754	-5.34208	-2.12367
H	5.665531	-2.96521	-1.12875
H	6.354822	-2.427	0.440652
H	4.83929	-3.36628	0.397784
H	5.716669	-0.45276	-1.77028
H	4.614674	0.597709	-0.81285
H	6.199355	0.069026	-0.12528
H	-3.22443	4.968532	1.244568
H	-3.01469	5.913818	-0.26269
H	-3.37613	4.157246	-0.33231
H	2.8779	3.920758	-0.9653
H	2.098123	2.398726	-0.41627
H	1.809983	2.990279	-2.05539
H	-2.96195	3.690155	-3.417
H	-1.50227	3.311699	-4.38353
H	-1.94233	2.275894	-2.97244
H	-0.27456	5.945997	-2.05016
H	-0.6286	5.659454	-3.77642
H	-1.96751	6.027189	-2.65015
H	-1.08705	0.71937	6.821813
H	-0.13048	2.179697	6.429376
H	-2.3042	2.744827	5.536958
H	-2.6223	1.06534	5.001606
H	-2.25598	-6.52402	0.063061
H	-0.73885	-5.6822	-0.38644
H	-0.57747	-5.74564	2.014552
H	-2.33227	-5.47152	2.241672
H	2.953514	-4.49287	0.790335
H	1.223173	-4.13863	1.124915
H	0.733438	-3.47138	-1.06483
H	1.983356	-4.73597	-1.40118
H	0.929952	3.814996	1.502012
H	1.719204	5.312158	0.900454
H	-0.40164	6.415057	0.528826
H	-0.73834	5.457293	2.011146

Table 4.27 Model Geometry for Gd^{M}.

Gd	0	0	0
P	0.053789	1.002421	3.391733
P	-1.95251	-2.84477	0.111786
P	2.851439	-1.42308	-0.3972
P	-0.72676	3.371117	-0.89273
N	1.343502	2.12637	3.250498
N	0.09312	0.347954	4.988019
N	-1.25722	2.030207	3.811582
N	0	0	2.238861
N	-3.43049	-2.17058	0.647563
N	-2.49082	-4.30064	-0.65017
N	-1.27932	-3.74762	1.412054
N	-1.08256	-1.84856	-0.66333
N	4.532254	-1.26426	-0.13382
N	2.342149	-2.46701	0.846119
N	2.657634	-2.66761	-1.58546
N	2.178058	-0.05207	-0.59587
N	-1.1041	3.907206	-2.46013
N	0.805111	4.105532	-0.60361
N	-1.46619	4.464043	0.199526
N	-0.99565	1.87145	-0.71353
C	2.552853	1.741777	2.540142
C	1.556779	3.134514	4.270263
C	1.309144	-0.2607	5.471121
C	-0.72775	1.081077	5.926274
C	-1.86747	1.643902	5.07379
C	-2.17874	2.41314	2.754799
C	-3.49995	-0.73386	0.871151
C	-4.31251	-2.95397	1.490223
C	-2.62354	-4.24831	-2.09479
C	-1.7838	-5.45828	-0.12367
C	-1.58394	-5.15871	1.363754
C	-1.02645	-3.12417	2.694507
C	5.368762	-2.44445	-0.08586
C	5.195705	-0.05651	-0.58548
C	2.66784	-2.22522	2.228582
C	2.034705	-3.81691	0.424532
C	1.761052	-3.71299	-1.07657
C	2.301853	-2.20154	-2.91993

C	-1.79901	3.033564	-3.38138
C	-1.02461	5.301316	-2.83056
C	1.976682	3.330044	-0.99356
C	0.813175	4.648387	0.753501
C	-0.54983	5.333709	0.897767
C	-2.86227	4.792307	0.13523
H	0.58837	3.452427	4.677437
H	2.199602	2.783056	5.105197
H	2.051081	4.016233	3.824034
H	3.31656	1.297685	3.21211
H	2.320617	1.019609	1.745966
H	3.003665	2.631843	2.067701
H	-4.06093	-2.8902	2.569131
H	-5.35356	-2.60357	1.371521
H	-4.27116	-4.00708	1.180866
H	-4.55405	-0.40914	0.824232
H	-3.08207	-0.4283	1.849407
H	-2.9459	-0.20781	0.082916
H	1.814384	-0.75749	4.631508
H	2.016171	0.468823	5.921427
H	1.085788	-1.02773	6.232994
H	-3.0168	1.695648	2.662868
H	-2.60138	3.411298	2.961408
H	-1.66326	2.444859	1.784743
H	2.907573	-1.16354	2.361047
H	1.804426	-2.44892	2.873783
H	3.536916	-2.82979	2.566908
H	1.232191	-1.92621	-2.99254
H	2.894958	-1.31237	-3.17108
H	2.515472	-2.99112	-3.66065
H	-1.8944	-3.19133	3.382702
H	-0.16932	-3.61341	3.190161
H	-0.76591	-2.06107	2.546226
H	-3.05671	-3.28142	-2.38219
H	-1.64822	-4.34349	-2.61269
H	-3.28924	-5.05569	-2.44506
H	5.751172	-2.73877	-1.08564
H	6.236298	-2.27174	0.576535
H	4.79831	-3.2928	0.312601
H	5.679644	-0.1854	-1.57714
H	4.437412	0.733421	-0.66159
H	5.978155	0.247088	0.134114
H	-3.31215	4.83335	1.144402

H	-3.05372	5.768796	-0.35954
H	-3.38892	4.010349	-0.4302
H	2.869675	3.976228	-0.95568
H	2.153825	2.431659	-0.37608
H	1.846913	2.980118	-2.02683
H	-2.84693	3.356463	-3.55031
H	-1.29067	3.012906	-4.36408
H	-1.80176	2.023902	-2.95011
H	-0.38653	5.831551	-2.11178
H	-0.57102	5.41358	-3.83342
H	-2.01951	5.793071	-2.85887
H	-1.11407	0.415749	6.719471
H	-0.17216	1.906269	6.426736
H	-2.34664	2.511186	5.561397
H	-2.64898	0.868035	4.920687
H	-2.3701	-6.38098	-0.27814
H	-0.79743	-5.59597	-0.61916
H	-0.75343	-5.75597	1.783378
H	-2.50193	-5.41791	1.939207
H	2.881367	-4.51035	0.636129
H	1.136834	-4.18816	0.945871
H	0.703596	-3.41977	-1.22939
H	1.956455	-4.67232	-1.58705
H	0.918734	3.853824	1.520437
H	1.642007	5.365859	0.872808
H	-0.5249	6.35476	0.451307
H	-0.82947	5.438308	1.962477

Table 4.28 Model Geometry for Tb^{M}.

Tb	0	0	0
P	-1.12289	3.272222	-0.75298
P	2.920777	-1.04269	-0.50047
P	-1.76925	-2.94854	0.061198
P	-0.16088	0.816388	3.44951
N	-1.12446	1.730391	-0.58026
N	-2.07716	4.191159	0.294279
N	0.267642	4.183178	-0.34776
N	-1.55973	3.709795	-2.31246
N	2.056425	0.239481	-0.67159
N	2.93845	-2.24237	-1.71393
N	2.371088	-2.14962	0.673331

N	4.538287	-0.67058	-0.23816
N	-0.95461	-1.82478	-0.62909
N	-1.03228	-3.8118	1.332668
N	-2.11147	-4.38369	-0.79219
N	-3.2955	-2.40121	0.5423
N	0	0	2.149845
N	-1.62162	1.5627	3.88941
N	-0.12029	-0.08475	4.899527
N	0.961595	2.091944	3.511803
C	-3.5115	4.282643	0.188111
C	-1.3425	5.144636	1.102526
C	0.118307	4.687357	1.017333
C	1.564714	3.620199	-0.69745
C	-1.55922	5.101112	-2.72579
C	-1.63047	2.727251	-3.38108
C	2.838481	-1.78306	-3.09246
C	2.035434	-3.33749	-1.34433
C	2.200137	-3.50241	0.166198
C	2.694178	-1.98183	2.072964
C	4.940873	0.683683	0.09778
C	5.5277	-1.70862	-0.01592
C	-0.91623	-3.23133	2.657345
C	-1.18437	-5.25103	1.210124
C	-1.32031	-5.50176	-0.29338
C	-2.27134	-4.28866	-2.2339
C	-4.18844	-3.30219	1.253841
C	-3.51722	-0.98873	0.815309
C	-2.49392	2.092306	2.856321
C	-2.26241	0.89747	5.016381
C	-1.11501	0.348049	5.865572
C	1.140203	-0.5888	5.400497
C	0.99405	2.98568	4.658532
C	2.22715	1.985621	2.800948
H	-1.69946	5.137149	2.146844
H	-1.45688	6.177453	0.711107
H	0.814463	5.522153	1.193275
H	0.315201	3.898381	1.771945
H	2.312301	-4.25568	-1.88629
H	0.981526	-3.07973	-1.57041
H	1.301756	-3.96064	0.60858
H	3.084826	-4.12922	0.406117
H	-2.08112	-5.62115	1.750431
H	-0.30598	-5.77331	1.62625

H	-0.31904	-5.53695	-0.77207
H	-1.8265	-6.45826	-0.5009
H	-2.92066	0.072914	4.672184
H	-2.88199	1.608881	5.586347
H	-0.72113	1.134163	6.5445
H	-1.44737	-0.49701	6.490983
H	-2.47521	5.334782	-3.29563
H	-0.68743	5.340643	-3.36267
H	-1.51912	5.752406	-1.84474
H	-1.61507	1.726475	-2.93412
H	-0.77842	2.822684	-4.07984
H	-2.5629	2.854622	-3.9577
H	1.54424	3.274667	-1.73936
H	1.850122	2.74948	-0.08172
H	2.336846	4.399823	-0.60487
H	-3.87591	3.487048	-0.47503
H	-3.83866	5.255987	-0.22687
H	-3.99258	4.152833	1.172786
H	5.210391	0.779232	1.166882
H	4.10239	1.355543	-0.12203
H	5.816881	0.984579	-0.50278
H	5.140635	-2.66724	-0.38285
H	5.790747	-1.81169	1.053899
H	6.453561	-1.48073	-0.57166
H	-2.86018	-5.1425	-2.60416
H	-1.3002	-4.27108	-2.76419
H	-2.80586	-3.36196	-2.47875
H	-0.73892	-2.14616	2.576947
H	-0.05453	-3.67297	3.18464
H	-1.81666	-3.40737	3.278334
H	3.164855	-2.58382	-3.77391
H	3.494662	-0.91445	-3.23621
H	1.808277	-1.48469	-3.36092
H	3.585632	-2.57147	2.36562
H	1.842892	-2.28233	2.700326
H	2.88631	-0.92094	2.276795
H	-1.92293	2.297413	1.94165
H	-2.97023	3.02631	3.197933
H	-3.2919	1.375725	2.590281
H	0.981532	-1.5044	5.992867
H	1.674495	0.143106	6.039402
H	1.787609	-0.84569	4.551994
H	-2.91846	-0.37157	0.134217

H	-3.25636	-0.7154	1.854723
H	-4.58079	-0.74989	0.650296
H	-4.02112	-4.33091	0.911036
H	-5.23591	-3.03527	1.037021
H	-4.04949	-3.26232	2.351819
H	2.535091	2.979836	2.436438
H	2.111666	1.319506	1.937283
H	3.039928	1.597588	3.446281
H	1.337891	3.984535	4.340887
H	1.677419	2.634534	5.456507
H	-0.01645	3.085587	5.073034

CHAPTER 5. INTERVALENCE CHARGE TRANSFER IN HOMOBIMETALLIC YTTERBIUM COMPLEXES

5.1 Background

Mixed valent compounds have shown many unusual electronic properties.[273] Intervalence charge transfer (IVCT) states in mixed valent compounds are of particular interest for lanthanide active phosphors by quenching and excitation loss.[274] To date, however, transition metal mixed valent compounds[275-277] have dominated the focus and lanthanide homometallic mixed valent compounds are scarce.[278, 279] Additionally, due to their broad absorption bands, low intensity, and lack of emission following absorption, there is a lack of experimental deliverables suitable for characterizing accurately IVCT features in the lanthanides. Recognition of broad IVCT features in mixed valent materials was, for many years, limited to a diffusive reflection spectrum of Ce-doped $LaPO_4$.[280] In the past few decades, however, interest in mixed valent material and their phenomenological properties has greatly increased, especially as it pertains to luminescence. Intervalence charge transfer has been notably investigated in Eu_4Cl_9 and Eu_5Cl_{11}.[281] The interpretation of which proved to be complicated given the many crystallographic locations for both the di- and trivalent europium ions. Following these studies, simplified spectra was recorded on KEu_2Cl_6 and $K_{1.6}Eu_{1.4}Cl_5$, both of which contain a singular mixed valent site.[282] Similarly, the deep violet phase $Na_5Eu_7Cl_{22}$ has been investigated and shown to exhibit a very prominent IVCT.[278]

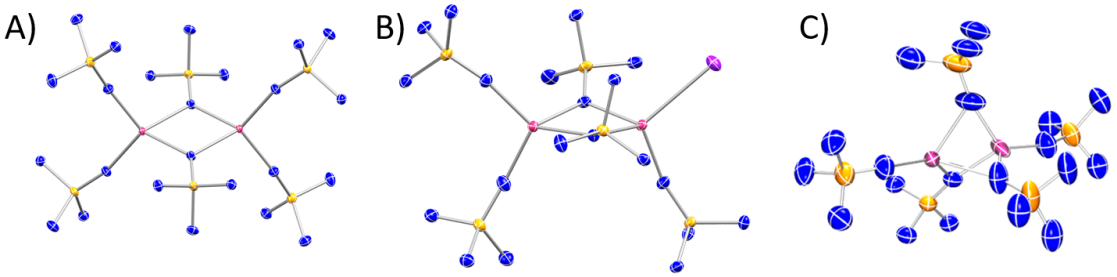

Figure 5.1 A) Molecular structure of 1-Yb^{6+} with thermal ellipsoids shown at 50% probability with hydrogen and carbon atoms omitted for clarity. B) Molecular structure of 2-Yb^{6+} with thermal ellipsoids shown at 50% probability with hydrogen and carbon atoms omitted for clarity. C) Molecular structure of 3-Yb^{5+} with thermal ellipsoids shown at 50% probability with hydrogen and carbon atoms omitted for clarity.

Mixed valent complexes are also promising candidates for realizing lanthanide-lanthanide bonding in the ground state. Computational and structure studies into bi- and tri-metallic complexes within endohedral fullerene cages have shown that single e- (half order) bonding is present.[107] Furthermore, the average oxidation state of these metal cations is determined to be +2.5, an average combination of the traditional trivalent oxidation state and a reduced divalent state. This compounds, due to their complexity, low yield, and low stability, have not served to be good analytes for more intensive spectroscopic investigation. Therefore, it is prudent to develop more computational and spectroscopically addressable mixed valent systems that have the potential to contain metal-metal bonding.

Herein, we report the synthesis and characterization of a series of molecular homobimetallic complexes of ytterbium, including one that exhibits a strikingly short interatomic ytterbium distance and, as a result, a prominent intervalence charge transfer. Additionally, an analogous series of samarium complexes are synthesized and characterized in order to highlight the critical importance of metal cation size on overall

structure, capacity for structural rearrangement in solution, and electronic communication between metal centers.

5.2 Results and Discussion

5.2.1 *Crystallographic Analysis*

The solid-state structural features of these ytterbium complexes were established by single-crystal X-ray diffraction (SCXRD). Some relevant bond lengths for the complexes described below are included in Table 5.1. The molecular structure of **1-Yb^{6+}** is shown in Figure 5.1A. It crystallized in the *P2$_1$/n* space group and notably features a diamond core with two bridging ligands. The Yb–N bond lengths average 2.20(1) Å, which is further delineated between four Yb-N bonds to terminal ligands and four Yb-N bonds to bridging ligands, which average 2.13(1) and 2.27(1) Å, respectively. The differences between terminal and bridging ligands is further exemplified through the Yb-N-P bond angles. For bridging ligands, the average bond angle is 131.08(7)°. For the terminal ligands, the bond angles are far closer to linear with an average bond angle of 164.80(9)°. The interatomic distance between ytterbium metal centers is 3.4126(6) Å, which is longer than two Shannon ionic radii for trivalent ytterbium (1.736 Å)[227] and Pyykkö covalent radius (3.40 Å).[283]

The molecular structure of **2-Yb^{6+}** is shown in Figure 5.1B. This structure crystallizes in the *P-1* space group and adopts a lower symmetry when compared to the homoleptic homobimetallic ytterbium complex described above. This is due to the inclusion of the heteroligand on one of the ytterbium metal centers. The average Yb-N

Table 5.1 Select bond lengths for 1-Yb^{6+}, 2-Yb^{6+}, and 3-Yb^{5+}. Subscript of a denotes terminal ligand and subscript of b denotes bridging ligand.

	1-Yb^{6+}	2-Yb^{6+}	3-Yb^{5+}
Yb1-N_a Distance (Å)	2.1288(14)	2.1428(15)	2.14(2)
Yb1-N_b Distance (Å)	2.2752(13)	2.2780(19)	2.28(1)
Yb2-N_a Distance (Å)	2.1288(14)	2.0648(13)	2.20(1)
Yb2-N_b Distance (Å)	2.2752(13)	2.2115(17)	2.40(1)
Yb1-Yb2 Distance (Å)	3.4126(8)	3.3680(6)	2.958(1)

bond length on the ytterbium metal center without an iodine is consistent with the bond lengths from Yb(3/3) in a similar coordination in environment, 2.131(1) Å. Likewise, bridging Yb-N bond length on the homoleptic ytterbium metal center are comparable to that of Yb(3/3), with an average of 2.282(2) Å. Inclusion of the iodide ligand on the other ytterbium metal center results in a general contraction of all Yb-N bond lengths for the bonded imidophospharanes. For the single terminal ligand on this ytterbium, the Yb-N bond length is 2.065(1) Å, a contraction of about 0.07 Å on average to analogous bonds for homoleptic ytterbiums. Similarly, the average Yb-N bond length for bridging imidophospharanes is 2.218(2) Å, which is on average 0.06 Å shorter than analogous bonds for homoleptic yetterbiums. The Yb-I bond distance is 2.9777(5) Å, which is generally in line with the expected both length based on an ionic bonding model. The effect of the heteroleptic iodine donor is further realized through a small decrease in Yb-N-P bond angles for the terminal ligands on the heteroleptic side versus the homoleptic side of the molecule, 164.7(1)° compared to 170.3(1)°, respectively. The interatomic distance

between ytterbium metal centers is 3.3680(6) Å, which, although slightly shorter than the interatomic distance for **1-Yb^{6+}**, is still much longer than two Shannon ionic radii for trivalent ytterbium (1.736 Å)[227] and comparable to Pyykkö covalent radius (3.40 Å).[283]

The molecular structure of **3-Yb^{5+}** is shown in Figure 5.1C. This compound crystallizes in the $P2_1$ space group. As apparent through the solid-state structure, upon reduction, this complex undergoes a ligand rearrangement and deviates from the diamond core present in both homobimetallic complexes presented above. This complex contains one terminal ligand on each metal center and is bridged by three ligands. The structure lacks a formal inversion center and bond metrics can be used to determine whether charge localization is present. A different is most obviously seen when comparing the Yb-N bond lengths to the three bridging ligands. The average bond length for one of the ytterbium metal centers is 2.39(1) Å, while the average analogous bond length for the other ytterbium metal center is 2.27(1) Å. This difference of around 0.12 Å is consistent with the difference in ionic radii for divalent and trivalent ytterbium in similar coordination environments (0.15 Å).[227] Similarly, the two terminal Yb-N bond lengths are 2.20(1) Å and 2.14(2) Å,

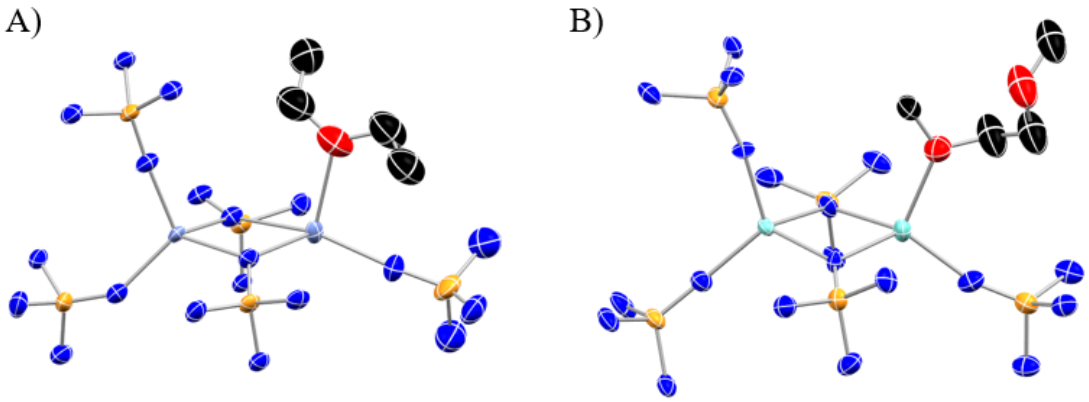

Figure 5.2 A) Molecular structure of 4-Sm^{5+}(Et_2O) with thermal ellipsoids shown at 50% probability with hydrogen and non-solvent carbon atoms omitted for clarity. B) Molecular structure of 4-Yb^{5+}(DME) with thermal ellipsoids shown at 50% probability with hydrogen and non-solvent carbon atoms omitted for clarity.

which show a difference as well, although not as drastic as for the bridging ligands. Due to the lack of bond length homology, it is fairly safe to say that, at the temperature of data collection, this structure does not exhibit the characteristics of a Robin-Day class III compound and is more probably a class II compound.[284] The analogous Yb-N-P bond angles for each ytterbium metal center does not appear to deviate substantially based on formal oxidation state of the metal and the only a small difference is seen in this bond angle for the terminal ligands, 168(1)° versus 172(1)° for the "divalent" and "trivalent" sides, respectively. The interatomic distance between ytterbium metal centers is 2.958(1) Å, which is substantially shorter than the interatomic distance for the ytterbium metal centers in both **1-Yb^{6+}** and **2-Yb^{6+}**. Given that the Shannon ionic radii for divalent ytterbium is about 0.15 Å larger than that of trivalent ytterbium, is it is reasonable to expect an elongation of the interatomic ytterbium distance upon reduction in a purely ionic model. However, instead there is a contraction of the interatomic bond distance of 0.41 Å when compared to the precursor **2-Yb^{6+}**. This certainly is accomplished in part by the ligand

rearrangement such that there are three bridging imido-phosphorane ligands as opposed to two in both **1-Yb^{6+}** and **2-Yb^{6+}**. This interatomic distance is still longer than the sum of the Shannon ionic radii for a trivalent and divalent ytterbium (1.888 Å)[227] but is well within the expected Pyykkö covalent radius (3.40 Å).[283] The molecular structure of **3-Yb^{5+}** contains the shortest interatomic ytterbium distance known in a molecular complex, which highlights its potential to exhibit a strong intervalence charge transfer and electronic communication.

Analogous samarium complexes were synthesized in a similar faction and the solid-state structural features of these complexes was established by single-crystal X-ray diffraction (SC-XRD). The molecular structures of **1-Sm^{6+}** and **2-Sm^{6+}** are shown in Figure 5.17 and Figure 5.18, respectively. The solid-state structure of these two complexes deviates very minorly from the structure for **1-Yb^{6+}** and **2-Yb^{6+}**, the primary difference between a general elongation of all bond lengths due to the increased size of samarium when compared to ytterbium.[227] The samarium interatomic distances in these compounds are 3.6475(7) Å and 3.6049(8) Å for **1-Sm^{6+}** and **2-Sm^{6+}**, respectively. The reduced samarium complex, **4-Sm^{5+}(Et$_2$O)** crystallizes from diethyl ether and deviates from **3-Yb^{5+}** by not undergoing a ligand rearrangement. The structure retains the diamond core of the

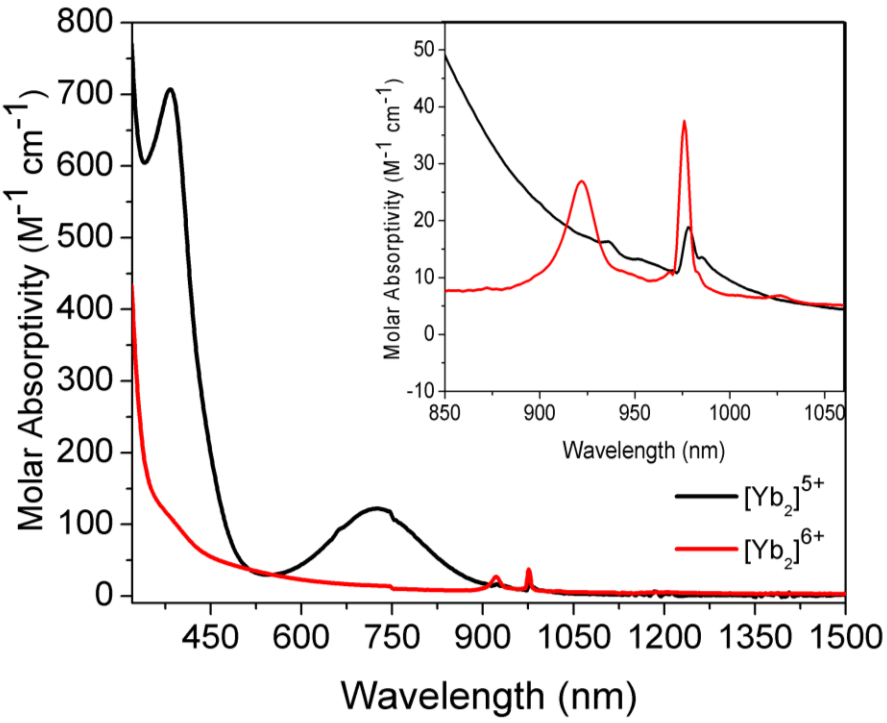

Figure 5.3 UV/vis/NIR spectra for 1-Yb^{6+} (red) and 3-Yb^{5+} (black).

trivalent counterparts and has an interatomic distance of 3.695(3) Å, which is similar to the interatomic distances of **1-Sm^{6+}** and **2-Sm^{6+}** despite the presence of the larger divalent samarium cation, indicative of a small contraction of this interatomic distance.

An "open" configuration of **3-Yb^{5+}** (**4-Yb^{5+}(DME)**, shown in Figure 5.2B), or one in which the ytterbium metal centers are bridged by only two ligands, can be obtained through the recrystallization with a Lewis basic solvent such as 1,2-dimethoxyethane (DME). In this configuration, the interatomic distance between ytterbium metal centers is much longer at 3.3786 Å and more in line with distances of its purely trivalent counterparts (3.4126(6) Å and 3.3680(6) Å for **1-Yb^{6+}** and **2-Yb^{6+}**, respectively). There is still a small contraction from the expected interatomic distance given that divalent ytterbium is approximately 0.15 Å large than trivalent ytterbium in a similar coordination environment.

5.2.2 *Uv/vis Spectroscopy*

Mixed valent compounds are distinguished by their intense colors, especially if the local environment of each of the metal cations are similar. Following this trend, the **3-Yb^{5+}** compound is vibrantly green, a striking difference when compared to the pale brown/tan hexakis dimer – a difference that will be easily seen in the UV/vis spectra, shown in Figure 5.3. Both spectra have two low molar absorptivity peaks between 900-1000 (outside the visible). These correspond to two unique *f-f* transitions – easily identified by their low molar absorptivity and general sharpness. The presence of two features here is likely due to resolution of CF splitting in this confined coordination. This is further confirmed through the comparison between the spectra for **1-Yb^{6+}** and **5-Yb^{3+}**, a monometallic complex. As shown in Figure 5.4, the four-coordinate monometallic complex shows only one transition in the early NIR region, corresponding to a singular $^2F_{7/2}$ to $^2F_{5/2}$ transition. The spectrum for **1-Yb^{6+}** lacks any absorption features in the visible while the **3-Yb^{5+}**

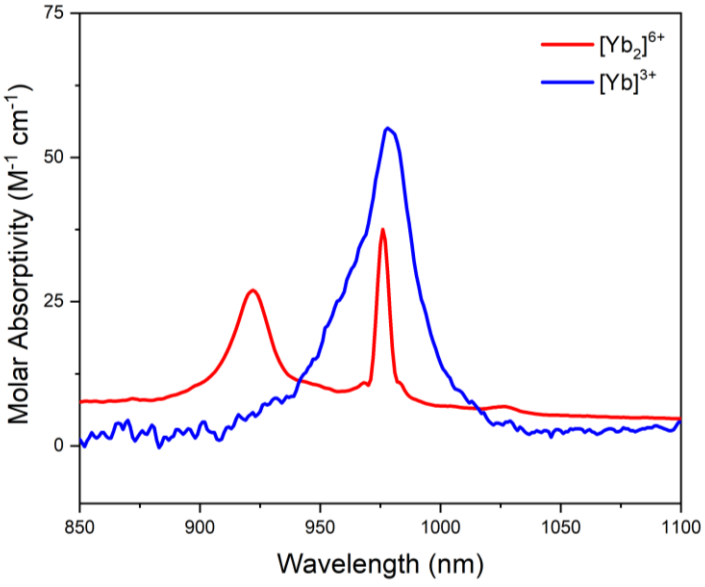

Figure 5.4 NIR spectra of 1-Yb^{6+} (red) and 5-Yb^{3+} (blue).

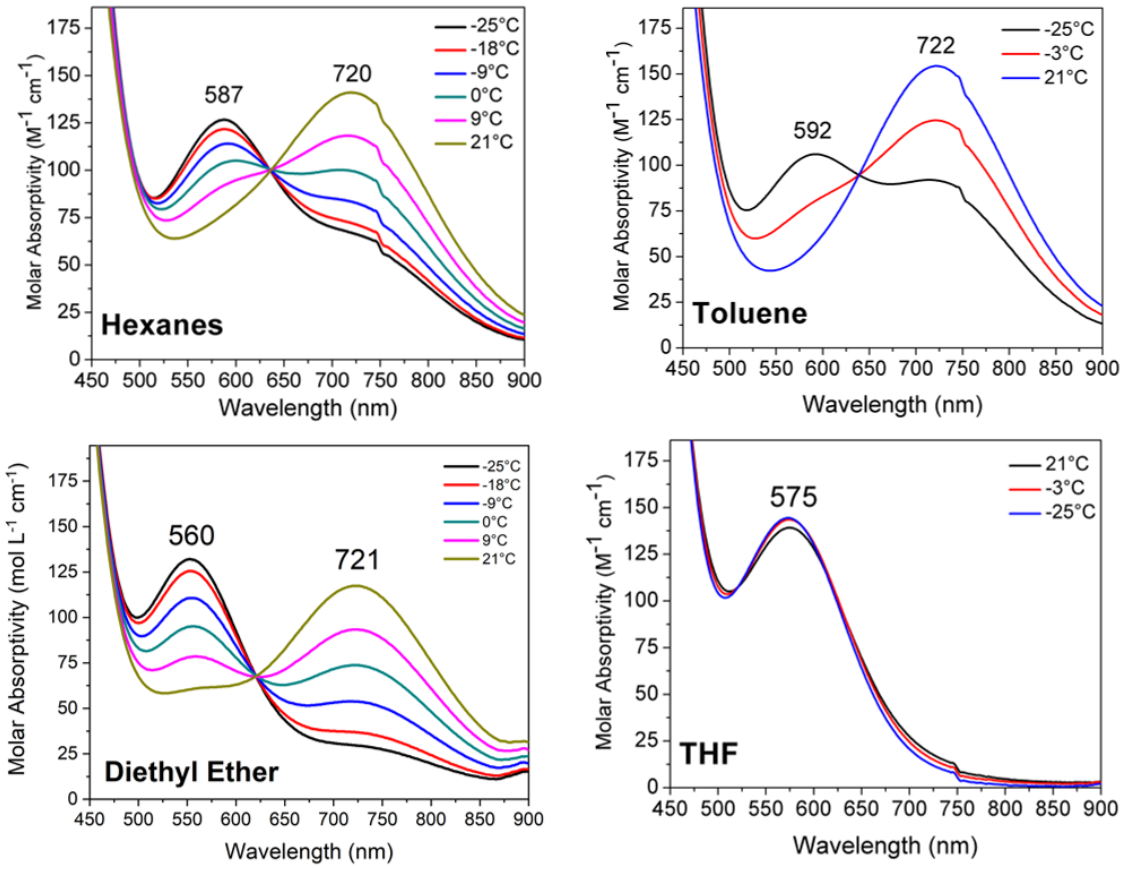

Figure 5.5 UV/vis spectra of 3-Yb^{5+} in various solvents at various temperatures.

spectrum contains two broad features, shown in Figure 5.3. The higher energy feature, with a molar absorptivity around 700 and centered around 379 nm, most likely corresponds to a f-d transition, which is not uncommon for a complex containing divalent ytterbium. More interesting is the broader, lower intensity peak centered around 720. This feature is sensitive to both temperature and solvent. At room temperature, in all solvents with the exception of THF, the 720 peak remains unchanged. However, when cooling down the solution, this feature is shifted to higher energy – the final apparent lambda max is dependent on the solvent system. Figure 5.5 shows the UV/vis spectra for **3-Yb^{5+}** in various solvents and temperatures, highlighting the sensitivity of this CT feature to both solvent dielectric and temperature. The solvent dependance along the broadness and molar

absorptivity of the lower energy feature all help to implicate this feature as an intervalence charge transfer feature (IVCT). This is a strong indicator of electronic communication between the metal centers. The temperature dependence of this feature is unique for IVCTs and implies a switch in electronic states over a temperature range near room temperature. Due to the varied equilibrium between the higher energy feature and the lower energy feature in each of the solvents, direct determination of the spectral qualities of each of these features cannot be done from the spectra as is. Spectral deconvolution was achieved through fitting of each feature in the visible region with a Gaussian function of the general form:

$$f(x) = ae^{(-\frac{x-b}{c})^2} \tag{5.3}$$

Where a represents the amplitude of the function, b represents the wavelength at which the function is centered, and c represents the factor related to the width of the function. The c parameter can be converted to the functions full width at high maximum (FWHM) by the Equation 5.2:

$$\text{FWHM} = \frac{2\sqrt{2\ \text{Ln}\ 2}\ c}{\sqrt{2}} \tag{5.2}$$

Due to the concentrations at which good data is acquired for the features in the 450 nm to 900 nm range, the highest energy feature attributable to an f-d transition is capped out and cannot be precisely modeled. However, using the downward slope of the feature

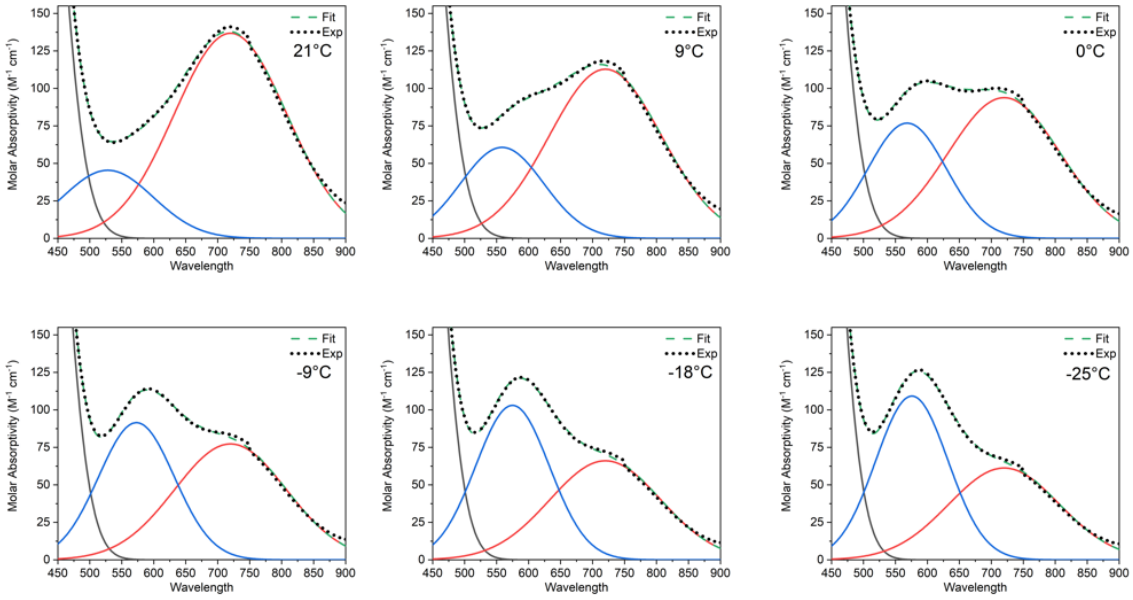

Figure 5.6 Gaussian fits of UV/vis spectra for 3-Yb^{5+} at various temperatures in hexanes.

from 450 to 900, an approximation is possible and, in practice, appears to be represent the feature well. Figure 5.6 shows the result of this fitting strategy for each temperature for **3-Yb^{5+}** in hexanes and Table 5.2 lists the fit parameters for these features at each temperature.

Figure 5.7 provides side-by-side comparison of the Gaussian fits for each solvent (except THF) in both the highest and lowest temperatures collected. When looking at the lower energy feature at the highest temperature, where this feature is most prominent, it is clear that the feature characteristics appear to be relatively invariable to solvent. The energy location is steady at 720 nm and the c parameter, which is indicative of feature broadness, remains relatively constant for all three solvents. The main factors that cause broadening of the spectral line are the distributions of vibrational and rotational energies of the molecules in the sample (and also those of their excited states). Therefore, comparison of these c parameters provides insight into the vibrational and rotational freedom of each of these

Table 5.2 Gaussian fit parameters for 3-Yb^{5+} spectra in hexanes (Figure 5.6).

	Higher Energy Feature			Lower Energy Feature		
	a	b	c	a	b	c
21°C	45.43	528.1	100.4	136.8	720.3	124.4
9°C	60.71	558.5	91.74	112.8	719.4	124.2
0°C	76.87	568.3	86.65	93.84	717.3	124.2
-9°C	91.49	572.9	83.66	77.29	718.4	123.6
-18°C	103	574.8	81.69	66.06	716.9	122.8
-25°C	109.2	575.7	79.95	61.25	716.3	122.3

structural configurations and their excited states. This analysis is supportive, qualitatively, that at higher temperatures, the closed configuration is preferred while at lower temperatures, the open configuration is prevalent. The fit absorptivity is varied as each solvent is in a different equilibrium with the higher energy feature at this temperature. When looking at the higher energy feature at the lowest temperature, where this feature is most prominent, it is clear that the feature characteristics appear to subtly vary with solvent, in both the energy of transition as well as the peak broadness. Again, the broadness of this feature is reduced when compared to the feature at higher temperatures.

5.2.2.1 TD-DFT

Typically, UV/vis spectra are interpreted using Time-Dependent Density Functional Theory (TDDFT). The effects of spin-orbit coupling are crucial to the description of lanthanide/actinide electronic structure. This description is especially important in f^1/f^{13} TDDFT methods can only treat spin-orbit coupling in closed shell systems. Therefore, it was chosen to also use Complete Active Space Self Consistent Field Theory (CASSCF) calculations to rationalize the experimental results. These calculations have the advantage of being able to consider both the ligand field and spin-orbit coupling

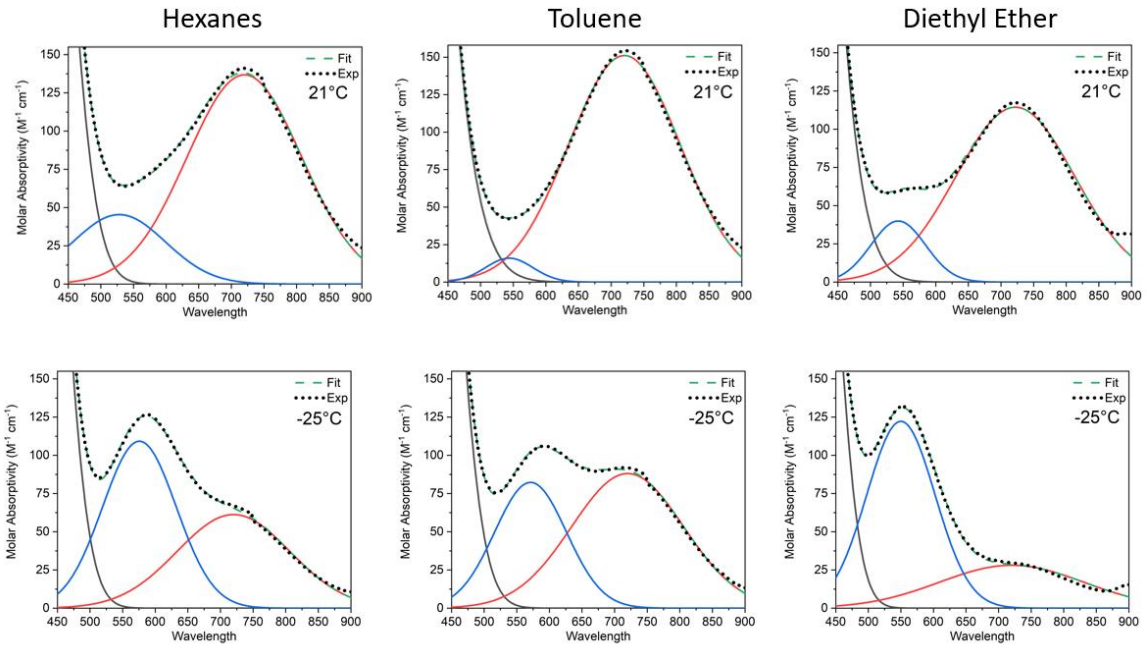

Figure 5.7 Gaussian fits of UV/vis spectra for 3-Yb^{5+} at high and low temperatures in hexanes, toluene, and diethyl ether.

effects. For simplicity, only metal-based orbitals were included in the active space. This means that transitions of the ligand-metal or metal-ligand charge transfer types, as well as ligand-based transitions, will not be observed in these calculations. However, the physics describing the electronic structure of the metal is well treated.

The calculated TDDFT absorption spectrum of **5-Yb^{3+}** is in excellent agreement with the experimentally observed spectrum. The calculation shows that the, as expected, the high energy portion of the spectrum is dominated by ligand to metal charge transfer (LMCT) and ligand to ligand excitations (Figure 5.8a). The *f-f* transitions are predicted to occur at far too low energy in the TDDFT calculation. The transition energy of an *f-f* transition of an f^{13} system can be estimated from the Landè interval rule as $^{7}/_{2}\zeta$ or 10150 cm^{-1} (for Yb(III), $\zeta \approx 2900$ cm^{-1}). Indeed, the CASSCF + SOC calculated and experimentally observed spectra both show transitions at ~10300 cm^{-1} (Figure 5.8b).

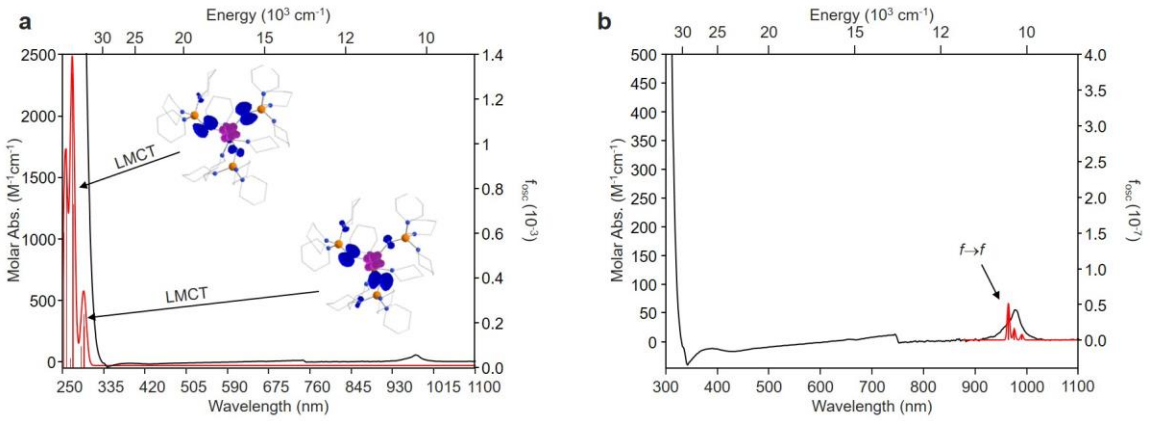

Figure 5.8 Calculated optical spectra of 5-Yb^{3+}. a) TDDFT calculated absorption spectrum of 5-Yb^{3+}. The diagrams within the figure are electron difference densities and show where electron density is lost in the ground state (blue) and gained in the excited state (purple). b) Calculated absorption spectrum of 5-Yb^{3+} at the CASSCF + SOC level of theory. In both figures the black trace is the experimental spectrum while the red trace is the calculated spectrum. The vertical lines show the calculated oscillator strength of each transition.

The experimentally observed UV/vis spectrum of **1-Yb^{6+}** is qualitatively similar to that of **5-Yb^{3+}** with the exception that the tail of the high energy feature appears to shift to slightly lower energy and that there are two predominate features in the 900-1000 nm range in **1-Yb^{6+}** compared to **5-Yb^{3+}**. The TDDFT calculated absorption spectrum of **1-Yb^{6+}** reproduces this observation and shows that as in **5-Yb^{3+}** the high energy features are dominated by LMCT transitions (Figure 5.9a). The CASSCF + SOC calculation included all 14 *f* orbitals and 26 *f* electrons associated with two Yb(III) ions. This calculation indeed reproduces the experimentally observed features around 940 and 980 nm and confirm that they arise from *f-f* type transitions (Figure 5.9b). The CASSCF + SOC calculations also predict and exceedingly weak intervalence charge transfer (IVCT) transitions ~480 nm.

The experimentally observed UV/vis spectrum of **3-Yb^{5+}** displays a marked difference from both **1-Yb^{6+}** and **5-Yb^{3+}** in that there is an intense, broad feature centered

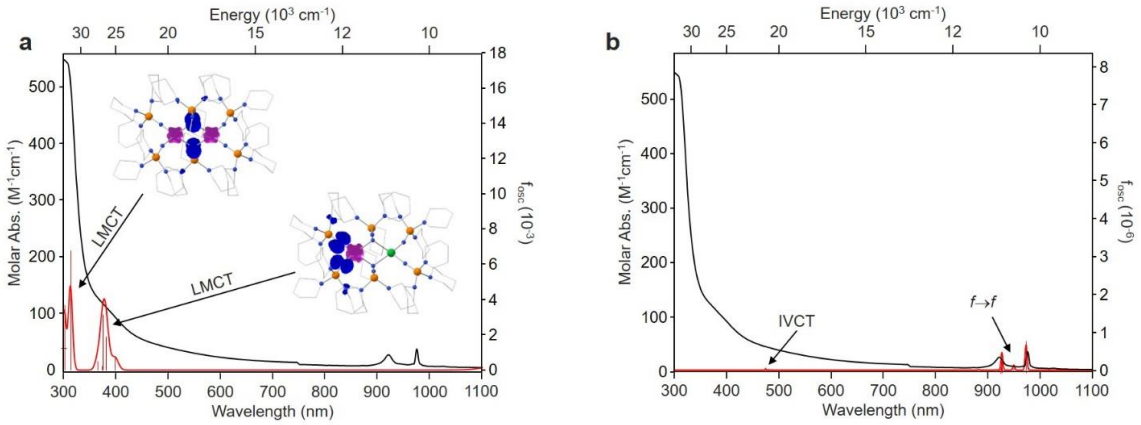

Figure 5.10 Calculated optical spectra of 3-Yb^{5+}. a) TDDFT calculated absorption spectrum of 3-Yb^{5+}. The diagrams within the figure are electron difference densities and show where electron density is lost in the ground state (blue) and gained in the excited state (purple). b) Calculated absorption spectrum of 3-Yb^{5+} at the CASSCF + SOC level of theory. In both figures the black trace is the experimental spectrum while the red trace is the calculated spectrum. The vertical lines show the calculated oscillator strength of each transition.

at ~730 nm. It is instructive to look at the ground state electronic structure to address any electron delocalization between the two Yb sites that may be present. A DFT calculation suggests that the system is best described as a localized mixed valent Yb(II)/Yb(III) bimetallic, which is in good agreement with the earlier analysis of the structural parameters. The TDDFT calculated absorption spectrum of **3-Yb^{5+}** reproduces the newly observed transition and suggests that it originates from an excitation from the *f* –orbital of the Yb(II) site to an orbital that is best described as an *s*/*p* hybrid localized on the Yb(II) site as depicted by the electron difference density map in Figure 5.10a. To explain why we do not observe a similar transition in the remaining compounds with formally Yb(III) sites, we perform a TDDFT calculation on Yb(II) and Yb(III) free ions to observe how the relative energies of the s/p/d/f orbitals change as a function of oxidation state. This simple calculation reveals a dramatic decrease in separation between *f* and s/p/d orbitals consistent with the experimental assignment. Finally, we perform a CASSCF + SOC calculation that

included all 14 *f* orbitals and 27 *f* electrons associated with one Yb(III) and one Yb(II) ion. This calculation indeed reproduces the f-f transition ~1000 nm and also predicts a pair of moderately intense groupings of IVCT transitions. Unsurprisingly, the IVCT transitions calculated at the TDDFT and CASSCF + SOC levels of theory occur at very different energies. This is likely a result of the physical limitations of DFT to properly account for the physical phenomenon required to accurately model the *f*-states and also the computational limitation of wavefunction based methods to capture all of the orbitals important for describing the transition.

5.2.3 *SQUID measurements*

Variable temperature dc magnetic susceptibility data for all compounds is shown in Figure 5.11. Magnetic data on these compounds is useful to gain insight into how this unique electronic configuration in these compounds affects the moments and to what extent

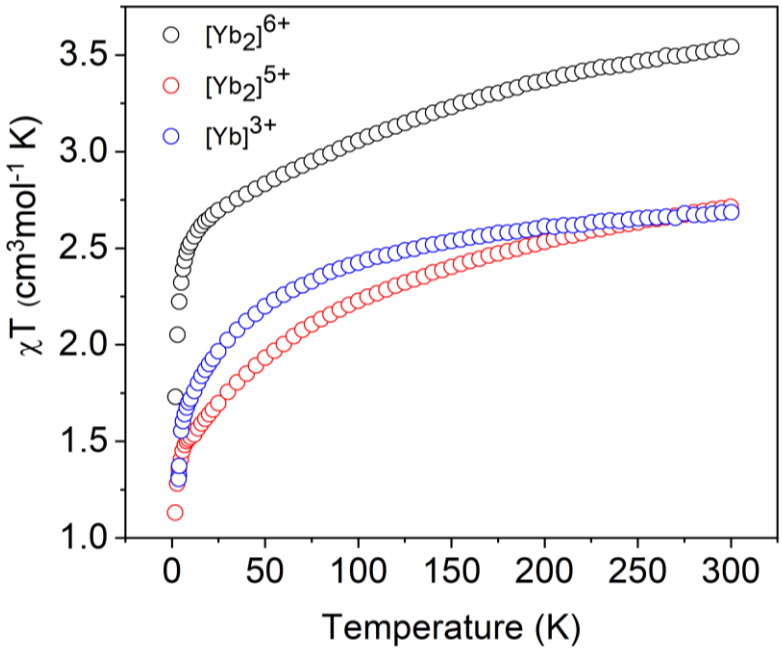

Figure 5.11 Variable-temperature molar magnetic susceptibility times temperature ($\chi_M T$) for 1-Yb^{6+} (black), 5-Yb^{3+}(blue), and 3-Yb^{5+} (red) collected under dc field of 1 T.

these ytterbium metal centers are isolated. Focusing on the room temperature magnetic moments, determining whether the moment is simply a sum of each individual metal's calculated moment or something deviant from that is telling of the nature of the interaction between the two ytterbium centers. Trivalent ytterbium is a $^2F_{7/2}$ ground state, corresponding to a calculated moment of 4.54 μ_B, in simple LS coupling schemes. Divalent ytterbium ion, on the other hand, is a $^1S_0$ ground state with a completely filled 4*f* orbital set, corresponding to an expected moment of 0 μ_B. As a result, the expected moment of the isolated metal centers could be calculated to be 4.54 μ_B per molecule, identical to that expected for **5-Yb^{3+}**. In a 1T field, **3-Yb^{5+}** has a room temperature moment to be 4.58 μ_B – only slightly higher than what would be expected for a purely isolated $4f^{14}$ – $4f^{13}$. Additionally, a field dependence is observed over 4 fields investigated – 0.5T, 1T, 2.5T, and 5T. Magnetic exchange coupling at low temperatures is common for mixed-valent

compounds who exhibit prominent intervalence charge transfers. As such, deviation at low temperatures from the quick asymptotic saturation of the magnetic moment, as seen for **5-Yb^{3+}**, is a strong indicator for magnetic exchange coupling phenomenon.

5.3 Conclusion

The synthetic approach for mixed valent lanthanide complexes with samarium and ytterbium was developed. The structural differences between **4-Sm^{5+}(Et$_2$O)** and **3-Yb^{5+}** highlights the flexibility of this class of compounds and the importance coordinating solvents and cation size plays in the phenological properties of these compounds. Recrystallization of **3-Yb^{5+}** with DME allows for the isolation of a complex, **4-Yb^{5+}(DME)**, that exhibits an "open" configuration similar to that of **4-Sm^{5+}(Et$_2$O)**.

The mixed valent ytterbium complex, **3-Yb^{5+}**, contains two prominent features in its room temperature UV/vis spectra, attributable to a f-d transition and a broad IVCT feature. The IVCT feature exhibits both temperature and solvent dependance, the latter of which is commonly characteristic of intervalence charge transfers. Gaussian fits of the UV/vis spectra in the visible region deconvolutes the equilibrium contributions of two contributing features at each temperature. Through this analysis, it is apparent higher energy feature, prominent at lower temperatures, is more sensitive to dielectric of solvent. Due to the general invariance of the spectra in THF at all temperatures, it is likely that the higher energy feature is representative of an IVCT for **3-Yb^{5+}** in an "open" configuration. This is further rationalized by the increased interatomic distance between ytterbiums in this configuration resulting in higher energy requirement for the charge transfer.

Spectral simulation through TDDFT reproduces the experimentally observed spectra well. Calculations confirm a charge localization, shown in the solid-state crystal structure, between divalent and trivalent ytterbium in **3-Yb^{5+}**. The IVCT feature is reproduced at both levels of theory (TDDFT and CASSCF + SOC), although the energies at which they occur differ due to the physical limitations of the DFT calculations.

The room temperature moment for the **3-Yb^{5+}** complex is similar to that of **5-Yb^{3+}** which is expected as divalent ytterbium is diamagnetic in its ground state. The low temperature moment is informative as it deviates from the purely trivalent monometallic complex, highlighting the low temperature magnetic coupling characteristic of complexes with IVCT behavior.

Analysis of this class of compounds is a crucial steppingstone to realizing lanthanide-lanthanide bonding in molecular complexes. Creating similar systems in which *d*-orbital population is present could be the key to developing a bonded lanthanide system. This can be achieved through interrogating an excited state of a pure 4*f*^{n} complex such as the ones in this study or by moving to new systems that can support non-traditional divalent in a similar fashion.

5.4 Experimental

5.4.1 *General Considerations*

Unless otherwise noted, all reagents were obtained from commercial suppliers. The syntheses and manipulations were conducted under argon with exclusion of oxygen and water using Schlenk techniques or in an inert atmosphere box (Vigor) under a dinitrogen (<0.1 ppm O_2/H_2O) atmosphere. The glovebox is equipped with two -35 ˚C freezers. All glassware and cannula were stored in an oven over-night (>8 h) at a temperature of ca. 160˚C. Celite and molecular sieves were dried under vacuum at a temperature >250˚C for a minimum of 24 h. C_6D_6 was stored over 3 Å molecular sieves and then vacuum-transferred from purple sodium/benzophenone prior to use. Pyridine-d_5 was degassed and stored over 3 Å molecular sieves and then transferred onto fresh 3 Å molecular sieves after 24h. Hexanes, diethyl ether and tetrahydrofuran were purged with UHP-grade argon (Airgas) and passed through columns containing Q-5 and molecular sieves in a solvent purification system (JC Meyer Solvent Systems). All solvents in the glovebox were stored in bottles over 3 Å molecular sieves. NMR spectra were obtained on a Bruker Advance III 400 MHz spectrometer at 298 K, unless otherwise noted. ^{1}H NMR chemical shifts are reported in δ, parts per million. ^{1}H NMR are references to the residual ^{1}H resonances of the deuterated solvent. Peak position is listed, followed by peak multiplicity, integration value, and proton assignment, where applicable. Multiplicity and shape are indicated by one or more of the following abbreviations: s (singlet); d (doublet); t (triplet); q (quartet); dd (doublet of doublets); td (triplet of doublets); m (multiplet); br (broad). Infrared (IR) samples were taken on a Bruker ALPHA FTIR spectrometer from 400 to 4000 cm^{-1}. IR samples were prepared as Nujol mulls sandwiched between two KBr plates. The peaks are

listed in wavenumber [cm^{-1}] and intensity by using the following abbreviations: vw (very weak); w (weak); m (medium); s (strong); vs (very strong); br (broad). UV/vis/NIR spectroscopy was performed in Teflon-valve sealed quartz cuvettes with a 1 cm path length on a Hitachi UH4150 UV–vis–NIR scanning spectrophotometer between 2500 and 240 nm. Elemental analyses were determined at Robertson Microlit Laboratories (Ledgewood, NJ). The ligand salt, [$((CH_2)_5N)_3PN$]K, was prepared according to previously reported procedures.[176]

Magnetic measurements were performed on a Quantum Design MPMS-5S magnetometer. Inside of a glovebox, a measured amount of quartz wool (10–20 mg) was loaded and packed tightly into a quartz tube. Powdered samples were loaded inside of the tube and onto the glass wool plug by tapping the compound through a glass pipet. Another pre-massed amount of quartz wool (10–20 mg) was loaded on top of the sample, and the contents were packed tightly again. The top of the tube was affixed to an Ultra Torr Swagelok adaptor while the bottom was plugged with a piece of snug tubing tightly closed with a stopper and copper wire. This was transported from the glovebox to a Schlenk line where it was sealed above and below the sample using a O_2/H_2 torch while the sample was under vacuum. The vacuum sealed tubing was taped to a straw, and the straw was loaded into the instrument. Diamagnetic corrections for the quartz wool and the complex were performed using Pascal's constants.[183]

Crystals suitable for X-ray diffraction were covered in paratone oil in a glove box and transferred to the diffractometer in a 20 mL capped vial. Crystals were mounted on a loop with paratone oil on a Bruker D8 VENTURE diffractometer. The crystals were cooled and kept at T = 100(2) K during data collections. The structures were solved with the

ShelXT structure solution program using the Intrinsic Phasing solution method and by using Olex2 as the graphical interface.[145, 146] The model was refined with version 2014/7 of XL using Least Squares minimization.[147] Structures are visualized in Ortep3 and graphics are generated with POV-ray.[185]

5.4.2 *Synthesis of 1-Yb^{6+}*

Inside a glovebox, $YbI_3(THF)_{3.5}$ (0.230 g, 0.285 mmol) was added to a 20 mL scintillation vial charged with a stir bar and 1 mL of THF. $[((CH_2)_5N)_3PN]K$ (0.302 g, 0.857 mmol, 3.0 eq.) was added to the stirring mixture as a solution in 4 mL of THF. The reaction mixture was stirred overnight. The mixture was filtered through a fine porosity frit packed with Celite. The filtrate was concentrated *in vacuo* to give a tan solid. The residue was triturated three times with 1 mL of *n*-pentane and then taken up in 8 mL of toluene and filtered through a pipet filter packed with Celite and glass filter paper. The solution was concentrated *in vacuo* and placed inside a −35 °C freezer overnight, during which time yellow crystals were obtained (0.491 g, 81%). No ^{1}H, ^{13}C, or ^{31}P NMR signals were observed. IR: ν [cm^{-1}] = 1260 (m), 1208 (w), 1172 (s), 1103 (m), 1063 (m), 1027 (m), 938 (s), 800 (m), 573 (m), 488 (w). Elemental analysis found (calculated): C, 46.13 (45.96), H, 7.77 (7.71), N, 14.39 (14.29). XRD quality crystals were grown from a saturated toluene solution at -35 °C.

5.4.3 *Synthesis of 2-Yb^{6+}*

Inside a glovebox, $YbI_3(THF)_{3.5}$ (0.300 g, 0.372 mmol) was added to a 20 mL scintillation vial charged with a stir bar and 1 mL of THF. $[((CH_2)_5N)_3PN]K$ (0.300 g, 0.857 mmol, 2.3 eq.) was dissolved separately in 5mL of THF. 2 mL of the $[(Pip)_3PN]K$

solution was added directly to the stirring slurry of $YbI_3(THF)_{3.5}$. The remaining 3 mL of $[(Pip)_3PN]K$ solution was added dropwise over 10 minutes under vigorous stirring. The reaction mixture was stirred overnight. The mixture was filtered through a fine porosity frit packed with Celite. The filtrate was concentrated *in vacuo* to give a yellow solid. The residue was triturated three times with 1 mL of *n*-pentane and then taken up in 5 mL of 1,2-dimethoxyethane and filtered through a pipet filter packed with Celite and glass filter paper. The dark yellow/orange solution was placed inside a −35 °C freezer overnight, during which time yellow crystals were obtained (0.561 g, 83%). No ^{1}H, ^{13}C, or ^{31}P NMR signals were observed. IR: ν [cm^{-1}] = 1260 (m), 1208 (w), 1172 (s), 1103 (m), 1063 (m), 1027 (m), 938 (s), 800 (m), 573 (m), 488 (w). Elemental analysis found (calculated): C, 46.13 (45.96), H, 7.77 (7.71), N, 14.39 (14.29). XRD quality crystals were grown through evaporation of 1,2-dimethoxyethane solution at room temperature.

5.4.4 *Synthesis of 3-Yb^{5+}*

Inside a glovebox, **2-Yb^{6+}** (0.400 g, 0.204 mmol) was added to a 20 mL scintillation vial charged with a glass stir bar and 4 mL of diethyl ether. Potassium graphite (KC_8) (0.028 g, 0.204 mmol, 1.0 eq.) was added to the stirring mixture as the solution in 4 mL of diethyl ether. The reaction mixture was stirred for 2h. The mixture was filtered through a fine porosity frit packed with Celite. The filtrate was concentrated *in vacuo* to give green solid. The residue was triturated three times with 1 mL of *n*-pentane and then taken up in 5 mL of n-hexanes and filtered through a pipet filter packed with Celite and glass filter paper. The solution is stored overnight inside a −35 °C freezer. The next day, purple solid has precipitated from the solution. The solution is filtered through a pipet filter packed with Celite and glass filter paper. The filtrate was concentrated *in vacuo* to give green solid. The

solid is redissolved in 1-2mL of n-pentane. The solution was concentrated *in vacuo* and placed inside a −35 °C freezer in an evaporation setup, during which time green crystals were obtained (0.220 g, 59%). No ^{1}H, ^{13}C, or ^{31}P NMR signals were observed. IR: ν [cm^{-1}] = 1264 (m), 1208 (w), 1100 (m), 1030 (m), 1024 (m), 938 (s), 800 (m), 725 (w), 573 (m), 488 (w). Elemental analysis found (calculated): C, 48.13 (49.14), H, 8.00 (8.25), N, 15.14 (15.28). XRD quality crystals were grown from an evaporating saturated n-pentane solution at -35 °C.

5.4.5 *Synthesis of 5-Yb^{3+}*

Inside a glovebox, $YbI_3(THF)_{3.5}$ (0.230 g, 0.285 mmol) was added to a 20 mL scintillation vial charged with a stir bar and 1 mL of THF. $[((CH_2)_5N)_3PN]K$ (0.394 g, 1.14 mmol, 4.0 eq.) was added to the stirring mixture as a solution in 5 mL of THF. The reaction mixture was stirred overnight. The mixture was filtered through a fine porosity frit packed with Celite. The filtrate was concentrated *in vacuo* to give a tan solid. The residue was triturated three times with 1 mL of *n*-pentane. Dry [2.2.2]Cryptand (0.107 g, 0.285 mmol, 1.0 eq.) was dissolved in 6 mL of DME. This solution is added to the tan solid to dissolve it. The mixture was filtered through a fine porosity frit packed with Celite. The solution was concentrated *in vacuo* and placed inside a −35 °C freezer overnight, during which time clear crystals were obtained (0.491 g, 81%). No ^{1}H, ^{13}C, or ^{31}P NMR signals were observed. IR: ν [cm^{-1}] = 1438 (m), 1355 (m), 1322 (m), 1258 (w), 1192 (vs), 1150 (m), 1105 (s), 1080 (w), 1043 (s), 1027 (s), 923 (s), 852 (m), 830 (m), 752 (w), 696 (s), 664 (m), 559 (s), 550 (s), 479 (s), 468 (s). Elemental analysis found (calculated): C, 46.13 (45.96), H, 7.77 (7.71), N, 14.39 (14.29). XRD quality crystals were grown from a saturated DME solution at -35 °C.

5.4.6 *Synthesis of 1-Sm^{6+}*

Inside a glovebox, $SmI_3(THF)_{3.5}$ (0.230 g, 0.293 mmol) was added to a 20 mL scintillation vial charged with a stir bar and 1 mL of THF. $[((CH_2)_5N)_3PN]K$ (0.310 g, 0.880 mmol, 3.0 eq.) was added to the stirring mixture as a solution in 4 mL of THF. The reaction mixture was stirred overnight. The mixture was filtered through a fine porosity frit packed with Celite. The filtrate was concentrated *in vacuo* to give a tan solid. The residue was triturated three times with 1 mL of *n*-pentane and then taken up in 8 mL of toluene and filtered through a pipet filter packed with Celite and glass filter paper. The solution was concentrated *in vacuo* and placed inside a −35 °C freezer overnight, during which time yellow crystals were obtained (0.470 g, 77%). No ^{1}H, ^{13}C, or ^{31}P NMR signals were observed. IR: ν [cm^{-1}] = 1258 (m), 1208 (w), 1170 (s), 1103 (m), 1061 (m), 1026 (m), 935 (s), 800 (m), 573 (m), 488 (w). Elemental analysis found (calculated): C, 51.96 (51.84), H, 8.71 (8.70), N, 16.10 (16.12). XRD quality crystals were grown from a saturated toluene solution at -35 °C.

5.4.7 *Synthesis of 2-Sm^{6+}*

Inside a glovebox, $SmI_3(THF)_{3.5}$ (0.250 g, 0.319 mmol) was added to a 20 mL scintillation vial charged with a stir bar and 1 mL of THF. $[((CH_2)_5N)_3PN]K$ (0.259 g, 0.734 mmol, 2.3 eq.) was dissolved separately in 5mL of THF. 2 mL of the $[(Pip)_3PN]K$ solution was added directly to the stirring slurry of $YbI_3(THF)_{3.5}$. The remaining 3 mL of $[(Pip)_3PN]K$ solution was added dropwise over 10 minutes under vigorous stirring. The reaction mixture was stirred overnight. The mixture was filtered through a fine porosity frit packed with Celite. The filtrate was concentrated *in vacuo* to give a yellow solid. The

residue was triturated three times with 1 mL of *n*-pentane and then taken up in 5 mL of 1,2-dimethoxyethane and filtered through a pipet filter packed with Celite and glass filter paper. The light-yellow solution was concentrated *in vacuo* and evaporated at room temperature using paratone oil, during which time clear crystals were obtained (0.426 g, 77%). No ^{1}H, ^{13}C, or ^{31}P NMR signals were observed. IR: ν [cm^{-1}] = 1260 (m), 1208 (w), 1172 (s), 1103 (m), 1063 (m), 1027 (m), 938 (s), 800 (m), 573 (m), 488 (w). Elemental analysis found (calculated): C, 47.25 (47.05), H, 7.87 (7.90), N, 14.60 (14.63). XRD quality crystals were grown through evaporation of 1,2-dimethoxyethane solution at room temperature.

5.4.8 *Synthesis of 4-Sm^{5+}(Et_2O)*

Inside a glovebox, **2-Sm^{6+}** (0.300 g, 0.157 mmol) was added to a 20 mL scintillation vial charged with a glass stir bar and 3 mL of diethyl ether. Potassium graphite (KC_8) (0.021 g, 0.157 mmol, 1.0 eq.) was added to the stirring mixture as a solution in 3 mL of THF. The reaction mixture was stirred for 2h. The mixture was filtered through a fine porosity frit packed with Celite. The filtrate was concentrated *in vacuo* to give dark green solid. The residue was triturated three times with 1 mL of *n*-pentane and then taken up in 5 mL of n-hexanes and filtered through a pipet filter packed with Celite and glass filter paper. The solution is stored overnight inside a −35 °C freezer. The next day, dark solid has precipitated from the solution. The solution is filtered through a pipet filter packed with Celite and glass filter paper. The filtrate was concentrated *in vacuo* to give green solid. The solid is redissolved in 1-2mL of diethyl ether. The solution was concentrated *in vacuo* and placed inside a −35 °C freezer in an evaporation setup, during which time green crystals were obtained (0.154 g, 55%). No ^{1}H, ^{13}C, or ^{31}P NMR signals were observed. IR: ν [cm^{-}

^{1}] = 1333(w), 1260 (m), 1205 (w), 1168 (s), 1113 (s), 1057 (s), 1030(m), 1024(m), 938 (s), 856(w), 830 (m), 800 (m), 718 (w), 575 (m), 507 (w), 478 (w). Elemental analysis found (calculated): C, 50.01 (50.96), H, 8.56 (8.66), N, 14.96 (15.05). XRD quality crystals were grown from an evaporating saturated diethyl ether solution at -35 °C.

5.5 Crystallographic Information

5.5.1 *1-Yb*$^{6+}$

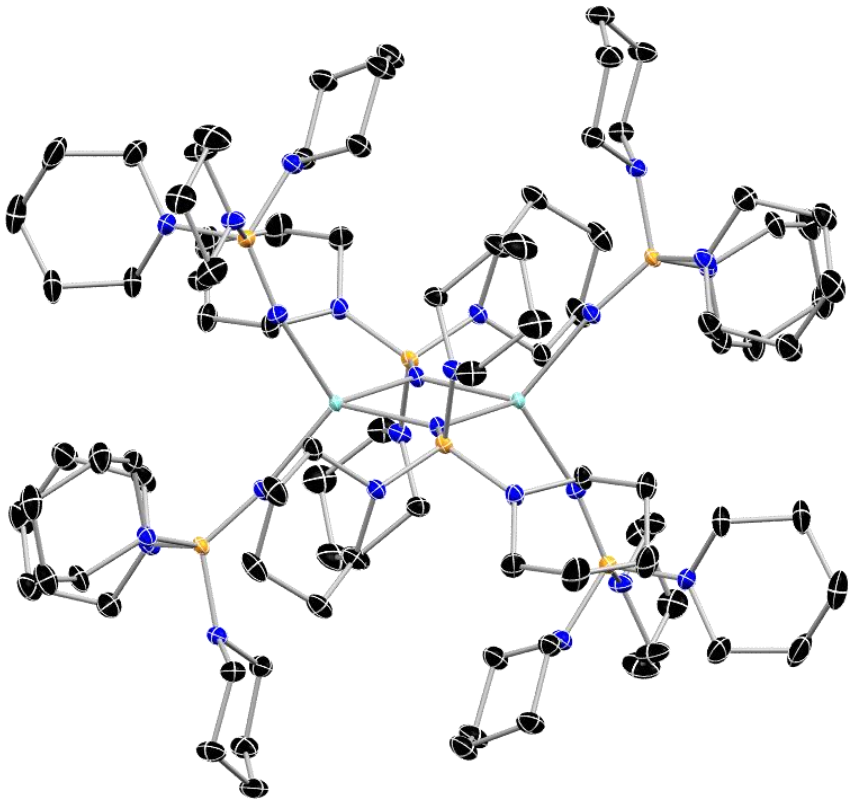

Figure 5.12 Molecular structure of 1-Yb^{6+} with thermal ellipsoids shown at 50% probability with hydrogen atoms omitted for clarity. Color code: C, black; N, blue; O, red; P, orange; Yb, blue.

Table 5.3 Crystal data and structure refinement for 1-Yb^{6+}.

Identification code	1-Yb^{6+}
Empirical formula	$C_{90}H_{180}N_{24}P_6Yb_2$
Formula weight	2130.47
Temperature/K	102(1)
Crystal system	monoclinic
Space group	$P2_1/n$
a/Å	15.74771(17)
b/Å	16.22747(17)
c/Å	22.5600(3)

α/°	90
β/°	90.1873(11)
γ/°	90
Volume/Å^3	5765.08(11)
Z	2
ρ_{calc}g/cm^3	1.227
μ/mm^{-1}	1.744
F(000)	2236.0
Crystal size/mm^3	0.398 × 0.315 × 0.179
Radiation	MoKα (λ = 0.71073)
2Θ range for data collection/°	3.604 to 80.768
Index ranges	-28 ≤ h ≤ 28, -25 ≤ k ≤ 29, -40 ≤ l ≤ 40
Reflections collected	96220
Independent reflections	34895 [R_{int} = 0.0735, R_{sigma} = 0.0681]
Data/restraints/parameters	34895/0/550
Goodness-of-fit on F^2	1.009
Final R indexes [I>=2σ (I)]	R_1 = 0.0409, wR_2 = 0.1073
Final R indexes [all data]	R_1 = 0.0516, wR_2 = 0.1121
Largest diff. peak/hole / e Å^{-3}	2.69/-0.85

Table 5.4 Fractional Atomic Coordinates (×10^4) and Equivalent Isotropic Displacement Parameters (Å^2×10^3) for 1-Yb^{6+}. U_{eq} is defined as 1/3 of the trace of the orthogonalised U_{IJ} tensor.

Atom	*x*	*y*	*z*	U(eq)
Yb1	5523.2(2)	5544.9(2)	5535.1(2)	9.05(2)
P8	6364.6(2)	3662.6(2)	5006.9(2)	11.15(6)
P28	5411.8(3)	5517.2(2)	7147.9(2)	12.30(6)
P48	7052.6(3)	7088.3(2)	5085.2(2)	13.59(6)
N2	6493.6(9)	3111.5(8)	4387.2(6)	14.2(2)
N9	5709.7(8)	4381.3(7)	4990.8(6)	11.97(18)
N10	7368.1(8)	3924.7(8)	5159.0(6)	15.3(2)
N16	6140.0(9)	2976.9(8)	5525.8(6)	15.2(2)
N22	6202.4(9)	5037.1(9)	7514.7(6)	18.0(2)
N29	5447.9(9)	5398.9(8)	6474.2(6)	15.4(2)
N30	4578.4(9)	5185.2(8)	7553.0(6)	14.8(2)
N36	5421.1(9)	6526.5(8)	7352.9(6)	15.4(2)
N42	7933.1(9)	7094.8(10)	5509.9(7)	19.8(2)
N49	6336.5(9)	6554.9(8)	5336.1(6)	15.5(2)
N50	6765.0(9)	8083.3(8)	4977.9(6)	17.7(2)
N56	7479.0(9)	6876.1(9)	4412.7(6)	16.6(2)

Atom	*x*	*y*	*z*	U(eq)
C3	5904.1(11)	2430.0(10)	4263.3(7)	19.0(3)
C4	6330.8(15)	1808.1(11)	3857.7(8)	26.2(4)
C5	6632.9(15)	2216.3(11)	3285.8(8)	26.0(4)
C6	7184.2(12)	2963.4(11)	3420.4(8)	21.8(3)
C7	6707.3(11)	3553.8(10)	3836.2(7)	17.2(3)
C11	8120.7(11)	3784.8(12)	4789.2(8)	22.7(3)
C12	8904.5(13)	3600.0(16)	5154.8(12)	34.8(5)
C13	9055.2(12)	4274.3(15)	5613.7(11)	30.2(4)
C14	8266.3(12)	4355.5(11)	6001.8(9)	22.5(3)
C15	7481.2(11)	4535.4(10)	5630.7(8)	16.9(2)
C17	5307.9(10)	2890.2(10)	5808.3(7)	17.3(3)
C18	5401.7(13)	2875.3(13)	6476.5(8)	25.5(3)
C19	6012.2(16)	2196.0(17)	6670.5(10)	37.0(5)
C20	6861.3(14)	2281.6(15)	6345.5(10)	33.8(5)
C21	6728.2(12)	2312.9(11)	5679.5(9)	23.0(3)
C23	6175.4(13)	4715.2(12)	8120.5(8)	23.7(3)
C24	6918.5(13)	5018.0(13)	8498.4(8)	25.2(3)
C25	7760.1(14)	4858.7(16)	8192.8(10)	32.4(4)
C26	7750.2(13)	5202.5(16)	7563.3(10)	32.4(4)
C27	6999.0(12)	4866.4(13)	7214.9(8)	25.4(3)
C31	3797.2(11)	5669.1(10)	7600.9(8)	19.3(3)
C32	3346.5(14)	5458.6(11)	8182.3(9)	24.1(3)
C33	3132.6(14)	4538.5(12)	8193.0(9)	26.2(4)
C34	3926.6(13)	4018.4(11)	8082.2(8)	23.9(3)
C35	4394.6(12)	4302.4(10)	7522.6(8)	19.5(3)
C37	5531.4(13)	6716.5(10)	7985.6(7)	21.1(3)
C38	5308.6(15)	7609.7(12)	8116.7(9)	27.6(4)
C39	5856.1(16)	8178.8(12)	7750.4(10)	30.1(4)
C40	5774.1(15)	7959.4(11)	7096.3(9)	28.2(4)
C41	5974.6(12)	7052.8(10)	6992.6(8)	20.6(3)
C43	8780.1(13)	7341.8(15)	5311.0(11)	31.1(4)
C44	9226.8(14)	7867.8(16)	5774.6(12)	37.8(5)
C45	9243.4(14)	7449.3(14)	6375.5(12)	35.2(5)
C46	8347.9(15)	7188.9(13)	6556.8(10)	29.8(4)
C47	7951.0(12)	6658.6(11)	6075.2(8)	22.3(3)
C51	7392.1(14)	8678.9(11)	4757.9(10)	29.0(4)
C52	6950(2)	9459.2(12)	4544.6(12)	37.6(6)
C53	6418.7(15)	9846.1(11)	5033.4(10)	29.2(4)
C54	5802.3(13)	9204.6(12)	5278.0(11)	28.2(4)
C55	6274.9(12)	8434.0(10)	5468.9(8)	20.7(3)
C57	7895.5(11)	6069.5(10)	4383.8(8)	19.0(3)

Atom	*x*	*y*	*z*	U(eq)
C58	8492.9(12)	6034.0(12)	3852.6(8)	23.6(3)
C59	8005.1(14)	6203.5(13)	3281.2(8)	26.8(4)
C60	7506.5(14)	7011.4(13)	3330.3(8)	27.4(4)
C61	6951.9(12)	7010.6(12)	3886.6(8)	22.1(3)

Table 5.5 Anisotropic Displacement Parameters ($Å^2×10^3$) for 1-Yb^{6+}. The Anisotropic displacement factor exponent takes the form: $-2\pi^2[h^2a^{*2}U_{11}+2hka^*b^*U_{12}+\ldots]$.

Atom	U_{11}	U_{22}	U_{33}	U_{23}	U_{13}	U_{12}
Yb1	10.54(3)	9.40(3)	7.22(3)	-0.97(1)	-1.24(2)	-0.09(1)
P8	11.84(14)	11.45(13)	10.16(14)	-1.08(10)	-0.64(11)	2.66(10)
P28	14.81(15)	13.76(15)	8.32(14)	-0.42(10)	-0.64(12)	-0.28(11)
P48	12.87(15)	14.96(15)	12.95(15)	-0.97(11)	0.89(12)	-2.06(11)
N2	16.6(5)	14.2(5)	11.9(5)	-2.2(4)	0.7(4)	1.4(4)
N9	12.5(5)	12.2(4)	11.1(5)	-1.6(3)	-2.0(4)	3.2(3)
N10	13.0(5)	18.6(5)	14.5(5)	-3.1(4)	-1.2(4)	1.9(4)
N16	16.0(5)	15.4(5)	14.1(5)	2.6(4)	1.3(4)	5.2(4)
N22	17.9(6)	24.2(6)	11.9(5)	2.3(4)	-1.4(4)	4.2(4)
N29	19.1(6)	17.8(5)	9.3(5)	-0.3(4)	-1.2(4)	-1.3(4)
N30	16.6(5)	14.9(5)	12.8(5)	0.3(4)	2.2(4)	-0.2(4)
N36	19.8(5)	13.7(5)	12.6(5)	-1.7(4)	-0.1(4)	-0.9(4)
N42	13.4(5)	29.1(7)	17.1(6)	-1.9(5)	-1.9(4)	-4.3(5)
N49	15.5(5)	15.8(5)	15.3(5)	1.2(4)	0.1(4)	-2.7(4)
N50	20.6(6)	14.0(5)	18.6(6)	0.4(4)	5.6(5)	-1.7(4)
N56	17.3(5)	19.6(5)	13.0(5)	0.2(4)	0.9(4)	0.9(4)
C3	23.6(7)	18.1(6)	15.2(6)	-4.1(5)	-0.4(5)	-2.2(5)
C4	43.0(11)	16.3(7)	19.3(7)	-5.4(5)	0.3(7)	2.6(6)
C5	40.2(11)	22.9(8)	15.0(7)	-6.2(5)	0.4(7)	8.3(7)
C6	23.7(8)	27.3(8)	14.5(6)	-2.4(5)	3.4(6)	9.2(6)
C7	20.7(7)	18.2(6)	12.8(6)	-0.3(4)	2.6(5)	4.2(5)
C11	14.8(6)	29.6(8)	23.9(8)	-6.2(6)	2.6(6)	3.1(5)
C12	15.1(7)	46.3(12)	43.1(13)	-13.0(10)	-3.2(8)	10.1(7)
C13	16.2(7)	39.1(10)	35.2(11)	-3.9(8)	-10.4(7)	2.0(7)
C14	19.4(7)	25.1(8)	22.9(8)	0.1(6)	-9.3(6)	0.5(5)
C15	15.8(6)	19.9(6)	15.1(6)	-1.6(5)	-4.1(5)	2.5(4)
C17	17.3(6)	19.4(6)	15.1(6)	5.1(5)	0.5(5)	1.4(5)
C18	28.3(9)	33.0(9)	15.1(7)	4.7(6)	2.9(6)	4.1(7)
C19	35.6(11)	52.1(13)	23.4(9)	21.2(9)	-1.6(8)	7.9(9)
C20	27.1(9)	40.9(11)	33.2(10)	19.8(9)	-5.0(8)	8.2(8)
C21	22.2(7)	18.5(7)	28.3(8)	7.2(6)	1.8(6)	8.2(5)

Atom	U_{11}	U_{22}	U_{33}	U_{23}	U_{13}	U_{12}
C23	25.0(8)	28.1(8)	18.1(7)	9.0(6)	-5.3(6)	0.0(6)
C24	27.2(8)	32.0(9)	16.2(7)	4.5(6)	-6.3(6)	4.3(7)
C25	24.0(9)	49.1(13)	24.0(9)	-0.4(8)	-9.8(7)	12.0(8)
C26	18.7(8)	57.0(14)	21.5(8)	-2.3(8)	-2.3(6)	5.6(8)
C27	22.2(8)	37.2(10)	16.7(7)	-3.9(6)	-2.5(6)	10.3(7)
C31	18.1(7)	19.9(6)	19.7(7)	2.5(5)	3.3(6)	0.9(5)
C32	26.1(8)	24.4(8)	22.1(8)	-1.6(6)	10.8(7)	0.5(6)
C33	27.4(9)	29.2(9)	21.9(8)	0.8(6)	9.9(7)	-5.5(6)
C34	31.2(9)	19.1(7)	21.6(8)	4.0(5)	5.2(7)	-3.5(6)
C35	24.8(7)	15.1(6)	18.6(7)	-2.0(5)	3.8(6)	-3.6(5)
C37	32.7(9)	17.5(6)	13.2(6)	-4.0(5)	-2.7(6)	0.3(6)
C38	37.4(10)	22.8(8)	22.7(8)	-9.9(6)	-1.9(7)	5.0(7)
C39	41.6(11)	18.3(7)	30.2(10)	-7.9(6)	-10.6(8)	-1.3(7)
C40	41.7(11)	16.5(7)	26.2(9)	0.3(6)	-8.4(8)	-9.4(7)
C41	24.1(7)	20.1(7)	17.6(7)	-0.9(5)	-1.3(6)	-7.5(5)
C43	16.3(7)	44.6(12)	32.5(10)	-8.8(8)	1.1(7)	-7.5(7)
C44	21.4(9)	44.4(13)	47.5(14)	-9.2(10)	-6.3(9)	-12.8(8)
C45	28.1(9)	34.3(10)	43.2(13)	-10.4(9)	-17.7(9)	-1.3(7)
C46	34.6(10)	31.1(9)	23.5(9)	-5.1(7)	-13.7(7)	-4.8(7)
C47	25.7(8)	19.4(7)	21.7(7)	-2.8(5)	-10.9(6)	-0.1(6)
C51	30.4(9)	19.6(7)	37.2(11)	1.2(7)	15.8(8)	-5.1(6)
C52	56.9(17)	21.6(9)	34.4(12)	9.0(7)	14.0(12)	-3.5(8)
C53	37.0(10)	15.1(7)	35.6(11)	3.4(6)	1.2(8)	0.9(6)
C54	25.9(9)	19.1(7)	39.7(11)	0.7(7)	2.8(8)	2.1(6)
C55	22.8(7)	18.5(7)	20.7(7)	0.0(5)	5.4(6)	0.0(5)
C57	18.9(7)	21.3(7)	16.7(6)	-0.6(5)	1.6(5)	1.1(5)
C58	20.9(7)	29.8(8)	20.2(7)	0.0(6)	5.8(6)	4.3(6)
C59	28.0(9)	37.2(10)	15.3(7)	-2.1(6)	4.8(6)	5.3(7)
C60	29.6(9)	36.8(10)	15.7(7)	4.9(6)	3.8(7)	5.9(7)
C61	19.6(7)	30.4(8)	16.3(7)	0.4(6)	1.2(6)	5.3(6)

Table 5.6 Bond Lengths for 1-Yb^{6+}.

Atom	Atom	Length/Å	Atom	Atom	Length/Å
Yb1	$N9^1$	2.2751(13)	C4	C5	1.528(3)
Yb1	N9	2.2719(12)	C5	C6	1.521(3)
Yb1	N29	2.1356(13)	C6	C7	1.538(2)
Yb1	N49	2.1289(13)	C11	C12	1.512(3)
P8	N2	1.6725(13)	C12	C13	1.524(3)
P8	N9	1.5572(12)	C13	C14	1.528(3)

Atom	Atom	Length/Å	Atom	Atom	Length/Å
P8	N10	1.6711(14)	C14	C15	1.519(2)
P8	N16	1.6542(13)	C17	C18	1.514(2)
P28	N22	1.6837(15)	C18	C19	1.526(3)
P28	N29	1.5331(14)	C19	C20	1.533(3)
P28	N30	1.6900(13)	C20	C21	1.517(3)
P28	N36	1.7019(13)	C23	C24	1.527(3)
P48	N42	1.6827(16)	C24	C25	1.518(3)
P48	N49	1.5316(13)	C25	C26	1.526(3)
P48	N50	1.6941(14)	C26	C27	1.520(3)
P48	N56	1.6966(13)	C31	C32	1.532(2)
N2	C3	1.470(2)	C32	C33	1.531(3)
N2	C7	1.475(2)	C33	C34	1.530(3)
N10	C11	1.469(2)	C34	C35	1.535(2)
N10	C15	1.465(2)	C37	C38	1.521(2)
N16	C17	1.466(2)	C38	C39	1.511(3)
N16	C21	1.462(2)	C39	C40	1.523(3)
N22	C23	1.464(2)	C40	C41	1.523(3)
N22	C27	1.454(2)	C43	C44	1.521(3)
N30	C31	1.464(2)	C44	C45	1.516(4)
N30	C35	1.463(2)	C45	C46	1.529(3)
N36	C37	1.470(2)	C46	C47	1.519(3)
N36	C41	1.468(2)	C51	C52	1.523(3)
N42	C43	1.465(2)	C52	C53	1.522(3)
N42	C47	1.459(2)	C53	C54	1.528(3)
N50	C51	1.469(2)	C54	C55	1.517(3)
N50	C55	1.467(2)	C57	C58	1.527(2)
N56	C57	1.466(2)	C58	C59	1.524(3)
N56	C61	1.463(2)	C59	C60	1.532(3)
C3	C4	1.520(2)	C60	C61	1.531(2)

Table 5.7 Bond Angles for 1-Yb^{6+}.

Atom	Atom	Atom	Angle/°	Atom	Atom	Atom	Angle/°
N9	Yb1	N9^{1}	82.74(4)	C43	N42	P48	125.23(14)
N29	Yb1	N9	116.85(5)	C47	N42	P48	120.54(12)
N29	Yb1	N9^{1}	118.24(5)	C47	N42	C43	112.68(16)
N49	Yb1	N9	116.55(5)	P48	N49	Yb1	163.20(9)
N49	Yb1	N9^{1}	111.25(5)	C51	N50	P48	119.71(12)
N49	Yb1	N29	109.27(5)	C55	N50	P48	113.76(11)
Yb1^{1}	P8	Yb1	58.370(6)	C55	N50	C51	110.83(14)

Atom	Atom	Atom	Angle/°	Atom	Atom	Atom	Angle/°
N2	P8	Yb1	142.17(5)	C57	N56	P48	113.55(11)
N2	P8	Yb1[1]	90.57(5)	C61	N56	P48	118.05(11)
N9	P8	Yb1[1]	31.23(5)	C61	N56	C57	110.50(13)
N9	P8	Yb1	27.43(5)	N2	C3	C4	109.50(14)
N9	P8	N2	117.60(7)	C3	C4	C5	111.10(14)
N9	P8	N10	116.10(7)	C6	C5	C4	110.86(15)
N9	P8	N16	112.16(7)	C5	C6	C7	109.80(15)
N10	P8	Yb1	93.79(5)	N2	C7	C6	108.90(13)
N10	P8	Yb1[1]	142.10(5)	N10	C11	C12	112.30(16)
N10	P8	N2	100.97(7)	C11	C12	C13	110.67(17)
N16	P8	Yb1[1]	108.35(5)	C12	C13	C14	109.03(17)
N16	P8	Yb1	105.14(5)	C15	C14	C13	111.26(17)
N16	P8	N2	104.99(7)	N10	C15	C14	111.54(13)
N16	P8	N10	103.30(7)	N16	C17	C18	110.49(14)
N22	P28	N30	99.26(7)	C17	C18	C19	110.87(16)
N22	P28	N36	107.82(8)	C18	C19	C20	110.30(16)
N29	P28	N22	113.54(8)	C21	C20	C19	111.02(19)
N29	P28	N30	121.84(8)	N16	C21	C20	110.18(15)
N29	P28	N36	112.93(7)	N22	C23	C24	112.45(15)
N30	P28	N36	99.55(6)	C25	C24	C23	111.12(17)
N42	P48	N50	107.15(8)	C24	C25	C26	110.75(16)
N42	P48	N56	100.52(7)	C27	C26	C25	110.84(19)
N49	P48	N42	113.55(8)	N22	C27	C26	111.25(15)
N49	P48	N50	113.24(7)	N30	C31	C32	109.60(15)
N49	P48	N56	120.65(7)	C33	C32	C31	109.48(15)
N50	P48	N56	99.91(7)	C34	C33	C32	110.83(16)
C3	N2	P8	118.87(10)	C33	C34	C35	111.32(15)
C3	N2	C7	110.57(13)	N30	C35	C34	110.54(13)
C7	N2	P8	118.22(10)	N36	C37	C38	111.24(15)
Yb1	N9	Yb1[1]	97.26(4)	C39	C38	C37	110.10(16)
P8	N9	Yb1	134.16(8)	C38	C39	C40	109.90(16)
P8	N9	Yb1[1]	127.99(7)	C41	C40	C39	110.95(16)
C11	N10	P8	127.46(12)	N36	C41	C40	110.69(15)
C15	N10	P8	115.72(10)	N42	C43	C44	111.26(18)
C15	N10	C11	114.88(13)	C45	C44	C43	111.72(19)
C17	N16	P8	124.45(10)	C44	C45	C46	110.47(19)
C21	N16	P8	121.80(11)	C47	C46	C45	110.06(18)
C21	N16	C17	113.13(13)	N42	C47	C46	110.92(16)
C23	N22	P28	126.89(12)	N50	C51	C52	110.27(18)
C27	N22	P28	119.82(12)	C53	C52	C51	111.47(19)
C27	N22	C23	113.21(15)	C52	C53	C54	109.39(16)

Atom	Atom	Atom	Angle/°	Atom	Atom	Atom	Angle/°
P28	N29	Yb1	166.39(9)	C55	C54	C53	110.64(16)
C31	N30	P28	121.55(10)	N50	C55	C54	111.36(15)
C35	N30	P28	116.15(10)	N56	C57	C58	110.21(14)
C35	N30	C31	111.26(13)	C59	C58	C57	110.31(15)
C37	N36	P28	117.82(11)	C58	C59	C60	110.51(16)
C41	N36	P28	114.46(10)	C61	C60	C59	110.63(15)
C41	N36	C37	110.31(13)	N56	C61	C60	109.97(15)

Table 5.8 Hydrogen Atom Coordinates (Å×10^4) and Isotropic Displacement Parameters (Å^2×10^3) for 1-Yb^{6+}.

Atom	*x*	*y*	*z*	U(eq)
H3A	5394.2	2641.59	4075.01	23
H3B	5742.57	2164.71	4631.33	23
H4A	5932.91	1371.09	3762.31	31
H4B	6812.13	1563.72	4061.42	31
H5A	6955.54	1822.17	3054.6	31
H5B	6145.01	2385.55	3052.16	31
H6A	7323.64	3245.75	3054.42	26
H6B	7709.83	2787.3	3606.45	26
H7A	7060.83	4027.18	3926.58	21
H7B	6192.42	3748.31	3644.93	21
H11A	8223.59	4270.39	4549.25	27
H11B	8011.58	3326.85	4523.32	27
H12A	9393.8	3560	4896.37	42
H12B	8835.18	3074.53	5353.88	42
H13A	9168.9	4793.44	5416.23	36
H13B	9543.5	4135.98	5857.3	36
H14A	8182.01	3848.02	6221.09	27
H14B	8350.91	4797.04	6285.72	27
H15A	6984.79	4534.36	5884.08	20
H15B	7531.9	5079.37	5456.08	20
H17A	5040.58	2384.01	5675.52	21
H17B	4946.39	3347.19	5692.86	21
H18A	4850.71	2783.75	6655.89	31
H18B	5612.98	3404.19	6612.66	31
H19A	5764.53	1661.85	6583.93	44
H19B	6106.69	2230.84	7094.83	44
H20A	7144.79	2781.01	6475.2	41
H20B	7223.38	1817.61	6444.26	41

Atom	*x*	*y*	*z*	U(eq)
H21A	7268.17	2404.01	5484.5	28
H21B	6501.17	1790.65	5542.53	28
H23A	6184.51	4117.82	8107.29	28
H23B	5647.14	4882.95	8304.7	28
H24A	6856.44	5604.03	8571.07	30
H24B	6912.47	4737.6	8878.09	30
H25A	7867.58	4270.4	8180.07	39
H25B	8214.79	5115.85	8417.18	39
H26A	7716.54	5799.05	7578.03	39
H26B	8273.75	5054.33	7364.58	39
H27A	6988.61	5114.99	6823.87	30
H27B	7063.39	4275.84	7166.02	30
H31A	3426.3	5547.63	7268.12	23
H31B	3931.88	6252.2	7591.67	23
H32A	3711.29	5593.81	8515.67	29
H32B	2829.48	5779.92	8215.94	29
H33A	2893.12	4395.53	8574.97	31
H33B	2710.82	4419.48	7890.56	31
H34A	3764.87	3444.74	8038.73	29
H34B	4304.65	4061.33	8421.12	29
H35A	4921.38	3997.63	7483.68	23
H35B	4047.2	4189.01	7176.27	23
H37A	6116	6613.41	8100.3	25
H37B	5170.51	6357.09	8218.36	25
H38A	4714.67	7706.62	8025.31	33
H38B	5397.16	7722.28	8534.66	33
H39A	6444.32	8128.11	7874.05	36
H39B	5680.19	8745.09	7811.96	36
H40A	5200.59	8075.49	6962.08	34
H40B	6160.95	8297.11	6867.08	34
H41A	5895.49	6922.04	6576.52	25
H41B	6563.32	6946.49	7094.61	25
H43A	8730.58	7650.82	4944.48	37
H43B	9117.07	6853.69	5232.5	37
H44A	9804.46	7974.83	5647.94	45
H44B	8936.76	8392.95	5808.26	45
H45A	9474.19	7824.82	6669.19	42
H45B	9608.27	6968.36	6359.09	42
H46A	8373.08	6880.96	6924.96	36
H46B	8000.72	7674.26	6621.11	36
H47A	8275	6153.7	6033.16	27

Atom	*x*	*y*	*z*	U(eq)
H47B	7376.65	6512	6188.02	27
H51A	7708.94	8436.25	4433.86	35
H51B	7789.57	8814.95	5072.34	35
H52A	7372.16	9852.59	4412.05	45
H52B	6586.2	9327.5	4209.79	45
H53A	6104.27	10312.17	4876.79	35
H53B	6786.73	10043.05	5348.56	35
H54A	5501.41	9433.65	5614.38	34
H54B	5387.32	9063.84	4975.84	34
H55A	6655.94	8567.89	5793.6	25
H55B	5871.12	8028.07	5610.04	25
H57A	7469.67	5640.22	4348.4	23
H57B	8214.8	5974.25	4745.81	23
H58A	8939.75	6440.14	3900.61	28
H58B	8754.75	5493.76	3831.73	28
H59A	7615.98	5752.86	3202.78	32
H59B	8399.54	6238.55	2952.78	32
H60A	7899.32	7471.33	3347	33
H60B	7150.46	7079.74	2982.07	33
H61A	6658.4	7533.99	3920.2	26
H61B	6528.94	6578.02	3856.46	26

5.5.2 *2-Yb*$^{6+}$

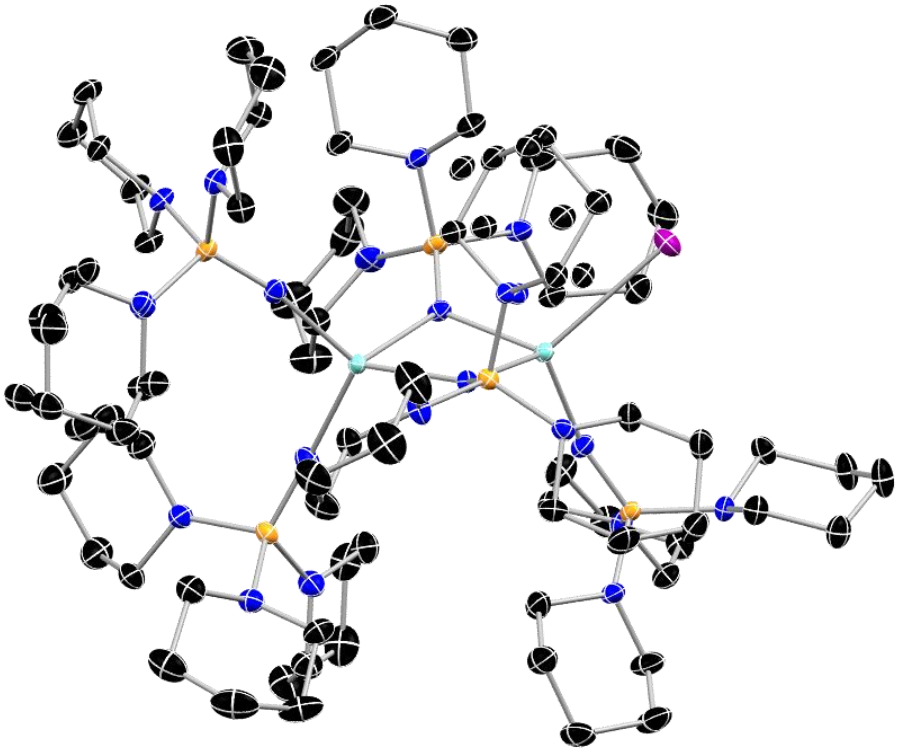

Figure 5.13 Molecular structure of 2-Yb^{6+} with thermal ellipsoids shown at 50% probability with hydrogen atoms omitted for clarity. Color code: C, black; N, blue; O, red; P, orange; I, purple; Yb, blue.

Table 5.9 Crystal data and structure refinement for 2-Yb^{6+}.

Identification code	2-Yb^{6+}
Empirical formula	$C_{75}H_{150}IN_{20}P_5Yb_2$
Formula weight	1959.97
Temperature/K	109.78
Crystal system	triclinic
Space group	P-1
a/Å	14.6571(8)
b/Å	14.7761(9)
c/Å	25.5541(15)
α/°	92.705(2)

β/°	97.818(2)
γ/°	116.804(2)
Volume/Å^3	4856.8(5)
Z	2
ρ_{calc}g/cm^3	1.340
μ/mm^{-1}	2.361
F(000)	2016.0
Crystal size/mm^3	0.471 × 0.316 × 0.232
Radiation	MoKα (λ = 0.71073)
2Θ range for data collection/°	4.468 to 66.262
Index ranges	-22 ≤ h ≤ 22, -22 ≤ k ≤ 22, -39 ≤ l ≤ 38
Reflections collected	93121
Independent reflections	36939 [R_{int} = 0.0345, R_{sigma} = 0.0391]
Data/restraints/parameters	36939/44/966
Goodness-of-fit on F^2	1.029
Final R indexes [I>=2σ (I)]	R_1 = 0.0267, wR_2 = 0.0675
Final R indexes [all data]	R_1 = 0.0320, wR_2 = 0.0700
Largest diff. peak/hole / e Å^{-3}	1.78/-0.79

Table 5.10 Fractional Atomic Coordinates (×10^4) and Equivalent Isotropic Displacement Parameters (Å^2×10^3) for 2-Yb^{6+}. U_{eq} is defined as 1/3 of the trace of the orthogonalised U_{IJ} tensor.

Atom	*x*	*y*	*z*	U(eq)
C1	5422.3(16)	3643.9(15)	7621.5(9)	26.1(4)
C2	6239.6(19)	3413.8(19)	7933.4(12)	39.3(6)
C3	6205(2)	3488(2)	8523.9(12)	45.6(7)
C4	6269(2)	4511(2)	8721.5(10)	40.6(6)
C5	5458.0(17)	4706.1(17)	8377.0(8)	27.0(4)
C6	6505.2(15)	5425.1(19)	6797.9(9)	29.1(4)
C7	6793.8(18)	6032(2)	6332.8(10)	38.2(6)
C8	6059.3(19)	5436(2)	5819.2(10)	42.8(6)
C9	4933.0(19)	5094(2)	5888.4(9)	40.6(6)
C10	4696.2(17)	4508.2(19)	6363.8(9)	32.4(5)
C11	6863.9(16)	6882.7(17)	8001.8(10)	30.1(4)
C12	7615.4(19)	7818.5(19)	7771.6(12)	41.5(6)
C13	7216(2)	8610.2(18)	7728.3(12)	41.5(6)
C14	6119(2)	8125.3(17)	7414.0(10)	34.3(5)
C15	5415.8(18)	7190.9(16)	7659.6(9)	28.1(4)
C16	2056.8(15)	3333.2(15)	5589.1(8)	23.5(4)
C17	1847.7(17)	3848.8(17)	5116.5(8)	27.3(4)
C18	1387.0(17)	3104.4(18)	4607.0(8)	28.8(4)

Atom	*x*	*y*	*z*	U(eq)
C19	431.0(16)	2153.1(17)	4690.5(8)	27.0(4)
C20	707.0(15)	1677.4(15)	5161.6(7)	22.4(3)
C26	-920.2(15)	1278.1(16)	6025.6(8)	23.6(4)
C27	-1922.5(18)	301(2)	5824.1(10)	36.6(5)
C28	-2174.1(19)	-431.4(19)	6247.7(11)	38.3(5)
C29	-1250.5(19)	-615.9(17)	6438.9(11)	34.7(5)
C30	-265.4(16)	386.6(16)	6614.3(8)	25.1(4)
C31	2261.4(16)	2383.2(16)	8066.4(8)	24.1(4)
C32	2856.3(18)	1885.4(17)	8346.6(11)	32.4(5)
C33	2133(2)	774.6(18)	8395.0(12)	38.4(6)
C34	1252(2)	700.9(19)	8671.0(13)	43.0(6)
C35	696(2)	1224.0(17)	8394.3(13)	40.6(6)
C41	2074.8(16)	3533.8(18)	9403.3(8)	26.7(4)
C42	1901(2)	3543(2)	9977.4(9)	36.3(5)
C43	1675.1(19)	4415(2)	10143.1(9)	33.6(5)
C44	778.9(17)	4380.8(18)	9754.2(8)	27.4(4)
C45	975.6(17)	4345.6(16)	9185.4(8)	23.9(4)
C46	4523.2(18)	6570.4(18)	9141.0(8)	28.3(4)
C47	4799.2(19)	6025.6(18)	9578.4(9)	30.4(4)
C48	5658.0(18)	6791.7(19)	10017.7(10)	33.2(5)
C49	5341(2)	7568(2)	10224.9(9)	37.7(6)
C50	5047.5(18)	8075.1(16)	9776.0(9)	30.3(5)
C51	2395.8(16)	7298.4(15)	9784.3(8)	22.6(4)
C52	2294.9(18)	7848.4(17)	10273.6(8)	26.9(4)
C53	1725(2)	8467.9(19)	10117.3(10)	34.0(5)
C54	2231.9(19)	9169.3(17)	9710.3(9)	30.3(4)
C55	2313.5(16)	8557.6(16)	9238.4(8)	22.6(4)
C56	4779.5(15)	9717.3(14)	9059.6(8)	23.0(4)
C57	4764.5(17)	10603.7(15)	8780.1(9)	26.9(4)
C58	5035.8(18)	10597.7(17)	8230.5(9)	31.5(5)
C59	4368.6(19)	9552.7(17)	7907.1(9)	31.0(4)
C60	4421.3(16)	8711.5(15)	8211.3(8)	24.0(4)
C61	177.6(17)	4274.4(17)	6007.9(8)	26.7(4)
C62	-755.7(18)	3890.5(19)	5558.7(8)	32.0(5)
C63	-1765.9(18)	3426.0(18)	5775.6(9)	33.9(5)
C64	-1764.0(17)	4165.8(18)	6213.4(9)	30.8(4)
C65	-787.5(16)	4552.0(16)	6639.7(8)	25.1(4)
C66	1774(2)	6661(2)	5858.6(9)	36.7(5)
C67	2619(2)	7699(2)	5784.3(10)	40.9(6)
C68	3644(2)	7673(2)	5797.9(10)	42.6(6)
C69	3919.8(19)	7280(2)	6310.4(11)	39.9(6)

Atom	*x*	*y*	*z*	U(eq)
C70	3038.0(16)	6252.4(16)	6372.0(8)	25.0(4)
C71	238.1(18)	7032.8(17)	6683.2(9)	30.4(5)
C72	-281.5(19)	7423.8(19)	7046.4(12)	39.5(6)
C73	527.5(19)	8342.9(17)	7430.5(10)	33.6(5)
C74	1326.2(17)	8069.3(15)	7736.2(8)	25.5(4)
C75	1779.2(15)	7625.6(14)	7356.5(8)	21.3(3)
I1	-561.6(2)	5396.7(2)	8257.0(2)	25.42(3)
N1	3892.4(13)	4899.8(13)	7358.4(7)	22.4(3)
N2	5582.5(12)	4658.2(13)	7819.0(7)	20.8(3)
N3	5425.8(12)	5117.1(14)	6843.8(7)	24.3(3)
N4	5812.8(13)	6448.1(13)	7694.5(7)	23.4(3)
N5	1488.9(12)	2903.4(12)	6707.5(6)	18.6(3)
N6	1121.1(12)	2408.4(12)	5648.0(6)	18.6(3)
N8	-57.1(12)	1041.1(12)	6183.3(6)	18.8(3)
N9	1627.4(11)	4101.6(11)	8074.0(6)	14.4(2)
N10	1406.3(13)	2286.3(12)	8333.7(7)	21.3(3)
N12	1167.0(11)	3475.0(12)	9046.8(6)	16.9(3)
N13	2698.9(12)	6764.6(12)	8522.6(6)	18.6(3)
N14	4229.2(12)	7317.7(12)	9362.1(6)	19.2(3)
N15	2932.7(12)	8040.4(11)	9425.9(6)	16.8(3)
N16	4103.5(12)	8741.4(11)	8727.0(6)	17.9(3)
N17	1710.9(11)	5432.0(11)	7240.1(6)	15.7(3)
N18	137.8(12)	5030.1(12)	6388.8(6)	19.6(3)
N19	2069.2(14)	6317.9(15)	6353.5(7)	26.1(3)
N20	948.2(13)	6732.3(12)	7005.0(6)	20.4(3)
P1	5052.2(3)	5238.8(4)	7422.0(2)	17.50(8)
P2	1151.7(4)	2035.7(3)	6267.9(2)	16.20(8)
P3	1043.4(3)	3193.8(3)	8389.5(2)	14.32(7)
P4	3427.2(3)	7633.0(3)	8965.2(2)	14.58(7)
P5	1260.3(4)	5845.0(4)	6777.9(2)	16.53(8)
Yb1	2258.2(2)	4215.6(2)	7297.0(2)	12.49(2)
Yb2	1449.9(2)	5519.2(2)	8069.2(2)	13.06(2)
C36A	-635(3)	2240(4)	7608.6(17)	20.6(5)
C37A	-1618(3)	2338(4)	7437.3(16)	23.7(5)
C38A	-2449(3)	1730(4)	7762.0(16)	23.7(7)
C39A	-2001(3)	2103(4)	8352.0(16)	23.7(5)
C40A	-1017(3)	1996(4)	8509.8(17)	19.5(5)
N11A	-240(3)	2570(16)	8181.9(18)	16.5(12)
C36B	-697(2)	2681(2)	7668.7(10)	20.6(5)
C37B	-1613(2)	1647(2)	7455.6(11)	23.7(5)
C38B	-2433(2)	1337(3)	7812.0(10)	23.7(7)

Atom	*x*	*y*	*z*	U(eq)
C39B	-1933(2)	1366(2)	8380.6(11)	23.7(5)
C40B	-1012(2)	2408(2)	8580.2(11)	19.5(5)
N11B	-246(2)	2695(8)	8221.2(10)	16.5(12)
C21A	2934(2)	1914.4(19)	6643.6(11)	23.8(5)
C22A	3156(2)	1134(2)	6930.0(12)	32.5(6)
C23A	3002(2)	247(2)	6534.6(13)	30.4(6)
C24A	1928(3)	-199(3)	6173(3)	39.9(9)
C25A	1726(2)	599(2)	5931.5(10)	24.1(5)
N7A	1877(6)	1421(4)	6335(3)	19.7(3)
C21B	2639(8)	1562(9)	6770(5)	23.8(5)
C22B	3529(8)	1443(8)	6590(5)	32.5(6)
C23B	3159(9)	376(8)	6300(6)	30.4(6)
C24B	1977(10)	-256(10)	6249(15)	39.9(9)
C25B	1394(9)	289(9)	6050(5)	24.1(5)
N7B	1820(30)	1340(20)	6309(16)	19.7(3)

Table 5.11 Anisotropic Displacement Parameters ($Å^2×10^3$) for 2-Yb^{6+}. The Anisotropic displacement factor exponent takes the form: $-2\pi^2[h^2a^{*2}U_{11}+2hka^*b^*U_{12}+\ldots]$.

Atom	U_{11}	U_{22}	U_{33}	U_{23}	U_{13}	U_{12}
C1	24.3(9)	17.0(8)	34.2(11)	2.4(8)	4.1(8)	7.4(7)
C2	31.4(12)	25.8(11)	63.1(17)	11.6(11)	5.9(11)	15.4(9)
C3	37.9(13)	34.1(13)	59.2(17)	18.2(12)	-7.3(12)	15.0(11)
C4	36.7(13)	34.6(12)	35.2(12)	9.3(10)	-11.2(10)	7.7(10)
C5	29.1(10)	26.3(10)	20.3(9)	3.9(7)	1.1(7)	9.0(8)
C6	17.3(8)	41.9(12)	27.1(10)	1.8(9)	7.8(7)	12.0(8)
C7	24.1(10)	47.3(14)	31.7(12)	3.2(10)	12.2(9)	4.9(10)
C8	28.4(11)	60.3(17)	25.7(11)	4.0(11)	10.0(9)	7.1(11)
C9	28.3(11)	61.4(17)	21.6(10)	5.5(10)	5.6(8)	11.3(11)
C10	23.7(10)	39.8(12)	24.6(10)	-3.1(9)	6.4(8)	6.8(9)
C11	21.7(9)	24.2(10)	36.8(12)	0.1(8)	2.4(8)	5.2(8)
C12	26.9(11)	26.2(11)	60.6(17)	2.1(11)	12.6(11)	2.0(9)
C13	45.8(14)	20.4(10)	50.8(15)	4.9(10)	17.0(12)	6.4(10)
C14	46.3(14)	22.4(10)	34.4(12)	7.3(9)	13.0(10)	14.1(10)
C15	32.8(11)	22.2(9)	32.3(11)	4.1(8)	8.5(8)	14.4(8)
C16	22.1(9)	22.8(9)	17.4(8)	3.0(7)	0.7(6)	4.2(7)
C17	31.3(10)	25.9(9)	19.0(9)	6.3(7)	5.2(7)	7.8(8)
C18	29.9(10)	33.9(11)	16.1(8)	6.7(8)	5.3(7)	8.5(9)
C19	26.5(9)	33.3(11)	14.0(8)	1.8(7)	1.0(7)	8.4(8)
C20	25.0(9)	21.8(8)	15.6(8)	-1.8(6)	3.5(6)	7.2(7)

Atom	U_{11}	U_{22}	U_{33}	U_{23}	U_{13}	U_{12}
C26	24.0(9)	23.9(9)	23.5(9)	6.2(7)	5.1(7)	11.0(7)
C27	23.2(10)	37.6(13)	36.6(12)	6.8(10)	2.1(8)	4.1(9)
C28	29.3(11)	29.3(11)	45.8(14)	6.9(10)	11.9(10)	2.7(9)
C29	40.2(12)	19.7(9)	45.9(14)	10.2(9)	20.8(10)	11.0(9)
C30	30.3(10)	21.9(9)	26.2(9)	9.8(7)	9.6(8)	12.9(8)
C31	27.8(9)	24.0(9)	25.1(9)	6.5(7)	8.2(7)	14.6(8)
C32	29.1(10)	24.5(10)	47.5(13)	9.6(9)	4.1(9)	16.0(9)
C33	39.6(13)	21.3(10)	60.4(16)	9.4(10)	6.9(11)	19.4(10)
C34	50.3(15)	24.4(11)	60.4(17)	21.1(11)	19.2(13)	18.4(11)
C35	37.8(13)	18.1(9)	71.8(19)	19.6(11)	25.6(12)	12.3(9)
C41	21.8(9)	33.9(11)	24.4(9)	-0.2(8)	-2.3(7)	15.1(8)
C42	44.2(13)	48.6(14)	20.5(10)	1.6(9)	-4.8(9)	28.4(12)
C43	38.7(12)	38.8(12)	20.5(9)	-3.1(9)	2.6(8)	16.7(10)
C44	32.1(10)	32.2(11)	23.6(9)	2.9(8)	9.5(8)	18.5(9)
C45	31.9(10)	26.5(9)	21.0(9)	6.3(7)	8.9(7)	18.7(8)
C46	37.2(11)	32.3(11)	23.9(9)	-1.9(8)	-0.4(8)	25.5(9)
C47	38.0(12)	28.2(10)	29.8(10)	-0.8(8)	-3.4(8)	22.3(9)
C48	32.2(11)	34.5(12)	35.2(12)	1.7(9)	-8.3(9)	21.4(10)
C49	47.7(14)	36.1(12)	28.2(11)	-7.5(9)	-15.4(10)	25.6(11)
C50	32.8(11)	21.6(9)	31.2(11)	-5.7(8)	-12.5(8)	13.7(8)
C51	28.4(9)	19.4(8)	21.7(9)	5.5(7)	8.4(7)	11.1(7)
C52	35.7(11)	28.6(10)	20.4(9)	6.5(8)	12.3(8)	15.9(9)
C53	44.7(13)	36.5(12)	33.6(11)	9.1(10)	22.9(10)	24.9(11)
C54	41.5(12)	27.1(10)	35.9(11)	8.8(9)	19.0(9)	23.9(9)
C55	25.9(9)	25.1(9)	24.1(9)	9.3(7)	9.0(7)	16.3(8)
C56	23.3(9)	14.3(7)	24.5(9)	-1.8(7)	1.2(7)	4.0(7)
C57	26.9(10)	14.8(8)	36.8(11)	3.0(8)	8.1(8)	7.1(7)
C58	29.5(10)	22.5(9)	35.7(12)	10.3(9)	7.6(9)	5.0(8)
C59	36.1(11)	26.0(10)	23.3(10)	7.5(8)	9.2(8)	6.3(9)
C60	24.6(9)	22.3(9)	24.0(9)	0.8(7)	10.6(7)	8.3(7)
C61	31.9(10)	28.5(10)	19.5(9)	-6.6(7)	-5.5(7)	17.4(8)
C62	37.3(12)	34.6(11)	20.1(9)	-9.6(8)	-9.2(8)	18.3(10)
C63	32.8(11)	29.6(11)	31.5(11)	-9.0(9)	-10.8(9)	13.5(9)
C64	23.2(10)	29.8(11)	34.2(11)	-3.5(9)	-3.5(8)	10.7(8)
C65	25.1(9)	22.4(9)	22.2(9)	-0.8(7)	-0.6(7)	7.7(7)
C66	41.8(13)	52.3(15)	23.9(10)	20.9(10)	7.4(9)	26.5(12)
C67	76.2(19)	33.1(12)	22.9(10)	13.3(9)	11.4(11)	31.9(13)
C68	46.9(14)	36.2(13)	32.5(12)	18.7(11)	10.0(10)	6.4(11)
C69	29.9(11)	40.9(13)	36.9(13)	19.2(11)	4.7(9)	4.8(10)
C70	28.2(10)	24.9(9)	23.2(9)	7.9(7)	6.4(7)	12.4(8)
C71	33.6(11)	22.2(9)	34.2(11)	-1.8(8)	-13.1(8)	17.5(8)

Atom	U_{11}	U_{22}	U_{33}	U_{23}	U_{13}	U_{12}
C72	28.9(11)	30.5(11)	59.1(16)	-7.3(11)	-8.4(10)	19.3(10)
C73	33.2(11)	22.6(10)	47.1(13)	-3.7(9)	0.3(9)	17.2(9)
C74	33.7(10)	16.1(8)	25.8(9)	0.0(7)	2.5(8)	11.7(8)
C75	25.5(9)	15.2(7)	20.7(8)	0.2(6)	-3.6(6)	9.5(7)
I1	19.49(6)	25.87(6)	35.10(7)	6.35(5)	7.89(5)	13.03(5)
N1	19.9(7)	24.8(8)	25.3(8)	7.8(6)	10.6(6)	10.6(6)
N2	19.6(7)	19.5(7)	22.8(7)	2.3(6)	1.7(6)	9.1(6)
N3	16.4(7)	33.6(9)	20.6(7)	0.0(7)	4.6(6)	9.4(7)
N4	20.5(7)	18.5(7)	29.2(8)	1.2(6)	4.1(6)	7.4(6)
N5	22.4(7)	19.3(7)	15.6(6)	2.1(5)	2.8(5)	11.1(6)
N6	20.9(7)	15.9(6)	13.5(6)	0.0(5)	0.8(5)	4.5(6)
N8	22.5(7)	15.2(6)	18.2(7)	2.2(5)	4.5(5)	7.9(6)
N9	15.1(6)	12.8(6)	15.0(6)	3.8(5)	4.6(5)	5.6(5)
N10	24.1(8)	13.9(6)	30.5(8)	8.9(6)	13.8(6)	9.8(6)
N12	16.0(6)	20.4(7)	16.0(6)	5.0(5)	3.3(5)	9.6(6)
N13	21.8(7)	17.2(7)	15.6(7)	-0.8(5)	0.2(5)	9.1(6)
N14	21.1(7)	18.1(7)	18.0(7)	-3.2(5)	-4.1(5)	11.1(6)
N15	22.3(7)	15.7(6)	14.8(6)	2.9(5)	5.5(5)	10.2(6)
N16	21.8(7)	12.7(6)	17.0(7)	0.0(5)	4.3(5)	6.1(5)
N17	18.8(7)	13.8(6)	14.0(6)	2.5(5)	0.2(5)	7.8(5)
N18	22.4(7)	19.0(7)	15.3(7)	-2.7(5)	-3.3(5)	10.0(6)
N19	29.3(9)	35.1(9)	18.6(7)	13.3(7)	4.9(6)	17.9(8)
N20	23.0(7)	15.3(7)	21.6(7)	-0.2(6)	-4.7(6)	10.4(6)
P1	14.35(19)	18.9(2)	19.6(2)	3.65(16)	5.44(15)	7.26(16)
P2	21.2(2)	14.06(18)	13.08(18)	-0.13(15)	1.76(15)	8.46(16)
P3	13.70(18)	13.27(18)	16.08(19)	4.88(15)	4.47(14)	5.52(15)
P4	16.88(19)	12.62(18)	13.59(18)	-0.56(14)	0.33(14)	7.09(15)
P5	20.9(2)	15.16(19)	13.34(18)	2.39(15)	-1.35(15)	9.24(16)
Yb1	13.20(3)	11.98(3)	12.51(3)	1.51(2)	2.74(2)	5.87(2)
Yb2	14.05(3)	11.55(3)	13.26(3)	0.00(2)	0.97(2)	6.17(2)
C36A	17.4(10)	23.1(14)	17.2(11)	4.7(11)	3.7(8)	5.5(11)
C37A	19.8(11)	27.9(12)	16.3(11)	-1.9(10)	2.7(8)	5.3(10)
C38A	15.2(9)	25.4(17)	21.7(11)	-1.2(13)	3.8(8)	1.9(12)
C39A	17.0(11)	26.1(12)	21.7(12)	2.1(10)	5.2(9)	4.3(9)
C40A	16.7(9)	18.5(14)	18.2(11)	2.7(11)	7.4(8)	2.7(12)
N11A	12.8(6)	19(3)	14.6(7)	2.1(11)	3.8(5)	4.1(6)
C36B	17.4(10)	23.1(14)	17.2(11)	4.7(11)	3.7(8)	5.5(11)
C37B	19.8(11)	27.9(12)	16.3(11)	-1.9(10)	2.7(8)	5.3(10)
C38B	15.2(9)	25.4(17)	21.7(11)	-1.2(13)	3.8(8)	1.9(12)
C39B	17.0(11)	26.1(12)	21.7(12)	2.1(10)	5.2(9)	4.3(9)
C40B	16.7(9)	18.5(14)	18.2(11)	2.7(11)	7.4(8)	2.7(12)

Atom	U_{11}	U_{22}	U_{33}	U_{23}	U_{13}	U_{12}
N11B	12.8(6)	19(3)	14.6(7)	2.1(11)	3.8(5)	4.1(6)
C21A	24.3(12)	15.0(11)	29.8(13)	0.6(9)	-1.8(9)	9.1(9)
C22A	35.5(14)	27.0(12)	34.2(14)	-0.2(10)	-5.8(10)	17.3(11)
C23A	28.0(12)	22.1(11)	42.5(17)	1.4(11)	-0.6(12)	14.8(10)
C24A	40.9(14)	25.6(12)	51(3)	-3.6(12)	-4.7(13)	18.0(11)
C25A	30.7(14)	20.8(12)	21.9(12)	-1.9(9)	1.1(9)	14.2(11)
N7A	23.2(11)	18.6(12)	17.3(12)	-2.7(8)	-0.2(6)	11.0(11)
C21B	24.3(12)	15.0(11)	29.8(13)	0.6(9)	-1.8(9)	9.1(9)
C22B	35.5(14)	27.0(12)	34.2(14)	-0.2(10)	-5.8(10)	17.3(11)
C23B	28.0(12)	22.1(11)	42.5(17)	1.4(11)	-0.6(12)	14.8(10)
C24B	40.9(14)	25.6(12)	51(3)	-3.6(12)	-4.7(13)	18.0(11)
C25B	30.7(14)	20.8(12)	21.9(12)	-1.9(9)	1.1(9)	14.2(11)
N7B	23.2(11)	18.6(12)	17.3(12)	-2.7(8)	-0.2(6)	11.0(11)

Table 5.12 Bond Lengths for 2-Yb^{6+}.

Atom	Atom	Length/Å	Atom	Atom	Length/Å
C1	C2	1.523(3)	C66	N19	1.467(3)
C1	N2	1.461(3)	C67	C68	1.516(4)
C2	C3	1.517(4)	C68	C69	1.535(3)
C3	C4	1.528(4)	C69	C70	1.520(3)
C4	C5	1.523(3)	C70	N19	1.461(3)
C5	N2	1.464(3)	C71	C72	1.521(4)
C6	C7	1.514(3)	C71	N20	1.475(2)
C6	N3	1.459(2)	C72	C73	1.523(3)
C7	C8	1.520(4)	C73	C74	1.534(3)
C8	C9	1.532(3)	C74	C75	1.523(3)
C9	C10	1.513(3)	C75	N20	1.474(2)
C10	N3	1.459(3)	I1	Yb2	2.9777(2)
C11	C12	1.533(3)	N1	P1	1.5220(17)
C11	N4	1.461(3)	N1	Yb1	2.1173(16)
C12	C13	1.528(4)	N2	P1	1.6848(16)
C13	C14	1.517(4)	N3	P1	1.6730(17)
C14	C15	1.529(3)	N4	P1	1.6720(18)
C15	N4	1.457(3)	N5	P2	1.5137(16)
C16	C17	1.526(3)	N5	Yb1	2.1425(16)
C16	N6	1.468(2)	N6	P2	1.7030(16)
C17	C18	1.522(3)	N8	P2	1.6921(16)
C18	C19	1.522(3)	N9	P3	1.5608(14)
C19	C20	1.520(3)	N9	Yb1	2.2839(14)
C20	N6	1.469(2)	N9	Yb2	2.2245(14)

Atom	Atom	Length/Å	Atom	Atom	Length/Å
C26	C27	1.523(3)	N10	P3	1.6575(16)
C26	N8	1.470(2)	N12	P3	1.6762(16)
C27	C28	1.529(3)	N13	P4	1.5376(16)
C28	C29	1.520(4)	N13	Yb2	2.0649(15)
C29	C30	1.521(3)	N14	P4	1.6858(15)
C30	N8	1.472(2)	N15	P4	1.6829(15)
C31	C32	1.507(3)	N16	P4	1.6821(16)
C31	N10	1.462(2)	N17	P5	1.5565(15)
C32	C33	1.523(3)	N17	Yb1	2.2778(14)
C33	C34	1.518(4)	N17	Yb2	2.2117(15)
C34	C35	1.492(4)	N18	P5	1.6735(16)
C35	N10	1.471(3)	N19	P5	1.6565(18)
C41	C42	1.523(3)	N20	P5	1.6753(17)
C41	N12	1.472(2)	P2	N7A	1.680(3)
C42	C43	1.524(3)	P2	N7B	1.715(14)
C43	C44	1.515(3)	P3	N11A	1.670(4)
C44	C45	1.523(3)	P3	N11B	1.671(3)
C45	N12	1.473(2)	Yb1	Yb2	3.36793(16)
C46	C47	1.522(3)	C36A	C37A	1.521(4)
C46	N14	1.470(2)	C36A	N11A	1.472(5)
C47	C48	1.529(3)	C37A	C38A	1.528(3)
C48	C49	1.517(3)	C38A	C39A	1.527(3)
C49	C50	1.517(3)	C39A	C40A	1.523(4)
C50	N14	1.464(2)	C40A	N11A	1.475(4)
C51	C52	1.520(3)	C36B	C37B	1.519(3)
C51	N15	1.474(2)	C36B	N11B	1.470(4)
C52	C53	1.525(3)	C37B	C38B	1.524(3)
C53	C54	1.525(3)	C38B	C39B	1.526(3)
C54	C55	1.523(3)	C39B	C40B	1.522(3)
C55	N15	1.476(2)	C40B	N11B	1.473(3)
C56	C57	1.528(3)	C21A	C22A	1.525(3)
C56	N16	1.466(2)	C21A	N7A	1.465(4)
C57	C58	1.512(3)	C22A	C23A	1.528(4)
C58	C59	1.524(3)	C23A	C24A	1.543(4)
C59	C60	1.522(3)	C24A	C25A	1.480(4)
C60	N16	1.461(2)	C25A	N7A	1.470(5)
C61	C62	1.524(3)	C21B	C22B	1.519(9)
C61	N18	1.473(3)	C21B	N7B	1.465(10)
C62	C63	1.521(4)	C22B	C23B	1.529(9)
C63	C64	1.526(3)	C23B	C24B	1.536(10)
C64	C65	1.530(3)	C24B	C25B	1.475(9)

Atom	Atom	Length/Å	Atom	Atom	Length/Å
C65	N18	1.471(3)	C25B	N7B	1.467(10)
C66	C67	1.517(4)			

Table 5.13 Bond Angles for 2-Yb^{6+}.

Atom	Atom	Atom	Angle/°	Atom	Atom	Atom	Angle/°
N2	C1	C2	109.85(18)	C65	N18	P5	117.77(12)
C3	C2	C1	110.7(2)	C66	N19	P5	121.92(15)
C2	C3	C4	110.9(2)	C70	N19	C66	112.70(17)
C5	C4	C3	110.8(2)	C70	N19	P5	124.32(13)
N2	C5	C4	110.03(19)	C71	N20	P5	123.33(14)
N3	C6	C7	110.76(19)	C75	N20	C71	110.15(15)
C6	C7	C8	111.0(2)	C75	N20	P5	116.84(13)
C7	C8	C9	110.0(2)	N1	P1	N2	119.67(9)
C10	C9	C8	110.7(2)	N1	P1	N3	112.65(9)
N3	C10	C9	110.6(2)	N1	P1	N4	114.76(9)
N4	C11	C12	111.4(2)	N3	P1	N2	102.61(9)
C13	C12	C11	110.8(2)	N4	P1	N2	98.98(9)
C14	C13	C12	110.3(2)	N4	P1	N3	106.37(9)
C13	C14	C15	110.2(2)	N5	P2	N6	113.12(8)
N4	C15	C14	111.74(18)	N5	P2	N8	119.85(9)
N6	C16	C17	111.53(16)	N5	P2	N7A	113.05(14)
C18	C17	C16	111.20(18)	N5	P2	N7B	116.6(5)
C17	C18	C19	109.86(16)	N6	P2	N7B	108.2(17)
C20	C19	C18	110.09(17)	N8	P2	N6	99.27(8)
N6	C20	C19	110.73(17)	N8	P2	N7B	97.4(13)
N8	C26	C27	110.42(18)	N7A	P2	N6	109.3(4)
C26	C27	C28	110.82(19)	N7A	P2	N8	100.8(3)
C29	C28	C27	110.24(19)	N9	P3	N10	112.73(8)
C28	C29	C30	111.21(19)	N9	P3	N12	116.76(8)
N8	C30	C29	110.95(18)	N9	P3	N11A	114.3(5)
N10	C31	C32	110.96(17)	N9	P3	N11B	112.3(3)
C31	C32	C33	110.76(19)	N10	P3	N12	104.58(8)
C34	C33	C32	110.4(2)	N10	P3	N11A	103.4(8)
C35	C34	C33	110.8(2)	N10	P3	N11B	110.3(4)
N10	C35	C34	112.2(2)	N11A	P3	N12	103.7(2)
N12	C41	C42	109.84(17)	N11B	P3	N12	99.19(15)
C41	C42	C43	111.85(19)	N13	P4	N14	112.30(8)
C44	C43	C42	110.20(18)	N13	P4	N15	120.08(9)
C43	C44	C45	110.75(17)	N13	P4	N16	112.62(8)
N12	C45	C44	111.37(16)	N15	P4	N14	100.17(8)

Atom	Atom	Atom	Angle/°	Atom	Atom	Atom	Angle/°
N14	C46	C47	110.74(17)	N16	P4	N14	110.78(8)
C46	C47	C48	110.97(19)	N16	P4	N15	99.67(8)
C49	C48	C47	109.78(18)	N17	P5	N18	118.13(8)
C50	C49	C48	111.2(2)	N17	P5	N19	112.08(8)
N14	C50	C49	111.29(18)	N17	P5	N20	111.79(8)
N15	C51	C52	110.04(16)	N18	P5	N20	100.61(8)
C51	C52	C53	110.99(18)	N19	P5	N18	103.83(9)
C54	C53	C52	110.51(18)	N19	P5	N20	109.48(9)
C55	C54	C53	110.31(18)	N1	Yb1	N5	111.84(6)
N15	C55	C54	109.50(16)	N1	Yb1	N9	116.94(6)
N16	C56	C57	110.48(16)	N1	Yb1	N17	109.94(6)
C58	C57	C56	112.10(18)	N1	Yb1	Yb2	113.53(5)
C57	C58	C59	110.69(17)	N5	Yb1	N9	117.12(6)
C60	C59	C58	110.90(18)	N5	Yb1	N17	117.08(5)
N16	C60	C59	110.59(17)	N5	Yb1	Yb2	134.42(4)
N18	C61	C62	109.21(17)	N9	Yb1	Yb2	41.00(4)
C63	C62	C61	110.87(19)	N17	Yb1	N9	80.41(5)
C62	C63	C64	110.94(19)	N17	Yb1	Yb2	40.66(4)
C63	C64	C65	110.98(18)	I1	Yb2	P3	97.973(8)
N18	C65	C64	109.35(17)	I1	Yb2	P5	99.103(9)
N19	C66	C67	110.9(2)	I1	Yb2	Yb1	137.524(5)
C68	C67	C66	110.6(2)	N9	Yb2	I1	118.00(4)
C67	C68	C69	110.3(2)	N9	Yb2	P3	22.23(4)
C70	C69	C68	110.7(2)	N9	Yb2	P5	102.79(4)
N19	C70	C69	110.64(19)	N9	Yb2	Yb1	42.34(4)
N20	C71	C72	109.76(19)	N13	Yb2	I1	111.62(4)
C71	C72	C73	110.6(2)	N13	Yb2	N9	112.82(6)
C72	C73	C74	109.81(18)	N13	Yb2	N17	109.77(6)
C75	C74	C73	111.10(18)	N13	Yb2	P3	116.68(4)
N20	C75	C74	110.75(17)	N13	Yb2	P5	111.08(4)
P1	N1	Yb1	171.50(11)	N13	Yb2	Yb1	110.84(4)
C1	N2	C5	110.90(16)	N17	Yb2	I1	118.58(4)
C1	N2	P1	118.18(13)	N17	Yb2	N9	83.17(5)
C5	N2	P1	115.90(13)	N17	Yb2	P3	101.71(4)
C6	N3	P1	123.03(14)	N17	Yb2	P5	22.50(4)
C10	N3	C6	112.87(16)	N17	Yb2	Yb1	42.14(4)
C10	N3	P1	122.94(13)	P5	Yb2	P3	117.859(11)
C11	N4	P1	127.75(15)	P5	Yb2	Yb1	63.922(9)
C15	N4	C11	112.46(17)	Yb1	Yb2	P3	63.457(8)
C15	N4	P1	119.72(14)	N11A	C36A	C37A	111.1(6)
P2	N5	Yb1	169.02(10)	C36A	C37A	C38A	110.7(3)

Atom	Atom	Atom	Angle/°	Atom	Atom	Atom	Angle/°
C16	N6	C20	111.41(15)	C39A	C38A	C37A	108.6(3)
C16	N6	P2	114.00(12)	C40A	C39A	C38A	110.7(3)
C20	N6	P2	122.49(13)	N11A	C40A	C39A	110.3(6)
C26	N8	C30	110.67(15)	C36A	N11A	P3	118.4(4)
C26	N8	P2	116.16(13)	C36A	N11A	C40A	112.4(5)
C30	N8	P2	115.48(13)	C40A	N11A	P3	125.6(4)
P3	N9	Yb1	133.61(8)	N11B	C36B	C37B	111.3(4)
P3	N9	Yb2	125.15(8)	C36B	C37B	C38B	111.4(2)
Yb2	N9	Yb1	96.66(5)	C37B	C38B	C39B	109.4(2)
C31	N10	C35	113.46(17)	C40B	C39B	C38B	111.2(2)
C31	N10	P3	123.20(13)	N11B	C40B	C39B	111.2(4)
C35	N10	P3	120.64(14)	C36B	N11B	P3	118.75(19)
C41	N12	C45	111.25(16)	C36B	N11B	C40B	112.9(3)
C41	N12	P3	119.10(13)	C40B	N11B	P3	127.50(19)
C45	N12	P3	113.21(12)	N7A	C21A	C22A	110.1(4)
P4	N13	Yb2	164.70(10)	C21A	C22A	C23A	110.9(2)
C46	N14	P4	118.84(13)	C22A	C23A	C24A	110.4(3)
C50	N14	C46	112.45(16)	C25A	C24A	C23A	112.4(3)
C50	N14	P4	120.57(13)	N7A	C25A	C24A	111.9(4)
C51	N15	C55	109.78(15)	C21A	N7A	P2	121.4(2)
C51	N15	P4	116.19(12)	C21A	N7A	C25A	111.8(5)
C55	N15	P4	116.77(12)	C25A	N7A	P2	121.8(2)
C56	N16	P4	124.40(13)	N7B	C21B	C22B	109.5(16)
C60	N16	C56	111.64(15)	C21B	C22B	C23B	111.5(8)
C60	N16	P4	118.80(12)	C22B	C23B	C24B	110.5(10)
P5	N17	Yb1	135.22(9)	C25B	C24B	C23B	113.7(11)
P5	N17	Yb2	124.56(8)	N7B	C25B	C24B	113.9(10)
Yb2	N17	Yb1	97.20(5)	C21B	N7B	P2	119.8(13)
C61	N18	P5	116.55(13)	C21B	N7B	C25B	112.1(12)
C65	N18	C61	110.59(16)	C25B	N7B	P2	123.2(11)

Table 5.14 Torsion Angles for 2-Yb^{6+}.

A	B	C	D	Angle/°	A	B	C	D	Angle/°
C1	C2	C3	C4	-52.6(3)	C59	C60	N16	P4	143.76(15)
C1	N2	P1	N1	76.27(17)	C60	N16	P4	N13	-33.67(17)
C1	N2	P1	N3	-49.29(16)	C60	N16	P4	N14	93.03(15)

A	B	C	D	Angle/°	A	B	C	D	Angle/°
C1	N2	P1	N4	-158.42(15)	C60	N16	P4	N15	-162.13(14)
C2	C1	N2	C5	-62.5(2)	C61	C62	C63	C64	52.6(3)
C2	C1	N2	P1	160.21(16)	C61	N18	P5	N17	-73.48(16)
C2	C3	C4	C5	52.1(3)	C61	N18	P5	N19	51.32(16)
C3	C4	C5	N2	-56.2(3)	C61	N18	P5	N20	164.63(14)
C4	C5	N2	C1	62.0(2)	C62	C61	N18	C65	63.5(2)
C4	C5	N2	P1	-159.68(15)	C62	C61	N18	P5	-158.37(16)
C5	N2	P1	N1	-58.98(17)	C62	C63	C64	C65	-52.0(3)
C5	N2	P1	N3	175.46(14)	C63	C64	C65	N18	56.6(2)
C5	N2	P1	N4	66.34(15)	C64	C65	N18	C61	-62.9(2)
C6	C7	C8	C9	54.1(3)	C64	C65	N18	P5	159.56(14)
C6	N3	P1	N1	177.78(17)	C65	N18	P5	N17	61.56(16)
C6	N3	P1	N2	-52.2(2)	C65	N18	P5	N19	-173.64(14)
C6	N3	P1	N4	51.2(2)	C65	N18	P5	N20	-60.34(15)
C7	C6	N3	C10	58.1(3)	C66	C67	C68	C69	-54.4(3)
C7	C6	N3	P1	-133.86(19)	C66	N19	P5	N17	173.98(18)
C7	C8	C9	C10	-54.3(3)	C66	N19	P5	N18	45.4(2)
C8	C9	C10	N3	56.0(3)	C66	N19	P5	N20	-61.4(2)
C9	C10	N3	C6	-58.4(3)	C67	C66	N19	C70	-58.3(3)
C9	C10	N3	P1	133.51(19)	C67	C66	N19	P5	133.01(19)
C10	N3	P1	N1	-15.4(2)	C67	C68	C69	C70	54.3(3)
C10	N3	P1	N2	114.65(19)	C68	C69	C70	N19	-55.5(3)

A	B	C	D	Angle/°	A	B	C	D	Angle/°
C10	N3	P1	N4	-141.91(18)	C69	C70	N19	C66	58.0(3)
C11	C12	C13	C14	-54.2(3)	C69	C70	N19	P5	-133.68(18)
C11	N4	P1	N1	152.73(18)	C70	N19	P5	N17	6.7(2)
C11	N4	P1	N2	24.1(2)	C70	N19	P5	N18	-121.94(18)
C11	N4	P1	N3	-81.99(19)	C70	N19	P5	N20	131.31(18)
C12	C11	N4	C15	-56.5(3)	C71	C72	C73	C74	-54.5(3)
C12	C11	N4	P1	126.5(2)	C71	N20	P5	N17	-161.34(16)
C12	C13	C14	C15	54.6(3)	C71	N20	P5	N18	-35.08(19)
C13	C14	C15	N4	-56.3(3)	C71	N20	P5	N19	73.85(19)
C14	C15	N4	C11	57.5(2)	C72	C71	N20	C75	-62.2(2)
C14	C15	N4	P1	-125.25(18)	C72	C71	N20	P5	152.99(16)
C15	N4	P1	N1	-24.02(19)	C72	C73	C74	C75	52.7(3)
C15	N4	P1	N2	-152.68(16)	C73	C74	C75	N20	-56.0(2)
C15	N4	P1	N3	101.26(16)	C74	C75	N20	C71	60.6(2)
C16	C17	C18	C19	53.7(2)	C74	C75	N20	P5	-152.06(13)
C16	N6	P2	N5	47.75(16)	C75	N20	P5	N17	56.03(16)
C16	N6	P2	N8	175.93(14)	C75	N20	P5	N18	-177.71(14)
C16	N6	P2	N7A	-79.1(3)	C75	N20	P5	N19	-68.78(16)
C16	N6	P2	N7B	-83.0(10)	N2	C1	C2	C3	57.5(2)
C17	C16	N6	C20	57.1(2)	N3	C6	C7	C8	-55.6(3)
C17	C16	N6	P2	-159.20(14)	N4	C11	C12	C13	54.7(3)
C17	C18	C19	C20	-55.8(2)	N5	P2	N7A	C21A	-23.0(10)

A	B	C	D	Angle/°	A	B	C	D	Angle/°
C18	C19	C20	N6	58.8(2)	N5	P2	N7A	C25A	-175.8(6)
C19	C20	N6	C16	-59.4(2)	N5	P2	N7B	C21B	3(4)
C19	C20	N6	P2	160.42(14)	N5	P2	N7B	C25B	157(3)
C20	N6	P2	N5	-173.02(14)	N6	C16	C17	C18	-54.4(2)
C20	N6	P2	N8	-44.83(16)	N6	P2	N7A	C21A	104.0(8)
C20	N6	P2	N7A	60.1(3)	N6	P2	N7A	C25A	-48.8(9)
C20	N6	P2	N7B	56.2(10)	N6	P2	N7B	C21B	132(3)
C26	C27	C28	C29	-53.3(3)	N6	P2	N7B	C25B	-74(4)
C26	N8	P2	N5	64.75(16)	N8	C26	C27	C28	57.4(3)
C26	N8	P2	N6	-58.79(15)	N8	P2	N7A	C21A	-152.1(8)
C26	N8	P2	N7A	-170.6(4)	N8	P2	N7A	C25A	55.1(9)
C26	N8	P2	N7B	-168.7(15)	N8	P2	N7B	C21B	-125(3)
C27	C26	N8	C30	-60.6(2)	N8	P2	N7B	C25B	28(4)
C27	C26	N8	P2	165.14(14)	N9	P3	N11A	C36A	49.3(17)
C27	C28	C29	C30	52.7(3)	N9	P3	N11A	C40A	-153.7(14)
C28	C29	C30	N8	-56.2(2)	N9	P3	N11B	C36B	33.5(9)
C29	C30	N8	C26	60.0(2)	N9	P3	N11B	C40B	-135.3(8)
C29	C30	N8	P2	-165.43(14)	N10	C31	C32	C33	55.3(3)
C30	N8	P2	N5	-67.31(16)	N10	P3	N11A	C36A	-73.6(15)
C30	N8	P2	N6	169.15(14)	N10	P3	N11A	C40A	83.4(16)
C30	N8	P2	N7A	57.3(4)	N10	P3	N11B	C36B	-93.2(8)
C30	N8	P2	N7B	59.3(15)	N10	P3	N11B	C40B	98.0(10)

A	B	C	D	Angle/°	A	B	C	D	Angle/°
C31	C32	C33	C34	-55.4(3)	N12	C41	C42	C43	-56.5(3)
C31	N10	P3	N9	6.35(19)	N12	P3	N11A	C36A	177.5(13)
C31	N10	P3	N12	-121.49(17)	N12	P3	N11A	C40A	-25.5(18)
C31	N10	P3	N11A	130.3(2)	N12	P3	N11B	C36B	157.5(8)
C31	N10	P3	N11B	132.74(18)	N12	P3	N11B	C40B	-11.3(10)
C32	C31	N10	C35	-55.1(3)	N14	C46	C47	C48	-55.9(3)
C32	C31	N10	P3	143.43(17)	N15	C51	C52	C53	57.0(2)
C32	C33	C34	C35	54.5(3)	N16	C56	C57	C58	-54.4(2)
C33	C34	C35	N10	-53.9(3)	N18	C61	C62	C63	-57.8(2)
C34	C35	N10	C31	54.9(3)	N19	C66	C67	C68	56.1(3)
C34	C35	N10	P3	-143.2(2)	N20	C71	C72	C73	59.6(3)
C35	N10	P3	N9	-153.82(19)	Yb1	N5	P2	N6	-76.0(5)
C35	N10	P3	N12	78.3(2)	Yb1	N5	P2	N8	167.5(5)
C35	N10	P3	N11A	-29.9(3)	Yb1	N5	P2	N7A	48.9(7)
C35	N10	P3	N11B	-27.4(2)	Yb1	N5	P2	N7B	50(2)
C41	C42	C43	C44	53.8(3)	Yb1	N9	P3	N10	33.28(14)
C41	N12	P3	N9	-84.53(16)	Yb1	N9	P3	N12	154.40(10)
C41	N12	P3	N10	40.80(17)	Yb1	N9	P3	N11A	-84.4(7)
C41	N12	P3	N11A	148.9(8)	Yb1	N9	P3	N11B	-92.0(4)
C41	N12	P3	N11B	154.7(4)	Yb1	N17	P5	N18	61.15(15)
C42	C41	N12	C45	59.0(2)	Yb1	N17	P5	N19	-59.49(15)
C42	C41	N12	P3	-166.54(15)	Yb1	N17	P5	N20	177.16(11)

A	B	C	D	Angle/°	A	B	C	D	Angle/°
C42	C43	C44	C45	-52.8(3)	Yb2	N9	P3	N10	-176.65(9)
C43	C44	C45	N12	56.2(2)	Yb2	N9	P3	N12	-55.53(12)
C44	C45	N12	C41	-59.6(2)	Yb2	N9	P3	N11A	65.6(7)
C44	C45	N12	P3	163.18(14)	Yb2	N9	P3	N11B	58.1(4)
C45	N12	P3	N9	49.10(15)	Yb2	N13	P4	N14	97.1(4)
C45	N12	P3	N10	174.43(13)	Yb2	N13	P4	N15	-20.2(4)
C45	N12	P3	N11A	-77.5(8)	Yb2	N13	P4	N16	-137.0(4)
C45	N12	P3	N11B	-71.7(4)	Yb2	N17	P5	N18	-94.39(11)
C46	C47	C48	C49	54.6(3)	Yb2	N17	P5	N19	144.98(10)
C46	N14	P4	N13	27.93(18)	Yb2	N17	P5	N20	21.63(13)
C46	N14	P4	N15	156.54(16)	C36A	C37A	C38A	C39A	56.5(5)
C46	N14	P4	N16	-98.95(16)	C37A	C36A	N11A	P3	-143.1(12)
C47	C46	N14	C50	57.3(2)	C37A	C36A	N11A	C40A	57.0(16)
C47	C46	N14	P4	-153.82(16)	C37A	C38A	C39A	C40A	-57.2(5)
C47	C48	C49	C50	-54.3(3)	C38A	C39A	C40A	N11A	57.6(8)
C48	C49	C50	N14	55.7(3)	C39A	C40A	N11A	P3	144.6(14)
C49	C50	N14	C46	-57.2(3)	C39A	C40A	N11A	C36A	-57.2(15)
C49	C50	N14	P4	154.54(17)	N11A	C36A	C37A	C38A	-56.6(8)
C50	N14	P4	N13	174.19(16)	C36B	C37B	C38B	C39B	-55.1(4)
C50	N14	P4	N15	-57.20(18)	C37B	C36B	N11B	P3	134.0(6)
C50	N14	P4	N16	47.31(19)	C37B	C36B	N11B	C40B	-55.7(9)
C51	C52	C53	C54	-52.6(3)	C37B	C38B	C39B	C40B	55.1(4)

A	B	C	D	Angle/°	A	B	C	D	Angle/°
C51	N15	P4	N13	65.19(16)	C38B	C39B	C40B	N11B	-55.6(5)
C51	N15	P4	N14	-58.13(15)	C39B	C40B	N11B	P3	-134.8(8)
C51	N15	P4	N16	-171.47(14)	C39B	C40B	N11B	C36B	55.9(9)
C52	C51	N15	C55	-62.4(2)	N11B	C36B	C37B	C38B	55.4(5)
C52	C51	N15	P4	162.32(14)	C21A	C22A	C23A	C24A	-51.8(4)
C52	C53	C54	C55	53.5(3)	C22A	C21A	N7A	P2	144.6(7)
C53	C54	C55	N15	-58.9(2)	C22A	C21A	N7A	C25A	-60.1(8)
C54	C55	N15	C51	63.5(2)	C22A	C23A	C24A	C25A	50.2(6)
C54	C55	N15	P4	-161.58(14)	C23A	C24A	C25A	N7A	-53.2(7)
C55	N15	P4	N13	-66.91(16)	C24A	C25A	N7A	P2	-146.2(7)
C55	N15	P4	N14	169.77(14)	C24A	C25A	N7A	C21A	58.7(9)
C55	N15	P4	N16	56.43(15)	N7A	C21A	C22A	C23A	57.2(5)
C56	C57	C58	C59	51.5(3)	C21B	C22B	C23B	C24B	2.9(19)
C56	N16	P4	N13	173.90(15)	C22B	C21B	N7B	P2	-143(3)
C56	N16	P4	N14	-59.39(17)	C22B	C21B	N7B	C25B	61(4)
C56	N16	P4	N15	45.45(17)	C22B	C23B	C24B	C25B	48(3)
C57	C56	N16	C60	58.8(2)	C23B	C24B	C25B	N7B	-46(3)
C57	C56	N16	P4	-147.07(14)	C24B	C25B	N7B	P2	-165(3)
C57	C58	C59	C60	-52.4(3)	C24B	C25B	N7B	C21B	-9(4)
C58	C59	C60	N16	56.8(2)	N7B	C21B	C22B	C23B	-56.8(18)
C59	C60	N16	C56	-60.5(2)					

Table 5.15 Hydrogen Atom Coordinates (Å×10^4) and Isotropic Displacement Parameters (Å^2×10^3) for 2-Yb^{6+}.

Atom	*x*	*y*	*z*	U(eq)
H1A	5470.88	3615.16	7238.96	31
H1B	4720.77	3123.96	7660.46	31
H2A	6114.57	2717.86	7805.32	47
H2B	6936.93	3905.21	7872.86	47
H3A	6791.98	3415.94	8723.37	55
H3B	5551.14	2923.83	8590.95	55
H4A	6156.16	4508.72	9094.74	49
H4B	6970.52	5068	8712.1	49
H5A	4753.77	4187.18	8412.71	32
H5B	5536.66	5387.87	8498.25	32
H6A	6606.41	4810.1	6747.38	35
H6B	6965.67	5845.4	7130.56	35
H7A	7513.49	6196.28	6295.16	46
H7B	6766.23	6683.65	6402.09	46
H8A	6153.04	4829.63	5723.26	51
H8B	6220.41	5869.65	5527.27	51
H9A	4817.7	5700.85	5938.43	49
H9B	4457.01	4655.79	5563.45	49
H10A	3979.35	4328.63	6414.53	39
H10B	4742.32	3865.68	6297.94	39
H11A	7109.59	6358.94	8000.36	36
H11B	6855.02	7083.64	8375.49	36
H12A	8306.44	8128.01	8003.74	50
H12B	7693.63	7603.36	7414.63	50
H13A	7225.35	8893.06	8089.09	50
H13B	7677.32	9179.13	7549.46	50
H14A	6123.18	7917.78	7040.62	41
H14B	5847.16	8629	7413.61	41
H15A	5360	7412.15	8020.48	34
H15B	4711.33	6864.5	7440.65	34
H16A	2613.59	3150.26	5538.59	28
H16B	2301.09	3818.17	5918.57	28
H17A	1360.61	4114.84	5188.61	33
H17B	2505.32	4434.35	5070.36	33
H18A	1909.75	2910.98	4505.74	35
H18B	1192.92	3434.98	4314.49	35
H19A	-117.9	2337.41	4756.53	32
H19B	159.26	1652.66	4365.89	32

Atom	*x*	*y*	*z*	U(eq)
H20A	80.13	1062.4	5214.11	27
H20B	1231.23	1463.13	5087.23	27
H26A	-759.46	1731.96	5742	28
H26B	-1008.59	1642.07	6334.56	28
H27A	-1850.74	-35.5	5499.15	44
H27B	-2500.14	471.26	5729.81	44
H28A	-2347.53	-137.51	6552.23	46
H28B	-2785.07	-1088.72	6096.9	46
H29A	-1149.55	-1009.49	6147.86	42
H29B	-1393.06	-1026.37	6740.76	42
H30A	-339.69	748.9	6928.75	30
H30B	328.68	244.54	6718.58	30
H31A	2736.12	3115.52	8061.05	29
H31B	1981.83	2057.97	7693.48	29
H32A	3203.38	2260.95	8705.93	39
H32B	3399.24	1918.4	8144.96	39
H33A	1844.97	381.26	8036.13	46
H33B	2528.22	474.6	8601.11	46
H34A	757.88	-26.76	8673.26	52
H34B	1533.91	1019.69	9044.89	52
H35A	329.74	841.78	8038.25	49
H35B	167.47	1218.5	8599.76	49
H41A	2703.28	4162.67	9367	32
H41B	2184.4	2939.12	9303.54	32
H42A	2527.44	3612.09	10215.38	44
H42B	1311.2	2884.76	10018.15	44
H43A	1499.47	4358.04	10504.8	40
H43B	2300.54	5076.83	10152.46	40
H44A	689.86	4992.78	9841.91	33
H44B	130.34	3769.23	9786.05	33
H45A	366.08	4288.29	8937.22	29
H45B	1584.3	4989.38	9145.25	29
H46A	5126.55	6924.27	8962.08	34
H46B	3939.03	6062.7	8872.13	34
H47A	5033.01	5555.35	9424.69	36
H47B	4174.69	5613.83	9731.98	36
H48A	5784.34	6427.39	10312.03	40
H48B	6309.92	7145.69	9875.53	40
H49A	4742.29	7222.64	10408.27	45
H49B	5923.18	8094.84	10487.22	45
H50A	4804.57	8545.59	9919.9	36

Atom	*x*	*y*	*z*	U(eq)
H50B	5667.7	8483.33	9618.42	36
H51A	2792.64	6925.16	9893.74	27
H51B	1697.38	6794.85	9594.91	27
H52A	2994.9	8309.78	10478.06	32
H52B	1910	7341.75	10505.05	32
H53A	990.27	7998.69	9964.69	41
H53B	1741.01	8882.04	10437.65	41
H54A	1813.33	9513.41	9585.37	36
H54B	2933.68	9701.53	9878.9	36
H55A	1610.52	8044.02	9059.68	27
H55B	2648.57	9019.49	8977.8	27
H56A	5498.42	9807.98	9132.84	28
H56B	4540.34	9713.96	9404	28
H57A	4064.8	10559.43	8751.18	32
H57B	5266.88	11257.02	8997.69	32
H58A	5778.22	10770.11	8261.12	38
H58B	4924.55	11122.57	8045.12	38
H59A	3639.26	9430.08	7825.78	37
H59B	4613.43	9538.73	7565.74	37
H60A	3960.17	8038.28	8000.7	29
H60B	5139.82	8799.64	8265.64	29
H61A	167.55	3695.04	6190.88	32
H61B	828.03	4592.35	5861.17	32
H62A	-717.7	4465.41	5362.87	38
H62B	-740.59	3370.4	5306.07	38
H63A	-1858.18	2785.75	5919.83	41
H63B	-2356.42	3255.29	5483.31	41
H64A	-2386.96	3817.06	6379.15	37
H64B	-1794.85	4753.29	6056.32	37
H65A	-782.92	5056.55	6910.44	30
H65B	-782.84	3974.78	6819.46	30
H66A	1119.93	6701.13	5868.36	44
H66B	1649.17	6157.65	5552.88	44
H67A	2420.5	7897.63	5439.06	49
H67B	2694.96	8216.83	6070.58	49
H68A	4199.06	8368.8	5779.97	51
H68B	3594.43	7221.5	5485.09	51
H69A	4558.26	7210.9	6300.01	48
H69B	4058.24	7779.51	6620.69	48
H70A	2950.67	5734.88	6082.74	30
H70B	3210.22	6033.09	6715.62	30

Atom	*x*	*y*	*z*	U(eq)
H71A	-296.77	6437.64	6435.16	37
H71B	631.78	7574.26	6469.97	37
H72A	-693.6	6873.4	7250.21	47
H72B	-760.89	7620.37	6828.87	47
H73A	183.58	8551.73	7684.26	40
H73B	882.04	8923.71	7230.23	40
H74A	1892.81	8689.63	7954.49	31
H74B	989.42	7565.15	7979.33	31
H75A	2178.03	8153.64	7138.18	26
H75B	2261.48	7419.64	7563.65	26
H36A	-784.46	1519.53	7527.66	25
H36B	-97.71	2662.71	7405.1	25
H37A	-1886.23	2082.78	7054.59	28
H37B	-1456.29	3067.06	7487.58	28
H38A	-3070.14	1830.68	7661.06	28
H38B	-2657.09	992.8	7690.47	28
H39A	-1840.78	2827.88	8425.15	28
H39B	-2522.98	1698.99	8568.05	28
H40A	-727.86	2259.07	8890.29	23
H40B	-1186.01	1265.31	8460.75	23
H36C	-159.3	2838.92	7442.35	25
H36D	-927.74	3215.29	7652.05	25
H37C	-1367.04	1125.17	7432.7	28
H37D	-1927.57	1674.98	7092.41	28
H38C	-2994.95	638.94	7680.59	28
H38D	-2741.3	1811.27	7803.82	28
H39C	-2453.44	1211.73	8616.69	28
H39D	-1696.56	834.95	8393.13	28
H40C	-1259.91	2927.55	8605.75	23
H40D	-676.59	2391.56	8940.68	23
H21A	3011.52	2468.31	6907.28	29
H21B	3439.79	2220.75	6403	29
H22A	2684.59	868.17	7190.71	39
H22B	3878.77	1468.82	7127.17	39
H23A	3058.93	-292.23	6730.87	37
H23B	3553	490.83	6313.84	37
H24A	1886.07	-697.48	5885.63	48
H24B	1383.5	-568.39	6384.16	48
H25A	2198.84	893.68	5674.43	29
H25B	1004.07	284.53	5733.68	29
H21C	2353.46	1087.15	7034.52	29

Atom	*x*	*y*	*z*	U(eq)
H21D	2893.39	2268.11	6941.04	29
H22C	4065.64	1567.35	6904.12	39
H22D	3848.72	1960.24	6349.99	39
H23C	3507.18	26.15	6500.15	37
H23D	3349.69	434.49	5941.97	37
H24C	1741.78	-888.62	6003.58	48
H24D	1811.34	-458.42	6601.37	48
H25C	1383.62	304.1	5662.76	29
H25D	667.08	-98.28	6104.72	29

Table 5.16 Atomic Occupancy for 2-Yb^{6+}.

Atom	*Occupancy*	Atom	*Occupancy*	Atom	*Occupancy*
C36A	0.374(2)	H36A	0.374(2)	H36B	0.374(2)
C37A	0.374(2)	H37A	0.374(2)	H37B	0.374(2)
C38A	0.374(2)	H38A	0.374(2)	H38B	0.374(2)
C39A	0.374(2)	H39A	0.374(2)	H39B	0.374(2)
C40A	0.374(2)	H40A	0.374(2)	H40B	0.374(2)
N11A	0.374(2)	C36B	0.626(2)	H36C	0.626(2)
H36D	0.626(2)	C37B	0.626(2)	H37C	0.626(2)
H37D	0.626(2)	C38B	0.626(2)	H38C	0.626(2)
H38D	0.626(2)	C39B	0.626(2)	H39C	0.626(2)
H39D	0.626(2)	C40B	0.626(2)	H40C	0.626(2)
H40D	0.626(2)	N11B	0.626(2)	C21A	0.817(3)
H21A	0.817(3)	H21B	0.817(3)	C22A	0.817(3)
H22A	0.817(3)	H22B	0.817(3)	C23A	0.817(3)
H23A	0.817(3)	H23B	0.817(3)	C24A	0.817(3)
H24A	0.817(3)	H24B	0.817(3)	C25A	0.817(3)
H25A	0.817(3)	H25B	0.817(3)	N7A	0.817(3)
C21B	0.183(3)	H21C	0.183(3)	H21D	0.183(3)
C22B	0.183(3)	H22C	0.183(3)	H22D	0.183(3)
C23B	0.183(3)	H23C	0.183(3)	H23D	0.183(3)
C24B	0.183(3)	H24C	0.183(3)	H24D	0.183(3)
C25B	0.183(3)	H25C	0.183(3)	H25D	0.183(3)
N7B	0.183(3)				

Table 5.17 Solvent masks information for 2-Yb^{6+}.

Number	X	Y	Z	Volume	Electron count	Content
1	0.000	0.000	0.000	297.1	40.2	?
2	0.500	0.000	0.500	444.2	108.5	?

5.5.3 *3-Yb*$^{5+}$

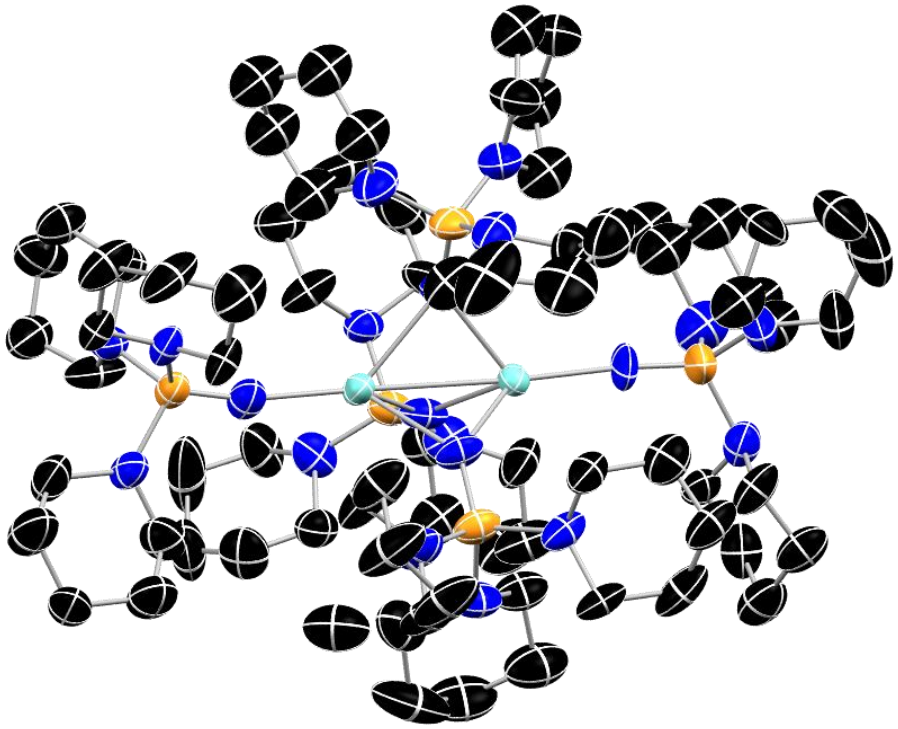

Figure 5.14 Molecular structure of 3-Yb^{5+} with thermal ellipsoids shown at 50% probability with hydrogen atoms omitted for clarity. Color code: C, black; N, blue; P, orange; Yb, blue.

Table 5.18 Crystal data and structure refinement for 3-Yb^{5+}.

Identification code	3-Yb^{5+}
Empirical formula	$C_{78}HN_{22}OP_5Yb_2$
Formula weight	1745.93
Temperature/K	100.15
Crystal system	monoclinic
Space group	$P2_1$
a/Å	13.934(6)
b/Å	27.807(7)
c/Å	14.069(6)
α/°	90

β/°	119.590(10)
γ/°	90
Volume/Å^3	4740(3)
Z	2
ρ_{calc}g/cm^3	1.223
μ/mm^{-1}	2.092
F(000)	1674.0
Crystal size/mm^3	? × ? × ?
Radiation	MoKα (λ = 0.71073)
2Θ range for data collection/°	4.434 to 52.64
Index ranges	-17 ≤ h ≤ 17, -34 ≤ k ≤ 34, -17 ≤ l ≤ 17
Reflections collected	79704
Independent reflections	19146 [R_{int} = 0.0950, R_{sigma} = 0.0835]
Data/restraints/parameters	19146/1/839
Goodness-of-fit on F^2	1.094
Final R indexes [I>=2σ (I)]	R_1 = 0.0627, wR_2 = 0.1577
Final R indexes [all data]	R_1 = 0.0862, wR_2 = 0.1743
Largest diff. peak/hole / e Å^{-3}	2.43/-0.92
Flack parameter	-0.004(18)

Table 5.19 Fractional Atomic Coordinates (×10^4) and Equivalent Isotropic Displacement Parameters (Å^2×10^3) for 3-Yb^{5+}. U_{eq} is defined as 1/3 of the trace of the orthogonalised U_{IJ} tensor.

Atom	*x*	*y*	*z*	U(eq)
Yb2	7115.0(5)	4419.3(2)	3554.0(5)	39.60(16)
Yb1	6495.5(5)	5416.9(2)	3747.9(5)	42.02(17)
P2	9452(4)	5142(2)	5173(4)	56.7(12)
P5	5831(3)	6700.5(15)	3715(4)	49.1(10)
P1	5674(4)	4997(2)	993(4)	66.7(14)
P3	5409(3)	4561.4(18)	4838(3)	53.7(11)
P4	7686(5)	3158.3(19)	3331(5)	75.3(16)
N6	8236(10)	5072(6)	4280(11)	56(4)
N21	5911(11)	6989(5)	2737(12)	51(3)
N7	10320(12)	4781(6)	4969(12)	60(4)
N15	6610(20)	2814(10)	3180(20)	120(3)
N8	9819(14)	4994(7)	6471(12)	72(5)
N19	6535(12)	7030(5)	4877(12)	58(4)
N4	4923(17)	5479(8)	438(14)	92(6)
N14	7455(18)	3689(6)	3345(15)	89(6)
N22	4513(11)	6849(5)	3344(10)	51(3)
N11	5384(13)	4987(6)	5642(14)	64(4)

Atom	*x*	*y*	*z*	U(eq)
N10	6302(12)	4667(6)	4508(11)	61(4)
N18	6166(12)	6179(5)	3879(13)	61(4)
N12	5596(13)	4033(6)	5478(13)	66(4)
N9	9839(13)	5712(6)	5284(15)	72(5)
N16	8070(20)	3002(7)	2455(16)	104(7)
N13	4059(11)	4540(5)	3843(10)	55(4)
N17	8677(13)	2894(5)	4513(14)	65(4)
C20	8048(17)	7615(8)	6693(19)	83(7)
C3	8800(30)	5175(16)	760(30)	131(13)
N2	6697(15)	5063(7)	700(13)	79(5)
N1	5940(12)	4913(6)	2173(10)	58(4)
N5	4992(16)	4555(7)	194(13)	82(5)
C15	11495(15)	4683(8)	5837(16)	70(6)
C1AA	9505(17)	4499(9)	6581(15)	74(6)
C70	4150(16)	6673(10)	4120(15)	84(7)
C19	10175(16)	4777(8)	3894(15)	64(5)
C13	3710(30)	4398(14)	-1710(20)	120(3)
C65	5590(14)	7508(6)	2436(15)	59(4)
C52	8050(50)	2413(13)	1110(40)	180(20)
C50	6760(30)	2291(12)	3240(30)	120(3)
C37	6490(20)	3422(11)	7360(20)	105(9)
C54	7680(20)	3247(10)	595(19)	94(8)
C69	6915(16)	6890(7)	2622(18)	66(5)
C74	3648(16)	6682(8)	2233(16)	71(5)
C33	4450(30)	5558(11)	6280(40)	149(16)
C10	4980(30)	4114(13)	560(30)	120(3)
C35	4908(19)	3850(8)	5930(20)	83(6)
C66	5325(19)	7602(10)	1270(20)	97(8)
C14	4730(20)	4577(10)	-944(17)	99(8)
C18	10410(20)	4262(8)	3670(20)	82(6)
C21	10140(20)	4324(13)	7790(20)	109(10)
C38	7220(20)	3620(11)	6880(20)	99(9)
C62	7120(20)	7843(9)	5590(30)	120(11)
C56	9827(17)	3098(9)	4820(20)	80(7)
C40	3814(17)	4100(8)	3146(16)	74(6)
C71	3050(20)	6884(11)	3880(18)	90(8)
C7	2980(30)	6070(12)	-850(30)	120(3)
C60	8504(14)	2970(7)	5413(15)	62(5)
C72	2168(18)	6746(10)	2739(19)	88(7)
C24	9470(19)	5349(11)	7040(20)	93(7)
C5	4270(30)	5677(12)	890(30)	120(3)

Atom	*x*	*y*	*z*	U(eq)
C61	6202(18)	7507(8)	5050(20)	97(8)
C43	2360(20)	4945(10)	2463(19)	84(7)
C46	4510(30)	2789(12)	2200(30)	120(3)
C31	6490(20)	5648(9)	6880(20)	88(7)
C57	10631(16)	2799(9)	5721(19)	77(6)
C25	9203(17)	6104(9)	4560(20)	88(7)
C17	11560(18)	4119(9)	4470(20)	84(7)
C36	5620(30)	3753(12)	7140(30)	120(3)
C59	9300(20)	2699(8)	6370(20)	84(7)
C51	8390(30)	2515(12)	2320(30)	146(15)
C30	6473(16)	5138(8)	6538(16)	65(5)
C1	7360(20)	4636(9)	813(19)	89(8)
C42	2084(18)	4523(16)	1714(19)	125(13)
C23	10060(30)	5196(16)	8300(20)	140(15)
C55	8340(30)	3419(13)	1760(30)	120(3)
C2	8100(30)	4705(14)	260(30)	122(11)
C68	6630(20)	6936(12)	1410(20)	105(9)
C41	2580(20)	4062(10)	2420(20)	94(8)
C34	4490(18)	5047(10)	5930(20)	89(7)
C29	11006(15)	5873(9)	6030(20)	85(7)
C67	6310(20)	7464(12)	1100(20)	106(10)
C16	11788(18)	4180(9)	5620(20)	90(8)
C32	5590(30)	5734(10)	7200(30)	110(10)
C39	6460(20)	3688(9)	5670(20)	86(7)
C48	4560(30)	2235(12)	2250(30)	120(3)
C58	10527(18)	2856(9)	6770(20)	88(7)
C12	3420(20)	3913(11)	-1360(20)	112(10)
C0AA	8190(30)	5594(15)	770(30)	147(16)
C53	8040(30)	2785(15)	390(30)	134(12)
C47	5610(30)	3039(12)	2050(30)	120(3)
C28	11561(19)	6035(10)	5440(30)	113(11)
C64	7368(19)	6811(8)	5893(18)	76(6)
C22	9850(30)	4677(13)	8470(20)	113(10)
C8	3680(30)	5859(12)	-1320(30)	120(3)
C44	3653(17)	4981(9)	3223(19)	79(7)
C4	7370(20)	5515(9)	1260(20)	91(7)
C26	9703(18)	6270(10)	3940(20)	97(8)
C6	3100(30)	5771(12)	120(30)	120(3)
C27	10920(20)	6440(10)	4600(30)	134(14)
C63	8400(20)	7117(10)	6490(20)	96(8)
C11	3630(30)	3896(12)	-120(30)	120(3)

Atom	*x*	*y*	*z*	U(eq)
C73	2547(16)	6896(9)	1893(17)	74(6)
C9	4790(30)	5754(12)	-530(30)	120(3)
C49	5820(30)	2100(12)	3270(30)	120(3)
C77	9830(30)	6057(14)	6730(30)	128(12)

Table 5.20 Anisotropic Displacement Parameters ($Å^2×10^3$) for 3-Yb^{5+}. The Anisotropic displacement factor exponent takes the form: $-2\pi^2[h^2a^{*2}U_{11}+2hka^*b^*U_{12}+\ldots]$.

Atom	U_{11}	U_{22}	U_{33}	U_{23}	U_{13}	U_{12}
Yb2	44.2(3)	40.4(3)	35.9(3)	-1.0(3)	21.1(3)	2.6(3)
Yb1	38.5(3)	37.3(3)	42.1(3)	1.1(3)	13.7(3)	3.3(3)
P2	37(2)	82(3)	48(2)	12(2)	18.6(19)	-2(2)
P5	41(2)	40(2)	57(2)	2.1(18)	17.4(19)	1.1(16)
P1	64(3)	98(4)	33(2)	4(2)	19(2)	13(3)
P3	43(2)	80(3)	41(2)	-2.9(19)	22.9(18)	-7.2(19)
P4	82(4)	55(3)	66(3)	-11(2)	19(3)	22(3)
N6	28(6)	83(10)	51(8)	12(7)	15(6)	-5(6)
N21	40(7)	42(7)	66(8)	8(6)	22(6)	8(5)
N7	44(8)	85(11)	55(8)	25(8)	27(7)	16(7)
N15	102(5)	122(6)	111(5)	9(5)	33(4)	20(5)
N8	65(11)	110(14)	42(8)	3(8)	25(8)	-4(10)
N19	56(8)	37(7)	60(8)	8(6)	13(7)	2(6)
N4	101(14)	116(16)	59(9)	23(11)	39(10)	46(13)
N14	123(16)	51(9)	75(11)	2(8)	34(11)	50(10)
N22	50(8)	53(7)	41(7)	2(6)	16(6)	1(6)
N11	55(9)	83(11)	76(11)	-14(8)	49(8)	-18(8)
N10	45(8)	99(12)	37(7)	-7(7)	18(6)	-13(8)
N18	47(8)	48(8)	74(10)	-2(7)	18(8)	-1(6)
N12	61(9)	91(12)	64(9)	12(8)	45(8)	3(8)
N9	42(8)	74(10)	78(11)	10(9)	13(8)	-1(7)
N16	150(20)	77(12)	73(12)	-11(10)	45(13)	47(13)
N13	48(7)	76(10)	39(7)	-1(6)	21(6)	7(6)
N17	55(9)	54(8)	83(11)	1(8)	32(8)	6(7)
C20	63(12)	66(12)	82(14)	-27(11)	6(11)	-6(9)
C3	170(30)	170(30)	90(20)	40(20)	90(20)	30(30)
N2	83(12)	112(15)	49(9)	20(9)	38(9)	36(11)
N1	57(9)	78(9)	33(7)	-3(6)	17(6)	6(7)
N5	84(12)	85(13)	54(9)	-2(8)	16(9)	20(9)
C15	41(10)	92(14)	58(11)	29(10)	10(8)	13(9)
C1AA	70(12)	101(17)	49(9)	25(11)	28(9)	-1(12)

Atom	U_{11}	U_{22}	U_{33}	U_{23}	U_{13}	U_{12}
C70	51(11)	150(20)	43(10)	13(11)	14(9)	-10(12)
C19	61(11)	84(14)	56(10)	20(9)	36(9)	23(10)
C13	102(5)	122(6)	111(5)	9(5)	33(4)	20(5)
C65	50(10)	55(10)	66(11)	12(8)	24(9)	17(8)
C52	270(60)	80(20)	210(40)	-50(30)	110(40)	20(30)
C50	102(5)	122(6)	111(5)	9(5)	33(4)	20(5)
C37	106(19)	130(20)	99(18)	60(17)	63(16)	14(17)
C54	110(20)	103(18)	60(13)	-34(12)	38(13)	-10(15)
C69	57(11)	62(11)	86(13)	25(10)	40(10)	25(9)
C74	54(11)	93(15)	58(11)	-14(10)	21(9)	2(10)
C33	83(19)	100(20)	270(50)	-70(30)	90(30)	0(15)
C10	102(5)	122(6)	111(5)	9(5)	33(4)	20(5)
C35	71(14)	79(14)	88(16)	-1(12)	32(12)	-19(11)
C66	54(12)	130(20)	104(18)	42(16)	35(13)	27(13)
C14	93(17)	130(20)	50(11)	-12(12)	21(11)	4(15)
C18	81(15)	81(15)	90(15)	22(11)	48(13)	10(11)
C21	84(16)	170(30)	68(14)	22(17)	38(13)	6(18)
C38	63(14)	130(20)	79(15)	33(15)	18(12)	-9(13)
C62	79(17)	75(15)	130(20)	-14(15)	-5(16)	5(13)
C56	48(11)	86(15)	104(18)	34(13)	38(12)	22(10)
C40	58(12)	97(16)	56(11)	-28(11)	20(9)	-21(11)
C71	81(16)	130(20)	60(12)	9(13)	39(12)	35(15)
C7	102(5)	122(6)	111(5)	9(5)	33(4)	20(5)
C60	42(9)	64(11)	61(11)	-3(9)	11(8)	4(8)
C72	56(12)	130(20)	80(15)	-25(14)	31(11)	-14(12)
C24	78(14)	130(20)	93(16)	-23(16)	60(13)	-2(15)
C5	102(5)	122(6)	111(5)	9(5)	33(4)	20(5)
C61	62(13)	68(13)	114(19)	-10(13)	9(13)	18(10)
C43	67(14)	117(18)	61(13)	1(13)	26(11)	5(12)
C46	102(5)	122(6)	111(5)	9(5)	33(4)	20(5)
C31	83(16)	71(13)	109(19)	-11(13)	48(15)	-22(12)
C57	45(11)	93(15)	88(15)	26(12)	29(10)	3(10)
C25	52(11)	87(15)	113(18)	42(14)	33(12)	16(10)
C17	58(12)	117(18)	86(15)	44(13)	43(11)	30(12)
C36	102(5)	122(6)	111(5)	9(5)	33(4)	20(5)
C59	90(17)	65(13)	110(20)	-1(12)	64(16)	2(11)
C51	190(40)	110(20)	120(20)	-18(19)	60(20)	80(20)
C30	51(11)	88(14)	56(11)	-5(10)	27(9)	3(10)
C1	106(18)	108(18)	72(14)	17(12)	57(14)	47(14)
C42	47(12)	250(40)	58(12)	30(20)	15(10)	22(19)
C23	110(20)	240(50)	70(16)	-60(20)	47(16)	-70(30)

Atom	U_{11}	U_{22}	U_{33}	U_{23}	U_{13}	U_{12}
C55	102(5)	122(6)	111(5)	9(5)	33(4)	20(5)
C2	120(20)	150(30)	120(20)	20(20)	70(20)	50(20)
C68	89(18)	150(20)	110(20)	24(18)	75(17)	24(17)
C41	80(16)	104(19)	89(17)	-45(15)	35(14)	-28(14)
C34	64(13)	114(19)	118(19)	-39(15)	66(14)	-7(12)
C29	32(9)	99(16)	84(15)	5(13)	-1(10)	-10(10)
C67	76(15)	170(30)	80(15)	66(17)	46(13)	57(17)
C16	57(12)	83(14)	114(19)	56(14)	30(13)	20(11)
C32	110(20)	80(16)	150(30)	-35(17)	70(20)	15(14)
C39	89(16)	91(16)	83(15)	33(13)	45(13)	46(13)
C48	102(5)	122(6)	111(5)	9(5)	33(4)	20(5)
C58	57(13)	89(16)	99(17)	11(13)	24(12)	5(11)
C12	89(18)	120(20)	87(18)	-30(16)	11(14)	13(16)
C0AA	160(30)	160(30)	170(30)	110(30)	120(30)	50(30)
C53	140(30)	140(30)	110(20)	-60(20)	50(20)	-10(20)
C47	102(5)	122(6)	111(5)	9(5)	33(4)	20(5)
C28	47(12)	97(18)	140(20)	44(17)	1(13)	-15(11)
C64	77(14)	66(12)	74(13)	-9(10)	29(11)	-13(10)
C22	110(20)	170(30)	61(14)	32(16)	40(14)	-14(19)
C8	102(5)	122(6)	111(5)	9(5)	33(4)	20(5)
C44	45(11)	97(16)	80(14)	40(12)	19(10)	6(10)
C4	81(15)	85(17)	110(18)	31(14)	49(14)	-1(12)
C26	54(12)	101(18)	120(20)	29(15)	34(13)	-5(12)
C6	102(5)	122(6)	111(5)	9(5)	33(4)	20(5)
C27	74(16)	89(17)	160(30)	54(19)	-5(17)	-8(14)
C63	65(14)	86(16)	94(17)	-8(13)	7(12)	-2(12)
C11	102(5)	122(6)	111(5)	9(5)	33(4)	20(5)
C73	47(10)	106(17)	69(12)	14(11)	29(9)	5(10)
C9	102(5)	122(6)	111(5)	9(5)	33(4)	20(5)
C49	102(5)	122(6)	111(5)	9(5)	33(4)	20(5)
C77	110(20)	150(30)	90(20)	-10(20)	25(18)	-20(20)

Table 5.21 Bond Lengths for 3-Yb^{5+}.

Atom	Atom	Length/Å	Atom	Atom	Length/Å
Yb2	Yb1	2.9576(10)	N2	C1	1.46(3)
Yb2	P2	3.536(5)	N2	C4	1.53(3)
Yb2	P1	3.528(5)	N5	C10	1.33(4)
Yb2	N6	2.282(14)	N5	C14	1.46(3)
Yb2	N14	2.137(15)	C15	C16	1.53(3)
Yb2	N10	2.250(15)	C1AA	C21	1.56(3)

Atom	Atom	Length/Å	Atom	Atom	Length/Å
Yb2	N1	2.281(14)	C70	C71	1.51(3)
Yb1	N6	2.360(13)	C19	C18	1.54(3)
Yb1	N10	2.418(16)	C13	C14	1.38(4)
Yb1	N18	2.195(15)	C13	C12	1.56(5)
Yb1	N1	2.404(14)	C65	C66	1.52(3)
P2	N6	1.544(13)	C52	C51	1.54(6)
P2	N7	1.702(16)	C52	C53	1.45(6)
P2	N8	1.686(16)	C50	C49	1.43(5)
P2	N9	1.657(17)	C37	C38	1.58(3)
P5	N21	1.643(15)	C37	C36	1.43(4)
P5	N19	1.700(15)	C54	C55	1.51(4)
P5	N22	1.694(15)	C54	C53	1.46(4)
P5	N18	1.506(15)	C69	C68	1.56(3)
P1	N4	1.64(2)	C74	C73	1.49(3)
P1	N2	1.678(19)	C33	C34	1.51(4)
P1	N1	1.529(14)	C33	C32	1.55(4)
P1	N5	1.620(19)	C10	C11	1.74(5)
P3	N11	1.649(17)	C35	C36	1.52(4)
P3	N10	1.555(15)	C66	C67	1.55(3)
P3	N12	1.675(17)	C18	C17	1.49(3)
P3	N13	1.704(14)	C21	C22	1.56(4)
P4	N15	1.70(3)	C38	C39	1.51(3)
P4	N14	1.514(15)	C62	C61	1.45(3)
P4	N16	1.63(2)	C56	C57	1.47(3)
P4	N17	1.716(17)	C40	C41	1.51(3)
N21	C65	1.51(2)	C71	C72	1.51(3)
N21	C69	1.51(2)	C7	C8	1.53(5)
N7	C15	1.51(2)	C7	C6	1.54(5)
N7	C19	1.42(2)	C60	C59	1.46(3)
N15	C50	1.46(4)	C72	C73	1.58(3)
N15	C47	1.63(4)	C24	C23	1.61(4)
N8	C1AA	1.47(3)	C5	C6	1.46(4)
N8	C24	1.49(3)	C43	C42	1.50(5)
N19	C61	1.46(3)	C43	C44	1.58(3)
N19	C64	1.46(3)	C46	C48	1.54(4)
N4	C5	1.46(4)	C46	C47	1.79(5)
N4	C9	1.50(4)	C31	C30	1.49(3)
N22	C70	1.49(2)	C31	C32	1.56(4)
N22	C74	1.50(2)	C57	C58	1.56(4)
N11	C30	1.48(2)	C25	C26	1.43(3)
N11	C34	1.50(2)	C17	C16	1.49(4)

Atom	Atom	Length/Å	Atom	Atom	Length/Å
N12	C35	1.48(3)	C59	C58	1.58(3)
N12	C39	1.45(3)	C1	C2	1.59(4)
N9	C25	1.46(3)	C42	C41	1.56(5)
N9	C29	1.50(2)	C23	C22	1.51(5)
N16	C51	1.47(3)	C68	C67	1.53(4)
N16	C55	1.68(4)	C29	C28	1.45(4)
N13	C40	1.50(2)	C48	C49	1.68(4)
N13	C44	1.45(2)	C12	C11	1.62(5)
N17	C56	1.55(3)	C0AA	C4	1.61(4)
N17	C60	1.42(3)	C28	C27	1.56(3)
C20	C62	1.58(3)	C64	C63	1.52(3)
C20	C63	1.55(3)	C8	C9	1.42(4)
C3	C2	1.57(5)	C26	C27	1.55(3)
C3	C0AA	1.45(5)			

Table 5.22 Bond Angles for 3-Yb^{5+}.

Atom	Atom	Atom	Angle/°	Atom	Atom	Atom	Angle/°
Yb1	Yb2	P2	68.02(9)	C25	N9	P2	126.4(15)
Yb1	Yb2	P1	67.79(10)	C25	N9	C29	109.9(17)
P1	Yb2	P2	106.13(13)	C29	N9	P2	122.7(14)
N6	Yb2	Yb1	51.6(4)	C51	N16	P4	126(2)
N6	Yb2	P2	18.2(4)	C55	N16	P4	120.8(17)
N6	Yb2	P1	90.7(4)	C55	N16	C51	113(2)
N14	Yb2	Yb1	176.4(6)	C40	N13	P3	111.7(12)
N14	Yb2	P2	115.6(6)	C44	N13	P3	114.2(13)
N14	Yb2	P1	110.2(5)	C44	N13	C40	113.8(16)
N14	Yb2	N6	131.9(7)	C56	N17	P4	109.7(13)
N14	Yb2	N10	125.8(8)	C60	N17	P4	113.0(12)
N14	Yb2	N1	124.7(6)	C60	N17	C56	108.0(16)
N10	Yb2	Yb1	53.2(4)	C63	C20	C62	111.0(19)
N10	Yb2	P2	90.9(4)	C0AA	C3	C2	116(3)
N10	Yb2	P1	105.6(4)	C1	N2	P1	116.9(17)
N10	Yb2	N6	85.7(5)	C1	N2	C4	115(2)
N10	Yb2	N1	87.8(5)	C4	N2	P1	110.0(14)
N1	Yb2	Yb1	52.7(4)	Yb2	N1	Yb1	78.2(4)
N1	Yb2	P2	104.6(4)	P1	N1	Yb2	134.8(9)
N1	Yb2	P1	17.9(4)	P1	N1	Yb1	134.9(9)
N1	Yb2	N6	87.0(5)	C10	N5	P1	123.2(19)
N6	Yb1	Yb2	49.3(4)	C10	N5	C14	115(2)
N6	Yb1	N10	80.3(5)	C14	N5	P1	118.2(18)

Atom	Atom	Atom	Angle/°	Atom	Atom	Atom	Angle/°
N6	Yb1	N1	82.4(5)	N7	C15	C16	107.0(18)
N10	Yb1	Yb2	48.2(4)	N8	C1AA	C21	112(2)
N18	Yb1	Yb2	174.8(4)	N22	C70	C71	112.3(18)
N18	Yb1	N6	126.2(5)	N7	C19	C18	107.1(16)
N18	Yb1	N10	136.2(6)	C14	C13	C12	113(3)
N18	Yb1	N1	130.9(6)	C66	C65	N21	110.4(17)
N1	Yb1	Yb2	49.0(4)	C53	C52	C51	122(3)
N1	Yb1	N10	81.4(5)	C49	C50	N15	105(3)
N6	P2	N7	112.0(9)	C36	C37	C38	110(2)
N6	P2	N8	118.4(8)	C55	C54	C53	114(3)
N6	P2	N9	111.8(8)	N21	C69	C68	110.8(16)
N8	P2	N7	100.3(9)	N22	C74	C73	112.4(17)
N9	P2	N7	110.8(9)	C34	C33	C32	113(2)
N9	P2	N8	102.7(10)	N5	C10	C11	109(2)
N21	P5	N19	107.3(7)	N12	C35	C36	110(2)
N21	P5	N22	97.7(7)	C65	C66	C67	111.1(17)
N22	P5	N19	100.9(7)	C13	C14	N5	116(3)
N18	P5	N21	117.0(9)	C17	C18	C19	111(2)
N18	P5	N19	112.5(8)	C22	C21	C1AA	107(2)
N18	P5	N22	119.3(8)	C39	C38	C37	107(2)
N4	P1	N2	102.4(10)	C61	C62	C20	110(2)
N1	P1	N4	113.4(9)	C57	C56	N17	105.9(17)
N1	P1	N2	120.2(9)	N13	C40	C41	108.4(18)
N1	P1	N5	112.4(10)	C72	C71	C70	110.1(19)
N5	P1	N4	105.8(10)	C6	C7	C8	111(3)
N5	P1	N2	100.9(11)	N17	C60	C59	111.1(17)
N11	P3	N12	108.1(8)	C71	C72	C73	109.4(19)
N11	P3	N13	101.5(8)	N8	C24	C23	107(2)
N10	P3	N11	111.1(8)	N4	C5	C6	117(3)
N10	P3	N12	113.1(9)	C62	C61	N19	114(2)
N10	P3	N13	118.9(7)	C42	C43	C44	110(2)
N12	P3	N13	103.1(8)	C47	C46	C48	112(3)
N14	P4	N15	111.8(14)	C30	C31	C32	110.6(19)
N14	P4	N16	114.9(12)	C56	C57	C58	112.0(19)
N14	P4	N17	118.7(9)	N9	C25	C26	110.8(19)
N16	P4	N15	110.8(14)	C18	C17	C16	111.5(19)
N16	P4	N17	102.2(9)	C37	C36	C35	112(3)
N17	P4	N15	96.8(11)	C60	C59	C58	112.2(19)
Yb2	N6	Yb1	79.1(4)	N16	C51	C52	111(3)
P2	N6	Yb2	134.2(9)	N11	C30	C31	113.1(19)
P2	N6	Yb1	138.6(9)	N2	C1	C2	112(2)

Atom	Atom	Atom	Angle/°	Atom	Atom	Atom	Angle/°
C65	N21	P5	124.6(12)	C43	C42	C41	108.5(18)
C65	N21	C69	107.8(13)	C22	C23	C24	113(2)
C69	N21	P5	116.7(11)	C54	C55	N16	103(2)
C15	N7	P2	123.3(14)	C3	C2	C1	107(2)
C19	N7	P2	116.3(12)	C69	C68	C67	105(2)
C19	N7	C15	112.7(15)	C40	C41	C42	112(2)
C50	N15	P4	117(2)	C33	C34	N11	111(2)
C50	N15	C47	118(3)	C28	C29	N9	113(2)
C47	N15	P4	100(2)	C68	C67	C66	111(2)
C1AA	N8	P2	113.2(13)	C17	C16	C15	112.7(17)
C1AA	N8	C24	111.7(17)	C33	C32	C31	110(2)
C24	N8	P2	114.4(16)	N12	C39	C38	111(2)
C61	N19	P5	124.5(13)	C46	C48	C49	105(3)
C64	N19	P5	121.4(12)	C57	C58	C59	103.3(18)
C64	N19	C61	112.4(16)	C13	C12	C11	115(2)
C5	N4	P1	119.4(18)	C3	C0AA	C4	116(2)
C5	N4	C9	113(2)	C52	C53	C54	112(3)
C9	N4	P1	127.7(18)	N15	C47	C46	96(2)
P4	N14	Yb2	172.4(14)	C29	C28	C27	113(3)
C70	N22	P5	113.7(12)	N19	C64	C63	112.9(19)
C74	N22	P5	115.9(12)	C23	C22	C21	112(2)
C74	N22	C70	105.8(15)	C9	C8	C7	115(3)
C30	N11	P3	115.4(13)	N13	C44	C43	109.3(18)
C30	N11	C34	112.3(16)	N2	C4	C0AA	106(3)
C34	N11	P3	124.6(14)	C25	C26	C27	117(3)
Yb2	N10	Yb1	78.5(5)	C5	C6	C7	110(3)
P3	N10	Yb2	146.3(10)	C28	C27	C26	106(2)
P3	N10	Yb1	125.2(9)	C64	C63	C20	108(2)
P5	N18	Yb1	168.1(11)	C10	C11	C12	99(2)
C35	N12	P3	124.9(14)	C74	C73	C72	109.2(18)
C35	N12	C39	110.1(18)	C8	C9	N4	114(3)
C39	N12	P3	125.1(14)	C50	C49	C48	118(3)

Table 5.23 Torsion Angles for 3-Yb^{5+}.

A	B	C	D	Angle/°	A	B	C	D	Angle/°
P2	N7	C15	C16	150.3(14)	N9	P2	N6	Yb1	-49.2(15)
P2	N7	C19	C18	-144.4(14)	N9	P2	N7	C15	69.7(16)
P2	N8	C1AA	C21	163.5(16)	N9	P2	N7	C19	-77.5(17)
P2	N8	C24	C23	-170.8(17)	N9	P2	N8	C1AA	177.2(14)
P2	N9	C25	C26	-111(2)	N9	P2	N8	C24	47.7(17)

A	B	C	D	Angle/°	A	B	C	D	Angle/°
P2	N9	C29	C28	111(2)	N9	C25	C26	C27	-56(3)
P5	N21	C65	C66	-157.3(14)	N9	C29	C28	C27	55(3)
P5	N21	C69	C68	148.8(17)	N16	P4	N15	C50	55(3)
P5	N19	C61	C62	-138(2)	N16	P4	N15	C47	-74(2)
P5	N19	C64	C63	136.5(18)	N16	P4	N17	C56	60.7(16)
P5	N22	C70	C71	169.9(17)	N16	P4	N17	C60	-178.6(15)
P5	N22	C74	C73	-170.2(14)	N13	P3	N11	C30	-172.9(14)
P1	N4	C5	C6	-129(3)	N13	P3	N11	C34	40(2)
P1	N4	C9	C8	132(3)	N13	P3	N10	Yb2	-62.3(19)
P1	N2	C1	C2	167(2)	N13	P3	N10	Yb1	65.9(12)
P1	N2	C4	C0AA	-170.8(16)	N13	P3	N12	C35	-53.4(18)
P1	N5	C10	C11	136(2)	N13	P3	N12	C39	126.5(18)
P1	N5	C14	C13	-143(2)	N13	C40	C41	C42	57(3)
P3	N11	C30	C31	151.3(16)	N17	P4	N15	C50	-51(2)
P3	N11	C34	C33	-157(2)	N17	P4	N15	C47	-179.6(17)
P3	N12	C35	C36	-122(2)	N17	P4	N16	C51	47(3)
P3	N12	C39	C38	117(2)	N17	P4	N16	C55	-122.3(19)
P3	N13	C40	C41	170.3(16)	N17	C56	C57	C58	-65(2)
P3	N13	C44	C43	-171.2(15)	N17	C60	C59	C58	61(2)
P4	N15	C50	C49	170(2)	C20	C62	C61	N19	-54(4)
P4	N15	C47	C46	-163.8(18)	C3	C0AA	C4	N2	-48(4)
P4	N16	C51	C52	146(3)	N2	P1	N4	C5	-152(2)
P4	N16	C55	C54	-130(2)	N2	P1	N4	C9	29(3)
P4	N17	C56	C57	-171.0(16)	N2	P1	N1	Yb2	-46.9(18)
P4	N17	C60	C59	174.2(14)	N2	P1	N1	Yb1	78.9(15)
N6	P2	N7	C15	-164.8(14)	N2	P1	N5	C10	109(2)
N6	P2	N7	C19	48.1(17)	N2	P1	N5	C14	-47.6(19)
N6	P2	N8	C1AA	53.5(18)	N2	C1	C2	C3	54(3)
N6	P2	N8	C24	-76.0(18)	N1	P1	N4	C5	-21(3)
N6	P2	N9	C25	-8(2)	N1	P1	N4	C9	160(2)
N6	P2	N9	C29	-175.1(18)	N1	P1	N2	C1	69(2)
N21	P5	N19	C61	66(2)	N1	P1	N2	C4	-63.5(17)
N21	P5	N19	C64	-129.6(16)	N1	P1	N5	C10	-20(3)
N21	P5	N22	C70	-175.8(14)	N1	P1	N5	C14	-176.9(17)
N21	P5	N22	C74	61.3(14)	N5	P1	N4	C5	102(2)
N21	P5	N18	Yb1	-37(5)	N5	P1	N4	C9	-77(3)
N21	C65	C66	C67	-57(3)	N5	P1	N2	C1	-54.8(18)
N21	C69	C68	C67	64(2)	N5	P1	N2	C4	172.3(14)
N7	P2	N6	Yb2	50.9(13)	N5	P1	N1	Yb2	71.7(15)
N7	P2	N6	Yb1	-174.2(10)	N5	P1	N1	Yb1	-162.6(11)
N7	P2	N8	C1AA	-68.6(16)	N5	C10	C11	C12	60(3)

A	B	C	D	Angle/°	A	B	C	D	Angle/°
N7	P2	N8	C24	162.0(16)	C15	N7	C19	C18	65(2)
N7	P2	N9	C25	118(2)	C1AA	N8	C24	C23	59(2)
N7	P2	N9	C29	-49(2)	C1AA	C21	C22	C23	-53(3)
N7	C15	C16	C17	53(2)	C70	N22	C74	C73	63(2)
N7	C19	C18	C17	-60(2)	C70	C71	C72	C73	-54(3)
N15	P4	N16	C51	-55(3)	C19	N7	C15	C16	-61(2)
N15	P4	N16	C55	136(2)	C19	C18	C17	C16	55(2)
N15	P4	N17	C56	173.8(16)	C13	C12	C11	C10	-50(3)
N15	P4	N17	C60	-65.6(16)	C65	N21	C69	C68	-65(2)
N15	C50	C49	C48	58(4)	C65	C66	C67	C68	57(3)
N8	P2	N6	Yb2	-65.0(15)	C50	N15	C47	C46	68(3)
N8	P2	N6	Yb1	69.9(15)	C37	C38	C39	N12	61(3)
N8	P2	N7	C15	-38.3(16)	C69	N21	C65	C66	59.9(19)
N8	P2	N7	C19	174.5(16)	C69	C68	C67	C66	-58(3)
N8	P2	N9	C25	-136(2)	C74	N22	C70	C71	-62(2)
N8	P2	N9	C29	57(2)	C10	N5	C14	C13	59(4)
N8	C1AA	C21	C22	59(3)	C35	N12	C39	C38	-63(3)
N8	C24	C23	C22	-53(3)	C14	N5	C10	C11	-67(3)
N19	P5	N21	C65	-53.8(15)	C14	C13	C12	C11	47(4)
N19	P5	N21	C69	86.1(14)	C18	C17	C16	C15	-52(3)
N19	P5	N22	C70	-66.5(15)	C38	C37	C36	C35	57(4)
N19	P5	N22	C74	170.6(13)	C62	C20	C63	C64	-54(3)
N19	P5	N18	Yb1	-162(5)	C56	N17	C60	C59	-64(2)
N19	C64	C63	C20	57(3)	C56	C57	C58	C59	59(2)
N4	P1	N2	C1	-163.9(17)	C40	N13	C44	C43	59(2)
N4	P1	N2	C4	63.3(15)	C71	C72	C73	C74	54(3)
N4	P1	N1	Yb2	-168.4(13)	C7	C8	C9	N4	48(4)
N4	P1	N1	Yb1	-42.6(16)	C60	N17	C56	C57	65(2)
N4	P1	N5	C10	-145(2)	C60	C59	C58	C57	-54(2)
N4	P1	N5	C14	59(2)	C24	N8	C1AA	C21	-66(2)
N4	C5	C6	C7	-51(4)	C24	C23	C22	C21	52(3)
N14	P4	N15	C50	-175(2)	C5	N4	C9	C8	-47(4)
N14	P4	N15	C47	56(2)	C61	N19	C64	C63	-58(3)
N14	P4	N16	C51	177(3)	C43	C42	C41	C40	-58(3)
N14	P4	N16	C55	8(2)	C46	C48	C49	C50	-56(4)
N14	P4	N17	C56	-66.8(19)	C25	N9	C29	C28	-58(3)
N14	P4	N17	C60	53.8(18)	C25	C26	C27	C28	49(4)
N22	P5	N21	C65	50.2(14)	C36	C37	C38	C39	-58(3)
N22	P5	N21	C69	-169.9(14)	C51	N16	C55	C54	59(3)
N22	P5	N19	C61	-35(2)	C51	C52	C53	C54	-37(6)
N22	P5	N19	C64	128.7(16)	C30	N11	C34	C33	55(3)

A	B	C	D	Angle/°	A	B	C	D	Angle/°
N22	P5	N18	Yb1	81(5)	C30	C31	C32	C33	-52(3)
N22	C70	C71	C72	60(3)	C1	N2	C4	C0AA	55(2)
N22	C74	C73	C72	-60(2)	C42	C43	C44	N13	-58(3)
N11	P3	N10	Yb2	-179.5(15)	C55	N16	C51	C52	-44(4)
N11	P3	N10	Yb1	-51.3(12)	C55	C54	C53	C52	56(4)
N11	P3	N12	C35	53.6(19)	C2	C3	C0AA	C4	49(4)
N11	P3	N12	C39	-126.5(19)	C34	N11	C30	C31	-58(3)
N11	P3	N13	C40	-166.6(13)	C34	C33	C32	C31	52(4)
N11	P3	N13	C44	62.6(16)	C29	N9	C25	C26	57(3)
N10	P3	N11	C30	-45.6(17)	C29	C28	C27	C26	-47(4)
N10	P3	N11	C34	167.4(19)	C32	C33	C34	N11	-53(4)
N10	P3	N12	C35	177.0(16)	C32	C31	C30	N11	56(3)
N10	P3	N12	C39	-3(2)	C39	N12	C35	C36	58(3)
N10	P3	N13	C40	71.3(15)	C48	C46	C47	N15	-60(3)
N10	P3	N13	C44	-59.5(17)	C12	C13	C14	N5	-43(4)
N18	P5	N21	C65	178.7(13)	C0AA	C3	C2	C1	-49(3)
N18	P5	N21	C69	-41.4(16)	C53	C52	C51	N16	34(6)
N18	P5	N19	C61	-163.6(19)	C53	C54	C55	N16	-65(3)
N18	P5	N19	C64	0.4(19)	C47	N15	C50	C49	-70(4)
N18	P5	N22	C70	57.2(17)	C47	C46	C48	C49	55(3)
N18	P5	N22	C74	-65.6(16)	C64	N19	C61	C62	57(3)
N12	P3	N11	C30	79.0(15)	C8	C7	C6	C5	48(4)
N12	P3	N11	C34	-68(2)	C44	N13	C40	C41	-59(2)
N12	P3	N10	Yb2	58.7(18)	C44	C43	C42	C41	57(3)
N12	P3	N10	Yb1	-173.0(8)	C4	N2	C1	C2	-63(3)
N12	P3	N13	C40	-54.7(14)	C6	C7	C8	C9	-49(4)
N12	P3	N13	C44	174.5(15)	C63	C20	C62	C61	54(4)
N12	C35	C36	C37	-57(3)	C9	N4	C5	C6	50(4)
N9	P2	N6	Yb2	175.9(11)					

5.5.4 *4-Yb^{5+}(DME)*

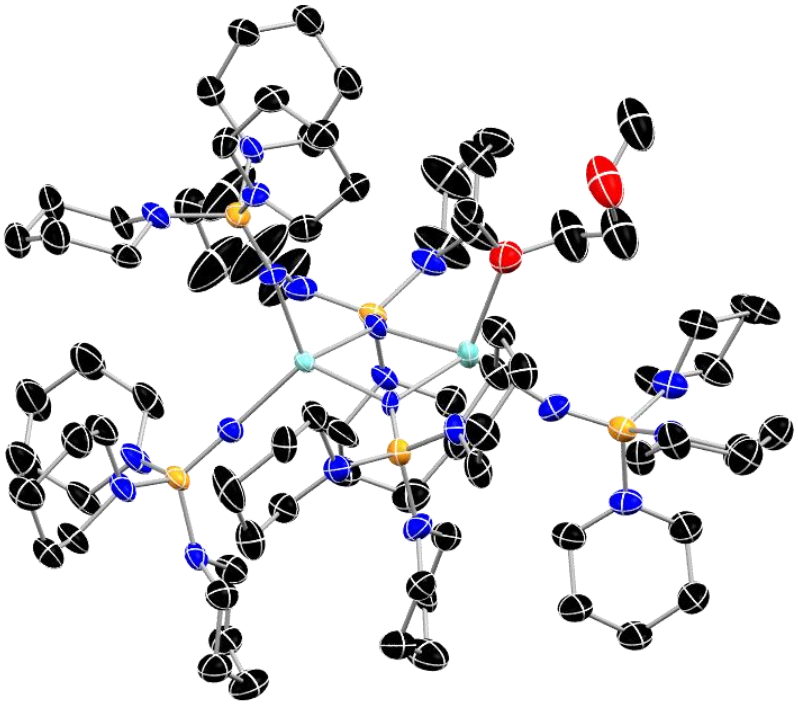

Figure 5.15 Molecular structure of 4-Yb^{5+}(DME) with thermal ellipsoids shown at 50% probability with hydrogen atoms omitted for clarity. Color code: C, black; N, blue; O, red; P, orange; Yb, blue. Structure contains approximately 10% Iodide heavy atom impurity.

Table 5.24 Crystal data and structure refinement for 4-Yb^{5+}(DME).

Identification code	4-Yb^{5+}(DME)
Empirical formula	$C_{78.39}H_{157.99}I_{0.15}N_{20}O_{1.7}P_5Yb_2$
Formula weight	1928.30
Temperature/K	?
Crystal system	orthorhombic
Space group	$P2_12_12_1$
a/Å	14.0140(4)
b/Å	14.0239(4)
c/Å	46.4722(11)
α/°	90
β/°	90
γ/°	90

Volume/Å^3	9133.2(4)
Z	4
ρ_{calc}g/cm^3	N/A
μ/mm^{-1}	N/A
F(000)	N/A
Crystal size/mm^3	N/A × N/A × N/A
Radiation	N/A (λ = 0.71073)
2Θ range for data collection/°	3.92 to 54.42
Index ranges	-17 ≤ h ≤ 18, 0 ≤ k ≤ 18, 0 ≤ l ≤ 59
Reflections collected	40529
Independent reflections	20280 [R_{int} = 0.0000, R_{sigma} = 1.3901]
Data/restraints/parameters	20280/N/A/N/A
Goodness-of-fit on F^2	N/A
Final R indexes [I>=2σ (I)]	R_1 = N/A, wR_2 = N/A
Final R indexes [all data]	R_1 = N/A, wR_2 = N/A
Largest diff. peak/hole / e Å^{-3}	1.16/N/A

Table 5.25 Fractional Atomic Coordinates (×10^4) and Equivalent Isotropic Displacement Parameters (Å^2×10^3) for 4-Yb^{5+}(DME). U_{eq} is defined as 1/3 of the trace of the orthogonalised U_{IJ} tensor.

Atom	*x*	*y*	*z*	U(eq)
Yb1	1371.38	5105.44	6110.28	22.143
Yb2	2689.25	6503.26	6549.25	28.293
C47	3501.42	6357.56	7453.81	90.42
C37	2836.75	5897.15	7899.79	90.42
O1	3176.42	5614.43	7637.44	90.42
C30A	2715.18	6672.42	7250.97	90.42
I1	2310.67	5885.07	7194.89	57.86
O2	2434.34	6034.28	7028.72	49.703
C4	1879.89	5287.45	7117.19	48.527
P1_1	570.25	7412.59	6274.15	28.5
N1_1	1183.96	6550.52	6326.54	28.267
N2_1	-514.53	7167.52	6140.9	41.73
N3_1	415.46	8068.92	6571.76	41.057
N4_1	933.18	8236.47	6035.82	30.667
C1_1	-935.25	6257.71	6195.37	125.173
C2_1	-1944.4	6259.89	6288.68	119.927
C3_1	-2569.65	6771.67	6077.49	62.887
C4_1	-2046.05	7503.66	5904.52	123.483
C5_1	-1212.08	7885.27	6056.45	108.343
C6_1	820.82	7823.12	6844.77	71.927

Atom	*x*	*y*	*z*	U(eq)
C7_1	100.87	7875.52	7081.16	65.873
C8_1	-371.12	8845.44	7098.63	63.593
C9_1	-760.83	9096.46	6807.32	89.42
C10_1	-52.88	9012.84	6577.63	88.013
C11_1	1725.05	8851.27	6125.25	49.93
C12_1	1760.77	9753.2	5946.54	56.263
C13_1	1822.02	9521.59	5630.24	59.053
C14_1	1043.49	8828.83	5543.32	65.387
C15_1	1046.18	7953.44	5739.54	70.58
P1_2	1040.82	4859.31	5334.06	30.51
N1_2	1170.44	4993.51	5652.38	30.25
N2_2	1023.12	3714.69	5227.42	40.467
N3_2	38.14	5370.93	5212.47	46.91
N4_2	1855.23	5303.93	5105.49	31.15
C1_2	515.11	3043.05	5402.27	52.957
C2_2	825.26	2036.69	5379.43	52.77
C3_2	878.81	1728.9	5070.52	54.383
C4_2	1404.82	2430.18	4886.36	45.34
C5_2	1062.65	3410.4	4927.24	43.317
C6_2	-640.27	5830.74	5396.36	51.22
C7_2	-1618.43	5425.37	5359.04	73.197
C8_2	-1950.1	5467.95	5049.05	79.62
C9_2	-1207.27	5010.81	4861.31	66.427
C10_2	-251.75	5402.54	4907.03	48.647
C11_2	1903.96	6346.34	5085.38	42.217
C12_2	2387.43	6659.56	4809.82	44.553
C13_2	3368.04	6223.45	4785.49	58.463
C14_2	3319.81	5151.31	4824.77	49.26
C15_2	2798.71	4896.93	5103.55	42.92
P1_3	-146.69	3478.72	6504.41	31.807
N1_3	570.55	4138.71	6369.86	32.987
N2_3	328.35	2618.52	6708.63	32.793
N3_3	-945.25	4065.99	6706.71	37.28
N4_3	-860	2824.44	6290.65	36.097
C1_3	1327.78	2603.61	6766.72	39.97
C2_3	1604.77	2494.46	7072.65	36.18
C3_3	1076.59	1683.86	7210.65	39.657
C4_3	26.52	1713.78	7151.83	42.217
C5_3	-187.51	1840.8	6844.97	39.81
C6_3	-703.32	4915.59	6862.43	46.703
C7_3	-734.68	4753.17	7180.12	47.463

Atom	*x*	*y*	*z*	U(eq)
C8_3	-1707.45	4408.34	7277.67	55.39
C9_3	-1969.71	3543.07	7104.6	53.247
C10_3	-1883.6	3684.48	6794.22	52.107
C11_3	-1513.13	3363.14	6105.15	41.54
C12_3	-2311.34	2740.52	5992.18	57.137
C13_3	-1917.65	1884.08	5835.91	58.227
C14_3	-1198.82	1363.77	6022.44	58.6
C15_3	-433.47	2049.27	6132.45	36.63
P1_4	3796.21	4604.19	6179.77	27.467
N1_4	2900.96	5133.22	6260.15	21.607
N2_4	4501.46	5183.37	5947.3	41.517
N3_4	4455.84	4331.36	6469.62	36.62
N4_4	3714.38	3541.05	6017.71	33.59
C1_4	4434.86	6196.53	5920.73	44.23
C2_4	4539.8	6582.08	5625.49	55.42
C3_4	5406.32	6179.61	5479.96	69.33
C4_4	5478.84	5118.97	5509.43	54.517
C5_4	5347.15	4798.11	5807.62	45.837
C6_4	4211.61	4628.67	6754.98	46.203
C7_4	4261.26	3822.93	6964.77	45.497
C8_4	5230.72	3344.35	6964.82	46.98
C9_4	5472.01	3061.07	6661.77	52.98
C10_4	5391.86	3849	6457.18	46.82
C11_4	3305.71	2754.82	6184.43	47.623
C12_4	3681.38	1805.36	6077.65	57.183
C13_4	3485.42	1686.99	5760.64	70.267
C14_4	3837.05	2541.23	5591.52	54.607
C15_4	3456.19	3472.17	5719.41	39.993
P1_5	4491.87	8364.91	6653.44	33.253
N1_5	3754.74	7655.47	6558.68	38.037
N2_5	5410.73	7890.34	6837.67	35.843
N3_5	4970.87	8967.72	6376.12	39.923
N4_5	4191	9258.31	6874.01	39.3
C1_5	5749.48	6971.6	6748.96	43.167
C2_5	6297.37	6425.32	6965.64	49.273
C3_5	7074.06	7023.77	7095.23	52.283
C4_5	6725.12	7985.99	7187.5	51.62
C5_5	6178.52	8466.53	6960.58	46.207
C6_5	4633.78	8863.88	6086.7	46.247
C7_5	5431.71	8897.89	5873.93	60.547
C8_5	6018.07	9801.32	5900.33	57.487

Atom	*x*	*y*	*z*	U(eq)
C9_5	6334.63	9906.83	6207.45	65.25
C10_5	5546.52	9843.94	6412.49	54.907
C11_5	3547.94	9992.48	6761.98	43.967
C12_5	3721.13	10935.29	6912.7	53.557
C13_5	3613.38	10825.57	7233.77	42.7
C14_5	4211.4	10006.11	7345.97	45.773
C15_5	4024.97	9092.48	7174.77	42.66

Table 5.26 Anisotropic Displacement Parameters ($Å^2×10^3$) for 4-Yb^{5+}(DME). The Anisotropic displacement factor exponent takes the form: $-2\pi^2[h^2a^{*2}U_{11}+2hka^*b^*U_{12}+\ldots]$.

Atom	U_{11}	U_{22}	U_{33}	U_{23}	U_{13}	U_{12}
Yb1	27.74	23.3	15.39	1.03	-2.29	-1.74
Yb2	27.16	28.13	29.59	-6.95	-5.06	1.24
C47	147.76	60.78	62.72	3.15	-32.78	-14.57
C37	147.76	60.78	62.72	3.15	-32.78	-14.57
O1	147.76	60.78	62.72	3.15	-32.78	-14.57
C30A	147.76	60.78	62.72	3.15	-32.78	-14.57
I1	72.76	76.91	23.91	6.66	8.41	18.72
O2	50.48	52.21	46.42	7.6	-1.03	-7.08
C4	59.92	55.16	30.5	1.47	-1.62	-14.35
P1_1	32.6	29.06	23.84	3.17	2.49	7.45
N1_1	34.43	23.6	26.77	-12.11	2.75	2.2
N2_1	43.84	50.42	30.93	11.01	6.46	0.22
N3_1	58.67	35.05	29.45	5.46	7.72	10.66
N4_1	38.02	31.9	22.08	-4.08	1.47	7.74
C1_1	51.53	80.97	243.02	87.39	-18.9	-14.32
C2_1	49.97	122.96	186.85	88.57	-28.69	-25.24
C3_1	49.09	84.75	54.82	-5.73	-4.76	-1.8
C4_1	44.66	135.61	190.18	81.88	-28.95	-15.69
C5_1	58.11	81.07	185.85	69.78	-32.7	-6.24
C6_1	86.29	93.05	36.44	-2.88	-2.82	51.72
C7_1	90.61	66.58	40.43	-18.83	3.29	10.76
C8_1	70.55	64.66	55.57	-15.83	24.99	4.33
C9_1	129.52	76.76	61.98	-17.81	12.37	41.66
C10_1	142.53	72.39	49.12	2.22	10.91	64.63
C11_1	50.35	60.17	39.27	11.62	-6.27	-12.27
C12_1	60.68	48.98	59.13	10.56	-11.84	-17.2
C13_1	64	53.41	59.75	11.95	5.99	-9.51
C14_1	91.31	66.97	37.88	1.92	14.88	-29.15

Atom	U_{11}	U_{22}	U_{33}	U_{23}	U_{13}	U_{12}
C15_1	129.92	56.44	25.38	-10.7	22.27	-22.53
P1_2	39.02	34.91	17.6	0.84	-1.44	-2.23
N1_2	31.67	34.35	24.73	1.43	-0.58	0.42
N2_2	60.48	41.26	19.66	-0.4	-3.62	-10.55
N3_2	46.07	77.33	17.33	-2.45	-10.43	16.5
N4_2	40.59	33.14	19.72	2.7	-8.35	-4.53
C1_2	88.9	33.74	36.23	-9.67	13.52	-16.92
C2_2	76.16	36.51	45.64	-4.9	-0.45	-12.67
C3_2	75.87	41.85	45.43	-2.7	6.21	0.66
C4_2	60.48	44.71	30.83	-8.64	0.69	3.6
C5_2	64.36	43.55	22.04	-2.39	-2.02	7.5
C6_2	52.71	72.57	28.38	-11.05	-16.67	23.29
C7_2	46.41	120.25	52.93	-34.15	-3.85	18.75
C8_2	59.48	123.12	56.26	-36.07	-14.15	21.63
C9_2	60.92	95.86	42.5	-13.38	-16.77	23.06
C10_2	61.31	65.84	18.79	-0.1	-12.13	26.9
C11_2	55.24	34.37	37.04	1.39	5.61	1.33
C12_2	56.92	33.93	42.81	10.68	5.68	-8.25
C13_2	49.18	63.62	62.59	21.89	8.5	-6.97
C14_2	44.66	60.83	42.29	11.78	2.24	-3.21
C15_2	43.89	49.28	35.59	8.92	-2.53	3.89
P1_3	37.63	34.59	23.2	4.9	-3.1	-6.9
N1_3	43.78	31.47	23.71	13.09	6.24	-18.45
N2_3	38.02	35.28	25.08	13.9	0.63	-8.32
N3_3	51.32	35.27	25.25	-12.13	3.65	-11.78
N4_3	52.61	35.17	20.51	-2.69	2.69	1.12
C1_3	39.98	38.66	41.27	8.97	6.29	4.18
C2_3	35.76	29.44	43.34	5.12	1.11	2.67
C3_3	45.43	36.86	36.68	11.31	-1.01	0.19
C4_3	45.29	48.83	32.53	24.08	0.43	-0.36
C5_3	46.82	37.68	34.93	16.66	-10.24	-18.54
C6_3	63.81	30.87	45.43	-7.53	-0.41	-8.52
C7_3	49.12	51.8	41.47	-19.31	-2.94	6.11
C8_3	46.36	83.99	35.82	-17.54	-0.33	5.75
C9_3	42.36	81.02	36.36	-11.98	7.16	-3.75
C10_3	58.67	58.84	38.81	-9.07	3.73	-18.97
C11_3	53.98	46.12	24.52	-12.68	-12.41	-0.33
C12_3	65.57	72.4	33.44	-11.26	-12.23	-18.26
C13_3	72.55	61.9	40.23	-8.61	-5.01	-27.31
C14_3	80.72	47.74	47.34	-10.24	-1.93	-20.05
C15_3	53.33	28.7	27.86	1.56	10.58	-4.34

Atom	U_{11}	U_{22}	U_{33}	U_{23}	U_{13}	U_{12}
P1_4	29.6	22.15	30.65	-1.13	-2.5	2.86
N1_4	17.1	22.78	24.94	-3.18	-6.65	-0.71
N2_4	37.26	37.07	50.22	-4.79	9.13	-11.53
N3_4	32.01	49.55	28.3	5.35	-13.35	4.46
N4_4	37.68	26.45	36.64	-3.91	4.53	-1.42
C1_4	50.71	39.11	42.87	-6.84	9	-10.52
C2_4	84.35	46.97	34.94	-15.84	-1.88	-24.18
C3_4	98.63	64.45	44.91	10.27	17.23	-6.8
C4_4	53.58	62.13	47.84	-0.09	12.83	-5.64
C5_4	33.17	59.09	45.25	-1.6	1.58	-4.71
C6_4	66.88	42.92	28.81	1.84	-13.28	11.29
C7_4	57.74	44.41	34.34	8.78	-4.66	8.24
C8_4	51.68	45.61	43.65	3.75	-16.74	5.49
C9_4	47.46	64.99	46.49	3.28	-14.63	23.81
C10_4	42.49	56.18	41.79	-7.33	-18.47	12.23
C11_4	70.7	46.69	25.48	-1.84	-0.52	-20.71
C12_4	63.37	53.79	54.39	-17.58	-4.41	-21.95
C13_4	131.99	25.97	52.84	-21.2	-13.7	-7.49
C14_4	68.55	37.92	57.35	-19.31	-6.83	-1.56
C15_4	47.8	33.36	38.82	-0.36	2.16	-0.36
P1_5	37.79	32.52	29.45	1.5	2.65	3.56
N1_5	34.28	33.93	45.9	5.09	5.45	-2.45
N2_5	37.52	26.75	43.26	1.04	7.8	0.67
N3_5	46.11	35.4	38.26	8.41	8.81	-0.94
N4_5	48.23	29.86	39.81	4.7	7.31	11.45
C1_5	40.29	38.46	50.75	-12.08	-5.94	10.72
C2_5	50.45	45.14	52.23	-11.3	-7.75	17.88
C3_5	39.67	51.58	65.6	3.06	-4.98	8.86
C4_5	44.32	47.64	62.9	1.93	-0.31	2.2
C5_5	43.27	32.79	62.56	-0.72	-0.92	-3.05
C6_5	52.37	49.92	36.45	3.61	8.23	-1.08
C7_5	67.93	64.55	49.16	-5.39	19.49	-25.89
C8_5	72.79	56.46	43.21	5.98	14.49	-23.18
C9_5	71.96	72.65	51.14	-3.55	8.64	-36.71
C10_5	66.71	50.86	47.15	5.26	4.95	-16.87
C11_5	58.13	38.85	34.92	2.68	4.33	20.14
C12_5	85.56	39.74	35.37	3.63	4.83	11.9
C13_5	64.72	28.98	34.4	-2.33	9.33	15.6
C14_5	65.74	44.07	27.51	4.64	7.1	21.36
C15_5	52.7	33.36	41.92	9.85	7.29	20.37

Table 5.27 Hydrogen Atom Coordinates (Å×10^4) and Isotropic Displacement Parameters (Å^2×10^3) for 4-Yb^{5+}(DME).

Atom	*x*	*y*	*z*	U(eq)
H47A	4044.19	6135	7343.05	108.504
H47B	3707.62	6895.75	7569.24	108.504
H37A	2401.8	6419.36	7874.57	135.63
H37B	3359.47	6096.05	8019.05	135.63
H37C	2510.54	5374.52	7989.91	135.63
H30A	2155.28	6815.19	7365.88	108.504
H30B	2915.84	7263.77	7161.19	108.504
H4A	1468.5	5093.58	6962.72	72.79
H4B	1500.64	5481.17	7278.98	72.79
H4C	2281.25	4763.26	7171.98	72.79
H1A_1	-560.57	5939.62	6342.29	150.208
H1B_1	-887.18	5879.4	6021.23	150.208
H2A_1	-1993.51	6567.18	6475.09	143.912
H2B_1	-2164.2	5607.58	6309.28	143.912
H3A_1	-2851.25	6308.8	5947.7	75.464
H3B_1	-3084.82	7081.06	6181.01	75.464
H4A_1	-1839.76	7219.48	5724.68	148.18
H4B_1	-2477.18	8023.33	5858.99	148.18
H5A_1	-900.4	8349.43	5933.51	130.012
H5B_1	-1428.76	8216.67	6227.61	130.012
H6A_1	1343.39	8254.29	6887.24	86.312
H6B_1	1077.32	7181.48	6835.21	86.312
H7A_1	411.31	7737.69	7263.03	79.048
H7B_1	-384.21	7393.29	7049.66	79.048
H8A_1	-883.64	8831.39	7238.85	76.312
H8B_1	90.64	9320.67	7158.71	76.312
H9A_1	-1294.69	8679.86	6764.36	107.304
H9B_1	-998.67	9745.83	6812	107.304
H10A_1	429.2	9501.84	6603.28	105.616
H10B_1	-362.29	9124	6393.96	105.616
H11A_1	2321.72	8507.5	6104.49	59.916
H11B_1	1649.55	9017.32	6326.59	59.916
H12A_1	1193.04	10130.24	5982.73	67.516
H12B_1	2311.41	10129.03	6002.5	67.516
H13A_1	2440.77	9244.49	5588.28	70.864
H13B_1	1760.24	10103.62	5519.01	70.864

Atom	*x*	*y*	*z*	U(eq)
H14A_1	1142.27	8630.13	5345.63	78.464
H14B_1	428.14	9143.17	5554.96	78.464
H15A_1	529.68	7529.56	5685.26	84.696
H15B_1	1642.61	7610.63	5716.81	84.696
H1A_2	-155.87	3076.43	5352.04	63.548
H1B_2	574.01	3238.83	5601.67	63.548
H2A_2	378.2	1631.97	5481.78	63.324
H2B_2	1447.06	1964.23	5468.48	63.324
H3A_2	1196.38	1115.35	5059.78	65.26
H3B_2	236.92	1650.37	4996.11	65.26
H4A_2	2079.52	2402.23	4932.18	54.408
H4B_2	1329.47	2253.6	4685.83	54.408
H5A_2	1478.8	3840.42	4822.46	51.98
H5B_2	429.34	3464.45	4844.6	51.98
H6A_2	-653.74	6507.42	5353.33	61.464
H6B_2	-443.19	5755.57	5595.16	61.464
H7A_2	-2062.63	5777.45	5478.77	87.836
H7B_2	-1619.94	4767.04	5423.06	87.836
H8A_2	-2552.56	5134.15	5028.72	95.544
H8B_2	-2044.12	6126.3	4991.66	95.544
H9A_2	-1194.51	4331.03	4899.67	79.712
H9B_2	-1384.15	5098.5	4661.26	79.712
H10A_2	-238.32	6058.4	4840.85	58.376
H10B_2	203.51	5043.31	4793.16	58.376
H11A_2	2255.13	6594.6	5248.91	50.66
H11B_2	1263.47	6607.66	5092.05	50.66
H12A_2	2003.31	6466.9	4646.2	53.464
H12B_2	2440.17	7349.17	4807.22	53.464
H13A_2	3783.07	6496.31	4930.83	70.156
H13B_2	3635.61	6369.07	4598.07	70.156
H14A_2	3961.22	4891.92	4830.03	59.112
H14B_2	2988.2	4868.31	4662.67	59.112
H15A_2	2754.12	4209.18	5121.22	51.504
H15B_2	3157.69	5135.77	5266.81	51.504
H1A_3	1603.24	3191.99	6695.02	47.964
H1B_3	1610.06	2083.88	6658.45	47.964
H2A_3	1466.34	3080.35	7175.43	43.416
H2B_3	2285.85	2378.34	7085.15	43.416
H3A_3	1333.2	1086.09	7139.67	47.588
H3B_3	1180.05	1704.11	7416.94	47.588
H4A_3	-261.84	1124.8	7218.28	50.66

Atom	*x*	*y*	*z*	U(eq)
H4B_3	-255.69	2234.41	7259.72	50.66
H5A_3	-37.71	1253.2	6744.55	47.772
H5B_3	-866.58	1954.31	6823.56	47.772
H6A_3	-1146.98	5419.39	6811.9	56.044
H6B_3	-67.78	5120.98	6807.69	56.044
H7A_3	-581.48	5343.32	7278.7	56.956
H7B_3	-256.56	4283.86	7232.29	56.956
H8A_3	-1690.22	4249.59	7480.75	66.468
H8B_3	-2178.66	4906.1	7249.16	66.468
H9A_3	-1560.93	3017.69	7161.47	63.896
H9B_3	-2622.3	3366.01	7149.15	63.896
H10A_3	-2378.1	4121.21	6731.29	62.528
H10B_3	-1988.32	3079.81	6697.92	62.528
H11A_3	-1159.59	3627.13	5944.36	49.848
H11B_3	-1783.17	3889.42	6213.38	49.848
H12A_3	-2706.41	2529.74	6151.32	68.564
H12B_3	-2708.27	3108.37	5862.11	68.564
H13A_3	-1613	2088.15	5658.89	69.872
H13B_3	-2435.32	1455.35	5786.32	69.872
H14A_3	-900.24	859.54	5911.5	70.32
H14B_3	-1524.12	1073.87	6184.58	70.32
H15A_3	6.71	1707.53	6256.19	43.956
H15B_3	-75.37	2301.8	5970.9	43.956
H1A_4	4922.4	6481.93	6041.28	53.076
H1B_4	3820.34	6396.39	5995.49	53.076
H2A_4	4592.24	7271.16	5634.21	66.504
H2B_4	3976.51	6425.65	5513.76	66.504
H3A_4	5386.96	6343.45	5277.26	83.196
H3B_4	5972.15	6470.33	5562.16	83.196
H4A_4	4999.28	4821.49	5388.62	65.42
H4B_4	6100.35	4912.9	5441.8	65.42
H5A_4	5307.94	4107.57	5809.35	55.004
H5B_4	5904.33	4979.37	5918.73	55.004
H6A_4	3570.48	4889.34	6754.58	55.444
H6B_4	4644.97	5129.42	6815.43	55.444
H7A_4	3776.55	3355.46	6916.79	54.596
H7B_4	4125.61	4061.82	7156.34	54.596
H8A_4	5709.73	3779.97	7038.45	56.376
H8B_4	5217.83	2784.98	7087.53	56.376
H9A_4	6119.22	2816.34	6657.16	63.576
H9B_4	5048.35	2550.93	6602.22	63.576

Atom	*x*	*y*	*z*	U(eq)
H10A_4	5492.44	3606.65	6264.06	56.184
H10B_4	5889.91	4310.94	6496.91	56.184
H11A_4	2615.95	2766.32	6167.41	57.148
H11B_4	3467.91	2833.02	6385.97	57.148
H12A_4	4363.24	1769.67	6111.87	68.62
H12B_4	3378.08	1291.98	6183.49	68.62
H13A_4	2804.78	1610.58	5730.52	84.32
H13B_4	3801.08	1115.88	5691.34	84.32
H14A_4	3629.4	2486.1	5393.11	65.528
H14B_4	4529.11	2551.6	5593.34	65.528
H15A_4	3719.17	4009.87	5614.77	47.992
H15B_4	2767.11	3491.41	5700.61	47.992
H1A_5	6149.26	7056.51	6580.51	51.8
H1B_5	5204.14	6591.34	6691.03	51.8
H2A_5	6576.23	5867.35	6875.4	59.128
H2B_5	5870	6209.63	7116.37	59.128
H3A_5	7337.73	6693.8	7260.55	62.74
H3B_5	7581.57	7103.5	6955.35	62.74
H4A_5	6325.77	7915.24	7356.64	61.944
H4B_5	7267.42	8379.23	7239.86	61.944
H5A_5	5905.71	9046.48	7039.13	55.448
H5B_5	6612.55	8648.43	6807.54	55.448
H6A_5	4183.53	9370.26	6044.5	55.496
H6B_5	4300.8	8260.55	6068.34	55.496
H7A_5	5170.85	8857.57	5680.98	72.656
H7B_5	5843.52	8350.36	5903	72.656
H8A_5	6569.76	9766.47	5774.71	68.984
H8B_5	5637.93	10348.21	5843.86	68.984
H9A_5	6796.84	9412.65	6251.05	78.3
H9B_5	6649.13	10518.31	6230.3	78.3
H10A_5	5136.2	10395.43	6388.84	65.888
H10B_5	5801.65	9859.66	6606.47	65.888
H11A_5	2891.34	9796.25	6791.25	52.76
H11B_5	3651.36	10068.27	6556.87	52.76
H12A_5	4359.11	11160.48	6868.7	64.268
H12B_5	3269.03	11405.45	6843.06	64.268
H13A_5	2947.89	10712.51	7279.92	51.24
H13B_5	3807.97	11411.46	7327.92	51.24
H14A_5	4062.11	9896.99	7547.11	54.928
H14B_5	4881.94	10171.68	7332.45	54.928
H15A_5	4443.55	8589.62	7242.65	51.192

Atom	*x*	*y*	*z*	U(eq)
H15B_5	3370.72	8888.19	7203.78	51.192

Table 5.28 Atomic Occupancy for 4-Yb^{5+}(DME).

Atom	*Occupancy*	Atom	*Occupancy*	Atom	*Occupancy*
C47	0.849	H47A	0.849	H47B	0.849
C37	0.849	H37A	0.849	H37B	0.849
H37C	0.849	O1	0.849	C30A	0.849
H30A	0.849	H30B	0.849	I1	0.151
O2	0.849	C4	0.849	H4A	0.849
H4B	0.849	H4C	0.849	H2A_1	0.5

5.5.5 *5-Yb*$^{3+}$

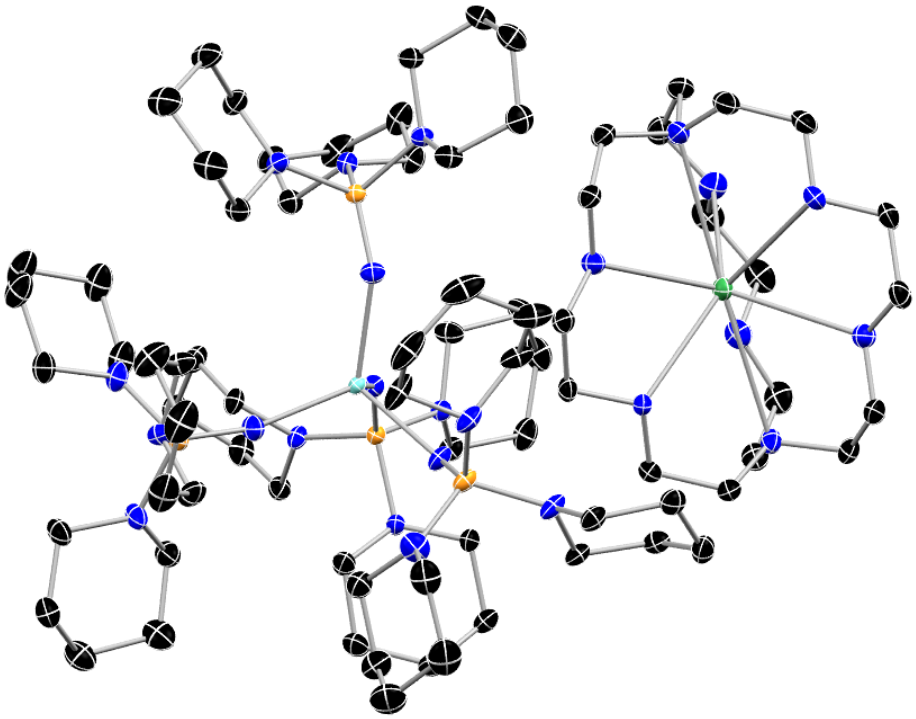

Figure 5.16 Molecular structure of 3-Yb^{5+} with thermal ellipsoids shown at 50% probability with hydrogen atoms omitted for clarity. Color code: C, black; N, blue; O, red; P, orange; K, green; Yb, blue.

Table 5.29 Crystal data and structure refinement for 5-Yb^{3+}.

Identification code	5-Yb^{3+}
Empirical formula	$C_{4.8}H_{9.71}K_{0.06}N_{1.03}O_{0.51}P_{0.23}Yb_{0.06}$
Formula weight	109.28
Temperature/K	99.99
Crystal system	triclinic
Space group	P-1
a/Å	13.9780(17)
b/Å	15.9280(16)
c/Å	23.929(3)
α/°	95.044(7)

β/°	105.496(5)
γ/°	101.582(6)
Volume/Å^3	4972.4(10)
Z	35
ρ_{calc}g/cm^3	1.277
μ/mm^{-1}	1.106
F(000)	2042.0
Crystal size/mm^3	0.411 × 0.272 × 0.222
Radiation	MoKα (λ = 0.71073)
2Θ range for data collection/°	4.36 to 56.548
Index ranges	-18 ≤ h ≤ 18, -21 ≤ k ≤ 20, -31 ≤ l ≤ 30
Reflections collected	105367
Independent reflections	24579 [R_{int} = 0.0501, R_{sigma} = 0.0405]
Data/restraints/parameters	24579/16/1079
Goodness-of-fit on F^2	1.032
Final R indexes [I>=2σ (I)]	R_1 = 0.0259, wR_2 = 0.0602
Final R indexes [all data]	R_1 = 0.0295, wR_2 = 0.0621
Largest diff. peak/hole / e Å^{-3}	0.96/-0.67

Table 5.30 Fractional Atomic Coordinates (×10^4) and Equivalent Isotropic Displacement Parameters (Å^2×10^3) for 5-Yb^{3+}. U_{eq} is defined as 1/3 of the trace of the orthogonalised U_{IJ} tensor.

Atom	*x*	*y*	*z*	U(eq)
Yb1	5357.3(2)	2264.1(2)	2493.2(2)	11.04(2)
P1	3840.9(3)	3091.6(3)	1326.2(2)	13.94(8)
P2	5625.9(3)	3170.4(3)	3898.6(2)	18.44(9)
P3	7660.8(3)	2083.1(3)	2220.9(2)	12.68(8)
P4	3823.7(3)	90.0(3)	2437.7(2)	19.23(9)
N1	4349.6(11)	2954.2(9)	1949.4(6)	18.4(3)
N2	2711.5(11)	2385.5(10)	985.3(6)	17.6(3)
N3	4430.3(11)	3043.5(9)	789.8(6)	15.9(3)
N4	3610.5(11)	4107.6(9)	1297.3(6)	16.2(3)
N5	6042.6(11)	2912.2(10)	3397.7(6)	19.6(3)
N6	5356.0(14)	2362.9(11)	4281.1(7)	29.1(4)
N7	4538.5(11)	3543.5(11)	3762.8(7)	22.9(3)
N8	6406.4(11)	4039.0(10)	4379.9(6)	21.3(3)
N9	6638.2(10)	2327.3(9)	2136.7(6)	16.1(3)
N10	7575.4(11)	1147.5(9)	1799.0(6)	16.4(3)
N11	8556.3(10)	2860.7(9)	2078.2(6)	15.4(3)
N12	8357.0(11)	1923.9(9)	2890.7(6)	15.4(3)
N13	4586.4(11)	949.9(9)	2522.4(7)	21.5(3)

Atom	*x*	*y*	*z*	U(eq)
N15	2764.9(11)	11.2(10)	2674.2(7)	21.4(3)
N16	3245.2(11)	-347.6(10)	1725.0(7)	22.6(3)
C1	2249.9(14)	1789.8(12)	1321.2(8)	22.6(4)
C2	1108.4(15)	1742.5(15)	1180.1(10)	32.9(5)
C3	581.7(16)	1480.9(16)	523.6(11)	39.2(6)
C4	1104.1(15)	2092.2(15)	179.8(10)	33.6(5)
C5	2249.9(14)	2146.8(13)	353.7(8)	24.1(4)
C6	5315.5(13)	3754.4(12)	842.6(8)	20.8(4)
C7	5622.6(15)	3712.7(14)	278.2(9)	29.5(4)
C8	5837.1(15)	2836.4(15)	111.8(9)	31.7(5)
C9	4945.9(15)	2100.9(13)	110.3(8)	25.4(4)
C10	4696.4(14)	2199.0(12)	691.7(8)	21.2(4)
C11	3219.4(15)	4384.8(12)	1777.7(8)	22.5(4)
C12	3285.0(17)	5355.3(13)	1848.0(9)	29.1(4)
C13	2718.7(16)	5615.9(13)	1278.7(9)	29.0(4)
C14	3093.1(16)	5286.1(13)	776.0(9)	26.9(4)
C15	3027.8(14)	4314.4(12)	739.5(8)	20.8(4)
C16	4924.0(17)	2425.2(15)	4769.5(9)	33.3(5)
C17	5650(2)	2292.4(16)	5334.6(10)	41.6(6)
C18	5966(2)	1436.7(17)	5254.1(10)	43.9(6)
C19	6389.1(17)	1382.6(15)	4729.1(9)	33.2(5)
C20	5638.9(15)	1542.6(13)	4182.9(9)	25.6(4)
C21	4605.2(15)	4333.9(14)	3478.2(8)	27.0(4)
C22	3730.4(17)	4755.1(16)	3512.7(9)	35.9(5)
C23	2710.8(17)	4125.6(18)	3231.3(10)	42.8(6)
C24	2665.9(15)	3256.9(17)	3457.1(10)	40.2(6)
C25	3598.6(15)	2899.6(15)	3433.1(9)	33.8(5)
C26	6110.0(14)	4510.2(12)	4834.2(8)	21.9(4)
C27	6685.0(15)	5457.1(12)	4959.7(8)	24.0(4)
C28	7835.5(15)	5532.4(12)	5153.3(8)	25.2(4)
C29	8134.4(14)	4982.5(12)	4699.0(8)	22.8(4)
C30	7493.8(13)	4052.7(12)	4560.9(8)	19.9(4)
C31	8376.6(14)	673.2(11)	1856.3(8)	20.0(4)
C32	8456.6(15)	344.2(13)	1256.0(9)	26.2(4)
C33	7424.6(16)	-193.5(13)	859.7(8)	27.3(4)
C34	6597.1(15)	313.3(13)	837.8(8)	25.7(4)
C35	6579.3(13)	623.8(12)	1453.1(8)	20.0(4)
C36	8162.7(14)	3274.2(13)	1571.1(8)	22.9(4)
C37	8860.4(17)	4153.7(14)	1599.6(10)	32.2(5)
C38	9949.8(16)	4072.4(14)	1651.4(10)	32.5(5)
C39	10318.1(14)	3596.6(13)	2160.7(9)	27.6(4)

Atom	*x*	*y*	*z*	U(eq)
C40	9579.3(13)	2733.9(12)	2112.0(8)	19.9(3)
C41	7795.8(14)	1221.4(12)	3124.4(8)	21.7(4)
C42	8497.7(17)	999.5(13)	3667.6(8)	28.8(4)
C43	8966.7(17)	1794.5(13)	4141.3(8)	30.0(4)
C44	9490.8(16)	2534.3(13)	3884.9(8)	27.3(4)
C45	8747.5(14)	2707.5(11)	3337.4(8)	20.6(4)
C51	2976.9(16)	145.2(14)	3317.2(8)	29.2(4)
C52	1994.3(19)	-91.5(16)	3488.6(10)	41.7(6)
C53	1270.6(18)	450.2(18)	3226.3(10)	43.2(6)
C54	1081.9(16)	344.1(18)	2563.4(10)	38.9(5)
C55	2086.0(14)	556.1(14)	2411.7(8)	25.7(4)
C56	2378.7(15)	-1096.2(13)	1513.3(9)	28.3(4)
C57	1770.1(16)	-1055.8(15)	893.5(9)	34.5(5)
C58	2444.4(18)	-1005.9(17)	481.5(10)	41.0(6)
C59	3370.3(17)	-238.2(15)	728.0(10)	35.8(5)
C60	3930.8(15)	-297.1(15)	1353.5(10)	32.2(5)
N14A	4384(6)	-736(6)	2679(8)	25.0(7)
C46A	3860(7)	-1655(6)	2540(4)	27.4(6)
C47A	4218(7)	-2119(6)	3056(5)	33.7(6)
C48A	5373(7)	-2005(6)	3224(6)	32.7(7)
C49A	5904(6)	-1045(6)	3324(5)	33.3(6)
C50A	5488(6)	-608(6)	2805(5)	26.3(5)
N14B	4325.6(16)	-656.6(14)	2794.3(14)	25.0(7)
C46B	3748.8(18)	-1519.2(15)	2818.0(13)	27.4(6)
C47B	4242(2)	-2212.3(16)	2620.4(12)	33.7(6)
C48B	5352(2)	-2050.1(16)	2992.6(13)	32.7(7)
C49B	5923.4(19)	-1125.9(17)	2994.2(14)	33.3(6)
C50B	5374.8(17)	-463.4(15)	3172.2(11)	26.3(5)
K1	8814.8(3)	6612.4(2)	2599.6(2)	17.41(7)
O1K	8489.5(9)	5271.7(7)	3259.7(5)	18.3(2)
O2K	6987.4(9)	5350.5(8)	2245.2(6)	20.9(3)
O3K	10707.9(10)	6450.3(9)	2415.5(6)	26.1(3)
O4K	9155.9(11)	6838.4(9)	1497.7(6)	26.6(3)
O5K	9783.3(10)	8025.5(8)	3524.0(6)	23.2(3)
O6K	7990.8(10)	8113.1(8)	2638.6(6)	22.9(3)
N1K	10556.9(11)	6462.5(10)	3622.2(7)	20.5(3)
N2K	7093.8(12)	6814.8(10)	1558.9(7)	22.2(3)
C1K	7689.1(13)	4517.1(11)	2959.7(8)	19.7(3)
C2K	6755.9(14)	4808.5(12)	2662.5(8)	21.1(4)
C3K	10913.0(16)	6901.9(14)	1956.8(10)	32.0(5)
C4K	10036.6(17)	6587.2(14)	1413.3(9)	32.0(5)

Atom	*x*	*y*	*z*	U(eq)
C5K	9213.2(16)	8659.8(12)	3578.8(8)	25.0(4)
C6K	8740.9(15)	8855.1(12)	2978.1(9)	25.0(4)
C7K	9378.8(14)	5035.8(11)	3583.1(8)	19.8(3)
C8K	10126.4(14)	5833.3(12)	3957.6(8)	22.1(4)
C9K	11317.8(14)	6144.9(13)	3391.4(9)	27.1(4)
C10K	11582.1(15)	6614.8(14)	2913.8(10)	31.1(4)
C11K	11036.7(15)	7304.3(12)	4003.0(9)	26.9(4)
C12K	10283.2(16)	7828.1(12)	4084.3(8)	26.4(4)
C13K	6302.7(15)	5999.0(13)	1414.2(8)	26.1(4)
C14K	6110.5(14)	5631.9(12)	1945.2(8)	22.8(4)
C15K	7466.3(16)	6969.1(13)	1047.2(8)	28.0(4)
C16K	8281.2(16)	6498.7(13)	1003.6(8)	29.1(4)
C17K	6680.0(15)	7538.9(12)	1731.7(9)	26.3(4)
C18K	7503.6(16)	8314.1(12)	2078.8(9)	25.8(4)
O1D	7951.6(12)	7280.1(10)	4349.5(7)	33.9(3)
O2D	8883.5(14)	8992.1(11)	5076.0(8)	47.3(4)
C1D	8536(2)	9699.9(16)	4876.6(12)	48.6(6)
C2D	8119(2)	8330.0(15)	5165.6(11)	40.2(5)
C3D	7409.0(18)	7773.7(14)	4609.0(10)	35.2(5)
C4D	7358.2(19)	6813.2(14)	3787.4(10)	36.0(5)
C5D	1362.1(19)	6703.0(15)	33.5(11)	43.5(6)
C6D	221(2)	5396.4(17)	-53.8(13)	65.7(9)
O3D	825.4(19)	6025.1(15)	289.6(10)	37.4(5)
O4D	965(3)	5774.7(19)	-190.1(17)	37.4(5)

Table 5.31 Anisotropic Displacement Parameters ($Å^2×10^3$) for 5-Yb^{3+}. The Anisotropic displacement factor exponent takes the form: $-2\pi^2[h^2a^{*2}U_{11}+2hka^*b^*U_{12}+\ldots]$.

Atom	U_{11}	U_{22}	U_{33}	U_{23}	U_{13}	U_{12}
Yb1	9.37(4)	13.08(4)	10.29(4)	0.88(2)	2.98(2)	2.01(2)
P1	11.18(19)	16.7(2)	14.7(2)	3.51(15)	4.13(15)	3.81(16)
P2	15.0(2)	25.6(2)	13.0(2)	-2.65(17)	2.71(16)	5.03(17)
P3	11.18(19)	13.87(19)	13.15(19)	1.30(15)	4.54(15)	2.26(15)
P4	12.6(2)	17.6(2)	26.0(2)	7.14(18)	4.79(17)	-0.14(16)
N1	16.7(7)	22.9(7)	17.3(7)	4.8(6)	5.7(6)	7.0(6)
N2	14.5(7)	21.0(7)	16.1(7)	4.4(6)	4.5(6)	0.4(6)
N3	13.7(7)	17.2(7)	17.2(7)	2.1(5)	5.9(5)	3.1(5)
N4	16.1(7)	18.5(7)	15.1(7)	3.4(5)	4.6(6)	6.3(6)

Atom	U_{11}	U_{22}	U_{33}	U_{23}	U_{13}	U_{12}
N5	16.4(7)	25.3(8)	13.8(7)	-3.5(6)	2.4(6)	3.1(6)
N6	37.0(10)	30.0(9)	27.2(9)	4.7(7)	18.8(8)	10.7(8)
N7	13.9(7)	32.4(9)	18.8(7)	-5.3(6)	1.7(6)	5.1(6)
N8	14.8(7)	30.4(8)	15.5(7)	-6.5(6)	0.6(6)	7.2(6)
N9	13.9(7)	19.0(7)	16.7(7)	3.1(5)	7.2(5)	2.9(5)
N10	12.0(7)	17.9(7)	17.8(7)	-2.4(5)	3.0(5)	3.7(5)
N11	10.9(6)	17.6(7)	17.8(7)	4.1(5)	4.8(5)	2.5(5)
N12	17.0(7)	13.5(7)	14.4(7)	1.3(5)	3.7(5)	2.0(5)
N13	17.8(7)	19.8(7)	25.2(8)	5.0(6)	6.3(6)	-0.6(6)
N15	16.2(7)	28.3(8)	18.9(8)	9.3(6)	5.3(6)	0.7(6)
N16	15.3(7)	23.3(8)	26.7(8)	0.2(6)	9.0(6)	-3.4(6)
C1	17.7(9)	23.3(9)	26.6(10)	8.6(7)	7.0(7)	1.2(7)
C2	18.3(9)	42.8(12)	42.4(12)	18.6(10)	14.5(9)	5.2(9)
C3	16.2(9)	47.5(14)	47.4(14)	19.8(11)	2.4(9)	-2.9(9)
C4	18.2(9)	41.4(12)	32.7(11)	13.6(9)	-1.5(8)	-3.4(9)
C5	20.4(9)	27.5(10)	19.5(9)	2.0(7)	3.3(7)	-1.2(7)
C6	13.4(8)	25.3(9)	21.2(9)	-0.8(7)	6.5(7)	-1.3(7)
C7	23.0(10)	36.6(11)	25.7(10)	0.0(8)	12.7(8)	-5.9(8)
C8	22.1(10)	50.8(13)	22.1(10)	-3.6(9)	11.1(8)	5.7(9)
C9	23.0(9)	31.5(10)	21.5(9)	-2.7(8)	6.2(7)	9.2(8)
C10	22.3(9)	21.0(9)	22.6(9)	2.2(7)	7.9(7)	8.8(7)
C11	25.6(9)	27.5(10)	20.2(9)	5.6(7)	10.2(7)	13.8(8)
C12	33.3(11)	27.4(10)	29.2(10)	-0.7(8)	10.4(9)	13.4(9)
C13	33.2(11)	24.9(10)	36.2(11)	9.4(8)	14.5(9)	15.5(8)
C14	29.5(10)	26.6(10)	30.8(10)	11.1(8)	11.9(8)	13.1(8)
C15	22.2(9)	22.9(9)	18.7(9)	5.6(7)	4.9(7)	8.8(7)
C16	37.7(12)	34.4(11)	34.3(11)	3.9(9)	24.8(10)	4.5(9)
C17	57.6(16)	42.3(13)	27.6(11)	3.0(9)	23.8(11)	3.5(11)
C18	56.7(16)	47.6(14)	27.6(12)	10.8(10)	12.0(11)	11.1(12)
C19	31.0(11)	37.4(12)	28.5(11)	3.9(9)	5.5(9)	6.6(9)
C20	25.5(10)	25.8(10)	24.2(10)	1.3(7)	6.1(8)	5.3(8)
C21	22.9(9)	43.6(12)	16.1(9)	3.6(8)	4.1(7)	14.2(9)
C22	37.3(12)	56.1(14)	23.4(10)	9.8(9)	9.9(9)	28.0(11)
C23	26.4(11)	80.3(19)	26.1(11)	3.1(11)	5.9(9)	27.0(12)
C24	15.5(9)	65.8(16)	30.3(11)	-18.2(11)	4.5(8)	3.2(10)
C25	16.7(9)	46.4(13)	29.2(11)	-16.7(9)	2.3(8)	2.3(9)
C26	22.1(9)	27.9(9)	14.9(8)	-3.0(7)	5.1(7)	7.1(7)
C27	28.6(10)	25.5(9)	18.4(9)	-0.1(7)	7.0(7)	8.4(8)
C28	28.0(10)	22.3(9)	21.7(9)	-0.8(7)	6.2(8)	0.7(8)
C29	19.4(9)	28.2(10)	19.8(9)	4.6(7)	4.2(7)	5.1(7)
C30	15.4(8)	26.8(9)	15.3(8)	-0.8(7)	0.9(6)	6.0(7)

Atom	U_{11}	U_{22}	U_{33}	U_{23}	U_{13}	U_{12}
C31	18.8(8)	17.4(8)	23.2(9)	0.5(7)	4.1(7)	6.9(7)
C32	23.6(9)	25.7(10)	31.7(10)	-2.5(8)	11.7(8)	9.1(8)
C33	35.4(11)	24.0(9)	21.6(9)	-4.8(7)	8.7(8)	8.2(8)
C34	25.4(10)	25.9(10)	20.3(9)	-4.9(7)	1.3(7)	4.4(8)
C35	14.7(8)	19.2(8)	22.5(9)	-2.7(7)	3.7(7)	0.4(7)
C36	18.8(9)	29.8(10)	24.0(9)	12.6(8)	9.1(7)	7.2(7)
C37	35.5(11)	27.8(10)	43.6(13)	18.7(9)	22.9(10)	9.7(9)
C38	29.1(11)	27.3(10)	44.7(13)	10.3(9)	20.5(10)	-1.1(8)
C39	16.4(9)	30.9(10)	30.6(10)	-1.8(8)	8.5(8)	-4.9(8)
C40	12.6(8)	25.4(9)	21.8(9)	2.7(7)	6.0(7)	3.7(7)
C41	25.7(9)	19.9(9)	18.3(9)	4.8(7)	6.8(7)	0.9(7)
C42	40.6(12)	22.2(9)	21.8(9)	7.7(7)	5.5(8)	6.4(8)
C43	39.6(12)	30.9(11)	16.5(9)	4.7(8)	2.6(8)	8.5(9)
C44	28.8(10)	27.4(10)	18.2(9)	-0.7(7)	-2.5(8)	4.2(8)
C45	25.3(9)	15.9(8)	17.2(8)	-0.2(6)	2.5(7)	3.5(7)
C51	29.5(10)	33.9(11)	18.2(9)	6.5(8)	3.2(8)	-2.5(8)
C52	49.5(14)	45.1(14)	25.8(11)	0.8(10)	20.4(10)	-10.6(11)
C53	30.3(12)	58.6(16)	38.2(13)	-6.4(11)	22.2(10)	-5.8(11)
C54	18.4(10)	61.5(16)	34.2(12)	-0.9(11)	8.9(9)	5.7(10)
C55	17.2(9)	40.1(11)	21.8(9)	8.3(8)	6.7(7)	8.1(8)
C56	21.9(9)	23.6(10)	35.2(11)	2.4(8)	9.0(8)	-4.2(8)
C57	22.2(10)	39.9(12)	33.1(11)	-1.2(9)	6.9(9)	-7.0(9)
C58	34.6(12)	47.6(14)	30.5(12)	-6.9(10)	11.2(10)	-10.4(10)
C59	30.6(11)	39.2(12)	34.2(12)	-3.0(9)	17.5(9)	-6.7(9)
C60	21.0(10)	36.0(11)	37.1(12)	-4.2(9)	14.4(9)	-3.0(8)
N14A	14.3(8)	17.1(9)	39.1(17)	8.1(9)	1.9(8)	-0.4(6)
C46A	19.5(11)	19.8(11)	40.8(16)	11.0(11)	5.9(11)	1.2(9)
C47A	38.5(14)	20.5(12)	37.6(14)	2.7(10)	6.4(12)	4.1(10)
C48A	33.1(12)	30.1(12)	42.9(18)	9.6(13)	15.8(13)	17.1(10)
C49A	20.0(11)	37.0(14)	48.0(18)	13.8(13)	13.6(12)	10.5(10)
C50A	18.3(11)	23.9(11)	33.9(13)	7.0(10)	3.8(10)	3.0(9)
N14B	14.3(8)	17.1(9)	39.1(17)	8.1(9)	1.9(8)	-0.4(6)
C46B	19.5(11)	19.8(11)	40.8(16)	11.0(11)	5.9(11)	1.2(9)
C47B	38.5(14)	20.5(12)	37.6(14)	2.7(10)	6.4(12)	4.1(10)
C48B	33.1(12)	30.1(12)	42.9(18)	9.6(13)	15.8(13)	17.1(10)
C49B	20.0(11)	37.0(14)	48.0(18)	13.8(13)	13.6(12)	10.5(10)
C50B	18.3(11)	23.9(11)	33.9(13)	7.0(10)	3.8(10)	3.0(9)
K1	16.80(17)	16.05(17)	18.67(17)	2.11(13)	5.63(14)	1.82(13)
O1K	17.7(6)	13.6(6)	19.7(6)	1.5(5)	1.1(5)	1.4(5)
O2K	15.3(6)	21.9(6)	23.6(7)	8.1(5)	4.1(5)	0.1(5)
O3K	21.3(7)	27.3(7)	31.9(7)	6.9(6)	13.4(6)	2.2(5)

Atom	U_{11}	U_{22}	U_{33}	U_{23}	U_{13}	U_{12}
O4K	28.8(7)	30.6(7)	22.6(7)	2.6(5)	12.6(6)	5.7(6)
O5K	29.8(7)	19.6(6)	19.5(6)	0.3(5)	5.0(5)	8.4(5)
O6K	27.2(7)	15.1(6)	25.7(7)	5.7(5)	6.0(6)	4.5(5)
N1K	15.7(7)	17.3(7)	25.2(8)	0.5(6)	3.0(6)	2.0(6)
N2K	23.5(8)	19.8(8)	20.8(8)	5.9(6)	4.4(6)	0.9(6)
C1K	20.2(9)	14.5(8)	21.2(9)	1.4(6)	5.5(7)	-1.7(7)
C2K	18.2(8)	20.3(9)	22.0(9)	4.8(7)	5.3(7)	-1.3(7)
C3K	27.8(10)	32.3(11)	44.3(13)	11.8(9)	23.4(10)	6.0(9)
C4K	39.7(12)	34.3(11)	32.3(11)	8.8(9)	24.3(10)	11.3(9)
C5K	33.6(11)	16.1(8)	25.9(10)	0.2(7)	10.0(8)	6.6(8)
C6K	30.4(10)	14.9(8)	28.8(10)	3.8(7)	8.1(8)	3.8(7)
C7K	21.3(9)	17.5(8)	21.2(9)	4.4(7)	5.4(7)	6.6(7)
C8K	21.4(9)	21.3(9)	20.5(9)	3.0(7)	1.0(7)	4.9(7)
C9K	17.3(9)	27.5(10)	35.8(11)	4.6(8)	5.3(8)	7.0(8)
C10K	16.2(9)	33.4(11)	43.8(12)	5.5(9)	11.5(9)	2.7(8)
C11K	21.8(9)	20.9(9)	28.3(10)	-0.4(7)	-3.8(8)	-0.1(7)
C12K	34.5(11)	19.7(9)	19.3(9)	-1.1(7)	1.6(8)	3.5(8)
C13K	23.6(9)	26.2(10)	20.9(9)	5.3(7)	-1.2(7)	-1.8(8)
C14K	17.9(9)	22.8(9)	22.5(9)	3.6(7)	0.6(7)	0.3(7)
C15K	33.5(11)	27.0(10)	19.8(9)	9.5(8)	3.8(8)	1.4(8)
C16K	38.8(12)	27.5(10)	18.7(9)	2.3(7)	9.3(8)	1.7(9)
C17K	22.9(9)	24.3(10)	30.8(10)	10.7(8)	3.4(8)	6.4(8)
C18K	30.4(10)	19.9(9)	29.6(10)	9.7(7)	8.3(8)	9.5(8)
O1D	39.2(9)	34.3(8)	36.0(8)	7.6(6)	17.6(7)	16.1(7)
O2D	49.6(10)	32.3(9)	58.0(11)	13.6(8)	13.6(9)	5.1(8)
C1D	76.1(19)	31.8(12)	44.7(14)	11.0(11)	24.7(14)	15.8(12)
C2D	50.0(14)	31.5(12)	40.8(13)	6.3(10)	19.8(11)	4.5(10)
C3D	36.5(12)	29.7(11)	46.0(13)	4.6(9)	21.8(10)	10.1(9)
C4D	46.4(13)	31.1(11)	37.0(12)	7.0(9)	19.6(10)	13.1(10)
C5D	38.0(13)	27.4(11)	60.9(16)	12.2(11)	12.6(12)	-1.6(10)
C6D	37.5(14)	40.2(15)	102(3)	30.5(16)	-4.2(15)	-7.2(12)
O3D	39.3(12)	35.0(11)	36.8(12)	-0.1(9)	17.8(10)	-0.4(9)
O4D	39.3(12)	35.0(11)	36.8(12)	-0.1(9)	17.8(10)	-0.4(9)

Table 5.32 Bond Lengths for 5-Yb^{3+}.

Atom	Atom	Length/Å	Atom	Atom	Length/Å
Yb1	N1	2.1863(13)	C37	C38	1.527(3)
Yb1	N5	2.1840(13)	C38	C39	1.519(3)
Yb1	N9	2.1686(12)	C39	C40	1.519(3)
Yb1	N13	2.1697(13)	C41	C42	1.522(3)

Atom	Atom	Length/Å	Atom	Atom	Length/Å
P1	N1	1.5265(14)	C42	C43	1.528(3)
P1	N2	1.6911(15)	C43	C44	1.524(3)
P1	N3	1.7044(15)	C44	C45	1.524(3)
P1	N4	1.7160(15)	C51	C52	1.522(3)
P2	N5	1.5256(14)	C52	C53	1.506(4)
P2	N6	1.6825(18)	C53	C54	1.525(3)
P2	N7	1.7035(16)	C54	C55	1.523(3)
P2	N8	1.6950(15)	C56	C57	1.514(3)
P3	N9	1.5226(14)	C57	C58	1.532(3)
P3	N10	1.6894(14)	C58	C59	1.532(3)
P3	N11	1.7023(14)	C59	C60	1.513(3)
P3	N12	1.7079(15)	N14A	C46A	1.463(5)
P4	N13	1.5176(14)	N14A	C50A	1.459(5)
P4	N15	1.7065(16)	C46A	C47A	1.517(6)
P4	N16	1.6959(17)	C47A	C48A	1.524(6)
P4	N14A	1.728(8)	C48A	C49A	1.527(6)
P4	N14B	1.682(2)	C49A	C50A	1.515(5)
N2	C1	1.459(2)	N14B	C46B	1.461(3)
N2	C5	1.458(2)	N14B	C50B	1.458(3)
N3	C6	1.469(2)	C46B	C47B	1.518(3)
N3	C10	1.481(2)	C47B	C48B	1.526(4)
N4	C11	1.469(2)	C48B	C49B	1.527(3)
N4	C15	1.469(2)	C49B	C50B	1.518(3)
N6	C16	1.456(2)	K1	O1K	2.8016(13)
N6	C20	1.457(2)	K1	O2K	2.7865(13)
N7	C21	1.482(3)	K1	O3K	2.8532(14)
N7	C25	1.471(2)	K1	O4K	2.8424(14)
N8	C26	1.462(2)	K1	O5K	2.8448(13)
N8	C30	1.460(2)	K1	O6K	2.8589(13)
N10	C31	1.456(2)	K1	N1K	3.0211(16)
N10	C35	1.455(2)	K1	N2K	3.0567(16)
N11	C36	1.462(2)	O1K	C1K	1.446(2)
N11	C40	1.466(2)	O1K	C7K	1.418(2)
N12	C41	1.474(2)	O2K	C2K	1.435(2)
N12	C45	1.476(2)	O2K	C14K	1.423(2)
N15	C51	1.474(2)	O3K	C3K	1.424(2)
N15	C55	1.468(2)	O3K	C10K	1.422(2)
N16	C56	1.460(2)	O4K	C4K	1.426(2)
N16	C60	1.467(2)	O4K	C16K	1.426(2)
C1	C2	1.525(3)	O5K	C5K	1.424(2)
C2	C3	1.526(3)	O5K	C12K	1.431(2)

Atom	Atom	Length/Å	Atom	Atom	Length/Å
C3	C4	1.528(3)	O6K	C6K	1.426(2)
C4	C5	1.526(3)	O6K	C18K	1.427(2)
C6	C7	1.522(3)	N1K	C8K	1.472(2)
C7	C8	1.527(3)	N1K	C9K	1.474(2)
C8	C9	1.528(3)	N1K	C11K	1.475(2)
C9	C10	1.525(3)	N2K	C13K	1.473(2)
C11	C12	1.522(3)	N2K	C15K	1.474(2)
C12	C13	1.520(3)	N2K	C17K	1.466(2)
C13	C14	1.527(3)	C1K	C2K	1.493(3)
C14	C15	1.525(3)	C3K	C4K	1.493(3)
C16	C17	1.519(3)	C5K	C6K	1.501(3)
C17	C18	1.526(4)	C7K	C8K	1.508(2)
C18	C19	1.528(3)	C9K	C10K	1.506(3)
C19	C20	1.519(3)	C11K	C12K	1.509(3)
C21	C22	1.525(3)	C13K	C14K	1.509(3)
C22	C23	1.512(3)	C15K	C16K	1.504(3)
C23	C24	1.525(4)	C17K	C18K	1.509(3)
C24	C25	1.536(3)	O1D	C3D	1.409(2)
C26	C27	1.522(3)	O1D	C4D	1.425(3)
C27	C28	1.526(3)	O2D	C1D	1.388(3)
C28	C29	1.532(3)	O2D	C2D	1.418(3)
C29	C30	1.526(3)	C2D	C3D	1.509(3)
C31	C32	1.526(3)	C5D	O3D	1.463(3)
C32	C33	1.531(3)	C5D	O4D	1.467(3)
C33	C34	1.530(3)	C6D	C6D^{1}	1.368(5)
C34	C35	1.520(2)	C6D	O3D	1.240(3)
C36	C37	1.522(3)	C6D	O4D	1.232(3)

Table 5.33 Bond Angles for 5-Yb^{3+}.

Atom	Atom	Atom	Angle/°	Atom	Atom	Atom	Angle/°
N5	Yb1	N1	113.37(6)	N11	C40	C39	110.55(15)
N9	Yb1	N1	105.56(5)	N12	C41	C42	110.59(15)
N9	Yb1	N5	104.38(5)	C41	C42	C43	110.96(16)
N9	Yb1	N13	113.32(6)	C44	C43	C42	109.37(16)
N13	Yb1	N1	112.60(6)	C43	C44	C45	110.40(16)
N13	Yb1	N5	107.42(6)	N12	C45	C44	110.49(14)
N1	P1	N2	114.87(8)	N15	C51	C52	110.89(16)
N1	P1	N3	121.60(8)	C53	C52	C51	110.33(19)
N1	P1	N4	112.52(8)	C52	C53	C54	109.5(2)
N2	P1	N3	99.99(7)	C55	C54	C53	110.81(17)

Atom	Atom	Atom	Angle/°	Atom	Atom	Atom	Angle/°
N2	P1	N4	106.11(7)	N15	C55	C54	110.99(17)
N3	P1	N4	99.57(7)	N16	C56	C57	110.37(17)
N5	P2	Yb1	26.86(5)	C56	C57	C58	111.03(18)
N5	P2	N6	113.76(9)	C57	C58	C59	109.35(18)
N5	P2	N7	120.54(8)	C60	C59	C58	110.63(19)
N5	P2	N8	113.43(8)	N16	C60	C59	111.04(17)
N6	P2	Yb1	108.12(6)	C46A	N14A	P4	124.0(6)
N6	P2	N7	101.70(9)	C50A	N14A	P4	118.7(6)
N6	P2	N8	108.02(9)	C50A	N14A	C46A	112.2(7)
N7	P2	Yb1	98.40(5)	N14A	C46A	C47A	110.2(6)
N8	P2	Yb1	136.31(6)	C46A	C47A	C48A	110.5(6)
N8	P2	N7	97.49(8)	C47A	C48A	C49A	110.3(6)
N9	P3	Yb1	21.50(5)	C50A	C49A	C48A	111.4(6)
N9	P3	N10	113.06(8)	N14A	C50A	C49A	110.0(6)
N9	P3	N11	112.94(7)	C46B	N14B	P4	124.73(17)
N9	P3	N12	121.44(7)	C50B	N14B	P4	122.28(17)
N10	P3	Yb1	113.82(5)	C50B	N14B	C46B	112.6(2)
N10	P3	N11	107.28(7)	N14B	C46B	C47B	110.6(2)
N10	P3	N12	101.40(7)	C46B	C47B	C48B	110.2(2)
N11	P3	Yb1	128.74(5)	C47B	C48B	C49B	110.5(2)
N11	P3	N12	98.93(7)	C50B	C49B	C48B	111.6(2)
N12	P3	Yb1	101.53(5)	N14B	C50B	C49B	110.0(2)
N13	P4	N15	121.37(9)	O1K	K1	O3K	100.48(4)
N13	P4	N16	113.92(8)	O1K	K1	O4K	138.67(4)
N13	P4	N14A	113.3(3)	O1K	K1	O5K	99.69(4)
N13	P4	N14B	113.29(10)	O1K	K1	O6K	124.41(4)
N15	P4	N14A	106.9(5)	O1K	K1	N1K	61.39(4)
N16	P4	N15	98.84(8)	O1K	K1	N2K	120.37(4)
N16	P4	N14A	99.5(6)	O2K	K1	O1K	59.78(4)
N14B	P4	N15	98.86(11)	O2K	K1	O3K	126.51(4)
N14B	P4	N16	108.62(11)	O2K	K1	O4K	100.62(4)
P1	N1	Yb1	145.85(9)	O2K	K1	O5K	136.84(4)
C1	N2	P1	118.93(12)	O2K	K1	O6K	98.54(4)
C5	N2	P1	126.26(12)	O2K	K1	N1K	120.87(4)
C5	N2	C1	113.01(14)	O2K	K1	N2K	60.90(4)
C6	N3	P1	116.77(11)	O3K	K1	O6K	129.08(4)
C6	N3	C10	109.87(14)	O3K	K1	N1K	60.20(4)
C10	N3	P1	112.46(11)	O3K	K1	N2K	118.90(4)
C11	N4	P1	112.03(11)	O4K	K1	O3K	60.14(4)
C15	N4	P1	119.35(11)	O4K	K1	O5K	116.17(4)
C15	N4	C11	110.67(14)	O4K	K1	O6K	92.49(4)

Atom	Atom	Atom	Angle/°	Atom	Atom	Atom	Angle/°
P2	N5	Yb1	134.74(9)	O4K	K1	N1K	119.74(4)
C16	N6	P2	125.16(14)	O4K	K1	N2K	59.16(4)
C16	N6	C20	113.16(17)	O5K	K1	O3K	92.58(4)
C20	N6	P2	121.42(13)	O5K	K1	O6K	60.03(4)
C21	N7	P2	113.44(12)	O5K	K1	N1K	59.40(4)
C25	N7	P2	115.16(13)	O5K	K1	N2K	119.54(4)
C25	N7	C21	109.25(16)	O6K	K1	N1K	119.03(4)
C26	N8	P2	124.15(13)	O6K	K1	N2K	60.13(4)
C30	N8	P2	116.68(12)	N1K	K1	N2K	178.23(4)
C30	N8	C26	111.82(14)	C1K	O1K	K1	115.89(10)
P3	N9	Yb1	143.59(9)	C7K	O1K	K1	115.74(10)
C31	N10	P3	125.50(11)	C7K	O1K	C1K	111.50(13)
C35	N10	P3	119.87(11)	C2K	O2K	K1	117.75(10)
C35	N10	C31	112.56(14)	C14K	O2K	K1	115.59(10)
C36	N11	P3	114.20(11)	C14K	O2K	C2K	110.63(13)
C36	N11	C40	111.34(14)	C3K	O3K	K1	111.69(11)
C40	N11	P3	121.28(12)	C10K	O3K	K1	117.97(11)
C41	N12	P3	112.32(11)	C10K	O3K	C3K	111.58(15)
C41	N12	C45	109.38(14)	C4K	O4K	K1	115.28(11)
C45	N12	P3	114.56(11)	C4K	O4K	C16K	111.43(15)
P4	N13	Yb1	165.65(10)	C16K	O4K	K1	114.49(11)
C51	N15	P4	114.57(12)	C5K	O5K	K1	115.93(11)
C55	N15	P4	113.99(12)	C5K	O5K	C12K	111.46(14)
C55	N15	C51	109.97(16)	C12K	O5K	K1	117.38(10)
C56	N16	P4	125.57(13)	C6K	O6K	K1	111.69(10)
C56	N16	C60	112.07(15)	C6K	O6K	C18K	109.83(14)
C60	N16	P4	114.57(12)	C18K	O6K	K1	114.76(10)
N2	C1	C2	110.46(15)	C8K	N1K	K1	107.03(10)
C1	C2	C3	110.99(18)	C8K	N1K	C9K	110.31(15)
C2	C3	C4	110.15(18)	C8K	N1K	C11K	109.66(15)
C5	C4	C3	110.80(17)	C9K	N1K	K1	108.58(11)
N2	C5	C4	111.59(16)	C9K	N1K	C11K	109.92(15)
N3	C6	C7	110.18(14)	C11K	N1K	K1	111.30(11)
C6	C7	C8	111.96(17)	C13K	N2K	K1	106.96(10)
C7	C8	C9	110.34(16)	C13K	N2K	C15K	109.56(15)
C10	C9	C8	110.33(15)	C15K	N2K	K1	110.92(11)
N3	C10	C9	109.79(15)	C17K	N2K	K1	108.88(11)
N4	C11	C12	111.54(16)	C17K	N2K	C13K	110.21(15)
C13	C12	C11	110.93(16)	C17K	N2K	C15K	110.25(15)
C12	C13	C14	110.07(16)	O1K	C1K	C2K	108.73(14)
C15	C14	C13	111.09(16)	O2K	C2K	C1K	108.87(14)

Atom	Atom	Atom	Angle/°	Atom	Atom	Atom	Angle/°
N4	C15	C14	110.82(15)	O3K	C3K	C4K	109.09(16)
N6	C16	C17	111.53(18)	O4K	C4K	C3K	109.55(17)
C16	C17	C18	110.80(19)	O5K	C5K	C6K	108.46(15)
C17	C18	C19	110.49(19)	O6K	C6K	C5K	109.88(15)
C20	C19	C18	110.80(19)	O1K	C7K	C8K	109.29(14)
N6	C20	C19	111.44(17)	N1K	C8K	C7K	114.17(15)
N7	C21	C22	110.13(17)	N1K	C9K	C10K	113.57(16)
C23	C22	C21	110.80(19)	O3K	C10K	C9K	109.51(15)
C22	C23	C24	112.04(18)	N1K	C11K	C12K	113.64(15)
C23	C24	C25	111.55(19)	O5K	C12K	C11K	108.17(16)
N7	C25	C24	109.54(17)	N2K	C13K	C14K	113.74(15)
N8	C26	C27	110.12(15)	O2K	C14K	C13K	108.65(15)
C26	C27	C28	110.49(16)	N2K	C15K	C16K	113.03(16)
C27	C28	C29	109.97(15)	O4K	C16K	C15K	108.52(16)
C30	C29	C28	111.57(15)	N2K	C17K	C18K	112.61(16)
N8	C30	C29	110.65(15)	O6K	C18K	C17K	109.57(15)
N10	C31	C32	110.99(15)	C3D	O1D	C4D	112.70(17)
C31	C32	C33	111.08(16)	C1D	O2D	C2D	114.2(2)
C34	C33	C32	110.28(15)	O2D	C2D	C3D	114.3(2)
C35	C34	C33	110.71(16)	O1D	C3D	C2D	109.62(19)
N10	C35	C34	110.56(15)	O3D	C6D	C6D^{1}	130.0(4)
N11	C36	C37	111.08(16)	O4D	C6D	C6D^{1}	141.8(4)
C36	C37	C38	111.04(17)	C6D	O3D	C5D	117.1(2)
C39	C38	C37	109.84(16)	C6D	O4D	C5D	117.4(2)
C40	C39	C38	111.47(16)				

Table 5.34 Hydrogen Atom Coordinates (Å×10^{4}) and Isotropic Displacement Parameters (Å^{2}×10^{3}) for 5-Yb^{3+}.

Atom	*x*	*y*	*z*	U(eq)
H1A	2580.9	1989.59	1745.74	27
H1B	2359.37	1205.6	1225.69	27
H2A	1001.69	2314.68	1310.81	39
H2B	801.02	1314.46	1396.27	39
H3A	-145.31	1503.03	437.64	47
H3B	611.33	878.88	401.25	47
H4A	805.35	1880.32	-245.55	40
H4B	983.81	2677.04	258.01	40
H5A	2370.41	1578.85	226.19	29
H5B	2579.15	2582.36	150.53	29
H6A	5894.82	3710.58	1174.49	25

Atom	*x*	*y*	*z*	U(eq)
H6B	5143.18	4317.14	923.41	25
H7A	6241.28	4176.12	327.91	35
H7B	5067.7	3818.39	-43.99	35
H8A	6469.76	2773.92	395.96	38
H8B	5940.74	2804.57	-282.23	38
H9A	4338.92	2109.52	-215.12	30
H9B	5126.12	1537.1	46.92	30
H10A	4115.82	1721.9	685.48	25
H10B	5293.04	2165.6	1016.16	25
H11A	3619.47	4236.39	2148.36	27
H11B	2499.33	4068.49	1697.71	27
H12A	2986.07	5515.38	2161.76	35
H12B	4010.26	5673.54	1965.83	35
H13A	2834.82	6255.12	1320.1	35
H13B	1976.59	5369.32	1191.26	35
H14A	2673	5407.39	401.45	32
H14B	3809.4	5597.9	836.64	32
H15A	2304.31	3998.48	643.9	25
H15B	3301.1	4121.98	421.5	25
H16A	4274.09	1982.23	4677.64	40
H16B	4772.31	3002.76	4823.32	40
H17A	5313.42	2292.22	5649.73	50
H17B	6265.2	2777.21	5454.46	50
H18A	5367.38	947.44	5191.6	53
H18B	6492.24	1390.42	5613.07	53
H19A	7043.11	1819.16	4816.25	40
H19B	6524.67	801.87	4658.37	40
H20A	5950.11	1548.19	3856.58	31
H20B	5017.93	1063.98	4067.85	31
H21A	4571.92	4179.99	3062.35	32
H21B	5265.88	4748.74	3676.18	32
H22A	3794.79	4947.83	3928.61	43
H22B	3769.43	5271.79	3310.59	43
H23A	2586.01	4030.43	2800.89	51
H23B	2163.19	4380.34	3313.31	51
H24A	2036.2	2835.63	3216.81	48
H24B	2636.49	3329.22	3866.94	48
H25A	3570.77	2355.19	3604.83	41
H25B	3594.34	2769.68	3020.06	41
H26A	6265.38	4245.55	5197.31	26
H26B	5365.92	4470.56	4702.58	26

Atom	*x*	*y*	*z*	U(eq)
H27A	6488.04	5768.63	5272.01	29
H27B	6498.84	5729.75	4602.14	29
H28A	8036.04	5331.85	5538.62	30
H28B	8200.21	6146.09	5196.69	30
H29A	8040.21	5245.35	4334.11	27
H29B	8865.31	4978.94	4850.59	27
H30A	7665.57	3728.66	4243.25	24
H30B	7654.03	3763.5	4912.78	24
H31A	8226.87	175.88	2065.13	24
H31B	9037.67	1057.56	2091.84	24
H32A	8965.83	-15.68	1304.91	31
H32B	8694.31	843.55	1068.61	31
H33A	7473.98	-337.88	458.99	33
H33B	7239.64	-742.66	1011.9	33
H34A	6730.36	818.31	632.97	31
H34B	5922.98	-62.13	614.05	31
H35A	6060.65	971.15	1430.74	24
H35B	6387.2	117.56	1646.05	24
H36A	7471.81	3348.92	1559.58	27
H36B	8105.6	2896.05	1206.84	27
H37A	8861.36	4551.12	1942.08	39
H37B	8597.36	4404.71	1241.51	39
H38A	9969.38	3750.8	1282.78	39
H38B	10405.93	4656.52	1715.54	39
H39A	10996.79	3495.48	2167.27	33
H39B	10392.94	3961.4	2533.8	33
H40A	9549.49	2348.12	1756.96	24
H40B	9824.63	2451.75	2457.84	24
H41A	7513.4	701.02	2820.8	26
H41B	7218.63	1404.06	3225.4	26
H42A	9048.9	779.68	3560.4	35
H42B	8104.89	535.71	3823.03	35
H43A	8426.52	1971.3	4287.08	36
H43B	9469.87	1652.58	4475.41	36
H44A	10083.34	2382.73	3783.77	33
H44B	9744.94	3064.59	4180.54	33
H45A	8169.85	2883.84	3441.98	25
H45B	9097.75	3188.32	3175.2	25
H51A	3319.21	759.8	3474.82	35
H51B	3443.95	-216.79	3491.19	35
H52A	1667.8	-713.19	3347.76	50

Atom	*x*	*y*	*z*	U(eq)
H52B	2153.09	6.1	3921.24	50
H53A	1566.13	1067.33	3397.3	52
H53B	616.32	264.59	3317.25	52
H54A	713.11	-259.67	2389.13	47
H54B	648.73	734.08	2394.58	47
H55A	1947.31	462.03	1980.26	31
H55B	2426.91	1174.12	2557.31	31
H56A	1934.38	-1105.7	1774	34
H56B	2628.12	-1635.77	1521.64	34
H57A	1474.85	-540.41	891.59	41
H57B	1200.26	-1577.31	751.02	41
H58A	2048.17	-931.14	86.72	49
H58B	2676.1	-1550.74	445.09	49
H59A	3838.66	-235.45	482.1	43
H59B	3140.85	310.71	716.11	43
H60A	4217.47	-817.46	1359.9	39
H60B	4504.77	218.6	1511.51	39
H46A	4003.81	-1923.12	2191.39	33
H46B	3113.98	-1713.21	2447.02	33
H47A	3880.98	-2743.41	2952.1	40
H47B	4023.94	-1881.78	3395.38	40
H48A	5559.36	-2315.33	2906.24	39
H48B	5604.24	-2257.67	3585.37	39
H49A	5802.93	-753.53	3680.23	40
H49B	6645.92	-983.77	3391.28	40
H50A	5812.71	20.32	2892.57	32
H50B	5653.02	-854.3	2457.24	32
H46C	3039.94	-1614.04	2561.35	33
H46D	3722.47	-1561.09	3224.19	33
H47C	4211.82	-2206.18	2202.74	40
H47D	3862.37	-2789.96	2658.07	40
H48C	5686.58	-2466.68	2833.5	39
H48D	5376.77	-2142.44	3399.55	39
H49C	6618.96	-1013.42	3270.37	40
H49D	5990.35	-1063.46	2597.46	40
H50C	5377.51	-475.43	3585.58	32
H50D	5734.79	124.41	3139.94	32
H1KA	7539.34	4133.64	3244.71	24
H1KB	7910.03	4187.33	2666.42	24
H2KA	6194.63	4299.29	2460.24	25
H2KB	6533.24	5135.7	2956.25	25

Atom	*x*	*y*	*z*	U(eq)
H3KA	11547.17	6799.04	1883.34	38
H3KB	11009.31	7532.52	2071.99	38
H4KA	10210.01	6837.19	1078.54	38
H4KB	9894.45	5948.04	1322.51	38
H5KA	9668.01	9194.05	3831.1	30
H5KB	8673.7	8438.05	3761.18	30
H6KA	8419.1	9349.96	3010.87	30
H6KB	9276.07	9017.56	2781.36	30
H7KA	9693.45	4767.65	3310.8	24
H7KB	9196	4607.03	3835.15	24
H8KA	9778.38	6123.88	4199.67	27
H8KB	10693.18	5651.89	4227.77	27
H9KA	11050.48	5519.87	3236.19	33
H9KB	11948.35	6207.49	3717.87	33
H10C	11815.54	7245.42	3056.08	37
H10D	12143.3	6414.42	2805.04	37
H11C	11530.33	7646.52	3831.88	32
H11D	11423.13	7200.71	4392.14	32
H12C	9775.3	7492.47	4249.27	32
H12D	10643.2	8370.18	4359.17	32
H13C	6510.73	5564.26	1179.17	31
H13D	5656.95	6101.75	1168.46	31
H14C	5976.82	6080.83	2208.4	27
H14D	5505.48	5137.91	1822.16	27
H15C	7742.26	7598.8	1072.26	34
H15D	6884.66	6780.87	685.64	34
H16C	8028.92	5870.37	998.78	35
H16D	8462.63	6580.54	636.27	35
H17C	6221.69	7344.24	1970.54	32
H17D	6267.75	7712.99	1375.08	32
H18C	8012.9	8471.22	1863.99	31
H18D	7200.04	8815.61	2130.18	31
H1DA	8061.34	9522.53	4480.24	73
H1DB	9116.28	10155.71	4868.64	73
H1DC	8183.41	9921.22	5140.02	73
H2DA	7709.45	8601.02	5375.12	48
H2DB	8454.88	7953.04	5421.55	48
H3DA	6841.63	7382.94	4699.4	42
H3DB	7114.36	8146.11	4332.73	42
H4DA	7209.51	7222.56	3511.67	54
H4DB	6716.52	6464.36	3817.81	54

Atom	*x*	*y*	*z*	U(eq)
H4DC	7740.5	6431.5	3646.02	54
H5DA	1814.51	7161.51	346.84	65
H5DB	1767.38	6454.16	-184.01	65
H5DC	863.75	6947.33	-233.83	65
H5DD	1950.07	6926.61	-104.79	65
H5DE	827.41	7013.22	-108.64	65
H5DF	1573.61	6789.09	463.31	65
H6D	35.68	5477.68	-453.78	79
H6DA	-188.16	5791.91	-7.4	79

Table 5.35 Atomic Occupancy for 5-Yb^{3+}.

Atom	*Occupancy*	Atom	*Occupancy*	Atom	*Occupancy*
N14A	0.182(2)	C46A	0.182(2)	H46A	0.182(2)
H46B	0.182(2)	C47A	0.182(2)	H47A	0.182(2)
H47B	0.182(2)	C48A	0.182(2)	H48A	0.182(2)
H48B	0.182(2)	C49A	0.182(2)	H49A	0.182(2)
H49B	0.182(2)	C50A	0.182(2)	H50A	0.182(2)
H50B	0.182(2)	N14B	0.818(2)	C46B	0.818(2)
H46C	0.818(2)	H46D	0.818(2)	C47B	0.818(2)
H47C	0.818(2)	H47D	0.818(2)	C48B	0.818(2)
H48C	0.818(2)	H48D	0.818(2)	C49B	0.818(2)
H49C	0.818(2)	H49D	0.818(2)	C50B	0.818(2)
H50C	0.818(2)	H50D	0.818(2)	H5DA	0.617(3)
H5DB	0.617(3)	H5DC	0.617(3)	H5DD	0.383(3)
H5DE	0.383(3)	H5DF	0.383(3)	H6D	0.617(3)
H6DA	0.383(3)	O3D	0.617(3)	O4D	0.383(3)

5.5.6 *1-Sm*$^{6+}$

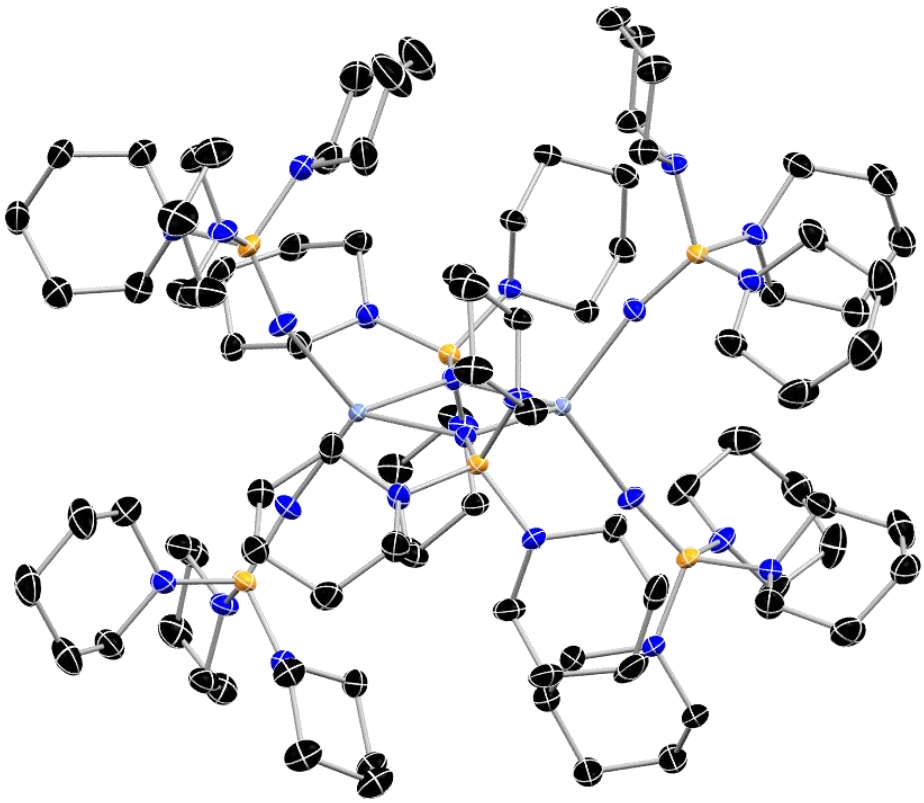

Figure 5.17 Molecular structure of 1-Sm^{6+} with thermal ellipsoids shown at 50% probability with hydrogen atoms omitted for clarity. Color code: C, black; N, blue; O, red; P, orange; Sm, blue.

Table 5.36 Crystal data and structure refinement for 1-Sm^{6+}.

Identification code	1-Sm^{6+}
Empirical formula	$C_{90}H_{180}N_{24}P_6Sm_2$
Formula weight	2085.09
Temperature/K	100(2)
Crystal system	monoclinic
Space group	$P2_1/c$
a/Å	15.4034(6)
b/Å	24.8126(11)
c/Å	29.2672(12)
α/°	90

β/°	99.8760(15)
γ/°	90
Volume/Å^3	11020.1(8)
Z	4
ρ_{calc}g/cm^3	1.257
μ/mm^{-1}	1.193
F(000)	4408.0
Crystal size/mm^3	0.326 × 0.321 × 0.272
Radiation	MoKα (λ = 0.71073)
2Θ range for data collection/°	4.322 to 62.044
Index ranges	-22 ≤ h ≤ 22, -35 ≤ k ≤ 35, -42 ≤ l ≤ 42
Reflections collected	285162
Independent reflections	35126 [R_{int} = 0.0471, R_{sigma} = 0.0276]
Data/restraints/parameters	35126/0/1099
Goodness-of-fit on F^2	1.030
Final R indexes [I>=2σ (I)]	R_1 = 0.0304, wR_2 = 0.0734
Final R indexes [all data]	R_1 = 0.0380, wR_2 = 0.0782
Largest diff. peak/hole / e Å^{-3}	1.41/-0.65

Table 5.37 Fractional Atomic Coordinates (×10^4) and Equivalent Isotropic Displacement Parameters (Å^2×10^3) for 1-Sm^{6+}. U_{eq} is defined as 1/3 of the trace of the orthogonalised U_{IJ} tensor.

Atom	*x*	*y*	*z*	U(eq)
Sm1	7471.8(2)	2277.2(2)	3912.6(2)	11.74(2)
Sm2	6832.5(2)	3611.3(2)	3449.8(2)	13.10(2)
P4	8033.6(3)	3435.2(2)	4609.0(2)	15.28(8)
P1	6278.9(3)	2402.0(2)	2762.4(2)	14.33(8)
P5	6260.7(3)	1293.2(2)	4529.3(2)	16.85(9)
P2	8263.9(3)	4454.1(2)	2837.2(2)	19.44(9)
P6	9625.8(3)	1578.1(2)	3912.3(2)	18.94(9)
P3	4730.7(3)	4234.2(2)	3609.1(2)	22.66(10)
N1	7543.5(10)	3196.7(6)	4143.5(5)	15.4(3)
N2	6698.3(10)	2693.1(6)	3217.1(5)	15.4(3)
N17	6683.6(11)	1745.5(6)	4284.8(6)	19.3(3)
N6	7733.0(12)	4159.0(7)	3158.8(6)	23.3(3)
N21	8785.8(11)	1909.6(7)	3915.1(6)	22.1(3)
N10	5542.4(11)	4016.3(7)	3432.8(6)	23.7(3)
N3	6905.4(11)	1969.5(6)	2520.5(6)	18.7(3)
N14	7921.5(10)	3111.3(6)	5100.8(5)	17.3(3)
N15	7727.1(12)	4060.1(7)	4731.2(6)	21.2(3)
N16	9114.0(11)	3462.6(7)	4625.8(6)	20.4(3)

Atom	*x*	*y*	*z*	U(eq)
N18	5291.5(10)	1406.1(7)	4711.7(6)	18.5(3)
N4	5434.6(11)	2012.6(7)	2839.7(6)	21.1(3)
N5	5969.6(12)	2817.8(7)	2308.6(5)	20.9(3)
N22	9576.2(11)	906.6(7)	3810.3(6)	20.4(3)
N7	9136.0(12)	4808.1(7)	3120.8(6)	24.2(3)
N8	8771.8(11)	4096.6(7)	2466.7(6)	20.3(3)
N23	10292.0(11)	1567.1(7)	4433.0(6)	23.7(3)
N19	6027.3(12)	745.5(7)	4195.5(6)	24.1(3)
N20	6862.3(11)	1089.5(7)	5034.7(6)	23.0(3)
N24	10194.4(12)	1775.3(7)	3500.3(7)	28.8(4)
N9	7650.7(12)	4880.4(7)	2469.1(6)	25.7(4)
N11	4869.1(14)	4869.3(8)	3808.5(8)	32.6(4)
N12	3799.7(11)	4188.5(8)	3211.6(7)	28.7(4)
C46	7001.9(13)	2989.2(8)	5148.1(7)	20.9(4)
C50	8496.7(13)	2650.6(8)	5254.3(7)	20.7(4)
N13	4378.5(13)	3937.0(7)	4063.5(6)	27.0(4)
C51	7478.1(14)	4423.6(8)	4335.9(7)	23.7(4)
C6	4960.2(13)	2078.9(9)	3229.6(7)	23.4(4)
C56	9548.3(13)	3301.9(8)	4240.2(7)	23.1(4)
C1	7110.1(15)	1446.5(8)	2744.2(7)	25.5(4)
C21	9430.3(14)	3703.7(9)	2682.9(7)	25.3(4)
C7	4092.9(14)	2376.1(10)	3086.6(8)	30.3(5)
C57	10009.8(15)	3779.3(9)	4060.3(8)	27.1(4)
C61	4489.9(13)	1424.3(9)	4361.6(7)	25.7(4)
C5	7686.8(15)	2204.9(10)	2369.1(8)	29.4(4)
C55	7436.8(14)	4238.3(8)	5160.5(7)	24.9(4)
C47	6946.1(14)	2889.1(9)	5656.2(7)	24.5(4)
C11	5428.5(16)	3292.7(9)	2380.1(7)	28.9(4)
C10	4909.3(14)	1722.4(9)	2451.3(8)	28.0(4)
C62	3688.9(14)	1324.0(10)	4591.0(8)	30.7(5)
C60	9701.2(14)	3717.9(10)	5012.3(7)	28.1(4)
C71	7824.3(13)	1089.8(9)	5087.1(8)	26.4(4)
C16	8897.2(16)	5211.6(9)	3444.6(8)	30.6(5)
C65	5287.8(13)	1846.5(9)	5047.1(8)	24.5(4)
C25	8196.0(14)	3854.4(9)	2068.9(8)	28.0(4)
C48	7561.2(14)	2432.7(9)	5851.0(7)	24.6(4)
C86	10065.3(15)	2320.1(9)	3303.6(8)	29.6(5)
C54	7761.6(16)	4809.6(9)	5285.6(8)	29.1(4)
C81	10209.5(15)	1965.0(10)	4785.8(8)	32.2(5)
C41	5012.4(18)	3958.6(10)	4501.9(8)	35.7(5)
C22	10013.0(14)	3533.6(10)	2336.1(8)	29.3(4)

Atom	*x*	*y*	*z*	U(eq)
C12	5652.4(18)	3772.4(10)	2108.7(9)	35.2(5)
C36	3885.5(16)	4324.2(13)	2738.6(9)	41.5(6)
C49	8493.0(14)	2538.3(9)	5765.7(7)	24.8(4)
C87	10892.1(16)	2658.9(9)	3431.1(9)	32.0(5)
C76	9217.1(17)	718.2(9)	3343.6(8)	32.1(5)
C20	9890.7(15)	4988.7(9)	2913.5(8)	28.7(4)
C53	7437.3(15)	5196.3(9)	4888.6(8)	29.0(4)
C80	9214.4(16)	585.2(9)	4153.8(8)	30.3(5)
C52	7761.7(14)	5003.3(8)	4455.2(8)	25.5(4)
C75	6549.3(15)	844.4(10)	5432.1(8)	30.1(5)
C66	6067.5(17)	741.3(9)	3703.8(8)	32.1(5)
C59	10191.6(15)	4193.6(10)	4852.2(8)	31.7(5)
C72	8203.0(16)	529.3(10)	5172.1(8)	31.8(5)
C83	11204.9(17)	1410.8(10)	5372.2(9)	35.3(5)
C13	5531.5(19)	3628.4(10)	1587.3(8)	37.0(6)
C70	5610.0(18)	266.1(9)	4351.6(9)	34.7(5)
C9	4030.2(15)	1998.5(11)	2279.4(8)	34.4(5)
C63	3637.0(14)	1747.7(10)	4962.2(9)	31.7(5)
C17	9664.5(17)	5348.4(10)	3825.8(8)	34.4(5)
C58	10660.8(15)	4030.5(10)	4454.2(8)	31.4(5)
C4	7975.2(18)	1843.2(11)	2001.7(9)	38.5(6)
C26	8067.3(16)	5245.7(10)	2173.5(8)	32.9(5)
C85	11151.6(15)	1304.0(10)	4515.4(8)	32.5(5)
C73	7908.2(16)	275.8(10)	5598.1(8)	33.7(5)
C45	4030(2)	3389.0(10)	3986.4(10)	41.8(6)
C31	4280.7(19)	5147.0(10)	4076.8(9)	37.0(5)
C67	6543(2)	244.9(11)	3576.1(11)	44.9(7)
C68	6121(2)	-268.4(11)	3722.3(10)	46.9(7)
C64	4507.6(14)	1786.3(10)	5300.1(8)	30.5(5)
C2	7396.5(19)	1054.8(9)	2397.3(8)	36.1(5)
C8	3518.5(15)	2097.3(12)	2674.8(9)	38.0(6)
C23	9460.1(16)	3296.3(11)	1898.3(9)	36.8(5)
C42	4574(2)	3816.2(12)	4911.5(10)	49.3(7)
C78	9174.1(18)	-230.0(10)	3639.4(10)	36.7(5)
C74	6902.9(16)	281.5(10)	5533.9(9)	34.9(5)
C84	11315.5(19)	1023.7(10)	4983.0(10)	43.0(6)
C77	9488(2)	134.3(10)	3283.6(10)	41.3(6)
C15	5816.5(16)	2666.4(9)	1816.8(7)	28.9(4)
C88	11665.2(17)	2384.9(11)	3266.7(11)	42.9(7)
C27	7452.1(18)	5350.7(11)	1726.8(9)	40.3(6)
C34	5194.4(18)	5699.0(10)	3426.7(9)	37.5(5)

Atom	*x*	*y*	*z*	U(eq)
C69	6059(2)	-242.6(10)	4240.2(11)	49.4(7)
C14	6044.7(17)	3122.7(10)	1519.2(8)	33.7(5)
C24	8730.7(16)	3693.0(11)	1698.5(8)	34.5(5)
C37	3235.5(17)	4001.6(15)	2396.5(9)	49.0(7)
C3	8159(2)	1273.0(12)	2189.8(9)	45.0(7)
C19	10692.3(16)	5079.3(10)	3292.7(9)	34.4(5)
C35	5564.5(17)	5209.9(10)	3700.1(9)	36.1(5)
C40	2919.9(15)	4311.9(11)	3305.9(10)	35.9(5)
C18	10482.2(17)	5513.3(10)	3628.5(9)	36.3(5)
C82	10321.6(16)	1703.4(13)	5260.7(9)	40.9(6)
C89	11783.1(18)	1815.0(12)	3464.7(13)	57.0(10)
C28	6566.1(18)	5565.9(11)	1802.5(11)	44.4(7)
C79	9475.4(19)	-2.8(10)	4124.7(10)	42.2(6)
C90	10924.8(19)	1498.6(10)	3346.4(11)	45.0(7)
C29	6182.5(17)	5213.2(12)	2145.1(12)	48.9(8)
C39	2231.7(16)	3987.9(12)	2979.1(10)	43.0(6)
C32	3889.6(19)	5646.6(10)	3832.1(10)	40.8(6)
C38	2300.8(17)	4104.4(14)	2474.1(10)	47.6(7)
C30	6824.4(17)	5096.1(11)	2575.6(10)	38.8(6)
C43	4113(3)	3273.4(14)	4840.8(12)	69.0(11)
C33	4598.9(19)	6017.0(10)	3696.2(9)	38.3(6)
C44	3522(3)	3240.6(15)	4370.6(12)	66.1(10)

Table 5.38 Anisotropic Displacement Parameters ($Å^2×10^3$) for 1-Sm^{6+}. The Anisotropic displacement factor exponent takes the form: $-2\pi^2[h^2a^{*2}U_{11}+2hka^*b^*U_{12}+\ldots]$.

Atom	U_{11}	U_{22}	U_{33}	U_{23}	U_{13}	U_{12}
Sm1	10.99(4)	11.45(4)	12.82(4)	0.32(3)	2.15(3)	0.93(3)
Sm2	12.55(4)	12.41(4)	14.80(4)	1.06(3)	3.62(3)	1.62(3)
P4	16.5(2)	15.3(2)	14.1(2)	-1.96(15)	2.64(16)	-2.47(16)
P1	14.3(2)	15.6(2)	12.83(19)	-0.99(15)	1.48(15)	1.25(16)
P5	15.6(2)	16.1(2)	19.9(2)	2.99(16)	5.99(17)	-0.10(16)
P2	19.0(2)	20.2(2)	20.1(2)	3.63(18)	6.12(17)	-1.49(18)
P6	14.1(2)	19.5(2)	24.1(2)	1.08(18)	5.93(17)	3.94(17)
P3	19.8(2)	22.2(2)	27.5(3)	1.27(19)	7.99(19)	8.36(19)
N1	16.8(7)	13.8(6)	15.1(7)	-0.5(5)	1.6(5)	-1.4(5)
N2	16.2(7)	15.7(7)	13.9(7)	-0.7(5)	1.6(5)	1.3(5)
N17	19.3(7)	18.0(7)	21.1(8)	3.0(6)	4.8(6)	-1.2(6)
N6	24.1(8)	23.7(8)	23.1(8)	3.6(6)	7.1(6)	-5.1(7)
N21	15.4(7)	26.3(8)	25.1(8)	-1.4(6)	5.0(6)	5.6(6)

Atom	U_{11}	U_{22}	U_{33}	U_{23}	U_{13}	U_{12}
N10	18.1(8)	28.1(9)	25.1(8)	-3.3(7)	4.0(6)	7.7(6)
N3	18.6(7)	19.1(7)	18.9(7)	-3.0(6)	4.7(6)	2.0(6)
N14	15.8(7)	21.1(7)	15.2(7)	1.1(6)	3.2(5)	0.0(6)
N15	29.3(9)	16.7(7)	17.9(7)	-2.8(6)	5.2(6)	0.3(6)
N16	16.7(7)	27.5(8)	16.9(7)	-4.4(6)	2.2(6)	-6.4(6)
N18	13.2(7)	22.8(8)	19.9(7)	-1.0(6)	3.6(6)	0.1(6)
N4	17.9(7)	25.4(8)	20.6(8)	-5.4(6)	5.3(6)	-4.2(6)
N5	27.9(9)	21.5(8)	12.2(7)	1.0(6)	0.5(6)	4.5(6)
N22	20.9(8)	19.7(8)	21.7(8)	2.3(6)	7.3(6)	1.9(6)
N7	26.0(9)	24.0(8)	25.3(8)	-2.4(7)	12.1(7)	-7.1(7)
N8	17.7(7)	23.0(8)	19.7(7)	0.2(6)	1.4(6)	-0.5(6)
N23	14.7(7)	25.5(8)	30.0(9)	-3.5(7)	1.6(6)	5.2(6)
N19	29.1(9)	17.7(8)	28.6(9)	-2.3(6)	13.1(7)	-5.1(7)
N20	16.1(7)	28.4(9)	25.5(8)	11.0(7)	6.8(6)	2.6(6)
N24	27.1(9)	21.8(8)	42.9(11)	8.2(7)	21.4(8)	9.0(7)
N9	23.8(8)	29.2(9)	25.8(9)	9.4(7)	9.3(7)	6.5(7)
N11	34.9(10)	22.6(9)	45.5(12)	-0.6(8)	21.6(9)	6.5(8)
N12	16.1(8)	39.6(11)	31.9(10)	9.5(8)	8.4(7)	8.4(7)
C46	18.0(8)	26.4(9)	19.1(9)	2.2(7)	5.7(7)	-0.6(7)
C50	21.6(9)	21.5(9)	19.7(9)	0.1(7)	5.3(7)	1.7(7)
N13	31.6(9)	23.7(8)	27.5(9)	3.0(7)	10.4(7)	7.6(7)
C51	29.9(10)	18.0(9)	22.9(9)	-2.4(7)	4.0(8)	-1.6(7)
C6	19.2(9)	30.2(10)	21.8(9)	2.0(8)	5.9(7)	-1.3(8)
C56	20.9(9)	22.9(9)	26.9(10)	-3.7(7)	8.1(7)	-2.1(7)
C1	31.4(11)	23.4(9)	21.3(9)	-0.5(7)	2.8(8)	9.5(8)
C21	24.9(10)	25.0(10)	25.4(10)	3.2(8)	2.7(8)	3.3(8)
C7	22.1(10)	42.8(13)	27.8(11)	1.9(9)	9.6(8)	5.0(9)
C57	26.5(10)	29.2(10)	27.6(10)	-2.8(8)	9.8(8)	-8.0(8)
C61	19.9(9)	34.9(11)	21.4(9)	0.6(8)	1.1(7)	1.6(8)
C5	25.1(10)	33.4(11)	32.9(11)	-4.3(9)	14.0(9)	-1.2(8)
C55	28.5(10)	23.6(9)	23.8(10)	-6.4(7)	8.0(8)	-2.6(8)
C47	26.0(10)	28.4(10)	21.4(9)	1.4(8)	10.3(7)	0.6(8)
C11	42.1(13)	22.1(10)	21.8(10)	1.0(7)	3.9(9)	7.6(9)
C10	23.3(10)	31.4(11)	29.3(11)	-10.3(8)	4.5(8)	-7.5(8)
C62	15.0(9)	41.6(13)	34.6(12)	-2.9(9)	1.4(8)	-2.0(8)
C60	22.1(10)	41.1(12)	19.9(9)	-4.8(8)	0.4(7)	-10.9(9)
C71	18.8(9)	29.6(10)	30.9(11)	8.4(8)	4.8(8)	2.7(8)
C16	33.9(12)	29.7(11)	31.3(11)	-4.6(9)	14.0(9)	-6.4(9)
C65	18.1(9)	26.7(10)	29.7(10)	-6.5(8)	6.7(7)	-3.0(7)
C25	22.3(10)	32.2(11)	28.4(10)	-6.1(8)	1.1(8)	-1.0(8)
C48	29.4(10)	27.5(10)	17.8(9)	2.7(7)	7.0(7)	-1.1(8)

Atom	U_{11}	U_{22}	U_{33}	U_{23}	U_{13}	U_{12}
C86	28.0(11)	27.8(11)	35.6(12)	8.6(9)	12.6(9)	7.7(8)
C54	33.5(11)	25.7(10)	29.2(11)	-11.3(8)	8.7(9)	-1.7(8)
C81	26.6(11)	36.4(12)	31.5(11)	-8.7(9)	-1.3(9)	10.4(9)
C41	45.6(14)	35.1(12)	26.5(11)	0.5(9)	6.9(10)	12.8(10)
C22	21.3(10)	32.6(11)	33.1(11)	-2.8(9)	2.4(8)	5.7(8)
C12	43.5(14)	29.4(11)	35.1(12)	6.5(9)	13.8(10)	9.1(10)
C36	21.3(11)	68.2(19)	34.6(13)	15.9(12)	4.1(9)	-0.2(11)
C49	25.0(10)	29.1(10)	19.7(9)	4.9(8)	2.3(7)	1.0(8)
C87	31.7(12)	28.0(11)	39.1(13)	7.4(9)	13.7(10)	4.7(9)
C76	41.8(13)	29.9(11)	24.4(10)	-0.4(8)	5.3(9)	3.5(10)
C20	29.4(11)	27.4(10)	31.9(11)	-2.0(8)	12.5(9)	-8.0(8)
C53	27.5(10)	20.4(9)	40.2(12)	-10.5(8)	9.3(9)	0.1(8)
C80	36.4(12)	30.0(11)	27.2(11)	0.2(8)	12.5(9)	-8.3(9)
C52	26.5(10)	18.2(9)	32.2(11)	-2.9(8)	6.5(8)	-1.6(7)
C75	25.5(10)	38.3(12)	27.5(11)	9.6(9)	7.6(8)	-0.4(9)
C66	39.4(13)	27.9(11)	31.5(11)	-4.5(9)	13.3(9)	-8.3(9)
C59	26.7(11)	35.5(12)	32.0(11)	-8.9(9)	2.3(9)	-12.4(9)
C72	31.1(11)	32.2(11)	32.3(11)	7.5(9)	6.2(9)	6.7(9)
C83	33.3(12)	37.7(13)	32.1(12)	7.0(10)	-2.1(9)	-2.7(10)
C13	46.6(14)	39.7(13)	27.6(11)	15.6(10)	14.1(10)	17.4(11)
C70	44.9(14)	23.4(10)	37.4(13)	1.4(9)	11.2(10)	-10.4(10)
C9	21.1(10)	51.8(15)	28.9(11)	-5.3(10)	0.3(8)	-7.0(10)
C63	17.0(9)	40.1(13)	40.3(13)	-2.5(10)	11.5(9)	1.2(8)
C17	44.4(14)	28.7(11)	31.9(12)	-4.5(9)	11.9(10)	-13.1(10)
C58	26.2(11)	35.0(12)	33.9(12)	-4.1(9)	8.2(9)	-13.5(9)
C4	41.9(14)	45.5(14)	33.3(12)	1.9(10)	21.5(10)	12.8(11)
C26	33.5(12)	34.1(12)	31.9(12)	9.2(9)	7.5(9)	-0.7(9)
C85	21.6(10)	39.5(13)	34.7(12)	-4.5(10)	-0.4(9)	14.2(9)
C73	32.8(12)	36.2(12)	31.6(12)	14.7(10)	3.9(9)	6.6(10)
C45	59.0(17)	27.1(12)	39.3(14)	5.3(10)	8.0(12)	3.8(11)
C31	49.2(15)	30.5(12)	35.7(13)	1.7(9)	19.7(11)	12.1(11)
C67	48.2(16)	41.9(14)	50.1(16)	-22.3(12)	23.6(13)	-9.3(12)
C68	62.3(18)	27.3(12)	50.9(16)	-15.5(11)	9.3(14)	-4.5(12)
C64	24.8(10)	39.1(12)	30.3(11)	-8.8(9)	12.2(8)	-3.4(9)
C2	54.5(15)	24.9(11)	27.9(11)	-3.3(9)	4.0(10)	16.0(10)
C8	17.8(10)	62.0(17)	33.9(12)	3.0(11)	3.4(9)	-0.8(10)
C23	30.3(12)	39.7(13)	40.4(13)	-13.8(11)	6.5(10)	3.2(10)
C42	79(2)	42.0(15)	31.0(13)	2.2(11)	20.9(13)	15.1(15)
C78	38.0(13)	24.0(11)	51.7(15)	-5.8(10)	18.1(11)	-1.1(9)
C74	35.4(12)	37.3(13)	31.3(12)	12.8(10)	3.8(9)	-3.7(10)
C84	46.2(15)	29.8(12)	45.7(15)	0.7(11)	-12.4(12)	10.8(11)

Atom	U_{11}	U_{22}	U_{33}	U_{23}	U_{13}	U_{12}
C77	52.1(16)	34.0(13)	43.3(14)	-11.0(11)	23.8(12)	-1.6(11)
C15	38.7(12)	26.9(10)	20.6(10)	-1.0(8)	3.1(8)	3.3(9)
C88	29.8(12)	38.2(13)	66.1(18)	19.0(13)	23.5(12)	9.8(10)
C27	41.2(14)	40.5(14)	36.6(13)	18.2(11)	-0.5(10)	-4.9(11)
C34	44.4(14)	34.7(13)	34.9(13)	5.7(10)	11.3(11)	4.1(11)
C69	73(2)	21.2(11)	50.2(17)	-2.3(11)	1.3(15)	-5.0(12)
C14	38.2(13)	40.7(13)	23.3(10)	2.0(9)	8.4(9)	9.4(10)
C24	29.1(11)	44.4(14)	28.1(11)	-10.9(10)	-0.2(9)	0.0(10)
C37	27.1(12)	87(2)	31.8(13)	7.9(14)	2.5(10)	4.7(13)
C3	53.9(17)	53.4(16)	31.6(13)	1.2(11)	18.0(12)	31.2(13)
C19	28.0(11)	31.2(12)	44.4(14)	0.8(10)	7.7(10)	-9.6(9)
C35	36.4(13)	30.4(12)	42.7(14)	4.2(10)	10.7(10)	5.8(10)
C40	20.2(10)	42.2(13)	46.7(14)	3.0(11)	9.9(9)	8.2(9)
C18	37.7(13)	31.6(12)	39.5(13)	-4.1(10)	6.5(10)	-14.8(10)
C82	26.1(11)	66.0(18)	30.6(12)	-3.6(12)	4.6(9)	1.1(11)
C89	35.7(14)	47.1(16)	99(3)	36.5(17)	42.2(16)	21.6(12)
C28	37.2(14)	35.3(13)	57.1(17)	21.8(12)	-2.4(12)	4.9(11)
C79	46.8(15)	29.8(12)	49.2(16)	12.9(11)	5.9(12)	-5.2(11)
C90	49.2(16)	31.3(12)	65.2(18)	14.8(12)	40.4(14)	17.1(11)
C29	24.9(12)	43.0(15)	77(2)	28.4(14)	2.7(12)	5.6(10)
C39	22.0(11)	53.3(16)	55.1(17)	1.4(13)	10.8(11)	0.7(11)
C32	53.5(16)	30.3(12)	43.9(14)	7.2(10)	23.6(12)	19.0(11)
C38	23.1(12)	68(2)	48.9(16)	9.1(14)	-1.7(11)	3.5(12)
C30	36.3(13)	34.6(13)	48.4(15)	3.2(11)	15.7(11)	8.1(10)
C43	124(3)	45.9(18)	44.6(18)	11.6(14)	35(2)	-5(2)
C33	59.0(17)	23.6(11)	35.1(13)	6.2(9)	16.0(11)	11.3(11)
C44	93(3)	50.5(19)	59(2)	15.0(16)	26.3(19)	-23.0(19)

Table 5.39 Bond Lengths for 1-Sm^{6+}.

Atom	Atom	Length/Å	Atom	Atom	Length/Å
Sm1	N1	2.3767(15)	C51	C52	1.526(3)
Sm1	N2	2.4073(15)	C6	C7	1.520(3)
Sm1	N17	2.2035(16)	C56	C57	1.521(3)
Sm1	N21	2.2190(16)	C1	C2	1.525(3)
Sm2	N1	2.3700(15)	C21	C22	1.525(3)
Sm2	N2	2.3766(15)	C7	C8	1.532(3)
Sm2	N6	2.2141(17)	C57	C58	1.525(3)
Sm2	N10	2.2198(16)	C61	C62	1.523(3)
P4	N1	1.5567(15)	C5	C4	1.524(3)
P4	N14	1.6832(16)	C55	C54	1.527(3)

Atom	Atom	Length/Å	Atom	Atom	Length/Å
P4	N15	1.6772(17)	C47	C48	1.523(3)
P4	N16	1.6578(17)	C11	C12	1.503(3)
P1	N2	1.5541(15)	C10	C9	1.524(3)
P1	N3	1.6787(16)	C62	C63	1.524(3)
P1	N4	1.6664(17)	C60	C59	1.518(3)
P1	N5	1.6849(16)	C71	C72	1.512(3)
P5	N17	1.5348(16)	C16	C17	1.518(3)
P5	N18	1.6927(16)	C65	C64	1.523(3)
P5	N19	1.6762(18)	C25	C24	1.523(3)
P5	N20	1.6828(17)	C48	C49	1.521(3)
P2	N6	1.5346(17)	C86	C87	1.518(3)
P2	N7	1.6977(18)	C54	C53	1.524(3)
P2	N8	1.6928(18)	C81	C82	1.517(4)
P2	N9	1.6800(18)	C41	C42	1.515(4)
P6	N21	1.5343(17)	C22	C23	1.530(3)
P6	N22	1.6921(17)	C12	C13	1.547(3)
P6	N23	1.6851(18)	C36	C37	1.517(4)
P6	N24	1.6802(19)	C87	C88	1.519(3)
P3	N10	1.5307(17)	C76	C77	1.526(3)
P3	N11	1.681(2)	C20	C19	1.529(3)
P3	N12	1.6883(19)	C53	C52	1.518(3)
P3	N13	1.6892(19)	C80	C79	1.520(3)
N3	C1	1.463(3)	C75	C74	1.510(3)
N3	C5	1.473(3)	C66	C67	1.512(4)
N14	C46	1.478(2)	C59	C58	1.527(3)
N14	C50	1.469(2)	C72	C73	1.533(3)
N15	C51	1.465(3)	C83	C84	1.522(4)
N15	C55	1.472(3)	C83	C82	1.527(4)
N16	C56	1.463(3)	C13	C14	1.514(3)
N16	C60	1.466(2)	C70	C69	1.502(4)
N18	C61	1.464(2)	C9	C8	1.527(3)
N18	C65	1.470(3)	C63	C64	1.527(3)
N4	C6	1.466(3)	C17	C18	1.529(3)
N4	C10	1.466(3)	C4	C3	1.527(4)
N5	C11	1.479(3)	C26	C27	1.500(3)
N5	C15	1.467(3)	C85	C84	1.517(4)
N22	C76	1.460(3)	C73	C74	1.528(3)
N22	C80	1.466(3)	C45	C44	1.521(4)
N7	C16	1.468(3)	C31	C32	1.505(3)
N7	C20	1.470(3)	C67	C68	1.524(4)
N8	C21	1.469(3)	C68	C69	1.536(4)

Atom	Atom	Length/Å	Atom	Atom	Length/Å
N8	C25	1.466(3)	C2	C3	1.512(4)
N23	C81	1.450(3)	C23	C24	1.532(3)
N23	C85	1.459(3)	C42	C43	1.520(5)
N19	C66	1.451(3)	C78	C77	1.519(4)
N19	C70	1.462(3)	C78	C79	1.525(4)
N20	C71	1.463(3)	C15	C14	1.506(3)
N20	C75	1.465(3)	C88	C89	1.527(4)
N24	C86	1.469(3)	C27	C28	1.517(4)
N24	C90	1.454(3)	C34	C35	1.511(3)
N9	C26	1.474(3)	C34	C33	1.528(4)
N9	C30	1.463(3)	C37	C38	1.517(4)
N11	C31	1.469(3)	C19	C18	1.529(4)
N11	C35	1.442(3)	C40	C39	1.529(4)
N12	C36	1.453(3)	C89	C90	1.526(4)
N12	C40	1.461(3)	C28	C29	1.524(4)
C46	C47	1.525(3)	C29	C30	1.491(4)
C50	C49	1.523(3)	C39	C38	1.527(4)
N13	C41	1.474(3)	C32	C33	1.532(4)
N13	C45	1.465(3)	C43	C44	1.517(5)

Table 5.40 Bond Angles for 1-Sm^{6+}.

Atom	Atom	Atom	Angle/°	Atom	Atom	Atom	Angle/°
N1	Sm1	N2	79.69(5)	C30	N9	P2	120.52(16)
N17	Sm1	N1	115.90(6)	C30	N9	C26	112.48(19)
N17	Sm1	N2	116.10(6)	C31	N11	P3	124.90(17)
N17	Sm1	N21	109.38(6)	C35	N11	P3	121.85(16)
N21	Sm1	N1	113.31(6)	C35	N11	C31	113.1(2)
N21	Sm1	N2	119.87(6)	C36	N12	P3	115.84(15)
N1	Sm2	N2	80.45(5)	C36	N12	C40	111.73(19)
N6	Sm2	N1	111.59(6)	C40	N12	P3	124.16(17)
N6	Sm2	N2	120.51(6)	N14	C46	C47	109.87(16)
N6	Sm2	N10	109.33(7)	N14	C50	C49	109.83(16)
N10	Sm2	N1	119.74(6)	C41	N13	P3	114.53(16)
N10	Sm2	N2	113.21(6)	C45	N13	P3	116.27(16)
N1	P4	N14	117.49(8)	C45	N13	C41	109.78(19)
N1	P4	N15	115.21(8)	N15	C51	C52	111.93(17)
N1	P4	N16	112.03(8)	N4	C6	C7	111.83(17)
N15	P4	N14	100.67(8)	N16	C56	C57	110.94(17)
N16	P4	N14	104.13(8)	N3	C1	C2	109.40(17)
N16	P4	N15	105.87(9)	N8	C21	C22	109.79(17)

Atom	Atom	Atom	Angle/°	Atom	Atom	Atom	Angle/°
N2	P1	N3	118.28(8)	C6	C7	C8	111.0(2)
N2	P1	N4	111.88(8)	C56	C57	C58	110.01(18)
N2	P1	N5	114.22(8)	N18	C61	C62	109.66(17)
N3	P1	N5	99.45(8)	N3	C5	C4	109.33(19)
N4	P1	N3	101.84(8)	N15	C55	C54	110.40(17)
N4	P1	N5	109.89(9)	C48	C47	C46	110.53(17)
N17	P5	N18	119.58(9)	N5	C11	C12	111.72(19)
N17	P5	N19	112.76(9)	N4	C10	C9	112.10(18)
N17	P5	N20	114.56(9)	C61	C62	C63	110.31(19)
N19	P5	N18	101.85(9)	N16	C60	C59	111.82(18)
N19	P5	N20	107.43(9)	N20	C71	C72	111.84(18)
N20	P5	N18	98.92(8)	N7	C16	C17	112.2(2)
N6	P2	N7	114.02(9)	N18	C65	C64	110.22(17)
N6	P2	N8	119.75(9)	N8	C25	C24	110.22(17)
N6	P2	N9	113.18(9)	C49	C48	C47	110.76(17)
N8	P2	N7	99.81(8)	N24	C86	C87	111.20(19)
N9	P2	N7	107.37(10)	C53	C54	C55	110.54(18)
N9	P2	N8	100.96(9)	N23	C81	C82	110.6(2)
N21	P6	N22	121.07(9)	N13	C41	C42	111.2(2)
N21	P6	N23	112.78(9)	C21	C22	C23	110.94(19)
N21	P6	N24	113.05(9)	C11	C12	C13	109.8(2)
N23	P6	N22	98.38(9)	N12	C36	C37	110.4(2)
N24	P6	N22	99.98(9)	C48	C49	C50	110.82(17)
N24	P6	N23	110.01(10)	C86	C87	C88	110.2(2)
N10	P3	N11	112.69(10)	N22	C76	C77	110.2(2)
N10	P3	N12	112.97(10)	N7	C20	C19	110.04(19)
N10	P3	N13	120.15(10)	C52	C53	C54	109.06(17)
N11	P3	N12	110.14(10)	N22	C80	C79	110.39(19)
N11	P3	N13	100.06(10)	C53	C52	C51	111.48(18)
N12	P3	N13	99.42(10)	N20	C75	C74	112.57(19)
Sm2	N1	Sm1	100.42(5)	N19	C66	C67	110.9(2)
P4	N1	Sm1	127.28(8)	C60	C59	C58	110.79(19)
P4	N1	Sm2	131.94(8)	C71	C72	C73	110.6(2)
Sm2	N2	Sm1	99.36(5)	C84	C83	C82	110.5(2)
P1	N2	Sm1	126.69(8)	C14	C13	C12	110.12(19)
P1	N2	Sm2	133.94(9)	N19	C70	C69	111.9(2)
P5	N17	Sm1	169.17(11)	C10	C9	C8	111.5(2)
P2	N6	Sm2	164.53(11)	C62	C63	C64	110.95(18)
P6	N21	Sm1	171.85(11)	C16	C17	C18	111.7(2)
P3	N10	Sm2	158.78(11)	C57	C58	C59	110.43(18)
C1	N3	P1	118.26(13)	C5	C4	C3	110.5(2)

Atom	Atom	Atom	Angle/°	Atom	Atom	Atom	Angle/°
C1	N3	C5	111.21(17)	N9	C26	C27	110.2(2)
C5	N3	P1	115.60(13)	N23	C85	C84	111.1(2)
C46	N14	P4	114.74(12)	C74	C73	C72	109.35(18)
C50	N14	P4	119.22(13)	N13	C45	C44	109.4(2)
C50	N14	C46	110.46(15)	N11	C31	C32	111.4(2)
C51	N15	P4	116.48(13)	C66	C67	C68	111.3(2)
C51	N15	C55	114.36(16)	C67	C68	C69	110.1(2)
C55	N15	P4	126.69(14)	C65	C64	C63	111.71(19)
C56	N16	P4	123.75(13)	C3	C2	C1	111.9(2)
C56	N16	C60	114.20(16)	C9	C8	C7	111.40(19)
C60	N16	P4	121.61(14)	C22	C23	C24	109.80(19)
C61	N18	P5	117.92(13)	C41	C42	C43	111.1(2)
C61	N18	C65	110.19(16)	C77	C78	C79	109.7(2)
C65	N18	P5	116.00(13)	C75	C74	C73	110.9(2)
C6	N4	P1	123.05(14)	C85	C84	C83	111.3(2)
C10	N4	P1	121.28(14)	C78	C77	C76	111.2(2)
C10	N4	C6	112.09(16)	N5	C15	C14	111.13(18)
C11	N5	P1	117.80(13)	C87	C88	C89	110.0(2)
C15	N5	P1	126.35(14)	C26	C27	C28	112.6(2)
C15	N5	C11	110.08(16)	C35	C34	C33	110.3(2)
C76	N22	P6	118.62(14)	C70	C69	C68	111.0(2)
C76	N22	C80	109.86(17)	C15	C14	C13	111.6(2)
C80	N22	P6	115.18(14)	C25	C24	C23	110.4(2)
C16	N7	P2	113.80(14)	C38	C37	C36	110.4(3)
C16	N7	C20	111.21(17)	C2	C3	C4	111.6(2)
C20	N7	P2	124.83(15)	C20	C19	C18	109.7(2)
C21	N8	P2	115.63(13)	N11	C35	C34	111.1(2)
C25	N8	P2	116.13(13)	N12	C40	C39	109.7(2)
C25	N8	C21	110.43(17)	C17	C18	C19	109.46(19)
C81	N23	P6	121.25(14)	C81	C82	C83	110.9(2)
C81	N23	C85	112.02(17)	C90	C89	C88	110.4(2)
C85	N23	P6	123.47(15)	C27	C28	C29	110.7(2)
C66	N19	P5	122.86(14)	C80	C79	C78	111.5(2)
C66	N19	C70	113.56(18)	N24	C90	C89	111.9(2)
C70	N19	P5	122.64(15)	C30	C29	C28	113.1(2)
C71	N20	P5	119.15(14)	C38	C39	C40	110.5(2)
C71	N20	C75	112.46(16)	C31	C32	C33	111.9(2)
C75	N20	P5	128.01(14)	C37	C38	C39	109.8(2)
C86	N24	P6	119.79(14)	N9	C30	C29	111.5(2)
C90	N24	P6	127.67(16)	C44	C43	C42	111.4(3)
C90	N24	C86	111.91(18)	C34	C33	C32	110.0(2)

Atom	Atom	Atom	Angle/°	Atom	Atom	Atom	Angle/°
C26	N9	P2	120.67(15)	C43	C44	C45	110.7(3)

Table 5.41 Hydrogen Atom Coordinates (Å×10^4) and Isotropic Displacement Parameters (Å^2×10^3) for 1-Sm^{6+}.

Atom	*x*	*y*	*z*	U(eq)
H46A	6795.87	2665.93	4962.45	25
H46B	6616.19	3295.28	5029.21	25
H50A	9104.73	2730.48	5207.04	25
H50B	8286.77	2328.45	5068.16	25
H51A	6830.96	4411.89	4235.89	28
H51B	7755.05	4298.12	4073.65	28
H6A	5334.49	2281.91	3480.45	28
H6B	4842.38	1719.61	3352.87	28
H56A	9105.06	3153.43	3986.23	28
H56B	9984.8	3015.59	4344.92	28
H1A	6583.59	1303.89	2855.74	31
H1B	7588.32	1488.26	3014.74	31
H21A	9129.68	3383.9	2784.57	30
H21B	9797.74	3866.24	2959.26	30
H7A	4212.89	2751.3	3000.75	36
H7B	3772.09	2388.62	3351.98	36
H57A	9567.85	4051.61	3927.6	33
H57B	10326.85	3658.09	3811.72	33
H61A	4519.85	1146.21	4122.24	31
H61B	4438.05	1781.24	4208.21	31
H5A	8171.35	2239	2637.48	35
H5B	7544.7	2569.02	2239.34	35
H55A	7670.91	3989.72	5416.75	30
H55B	6785.37	4229.11	5117.78	30
H47A	7109.89	3221.77	5837.26	29
H47B	6333.03	2795.08	5684.59	29
H11A	5525.27	3384.55	2714.16	35
H11B	4797.4	3203.01	2283.46	35
H10A	4799.5	1350.89	2550.77	34
H10B	5247.15	1698.51	2193.16	34
H62A	3730.45	960.91	4733.31	37
H62B	3146.95	1337.35	4354.06	37
H60A	10132.58	3448.87	5162.49	34
H60B	9350.6	3842.29	5245.67	34
H71A	8071.75	1325.7	5350.18	32

Atom	*x*	*y*	*z*	U(eq)
H71B	7999.81	1239.3	4802.83	32
H16A	8402.43	5072.49	3586.25	37
H16B	8694.26	5543.72	3271.09	37
H65A	5249.66	2196.84	4883.04	29
H65B	5843.66	1840.54	5274.27	29
H25A	7734.89	4116.08	1937.56	34
H25B	7901.66	3532.66	2171.6	34
H48A	7565.21	2398.77	6188.36	29
H48B	7343.61	2088.98	5701.85	29
H86A	9571.05	2496.91	3421.19	36
H86B	9908.05	2295.44	2961.83	36
H54A	7543.64	4929.2	5568.21	35
H54B	8413.81	4812.83	5352.44	35
H81A	9622.78	2138.14	4714.79	39
H81B	10662.67	2247.87	4785.59	39
H41A	5265.08	4325.69	4545.18	43
H41B	5500.67	3703.44	4486.55	43
H22A	10445.11	3261.96	2480.77	35
H22B	10343.69	3850.12	2251.81	35
H12A	6270.06	3882.27	2221.01	42
H12B	5264.15	4078.5	2154.5	42
H36A	4493.27	4246.06	2689.8	50
H36B	3774.43	4714.02	2685.38	50
H49A	8867.38	2220.81	5864.87	30
H49B	8743.45	2851.4	5952.93	30
H87A	11025.17	2708.21	3771.59	38
H87B	10795.3	3018.97	3285.55	38
H76A	9438.24	948.22	3112.1	39
H76B	8566.28	745.37	3290.55	39
H20A	9739.05	5328.3	2740.63	34
H20B	10031.09	4713.51	2692.33	34
H53A	6785.28	5209.77	4831.77	35
H53B	7663.05	5563.62	4970.34	35
H80A	8564.02	616.25	4096.92	36
H80B	9438.72	724.99	4468.8	36
H52A	8412.66	5026.54	4504.19	31
H52B	7523.68	5241.37	4191.96	31
H75A	5897.31	831.54	5369.14	36
H75B	6731.01	1073.14	5709.18	36
H66A	6378.92	1067.87	3623.89	38
H66B	5462.24	748.03	3523.1	38

Atom	*x*	*y*	*z*	U(eq)
H59A	10629.23	4329.21	5114.69	38
H59B	9770.08	4488.13	4748.69	38
H72A	8854.45	547.76	5221.46	38
H72B	8003.48	301.37	4896.48	38
H83A	11690.15	1677.53	5413.71	42
H83B	11235.24	1208.23	5665.92	42
H13A	4898.54	3570.62	1464.54	44
H13B	5741.49	3930.44	1413.98	44
H70A	4983.83	255.22	4200.54	42
H70B	5628.5	288.32	4690.87	42
H9A	3673.21	1770.45	2040.38	41
H9B	4136.99	2347.01	2134.01	41
H63A	3158.72	1652.44	5134.41	38
H63B	3495.22	2102.25	4812.86	38
H17A	9806.52	5031.27	4030.25	41
H17B	9491.92	5647.03	4015.9	41
H58A	10936.45	4351.7	4338.33	38
H58B	11132.98	3768.12	4567.75	38
H4A	8513.84	1992.75	1907.79	46
H4B	7506.34	1832.3	1724.36	46
H26A	8618.33	5081.61	2107.42	40
H26B	8219.28	5590.43	2338.25	40
H85A	11617.76	1576.09	4504.51	39
H85B	11180.49	1036.58	4267.49	39
H73A	8125.8	-99.62	5637.37	40
H73B	8158.12	481.59	5879.93	40
H45A	4520.9	3131.97	3984.37	50
H45B	3635.39	3368.42	3681.95	50
H31A	4615.44	5246.56	4384.82	44
H31B	3800.55	4899.7	4125.58	44
H67A	7167.49	259.62	3729.57	54
H67B	6528.44	238.87	3236.62	54
H68A	6477.6	-584.46	3663.05	56
H68B	5523.57	-310.79	3536.87	56
H64A	4487.9	2099.95	5507.14	37
H64B	4587.56	1457.97	5494.96	37
H2A	7571.41	708.67	2554.82	43
H2B	6892.46	983.59	2145.68	43
H8A	3305.86	1748.75	2777.87	46
H8B	2998.01	2324.74	2561.53	46
H23A	9194.87	2951.24	1974.02	44

Atom	*x*	*y*	*z*	U(eq)
H23B	9841.09	3223.22	1665.14	44
H42A	4138.25	4098.12	4951.73	59
H42B	5023.14	3805.05	5197.15	59
H78A	9417.87	-596.72	3619.11	44
H78B	8523.16	-255.27	3574.84	44
H74A	6658.34	39.41	5274.72	42
H74B	6712.8	145.3	5818.98	42
H84A	11920.37	874.23	5040.71	52
H84B	10897.01	720.28	4979.41	52
H77A	9232.89	9.48	2967.78	50
H77B	10137.29	112.25	3317.97	50
H15A	5189.64	2567.16	1718.9	35
H15B	6180.12	2347.65	1773.01	35
H88A	12209.18	2596.16	3368.74	51
H88B	11558.63	2369.06	2923.59	51
H27A	7360.3	5011.38	1547.04	48
H27B	7726.64	5614.39	1541.47	48
H34A	4852.6	5583.82	3124.81	45
H34B	5683.5	5931.86	3365.25	45
H69A	5724.23	-558.03	4323.39	59
H69B	6658.32	-257.85	4426.83	59
H14A	5913.58	3013.91	1189.13	40
H14B	6683.6	3199.27	1598.2	40
H24A	8996.12	4017.96	1582.59	41
H24B	8338.03	3523.58	1434.27	41
H37A	3289.84	4105.13	2075.93	59
H37B	3372.13	3612.74	2435.38	59
H3A	8268.51	1033.19	1935.3	54
H3B	8697.18	1275.68	2429.79	54
H19A	11201.85	5193.62	3151	41
H19B	10849.66	4738.73	3463.13	41
H35A	5934.84	5002.29	3517.74	43
H35B	5942.38	5327.29	3991.39	43
H40A	2800.13	4702.03	3260.74	43
H40B	2886.28	4220.84	3631.7	43
H18A	10988.72	5558.19	3883.97	44
H18B	10375.26	5861.86	3463.9	44
H82A	9836.86	1443.57	5268.9	49
H82B	10289.21	1982.92	5498.55	49
H89A	12253.78	1628.12	3334.62	68
H89B	11963.95	1833.12	3805.65	68

Atom	*x*	*y*	*z*	U(eq)
H28A	6154.7	5574.63	1502.89	53
H28B	6637.26	5938.91	1923.08	53
H79A	9208.81	-215.86	4351.06	51
H79B	10123.87	-35.8	4207.73	51
H90A	10784.93	1443.71	3006.71	54
H90B	11001.88	1139.52	3495.42	54
H29A	5661.76	5396.05	2230.36	59
H29B	5981.06	4868.64	1992.12	59
H39A	2323.64	3598.31	3042.54	52
H39B	1634.74	4083.77	3034.79	52
H32A	3553.63	5845.35	4037.74	49
H32B	3473.66	5541.58	3549.68	49
H38A	1887.05	3869.86	2266.91	57
H38B	2138.34	4484.21	2399.31	57
H30A	6946.84	5431.34	2758.78	47
H30B	6563.16	4832.12	2766.49	47
H43A	4560.69	2983.48	4866.42	83
H43B	3755.88	3216.83	5087.41	83
H33A	4316.15	6316.85	3502.45	46
H33B	4955.97	6172.94	3978.82	46
H44A	3017.28	3489.25	4362.94	79
H44B	3287.35	2869.98	4319.43	79

Table 5.42 Solvent masks information for 1-Sm^{6+}.

Number	X	Y	Z	Volume	Electron count	Content
1	0.204	0.218	0.124	335.6	45.6	?
2	0.204	0.282	0.624	335.6	47.3	?
3	-0.204	0.718	0.376	335.6	44.1	?
4	-0.204	0.782	0.876	335.6	45.8	?

5.5.7 *2-Sm*$^{6+}$

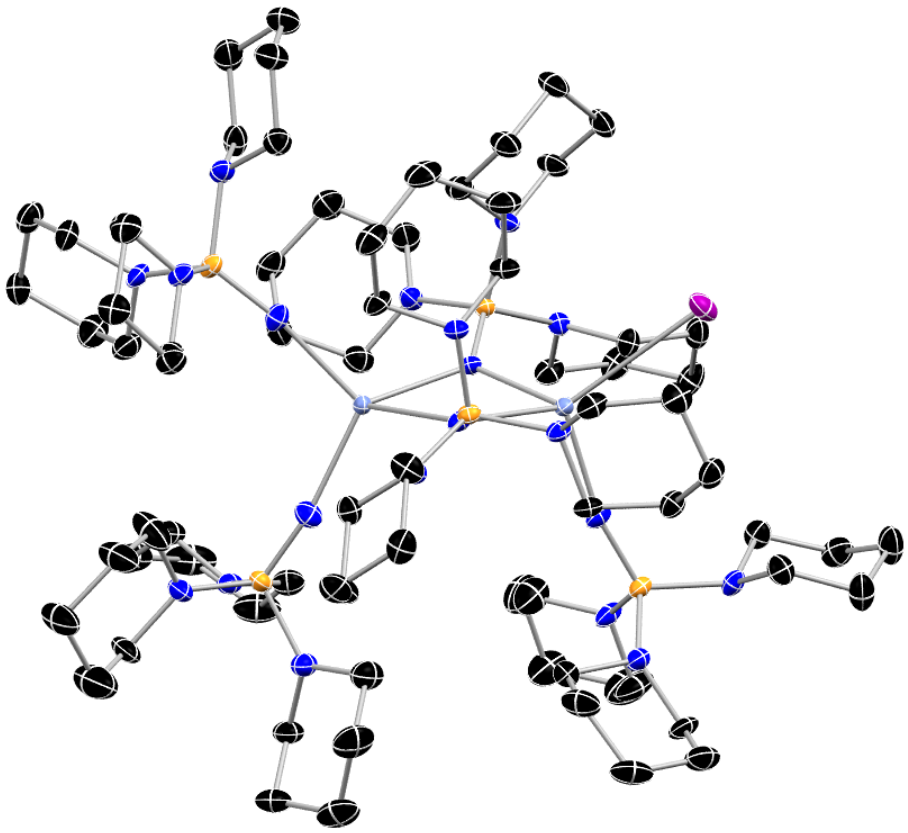

Figure 5.18 Molecular structure of 2-Sm^{6+} with thermal ellipsoids shown at 50% probability with hydrogen atoms omitted for clarity. Color code: C, black; N, blue; O, red; P, orange; I, purple; Sm, blue.

Table 5.43 Crystal data and structure refinement for 2-Sm^{6+}.

Identification code	2-Sm^{6+}
Empirical formula	$C_{81}H_{164}IN_{20}P_5Sm_2$
Formula weight	2000.76
Temperature/K	100(2)
Crystal system	triclinic
Space group	P-1
a/Å	14.871(3)
b/Å	14.894(3)
c/Å	25.625(5)
α/°	100.484(8)

β/°	90.506(8)
γ/°	117.103(7)
Volume/Å^3	4940.8(16)
Z	2
ρ_{calc}g/cm^3	1.345
μ/mm^{-1}	1.619
F(000)	2084.0
Crystal size/mm^3	0.526 × 0.27 × 0.217
Radiation	MoKα (λ = 0.71073)
2Θ range for data collection/°	4.876 to 51.362
Index ranges	-16 ≤ h ≤ 18, -18 ≤ k ≤ 18, -31 ≤ l ≤ 25
Reflections collected	33788
Independent reflections	18053 [R_{int} = 0.0429, R_{sigma} = 0.0655]
Data/restraints/parameters	18053/27/984
Goodness-of-fit on F^2	1.043
Final R indexes [I>=2σ (I)]	R_1 = 0.0369, wR_2 = 0.0907
Final R indexes [all data]	R_1 = 0.0438, wR_2 = 0.0957
Largest diff. peak/hole / e Å^{-3}	1.26/-0.75

Table 5.44 Fractional Atomic Coordinates (×10^4) and Equivalent Isotropic Displacement Parameters (Å^2×10^3) for 2-Sm^{6+}. U_{eq} is defined as 1/3 of the trace of the orthogonalised U_{IJ} tensor.

Atom	*x*	*y*	*z*	U(eq)
Sm1	4173.0(2)	2380.3(2)	7340.9(2)	13.14(6)
Sm2	5458.5(2)	1348.5(2)	8054.3(2)	13.74(6)
I1	5382.5(2)	-703.1(2)	8221.9(2)	27.98(7)
C1S	2566(5)	4191(5)	4864(3)	76.2(18)
C2S	1647(5)	4293(4)	5052(2)	62.6(15)
C3S	1873(5)	5092(4)	5547(2)	59.0(14)
C4S	972(5)	5235(4)	5724(2)	57.3(14)
C5S	1127(4)	5872(4)	6273(2)	60.3(15)
C6S	165(4)	5826(4)	6472(2)	55.9(14)
P1_1	5280.7(7)	5215.0(7)	7478.2(4)	17.9(2)
N1_1	4964(2)	4064(2)	7410.7(12)	23.2(7)
N2_1	4660(2)	5729(2)	7875.0(12)	19.2(7)
N3_1	6473(2)	6009(2)	7753.5(13)	22.6(7)
N4_1	5155(3)	5544(2)	6897.4(13)	24.6(8)
C1_1	3639(3)	5477(3)	7672.0(18)	30.7(10)
C2_1	3312(3)	6226(3)	7987(2)	43.0(13)
C3_1	3362(4)	6201(4)	8576(2)	52.1(15)
C4_1	4409(4)	6379(4)	8779.7(19)	43.8(13)

Atom	*x*	*y*	*z*	U(eq)
C5_1	4698(3)	5633(3)	8431.9(15)	26.9(9)
C6_1	7225(3)	5633(3)	7716.8(19)	33.8(10)
C7_1	8147(3)	6319(4)	7461(2)	43.4(12)
C8_1	8616(3)	7438(4)	7770(2)	44.5(13)
C9_1	7809(3)	7807(3)	7816.6(19)	37.9(11)
C10_1	6889(3)	7077(3)	8052.0(16)	27.2(9)
C11_1	4595(5)	4785(4)	6413.0(18)	51.6(15)
C12_1	5046(5)	5013(4)	5931.8(18)	54.1(16)
C13_1	5312(5)	6103(4)	5866.3(18)	55.4(17)
C14_1	5966(5)	6872(4)	6370(2)	62.1(17)
C15_1	5417(3)	6598(3)	6858.7(17)	30.8(10)
P1_2	1999.3(7)	1268.2(7)	6274.8(3)	17.3(2)
N1_2	2858(2)	1638(2)	6718.0(12)	21.0(7)
N2_2	1010(2)	68(2)	6193.3(12)	19.8(7)
N3_2	1367(2)	1968(2)	6343.5(12)	20.7(7)
N4_2	2385(2)	1197(2)	5653.5(11)	19.2(7)
C1_2	1288(3)	-771(3)	6052.3(16)	25.6(9)
C2_2	339(3)	-1803(3)	5870.4(18)	37.6(11)
C3_2	-379(3)	-2017(3)	6305(2)	39.9(12)
C4_2	-619(3)	-1114(3)	6470.3(19)	36.6(11)
C5_2	355(3)	-104(3)	6631.6(16)	26.2(9)
C6_2	1864(3)	3040(3)	6647.5(17)	30.1(10)
C7_2	1103(3)	3301(3)	6928.2(17)	34.3(10)
C8_2	236(3)	3121(3)	6532.2(16)	28.7(9)
C9_2	-241(3)	2026(3)	6202.5(18)	31.7(10)
C10_2	561(3)	1788(3)	5944.8(15)	26.3(9)
C11_2	3314(3)	2127(3)	5595.0(14)	23.0(9)
C12_2	3836(3)	1901(3)	5124.4(15)	26.1(9)
C13_2	3121(3)	1411(3)	4611.2(15)	29.6(10)
C14_2	2174(3)	469(3)	4691.8(15)	29.5(10)
C15_2	1676(3)	758(3)	5163.4(14)	22.9(9)
P1_3	3142.3(7)	1073.6(7)	8441.5(3)	13.86(19)
N1_3	4027(2)	1614(2)	8106.1(11)	15.4(6)
N2_3	3466(2)	1112(2)	9079.0(11)	16.6(6)
N3_3	2313(2)	1536(2)	8466.3(12)	19.2(7)
N4_3	2498(2)	-196(2)	8217.7(11)	18.0(7)
C1_3	4291(3)	842(3)	9139.8(14)	20.3(8)
C2_3	4345(3)	565(3)	9675.1(14)	26.4(9)
C3_3	4449(3)	1430(3)	10130.1(15)	30.6(10)
C4_3	3624(3)	1737(3)	10044.3(15)	30.4(10)
C5_3	3591(3)	1988(3)	9497.2(14)	24.4(9)

Atom	*x*	*y*	*z*	U(eq)
C6_3	2589(3)	2601(3)	8441.9(17)	28.4(9)
C7_3	1805(3)	2643(3)	8095.8(19)	36.3(11)
C8_3	751(3)	2107(3)	8287(2)	35.4(11)
C9_3	496(3)	1014(4)	8331(2)	38.5(11)
C10_3	1324(3)	1018(3)	8671.6(18)	32.1(10)
C11_3	2139(3)	-593(3)	7645.7(14)	25.7(9)
C12_3	2224(3)	-1563(3)	7438.1(15)	29.8(10)
C13_3	1647(3)	-2389(3)	7758.7(15)	29.9(10)
C14_3	2045(3)	-1935(3)	8352.9(15)	30.5(10)
C15_3	1938(3)	-979(3)	8535.2(15)	27.5(10)
P1_4	7573.7(7)	3409.6(7)	8980.2(4)	16.8(2)
N1_4	6706(2)	2653(2)	8545.3(12)	19.3(7)
N2_4	7997(2)	2950(2)	9426.8(11)	18.6(7)
N3_4	8669(2)	4081(2)	8731.4(12)	20.4(7)
N4_4	7251(2)	4214(2)	9385.6(12)	22.8(7)
C1_4	7283(3)	2461(3)	9805.6(15)	25.0(9)
C2_4	7837(3)	2365(3)	10271.8(16)	31.4(10)
C3_4	8418(4)	1768(4)	10084.9(18)	36.7(11)
C4_4	9098(3)	2239(4)	9662.2(18)	35.2(11)
C5_4	8472(3)	2308(3)	9211.2(16)	26.5(9)
C6_4	8605(3)	4472(3)	8253.1(16)	26.5(9)
C7_4	9422(3)	4466(3)	7899.1(17)	36.7(11)
C8_4	10472(3)	5070(3)	8211.6(19)	39.6(12)
C9_4	10503(3)	4711(3)	8723.6(19)	34.7(11)
C10_4	9657(3)	4717(3)	9052.8(16)	26.4(9)
C11_4	6479(4)	4455(4)	9179(2)	44.5(12)
C12_4	5969(4)	4776(4)	9613(2)	45.6(13)
C13_4	6752(4)	5690(4)	10034(2)	43.7(12)
C14_4	7547(4)	5422(4)	10233(2)	53.0(15)
C15_4	8019(3)	5080(4)	9781.0(19)	40.2(12)
C1_5	4477(3)	-685(3)	6621.8(14)	23.4(9)
C2_5	4032(3)	-1684(3)	6199.3(17)	33.5(10)
C3_5	3310(3)	-1671(3)	5774.9(17)	35.4(11)
C4_5	3834(3)	-696(3)	5550.9(16)	32.0(10)
C5_5	4273(3)	263(3)	5995.9(14)	24.4(9)
C6_5	6225(3)	3050(3)	6378.0(15)	23.6(9)
C7_5	7215(3)	3945(3)	6293.3(17)	32.5(10)
C8_5	7606(3)	3648(3)	5774.4(17)	34.0(11)
C9_5	7710(3)	2679(3)	5771.3(16)	31.7(10)
C10_5	6709(3)	1815(3)	5867.4(15)	28.2(10)
C11_5	7573(3)	1845(3)	7334.6(14)	20.2(8)

Atom	*x*	*y*	*z*	U(eq)
C12_5	7989(3)	1424(3)	7716.2(15)	22.7(8)
C13_5	8242(3)	595(3)	7419.1(17)	29.3(9)
C14_5	7327(3)	-234(3)	7034.8(18)	32.2(10)
C15_5	6949(3)	252(3)	6673.7(15)	24.9(9)
N1_5	5387(2)	1771(2)	7234.0(11)	17.7(7)
N2_5	5008(2)	203(2)	6363.3(11)	17.2(7)
N3_5	6352(2)	2131(2)	6361.5(12)	21.9(7)
N4_5	6663(2)	993(2)	6996.1(12)	18.0(7)
P1_5	5815.4(7)	1322.1(7)	6767.4(3)	15.2(2)

Table 5.45 Anisotropic Displacement Parameters ($Å^2×10^3$) for 2-Sm^{6+}. The Anisotropic displacement factor exponent takes the form: $-2\pi^2[h^2a^{*2}U_{11}+2hka^*b^*U_{12}+\ldots]$.

Atom	U_{11}	U_{22}	U_{33}	U_{23}	U_{13}	U_{12}
Sm1	14.05(10)	12.82(9)	12.70(9)	3.10(6)	0.28(7)	6.24(7)
Sm2	12.67(10)	12.89(9)	14.62(9)	1.68(7)	-1.11(7)	5.55(7)
I1	30.87(16)	20.12(13)	38.71(15)	11.81(11)	10.42(12)	14.57(11)
C1S	98(5)	78(5)	68(4)	9(3)	-7(3)	56(4)
C2S	85(4)	49(3)	56(3)	16(2)	-4(3)	32(3)
C3S	81(4)	39(3)	55(3)	21(2)	10(3)	23(3)
C4S	77(4)	35(3)	51(3)	18(2)	4(3)	16(3)
C5S	58(3)	41(3)	61(3)	4(2)	-1(3)	8(3)
C6S	60(3)	40(3)	50(3)	3(2)	-4(2)	11(3)
P1_1	18.5(5)	13.5(4)	21.4(5)	4.5(4)	2.0(4)	6.8(4)
N1_1	26.3(19)	19.5(16)	26.1(16)	4.5(13)	6.1(14)	12.6(14)
N2_1	13.9(16)	14.7(15)	26.8(16)	0.9(12)	1.4(13)	6.1(12)
N3_1	18.4(17)	18.1(16)	29.8(17)	2.2(13)	0.3(14)	8.2(13)
N4_1	28.7(19)	15.2(16)	26.2(17)	6.2(13)	-2.5(14)	6.4(14)
C1_1	23(2)	20(2)	44(2)	3.1(18)	3.4(19)	6.9(17)
C2_1	21(2)	29(2)	79(4)	5(2)	12(2)	14.2(19)
C3_1	33(3)	35(3)	76(4)	-7(2)	26(3)	12(2)
C4_1	42(3)	31(3)	39(3)	-8(2)	13(2)	6(2)
C5_1	23(2)	26(2)	26(2)	3.9(16)	6.3(17)	7.5(17)
C6_1	25(2)	28(2)	49(3)	4.3(19)	5(2)	14.0(19)
C7_1	23(2)	48(3)	56(3)	5(2)	11(2)	15(2)
C8_1	23(3)	45(3)	49(3)	11(2)	9(2)	2(2)
C9_1	27(2)	24(2)	49(3)	6.7(19)	0(2)	0.4(18)
C10_1	23(2)	19(2)	32(2)	1.2(16)	0.2(17)	5.0(16)
C11_1	92(4)	29(3)	28(2)	7.8(19)	2(2)	23(3)
C12_1	77(4)	28(3)	31(2)	9.1(19)	-9(2)	1(2)

Atom	U_{11}	U_{22}	U_{33}	U_{23}	U_{13}	U_{12}
C13_1	80(4)	32(3)	28(2)	15(2)	-13(2)	2(2)
C14_1	77(4)	36(3)	49(3)	12(2)	-5(3)	6(3)
C15_1	40(3)	15.2(19)	34(2)	8.6(16)	1.7(19)	9.3(18)
P1_2	15.4(5)	22.1(5)	13.3(4)	2.9(3)	-0.4(4)	8.1(4)
N1_2	19.9(17)	28.3(17)	16.4(14)	4.9(13)	1.6(13)	12.6(14)
N2_2	15.6(16)	21.6(16)	20.3(15)	6.7(12)	2.5(13)	6.2(13)
N3_2	14.6(16)	24.1(17)	21.4(15)	1.6(13)	-4.4(13)	8.6(13)
N4_2	15.6(16)	23.2(16)	14.8(14)	2.9(12)	0.0(12)	6.0(13)
C1_2	25(2)	26(2)	27(2)	6.0(16)	3.5(17)	11.5(17)
C2_2	36(3)	25(2)	42(3)	7.8(19)	-1(2)	6.4(19)
C3_2	26(2)	31(2)	58(3)	20(2)	5(2)	5.6(19)
C4_2	23(2)	43(3)	50(3)	25(2)	9(2)	14(2)
C5_2	24(2)	36(2)	26(2)	15.3(17)	7.5(17)	17.1(18)
C6_2	22(2)	26(2)	40(2)	-0.6(18)	-5.3(18)	11.3(17)
C7_2	36(3)	34(2)	36(2)	-3.4(18)	-2.8(19)	22(2)
C8_2	32(2)	32(2)	30(2)	8.3(17)	2.6(18)	20.7(19)
C9_2	23(2)	36(2)	40(2)	5.2(19)	-2.2(19)	17.6(19)
C10_2	27(2)	33(2)	23.2(19)	3.2(16)	-3.0(17)	18.0(18)
C11_2	20(2)	24(2)	20.3(18)	4.9(15)	0.1(15)	6.3(16)
C12_2	21(2)	30(2)	22.9(19)	5.8(16)	3.8(16)	8.4(17)
C13_2	35(3)	32(2)	18.9(19)	2.5(16)	6.8(17)	14.6(19)
C14_2	34(2)	31(2)	16.3(18)	-3.5(16)	-4.2(16)	12.2(18)
C15_2	22(2)	25(2)	18.4(18)	3.9(15)	-0.1(15)	8.2(16)
P1_3	12.2(5)	14.3(4)	14.7(4)	4.4(3)	1.0(3)	5.3(4)
N1_3	11.7(15)	14.2(14)	18.2(14)	3.5(11)	0.8(12)	4.1(12)
N2_3	19.4(17)	16.5(15)	14.8(14)	2.2(11)	1.8(12)	9.4(13)
N3_3	15.1(16)	19.2(16)	27.2(16)	8.5(13)	6.7(13)	9.8(13)
N4_3	19.9(17)	13.5(15)	15.4(14)	4.2(11)	1.4(12)	3.1(12)
C1_3	20(2)	26(2)	20.0(18)	3.9(15)	4.0(15)	15.5(16)
C2_3	26(2)	34(2)	24(2)	13.0(17)	3.0(17)	15.2(19)
C3_3	29(2)	48(3)	14.9(18)	3.0(17)	-1.6(16)	20(2)
C4_3	30(2)	44(3)	18.0(18)	-1.1(17)	2.1(17)	21(2)
C5_3	25(2)	23(2)	21.4(18)	-4.8(15)	0.2(16)	11.5(17)
C6_3	26(2)	23(2)	36(2)	4.7(17)	5.6(18)	12.0(17)
C7_3	34(3)	30(2)	49(3)	17(2)	1(2)	16(2)
C8_3	17(2)	38(3)	56(3)	9(2)	-1(2)	16.0(19)
C9_3	21(2)	38(3)	57(3)	16(2)	5(2)	12(2)
C10_3	21(2)	37(2)	44(2)	21(2)	9.7(19)	13.6(19)
C11_3	29(2)	22(2)	16.6(18)	3.4(15)	-4.1(16)	3.9(17)
C12_3	40(3)	19(2)	21.6(19)	1.8(15)	-1.9(17)	7.1(18)
C13_3	43(3)	15.2(19)	23.1(19)	4.0(15)	-0.2(18)	6.2(17)

Atom	U_{11}	U_{22}	U_{33}	U_{23}	U_{13}	U_{12}
C14_3	43(3)	21(2)	25(2)	10.2(16)	-4.1(18)	9.9(18)
C15_3	32(2)	20(2)	19.7(18)	8.9(15)	2.8(16)	0.6(17)
P1_4	13.6(5)	17.8(5)	17.0(4)	-0.4(3)	-1.0(4)	7.3(4)
N1_4	12.0(16)	22.3(16)	21.1(15)	0.3(12)	-0.8(12)	7.4(13)
N2_4	13.6(16)	27.0(17)	16.0(14)	4.8(12)	2.2(12)	10.0(13)
N3_4	16.5(17)	20.9(16)	21.0(15)	4.7(12)	-0.4(13)	6.3(13)
N4_4	15.1(17)	24.2(17)	26.3(16)	-5.0(13)	-4.8(13)	10.7(14)
C1_4	24(2)	31(2)	21.4(18)	7.2(16)	4.1(16)	13.1(17)
C2_4	28(2)	37(2)	24(2)	6.1(17)	2.1(17)	11.3(19)
C3_4	38(3)	52(3)	34(2)	25(2)	9(2)	26(2)
C4_4	34(3)	50(3)	36(2)	23(2)	11(2)	27(2)
C5_4	31(2)	27(2)	26(2)	7.3(16)	7.1(17)	17.0(18)
C6_4	26(2)	23(2)	30(2)	8.3(16)	-0.4(17)	9.4(17)
C7_4	37(3)	29(2)	31(2)	9.7(18)	11.2(19)	3.6(19)
C8_4	26(2)	27(2)	51(3)	5(2)	14(2)	1.1(19)
C9_4	19(2)	27(2)	51(3)	5.0(19)	3(2)	5.5(18)
C10_4	11.7(19)	25(2)	35(2)	-0.2(17)	-3.9(16)	4.9(16)
C11_4	42(3)	44(3)	49(3)	-8(2)	-4(2)	28(2)
C12_4	44(3)	50(3)	46(3)	-8(2)	-9(2)	30(2)
C13_4	42(3)	38(3)	49(3)	-14(2)	-3(2)	25(2)
C14_4	50(3)	50(3)	44(3)	-21(2)	-8(2)	22(3)
C15_4	24(2)	33(3)	50(3)	-18(2)	-10(2)	12.1(19)
C1_5	21(2)	19.2(19)	20.8(18)	0.7(15)	1.9(16)	3.3(16)
C2_5	28(2)	19(2)	40(2)	-2.7(17)	-3.0(19)	2.9(17)
C3_5	31(3)	26(2)	37(2)	-13.2(18)	-8.6(19)	8.9(18)
C4_5	32(3)	36(2)	22(2)	-9.3(17)	-6.8(17)	17.4(19)
C5_5	23(2)	25(2)	18.2(18)	-3.9(15)	-6.7(15)	8.4(17)
C6_5	27(2)	26(2)	22.2(18)	8.3(15)	4.6(16)	14.0(17)
C7_5	37(3)	24(2)	33(2)	9.8(17)	8.7(19)	10.1(19)
C8_5	30(2)	35(2)	33(2)	18.7(19)	9.8(19)	7.7(19)
C9_5	31(2)	46(3)	22.2(19)	10.8(18)	9.2(17)	21(2)
C10_5	36(3)	29(2)	20.8(19)	4.3(16)	12.6(17)	16.2(19)
C11_5	14.9(19)	17.4(18)	21.9(18)	-2.2(14)	2.4(15)	4.3(15)
C12_5	20(2)	27(2)	22.1(18)	2.3(15)	1.1(16)	13.0(17)
C13_5	23(2)	34(2)	34(2)	5.8(18)	-0.2(18)	17.2(18)
C14_5	34(3)	26(2)	40(2)	-2.1(18)	3(2)	20.7(19)
C15_5	19(2)	26(2)	27(2)	-5.8(16)	1.2(16)	12.3(17)
N1_5	14.6(16)	18.2(15)	16.9(14)	-0.1(12)	-1.3(12)	6.1(12)
N2_5	15.8(16)	15.3(15)	16.8(14)	0.8(11)	1.1(12)	5.0(12)
N3_5	25.2(18)	20.4(16)	18.6(15)	3.2(12)	8.2(13)	9.6(14)
N4_5	15.3(16)	16.1(15)	19.5(15)	-2.6(12)	-1.5(12)	7.2(12)

Atom	U_{11}	U_{22}	U_{33}	U_{23}	U_{13}	U_{12}
P1_5	14.6(5)	14.6(4)	13.5(4)	-0.1(3)	1.2(3)	5.4(4)

Table 5.46 Bond Lengths for 2-Sm^{6+}.

Atom	Atom	Length/Å	Atom	Atom	Length/Å
Sm1	N1_1	2.202(3)	N2_3	C5_3	1.467(4)
Sm1	N1_2	2.219(3)	N3_3	C6_3	1.460(5)
Sm1	N1_3	2.406(3)	N3_3	C10_3	1.471(5)
Sm1	N1_5	2.360(3)	N4_3	C11_3	1.472(4)
Sm2	I1	3.1142(7)	N4_3	C15_3	1.479(4)
Sm2	N1_3	2.337(3)	C1_3	C2_3	1.515(5)
Sm2	N1_4	2.141(3)	C2_3	C3_3	1.520(6)
Sm2	N1_5	2.316(3)	C3_3	C4_3	1.519(6)
C1S	C2S	1.516(9)	C4_3	C5_3	1.521(5)
C2S	C3S	1.489(8)	C6_3	C7_3	1.490(6)
C3S	C4S	1.510(8)	C7_3	C8_3	1.532(6)
C4S	C5S	1.499(7)	C8_3	C9_3	1.520(6)
C5S	C6S	1.499(8)	C9_3	C10_3	1.500(6)
P1_1	N1_1	1.531(3)	C11_3	C12_3	1.509(6)
P1_1	N2_1	1.687(3)	C12_3	C13_3	1.530(5)
P1_1	N3_1	1.675(3)	C13_3	C14_3	1.540(5)
P1_1	N4_1	1.683(3)	C14_3	C15_3	1.496(6)
N2_1	C1_1	1.454(5)	P1_4	N1_4	1.539(3)
N2_1	C5_1	1.463(5)	P1_4	N2_4	1.685(3)
N3_1	C6_1	1.458(5)	P1_4	N3_4	1.681(3)
N3_1	C10_1	1.467(5)	P1_4	N4_4	1.681(3)
N4_1	C11_1	1.458(5)	N2_4	C1_4	1.473(5)
N4_1	C15_1	1.459(5)	N2_4	C5_4	1.465(5)
C1_1	C2_1	1.518(6)	N3_4	C6_4	1.469(5)
C2_1	C3_1	1.518(8)	N3_4	C10_4	1.470(5)
C3_1	C4_1	1.526(8)	N4_4	C11_4	1.469(6)
C4_1	C5_1	1.514(6)	N4_4	C15_4	1.468(5)
C6_1	C7_1	1.529(6)	C1_4	C2_4	1.509(6)
C7_1	C8_1	1.530(7)	C2_4	C3_4	1.524(6)
C8_1	C9_1	1.528(7)	C3_4	C4_4	1.529(6)
C9_1	C10_1	1.522(5)	C4_4	C5_4	1.525(6)
C11_1	C12_1	1.430(6)	C6_4	C7_4	1.525(6)
C12_1	C13_1	1.528(7)	C7_4	C8_4	1.525(6)
C13_1	C14_1	1.532(7)	C8_4	C9_4	1.512(7)
C14_1	C15_1	1.517(7)	C9_4	C10_4	1.524(6)
P1_2	N1_2	1.527(3)	C11_4	C12_4	1.481(7)

Atom	Atom	Length/Å	Atom	Atom	Length/Å
P1_2	N2_2	1.693(3)	C12_4	C13_4	1.540(6)
P1_2	N3_2	1.683(3)	C13_4	C14_4	1.521(8)
P1_2	N4_2	1.699(3)	C14_4	C15_4	1.490(6)
N2_2	C1_2	1.474(5)	C1_5	C2_5	1.525(5)
N2_2	C5_2	1.474(5)	C1_5	N2_5	1.479(4)
N3_2	C6_2	1.471(5)	C2_5	C3_5	1.531(6)
N3_2	C10_2	1.462(5)	C3_5	C4_5	1.525(6)
N4_2	C11_2	1.479(4)	C4_5	C5_5	1.520(5)
N4_2	C15_2	1.472(5)	C5_5	N2_5	1.481(5)
C1_2	C2_2	1.524(5)	C6_5	C7_5	1.521(5)
C2_2	C3_2	1.524(6)	C6_5	N3_5	1.458(5)
C3_2	C4_2	1.532(7)	C7_5	C8_5	1.528(6)
C4_2	C5_2	1.519(6)	C8_5	C9_5	1.519(6)
C6_2	C7_2	1.505(6)	C9_5	C10_5	1.520(5)
C7_2	C8_2	1.525(6)	C10_5	N3_5	1.460(5)
C8_2	C9_2	1.520(6)	C11_5	C12_5	1.517(5)
C9_2	C10_2	1.515(6)	C11_5	N4_5	1.486(4)
C11_2	C12_2	1.508(5)	C12_5	C13_5	1.527(6)
C12_2	C13_2	1.520(5)	C13_5	C14_5	1.533(6)
C13_2	C14_2	1.518(5)	C14_5	C15_5	1.517(6)
C14_2	C15_2	1.520(5)	C15_5	N4_5	1.478(5)
P1_3	N1_3	1.557(3)	N1_5	P1_5	1.547(3)
P1_3	N2_3	1.683(3)	N2_5	P1_5	1.679(3)
P1_3	N3_3	1.660(3)	N3_5	P1_5	1.663(3)
P1_3	N4_3	1.663(3)	N4_5	P1_5	1.681(3)
N2_3	C1_3	1.469(5)			

Table 5.47 Bond Angles for 2-Sm^{6+}.

Atom	Atom	Atom	Angle/°	Atom	Atom	Atom	Angle/°
N1_1	Sm1	N1_2	110.97(12)	C5_3	N2_3	P1_3	119.6(3)
N1_1	Sm1	N1_3	121.69(11)	C5_3	N2_3	C1_3	111.6(3)
N1_1	Sm1	N1_5	108.19(11)	C6_3	N3_3	P1_3	123.4(3)
N1_2	Sm1	N1_3	117.61(10)	C6_3	N3_3	C10_3	112.3(3)
N1_2	Sm1	N1_5	115.88(11)	C10_3	N3_3	P1_3	122.0(3)
N1_5	Sm1	N1_3	77.91(10)	C11_3	N4_3	P1_3	118.6(2)
N1_3	Sm2	I1	121.52(7)	C11_3	N4_3	C15_3	111.5(3)
N1_4	Sm2	I1	110.93(9)	C15_3	N4_3	P1_3	126.7(2)
N1_4	Sm2	N1_3	108.39(11)	N2_3	C1_3	C2_3	111.7(3)
N1_4	Sm2	N1_5	106.66(11)	C1_3	C2_3	C3_3	111.0(3)
N1_5	Sm2	I1	125.13(8)	C4_3	C3_3	C2_3	110.3(3)

Atom	Atom	Atom	Angle/°	Atom	Atom	Atom	Angle/°
N1_5	Sm2	N1_3	80.18(10)	C3_3	C4_3	C5_3	112.3(3)
C3S	C2S	C1S	114.1(5)	N2_3	C5_3	C4_3	110.0(3)
C2S	C3S	C4S	114.6(5)	N3_3	C6_3	C7_3	110.7(3)
C5S	C4S	C3S	115.4(5)	C6_3	C7_3	C8_3	111.1(4)
C4S	C5S	C6S	113.5(5)	C9_3	C8_3	C7_3	110.4(4)
N1_1	P1_1	N2_1	119.31(17)	C10_3	C9_3	C8_3	110.4(4)
N1_1	P1_1	N3_1	114.94(18)	N3_3	C10_3	C9_3	111.0(3)
N1_1	P1_1	N4_1	112.60(17)	N4_3	C11_3	C12_3	111.3(3)
N3_1	P1_1	N2_1	99.42(16)	C11_3	C12_3	C13_3	111.1(3)
N3_1	P1_1	N4_1	106.83(16)	C12_3	C13_3	C14_3	108.7(3)
N4_1	P1_1	N2_1	101.97(17)	C15_3	C14_3	C13_3	110.1(3)
P1_1	N1_1	Sm1	167.3(2)	N4_3	C15_3	C14_3	111.2(3)
C1_1	N2_1	P1_1	116.8(3)	N1_4	P1_4	N2_4	119.60(17)
C1_1	N2_1	C5_1	110.9(3)	N1_4	P1_4	N3_4	113.06(16)
C5_1	N2_1	P1_1	115.2(3)	N1_4	P1_4	N4_4	111.95(17)
C6_1	N3_1	P1_1	119.2(3)	N3_4	P1_4	N2_4	99.50(16)
C6_1	N3_1	C10_1	112.7(3)	N4_4	P1_4	N2_4	101.15(16)
C10_1	N3_1	P1_1	128.1(3)	N4_4	P1_4	N3_4	110.38(16)
C11_1	N4_1	P1_1	122.8(3)	P1_4	N1_4	Sm2	166.6(2)
C11_1	N4_1	C15_1	113.3(3)	C1_4	N2_4	P1_4	116.2(3)
C15_1	N4_1	P1_1	122.8(3)	C5_4	N2_4	P1_4	116.1(2)
N2_1	C1_1	C2_1	110.1(3)	C5_4	N2_4	C1_4	109.8(3)
C1_1	C2_1	C3_1	110.3(4)	C6_4	N3_4	P1_4	117.2(3)
C2_1	C3_1	C4_1	110.8(4)	C10_4	N3_4	P1_4	124.5(3)
C5_1	C4_1	C3_1	110.3(4)	C10_4	N3_4	C6_4	111.9(3)
N2_1	C5_1	C4_1	110.4(4)	C11_4	N4_4	P1_4	118.8(3)
N3_1	C6_1	C7_1	111.3(4)	C15_4	N4_4	P1_4	120.1(3)
C6_1	C7_1	C8_1	110.6(4)	C15_4	N4_4	C11_4	112.4(3)
C9_1	C8_1	C7_1	110.1(4)	N2_4	C1_4	C2_4	110.6(3)
C10_1	C9_1	C8_1	111.0(4)	C1_4	C2_4	C3_4	111.2(3)
N3_1	C10_1	C9_1	112.0(3)	C2_4	C3_4	C4_4	110.1(4)
C12_1	C11_1	N4_1	115.1(4)	C5_4	C4_4	C3_4	110.1(4)
C11_1	C12_1	C13_1	112.8(5)	N2_4	C5_4	C4_4	109.5(3)
C12_1	C13_1	C14_1	108.8(4)	N3_4	C6_4	C7_4	110.2(4)
C15_1	C14_1	C13_1	110.0(4)	C8_4	C7_4	C6_4	110.8(4)
N4_1	C15_1	C14_1	111.1(4)	C9_4	C8_4	C7_4	111.6(3)
N1_2	P1_2	N2_2	119.79(17)	C8_4	C9_4	C10_4	111.1(4)
N1_2	P1_2	N3_2	113.49(17)	N3_4	C10_4	C9_4	109.7(3)
N1_2	P1_2	N4_2	113.20(17)	N4_4	C11_4	C12_4	111.8(4)
N2_2	P1_2	N4_2	99.35(15)	C11_4	C12_4	C13_4	110.8(4)
N3_2	P1_2	N2_2	99.83(16)	C14_4	C13_4	C12_4	109.9(4)

Atom	Atom	Atom	Angle/°	Atom	Atom	Atom	Angle/°
N3_2	P1_2	N4_2	109.58(16)	C15_4	C14_4	C13_4	111.1(4)
P1_2	N1_2	Sm1	172.5(2)	N4_4	C15_4	C14_4	111.6(4)
C1_2	N2_2	P1_2	114.4(2)	N2_5	C1_5	C2_5	109.5(3)
C5_2	N2_2	P1_2	115.2(2)	C1_5	C2_5	C3_5	110.8(4)
C5_2	N2_2	C1_2	110.5(3)	C4_5	C3_5	C2_5	110.3(3)
C6_2	N3_2	P1_2	120.2(3)	C5_5	C4_5	C3_5	111.0(3)
C10_2	N3_2	P1_2	122.4(3)	N2_5	C5_5	C4_5	109.0(3)
C10_2	N3_2	C6_2	111.8(3)	N3_5	C6_5	C7_5	110.5(3)
C11_2	N4_2	P1_2	113.6(2)	C6_5	C7_5	C8_5	110.7(3)
C15_2	N4_2	P1_2	123.0(2)	C9_5	C8_5	C7_5	110.3(3)
C15_2	N4_2	C11_2	111.1(3)	C8_5	C9_5	C10_5	110.2(4)
N2_2	C1_2	C2_2	110.4(3)	N3_5	C10_5	C9_5	111.1(3)
C3_2	C2_2	C1_2	110.6(4)	N4_5	C11_5	C12_5	110.1(3)
C2_2	C3_2	C4_2	109.7(4)	C11_5	C12_5	C13_5	111.6(3)
C5_2	C4_2	C3_2	110.5(4)	C12_5	C13_5	C14_5	110.2(3)
N2_2	C5_2	C4_2	110.8(3)	C15_5	C14_5	C13_5	110.7(3)
N3_2	C6_2	C7_2	110.5(3)	N4_5	C15_5	C14_5	110.2(3)
C6_2	C7_2	C8_2	111.0(4)	Sm2	N1_5	Sm1	100.88(11)
C9_2	C8_2	C7_2	110.3(4)	P1_5	N1_5	Sm1	137.40(18)
C10_2	C9_2	C8_2	110.8(3)	P1_5	N1_5	Sm2	118.35(18)
N3_2	C10_2	C9_2	111.2(3)	C1_5	N2_5	C5_5	109.8(3)
N4_2	C11_2	C12_2	111.5(3)	C1_5	N2_5	P1_5	116.2(2)
C11_2	C12_2	C13_2	112.0(3)	C5_5	N2_5	P1_5	115.4(2)
C14_2	C13_2	C12_2	109.7(3)	C6_5	N3_5	C10_5	113.7(3)
C13_2	C14_2	C15_2	110.3(3)	C6_5	N3_5	P1_5	122.7(3)
N4_2	C15_2	C14_2	110.6(3)	C10_5	N3_5	P1_5	121.1(3)
N1_3	P1_3	N2_3	116.82(16)	C11_5	N4_5	P1_5	115.9(2)
N1_3	P1_3	N3_3	112.61(16)	C15_5	N4_5	C11_5	109.6(3)
N1_3	P1_3	N4_3	113.14(15)	C15_5	N4_5	P1_5	123.5(3)
N3_3	P1_3	N2_3	105.72(16)	N1_5	P1_5	N2_5	117.80(16)
N3_3	P1_3	N4_3	107.50(16)	N1_5	P1_5	N3_5	112.60(17)
N4_3	P1_3	N2_3	99.92(15)	N1_5	P1_5	N4_5	110.96(16)
Sm2	N1_3	Sm1	98.93(10)	N2_5	P1_5	N4_5	100.42(16)
P1_3	N1_3	Sm1	134.30(18)	N3_5	P1_5	N2_5	104.88(15)
P1_3	N1_3	Sm2	123.87(17)	N3_5	P1_5	N4_5	109.27(16)
C1_3	N2_3	P1_3	113.3(2)				

Table 5.48 Hydrogen Atom Coordinates (Å×10^4) and Isotropic Displacement Parameters (Å^2×10^3) for 2-Sm^{6+}.

Atom	*x*	*y*	*z*	U(eq)
H1SA	2343.32	3567.02	4584.19	114
H1SB	2942.68	4144.61	5164.92	114
H1SC	3006.76	4795.83	4721.31	114
H2SA	1342.88	4463.58	4763.7	75
H2SB	1134.89	3618.52	5115.19	75
H3SA	2410.01	5758.71	5489.16	71
H3SB	2146.41	4902.2	5839.1	71
H4SA	789.14	5561.37	5466.12	69
H4SB	388.21	4545.87	5707	69
H5SA	1610.83	6598.73	6272.63	72
H5SB	1436.11	5630.78	6523.2	72
H6SA	-190.12	5981.12	6205.23	84
H6SB	327.44	6333.52	6806.86	84
H6SC	-271.96	5133.8	6533.1	84
H1A_1	3161.26	4764.18	7702.03	37
H1B_1	3622.28	5513.02	7290.37	37
H2A_1	2608.87	6036.89	7852.93	52
H2B_1	3762	6931.94	7936.85	52
H3A_1	2839.81	5524.09	8630.75	62
H3B_1	3216.06	6741.75	8780.8	62
H4A_1	4919.26	7095.95	8777.2	53
H4B_1	4404.09	6281.7	9151.93	53
H5A_1	5391.57	5778.59	8557.19	32
H5B_1	4223.35	4918.6	8460.32	32
H6A_1	6912.3	4919.86	7501.62	41
H6B_1	7448.27	5616.81	8078.66	41
H7A_1	7936.6	6282.92	7086.66	52
H7B_1	8659.36	6068.24	7458.03	52
H8A_1	8902.76	7489.49	8130.42	53
H8B_1	9174.32	7882.44	7582.47	53
H9A_1	8102.88	8506.26	8046.86	45
H9B_1	7594.54	7849.95	7458.98	45
H10A_1	7086.86	7110.31	8427.8	33
H10B_1	6357.13	7301.5	8049.27	33
H11A_1	4524.68	4107.52	6452.77	62
H11B_1	3903.88	4720.2	6378.02	62
H12A_1	4568.41	4509.45	5623.31	65
H12B_1	5670.52	4931.85	5930.61	65

Atom	*x*	*y*	*z*	U(eq)
H13A_1	4683.59	6162.54	5812.03	66
H13B_1	5690.68	6253.02	5550.66	66
H14A_1	6622.43	6857.85	6403.56	75
H14B_1	6106.79	7578.07	6342.77	75
H15A_1	5857.33	7081.4	7182.94	37
H15B_1	4790.46	6673.2	6838.58	37
H1A_2	1663.03	-795.35	6366.13	31
H1B_2	1738.33	-637.48	5762.75	31
H2A_2	-12.79	-1793.32	5543.07	45
H2B_2	534.89	-2360.96	5784.2	45
H3A_2	-59.81	-2108.78	6617.97	48
H3B_2	-1015.57	-2659.98	6170.81	48
H4A_2	-1013.78	-1077.65	6168.94	44
H4B_2	-1037.33	-1226.05	6773.57	44
H5A_2	187.62	472.77	6726.23	31
H5B_2	724.37	-120.96	6950.09	31
H6A_2	2186.44	3513.25	6402.24	36
H6B_2	2403.16	3132.71	6913.31	36
H7A_2	1443.55	4032.05	7118.33	41
H7B_2	825.35	2868.02	7196.05	41
H8A_2	-285.43	3237.75	6727.95	34
H8B_2	497.76	3617.32	6293.09	34
H9A_2	-591.86	1533.65	6434.83	38
H9B_2	-752	1941.63	5922.25	38
H10A_2	240.77	1058.45	5751.81	32
H10B_2	857.04	2227.56	5681.97	32
H11A_2	3787.73	2388.94	5924.46	28
H11B_2	3133.39	2672.22	5547.3	28
H12A_2	4102.63	1431.24	5195.95	31
H12B_2	4419.14	2551.65	5079.69	31
H13A_2	2931.01	1916.04	4508.2	35
H13B_2	3467.17	1206.91	4320.1	35
H14A_2	2357.48	-64.95	4756.71	35
H14B_2	1689.48	179.37	4365.29	35
H15A_2	1463.36	1267.46	5090.75	27
H15B_2	1061.72	136.85	5212.84	27
H1A_3	4945.35	1433.78	9104.99	24
H1B_3	4181.45	250.77	8851.12	24
H2A_3	4934.65	431.65	9711.55	32
H2B_3	3722.72	-73.91	9694.38	32
H3A_3	4394.54	1198.21	10472.31	37

Atom	*x*	*y*	*z*	U(eq)
H3B_3	5124.63	2033.19	10149.39	37
H4A_3	3745.43	2347.42	10322.71	36
H4B_3	2957.36	1166.09	10082.91	36
H5A_3	3018.3	2141.97	9449.16	29
H5B_3	4228.49	2605.58	9469.71	29
H6A_3	3254.06	2915.09	8298.1	34
H6B_3	2655.29	3002.66	8806.04	34
H7A_3	1790.15	2303.53	7723.59	44
H7B_3	1985.34	3372.18	8100.94	44
H8A_3	737.53	2502.35	8639.06	42
H8B_3	235.4	2087.93	8031.87	42
H9A_3	-153.31	701.81	8488.7	46
H9B_3	413.32	591.39	7970.11	46
H10A_3	1356.32	1378.04	9041.76	39
H10B_3	1166.94	299.29	8678.21	39
H11A_3	2547.68	-60.74	7443.79	31
H11B_3	1422.31	-738.92	7588.58	31
H12A_3	2948.37	-1402.22	7461.12	36
H12B_3	1944.43	-1831.5	7058.16	36
H13A_3	1751.83	-3000.22	7634.36	36
H13B_3	910.53	-2606.51	7707.61	36
H14A_3	1655.55	-2449.6	8567.61	37
H14B_3	2767.74	-1770	8406.04	37
H15A_3	1210.17	-1153.67	8500.57	33
H15B_3	2202.62	-690.1	8916.38	33
H1A_4	6757.75	1768.09	9621.56	30
H1B_4	6940.04	2880.11	9936.58	30
H2A_4	7340.94	2006.71	10513.05	38
H2B_4	8316.99	3062.11	10475.17	38
H3A_4	7932.57	1037.77	9933.43	44
H3B_4	8839.44	1787.71	10392.39	44
H4A_4	9642.07	2936.1	9826.43	42
H4B_4	9421.35	1807.04	9517.28	42
H5A_4	8915.17	2612.93	8938.5	32
H5B_4	7940.66	1609.16	9038.78	32
H6A_4	8695.76	5183.89	8359.99	32
H6B_4	7925.74	4035.07	8051.45	32
H7A_4	9284.1	3745.38	7759.43	44
H7B_4	9402.69	4776.03	7591.42	44
H8A_4	10978.07	4984.34	7988.12	47
H8B_4	10657	5812.85	8296.8	47

Atom	*x*	*y*	*z*	U(eq)
H9A_4	11168.54	5169.17	8935.34	42
H9B_4	10429.92	4003.87	8637.86	42
H10A_4	9667.16	4442.21	9375.34	32
H10B_4	9763.63	5433.25	9168.74	32
H11A_4	5965.19	3838.61	8926.84	53
H11B_4	6805.08	5014.88	8980.7	53
H12A_4	5574.35	4188.66	9784.68	55
H12B_4	5490.08	4977.27	9461.44	55
H13A_4	7084.39	6306.9	9874.77	52
H13B_4	6403.81	5852.03	10336.57	52
H14A_4	8079.99	6033.82	10479.08	64
H14B_4	7225.43	4865.26	10434.03	64
H15A_4	8408.09	5664.31	9606.24	48
H15B_4	8500.18	4868.53	9920.37	48
H1A_5	3926.78	-619.72	6812.06	28
H1B_5	4960.15	-696.54	6885.9	28
H2A_5	3659.8	-2276.69	6371.19	40
H2B_5	4589.59	-1770.9	6027.69	40
H3A_5	3093.59	-2285.42	5482.62	43
H3B_5	2696.55	-1697.88	5934.61	43
H4A_5	4385.41	-720.69	5345.28	38
H4B_5	3337.92	-663.11	5304.65	38
H5A_5	4617.55	886.59	5843.39	29
H5B_5	3720.9	309.61	6192.9	29
H6A_5	6009.87	3238.92	6727.73	28
H6B_5	5688	2904.48	6096.55	28
H7A_5	7730.04	4143.35	6597.14	39
H7B_5	7103.62	4547.56	6279.55	39
H8A_5	7127.37	3526.31	5466.97	41
H8B_5	8273.52	4219.95	5738.65	41
H9A_5	8246.2	2823.53	6053.27	38
H9B_5	7913.77	2463.55	5422.88	38
H10A_5	6193.65	1619.87	5564.26	34
H10B_5	6799	1202.75	5887.59	34
H11A_5	7387.73	2357.07	7539.67	24
H11B_5	8100.01	2197.16	7105.48	24
H12A_5	7481.1	1127.57	7965.31	27
H12B_5	8609.74	1994.73	7929.38	27
H13A_5	8428.76	274.84	7678.82	35
H13B_5	8830.89	913.38	7216.44	35
H14A_5	7524.08	-722.1	6815	39

Atom	*x*	*y*	*z*	U(eq)
H14B_5	6774.63	-625.77	7241.68	39
H15A_5	7487.74	612.13	6452.13	30
H15B_5	6352.19	-292.97	6431.97	30

5.5.8 *4-Sm^{5+}(Et2O)*

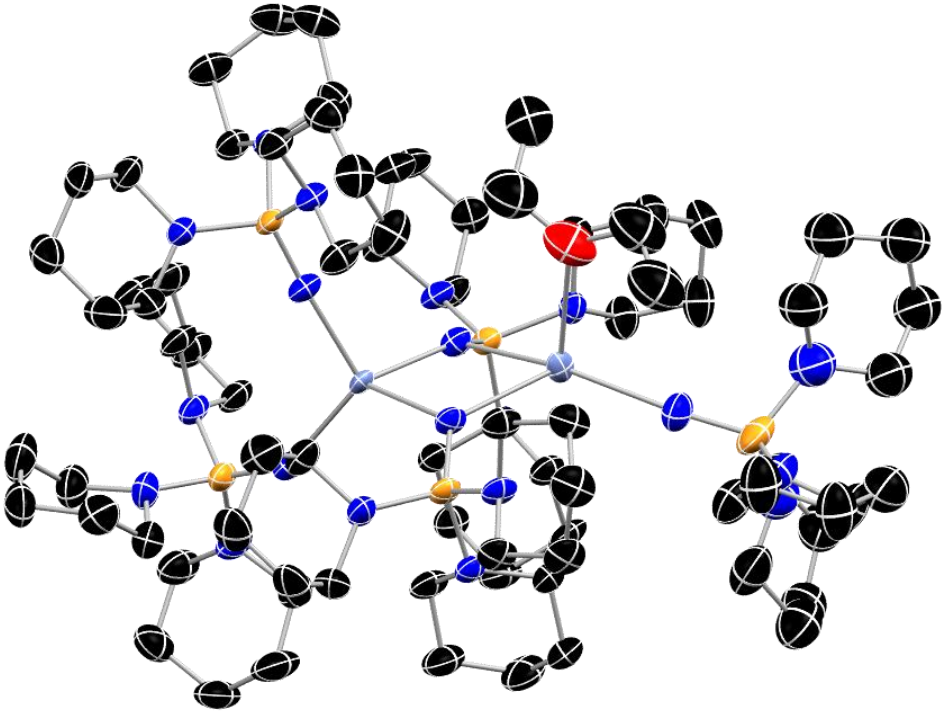

Figure 5.19 Molecular structure of 4-Sm^{5+}(Et$_2$O) with thermal ellipsoids shown at 50% probability with hydrogen atoms omitted for clarity. Color code: C, black; N, blue; O, red; P, orange; Sm, blue.

Table 5.49 Crystal data and structure refinement for 4-Sm^{5+}(Et$_2$O).

Identification code	4-Sm^{5+}(Et$_2$O)
Empirical formula	$C_{79}H_{160}N_{20}OP_5Sm_2$
Formula weight	1861.82
Temperature/K	100(2)
Crystal system	triclinic
Space group	P-1
a/Å	13.5758(4)
b/Å	14.8992(5)
c/Å	25.9079(8)
α/°	82.223(2)

β/°	88.2160(10)
γ/°	63.3200(10)
Volume/Å^3	4636.7(3)
Z	2
ρ_{calc}g/cm^3	1.334
μ/mm^{-1}	10.627
F(000)	1962.0
Crystal size/mm^3	0.333 × 0.243 × 0.132
Radiation	CuKα (λ = 1.54178)
2Θ range for data collection/°	6.702 to 149.106
Index ranges	-16 ≤ h ≤ 16, -18 ≤ k ≤ 18, -32 ≤ l ≤ 32
Reflections collected	68983
Independent reflections	18803 [R_{int} = 0.0670, R_{sigma} = 0.0568]
Data/restraints/parameters	18803/569/1055
Goodness-of-fit on F^2	1.077
Final R indexes [I>=2σ (I)]	R_1 = 0.0606, wR_2 = 0.1586
Final R indexes [all data]	R_1 = 0.0727, wR_2 = 0.1683
Largest diff. peak/hole / e Å^{-3}	2.36/-1.56

Table 5.50 Fractional Atomic Coordinates (×10^4) and Equivalent Isotropic Displacement Parameters (Å^2×10^3) for 4-Sm^{5+}(Et$_2$O). U_{eq} is defined as 1/3 of the trace of the orthogonalised U_{IJ} tensor.

Atom	*x*	*y*	*z*	U(eq)
Sm1A	4822.1(17)	7347.9(16)	3086.0(7)	30.2(3)
Sm1B	5001(3)	7155(2)	3169.8(10)	37.1(4)
Sm2	7011.6(2)	6647.9(2)	2120.3(2)	23.81(9)
P1	4095.3(11)	8437.6(10)	1880.2(5)	30.3(3)
P2	7810.1(11)	4064.1(10)	1777.2(5)	29.6(3)
P3	8266.5(14)	7754.8(12)	1161.3(5)	38.6(3)
P4	7825.0(12)	6624.2(11)	3376.5(5)	30.9(3)
O1	4623(5)	5652(5)	3250(3)	85.2(15)
N1	6973(4)	6532(4)	3038.2(16)	33.7(9)
N2	5114(4)	7501(3)	2129.5(17)	33.6(9)
N3	4021(4)	9596(3)	1884.3(16)	32.2(10)
N4	2963(4)	8562(3)	2224.1(18)	33.9(10)
N5	3857(4)	8439(4)	1254.9(19)	36.6(10)
N6	7504(4)	5130(3)	1896.5(18)	36.2(10)
N7	6985(4)	3853(3)	1388.4(17)	33.0(9)
N8	7886(4)	3252(3)	2319.9(18)	35.1(10)
N9	8994(4)	3552(4)	1461(2)	38.1(10)
N10	7890(4)	7484(4)	1696.0(18)	37.8(11)

Atom	*x*	*y*	*z*	U(eq)
N11	7713(5)	7640(4)	610.4(17)	40.3(11)
N12	8009(6)	8979(4)	1046(2)	53.5(15)
N13	9596(5)	7030(5)	1058(2)	50.0(13)
N14	7651(4)	7788(4)	3453.3(16)	34.5(10)
N15	7866(4)	6121(4)	4006.7(16)	35.5(10)
N16	9100(4)	6117(4)	3154.1(19)	39.6(11)
N17	3825(5)	8227(5)	3755(2)	54.0(13)
C1	5006(10)	4951(9)	2874(5)	103(2)
C2	4129(10)	4743(11)	2675(5)	116(4)
C3	4145(10)	5426(10)	3746(4)	107(3)
C4	4661(10)	5511(9)	4179(4)	102(3)
C5	4773(5)	9829(4)	1524(2)	37.0(12)
C6	4540(6)	10925(5)	1495(2)	42.0(13)
C7	4638(7)	11192(5)	2028(3)	52.2(17)
C8	3895(7)	10919(5)	2402(2)	50.3(16)
C9	4161(6)	9801(5)	2412(2)	40.6(13)
C10	2742(5)	7677(5)	2237(3)	45.5(14)
C11	2006(6)	7635(5)	2676(3)	53.6(17)
C12	934(6)	8602(6)	2635(3)	65(2)
C13	1206(6)	9488(6)	2622(3)	62(2)
C14	1932(5)	9518(5)	2167(3)	50.4(16)
C15	3005(5)	9280(5)	926(2)	41.0(13)
C16	2150(5)	8995(5)	731(2)	46.8(15)
C17	2697(6)	8066(5)	453(3)	48.3(15)
C18	3598(6)	7203(5)	799(3)	48.2(15)
C19	4406(5)	7534(5)	995(2)	44.3(14)
C20	6777(5)	4445(5)	862(2)	40.0(12)
C21	6376(6)	3971(6)	487(3)	56.1(16)
C22	5344(7)	3900(7)	686(3)	67(2)
C23	5527(6)	3373(6)	1243(3)	61.5(18)
C24	5958(5)	3872(5)	1590(3)	44.6(13)
C25	8381(6)	2174(5)	2271(3)	46.3(14)
C26	8167(7)	1570(6)	2749(3)	57.2(16)
C27	8604(7)	1732(6)	3245(3)	57.6(16)
C28	8102(7)	2876(6)	3281(3)	61.1(18)
C29	8299(6)	3435(5)	2793(2)	49.4(15)
C30	9280(5)	2806(5)	1095(3)	48.7(15)
C31	10423(5)	1940(5)	1220(3)	47.1(14)
C32	11281(6)	2308(5)	1258(3)	57.9(18)
C33	10925(6)	3114(6)	1628(4)	73(2)
C34	9811(6)	3934(5)	1473(3)	58.1(18)

Atom	*x*	*y*	*z*	U(eq)
C35	6589(6)	8423(5)	442(2)	45.9(15)
C36	6352(7)	8379(6)	-124(2)	54.8(18)
C37	6502(7)	7330(6)	-192(3)	61(2)
C38	7609(7)	6505(5)	32(2)	56(2)
C39	7807(6)	6624(5)	588(2)	46.8(16)
C40	7597(6)	9647(5)	1434(3)	52.4(17)
C41	8398(10)	10000(8)	1572(3)	83(3)
C42	8762(8)	10484(7)	1095(3)	69(2)
C43	9154(7)	9778(6)	685(3)	57.1(18)
C44	8307(8)	9435(6)	568(3)	62(2)
C45	10383(6)	6816(6)	1477(3)	57.9(18)
C46	11300(7)	5763(6)	1497(3)	66(2)
C47	11872(7)	5600(6)	957(3)	67(2)
C48	10994(7)	5924(6)	523(3)	70(2)
C49	10101(7)	6981(6)	539(3)	63(2)
C50	6713(5)	8377(5)	3768(2)	42.6(14)
C51	6747(6)	9329(5)	3872(3)	52.5(17)
C52	6746(8)	9980(5)	3375(3)	64(2)
C53	7677(8)	9360(6)	3040(3)	61(2)
C54	7620(6)	8407(5)	2950(2)	44.2(14)
C55	7810(6)	5150(5)	4089(2)	45.0(14)
C56	7445(6)	4988(6)	4637(2)	51.5(16)
C57	8221(7)	5010(6)	5042(3)	62(2)
C58	8351(6)	5980(6)	4927(2)	54.0(17)
C59	8684(6)	6123(6)	4370(2)	46.9(15)
C60	9434(5)	5399(5)	2768(2)	44.3(14)
C61	10487(6)	4451(6)	2930(3)	60.4(19)
C62	11411(6)	4727(6)	3041(3)	62(2)
C63	11061(6)	5479(7)	3423(3)	64(2)
C64	9984(6)	6403(6)	3248(3)	56.3(18)
P5	3116.6(19)	8763.9(14)	4186.9(8)	59.5(5)
N18_1	3722(8)	8434(10)	4750(3)	64.2(14)
C65_1	4885(9)	7857(9)	4863(4)	68(2)
C66_1	5117(10)	7082(8)	5343(4)	87(2)
C67_1	4518(10)	7555(10)	5806(3)	87(2)
C68_1	3303(9)	8256(10)	5678(4)	81(5)
C69_1	3157(9)	8996(8)	5183(4)	70(2)
N18_2	1887(6)	8678(8)	4205(5)	78.2(14)
C65_2	2065(7)	7643(8)	4289(6)	84(2)
C66_2	1078(8)	7549(8)	4098(6)	85(3)
C67_2	29(8)	8236(8)	4334(6)	86(3)

Atom	*x*	*y*	*z*	U(eq)
C68_2	-114(6)	9317(7)	4291(6)	80.7(15)
C69_2	929(8)	9328(8)	4488(5)	79.3(14)
N18_3	1968(8)	8580(10)	4399(5)	78.2(14)
C65_3	2042(8)	7698(10)	4732(6)	79(3)
C66_3	977(10)	7915(12)	5010(5)	80(3)
C67_3	2(9)	8335(11)	4637(6)	75(3)
C68_3	-27(8)	9205(11)	4244(7)	80.7(15)
C69_3	1089(10)	8919(12)	3994(5)	79.3(14)
N18_4	2640(10)	10058(5)	4070(4)	77.1(16)
C65_4	1912(9)	10672(7)	3634(5)	83(4)
C66_4	1283(8)	11765(7)	3729(5)	83(2)
C67_4	2035(10)	12197(6)	3863(5)	78.0(19)
C68_4	2893(10)	11500(7)	4285(5)	86(2)
C69_4	3465(8)	10416(7)	4155(5)	83(4)
N18_5	2621(13)	10046(5)	4158(5)	77.1(16)
C65_5	2644(14)	10581(9)	3657(5)	82(2)
C66_5	2823(13)	11496(9)	3708(6)	83(2)
C67_5	2010(14)	12182(7)	4056(6)	78.0(19)
C68_5	1896(15)	11604(9)	4567(5)	86(2)
C69_5	1718(13)	10699(9)	4468(6)	87(3)
N18_6	3713(10)	8390(13)	4806(4)	64.2(14)
C65_6	4783(11)	8362(13)	4805(4)	68(2)
C66_6	5537(9)	7568(14)	5229(5)	87(2)
C67_6	5043(11)	7705(15)	5756(4)	87(2)
C68_6	3862(12)	7843(14)	5751(5)	79(3)
C69_6	3176(9)	8648(14)	5304(5)	70(2)

Table 5.51 Anisotropic Displacement Parameters ($Å^2×10^3$) for 4-Sm^{5+}(Et_2O). The Anisotropic displacement factor exponent takes the form: $-2\pi^2[h^2a^{*2}U_{11}+2hka^*b^*U_{12}+\ldots]$.

Atom	U_{11}	U_{22}	U_{33}	U_{23}	U_{13}	U_{12}
Sm1A	31.4(5)	44.1(7)	14.4(4)	-0.7(4)	-2.5(3)	-17.1(4)
Sm1B	40.8(8)	50.7(9)	23.9(7)	-11.6(7)	7.0(6)	-22.8(6)
Sm2	29.52(15)	25.84(15)	18.12(13)	-9.93(10)	1.68(10)	-12.40(11)
P1	31.0(7)	27.7(7)	30.8(6)	-8.0(5)	-2.5(5)	-10.6(5)
P2	32.8(7)	27.2(6)	30.0(6)	-13.7(5)	1.6(5)	-11.8(5)
P3	55.9(9)	47.1(9)	27.1(6)	-16.1(6)	14.6(6)	-33.5(7)
P4	40.7(7)	36.4(7)	21.1(5)	-7.9(5)	-3.0(5)	-20.7(6)
O1	87(4)	85(3)	94(3)	10(2)	-5(3)	-53(3)
N1	46.3(16)	44(2)	18.9(13)	-7.3(13)	-0.7(9)	-27.0(14)

Atom	U_{11}	U_{22}	U_{33}	U_{23}	U_{13}	U_{12}
N2	36(2)	32(2)	31.2(16)	-7.3(15)	-2.7(11)	-12.7(19)
N3	43(3)	35(2)	24(2)	-10.2(18)	3.6(19)	-21(2)
N4	29(2)	33(2)	36(2)	-9.1(19)	4.1(19)	-9.2(19)
N5	39(3)	31(2)	39(3)	-14(2)	-5(2)	-12(2)
N6	46(3)	32(2)	33(2)	-12.4(18)	0(2)	-17(2)
N7	36(2)	34(2)	32(2)	-13.2(17)	0.4(17)	-16.8(19)
N8	44(3)	29(2)	33(2)	-7.8(17)	-0.5(18)	-16(2)
N9	36(2)	37(2)	45(3)	-20(2)	8(2)	-16.5(19)
N10	46(3)	42(3)	34(2)	-16(2)	6(2)	-24(2)
N11	66(3)	43(3)	25(2)	-13(2)	15(2)	-35(3)
N12	93(4)	58(3)	36(3)	-20(2)	22(3)	-55(3)
N13	51(3)	68(4)	38(3)	-24(3)	18(2)	-30(3)
N14	48(3)	39(3)	24(2)	-10.5(19)	2.5(19)	-25(2)
N15	47(3)	42(3)	22(2)	-5.2(19)	-8.8(19)	-24(2)
N16	36(3)	51(3)	37(2)	-21(2)	5(2)	-21(2)
N17	66(3)	63(3)	40(2)	-20(2)	19(2)	-33(2)
C1	113(5)	102(4)	110(4)	-6(4)	6(3)	-64(3)
C2	108(6)	147(8)	123(7)	-55(7)	35(5)	-75(5)
C3	113(5)	134(6)	94(3)	8(3)	-1(3)	-80(5)
C4	110(7)	116(8)	95(3)	11(4)	-4(3)	-70(7)
C5	44(3)	38(3)	33(3)	-10(2)	2(2)	-21(3)
C6	55(4)	43(3)	33(3)	-4(2)	1(3)	-26(3)
C7	80(5)	48(4)	45(3)	-11(3)	-2(3)	-41(4)
C8	81(5)	46(4)	35(3)	-21(3)	7(3)	-34(4)
C9	60(4)	42(3)	27(3)	-9(2)	2(3)	-29(3)
C10	41(3)	47(4)	49(4)	-5(3)	2(3)	-22(3)
C11	50(4)	52(4)	58(4)	-4(3)	10(3)	-23(3)
C12	46(4)	71(5)	70(5)	5(4)	14(4)	-24(4)
C13	39(4)	59(5)	59(4)	-3(4)	11(3)	1(3)
C14	38(3)	39(3)	57(4)	-1(3)	4(3)	-4(3)
C15	50(4)	40(3)	31(3)	-8(2)	-7(3)	-17(3)
C16	47(4)	54(4)	37(3)	-2(3)	-8(3)	-21(3)
C17	59(4)	50(4)	43(3)	-12(3)	-12(3)	-28(3)
C18	60(4)	40(3)	47(3)	-12(3)	-7(3)	-23(3)
C19	48(4)	44(4)	40(3)	-19(3)	-1(3)	-17(3)
C20	50(3)	43(3)	31(2)	-10(2)	-1(2)	-23(3)
C21	71(4)	62(4)	44(3)	-15(3)	-12(3)	-34(4)
C22	74(5)	79(5)	67(4)	-7(4)	-23(3)	-50(4)
C23	54(4)	72(5)	72(4)	-3(3)	-14(3)	-41(4)
C24	36(3)	52(4)	47(3)	-4(3)	0(2)	-21(3)
C25	59(4)	33(3)	48(3)	-13(2)	4(3)	-20(3)

Atom	U_{11}	U_{22}	U_{33}	U_{23}	U_{13}	U_{12}
C26	63(4)	49(4)	66(4)	-2(3)	3(3)	-32(3)
C27	63(4)	53(3)	49(3)	7(3)	1(3)	-23(3)
C28	75(5)	56(3)	37(3)	-1(3)	-1(3)	-17(3)
C29	69(4)	45(3)	34(3)	-9(2)	-5(3)	-24(3)
C30	47(3)	52(3)	46(3)	-26(3)	6(3)	-16(3)
C31	46(3)	40(3)	53(4)	-18(3)	17(3)	-16(2)
C32	42(3)	44(3)	85(5)	-17(3)	18(3)	-15(3)
C33	41(3)	55(4)	134(7)	-43(4)	13(4)	-22(3)
C34	48(3)	44(3)	92(5)	-29(3)	21(3)	-25(3)
C35	66(4)	43(4)	35(3)	-18(3)	9(3)	-28(3)
C36	85(5)	57(4)	31(3)	-15(3)	1(3)	-37(4)
C37	98(6)	71(5)	35(3)	-22(3)	8(4)	-53(5)
C38	112(6)	46(4)	28(3)	-16(3)	13(3)	-49(4)
C39	86(5)	42(3)	25(3)	-15(2)	11(3)	-38(3)
C40	66(4)	45(4)	55(4)	-18(3)	18(3)	-31(3)
C41	153(9)	98(7)	52(4)	-33(4)	25(5)	-100(7)
C42	105(6)	90(6)	55(4)	-19(4)	9(4)	-80(6)
C43	66(5)	72(5)	48(4)	1(3)	7(3)	-47(4)
C44	101(6)	70(5)	40(3)	-14(3)	11(4)	-58(5)
C45	60(4)	68(5)	58(4)	-28(4)	21(4)	-35(4)
C46	71(5)	69(5)	63(5)	-15(4)	6(4)	-36(4)
C47	60(5)	59(5)	84(6)	-26(4)	36(4)	-25(4)
C48	84(6)	64(5)	54(4)	-20(4)	31(4)	-26(4)
C49	77(5)	66(5)	54(4)	-19(4)	28(4)	-37(4)
C50	47(3)	46(4)	42(3)	-20(3)	7(3)	-23(3)
C51	62(4)	48(4)	57(4)	-28(3)	13(3)	-28(3)
C52	98(6)	39(4)	64(5)	-16(3)	12(4)	-38(4)
C53	105(6)	59(4)	44(4)	-16(3)	13(4)	-58(5)
C54	70(4)	45(4)	30(3)	-10(3)	-2(3)	-35(3)
C55	61(4)	44(3)	35(3)	-2(3)	-7(3)	-29(3)
C56	64(4)	64(4)	37(3)	5(3)	-8(3)	-40(4)
C57	80(5)	83(5)	30(3)	10(3)	-11(3)	-47(5)
C58	67(5)	77(5)	27(3)	-5(3)	-12(3)	-40(4)
C59	58(4)	64(4)	28(3)	-3(3)	-11(3)	-36(3)
C60	46(4)	44(3)	38(3)	-14(3)	-2(3)	-13(3)
C61	46(4)	53(4)	71(5)	-14(4)	-12(4)	-10(3)
C62	38(4)	77(5)	64(5)	-9(4)	-3(3)	-20(4)
C63	44(4)	112(7)	50(4)	-14(4)	-2(3)	-46(4)
C64	55(4)	76(5)	60(4)	-28(4)	12(3)	-45(4)
P5	82.9(14)	44.7(10)	52.6(10)	-24.3(8)	12.9(9)	-26.0(9)
N18_1	82(3)	66(4)	45(2)	-24(2)	11(2)	-30(3)

Atom	U_{11}	U_{22}	U_{33}	U_{23}	U_{13}	U_{12}
C65_1	82(3)	74(6)	49(3)	-20(3)	9(2)	-32(3)
C66_1	81(3)	108(6)	55(3)	-3(3)	10(2)	-31(3)
C67_1	81(3)	108(6)	55(3)	-3(3)	10(2)	-31(3)
C68_1	81(5)	81(5)	80(5)	-12(2)	3(2)	-36(3)
C69_1	83(3)	76(6)	44(3)	-23(3)	11(2)	-25(3)
N18_2	80.9(19)	76.1(19)	81(2)	-14.4(16)	1.7(15)	-36.7(14)
C65_2	79(3)	76(2)	99(8)	-16(2)	2(3)	-36.3(18)
C66_2	80(3)	78(3)	101(7)	-17(4)	2(3)	-37(2)
C67_2	79(3)	81(3)	102(9)	-18(3)	1(3)	-37(2)
C68_2	81.2(19)	81(2)	84(3)	-17(2)	2.0(16)	-37.6(17)
C69_2	81(2)	79(2)	81(2)	-16.3(18)	1.7(16)	-37.2(16)
N18_3	80.9(19)	76.1(19)	81(2)	-14.4(16)	1.7(15)	-36.7(14)
C65_3	83(3)	74(3)	81(5)	-16(3)	8(3)	-34(2)
C66_3	83(3)	77(6)	82(5)	-18(4)	8(2)	-35(3)
C67_3	81(3)	69(4)	76(4)	-28(4)	12(3)	-29(3)
C68_3	81.2(19)	81(2)	84(3)	-17(2)	2.0(16)	-37.6(17)
C69_3	81(2)	79(2)	81(2)	-16.3(18)	1.7(16)	-37.2(16)
N18_4	85(2)	73(2)	73(2)	-13.2(15)	9.0(17)	-34.2(16)
C65_4	68(7)	94(9)	76(7)	-40(7)	0(6)	-18(6)
C66_4	92(5)	75(2)	81(3)	-10(2)	11(4)	-36(2)
C67_4	79(2)	77(2)	78(2)	-11.3(10)	3.3(10)	-34.7(12)
C68_4	103(6)	73(3)	80(2)	-15.1(17)	14(2)	-36(3)
C69_4	68(7)	94(9)	76(7)	-40(7)	0(6)	-18(6)
N18_5	85(2)	73(2)	73(2)	-13.2(15)	9.0(17)	-34.2(16)
C65_5	92(6)	75(3)	77(2)	-10.6(17)	11(2)	-36(3)
C66_5	92(5)	75(2)	81(3)	-10(2)	11(4)	-36(2)
C67_5	79(2)	77(2)	78(2)	-11.3(10)	3.3(10)	-34.7(12)
C68_5	103(6)	73(3)	80(2)	-15.1(17)	14(2)	-36(3)
C69_5	101(5)	75(2)	86(4)	-19(2)	22(4)	-38(2)
N18_6	82(3)	66(4)	45(2)	-24(2)	11(2)	-30(3)
C65_6	82(3)	74(6)	49(3)	-20(3)	9(2)	-32(3)
C66_6	81(3)	108(6)	55(3)	-3(3)	10(2)	-31(3)
C67_6	81(3)	108(6)	55(3)	-3(3)	10(2)	-31(3)
C68_6	80(3)	95(7)	49(3)	-12(4)	11(3)	-28(3)
C69_6	83(3)	76(6)	44(3)	-23(3)	11(2)	-25(3)

Table 5.52 Bond Lengths for 4-Sm^{5+}(Et_2O).

Atom	Atom	Length/Å	Atom	Atom	Length/Å
Sm1A	Sm2	3.6935(19)	C23	C24	1.519(9)
Sm1A	P1	3.279(2)	C25	C26	1.528(9)

Atom	Atom	Length/Å	Atom	Atom	Length/Å
Sm1A	O1	2.637(7)	C26	C27	1.521(11)
Sm1A	N1	2.617(5)	C27	C28	1.540(10)
Sm1A	N2	2.493(5)	C28	C29	1.504(9)
Sm1A	N17	2.329(6)	C30	C31	1.515(9)
Sm1B	Sm2	3.695(3)	C31	C32	1.506(9)
Sm1B	O1	2.494(7)	C32	C33	1.534(11)
Sm1B	N1	2.438(6)	C33	C34	1.479(10)
Sm1B	N2	2.687(5)	C35	C36	1.527(8)
Sm1B	N17	2.369(6)	C36	C37	1.517(10)
Sm2	N1	2.361(4)	C37	C38	1.519(11)
Sm2	N2	2.306(5)	C38	C39	1.522(8)
Sm2	N6	2.207(4)	C40	C41	1.475(10)
Sm2	N10	2.251(5)	C41	C42	1.527(10)
P1	N2	1.535(5)	C42	C43	1.510(11)
P1	N3	1.685(5)	C43	C44	1.506(10)
P1	N4	1.701(5)	C45	C46	1.497(11)
P1	N5	1.661(5)	C46	C47	1.573(11)
P2	N6	1.524(5)	C47	C48	1.528(12)
P2	N7	1.686(4)	C48	C49	1.500(11)
P2	N8	1.699(5)	C50	C51	1.500(8)
P2	N9	1.680(5)	C51	C52	1.503(10)
P3	N10	1.527(5)	C52	C53	1.519(11)
P3	N11	1.696(5)	C53	C54	1.505(8)
P3	N12	1.680(6)	C55	C56	1.515(9)
P3	N13	1.671(6)	C56	C57	1.523(9)
P4	N1	1.537(4)	C57	C58	1.523(10)
P4	N14	1.681(5)	C58	C59	1.513(9)
P4	N15	1.694(5)	C60	C61	1.510(9)
P4	N16	1.668(5)	C61	C62	1.531(10)
O1	C1	1.437(13)	C62	C63	1.501(11)
O1	C3	1.487(12)	C63	C64	1.518(11)
N3	C5	1.485(7)	P5	N18_1	1.602(8)
N3	C9	1.477(6)	P5	N18_2	1.730(7)
N4	C10	1.473(8)	P5	N18_3	1.760(7)
N4	C14	1.475(7)	P5	N18_4	1.721(6)
N5	C15	1.452(7)	P5	N18_5	1.708(7)
N5	C19	1.462(7)	P5	N18_6	1.723(9)
N7	C20	1.481(7)	N18_1	C65_1	1.436(8)
N7	C24	1.462(7)	N18_1	C69_1	1.473(8)
N8	C25	1.459(7)	C65_1	C66_1	1.513(5)
N8	C29	1.469(7)	C66_1	C67_1	1.500(5)

Atom	Atom	Length/Å	Atom	Atom	Length/Å
N9	C30	1.468(7)	C67_1	C68_1	1.522(5)
N9	C34	1.459(8)	C68_1	C69_1	1.527(5)
N11	C35	1.479(9)	N18_2	C65_2	1.435(8)
N11	C39	1.471(7)	N18_2	C69_2	1.472(8)
N12	C40	1.432(8)	C65_2	C66_2	1.513(5)
N12	C44	1.466(8)	C66_2	C67_2	1.501(5)
N13	C45	1.447(9)	C67_2	C68_2	1.522(4)
N13	C49	1.487(8)	C68_2	C69_2	1.527(5)
N14	C50	1.476(7)	N18_3	C65_3	1.437(8)
N14	C54	1.481(7)	N18_3	C69_3	1.474(8)
N15	C55	1.468(8)	C65_3	C66_3	1.513(5)
N15	C59	1.481(7)	C66_3	C67_3	1.500(5)
N16	C60	1.475(7)	C67_3	C68_3	1.522(5)
N16	C64	1.477(8)	C68_3	C69_3	1.526(5)
N17	P5	1.517(6)	N18_4	C65_4	1.437(8)
C1	C2	1.480(15)	N18_4	C69_4	1.474(8)
C3	C4	1.390(15)	C65_4	C66_4	1.513(5)
C5	C6	1.508(8)	C66_4	C67_4	1.500(5)
C6	C7	1.514(8)	C67_4	C68_4	1.522(5)
C7	C8	1.524(10)	C68_4	C69_4	1.527(5)
C8	C9	1.534(8)	N18_5	C65_5	1.435(8)
C10	C11	1.506(9)	N18_5	C69_5	1.474(8)
C11	C12	1.513(10)	C65_5	C66_5	1.511(5)
C12	C13	1.520(12)	C66_5	C67_5	1.500(5)
C13	C14	1.522(10)	C67_5	C68_5	1.522(5)
C15	C16	1.524(8)	C68_5	C69_5	1.527(5)
C16	C17	1.515(9)	N18_6	C65_6	1.436(8)
C17	C18	1.515(9)	N18_6	C69_6	1.474(8)
C18	C19	1.514(9)	C65_6	C66_6	1.513(5)
C20	C21	1.518(8)	C66_6	C67_6	1.500(5)
C21	C22	1.522(11)	C67_6	C68_6	1.522(5)
C22	C23	1.516(11)	C68_6	C69_6	1.527(5)

Table 5.53 Bond Angles for 4-Sm^{5+}(Et_2O).

Atom	Atom	Atom	Angle/°	Atom	Atom	Atom	Angle/°
P1	Sm1A	Sm2	63.00(4)	N3	C9	C8	110.2(5)
O1	Sm1A	Sm2	99.57(17)	N4	C10	C11	111.3(5)
O1	Sm1A	P1	110.76(17)	C10	C11	C12	110.8(6)
N1	Sm1A	Sm2	39.51(9)	C11	C12	C13	108.2(6)
N1	Sm1A	P1	100.70(11)	C12	C13	C14	111.0(7)

Atom	Atom	Atom	Angle/°	Atom	Atom	Atom	Angle/°
N1	Sm1A	O1	97.70(19)	N4	C14	C13	108.7(5)
N2	Sm1A	Sm2	37.87(11)	N5	C15	C16	111.8(5)
N2	Sm1A	P1	26.66(11)	C17	C16	C15	110.8(5)
N2	Sm1A	O1	101.6(2)	C16	C17	C18	110.6(5)
N2	Sm1A	N1	77.20(15)	C19	C18	C17	110.9(5)
N17	Sm1A	Sm2	154.47(18)	N5	C19	C18	112.3(5)
N17	Sm1A	P1	118.22(17)	N7	C20	C21	110.2(5)
N17	Sm1A	O1	103.0(2)	C20	C21	C22	110.4(6)
N17	Sm1A	N1	124.4(2)	C23	C22	C21	111.1(6)
N17	Sm1A	N2	144.0(2)	C22	C23	C24	110.7(6)
O1	Sm1B	Sm2	102.39(19)	N7	C24	C23	109.9(6)
O1	Sm1B	N2	100.2(2)	N8	C25	C26	111.2(5)
N1	Sm1B	Sm2	38.90(10)	C27	C26	C25	110.8(6)
N1	Sm1B	O1	106.7(2)	C26	C27	C28	109.5(6)
N1	Sm1B	N2	76.82(16)	C29	C28	C27	110.5(6)
N2	Sm1B	Sm2	38.43(10)	N8	C29	C28	112.7(6)
N17	Sm1B	Sm2	151.1(2)	N9	C30	C31	111.3(5)
N17	Sm1B	O1	106.3(3)	C32	C31	C30	112.1(6)
N17	Sm1B	N1	131.3(2)	C31	C32	C33	110.8(6)
N17	Sm1B	N2	130.1(2)	C34	C33	C32	110.3(7)
N2	Sm2	N1	86.21(16)	N9	C34	C33	112.2(6)
N6	Sm2	N1	108.88(17)	N11	C35	C36	110.2(5)
N6	Sm2	N2	109.17(17)	C37	C36	C35	110.6(6)
N6	Sm2	N10	114.08(17)	C36	C37	C38	112.0(6)
N10	Sm2	N1	118.01(16)	C37	C38	C39	111.2(6)
N10	Sm2	N2	117.21(17)	N11	C39	C38	110.4(5)
N2	P1	N3	119.2(2)	N12	C40	C41	111.6(6)
N2	P1	N4	109.6(2)	C40	C41	C42	112.3(7)
N2	P1	N5	114.6(2)	C43	C42	C41	110.1(6)
N3	P1	N4	100.2(2)	C44	C43	C42	111.0(6)
N5	P1	N3	102.5(2)	N12	C44	C43	110.7(6)
N5	P1	N4	109.6(2)	N13	C45	C46	110.7(6)
N6	P2	N7	120.7(3)	C45	C46	C47	110.8(7)
N6	P2	N8	112.6(2)	C48	C47	C46	109.4(6)
N6	P2	N9	113.7(3)	C49	C48	C47	112.0(7)
N7	P2	N8	100.1(2)	N13	C49	C48	108.6(6)
N9	P2	N7	99.3(2)	N14	C50	C51	111.0(5)
N9	P2	N8	108.7(3)	C50	C51	C52	111.7(6)
N10	P3	N11	120.5(2)	C51	C52	C53	109.7(6)
N10	P3	N12	112.4(3)	C54	C53	C52	111.3(6)
N10	P3	N13	114.1(3)	N14	C54	C53	110.6(5)

Atom	Atom	Atom	Angle/°	Atom	Atom	Atom	Angle/°
N12	P3	N11	100.8(3)	N15	C55	C56	109.1(5)
N13	P3	N11	98.6(3)	C55	C56	C57	111.4(6)
N13	P3	N12	108.9(3)	C58	C57	C56	110.3(6)
N1	P4	N14	118.5(3)	C59	C58	C57	111.0(6)
N1	P4	N15	112.8(2)	N15	C59	C58	109.8(5)
N1	P4	N16	113.8(2)	N16	C60	C61	112.6(5)
N14	P4	N15	100.4(2)	C60	C61	C62	110.2(6)
N16	P4	N14	101.2(2)	C63	C62	C61	111.0(6)
N16	P4	N15	108.6(3)	C62	C63	C64	111.5(6)
C1	O1	Sm1A	120.3(6)	N16	C64	C63	111.6(6)
C1	O1	Sm1B	121.5(6)	N17	P5	N18_1	115.0(5)
C1	O1	C3	121.2(8)	N17	P5	N18_2	111.0(5)
C3	O1	Sm1A	118.5(7)	N17	P5	N18_3	121.7(6)
C3	O1	Sm1B	116.6(7)	N17	P5	N18_4	112.6(5)
Sm2	N1	Sm1A	95.64(16)	N17	P5	N18_5	119.7(5)
Sm2	N1	Sm1B	100.70(17)	N17	P5	N18_6	116.6(5)
P4	N1	Sm1A	129.9(3)	N18_1	P5	N18_2	111.6(6)
P4	N1	Sm1B	127.8(3)	N18_1	P5	N18_4	104.8(6)
P4	N1	Sm2	123.7(2)	N18_4	P5	N18_2	100.8(5)
Sm2	N2	Sm1A	100.55(17)	N18_5	P5	N18_3	102.1(7)
Sm2	N2	Sm1B	95.16(16)	N18_5	P5	N18_6	99.4(8)
P1	N2	Sm1A	106.5(2)	N18_6	P5	N18_3	91.9(6)
P1	N2	Sm1B	112.6(2)	C65_1	N18_1	P5	126.6(7)
P1	N2	Sm2	143.9(3)	C65_1	N18_1	C69_1	111.1(5)
C5	N3	P1	114.7(4)	C69_1	N18_1	P5	119.4(7)
C9	N3	P1	112.9(4)	N18_1	C65_1	C66_1	111.2(6)
C9	N3	C5	109.8(4)	C67_1	C66_1	C65_1	112.2(6)
C10	N4	P1	112.6(4)	C66_1	C67_1	C68_1	112.2(6)
C10	N4	C14	111.4(5)	C67_1	C68_1	C69_1	111.0(6)
C14	N4	P1	121.7(4)	N18_1	C69_1	C68_1	110.0(6)
C15	N5	P1	124.5(4)	C65_2	N18_2	P5	111.8(7)
C15	N5	C19	112.5(5)	C65_2	N18_2	C69_2	111.4(5)
C19	N5	P1	122.6(4)	C69_2	N18_2	P5	122.9(7)
P2	N6	Sm2	176.0(3)	N18_2	C65_2	C66_2	111.1(6)
C20	N7	P2	113.7(4)	C67_2	C66_2	C65_2	112.1(6)
C24	N7	P2	119.3(4)	C66_2	C67_2	C68_2	112.0(6)
C24	N7	C20	109.9(5)	C67_2	C68_2	C69_2	110.7(6)
C25	N8	P2	117.4(4)	N18_2	C69_2	C68_2	109.9(6)
C25	N8	C29	111.5(5)	C65_3	N18_3	P5	124.1(8)
C29	N8	P2	114.6(4)	C65_3	N18_3	C69_3	110.7(5)
C30	N9	P2	126.8(4)	C69_3	N18_3	P5	113.8(8)

Atom	Atom	Atom	Angle/°	Atom	Atom	Atom	Angle/°
C34	N9	P2	120.9(4)	N18_3	C65_3	C66_3	111.4(6)
C34	N9	C30	111.8(5)	C67_3	C66_3	C65_3	112.1(6)
P3	N10	Sm2	143.8(3)	C66_3	C67_3	C68_3	111.9(6)
C35	N11	P3	117.5(4)	C67_3	C68_3	C69_3	111.0(6)
C39	N11	P3	114.5(4)	N18_3	C69_3	C68_3	110.3(6)
C39	N11	C35	110.1(5)	C65_4	N18_4	P5	122.4(7)
C40	N12	P3	122.7(4)	C65_4	N18_4	C69_4	110.6(5)
C40	N12	C44	113.1(5)	C69_4	N18_4	P5	115.0(8)
C44	N12	P3	123.8(5)	N18_4	C65_4	C66_4	111.3(6)
C45	N13	P3	117.4(4)	C67_4	C66_4	C65_4	112.2(6)
C45	N13	C49	112.2(6)	C66_4	C67_4	C68_4	112.1(6)
C49	N13	P3	124.3(5)	C67_4	C68_4	C69_4	110.9(6)
C50	N14	P4	116.4(4)	N18_4	C69_4	C68_4	110.1(6)
C50	N14	C54	109.9(5)	C65_5	N18_5	P5	115.8(8)
C54	N14	P4	112.4(3)	C65_5	N18_5	C69_5	111.1(5)
C55	N15	P4	115.5(4)	C69_5	N18_5	P5	125.5(9)
C55	N15	C59	111.3(5)	N18_5	C65_5	C66_5	111.5(6)
C59	N15	P4	118.2(4)	C67_5	C66_5	C65_5	112.5(6)
C60	N16	P4	122.1(4)	C66_5	C67_5	C68_5	112.3(6)
C60	N16	C64	110.7(5)	C67_5	C68_5	C69_5	110.8(6)
C64	N16	P4	126.7(4)	N18_5	C69_5	C68_5	109.8(6)
P5	N17	Sm1A	175.6(4)	C65_6	N18_6	P5	110.8(8)
P5	N17	Sm1B	171.1(4)	C65_6	N18_6	C69_6	111.1(5)
O1	C1	C2	113.1(10)	C69_6	N18_6	P5	128.2(8)
C4	C3	O1	112.1(9)	N18_6	C65_6	C66_6	111.2(6)
N3	C5	C6	111.2(5)	C67_6	C66_6	C65_6	112.2(6)
C5	C6	C7	111.3(5)	C66_6	C67_6	C68_6	112.1(6)
C6	C7	C8	109.6(5)	C67_6	C68_6	C69_6	110.9(6)
C7	C8	C9	110.5(5)	N18_6	C69_6	C68_6	110.0(6)

Table 5.54 Torsion Angles for 4-Sm^{5+}(Et_2O).

A	B	C	D	Angle/°	A	B	C	D	Angle/°
Sm1A	O1	C1	C2	-122.1(9)	N17	P5	N18_4	C69_4	-75.9(8)
Sm1A	O1	C3	C4	-51.0(13)	N17	P5	N18_5	C65_5	17.0(13)
Sm1B	O1	C1	C2	-129.9(9)	N17	P5	N18_5	C69_5	163.8(9)
Sm1B	O1	C3	C4	-43.7(13)	N17	P5	N18_6	C65_6	48.9(11)
P1	N3	C5	C6	171.8(4)	N17	P5	N18_6	C69_6	-168.9(10)
P1	N3	C9	C8	-170.6(4)	C1	O1	C3	C4	126.8(12)
P1	N4	C10	C11	160.9(4)	C3	O1	C1	C2	60.1(14)
P1	N4	C14	C13	-164.5(5)	C5	N3	C9	C8	60.0(7)

A	B	C	D	Angle/°	A	B	C	D	Angle/°
P1	N5	C15	C16	-117.0(5)	C5	C6	C7	C8	-54.6(8)
P1	N5	C19	C18	117.4(5)	C6	C7	C8	C9	54.9(8)
P2	N7	C20	C21	160.9(5)	C7	C8	C9	N3	-58.4(7)
P2	N7	C24	C23	-163.6(5)	C9	N3	C5	C6	-59.7(6)
P2	N8	C25	C26	-167.7(5)	C10	N4	C14	C13	58.8(7)
P2	N8	C29	C28	166.3(5)	C10	C11	C12	C13	-56.1(9)
P2	N9	C30	C31	-132.4(5)	C11	C12	C13	C14	58.3(8)
P2	N9	C34	C33	128.5(6)	C12	C13	C14	N4	-59.7(8)
P3	N11	C35	C36	164.2(4)	C14	N4	C10	C11	-58.3(7)
P3	N11	C39	C38	-163.3(5)	C15	N5	C19	C18	-55.7(7)
P3	N12	C40	C41	115.8(7)	C15	C16	C17	C18	53.9(7)
P3	N12	C44	C43	-115.4(7)	C16	C17	C18	C19	-53.5(8)
P3	N13	C45	C46	144.3(5)	C17	C18	C19	N5	54.2(8)
P3	N13	C49	C48	-146.5(6)	C19	N5	C15	C16	56.0(7)
P4	N14	C50	C51	171.7(4)	C20	N7	C24	C23	62.5(6)
P4	N14	C54	C53	-169.4(5)	C20	C21	C22	C23	-52.6(9)
P4	N15	C55	C56	-159.8(4)	C21	C22	C23	C24	53.0(9)
P4	N15	C59	C58	161.2(5)	C22	C23	C24	N7	-57.9(8)
P4	N16	C60	C61	-130.1(6)	C24	N7	C20	C21	-62.4(7)
P4	N16	C64	C63	131.3(6)	C25	N8	C29	C28	-57.3(8)
N1	P4	N14	C50	69.4(5)	C25	C26	C27	C28	54.8(8)
N1	P4	N14	C54	-58.6(5)	C26	C27	C28	C29	-53.9(9)
N1	P4	N15	C55	42.1(5)	C27	C28	C29	N8	55.3(8)
N1	P4	N15	C59	177.6(5)	C29	N8	C25	C26	57.3(7)
N1	P4	N16	C60	-16.9(6)	C30	N9	C34	C33	-59.0(9)
N1	P4	N16	C64	154.4(5)	C30	C31	C32	C33	51.2(9)
N2	P1	N3	C5	72.2(4)	C31	C32	C33	C34	-53.0(10)
N2	P1	N3	C9	-54.7(5)	C32	C33	C34	N9	57.0(9)
N2	P1	N4	C10	-60.1(5)	C34	N9	C30	C31	55.6(8)
N2	P1	N4	C14	163.7(5)	C35	N11	C39	C38	61.7(7)
N2	P1	N5	C15	-174.2(5)	C35	C36	C37	C38	-51.3(8)
N2	P1	N5	C19	13.5(6)	C36	C37	C38	C39	50.8(8)
N3	P1	N2	Sm1A	81.3(3)	C37	C38	C39	N11	-55.7(8)
N3	P1	N2	Sm1B	81.7(3)	C39	N11	C35	C36	-62.3(6)
N3	P1	N2	Sm2	-55.7(5)	C40	N12	C44	C43	57.5(9)
N3	P1	N4	C10	173.8(4)	C40	C41	C42	C43	-52.2(11)
N3	P1	N4	C14	37.5(5)	C41	C42	C43	C44	52.2(10)
N3	P1	N5	C15	-43.6(5)	C42	C43	C44	N12	-54.8(9)
N3	P1	N5	C19	144.1(5)	C44	N12	C40	C41	-57.2(9)
N3	C5	C6	C7	57.4(7)	C45	N13	C49	C48	61.9(8)
N4	P1	N2	Sm1A	-33.1(3)	C45	C46	C47	C48	-51.3(9)

A	B	C	D	Angle/°	A	B	C	D	Angle/°
N4	P1	N2	Sm1B	-32.8(3)	C46	C47	C48	C49	53.1(9)
N4	P1	N2	Sm2	-170.2(4)	C47	C48	C49	N13	-57.6(9)
N4	P1	N3	C5	-168.4(4)	C49	N13	C45	C46	-62.0(8)
N4	P1	N3	C9	64.7(4)	C50	N14	C54	C53	59.3(7)
N4	P1	N5	C15	62.1(5)	C50	C51	C52	C53	-53.8(9)
N4	P1	N5	C19	-110.2(5)	C51	C52	C53	C54	53.9(9)
N4	C10	C11	C12	56.8(8)	C52	C53	C54	N14	-57.3(9)
N5	P1	N2	Sm1A	-156.8(2)	C54	N14	C50	C51	-59.2(6)
N5	P1	N2	Sm1B	-156.4(2)	C55	N15	C59	C58	-61.6(7)
N5	P1	N2	Sm2	66.2(5)	C55	C56	C57	C58	53.6(9)
N5	P1	N3	C5	-55.6(4)	C56	C57	C58	C59	-52.9(9)
N5	P1	N3	C9	177.6(4)	C57	C58	C59	N15	56.5(8)
N5	P1	N4	C10	66.5(4)	C59	N15	C55	C56	61.7(7)
N5	P1	N4	C14	-69.8(5)	C60	N16	C64	C63	-56.6(7)
N5	C15	C16	C17	-55.2(7)	C60	C61	C62	C63	53.0(9)
N6	P2	N7	C20	57.6(5)	C61	C62	C63	C64	-53.5(9)
N6	P2	N7	C24	-74.7(5)	C62	C63	C64	N16	55.5(8)
N6	P2	N8	C25	-168.2(4)	C64	N16	C60	C61	57.4(8)
N6	P2	N8	C29	-34.5(5)	P5	N18_1	C65_1	C66_1	-138.5(12)
N6	P2	N9	C30	-150.7(5)	P5	N18_1	C69_1	C68_1	136.5(11)
N6	P2	N9	C34	20.6(6)	P5	N18_2	C65_2	C66_2	-157.6(9)
N7	P2	N8	C25	62.2(5)	P5	N18_2	C69_2	C68_2	161.7(9)
N7	P2	N8	C29	-164.1(4)	P5	N18_3	C65_3	C66_3	158.1(11)
N7	P2	N9	C30	-21.1(6)	P5	N18_3	C69_3	C68_3	-153.5(11)
N7	P2	N9	C34	150.2(5)	P5	N18_4	C65_4	C66_4	158.1(9)
N7	C20	C21	C22	57.0(8)	P5	N18_4	C69_4	C68_4	-154.2(9)
N8	P2	N7	C20	-178.3(4)	P5	N18_5	C65_5	C66_5	-148.0(12)
N8	P2	N7	C24	49.4(5)	P5	N18_5	C69_5	C68_5	149.9(13)
N8	P2	N9	C30	83.1(6)	P5	N18_6	C65_6	C66_6	-150.1(12)
N8	P2	N9	C34	-105.7(6)	P5	N18_6	C69_6	C68_6	156.3(15)
N8	C25	C26	C27	-57.2(8)	N18_1	P5	N18_2	C65_2	-70.5(10)
N9	P2	N7	C20	-67.3(4)	N18_1	P5	N18_2	C69_2	66.2(10)
N9	P2	N7	C24	160.5(4)	N18_1	P5	N18_4	C65_4	-171.0(9)
N9	P2	N8	C25	-41.3(5)	N18_1	P5	N18_4	C69_4	49.9(9)
N9	P2	N8	C29	92.4(5)	N18_1	C65_1	C66_1	C67_1	-54.5(10)
N9	C30	C31	C32	-52.6(8)	C65_1	N18_1	C69_1	C68_1	-61.5(8)
N10	P3	N11	C35	75.8(5)	C65_1	C66_1	C67_1	C68_1	48.8(11)
N10	P3	N11	C39	-55.8(6)	C66_1	C67_1	C68_1	C69_1	-49.3(11)
N10	P3	N12	C40	6.5(7)	C67_1	C68_1	C69_1	N18_1	54.8(9)
N10	P3	N12	C44	178.7(6)	C69_1	N18_1	C65_1	C66_1	61.0(8)
N10	P3	N13	C45	-44.0(6)	N18_2	P5	N18_1	C65_1	140.9(10)

A	B	C	D	Angle/°	A	B	C	D	Angle/°
N10	P3	N13	C49	165.7(5)	N18_2	P5	N18_1	C69_1	-60.1(10)
N11	P3	N10	Sm2	17.3(7)	N18_2	P5	N18_4	C65_4	-55.0(9)
N11	P3	N12	C40	136.0(6)	N18_2	P5	N18_4	C69_4	165.9(8)
N11	P3	N12	C44	-51.8(7)	N18_2	C65_2	C66_2	C67_2	-54.3(10)
N11	P3	N13	C45	-173.0(5)	C65_2	N18_2	C69_2	C68_2	-61.5(8)
N11	P3	N13	C49	36.8(6)	C65_2	C66_2	C67_2	C68_2	49.2(11)
N11	C35	C36	C37	56.7(8)	C66_2	C67_2	C68_2	C69_2	-50.0(11)
N12	P3	N10	Sm2	135.8(5)	C67_2	C68_2	C69_2	N18_2	55.3(10)
N12	P3	N11	C35	-48.4(5)	C69_2	N18_2	C65_2	C66_2	60.6(9)
N12	P3	N11	C39	180.0(5)	N18_3	P5	N18_5	C65_5	-120.8(10)
N12	P3	N13	C45	82.4(6)	N18_3	P5	N18_5	C69_5	26.0(13)
N12	P3	N13	C49	-67.9(6)	N18_3	P5	N18_6	C65_6	176.1(11)
N12	C40	C41	C42	54.3(11)	N18_3	P5	N18_6	C69_6	-41.7(12)
N13	P3	N10	Sm2	-99.6(5)	N18_3	C65_3	C66_3	C67_3	54.9(10)
N13	P3	N11	C35	-159.7(4)	C65_3	N18_3	C69_3	C68_3	61.2(9)
N13	P3	N11	C39	68.7(5)	C65_3	C66_3	C67_3	C68_3	-49.0(11)
N13	P3	N12	C40	-120.9(6)	C66_3	C67_3	C68_3	C69_3	49.3(11)
N13	P3	N12	C44	51.3(7)	C67_3	C68_3	C69_3	N18_3	-54.9(10)
N13	C45	C46	C47	55.8(8)	C69_3	N18_3	C65_3	C66_3	-60.9(9)
N14	P4	N1	Sm1A	-52.4(4)	N18_4	P5	N18_1	C65_1	-110.9(10)
N14	P4	N1	Sm1B	-60.2(4)	N18_4	P5	N18_1	C69_1	48.2(10)
N14	P4	N1	Sm2	83.0(4)	N18_4	P5	N18_2	C65_2	178.7(8)
N14	P4	N15	C55	169.3(4)	N18_4	P5	N18_2	C69_2	-44.6(9)
N14	P4	N15	C59	-55.3(5)	N18_4	C65_4	C66_4	C67_4	54.5(10)
N14	P4	N16	C60	-145.2(5)	C65_4	N18_4	C69_4	C68_4	61.9(8)
N14	P4	N16	C64	26.1(6)	C65_4	C66_4	C67_4	C68_4	-48.5(11)
N14	C50	C51	C52	57.3(8)	C66_4	C67_4	C68_4	C69_4	49.3(11)
N15	P4	N1	Sm1A	64.5(4)	C67_4	C68_4	C69_4	N18_4	-55.3(9)
N15	P4	N1	Sm1B	56.7(4)	C69_4	N18_4	C65_4	C66_4	-61.2(9)
N15	P4	N1	Sm2	-160.1(3)	N18_5	P5	N18_3	C65_3	-146.3(10)
N15	P4	N14	C50	-53.8(4)	N18_5	P5	N18_3	C69_3	73.7(10)
N15	P4	N14	C54	178.2(4)	N18_5	P5	N18_6	C65_6	-81.3(11)
N15	P4	N16	C60	109.6(5)	N18_5	P5	N18_6	C69_6	60.9(13)
N15	P4	N16	C64	-79.1(6)	N18_5	C65_5	C66_5	C67_5	-53.3(11)
N15	C55	C56	C57	-57.6(8)	C65_5	N18_5	C69_5	C68_5	-62.0(9)
N16	P4	N1	Sm1A	-171.2(3)	C65_5	C66_5	C67_5	C68_5	47.8(11)
N16	P4	N1	Sm1B	-179.0(3)	C66_5	C67_5	C68_5	C69_5	-49.3(11)
N16	P4	N1	Sm2	-35.8(4)	C67_5	C68_5	C69_5	N18_5	55.6(10)
N16	P4	N14	C50	-165.4(4)	C69_5	N18_5	C65_5	C66_5	60.6(9)
N16	P4	N14	C54	66.7(5)	N18_6	P5	N18_3	C65_3	-46.2(12)
N16	P4	N15	C55	-85.0(5)	N18_6	P5	N18_3	C69_3	173.8(10)

A	B	C	D	Angle/°	A	B	C	D	Angle/°
N16	P4	N15	C59	50.5(5)	N18_6	P5	N18_5	C65_5	145.1(10)
N16	C60	C61	C62	-55.4(8)	N18_6	P5	N18_5	C69_5	-68.0(12)
N17	P5	N18_1	C65_1	13.3(13)	N18_6	C65_6	C66_6	C67_6	-54.4(10)
N17	P5	N18_1	C69_1	172.4(7)	C65_6	N18_6	C69_6	C68_6	-61.6(8)
N17	P5	N18_2	C65_2	59.2(8)	C65_6	C66_6	C67_6	C68_6	48.7(11)
N17	P5	N18_2	C69_2	-164.1(8)	C66_6	C67_6	C68_6	C69_6	-49.4(11)
N17	P5	N18_3	C65_3	77.0(11)	C67_6	C68_6	C69_6	N18_6	55.0(10)
N17	P5	N18_3	C69_3	-63.0(10)	C69_6	N18_6	C65_6	C66_6	61.0(9)
N17	P5	N18_4	C65_4	63.3(10)					

Table 5.55 Hydrogen Atom Coordinates (Å×10^4) and Isotropic Displacement Parameters (Å^2×10^3) for 4-Sm^{5+}(Et$_2$O).

Atom	*x*	*y*	*z*	U(eq)
H1A	5598.8	4317.95	3033.08	124
H1B	5303.17	5223.18	2583.24	124
H2A	4430.89	4267.85	2429.1	174
H2B	3548.79	5363.1	2507.34	174
H2C	3837.24	4463.92	2960.36	174
H3A	3365.34	5890.65	3740.7	128
H3B	4217.75	4743.1	3773.15	128
H4A	4504.45	6206.88	4178.17	154
H4B	5443.14	5103.25	4166.87	154
H4C	4391.04	5282.07	4490.36	154
H5A	4683.39	9686.05	1179.2	44
H5B	5531.29	9396.8	1644.4	44
H6A	3801.07	11356.04	1348.39	50
H6B	5056.06	11049.78	1265.09	50
H7A	4423.54	11911.61	2003.24	63
H7B	5397.19	10822.98	2157.81	63
H8A	3128.88	11344.5	2291.99	60
H8B	3999.25	11042.33	2749.1	60
H9A	4915.14	9373.13	2540.13	49
H9B	3675.62	9639.85	2647.72	49
H10A	3434.38	7062.1	2279.11	55
H10B	2393.16	7714.43	1908.46	55
H11A	2380.97	7537.49	3006.92	64
H11B	1850.6	7061.92	2666.51	64
H12A	486.63	8582.73	2931.65	78
H12B	521.75	8674.12	2319.86	78
H13A	1583.98	9427.6	2945.82	74

Atom	*x*	*y*	*z*	U(eq)
H13B	528.02	10117.03	2589.85	74
H14A	1551.22	9598.56	1840.56	61
H14B	2097.13	10088.21	2164.07	61
H15A	3341.67	9493.08	629.31	49
H15B	2641.74	9847.97	1121.05	49
H16A	1750.65	8858.37	1023.21	56
H16B	1623.91	9557.2	493.31	56
H17A	3010.84	8230.2	134.39	58
H17B	2150.44	7858.61	361.15	58
H18A	3270.79	6973.36	1093.11	58
H18B	3988.01	6638.91	603.38	58
H19A	4936.8	6986.05	1237.09	53
H19B	4805.84	7672.82	703.42	53
H20A	7451.51	4461.32	737.85	48
H20B	6226.91	5136.8	878.15	48
H21A	6950.22	3298.74	449.4	67
H21B	6214.3	4379.06	146.7	67
H22A	4737.31	4576.04	670.46	81
H22B	5146.43	3526.45	465.01	81
H23A	6053.46	2665.15	1251.48	74
H23B	4837.81	3402.25	1374.39	74
H24A	5412.88	4568.4	1599.99	54
H24B	6088.71	3515.81	1942	54
H25A	9169.38	1922.35	2231.69	56
H25B	8074.34	2077.49	1962.07	56
H26A	7381.23	1782.91	2773.38	69
H26B	8525.84	854.84	2712.84	69
H27A	9401.21	1449.06	3240.06	69
H27B	8409.66	1389.35	3546.07	69
H28A	7314.88	3138.33	3332.15	73
H28B	8431.36	2983.28	3579.17	73
H29A	7938.08	4156.23	2816.04	59
H29B	9083.97	3225.73	2766.36	59
H30A	9252.41	3135.97	742.98	58
H30B	8743.92	2540.53	1113.43	58
H31A	10414.94	1541.77	1547.57	57
H31B	10618	1501.79	950.03	57
H32A	11391.39	2593.98	915	70
H32B	11976.28	1741.37	1385.42	70
H33A	10923.06	2804.59	1981.75	88
H33B	11447.31	3395.59	1617.8	88

Atom	*x*	*y*	*z*	U(eq)
H34A	9589.74	4424.59	1717.19	70
H34B	9833.46	4278.62	1130.65	70
H35A	6522.37	9088.86	474.95	55
H35B	6053.37	8313.29	663.47	55
H36A	5601.35	8874.85	-226.28	66
H36B	6846.92	8547.1	-348.96	66
H37A	6445.69	7292.34	-559.57	73
H37B	5915.73	7216.22	-18.87	73
H38A	8192.47	6535.94	-184.13	67
H38B	7629.73	5846.81	27	67
H39A	7270.25	6521.26	812.38	56
H39B	8536.46	6114.62	713.61	56
H40A	7437.6	9297.21	1744.3	63
H40B	6914.75	10227.67	1304.71	63
H41A	9040.47	9430.4	1746.26	99
H41B	8068.25	10491.52	1814.07	99
H42A	8148.56	11119.3	953.29	82
H42B	9352.86	10627.93	1195.7	82
H43A	9298.53	10123.05	368.86	69
H43B	9838.79	9191.45	807	69
H44A	7653.34	10011.26	406.67	74
H44B	8600.17	8943.88	324.52	74
H45A	10012.74	6889.14	1806.39	69
H45B	10684.08	7300.44	1424.67	69
H46A	11008.27	5277.06	1585.5	79
H46B	11840.22	5648.43	1766.23	79
H47A	12276.74	5998.47	895.95	81
H47B	12389.83	4891.57	959.98	81
H48A	11339.63	5889.13	188.43	84
H48B	10670.35	5457.35	558.01	84
H49A	10407.14	7460.37	480.86	76
H49B	9544.68	7154.04	267.25	76
H50A	6738.62	7967.05	4096.21	51
H50B	6026.78	8550.41	3583.89	51
H51A	7405.12	9153.15	4080.69	63
H51B	6111.56	9710.85	4069.91	63
H52A	6841.31	10554.65	3454.94	77
H52B	6045.56	10236.51	3186.85	77
H53A	7632.82	9764.38	2706.57	73
H53B	8379.53	9182.93	3209.38	73
H54A	6944.1	8582.96	2755.96	53

Atom	*x*	*y*	*z*	U(eq)
H54B	8236.72	8015.59	2745.29	53
H55A	8529.15	4601.7	4039.43	54
H55B	7290.7	5156.31	3837.97	54
H56A	7425.84	4339.37	4696.21	62
H56B	6705.32	5513.84	4675.99	62
H57A	7928.88	4972.4	5386.34	74
H57B	8936.09	4427.6	5038.14	74
H58A	7659.75	6555.78	4983.32	65
H58B	8907.63	5951	5163.5	65
H59A	8726.63	6760.66	4299.57	56
H59B	9406.61	5579.79	4320.56	56
H60A	9533.62	5731.89	2436.5	53
H60B	8847.6	5212.33	2720.21	53
H61A	10699.36	4024.87	2654.7	72
H61B	10368.58	4072.31	3240.43	72
H62A	12059.59	4118.96	3180.14	74
H62B	11605.34	5012.76	2717.98	74
H63A	11631.42	5690.53	3460.18	77
H63B	10973.61	5157.3	3761.02	77
H64A	9759.33	6851.47	3513.2	68
H64B	10094.26	6767.5	2930.1	68
H65A_1	5195.07	8312.15	4917.18	82
H65B_1	5239.06	7514.44	4567.03	82
H66A_1	4894.71	6576.08	5270.25	104
H66B_1	5903.63	6742	5423.68	104
H67A_1	4861.97	7936.66	5929.4	104
H67B_1	4583.4	7023.49	6084.05	104
H68A_1	2977.78	8633.67	5966.61	97
H68B_1	2921.62	7856.05	5630.19	97
H69A_1	2378.21	9399.04	5093.33	84
H69B_1	3461.45	9451.75	5243.73	84
H65A_2	2201.26	7390.2	4657.88	100
H65B_2	2712.1	7232.3	4105.95	100
H66A_2	1004.98	7714.37	3721.71	102
H66B_2	1198.07	6852.75	4185.42	102
H67A_2	32.89	7975.52	4698.19	103
H67B_2	-592.96	8237.7	4158.13	103
H68A_2	-733.1	9708.54	4495.37	97
H68B_2	-274.09	9629.29	3930.79	97
H69A_2	844.12	10016.45	4435.01	95
H69B_2	1045.14	9085.04	4858.12	95

Atom	*x*	*y*	*z*	U(eq)
H65A_3	2640.19	7474.81	4987.71	95
H65B_3	2206.41	7153.93	4525.22	95
H66A_3	1037.56	7293.63	5211.79	96
H66B_3	862.54	8396.93	5249.85	96
H67A_3	-669.93	8572.57	4830.98	90
H67B_3	31.25	7799.32	4451.99	90
H68A_3	-220.99	9796.49	4417.74	97
H68B_3	-588.41	9377.11	3975.02	97
H69A_3	1243.95	8379.72	3785.31	95
H69B_3	1068.19	9500.25	3766.01	95
H65A_4	1393.66	10408.79	3576.22	100
H65B_4	2337.51	10636.34	3323.55	100
H66A_4	842.84	12166.95	3418	100
H66B_4	783.51	11809.15	4010.91	100
H67A_4	1599.25	12848.69	3981.9	94
H67B_4	2406.7	12306.6	3553.1	94
H68A_4	2537.94	11509.46	4616.91	103
H68B_4	3437.07	11745.34	4318.29	103
H69A_4	3887.61	10392.17	3844.23	100
H69B_4	3970.87	9975.27	4439.85	100
H65A_5	1951.55	10797.82	3468.28	98
H65B_5	3231.54	10128.43	3458.99	98
H66A_5	3564.17	11270.1	3847.55	100
H66B_5	2761.79	11873.97	3365.13	100
H67A_5	1295.82	12544.21	3874.91	94
H67B_5	2244.76	12679.23	4130.15	94
H68A_5	1276.88	12054.28	4751.4	103
H68B_5	2557.7	11368.24	4783.89	103
H69A_5	1696.78	10314.21	4797.63	105
H69B_5	1018.21	10936.99	4281.74	105
H65A_6	4709.49	9022.11	4856.66	82
H65B_6	5106.86	8213.42	4468.65	82
H66A_6	5688.92	6900.77	5150.31	104
H66B_6	6231.77	7604.66	5236.06	104
H67A_6	5053.55	8292.97	5871.44	104
H67B_6	5488.14	7116.35	6003.49	104
H68A_6	3532.08	8043.53	6079.73	95
H68B_6	3863.01	7203.95	5712.12	95
H69A_6	2443.61	8688.83	5291.14	84
H69B_6	3101.91	9304.68	5363.17	84

Table 5.56 Atomic Occupancy for 4-$Sm^{5+}(Et_2O)$.

Atom	*Occupancy*	Atom	*Occupancy*	Atom	*Occupancy*
Sm1A	0.572(4)	Sm1B	0.428(4)	N18_1	0.572(4)
C65_1	0.572(4)	H65A_1	0.572(4)	H65B_1	0.572(4)
C66_1	0.572(4)	H66A_1	0.572(4)	H66B_1	0.572(4)
C67_1	0.572(4)	H67A_1	0.572(4)	H67B_1	0.572(4)
C68_1	0.572(4)	H68A_1	0.572(4)	H68B_1	0.572(4)
C69_1	0.572(4)	H69A_1	0.572(4)	H69B_1	0.572(4)
N18_2	0.572(4)	C65_2	0.572(4)	H65A_2	0.572(4)
H65B_2	0.572(4)	C66_2	0.572(4)	H66A_2	0.572(4)
H66B_2	0.572(4)	C67_2	0.572(4)	H67A_2	0.572(4)
H67B_2	0.572(4)	C68_2	0.572(4)	H68A_2	0.572(4)
H68B_2	0.572(4)	C69_2	0.572(4)	H69A_2	0.572(4)
H69B_2	0.572(4)	N18_3	0.428(4)	C65_3	0.428(4)
H65A_3	0.428(4)	H65B_3	0.428(4)	C66_3	0.428(4)
H66A_3	0.428(4)	H66B_3	0.428(4)	C67_3	0.428(4)
H67A_3	0.428(4)	H67B_3	0.428(4)	C68_3	0.428(4)
H68A_3	0.428(4)	H68B_3	0.428(4)	C69_3	0.428(4)
H69A_3	0.428(4)	H69B_3	0.428(4)	N18_4	0.572(4)
C65_4	0.572(4)	H65A_4	0.572(4)	H65B_4	0.572(4)
C66_4	0.572(4)	H66A_4	0.572(4)	H66B_4	0.572(4)
C67_4	0.572(4)	H67A_4	0.572(4)	H67B_4	0.572(4)
C68_4	0.572(4)	H68A_4	0.572(4)	H68B_4	0.572(4)
C69_4	0.572(4)	H69A_4	0.572(4)	H69B_4	0.572(4)
N18_5	0.428(4)	C65_5	0.428(4)	H65A_5	0.428(4)
H65B_5	0.428(4)	C66_5	0.428(4)	H66A_5	0.428(4)
H66B_5	0.428(4)	C67_5	0.428(4)	H67A_5	0.428(4)
H67B_5	0.428(4)	C68_5	0.428(4)	H68A_5	0.428(4)
H68B_5	0.428(4)	C69_5	0.428(4)	H69A_5	0.428(4)
H69B_5	0.428(4)	N18_6	0.428(4)	C65_6	0.428(4)
H65A_6	0.428(4)	H65B_6	0.428(4)	C66_6	0.428(4)
H66A_6	0.428(4)	H66B_6	0.428(4)	C67_6	0.428(4)
H67A_6	0.428(4)	H67B_6	0.428(4)	C68_6	0.428(4)
H68A_6	0.428(4)	H68B_6	0.428(4)	C69_6	0.428(4)
H69A_6	0.428(4)	H69B_6	0.428(4)		

CHAPTER 6. CONCLUSION

6.1 Thesis Overview

This thesis outlines the development of several lanthanide complexes featuring weak-field ligand systems, as well as new lanthanide starting materials using low-polarity low-basicity supporting solvents. This body of work advances the synthetic approaches to low, high, and mixed-valent lanthanide complexes. Spectroscopic investigation of these complexes provided insight into their unique electronic structure as well as oxidation state dependance on covalent bonding.

Chapter two outlines a methodology for the synthesis of etherate based lanthanide triiodide starting materials for metathesis reactions. This method offers a consistent route for the production of trivalent lanthanide iodide precursors on reasonable scales for bulk synthesis (~1 g). Crystallographic investigation of the **1-Ln** complexes reveal that these solvated lanthanide triiodides are isostructural with three weakly bound diethyl ethers to each lanthanide metal center. These materials provide increased flexibility for complex formation in which more basic supporting solvents, such as THF, are undesirable. Similarly, through Soxhlet extraction, these materials can be converted to known THF adducts with consistent composition in situations where that is more desirable.

Chapter three details the synthesis of neutral homoleptic divalent complexes through oxidative transmetallation. This work relies on the use of oxidizing copper(I) ligand salts, a process that is scarcely seen for low valent lanthanide complex formation. Absorbance studies and variable-temperature dc magnetic susceptibility measurements

confirm the divalent nature of the compounds and suggest that the observed distorted coordination polyhedra enforced by the linear Si–N–Si ligand backbone support a homologous structure to the formally two-coordinate lanthanide complexes.

Chapter four establishes the first ever isostructural valency series for a $4f^7$ ground state spanning three oxidation states (Eu^{2+}, Gd^{3+}, and Tb^{4+}). High frequency and -field EPR, along with multi-field magnetic data fitting, highlights the increase in ZFS (as given by Δ_{8S}, which gives the effect of ZFS absent the complication of signage of traditional parameters) for Tb^{4+} when compared to Eu^{2+} and Gd^{3+} in a nearly conserved ligand environment. This work contributes to recent spectroscopic reevaluation of lanthanide covalent bonding and reveal that tetravalent lanthanides, even mid-lanthanides, have greater metal-ligand bond covalency than in their di- and trivalent counterparts.

Chapter five outlines the development of a series of ytterbium and samarium imidophosphorane complexes, each with a mixed valent complex. The mixed valent ytterbium complex, **3-Yb^{5+}**, contains two prominent features in its room temperature UV/vis spectra, attributable to a *f-d* transition and a broad IVCT feature. The IVCT feature exhibits both temperature and solvent dependance, the latter of which is commonly characteristic of intervalence charge transfers. Gaussian fits of the UV/vis spectra in the visible region deconvolutes the equilibrium contributions of two contributing features at each temperature. Through this analysis, it is apparent higher energy feature, prominent at lower temperatures, is more sensitive to dielectric of solvent. Spectral simulation through TDDFT reproduces the experimentally observed spectra well. Calculations confirm a charge localization, shown in the solid-state crystal structure, between divalent and trivalent ytterbium in **3-Yb^{5+}**. The room temperature moment for the **3-Yb^{5+}** complex is

similar to that of **5-Yb^{3+}** which is expected as divalent ytterbium is diamagnetic in its ground state. The low temperature moment is informative as it deviates from the purely trivalent monometallic complex, highlighting the low temperature magnetic coupling characteristic of complexes with IVCT behavior.

6.2 Future Work

6.2.1 *New Low-Valent f-element Complexes Supported by Bulky Disilyl Amides*

The development of oxidizing copper(I) reagents such as **1** opens up a lot of possibilities for expansion to other *f*-elements. The multidentate capacity of the bis(tri-tert-butoxysilyl)amide ligand allows for satisfying high coordination requirements of large divalent ions while still maintaining a neutral complex in the primary coordination sphere. Similarly, due to the vibronic coupling observed in **2-Eu**, which caused a large enhancement of molar absorptivity in formally forbidden transitions, this ligand set behaves similar to linear two-coordinate complexes. Because of this, these complexes, with the appropriate metal center, have the potential to be potent single molecular magnets.

Numerous excellent single molecular magnets (SMMs) have been developed featuring trivalent lanthanides due largely to their strong magnetic anisotropy. Recently, however, High-level ab initio calculations are reported for LnO (Ln = Tb, Dy, Ho) which show that divalent lanthanides can exhibit equally strong magnetic anisotropy and magnetization blocking barriers. In particular, detailed calculations predict a multilevel magnetization blocking barrier exceeding 3000 K for a [DyO] complex deposited on a hexagonal boron nitride surface, bringing the expected performance of single-molecule magnets to a qualitatively new level compared to the current state-of-the art complexes. In

practice, non-traditional divalent lanthanides ($4f^n5d^1$ ground states) are breaking norms and establishing new highs. This unique valence electronic structure leads to the highest magnetic moments observed for any ion in the cases of $DyCp_3'$and $HoCp_3'$.[65] This is particularly advantageous for single molecular magnets because larger moments help deter tunneling of magnetization. Combining the high moment potential of low-valent Dy and Ho with the high local symmetry ligand sets such as bis(tri-tert-butoxysilyl)amide ligand can enhance key SMM properties.

6.2.2 *Mixed-Valent Template for Exploring Metal-Metal Bonding in the Lanthanides*

The development of lanthanide bimetallics that exhibit prominent intervalence charge transfers (IVCT) is a crucial steppingstone to realizing stable metal-metal bonding lanthanide complexes. It is not unsurprising that **3-Yb^{5+}**, being of pure 4*f* character, did not form any metal-metal bonds. This is because to the general inertness of *f*-orbitals due to this poor radial extent and core-like nature. On the other hand, *d*-orbitals are very promising for achieving bonding. Although higher in energy, the 5*d* orbitals extend greatly from the [Xe] core. Therefore, it may be possible to realize bonding in an excited state of a pure 4*f* complex (by pumping an *f-d* band) or by moving to a system in which reduction populates a *d*-orbital (non-traditional divalent lanthanides).

To investigate bonding in an excited state, the two potential methods of investigation are SQUID magnetometry and SCXRD. During SQUID measurements, the complex will be irradiated with UV light (around 380 nm) during the collection. Assuming the compound's stability to extended exposure, the collected dc magnetic data should reveal key differences from the ground state data, especially due to the removal of the

diamagnetic $4f^{14}$ ytterbium ion. Fits on the magnetic data, as well as calculations, will be required in order to assess the nature of the electronic structure in the excited state and to assign the exchange interaction or potential bonding interaction. For SCXRD, a structural data set will be collected while the crystal is being irritated with UV light. The goal from this is to look at the bond metrics of the resultant structure. Useful things to look for include: a contraction of the interatomic ytterbium distance from the 2.958(1) Å, and a homology of all Yb-N bond lengths in the structure. The primary concerns for this process are radiation damage of the crystal from light exposure as well as temperature control of the crystal. If a set temperature cannot be maintained, such as 100K, it may be prudent to collect a structure at the steady state temperature achieved during irradiation without the UV light source for comparison of bond metrics.

The primary challenge of the later approach is the much higher reduction requirements of the nontraditional divalent lanthanides. For example, the reduction potential of ytterbium is around 1.2 V vs NHE while dysprosium, the most easily reduced non-traditional divalent lanthanide, is around 2.5 V vs NHE.[189] Therefore, to accomplish this, some adaptation of the current ligand system, as well as innovative use of new reductants might be necessary to successfully develop an analogous system to **3-Yb**$^{5+}$ featuring non-traditional divalent lanthanides.

APPENDIX A. COLLABORATOR CONTRIBUTIONS

A.1 Diethyl Ether Adducts of Trivalent Lanthanide Iodides

Natalie Rice, Brandon Yik, Luis Aguirre Quintana, and Dominic Russo contributed significantly to the isolation of several crystal structures in this work. Dr. John Bacsa collected and refined all SCXRD structures.

A.2 Synthesis of Homoleptic, Divalent Lanthanide (Sm, Eu) Complexes via Oxidative Transmetallation

Dr. John Bacsa and Ningxin Jiang collected and refined all SCXRD structures.

A.3 High-Frequency and -Field Electron Paramagnetic Spectroscopic Analysis of Metal-Ligand Covalency in $4f^7$ Valency Series (Eu^{2+}, Gd^{3+}, Tb^{4+})

Dr. Sam Greer assisted with data collection at NHMFL. He also performed spectral fits on EPR spectra and performed the quantum chemical calculations. Natalie Rice developed the synthetic methodology for the tetravalent terbium complex in this work. Ningxin Jiang collected and refined all SCXRD structures.

A.4 Intervalence Charge Transfer in Homobimetallic Ytterbium Complexes

Dr. Sam Greer performed all DFT and CASSCF calculations for this work.

APPENDIX B. PERMISSIONS TO REPRODUCE PUBLISHED MATERIALS

Part of these thesis chapters have been adapted with permission from articles co-written by the author:

B.1 Introduction

Gompa, T. P., Ramanathan, A., Rice, N. T., La Pierre, H. S. The chemical and physical properties of tetravalent lanthanides: Pr, Nd, Tb, and Dy. Dalton Trans., **2020**,*49*, 15945-15987

https://pubs.rsc.org/en/content/articlelanding/2020/dt/d0dt01400a (Accessed August 2021)

B.2 Diethyl Ether Adducts of Trivalent Lanthanide Iodides

Gompa, T. P., Rice, N. T., Russo, D. R., Quintana L. M. A., Yik, B. J. Bacsa, J., La Pierre, H. S. Diethyl ether adducts of trivalent lanthanide iodides. Dalton Trans., **2019**, *48*, 8030-8033.

https://pubs.rsc.org/en/content/articlelanding/2019/dt/c9dt00775j (Accessed August 2021)

B.3 Synthesis of Homoleptic, Divalent Lanthanide (Sm, Eu) Complexes via Oxidative Transmetallation

Gompa, T. P., Jiang, N., J. Bacsa, J., La Pierre, H. S. Synthesis of Homoleptic, Divalent Lanthanide (Sm, Eu) Complexes via Oxidative Transmetallation. Dalton Trans., **2019**, *48*, 16869-16872.

https://pubs.rsc.org/en/content/articlelanding/2019/dt/c9dt04230j (Accessed August 2021)

B.4 High-Frequency and -Field Electron Paramagnetic Spectroscopic Analysis of Metal-Ligand Covalency in $4f^7$ Valency Series (Eu^{2+}, Gd^{3+}, Tb^{4+})

Gompa, T. P., Greer, S. M., Rice, N. T., Jiang, N., Telser, J., Ozarowski, A., Stein, B. W., La Pierre, H. S. High-Frequency and -Field Electron Paramagnetic Resonance Spectroscopic Analysis of Metal–Ligand Covalency in a $4f^7$ Valence Series (Eu^{2+}, Gd^{3+}, and Tb^{4+}). Inorg. Chem., **2021**, *60*, 12, 9064-9073.

https://pubs.acs.org/doi/10.1021/acs.inorgchem.1c01062 (Accessed August 2021)

REFERENCES

[1] Kulkarni, P.; Chellam, S.; Fraser, M. P., *Atmos. Environ.* **2006,** *40* (3), 508-520.

[2] DeKalb, E. L.; Fassel, V. A., *Anal. Chem.* **1975,** *47* (14), 2354-2356.

[3] DOE, *Critical Materials Strategy* **2011**.

[4] Park, W. K.; Sun, L.; Noddings, A.; Kim, D.-J.; Fisk, Z.; Greene, L. H., *P. Natl. A. Sci.* **2016,** *113* (24), 6599.

[5] Allen, J. W.; Batlogg, B.; Wachter, P., *Phys. Rev. B.* **1979,** *20* (12), 4807-4813.

[6] Rinehart, J. D.; Fang, M.; Evans, W. J.; Long, J. R., *J. Am. Chem. Soc.* **2011,** *133* (36), 14236-14239.

[7] Molander, G. A., *Chem. Rev.* **1992,** *92* (1), 29-68.

[8] Xie, F.; Zhang, T. A.; Dreisinger, D.; Doyle, F., *Miner. Eng.* **2014,** *56*, 10-28.

[9] Taylor, M. D.; Carter, C. P., *J. Inorg. Nucl. Chem.* **1962,** *24* (4), 387-391.

[10] Kui, S. C. F.; Li, H.-W.; Lee, H. K., *Inorg. Chem.* **2003,** *42* (9), 2824-2826.

[11] Hazin, P. N.; Huffman, J. C.; Bruno, J. W., *Organometallics* **1987,** *6* (1), 23-27.

[12] Deacon, G. B.; Koplick, A. J., *Inorg. Nucl. Chem. Lett.* **1979,** *15* (5), 263-265.

[13] Taube, R.; Maiwald, S.; Sieler, J., *J. Organomet. Chem.* **2001,** *621* (1), 327-336.

[14] Izod, K.; Liddle, S. T.; Clegg, W., *Inorg. Chem.* **2004,** *43* (1), 214-218.

[15] Spedding, F. H.; Voigt, A. F.; Gladrow, E. M.; Sleight, N. R., *J. Am. Chem. Soc.* **1947,** *69* (11), 2777-2781.

[16] Spedding, F. H.; Voigt, A. F.; Gladrow, E. M.; Sleight, N. R.; Powell, J. E.; Wright, J. M.; Butler, T. A.; Figard, P., *J. Am. Chem. Soc.* **1947,** *69* (11), 2786-2792.

[17] Spedding, F. H.; Fulmer, E. I.; Butler, T. A.; Gladrow, E. M.; Gobush, M.; Porter, P. E.; Powell, J. E.; Wright, J. M., *J. Am. Chem. Soc.* **1947,** *69* (11), 2812-2818.

[18] Spedding, F. H.; Fulmer, E. I.; Butler, T. A.; Powell, J. E., *J. Am. Chem. Soc.* **1950,** *72* (6), 2349-2354.

[19] Spedding, F. H.; Fulmer, E. I.; Powell, J. E.; Butler, T. A., *J. Am. Chem. Soc.* **1950,** *72* (6), 2354-2361.

[20] Spedding, F. H.; Daane, A. H., *J. Am. Chem. Soc.* **1952,** *74* (11), 2783-2785.

[21] Spedding, F. H., *Discuss. Faraday Soc.* **1949,** *7* (0), 214-231.

[22] US2539282. US2539282, 1951.

[23] US2798789, 1957.

[24] Klemm, W., *Z. Anorg. Allg. Chem.* **1929,** *184* (1), 345-351.

[25] Meyer, G., *J. Solid State Chem.* **2019,** *270*, 324-334.

[26] Meyer, G., *Angew. Chem. Int. Edit.* **2014,** *53* (14), 3550-3551.

[27] Pol, A.; Barends, T. R. M.; Dietl, A.; Khadem, A. F.; Eygensteyn, J.; Jetten, M. S. M.; Op den Camp, H. J. M., *Environ. Microbiol.* **2014,** *16* (1), 255-264.

[28] Keltjens, J. T.; Pol, A.; Reimann, J.; Op den Camp, H. J. M., *Appl. Microbiol. Biot.* **2014,** *98* (14), 6163-6183.

[29] Martinez-Gomez, N. C.; Vu, H. N.; Skovran, E., *Inorg. Chem.* **2016,** *55* (20), 10083-10089.

[30] Lumpe, H.; Pol, A.; Op den Camp, H. J. M.; Daumann, L. J., *Dalton Trans.* **2018,** *47* (31), 10463-10472.

[31] Daumann, L. J., *Angew. Chem. Int. Edit.* **2019,** *58* (37), 12795-12802.

[32] Bogart, J. A.; Lewis, A. J.; Schelter, E. J., *Chem-Eur J* **2015,** *21* (4), 1743-1748.

[33] Dorfner, W. L.; Carroll, P. J.; Schelter, E. J., *Org. Lett.* **2015,** *17* (8), 1850-1853.

[34] Cotruvo, J. A., *ACS Cent. Sci.* **2019,** *5* (9), 1496-1506.

[35] Druding, L. F.; Corbett, J. D.; Ramsey, B. N., *Inorg. Chem.* **1963,** *2* (4), 869-871.

[36] Sallach, R. A.; Corbett, J. D., *Inorg. Chem.* **1963,** *2* (3), 457-459.

[37] Druding, L. F.; Corbett, J. D., *J. Am. Chem. Soc.* **1959,** *81* (20), 5512-5512.

[38] Corbett, J. D.; McCollum, B. C., *Inorg. Chem.* **1966,** *5* (5), 938-940.

[39] Lokken, D. A.; Corbett, J. D., *Inorg. Chem.* **1973,** *12* (3), 556-559.

[40] Loechner, U.; Corbett, J. D., *Inorg. Chem.* **1975,** *14* (2), 426-428.

[41] Meyer, G., *Chem. Rev.* **1988,** *88* (1), 93-107.

[42] Schleid, T.; Meyer, G., *Inorg. Chim. Acta* **1987,** *140*, 113-116.

[43] Meyer, G., *Prog. Solid State Ch.* **1982,** *14* (3), 141-219.

[44] Hammerich, S.; Pantenburg, I.; Meyer, G., *Z. Anorg. Allg. Chem.* **2006,** *632* (14), 2181-2183.

[45] Hammerich, S.; Pantenburg, I.; Meyer, G., *Z. Anorg. Allg. Chem.* **2006,** *632* (8-9), 1487-1490.

[46] Meyer, G.; Meyer, H. J., *Chem. Mater.* **1992,** *4* (6), 1157-1168.

[47] Felser, C.; Ahn, K.; Kremer, R. K.; Seshadri, R.; Simon, A., *J. Solid State Chem.* **1999,** *147* (1), 19-25.

[48] Cloke, F. G. N., *Chem. Soc. Rev.* **1993,** *22* (1), 17-24.

[49] Brennan, J. G.; Cloke, F. G. N.; Sameh, A. A.; Zalkin, A., *J. Chem. Soc. Chem. Comm.* **1987,** (21), 1668-1669.

[50] Anderson, D. M.; Cloke, F. G. N.; Cox, P. A.; Edelstein, N.; Green, J. C.; Pang, T.; Sameh, A. A.; Shalimoff, G., *J. Chem. Soc. Chem. Comm.* **1989,** (1), 53-55.

[51] Cloke, F. G. N.; Khan, K.; Perutz, R. N., *J. Chem. Soc. Chem. Comm.* **1991,** (19), 1372-1373.

[52] L. Arnold, P.; Geoffrey N. Cloke, F.; B. Hitchcock, P., *Chem. Commun.* **1997,** (5), 481-482.

[53] Arnold, P. L.; Petrukhina, M. A.; Bochenkov, V. E.; Shabatina, T. I.; Zagorskii, V. V.; Sergeev, G. B.; Cloke, F. G. N., *J. Organomet. Chem.* **2003,** *688* (1), 49-55.

[54] Bochkarev, M. N.; Fedushkin, I. L.; Fagin, A. A.; Petrovskaya, T. V.; Ziller, J. W.; Broomhall-Dillard, R. N. R.; Evans, W. J., *Angew. Chem. Int. Edit.* **1997,** *36* (1-2), 133-135.

[55] Evans, W. J.; Allen, N. T.; Ziller, J. W., *J. Am. Chem. Soc.* **2000,** *122* (47), 11749-11750.

[56] Bochkarev, M. N.; Fedushkin, I. L.; Dechert, S.; Fagin, A. A.; Schumann, H., *Angew. Chem. Int. Edit.* **2001,** *40* (17), 3176-3178.

[57] Bochkarev, M. N.; Fagin, A. A., *Chem-Eur J* **1999,** *5* (10), 2990-2992.

[58] L. Arnold, P.; Geoffrey N. Cloke, F.; F. Nixon, J., *Chem. Commun.* **1998,** (7), 797-798.

[59] Hitchcock, P. B.; Lappert, M. F.; Maron, L.; Protchenko, A. V., *Angew. Chem. Int. Edit.* **2008,** *47* (8), 1488-1491.

[60] MacDonald, M. R.; Ziller, J. W.; Evans, W. J., *J. Am. Chem. Soc.* **2011,** *133* (40), 15914-15917.

[61] MacDonald, M. R.; Bates, J. E.; Ziller, J. W.; Furche, F.; Evans, W. J., *J. Am. Chem. Soc.* **2013,** *135* (26), 9857-9868.

[62] MacDonald, M. R.; Fieser, M. E.; Bates, J. E.; Ziller, J. W.; Furche, F.; Evans, W. J., *J. Am. Chem. Soc.* **2013,** *135* (36), 13310-13313.

[63] Langeslay, R. R.; Fieser, M. E.; Ziller, J. W.; Furche, F.; Evans, W. J., *Chem. Sci.* **2015,** *6* (1), 517-521.

[64] Fieser, M. E.; MacDonald, M. R.; Krull, B. T.; Bates, J. E.; Ziller, J. W.; Furche, F.; Evans, W. J., *J. Am. Chem. Soc.* **2015,** *137* (1), 369-382.

[65] Meihaus, K. R.; Fieser, M. E.; Corbey, J. F.; Evans, W. J.; Long, J. R., *J. Am. Chem. Soc.* **2015,** *137* (31), 9855-9860.

[66] Windorff, C. J.; MacDonald, M. R.; Meihaus, K. R.; Ziller, J. W.; Long, J. R.; Evans, W. J., *Chem-Eur J* **2016,** *22* (2), 772-782.

[67] Woen, D. H.; Chen, G. P.; Ziller, J. W.; Boyle, T. J.; Furche, F.; Evans, W. J., *Angew. Chem. Int. Edit.* **2017,** *56* (8), 2050-2053.

[68] Windorff, C. J.; Chen, G. P.; Cross, J. N.; Evans, W. J.; Furche, F.; Gaunt, A. J.; Janicke, M. T.; Kozimor, S. A.; Scott, B. L., *J. Am. Chem. Soc.* **2017,** *139* (11), 3970-3973.

[69] Fieser, M. E.; Ferrier, M. G.; Su, J.; Batista, E.; Cary, S. K.; Engle, J. W.; Evans, W. J.; Lezama Pacheco, J. S.; Kozimor, S. A.; Olson, A. C.; Ryan, A. J.; Stein, B. W.; Wagner, G. L.; Woen, D. H.; Vitova, T.; Yang, P., *Chem. Sci.* **2017,** *8* (9), 6076-6091.

[70] Fieser, M. E.; Palumbo, C. T.; La Pierre, H. S.; Halter, D. P.; Voora, V. K.; Ziller, J. W.; Furche, F.; Meyer, K.; Evans, W. J., *Chem. Sci.* **2017,** *8* (11), 7424-7433.

[71] Huh, D. N.; Darago, L. E.; Ziller, J. W.; Evans, W. J., *Inorg. Chem.* **2018,** *57* (4), 2096-2102.

[72] Ryan, A. J.; Darago, L. E.; Balasubramani, S. G.; Chen, G. P.; Ziller, J. W.; Furche, F.; Long, J. R.; Evans, W. J., *Chem-Eur. J.* **2018,** *24* (30), 7702-7709.

[73] Su, J.; Windorff, C. J.; Batista, E. R.; Evans, W. J.; Gaunt, A. J.; Janicke, M. T.; Kozimor, S. A.; Scott, B. L.; Woen, D. H.; Yang, P., *J. Am. Chem. Soc.* **2018,** *140* (24), 7425-7428.

[74] Woen, D. H.; Huh, D. N.; Ziller, J. W.; Evans, W. J., *Organometallics* **2018,** *37* (18), 3055-3063.

[75] Huh, D. N.; Ziller, J. W.; Evans, W. J., *Inorg. Chem.* **2018,** *57* (18), 11809-11814.

[76] Palumbo, C. T.; Halter, D. P.; Voora, V. K.; Chen, G. P.; Ziller, J. W.; Gembicky, M.; Rheingold, A. L.; Furche, F.; Meyer, K.; Evans, W. J., *Inorg. Chem.* **2018,** *57* (20), 12876-12884.

[77] Jenkins, T. F.; Woen, D. H.; Mohanam, L. N.; Ziller, J. W.; Furche, F.; Evans, W. J., *Organometallics* **2018,** *37* (21), 3863-3873.

[78] Moehring, S. A.; Beltrán-Leiva, M. J.; Páez-Hernández, D.; Arratia-Pérez, R.; Ziller, J. W.; Evans, W. J., *Chem-Eur J* **2018,** *24* (68), 18059-18067.

[79] Huh, D. N.; Ziller, J. W.; Evans, W. J., *Dalton Trans.* **2018,** *47* (48), 17285-17290.

[80] Ryan, A. J.; Angadol, M. A.; Ziller, J. W.; Evans, W. J., *Chem. Commun.* **2019,** *55* (16), 2325-2327.

[81] Angadol, M. A.; Woen, D. H.; Windorff, C. J.; Ziller, J. W.; Evans, W. J., *Organometallics* **2019,** *38* (5), 1151-1158.

[82] Moehring, S. A.; Evans, W. J., *Chem-Eur J* **2020,** *26* (7), 1530-1534.

[83] Moehring, S. A.; Miehlich, M.; Hoerger, C. J.; Meyer, K.; Ziller, J. W.; Evans, W. J., *Inorg. Chem.* **2020,** *59* (5), 3207-3214.

[84] La Pierre, H. S.; Kameo, H.; Halter, D. P.; Heinemann, F. W.; Meyer, K., *Angew. Chem. Int. Edit.* **2014,** *53* (28), 7154-7157.

[85] La Pierre, H. S.; Scheurer, A.; Heinemann, F. W.; Hieringer, W.; Meyer, K., *Angew. Chem. Int. Edit.* **2014,** *53* (28), 7158-7162.

[86] Billow, B. S.; Livesay, B. N.; Mokhtarzadeh, C. C.; McCracken, J.; Shores, M. P.; Boncella, J. M.; Odom, A. L., *J. Am. Chem. Soc.* **2018,** *140* (50), 17369-17373.

[87] Kelly, R. P.; Maron, L.; Scopelliti, R.; Mazzanti, M., *Angew. Chem. Int. Edit.* **2017,** *56* (49), 15663-15666.

[88] Gould, C. A.; McClain, K. R.; Yu, J. M.; Groshens, T. J.; Furche, F.; Harvey, B. G.; Long, J. R., *J. Am. Chem. Soc.* **2019,** *141* (33), 12967-12973.

[89] Guo, F.-S.; Tsoureas, N.; Huang, G.-Z.; Tong, M.-L.; Mansikkamäki, A.; Layfield, R. A., *Angew. Chem. Int. Edit.* **2020,** *59* (6), 2299-2303.

[90] Martin, J. D.; Corbett, J. D., *Angew. Chem. Int. Edit.* **1995,** *34* (2), 233-235.

[91] Arnold, P. L.; Cloke, F. G. N.; Hitchcock, P. B.; Nixon, J. F., *J. Am. Chem. Soc.* **1996,** *118* (32), 7630-7631.

[92] Wadsworth, E.; Duke, F. R.; Goetz, C. A., *Anal. Chem.* **1957,** *29* (12), 1824-1825.

[93] Sofen, S. R.; Cooper, S. R.; Raymond, K. N., *Inorg. Chem.* **1979,** *18* (6), 1611-1616.

[94] Deblonde, G. J. P.; Sturzbecher-Hoehne, M.; Abergel, R. J., *Inorg. Chem.* **2013,** *52* (15), 8805-8811.

[95] Crosswhite, H. M.; Crosswhite, H.; Carnall, W. T.; Paszek, A. P., *J. Chem. Phys.* **1980,** *72* (9), 5103-5117.

[96] Cundari, T. R.; Stevens, W. J., *J. Chem. Phys.* **1993,** *98* (7), 5555-5565.

[97] Hong, G.; Schautz, F.; Dolg, M., *J. Am. Chem. Soc.* **1999,** *121* (7), 1502-1512.

[98] Maron, L.; Eisenstein, O., *J. Phys. Chem. A* **2000,** *104* (30), 7140-7143.

[99] Vetere, V.; Maldivi, P.; Adamo, C., *J. Comput. Chem.* **2003,** *24*, 850.

[100] Atanasov, M.; Daul, C.; Güdel, H. U.; Wesolowski, T. A.; Zbiri, M., *Inorg. Chem.* **2005,** *44* (8), 2954-2963.

[101] Löble, M. W.; Keith, J. M.; Altman, A. B.; Stieber, S. C. E.; Batista, E. R.; Boland, K. S.; Conradson, S. D.; Clark, D. L.; Lezama Pacheco, J.; Kozimor, S. A.; Martin, R. L.; Minasian, S. G.; Olson, A. C.; Scott, B. L.; Shuh, D. K.; Tyliszczak, T.; Wilkerson, M. P.; Zehnder, R. A., *J. Am. Chem. Soc.* **2015,** *137* (7), 2506-2523.

[102] Shahin, A. M.; Grandjean, F.; Long, G. J.; Schuman, T. P., *Chem. Mater.* **2005,** *17* (2), 315-321.

[103] Kotani, A.; Kvashnina, K. O.; Butorin, S. M.; Glatzel, P., *J. Electron Spectrosc.* **2011,** *184* (3), 210-215.

[104] Kvashnina, K. O.; Butorin, S. M.; Glatzel, P., *Journal of Analytical Atomic Spectrometry* **2011,** *26* (6), 1265-1272.

[105] Altman, A. B.; Pacold, J. I.; Wang, J.; Lukens, W. W.; Minasian, S. G., *Dalton Trans.* **2016,** *45* (24), 9948-9961.

[106] Minasian, S. G.; Batista, E. R.; Booth, C. H.; Clark, D. L.; Keith, J. M.; Kozimor, S. A.; Lukens, W. W.; Martin, R. L.; Shuh, D. K.; Stieber, S. C. E.; Tylisczcak, T.; Wen, X.-d., *J. Am. Chem. Soc.* **2017,** *139* (49), 18052-18064.

[107] Liu, F.; Spree, L.; Krylov, D. S.; Velkos, G.; Avdoshenko, S. M.; Popov, A. A., *Acc. Chem. Res.* **2019,** *52* (10), 2981-2993.

[108] Arnold, P. L.; Cowie, B. E.; Suvova, M.; Zegke, M.; Magnani, N.; Colineau, E.; Griveau, J.-C.; Caciuffo, R.; Love, J. B., *Angewandte Chemie International Edition* **2017,** *56* (36), 10775-10779.

[109] Mills, D. P.; Moro, F.; McMaster, J.; Slageren, V. J.; Lewis, W.; Blake, A. J.; Liddle, S. T., *Nature Chemistry* **2011,** *3*, 454-460.

[110] Hilgar, J. D.; Flores, B. S.; Rinehart, J. D., *Chemical Communications* **2017,** (53), 7322-7324.

[111] Chilton, N. F.; Goodwin, C. A. P.; Mills, D. P.; Winpenny, R. E. P., *Chem. Commun.* **2014,** *51* (1), 101-103.

[112] Guo, F. S.; Day, B. M.; Chen, Y. C.; Tong, M. L.; Mansikkamaki, A.; Leyfield, R. A., *Science* **2018,** *362* (6421), 1400-1403.

[113] Goodwin, C. A. P.; Ortu, F.; Reta, D.; Chilton, N. F.; Mills, D. P., *Nature* **2017,** *548* (7668), 439-442.

[114] King, D. M.; Tuna, F.; McMaster, J.; Lewis, W.; Blake, A. J.; McInnes, E. J. L.; Liddle, S. T., *Angewandte Chemie* **2013,** *52* (18), 4921-4924.

[115] Gould, C. A.; Darago, L. E.; Gonzalez, M. I.; Demir, S.; Long, J. R., *Angewandte Chemie* **2017,** *129* (34), 10237-10241.

[116] Galley, S. S.; Sperling, J. M.; Windorff, C. J.; Zeller, M.; Albrecht-Schmitt, T. E.; Bart, S. C., *Organometallics* **2019,** *38* (3), 606-609.

[117] Dutkiewicz, M. S.; Apostolidis, C.; Walter, O.; Arnold, P. L., *Chem. Sci.* **2017,** *8* (4), 2553-2561.

[118] Clark, D. L.; Sattelberger, A. P.; Bott, S. G.; Vrtis, R. N., *Inorg. Chem.* **1989,** *28* (10), 1771-1773.

[119] Schnaars, D. D.; Wu, G.; Hayton, T. W., *Dalton Trans.* **2008,** (44), 6121-6126.

[120] Kutscher, J.; Schneider, A., *Inorganic and Nuclear Chemistry Letters* **1971,** *7* (9), 815-819.

[121] Boyle, T. J.; Ottley, L. A. M.; Alam, T. M.; Rodriguez, M. A.; Yang, P.; McIntyre, S. K., *Polyhedron* **2010,** *29* (7), 1784-1795.

[122] Xie, Z.; Chiu, K.-y.; Wu, B.; Mak, T. C. W., *Inorg. Chem.* **1996,** *35* (20), 5957-5958.

[123] Brown, J. L.; Davis, B. L.; Scott, B. L.; Gaunt, A. J., *Inorg. Chem.* **2015,** *54* (24), 11958-11968.

[124] Evans, W. J.; Shreeve, J. L.; Ziller, J. W.; Doedens, R. J., *Inorg. Chem.* **1995,** *34* (3), 576-585.

[125] Young, R. C.; Hastings, J. L., *J. Am. Chem. Soc.* **1937,** *59* (4), 765-766.

[126] Carmichael, C. D.; Jones, N. A.; Arnold, P. L., *Inorg. Chem.* **2008,** *47* (19), 8577-8579.

[127] Windorff, C. J.; Dumas, M. T.; Ziller, J. W.; Gaunt, A. J.; Kozimor, S. A.; Evans, W. J., *Inorg. Chem.* **2017,** *56* (19), 11981-11989.

[128] Huebner, L.; Kornienko, A.; Emge, T. J.; Brennan, J. G., *Inorg. Chem.* **2004,** *43* (18), 5659-5664.

[129] La Pierre, H. S.; Heinemann, F. W.; Meyer, K., *Chem. Commun.* **2014,** *50* (30), 3962-3964.

[130] Avens, L. R.; Bott, S. G.; Clark, D. L.; Sattelberger, A. P.; Watkin, J. G.; Zwick, B. D., *Inorg. Chem.* **1994,** *33* (10), 2248-2256.

[131] Evans, W. J.; Kozimor, S. A.; Ziller, J. W.; Fagin, A. A.; Bochkarev, M. N., *Inorg. Chem.* **2005,** *44* (11), 3993-4000.

[132] Asprey, L. B.; Keenan, T. K.; Kruse, F. H., *Inorg. Chem.* **1964,** *3* (8), 1137-1141.

[133] Carter, F. L.; Murray, J. F., *Materials Research Bulletin* **1972,** *7* (6), 519-523.

[134] Corbett, J. D.; Simon, A., Lanthanum Triiodide (and Other Rare Earth Metal Triiodides). In *Inorganic Syntheses*, 1984; pp 519-523.

[135] Gaunt, A. J.; Reilly, S. D.; Enriquez, A. E.; Hayton, T. W.; Boncella, J. M.; Scott, B. L.; Neu, M. P., *Inorg. Chem.* **2008,** *47* (18), 8412-8419.

[136] Natrajan, L.; Mazzanti, M.; Bezombes, J.-P.; Pécaut, J., *Inorg. Chem.* **2005,** *44* (17), 6115-6121.

[137] Niemeyer, M., *Acta Crystallogr., Sect. E: Struct. Rep. Online* **2001,** *57* (8), m363-m364.

[138] Schwarzenbach, G.; Flaschka, H., *Complexometric Titrations*. Second ed.; United Kingdom, 1969.

[139] Shannon, R. D., *Acta Cryst.* **1976,** *A32*, 751-767.

[140] Raymond, K. N.; Eigenbrot, C. W., *Acc. Chem. Res.* **1980,** *13* (8), 276-283.

[141] Robinson, K.; Gibbs, G. V.; Ribbe, P. H., *Science* **1971,** *172* (3983), 567.

[142] Blatov, V. A.; Shevchenko, A. P.; Serenzhkin, V. N., *Acta Crystallographica Section A* **1995,** *51* (6), 909-916.

[143] Wooles, A. J.; Mills, D. P.; Lewis, W.; Blake, A. J.; Liddle, S. T., *Dalton Trans* **2010,** *39* (2), 500-510.

[144] Bradley, D. C.; Ghotra, J. S.; Hart, F. A., *Dalton Trans.* **1973,** (10), 1021-1023.

[145] Sheldrick, G. M., *Acta. Crystallogr. A* **2015,** *71* (1), 3-8.

[146] Dolomanov, O. V.; Bourhis, L. J.; Gildea, R. J.; Howard, J. A. K.; Puschmann, H., *J Appl Crystallogr* **2009,** *42* (2), 339-341.

[147] Sheldrick, G. M., *Acta Crystallogr C* **2015,** *71* (1), 3-8.

[148]

[149] Goodwin, C. A. P.; Reta, D.; Ortu, F.; Chilton, N. F.; Mills, D. P., *J. Am. Chem. Soc.* **2017,** *139* (51), 18714-18724.

[150] Goodwin, C. A. P.; Ortu, F.; Reta, D.; Chilton, N. F.; Mills, D. P., *Nature* **2017,** *548*, 439.

[151] Chilton, N. F.; Goodwin, C. A. P.; Mills, D. P.; Winpenny, R. E. P., *Chem. Commun.* **2015,** *51* (1), 101-103.

[152] Xémard, M.; Cordier, M.; Molton, F.; Duboc, C.; Le Guennic, B.; Maury, O.; Cador, O.; Nocton, G., *Inorg. Chem.* **2019,** *58* (4), 2872-2880.

[153] Xémard, M.; Zimmer, S.; Cordier, M.; Goudy, V.; Ricard, L.; Clavaguéra, C.; Nocton, G., *J. Am. Chem. Soc.* **2018,** *140* (43), 14433-14439.

[154] Hilgar, J. D.; Bernbeck, M. G.; Flores, B. S.; Rinehart, J. D., *Chem. Sci.* **2018,** *9* (36), 7204-7209.

[155] Fataftah, M. S.; Freedman, D. E., *Chem. Commun.* **2018,** *54* (98), 13773-13781.

[156] Atzori, M.; Sessoli, R., *J. Am. Chem. Soc.* **2019,** *141* (29), 11339-11352.

[157] Guo, F.-S.; Day, B. M.; Chen, Y.-C.; Tong, M.-L.; Mansikkamäki, A.; Layfield, R. A., *Angew. Chem. Int. Edit.* **2017,** *56* (38), 11445-11449.

[158] Rinehart, J. D.; Long, J. R., *Chem. Sci.* **2011,** *2* (11), 2078-2085.

[159] Shoshkin, A. N.; Bochkarev, L. N.; Khorshev, S. Y., *Russ. J. Gen. Chem.* **2002,** *72* (5), 715-716.

[160] Bochkarev, L. N.; Druzhkova, O. N.; Zhiltsov, S. F.; Zakharov, L. N.; Fukin, G. K.; Khorshev, S. Y.; Yanovsky, A. I.; Struchkov, Y. T., *Organometallics* **1997,** *16* (4), 500-502.

[161] Evans, W. J., *Polyhedron* **1987,** *6* (5), 803-835.

[162] Bochkarev, M. N., Zakharov, L.N., and Kalinina, G.S., *Organoderivatives of Rare Earth Elements*. Dordrecht: Kluwer Academic: 1995.

[163] James, A. M.; Laxman, R. K.; Fronczek, F. R.; Maverick, A. W., *Inorg. Chem.* **1998,** *37* (15), 3785-3791.

[164] Rad'kov, Y. F. F., E. A.; Khorshev, S. Ya.; Kalinina, G. S.; Bochkarev, M. N.; Razuvaev, G. A., *Zh. Obshch. Khim.* **1985,** *55* (10), 2153.

[165] Crease, A. E.; Legzdins, P., *J. Chem. Soc., Chem. Commun.* **1973,** (20), 775-776.

[166] Beletskaya, I. P.; Suleimanov, G. Z.; Shifrina, R. R.; Mekhdiev, R. Y.; Agdamskii, T. A.; Khandozhko, V. N.; Kolobova, N. E., *J. Organomet. Chem.* **1986,** *299* (2), 239-244.

[167] Ginsberg, A. P., *Inorganic Syntheses*. John Wiley & Sons, Inc: Hoboken NJ, 1990; Vol. 27, p 142-146.

[168] Kaesz, H. D., *Inorganic Syntheses*. John Wiley & Sons, Inc: Hoboken NJ, 1989; Vol. 26, p 17-23.

[169] Edelmann, F. T.; Herrmann, W. A., *Synthetic Methods of Organometallic and Inorganic Chemistry*. Thieme Medical Publishers, Inc: New York, 1997; Vol. 6, p 50-57.

[170] Gilman, H.; Jones, R. G., *J. Org. Chem.* **1945,** *10* (6), 505-515.

[171] Deacon, G. B.; Gardiner, M. G.; Junk, P. C.; Townley, J. P.; Wang, J., *Organometallics* **2012,** *31* (10), 3857-3864.

[172] Deacon, G. B.; Forsyth, C. M.; Nickel, S., *J. Organomet. Chem.* **2002,** *647* (1), 50-60.

[173] Graves, C. R.; Kiplinger, J. L., *Chem. Commun.* **2009,** (26), 3831-3853.

[174] Lewis, A. J.; Nakamaru-Ogiso, E.; Kikkawa, J. M.; Carroll, P. J.; Schelter, E. J., *Chem. Commun.* **2012,** *48* (41), 4977-4979.

[175] Graves, C. R.; Scott, B. L.; Morris, D. E.; Kiplinger, J. L., *J. Am. Chem. Soc.* **2007,** *129* (39), 11914-11915.

[176] Rice, N. T.; Su, J.; Gompa, T. P.; Russo, D. R.; Telser, J.; Palatinus, L.; Bacsa, J.; Yang, P.; Batista, E. R.; La Pierre, H. S., *Inorg. Chem.* **2019,** *58* (8), 5289-5304.

[177] Rice, N. T.; Popov, I. A.; Russo, D. R.; Bacsa, J.; Batista, E. R.; Yang, P.; Telser, J.; La Pierre, H. S., *J. Am. Chem. Soc.* **2019,** *141* (33), 13222-13233.

[178] Goodwin, C. A. P.; Joslin, K. C.; Lockyer, S. J.; Formanuik, A.; Morris, G. A.; Ortu, F.; Vitorica-Yrezabal, I. J.; Mills, D. P., *Organometallics* **2015,** *34* (11), 2314-2325.

[179] Goodwin, C. A. P.; Chilton, N. F.; Vettese, G. F.; Moreno Pineda, E.; Crowe, I. F.; Ziller, J. W.; Winpenny, R. E. P.; Evans, W. J.; Mills, D. P., *Inorg. Chem.* **2016,** *55* (20), 10057-10067.

[180] Willauer, A. R.; Toniolo, D.; Fadaei-Tirani, F.; Yang, Y.; Laurent, M.; Mazzanti, M., *Dalton Trans.* **2019,** *48* (18), 6100-6110.

[181] Yang, L.; Powell, D. R.; Houser, R. P., *Dalton Trans.* **2007,** (9), 955-964.

[182] Hänninen, P.; Härmä, H., *Lanthanide Luminescence: Photophysical, Analytical and Biological Aspects*. Springer: Berlin, 2013.

[183] Bain, G. A.; Berry, J. F., *J. Chem. Educ.* **2008,** *85* (4), 532.

[184] Beckmann, J.; Dakternieks, D.; Duthie, A.; Larchin, M. L.; Tiekink, E. R. T., *Appl. Organomet. Chem.* **2003,** *17* (1), 52-62.

[185] Ltd., P. o. V. P. Persistence of Vision Raytracer (Version 3.6) [Computer software]. Retrieved from http://www.povray.org/download/.

[186] Gompa, T. P.; Ramanathan, A.; Rice, N. T.; La Pierre, H. S., *Dalton Trans.* **2020,** *49* (45), 15945-15987.

[187] Piro, N. A.; Robinson, J. R.; Walsh, P. J.; Schelter, E. J., *Coord. Chem. Rev.* **2014,** *260*, 21-36.

[188] Evans, W. J.; Davis, B. L., *Chem. Rev.* **2002,** *102* (6), 2119-2136.

[189] Morss, L. R., *Chem. Rev.* **1976,** *76* (6), 827-841.

[190] Nocton, G.; Ricard, L., *Dalton Trans.* **2014,** *43* (11), 4380-4387.

[191] Cheisson, T.; Auffrant, A.; Nocton, G., *Organometallics* **2015,** *34* (22), 5470-5478.

[192] MacDonald, M. R.; Bates, J. E.; Fieser, M. E.; Ziller, J. W.; Furche, F.; Evans, W. J., *J. Am. Chem. Soc.* **2012,** *134* (20), 8420-8423.

[193] Evans, W. J., *Organometallics* **2016,** *35* (18), 3088-3100.

[194] Heitmann, D.; Jones, C.; Mills, D. P.; Stasch, A., *Dalton Trans.* **2010,** *39* (7), 1877-1882.

[195] Jacquot, L.; Xémard, M.; Clavaguéra, C.; Nocton, G., *Organometallics* **2014,** *33* (15), 4100-4106.

[196] Nocton, G.; Ricard, L., *Chem. Commun.* **2015,** *51* (17), 3578-3581.

[197] Andrez, J.; Bozoklu, G.; Nocton, G.; Pécaut, J.; Scopelliti, R.; Dubois, L.; Mazzanti, M., *Chem-Eur. J.* **2015,** *21* (43), 15188-15200.

[198] Xémard, M.; Goudy, V.; Braun, A.; Tricoire, M.; Cordier, M.; Ricard, L.; Castro, L.; Louyriac, E.; Kefalidis, C. E.; Clavaguéra, C.; Maron, L.; Nocton, G., *Organometallics* **2017,** *36* (23), 4660-4668.

[199] Cheisson, T.; Ricard, L.; Heinemann, F. W.; Meyer, K.; Auffrant, A.; Nocton, G., *Inorg. Chem.* **2018,** *57* (15), 9230-9240.

[200] Xémard, M.; Cordier, M.; Louyriac, E.; Maron, L.; Clavaguéra, C.; Nocton, G., *Dalton Trans.* **2018,** *47* (28), 9226-9230.

[201] Willauer, A. R.; Dabrowska, A. M.; Scopelliti, R.; Mazzanti, M., *Chem. Commun.* **2020,** *56* (63), 8936-8939.

[202] Toniolo, D.; Willauer, A. R.; Andrez, J.; Yang, Y.; Scopelliti, R.; Maron, L.; Mazzanti, M., *Chem-Eur. J.* **2019,** *25* (33), 7831-7834.

[203] Kelly, R. P.; Toniolo, D.; Tirani, F. F.; Maron, L.; Mazzanti, M., *Chem. Commun.* **2018,** *54* (73), 10268-10271.

[204] Plesniak, M. P.; Just-Baringo, X.; Ortu, F.; Mills, D. P.; Procter, D. J., *Chem. Commun.* **2016,** *52* (92), 13503-13506.

[205] Moutet, J.; Schleinitz, J.; La Droitte, L.; Tricoire, M.; Pointillart, F.; Gendron, F.; Simler, T.; Clavaguéra, C.; Le Guennic, B.; Cador, O.; Nocton, G., *Angew. Chem. Int. Edit.*, Accepted Author Manuscript.

[206] Woodruff, D. N.; Winpenny, R. E. P.; Layfield, R. A., *Chem. Rev.* **2013,** *113* (7), 5110-5148.

[207] Zhang, W.; Muhtadi, A.; Iwahara, N.; Ungur, L.; Chibotaru, L. F., *Angew. Chem. Int. Edit.* **2020,** *59* (31), 12720-12724.

[208] Rice, N. T.; Popov, I. A.; Russo, D. R.; Gompa, T. P.; Ramanathan, A.; Bacsa, J.; Batista, E. R.; Yang, P.; La Pierre, H. S., *Chem. Sci.* **2020,** *11* (24), 6149-6159.

[209] Willauer, A. R.; Palumbo, C. T.; Scopelliti, R.; Zivkovic, I.; Douair, I.; Maron, L.; Mazzanti, M., *Angew. Chem. Int. Edit.* **2020,** *59* (9), 3549-3553.

[210] Palumbo, C. T.; Zivkovic, I.; Scopelliti, R.; Mazzanti, M., *J. Am. Chem. Soc.* **2019,** *141* (25), 9827-9831.

[211] Willauer, A. R.; Palumbo, C. T.; Fadaei-Tirani, F.; Zivkovic, I.; Douair, I.; Maron, L.; Mazzanti, M., *J. Am. Chem. Soc.* **2020,** *142* (12), 5538-5542.

[212] Goldfarb, D.; Stoll, S., *EPR Spectroscopy*. eMagRes: 2017.

[213] Deblonde, G. J. P.; Sturzbecher-Hoehne, M.; Rupert, P. B.; An, D. D.; Illy, M.-C.; Ralston, C. Y.; Brabec, J.; de Jong, W. A.; Strong, R. K.; Abergel, R. J., *Nat. Chem.* **2017,** *9* (9), 843-849.

[214] Antonio, M. R.; Williams, C. W.; Soderholm, L., *Radiochim. Acta.* **2002,** *90* (12), 851-856.

[215] Cary, S. K.; Su, J.; Galley, S. S.; Albrecht-Schmitt, T. E.; Batista, E. R.; Ferrier, M. G.; Kozimor, S. A.; Mocko, V.; Scott, B. L.; Van Alstine, C. E.; White, F. D.; Yang, P., *Dalton Trans.* **2018,** *47* (41), 14452-14461.

[216] Sperling, J. M.; Warzecha, E. J.; Celis-Barros, C.; Sergentu, D.-C.; Wang, X.; Klamm, B. E.; Windorff, C. J.; Gaiser, A. N.; White, F. D.; Beery, D. A.; Chemey, A. T.; Whitefoot, M. A.; Long, B. N.; Hanson, K.; Kögerler, P.; Speldrich, M.; Zurek, E.; Autschbach, J.; Albrecht-Schönzart, T. E., *Nature* **2020,** *583* (7816), 396-399.

[217] Krzystek, J.; Ozarowski, A.; Telser, J., *Coord. Chem. Rev.* **2006,** *250* (17), 2308-2324.

[218] Hassan, A. K.; Pardi, L. A.; Krzystek, J.; Sienkiewicz, A.; Goy, P.; Rohrer, M.; Brunel, L. C., *J. Magn. Reson.* **2000,** *142* (2), 300-312.

[219] Telser, J.; Ozarowski, A.; Krzystek, J., High-frequency and -field electron paramagnetic resonance of transition metal ion (d block) coordination complexes. In *Electron Paramagnetic Resonance: Volume 23*, The Royal Society of Chemistry: 2013; Vol. 23, pp 209-263.

[220] Telser, J., *eMagRes* **2017,** *6* (2), 207-234.

[221] Telser, J., EPR Interactions - Zero Field Splittings. In *EPR Spectroscopy: Fundamentals and Methods*, Goldfarb, D.; Stoll, S., Eds. John Wiley & Sons, Ltd.: Chichester, UK, 2018; pp 29-63.

[222] Benmelouka, M.; Van Tol, J.; Borel, A.; Port, M.; Helm, L.; Brunel, L. C.; Merbach, A. E., *J. Am. Chem. Soc.* **2006,** *128* (24), 7807-7816.

[223] Clayton, J. A.; Keller, K.; Qi, M.; Wegner, J.; Koch, V.; Hintz, H.; Godt, A.; Han, S.; Jeschke, G.; Sherwin, M. S.; Yulikov, M., *Phys. Chem. Chem. Phys.* **2018,** *20* (15), 10470-10492.

[224] Newman, D. J.; Urban, W., *Adv. Phys.* **1975,** *24* (6), 793-844.

[225] Raitsimring, A. M.; Astashkin, A. V.; Baute, D.; Goldfarb, D.; Poluektov, O. G.; Lowe, M. P.; Zech, S. G.; Caravan, P., *Chem. Phys. Chem.* **2006,** *7* (7), 1590-1597.

[226] Attempts to prepare analogs of **1-Eu^{2+}** with one or both of the potassium cations sequestered as outer sphere cations in crypts or crowns uniformly resulted in the isolation of oxidized products.

[227] Shannon, R., *Acta Crystallogr., Sect. A: Cryst.. Phys., Diffr., Theor. Gen. Crystallogr.* **1976,** *32*, 751-767.

[228] Chilton, N. F.; Anderson, R. P.; Turner, L. D.; Soncini, A.; Murray, K. S., *J. Comput. Chem.* **2013,** *34* (13), 1164-1175.

[229] Stoll, S.; Schweiger, A., *J. Magn. Reson.* **2006,** *178* (1), 42-55.

[230] Azarkh, M.; Groenen, E. J. J., *J. Magn. Reson.* **2015,** *255*, 106-113.

[231] Abragam, A.; Bleaney, B., *Electron Paramagnetic Resonance of Trasition Ions*. Clarendon Press: 1970.

[232] Vazhenin, V. A.; Artyomov, M. Y.; Potapov, A. P.; Chernyshev, V. A.; Fokin, A. V.; Serdtsev, A. V., *Phys. Solid State* **2017,** *59* (5), 967-972.

[233] Vazhenin, V. A.; Potapov, A. P.; Asatryan, G. R.; Uspenskaya, Y. A.; Petrosyan, A. G.; Fokin, A. V., *Phys. Solid State* **2016,** *58* (8), 1627-1633.

[234] Yeom, T. H.; Lee, S. H.; Choh, S. H.; Han, T. J.; Kim, T. H.; Ro, J. H., *J. Appl. Phys.* **2003,** *94* (6), 3796-3799.

[235] Yeom, T. H.; Kim, I. G.; Lee, S. H.; Choh, S. H.; Kim, T. H.; Ro, J. H., *J. Appl. Phys.* **2000,** *87* (3), 1424-1428.

[236] Baker, J. M.; Chadwick, J. R.; Garton, G.; Hurrell, J. P.; Bleaney, B., *Proc. R. Soc. Lon. Ser-A.* **1965,** *286* (1406), 352-365.

[237] First-order perturbation theory gives these results, which for low rhombicity, $|E/D| < 0.1$, is accurate to better than 1% compared to an exact calculation. The complete analysis, here assuming $D > 0$ and setting the lowest doublet ($m_S = \pm 1/2$) at $[-5D-(37.5)E^2/D]$, gives the next doublet ($m_S = \pm 3/2$) at $[-3D + (27.9)E^2/D]$, the next ($m_S = \pm 5/2$) at $[D + (7.5)E^2/D]$, and the highest ($m_S = \pm 7/2$) at $[7D + (2.1)E^2/D]$. For example, 1-Eu^{2+}, the maximum splitting is 0.596 cm^{-1} from this equation which is close to $\Delta_{8S} = 0.58$ cm^{-1}.

[238] Freidzon, A. Y.; Kurbatov, I. A.; Vovna, V. I., *Phys. Chem. Chem. Phys.* **2018,** *20* (21), 14564-14577.

[239] Kramida, A., Ralchenko, Y., Reader, J., and NIST ASD Team (2020). NIST Atomic Spectra Database (ver. 5.8), [Online]. Available: https://physics.nist.gov/asd [2020, December 30]. National Institute of Standards and Technology, Gaithersburg, MD. DOI: https://doi.org/10.18434/T4W30F.

[240] Beck, D. R.; Domeier, E., *Can. J. Phys.* **2009,** *87* (1), 75-81.

[241] Hutton, D. R.; Milne, R. J., *J. Phys. C* **1969,** *2* (12), 2297-2300.

[242] Hansen, S.; Mosel, B. D.; Müller-Warmuth, W.; Fielding, P. E., *Z. Naturforsch. A* **1996,** *51* (8), 885-894.

[243] Ebendorff-Heidepriem, H.; Ehrt, D., *J. Phys. Condens. Matter* **1999,** *11* (39), 7627-7634.

[244] Andersson, K.; Malmqvist, P. Å.; Roos, B. O., *J. Chem. Phys.* **1992,** *96* (2), 1218-1226.

[245] Andersson, K.; Malmqvist, P. A.; Roos, B. O.; Sadlej, A. J.; Wolinski, K., *J. Phys. Chem.* **1990,** *94* (14), 5483-5488.

[246] Malmqvist, P.-Å.; Roos, B. O., *Chem. Phys. Lett.* **1989,** *155* (2), 189-194.

[247] Angeli, C.; Cimiraglia, R.; Evangelisti, S.; Leininger, T.; Malrieu, J.-P., *J. Chem. Phys.* **2001,** *114* (23), 10252-10264.

[248] Angeli, C.; Cimiraglia, R.; Malrieu, J.-P., *J. Chem. Phys.* **2002,** *117* (20), 9138-9153.

[249] Angeli, C.; Cimiraglia, R.; Malrieu, J.-P., *Chem. Phys. Lett.* **2001,** *350* (3), 297-305.

[250] Angeli, C.; Bories, B.; Cavallini, A.; Cimiraglia, R., *J. Chem. Phys.* **2006,** *124* (5), 054108.

[251] Jung, J.; Atanasov, M.; Neese, F., *Inorg. Chem.* **2017,** *56* (15), 8802-8816.

[252] Aravena, D.; Atanasov, M.; Neese, F., *Inorg. Chem.* **2016,** *55* (9), 4457-4469.

[253] Singh, S. K.; Eng, J.; Atanasov, M.; Neese, F., *Coord. Chem. Rev.* **2017,** *344*, 2-25.

[254] Neese, F.; Solomon, E. I., Interpretation and Calculation of Spin-Hamiltonian Parameters in Transition Metal Complexes. In *Magnetism: Molecules to Materials IV*, 2001; pp 345-466.

[255] Ballhausen, C. J., *Introduction to Ligand Field Theory*. McGraw-Hill Book Company Inc: 1962.

[256] Jo/rgensen, C. K.; Pappalardo, R.; Schmidtke, H. H., *J. Chem. Phys.* **1963,** *39* (6), 1422-1430.

[257] Neese, F.; Solomon, E. I., *Inorg. Chem.* **1998,** *37* (26), 6568-6582.

[258] The NIST Atomic Spectra Database Levels Data [73-74] gives extensive information on free ion Eu^{2+}, minimal on Gd^{3+}, and none on Tb^{4+}. Thus, direct comparison of the trends observed here for imidophosphorane complexes with the free-ions is not possible. It is clear, however, that the ^{6}P first excited state is closer in energy to the ^{8}S ground state in Eu^{2+} than in Gd^{3+} (by ~10 – 15%), which is consistent with the results in Table 4.2. The ground state character calculated here (Table 4.2) being ~97% ^{8}S and ~3% ^{6}P is also consistent with free-ion results.

[259] Atanasov, M.; Aravena, D.; Suturina, E.; Bill, E.; Maganas, D.; Neese, F., *Coord. Chem. Rev.* **2015,** *289-290*, 177-214.

[260] Su, J.; Batista, E. R.; Boland, K. S.; Bone, S. E.; Bradley, J. A.; Cary, S. K.; Clark, D. L.; Conradson, S. D.; Ditter, A. S.; Kaltsoyannis, N.; Keith, J. M.; Kerridge, A.; Kozimor, S. A.; Löble, M. W.; Martin, R. L.; Minasian, S. G.; Mocko, V.; La Pierre, H. S.; Seidler, G. T.; Shuh, D. K.; Wilkerson, M. P.; Wolfsberg, L. E.; Yang, P., *J. Am. Chem. Soc.* **2018,** *140* (51), 17977-17984.

[261] Gompa, T. P.; Rice, N. T.; Russo, D. R.; Aguirre Quintana, L. M.; Yik, B. J.; Bacsa, J.; La Pierre, H. S., *Dalton Trans.* **2019,** *48* (23), 8030-8033.

[262] Girard, P.; Namy, J. L.; Kagan, H. B., *J. Am. Chem. Soc.* **1980,** *102* (8), 2693-2698.

[263] Dolomanov, O. V.; Bourhis, L. J.; Gildea, R. J.; Howard, J. A. K.; Puschmann, H., *J. Appl. Crystallogr.* **2009,** *42*, 339-341.

[264] Sheldrick, G. M., *Acta. Crystallogr. A* **2015,** *71*, 3-8.

[265] Sheldrick, G. M., *Acta. Crystallogr. C* **2015,** *71*, 3-8.

[266] **Persistence of Vision Pty. Ltd. (2004) Persistence of Vision Raytracer (Version 3.6) [Computer Software]. Retrieved from http://www.povray.org/download/**.

[267] van Lenthe, E.; Baerends, E. J.; Snijders, J. G., *J. Chem. Phys.* **1994,** *101* (11), 9783-9792.

[268] van Lenthe, E.; Baerends, E. J.; Snijders, J. G., *J. Chem. Phys.* **1993,** *99* (6), 4597-4610.

[269] Hess, B. A., *Phys. Rev. A* **1986,** *33* (6), 3742-3748.

[270] Angeli, C.; Cimiraglia, R.; Evangelisti, S.; Leininger, T.; Malrieu, J. P., *J. Chem. Phys.* **2001,** *114* (23), 10252-10264.

[271] Ganyushin, D.; Neese, F., *J. Chem. Phys.* **2013,** *138* (10), 104113.

[272] Ganyushin, D.; Neese, F., *J. Chem. Phys.* **2006,** *125* (2), 024103.

[273] *Mixed Valency Systems: Applications in Chemistry, Physics, and Biology*. Kluwer Academic Publishers: Dordrecht, Boston, London, 1991; Vol. 343.

[274] Barandiarán, Z.; Seijo, L., *J. Chem. Phys.* **2014,** *141* (23), 234704.

[275] Cowan, D. O.; LeVanda, C.; Park, J.; Kaufman, F., *Acc. Chem. Res.* **1973,** *6* (1), 1-7.

[276] Demadis, K. D.; Hartshorn, C. M.; Meyer, T. J., *Chem. Rev.* **2001,** *101* (9), 2655-2686.

[277] Richardson, D. E.; Taube, H., *Coord. Chem. Rev.* **1984,** *60*, 107-129.

[278] Wickleder, C., *Z. Naturforsch. Pt. B.* **2002,** *57* (8), 901-907.

[279] Jiang, Y.; Zhu, X.; Chen, M.; Wang, Y.; Yao, Y.; Wu, B.; Shen, Q., *Organometallics* **2014,** *33* (8), 1972-1976.

[280] van Schaik, W.; Lizzo, S.; Smit, W.; Blasse, G., *J. Electrochem. Soc.* **1993,** *140* (1), 216-222.

[281] Lange, F. T.; Bärnighausen, H., *Z. Anorg. Allg. Chem.* **1993,** *619* (10), 1747-1754.

[282] Wickleder, C., *Z. Anorg. Allg. Chem.* **2002,** *628* (8), 1815-1820.

[283] Pyykkö, P.; Atsumi, M., *Chem-Eur. J.* **2009,** *15* (1), 186-197.

[284] Robin, M. B.; Day, P., Mixed Valence Chemistry-A Survey and Classification. In *Advances in Inorganic Chemistry and Radiochemistry*, Emeléus, H. J.; Sharpe, A. G., Eds. Academic Press: 1968; Vol. 10, pp 247-422.